PHD

Site Selective Catalytic C-H Functionalisation

Leitch, Jamie

Award date:
2017

Awarding institution:
University of Bath

Department of Chemistry | UNIVERSITY OF BATH | syngenta

Site Selective Catalytic C–H Functionalisation

Jamie Alexander Leitch

Thesis Submitted for the Degree of Doctor of Philosophy

Department of Chemistry

University of Bath

October 2017

Supervisors:

Prof. Christopher G. Frost and Dr. Yunas Bhonoah

Contents

Acknowledgments

I would first and foremost like to thank Christopher Frost for his continuing support, enthusiasm and supervision throughout my PhD studies. I would also like to thank Yunas Bhonoah for his supervision, especially during my CASE placement at Jealott's Hill.

I would also like to thank the rest of the Frost group, especially Sean and Baz for their invaluable input, discussion and help during my research, as well as Will, Andy, Sinéad, Callum, Ella and Sam for their day to day sanity check.

I also thank Ella, Hans, Janette and Liliane for allowing me to supervise their Masters projects and carrying out my hair-brained ideas.

I would greatly like to thank Claire McMullin for her ongoing professional collaboration even through maternity leave. I would also like to thank Philippe Wilson and Ian Williams for further computational collaborations.

I would also like to thank John Lowe, Catherine Lyall (both NMR), Mary Mahon, and Gabi Kociok-Koln (both Crystallography) for their invaluable help throughout my research.

Last but by no means least, I would like to thank Kathryn for her continued and unmatched support over the course of the last three years, I honestly couldn't have done it without her.

Abstract

Harnessing site selectivity in C–H functionalisation remains one of the greatest challenges in modern catalysis. In order to differentiate electronically and sterically similar C–H bonds, a variety of pioneering methods have been developed in recent years. One of the key developments is the use of Lewis basic directing groups to selectively direct a metal centre. The results herein report the manipulation of directing group chemistry to allow selective *ortho*, *meta* and *para* C–H functionalisation of arenes.

Chapter 1 reports the developments in moving beyond *ortho*-selectivity in transition metal catalysed C–H functionalisation chemistry.

Chapter 2 reports the use of the biologically relevant oxazolidinone and hydantoin heterocycles as weakly coordinating directing groups in ruthenium catalysed *ortho*-C–H alkenylation methodology.

Chapter 3 reports the application of ruthenium catalysed σ-activation to the remote C–H functionalisation of indoles at the C6 position and carbazoles at the C4 position.

Chapter 4 reports the manipulation of site selective cyclometalation and its application in the *para*-C–H alkylation of aniline derivatives.

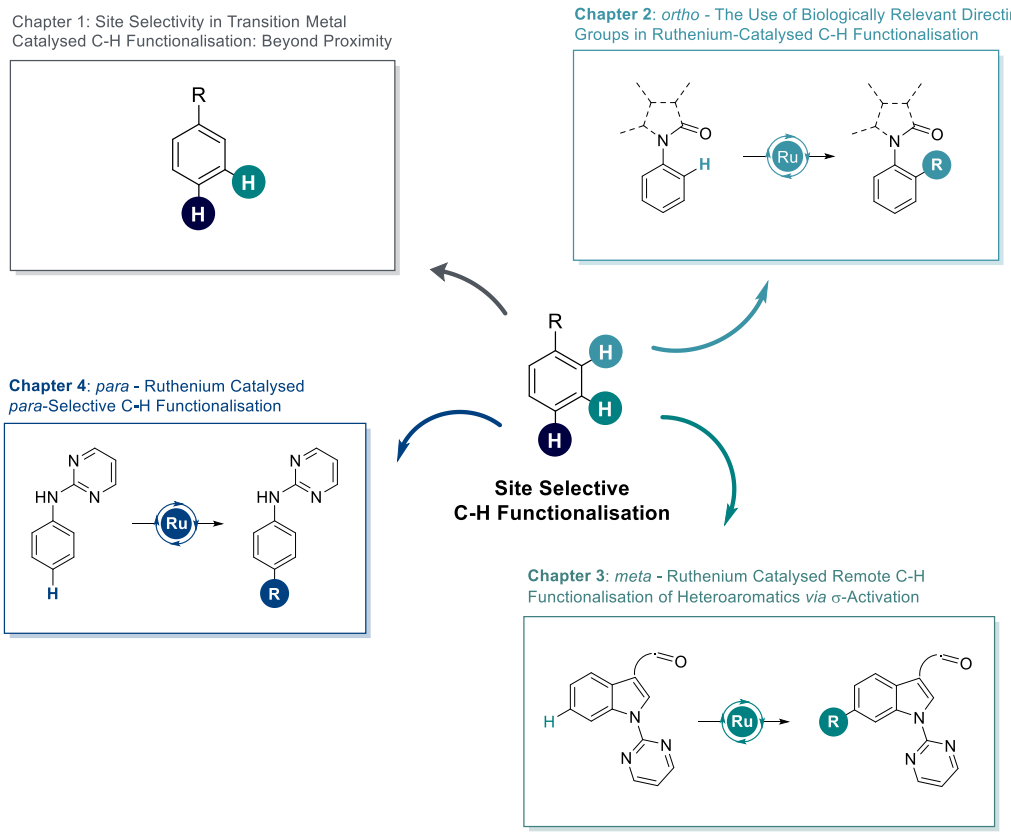

Publication List

7. “Ruthenium Catalyzed Remote C4-Selective C–H Functionalization of Carbazoles *via* σ-Activation.” **J. A. Leitch**, C. J. Heron, J. McKnight, G. Kociok-Köhn, Y. Bhonoah, and C. G. Frost, *Chem. Commun.*, 2017, **53**, 13039.

6. “Ruthenium-Catalyzed *para*-Selective C–H Alkylation of Aniline Derivatives via Ru-N σ-Activation.” **J. A. Leitch**, C. L. McMullin, A. J. Paterson, M. F. Mahon, Y. Bhonoah, and C. G. Frost, *Angew. Chem. Int. Ed.*, 2017, **129**, 15327.

5. “Ruthenium-Catalysed σ-Activation for Remote *meta*-C–H Functionalisation.” **J. A. Leitch** and C. G. Frost, *Chem. Soc. Rev.*, 2017, **46**, 7145.

4. “Beyond C2 & C3: Transition-Metal Catalyzed C–H Functionalization of Indole and other Related Heteroaromatics.” **J. A. Leitch**, Y. Bhonoah, and C. G. Frost, *ACS Catal.*, 2017, **7**, 5618.

3. “Remote C6-Selective Ruthenium Catalyzed C–H Alkylation of Indole Derivatives via σ-Activation.” **J. A. Leitch**, C. L. McMullin, M. F. Mahon, Y. Bhonoah, and C. G. Frost, *ACS Catal.*, 2017, **7**, 2616.

2. “Use of the Hydantoin Directing Group in Ruthenium(II)-Catalyzed C–H Functionalization.” **J. A. Leitch**, H. P. Cook, Y. Bhonoah, and C. G. Frost, *J. Org. Chem.*, 2016, **81**, 10081.

1. “Ruthenium(II)-Catalyzed C–H Functionalization Using the Oxazolidinone Heterocycle as a Weakly Coordinating Directing Group: Experimental and Computational Insights.” **J. A. Leitch**, P. B. Wilson, M. F. Mahon, Y. Bhonoah, C. L. McMullin, I. H. Williams, and C. G. Frost. *ACS Catal.*, 2016, **6**, 5520.

Abbreviations

2,4-DNPH – 2,4-dinitrophenylhydrazine
Ac – Acetyl
Acac - Acetylacetone
ACS – American Chemical Society
Ad – Adamantyl
Ala – Alanine
Alk – Alkyl
Ar – Aryl
Ar_F – Polyfluorinated aryl
AMLA – Ambiphilic metal-ligand activation
Atm – Atmosphere
Aux - Auxiliary
Bn – Benzyl
Boc – *tert*-butoxycarbonyl
Bz – Benzoyl
Bu – Butyl
Cat. - Catalytic
cm - Cymene
CMD – Concerted metalation deprotonation
COD – Cyclooctadiene
Cp – Cyclopentadiene
Cp* - Pentamethylcyclopentadiene
CPME – Cyclopentyl methyl ether
CSA – Camphor sulfonic acid ((7,7-dimethyl-2-oxobicyclo[2.2.1]heptan-1-yl)methanesulfonic acid)
Cy - Cyclohexyl
dba – Dibenzylideneacetone
DBU – 1,8-diazabicyclo[5.4.0]undec-7-ene
DCE – 1,2-dichloroethane
DBAD – Di-*tert*-butyl azodicarboxylate
DCM – Dichloromethane
DFT – Density Functional Theory
DIPEA - *N*,*N*-Diisopropylethylamine
DMA – *N,N*-dimethylacetamide

DME - 1,2-dimethoxyethane

DMEDA - *N*,*N*′-Dimethylethylenediamine

DMF – *N,N*-dimethylformamide

DMSO - Dimethylsulfoxide

DG – Directing group

DMPE – 1,2-bis(diphenylphosphino)methane

DPPE – 1,2-bis(diphenylphosphino)ethane

DTBP – Di-*tert*-butyl peroxide

dtbpy – 2,6-di-*tert*-butylpyridine

dtbbpy - 4,4′-di-tert-butyl-2,2′-dipyridyl

EN - ethylenediamine

ESI – Electrospray Ionisation

Et – Ethyl

EWG – Electron withdrawing group

Eq – Equivalent

FT-IR – Fourier Transform Infra-Red

Gly – Glycine

Hex - Hexane

HFIP – 1,1,1,3,3,3-hexafluoro-2-propanol

HMDS – Bis(trimethylsilyl)amide

HPLC – High Performance Liquid Chromatography

HRMS – High Resolution Mass Spectrometry

i – iso

IM – Imidazolinium

INT – Intermediate

IR – Infra-Red

In - Indole

Ind – Indene

KIE – Kinetic Isotope Effect

LC-MS – Liquid Chromatography Mass Spectrometry

LED – Light emitting diode

L_n – Unspecified ligand set

LUMO – Lowest unoccupied molecular orbital

LR – Lawesson's reagent (2,4-bis(4-methoxyphenyl)-1,3,2,4-dithiadiphosphetane-2,4-disulfide)

M – Metal

m – meta

Me – Methyl

Mes – 1,4,6-trimethyl

mp – Melting point

MS – Molecular sieves

MS – Mass Spectrometry

Ms - Methanesulfonyl

NBO – Natural Bond Order

NBS – *N*-bromosuccinimide

NFSI – *N*-fluorobenzenesulfonimide

NMP – *N*-methylpyrrolidnone

NMR – Nuclear Magnetic Resonance

Ns – 2-nitrotoluenesulfonyl

o – ortho

OLED – Organic Light Emitting Diode

o.n. - Overnight

p – para

PEPPSI-IPr – [1,3-bis(2,6-diisopropylphenyl)imidazol-2-ylidene](3-chloropyridyl)palladium(II) dichloride

Ph – Phenyl

Phe – Phenylalanine

Phen – 1,10-phenanthroline

Pin – Pinacol (2,3-dimethylbutane-2,3-diol)

Piv – 2,2-dimethylpropanoyl

Pm – Pyrimidine

Pr – Propyl

Py – Pyridine / pyridyl

Quant. – Quantitative

rt – Room temperature

s - sec

SCXRD – Single Crystal X-Ray Diffraction

S_EAr – Electrophilic aromatic substitution

SET – Single electron transfer

SOMO – Singly occupied molecular orbital

SPhos – 2-dicyclohexylphosphino-2′,6′-dimethoxybiphenyl

t – tert

*t*AmOH – 2-methyl-2-butanol

TBA – Tetrabutylammonium

TBAF – Tetrabutylammonium fluoride

TBAI – Tetrabutylammonium iodide

TBME – *tert*-butyl methyl ether

Tc – 2-thiophenecarboxylate

TEMPO – (2,2,6,6-tetramethyl-piperidin-1-yl)oxyl

Tf – trifyl (trifluoromethanesulfonyl)

TFA – Trifluoroacetic acid / trifluoroacetate

THF – Tetrahydrofuran

TIPP - Triisopropylphenyl

TIPS – Triisopropylsilyl

TLC – Thin Layer Chromatography

TM – Transition Metal

TMEDA – *N,N,N',N'*-tetramethylethylenediamine

TMP – 3,4,5-trimethoxyphenyl

TOF – Time of Flight

Tol – Toluene

Triphos - Bis(diphenylphosphinoethyl)phenylphosphine

TS – Transition State

Ts – *para*-toluenesulfonyl

TSA – toluenesulfonic acid

Val – Valine

Xantphos - 4,5-bis(diphenylphosphino)-9,9-dimethylxanthene

Chapter 1: Site Selectivity in Transition-Metal Catalysed C–H Functionalisation: Beyond Proximity

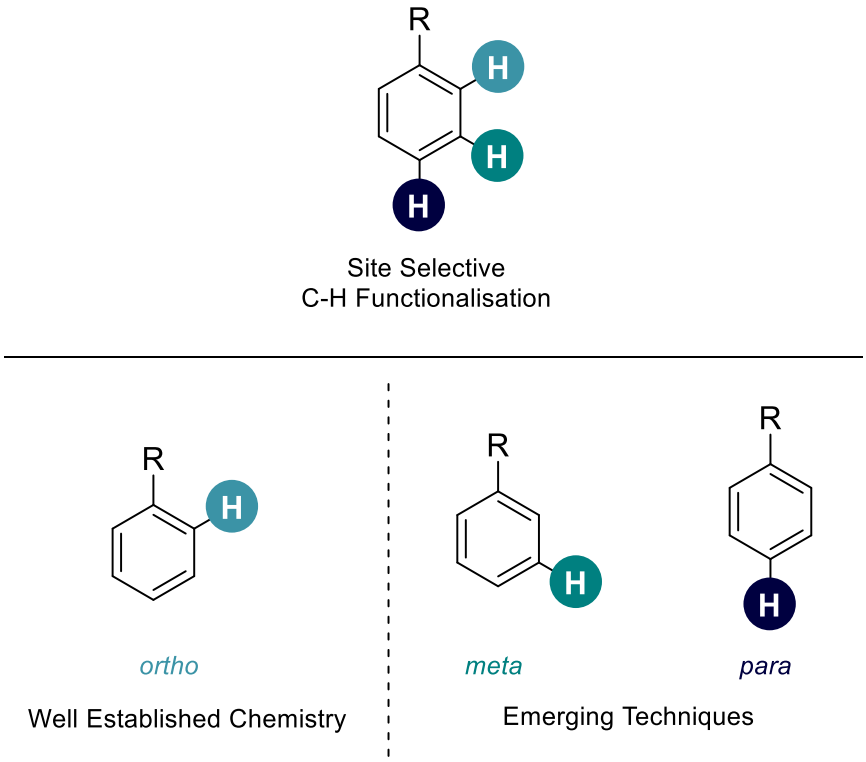

"Controlling the regioselectivity of C–H bond functionalization is imperative to harness its full potential." [1]

1.1: *ortho*: The Birth of Directed C–H Functionalisation

The ability to transform seemingly inert C–H bonds into reactive functional groups has become one of the greatest tasks in recent modern catalytic development. This is because one of the greatest assets of C–H functionalisation methodology is its potential use in late stage functionalisation for *inter alia* drug discovery and natural product synthesis.[2] This power to access untapped chemical space using modern transition metal catalysis is of great interest to both industry and academia. C–H functionalisation has its principle advantages over traditional cross coupling methodologies, such as the Suzuki, Negishi, and Stille reactions, in that at least one of the substrates do not need to be pre-functionalised with functional groups ($B(OR)_2$, ZnR, and SnR_3 respectively) that will eventually become atomic waste.

The major challenge in C–H functionalisation is the ability to selectively transform certain C–H bonds. This has been combatted by many through two clear methods. The first is direct C–H functionalisation where a highly active metal centre exploits the careful manipulation of steric and electronic effects to enable selective C–H activation. This C–H cleavage will take place at the most/least electron dense, most acidic or least hindered C–H bond, depending on the catalyst system employed (Scheme 1-1a).[3] The second is directed C–H activation, here a Lewis basic directing group can coordinate a metal centre and facilitate selective insertion *ortho* to the directing group (Scheme 1-1b). The latter of these will form the focus of the review from this point on.

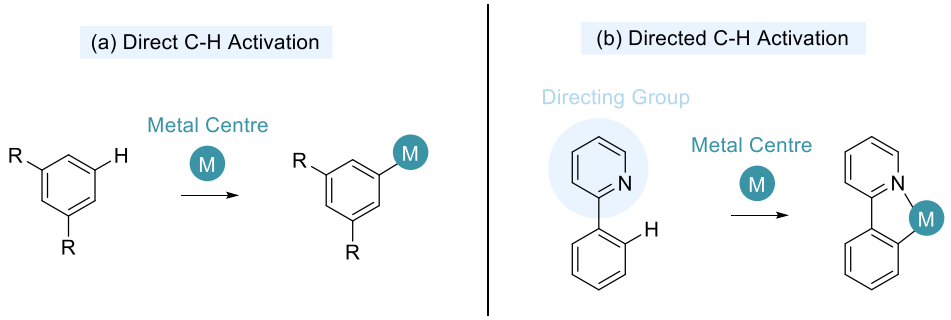

Scheme 1-1: Direct vs Directed C–H Activation

There are multiple pathways in which a metal centre/complex can enable C–H activation to form a cyclometalated intermediate. These include oxidative addition, electrophilic addition to a metal centre, σ-bond metathesis, and concerted metalation deprotonation (CMD, also known as AMLA). The first and last of these have become the

most widely used in C–H activation methodology (Scheme 1-2). A pure organometallic oxidative addition can be carried out with low-valent electron rich complexes of rare earth transition metals. This also leads to a net +2 change in the oxidation state. CMD, first proposed by McGregor[4] and Fagnou[5] relies on the use of its coordinated carboxylate ligand to act as a proton shuttle to enable C–H activation, and due to this there is no net oxidation state change in the metal. This allows CMD to be more widespread, especially to base metals. CMD was first applied to ruthenium catalysis by Dixneuf[6] and Ackermann.[7] It must be noted that both CMD and oxidative addition are also used in direct C–H activation.

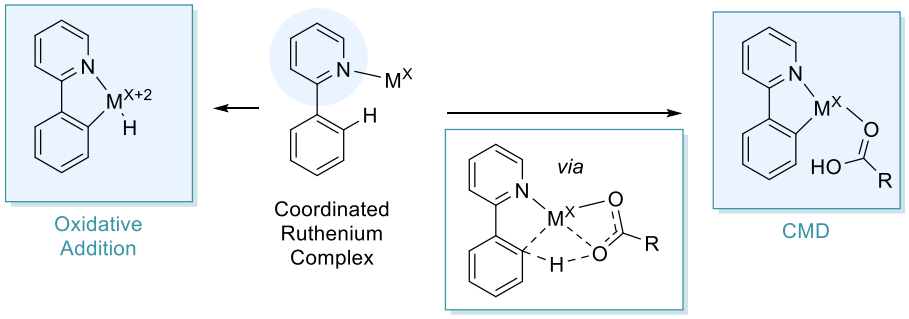

Scheme 1-2: Methods of C–H Activation where X = Oxidation State of Metal (M)

This cyclometalate can then coordinate a coupling partner and then cross couple this in a C-R bond forming reaction to create the *ortho*-substituted arene (Scheme 1-3). In the case of Scheme 1-3, a standard oxidative addition / reductive elimination pathway for the cross coupling is shown, however there are multiple ways in which a cyclometalated species can facilitate C–H functionalisation including (but not limited to) transmetalation, migratory insertion, and β-hydride elimination.[8]

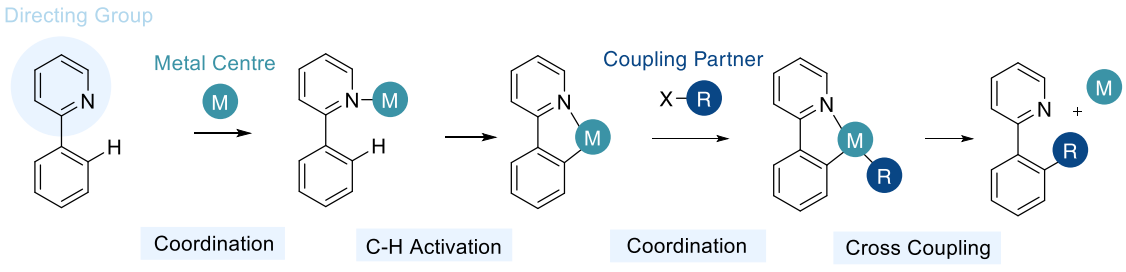

Scheme 1-3: Overcoming Site Selectivity using Directing Groups

The use of directing groups that strongly coordinate a metal centre, predominately based on N-based directing groups, has evolved rapidly to enable the use of a multitude of different metal-coordinating directing groups. Among these are the heteroaromatics:

pyrazole, pyrimidine, triazole, tetrazole, oxazoline and then acyclic derivatives such as ketimines (Scheme 1-4).[9] Through an influx of research output, a large variety of C-C and C-X bond forming reactions have also entered the synthetic toolkit including (but certainly not limited to) those shown below (Scheme 1-4c).[9] It also must be noted that despite C–H functionalisation's roots in rare earth metal catalysis such as palladium,[10] rhodium,[11] and ruthenium,[12] a variety of transformations are now available using first row transition metals such as cobalt,[13] manganese,[14] and iron.[15]

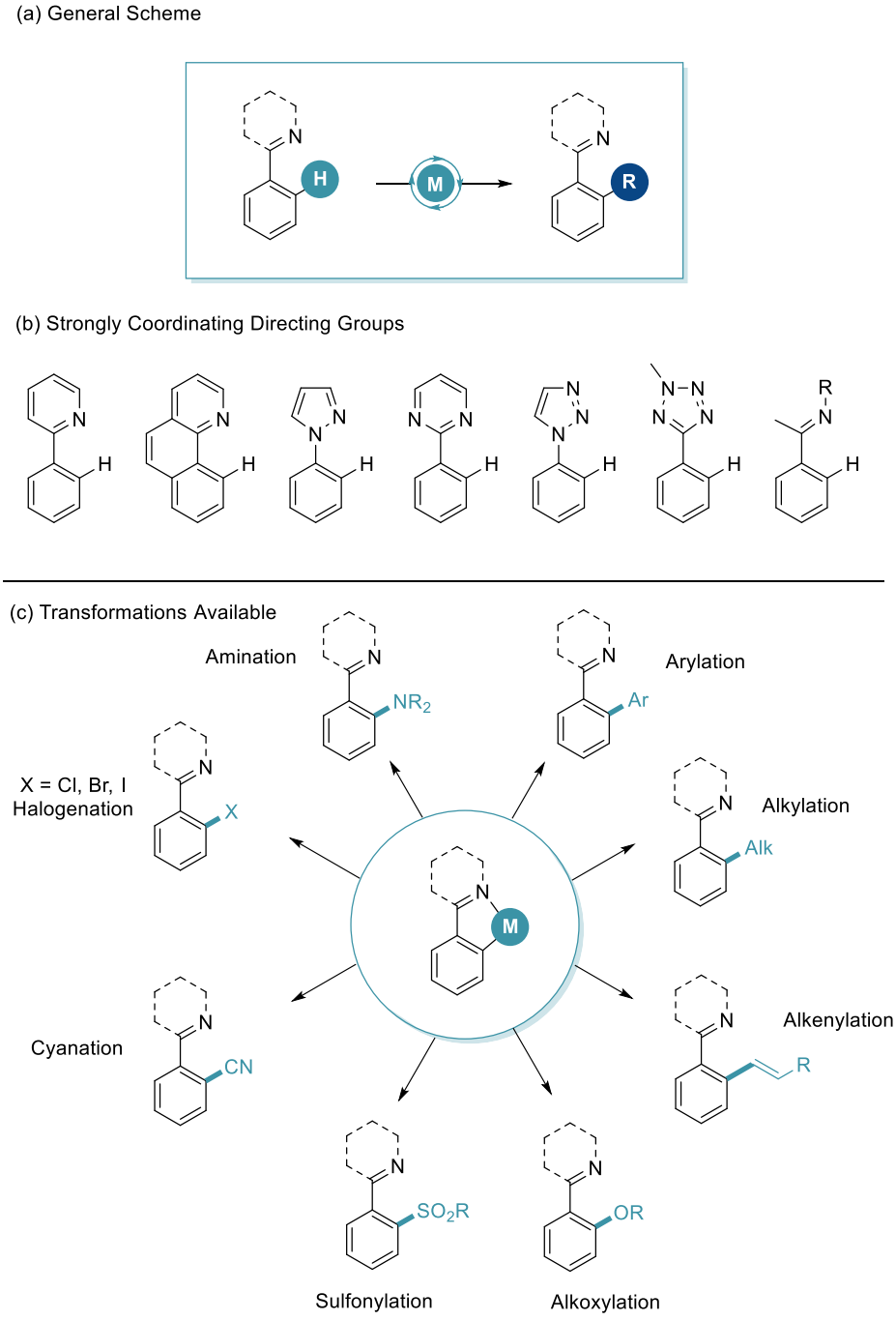

Scheme 1-4: Strongly Coordinating Directing Groups in C–H Functionalisation

Whilst the use of strongly coordinating directing groups has enabled efficient and selective C–H functionalisation, these structural motifs are not often ubiquitous in organic molecules. Therefore, there has been a large interest in the use of weakly coordinating directing groups (which generally coordinate metal centres through a carbonyl) which are more commonly found as organic functional groups, these include: carboxylic acids, aldehydes, esters, anilides, and carbamates (Scheme 1-5). Due to the weaker cyclometalated species formed as an intermediate in these reactions, these structures are less amenable to the widespread toolkit developed for strongly coordinating directing groups, and do more commonly rely on the use of rare earth metals such as palladium[16] and ruthenium.[17]

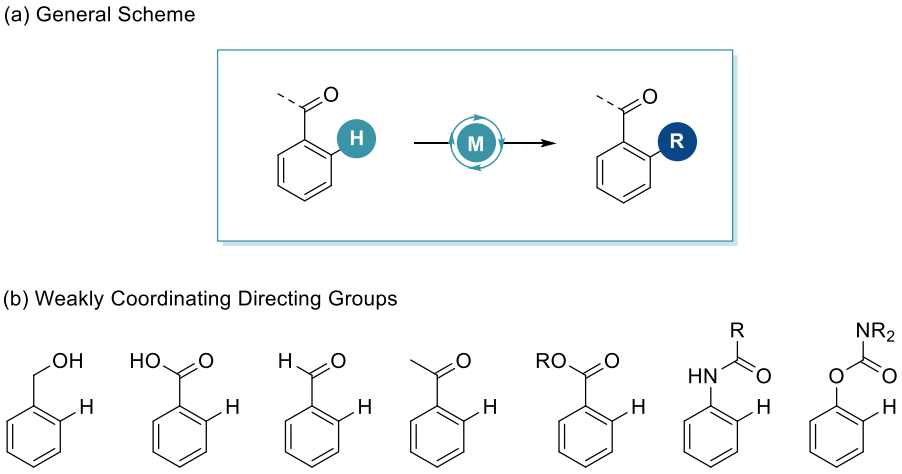

Scheme 1-5: Examples of Weakly Coordinating Directing Groups in C–H Functionalisation

Directed C–H activation has enabled a plethora of transformations, of which a huge majority enable selective C–H functionalisation *ortho* to the directing group. In order to gain access to the more remote *meta* and *para* C–H bonds, different techniques are necessary. The next section will explore in much greater detail how directed C–H functionalisation under careful reaction design has granted access to *meta* selectivity.

1.2: *meta*: Beyond *ortho*-Selectivity

1.2.1: Direct *meta* C–H Activation

The power of selectively accessing remote C–H bonds will heavily contribute to future research programmes in all arms of synthetic development.[18] The first reports of transition metal-catalysed process to overcome the cage of *ortho*-selectivity made use of direct C–H functionalisation, where steric and electronic properties of an arene can dictate selectivity.

Sterics were exploited in a report in 2002 by Smith and co-workers. Here they utilised iridium catalysis in the presence of phosphine ligands to selectively C–H borylate the least hindered site on steric grounds.[19] Therefore, on the use of a di-*meta*-substituted arene, C–H borylation takes place *meta* to the substituents already in place (Scheme 1-6). In this methodology, the arene is often used in vast excess as solvent, and for solid arenes, cyclohexane was used as solvent.

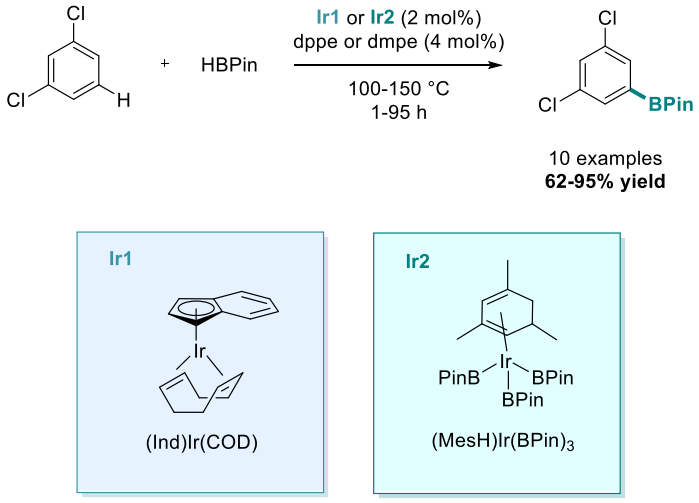

Scheme 1-6: Site Selective Iridium-Catalysed C–H Borylation

Hartwig and co-workers have applied this selective C–H borylation methodology to subsequent palladium-catalysed alkylation and allylation chemistry to give a wide range of structurally diverse building blocks.[21]

In 2009, Yu and co-workers disclosed the exploitation of the inherent electronic properties of an arene to exhibit *meta* selectivity. Here, they demonstrated that electron

deficient arenes could undergo selective direct C–H activation at the *meta* position employing palladium catalysis and a specialised sterically encumbered pyridine based ligand (Scheme 1-7). They showed that despite overall preference for direct C–H activation at the *meta* position, competing *para* C–H functionalisation was also observed in a majority of examples.[21] A full experimental and computational mechanistic paper on a similar methodology has been reported by Wu and Zeng.[22] A similar concept has also been explored by Sanford in the C–H acetoxylation of electronically biased arenes, where the *meta* / *para* selectivity issues were even more apparent.[23]

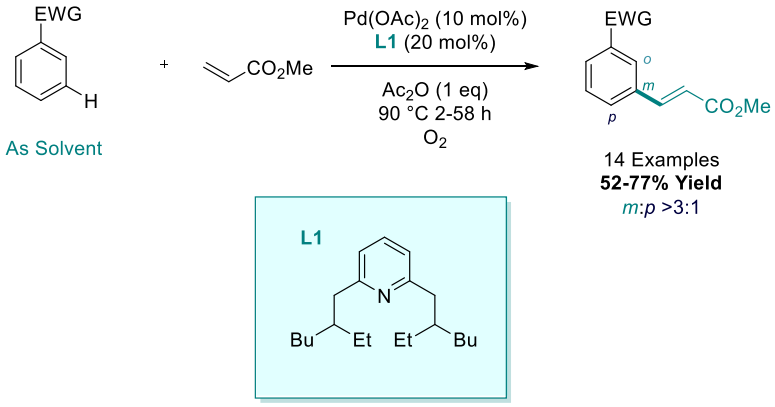

Scheme 1-7: Palladium Catalysed *meta* C–H alkenylation of Electronically Biased Arenes

Both methodologies shown above were shown to utilise a vast excess of arene in the reaction mixture, using them as solvent. Ritter and co-workers described the C–H imidation of electronically biased arenes employing dual palladium / silver catalysis and using the arene as the limiting reagent (Scheme 1-8).[24]

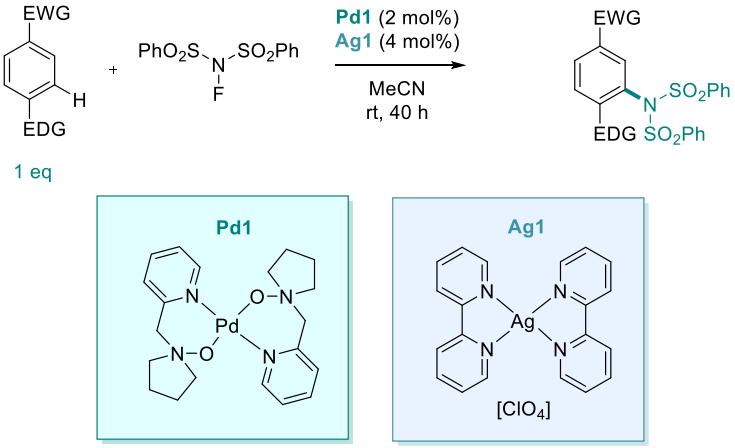

Scheme 1-8: Palladium / Silver Catalysed C–H Imidation at the *meta* Position of Electronically Biased Arenes

They demonstrated that a mixture of electron withdrawing *meta* directing and electron donating *ortho* / *para* substituents was necessary to elicit the greatest selectivity. It was also shown to undergo C–H functionalisation *via* a radical mechanism whereby the silver salt engages in a single electron transfer (SET) process which then interacts with the palladium.

1.2.2: Template Assisted *meta*-C–H Functionalisation

1.2.2.1: Covalent Templates

One of the most well-known and key methodologies that has been developed to enable the *meta*-selective activation of C–H bonds is the work pioneered by Yu and co-workers on the design of templated directing groups (Scheme 1-9).[25] These directing groups have been shown to form macrocyclic cyclometalates which have been meticulously designed to cyclometalate at the *meta* position.

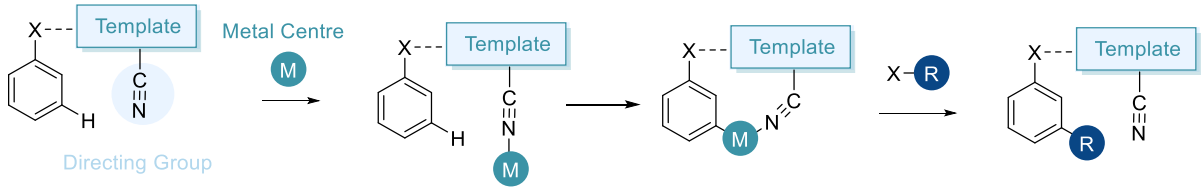

Scheme 1-9: Template Assisted *meta*-Selective C–H Functionalisation

The seminal example of this work was reported in 2012 on the *meta*-alkenylation of benzyl alcohol derivatives (Scheme 1-10).[26] The templated directing group that was disclosed is an incredibly sterically encumbered phenol derivative, which coordinates a palladium centre through a nitrile functional group. This mechanistic pathway has also been investigated from a purely computational standpoint in separate reports.[27-28]

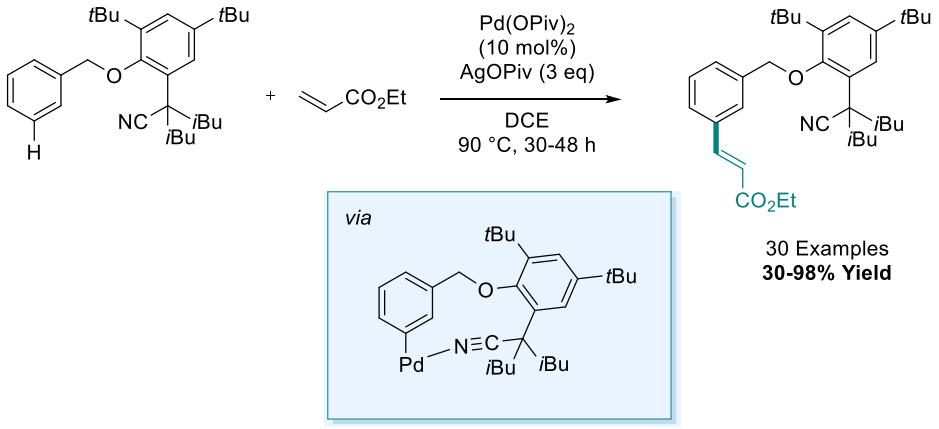

Scheme 1-10: Palladium Catalysed Template Assisted *meta*-Alkenylation

One of the major disadvantages to the methodology above is that a method of cleaving this high atomic weight template was not disclosed. To this end, at the end of the report they proposed a removable 'U' shaped template which could be furnished to a hydrocinnamic acid derivative (Scheme 1-11a).[26] This could direct functionalisation to the *meta*-C–H bond and was then readily cleaved *via* saponification, including recovery of the amine parent of the template which can then recycled. Yu reported that this U-shaped template could also be used to facilitate *meta*-C–H arylation chemistry (Scheme 1-12b).[29] Another report also detailed the use of this U-shaped template to a phenol derivative used again in *meta*-alkenylation chemistry.[30]

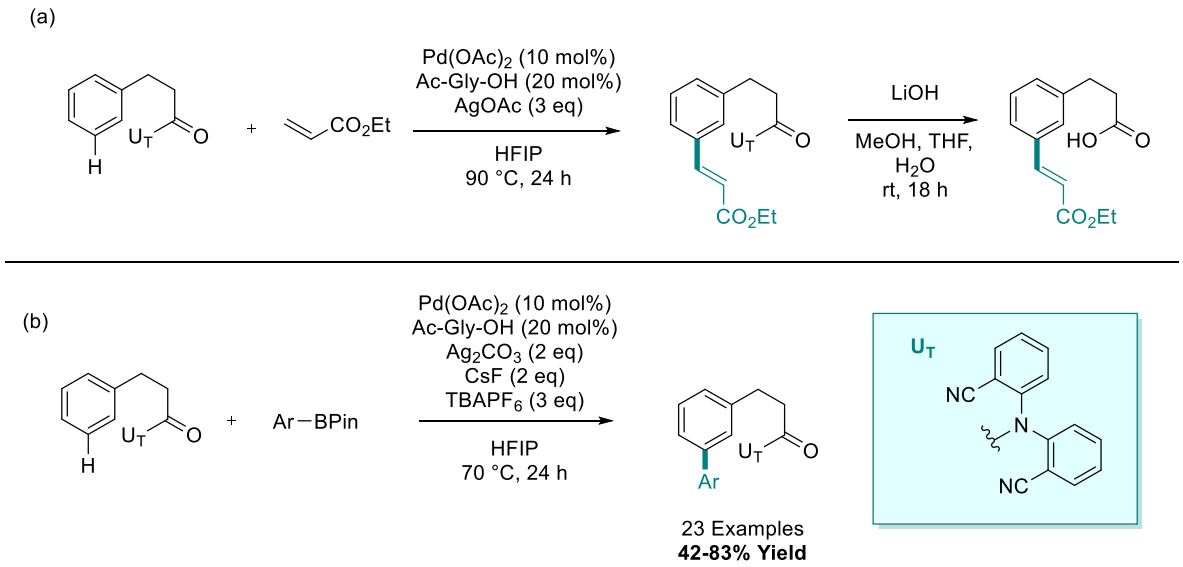

Scheme 1-11: Development of Cleavable Templates for *meta*-Functionalisation

In late 2013, Tan reported the *meta*-alkenylation of benzyl alcohol derivatives using a silyl-based template (Scheme 1-12). This has benefits over the previous methodologies described as a simple *in situ* treatment with TBAF at the end of the reaction reveals the free alcohol functional group. They also demonstrated that this template could be regenerated for recycling.[31]

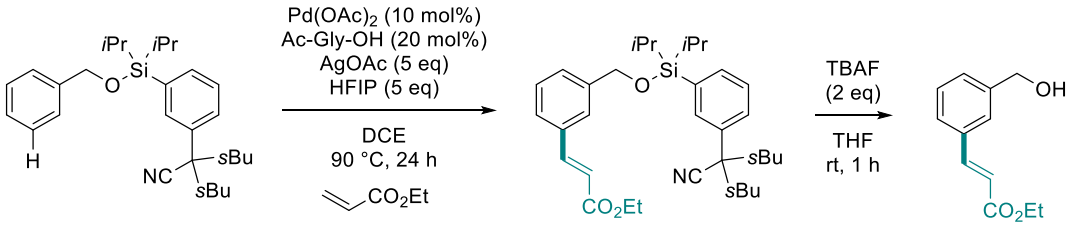

Scheme 1-12: Readily Cleaved Silyl Based Templates for *meta*-Functionalisation

Following these seminal reports Yu reported the *meta*-C–H functionalisation of amine derivatives using this template concept. A modified template was used to enable effective *meta*-alkenylation and acetoxylation of a wide range of amines, focussing on aniline derivatives (Scheme 1-13a).[32] This work was expanded into indoline derivatives which were furnished with a sulfonamide template linker. It was shown that the all of the previously developed alkenylation, arylation and acetoxylation methodologies were amenable to this scaffold (Scheme 1-13b).[33]

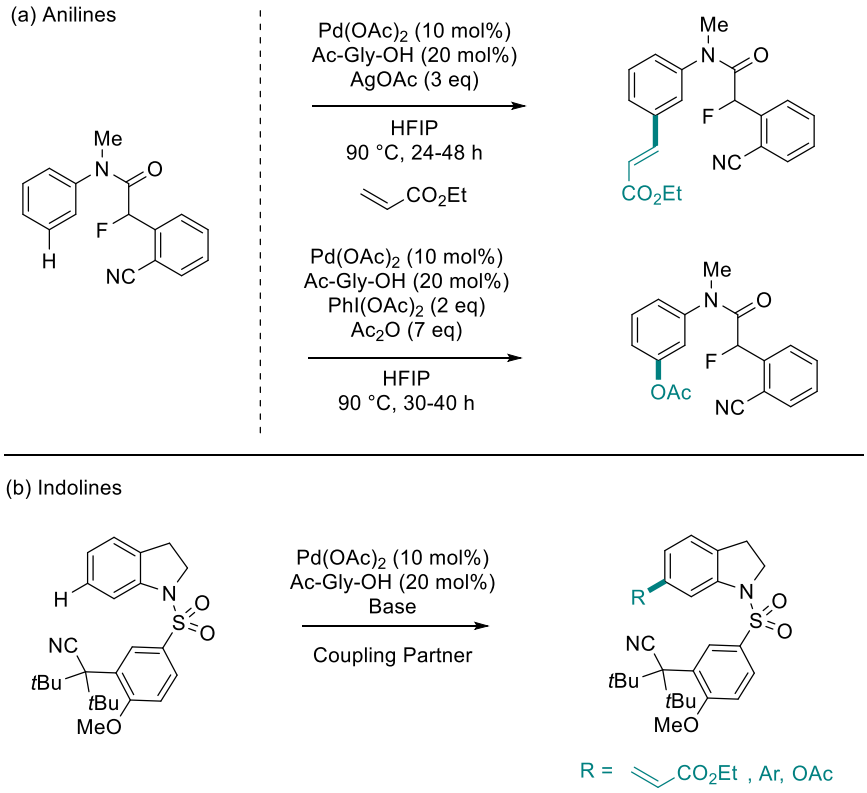

Scheme 1-13: Template Assisted *meta*-Functionalisation of Aniline and Indoline Derivatives

From this point on, this research area has received a colossal influx of reaction systems with further developments from Yu and vast contributions by Maiti and co-workers amongst others. A summary of the templates constructed and the transformations available with them is shown in Scheme 1-15. Firstly, Maiti and co-workers reported the *meta*-alkenylation phenylacetic acid derivatives (Scheme 1-14a).[34] Li and co-workers then showed that an *in situ* created phthalimide (from phenylethylamides derivatives) enabled *meta* selective alkenylation chemistry (Scheme 1-14b).[35] Yu then reported that his U-shaped template was also amenable to the *meta*-alkenylation of phenylacetic acid derivatives (Scheme 1-14c).[36] Maiti and co-workers demonstrated that sulfonates could be used as linkers for this methodology, and were shown to be able to undergo a Julia reaction give the di-vinylated benzene (Scheme 1-14d).[37] Yu and co-workers then reported that the use of a pyridine template enabled *meta*-alkenylation and iodination of benzyl alcohol derivatives. This was an important step as can potentially unlock other chemistry that pyridyl directing groups can carry out in palladium catalysis (Scheme 1-14e).[38] Li showed that amide linked templates could be used in *meta*-alkenylation reactions (Scheme 1-14g).[39] Maiti and co-workers demonstrated that their sulfonate template from before was amenable to *meta*-hydroxylation methodology (Scheme 1-14g)[40] and that increasing the linker size maintained reactivity in remote functionalisation (Scheme 1-14h).[41] The same group then

demonstrated that a biaryl system (Scheme 1-14i)[42] and phosphonate linkers (Scheme 1-14j)[43] were tolerated in catalysis. They also demonstrated that sulfonates furnished with pyrimidine (Scheme 1-14k)[44] and nitroquinoline (1-14l)[45] granted access to *meta*-functionalised arenes.

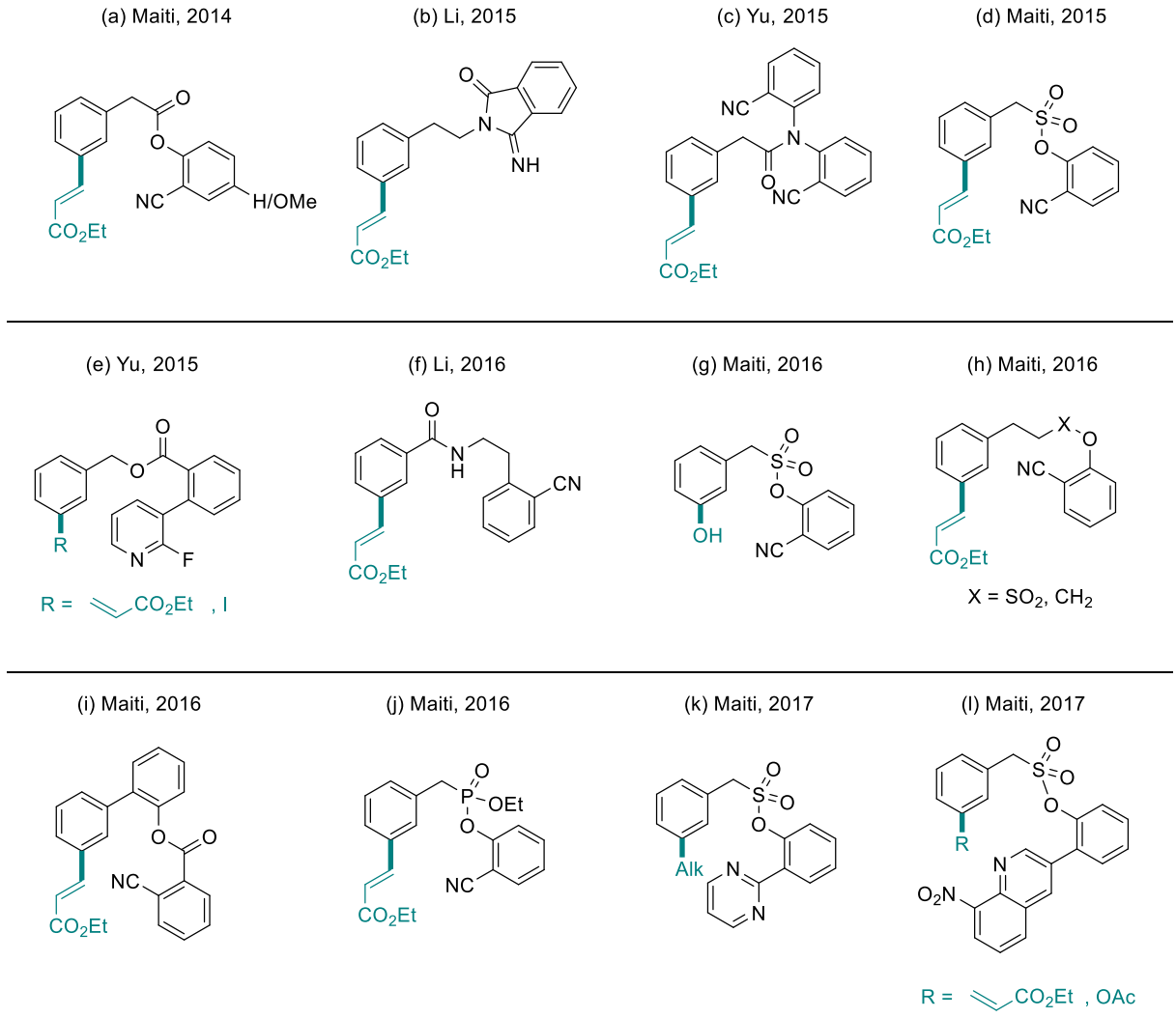

Scheme 1-14: Summary of Templates and Transformations used in Template-Assisted Remote *meta*-Functionalisation

All of the examples above have employed palladium catalysis to afford macrocyclic cyclometalates that can carry out C–H functionalisation chemistry. There have been two recent examples to date that have utilised rhodium catalysis in template-assisted chemistry. Both Lu, Sun and Yu,[46] and Maiti[47] have reported *meta*-alkenylation reaction methodologies (Scheme 1-15). Whilst this is inherently iterative of previous work, the importance of these findings is in the potential they hold to open up a vast field of potential chemistry of rhodium catalysed C–H activation.[48]

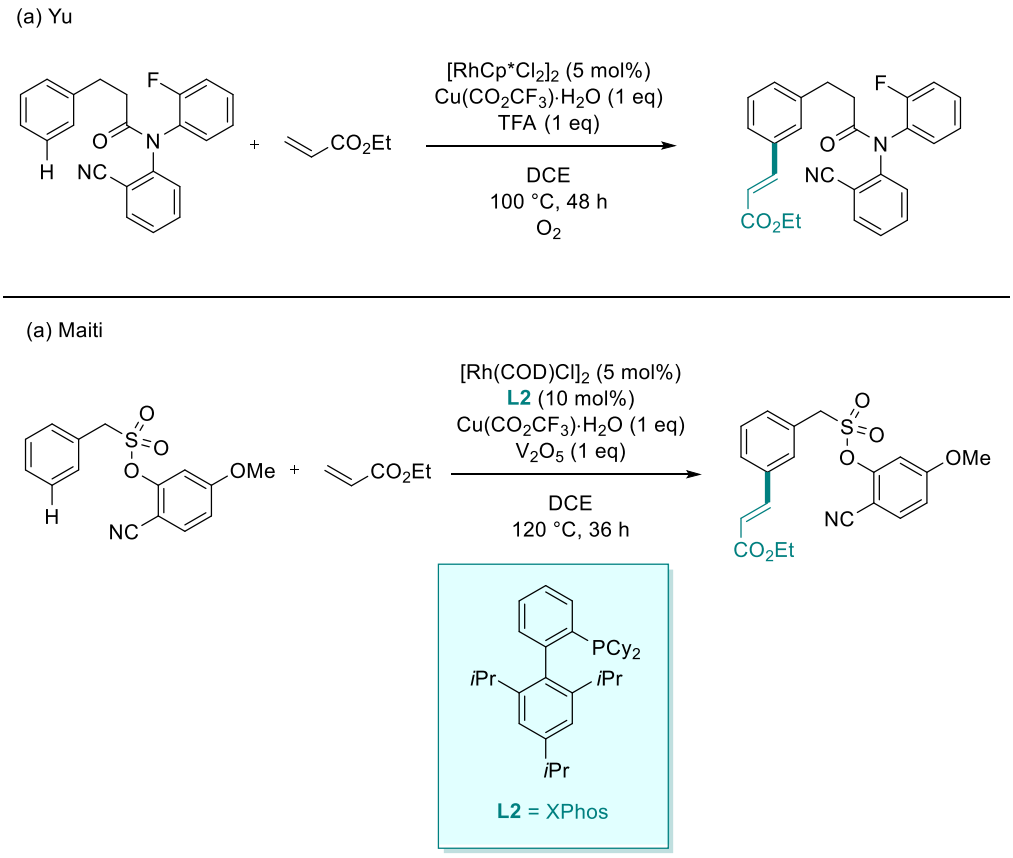

Scheme 1-15: Rhodium Catalysed *meta*-Alkenylation of Template Furnished Arenes

1.2.2.2: Non-Covalent Templates

Template-assisted *meta*-selective C–H functionalisation has become a widely-researched area in the past five years. Despite all the improvements and template developments, there is still a fundamental issue with this kind of chemistry. This is the high amount of atomic waste of the template, which is not found in the final product, and in separate pre-installation and removal steps. Due to this there has been efforts to create non-covalent templates that are in the reaction as part of the catalytic system (catalyst or ligand) than can direct cyclometalation at the *meta*-position and therefore subsequent *meta*-functionalisation. The power of non-covalent interactions in transition metal catalysis has also been explored in a recent review.[49]

The first example of this proposal was reported by Kanai and co-workers in 2015. Here they demonstrate the conceptually elegant iridium catalysed *meta*-borylation of benzamide derivatives (Scheme 1-16).[50] The regioselectivity was controlled by the meticulously designed ligand additive, which was shown to proposed to form a hydrogen

bond between the urea (ligand) and carbonyl (substrate), which templates the bipyridyl ligand proximal to the *meta*-C–H bond. This example highlights the power of non-covalent templates as the ligand is used in quantities as low as 1.5 mol%. Low amounts of competing *para*-selectivity were also observed in the reaction methodology.

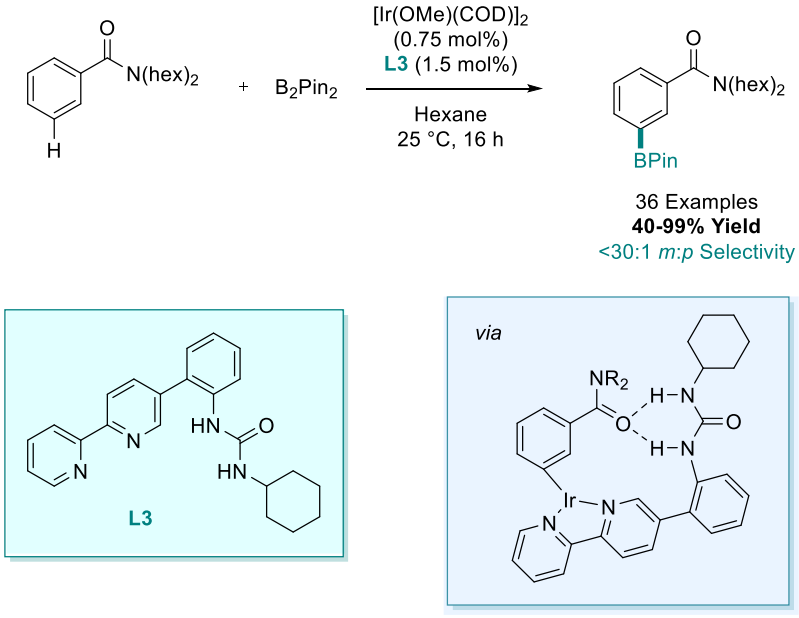

Scheme 1-16: Iridium Catalysed *meta*-Borylation using Non-Covalent Template

In 2016 Chattopadhyay reported the iridium catalysed *meta*-borylation of aldehydes (Scheme 1-17).[51] In this methodology, methylamine or *tert*-butylamine is reacted *in situ* to form an imine, and then they propose that one of two mechanisms are at play. Either (a) a hydrogen bond between the H on the imine and the oxygen on the boronate ligand enables templating of the octahedral iridium centre to the *meta*-C–H bond or (b) the imine can coordinate the boronate itself in a Lewis basic fashion. In this report, competing regioselectivity was present between *meta* and *ortho* functionalisation.

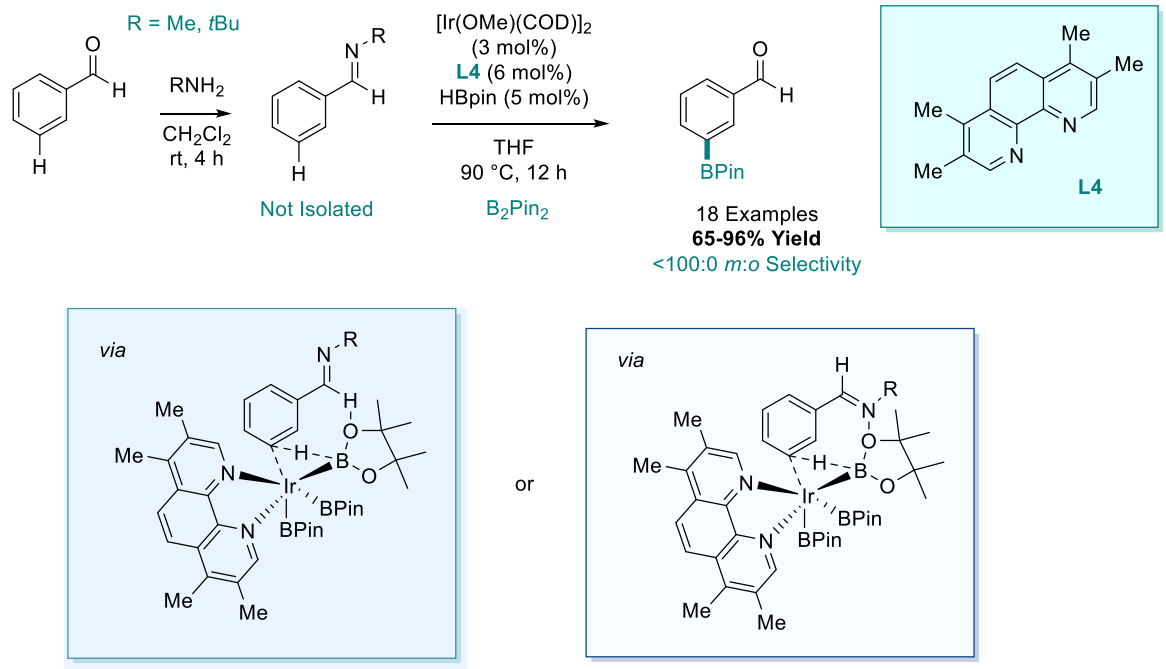

Scheme 1-17: Iridium Catalysed *meta*-Borylation of Aldehydes using Non-Covalent Template

The first two examples shown above have (or potentially have) made use of hydrogen bonding interactions to elicit *meta*-selectivity. In 2016, Phipps and co-workers described the *meta*-borylation of quaternary ammonium salts utilising electrostatic interactions between substrate and ligand to facilitate selective C–H iridation at the *meta* position (Scheme 1-18).[52]

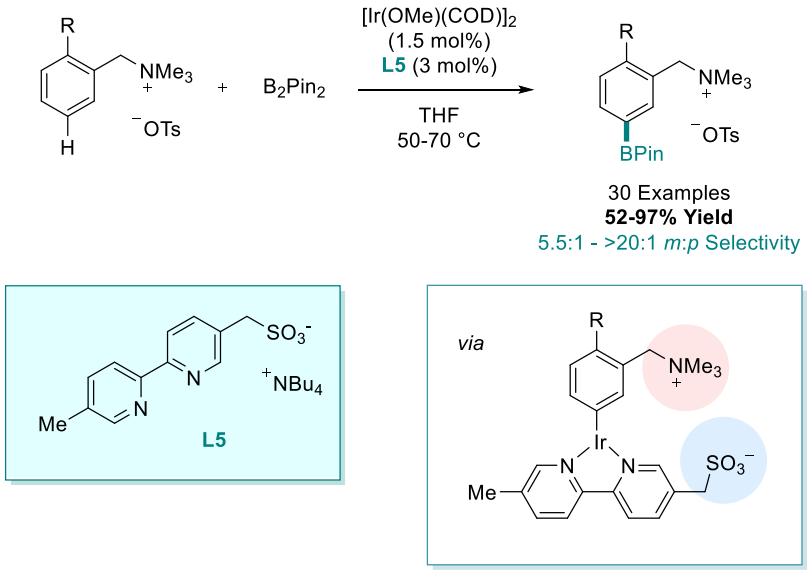

Scheme 1-18: Iridium Catalysed *meta*-Borylation using Electrostatic Template

In early 2017, Yu and co-workers reported the *meta*-alkenylation of 3-phenylpyridine derivatives utilising a catalytic quantity of a templating bipyridyl ligand (Scheme 1-19a).[53]

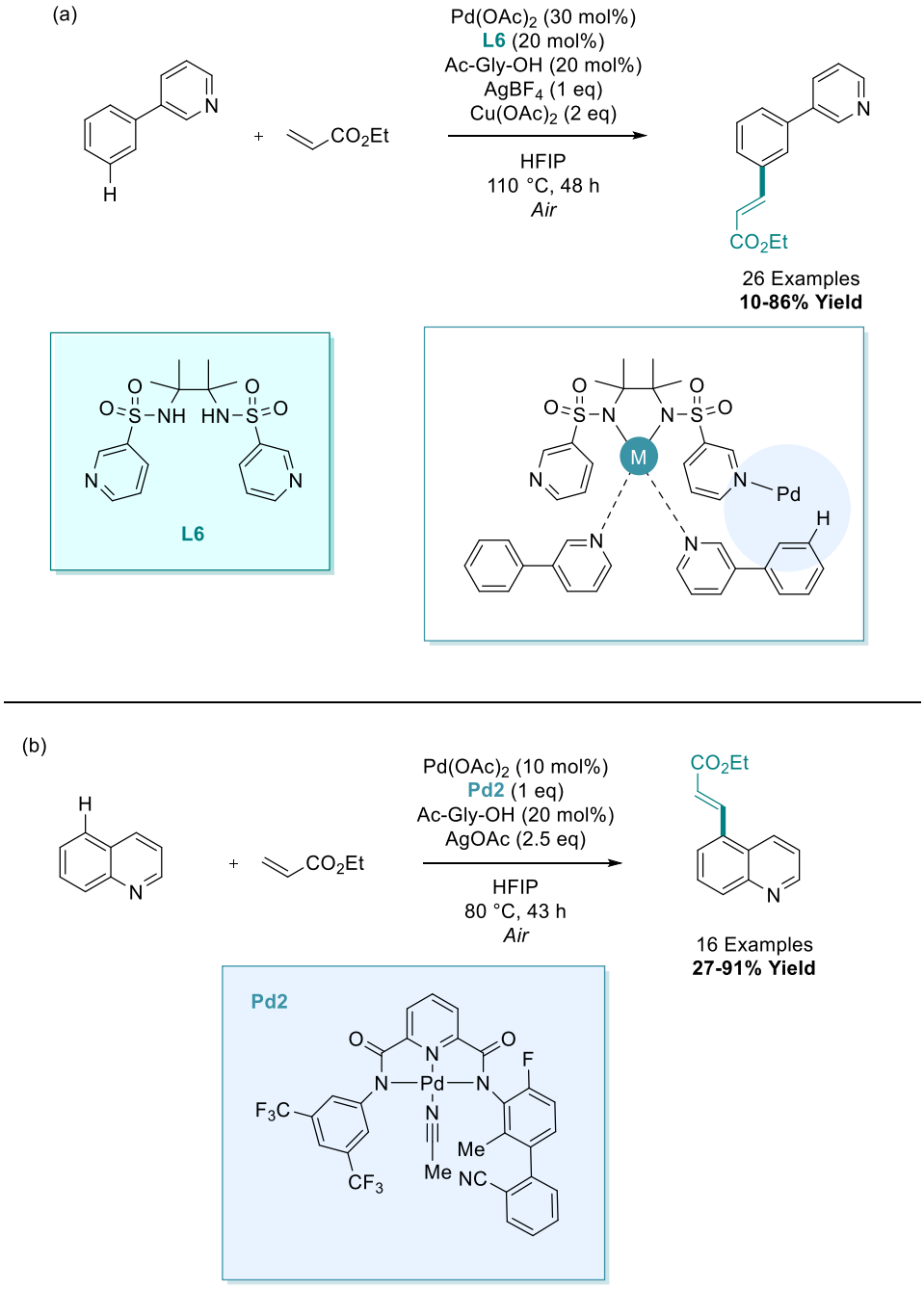

Scheme 1-19: Palladium Catalysed Remote Alkenylation using Non-Covalent Pyridyl and Nitrile Templates

They proposed that a metal centre (palladium or copper) can form a cyclometalate with the bidentate sulfonamide ligand. This cyclometalate can then coordinate the pyridine directing

group on the organic substrate. From this point, they propose that the pyridyl sections on the ligand can coordinate a palladium centre. Using their model, this palladium would then be proximal to the *meta*-C–H bond of 3-phenylpyridine. To this end, they propose that directed cyclometalation and C–H functionalisation affords the *meta*-alkenylated structure. In this same report, they looked to expand the scope of heteroaromatics to enable the remote C–H functionalisation of quinoline. They found that in this case, a drastically different scaffold was required to enable precise recognition of distance and geometry. They also found that preforming the template cyclometalate was more fruitful, therefore a variety of palladium bound templates were synthesised, with Pd2 being the most efficient. Unfortunately using catalytic quantities of this co-catalyst low conversion to product, however they found that using stoichiometric amounts of this cyclometalate they could access C5 alkenylation of quinoline derivatives (Scheme 1-19b).

1.2.3: Transient Mediator

In 2009, Gaunt and co-workers disclosed the *meta* arylation of anilides. Here, they employed copper catalysis and hypervalent iodines as coupling partners (Scheme 1-20).[54] A mechanism was also proposed which builds on their work using a similar system in the C3 arylation of indoles.[55] They suggest that a conjugate addition style carbocupration which causes dearomatisation, subsequent rearomatisation leaves the organocuprate in the *meta* position to the anilide directing group. This organometallic can then reductively eliminate to form the aryl-aryl bond in the product. This work was expanded to utilise α-aryl carbonyl compounds as structural motifs.[56]

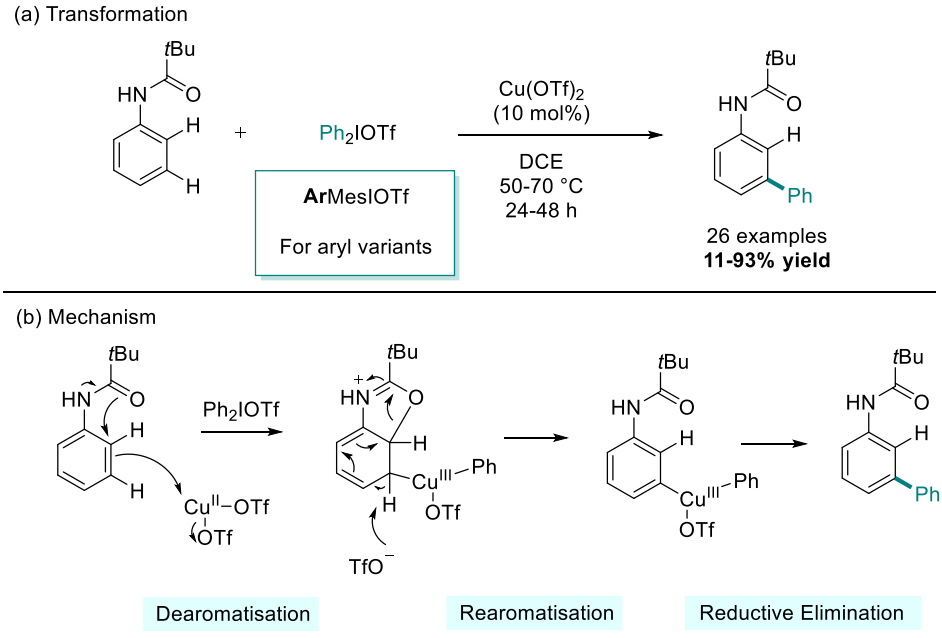

Scheme 1-20: Copper Catalysed Remote *meta*-Arylation of Anilides

The above report introduces the concept of the use of a transient mediator in *meta*-selective C–H functionalisation. In this method of accessing remote C–H bonds, one utilises an *ortho* / *ortho* C–H functionalisation pathway, which gives the net *meta*-substituted products (Scheme 1-21). This methodology enables the insertion at the *ortho* position, which is labelled 'X' as this could be a metal centre or an organic structure (such as part of the directing group shown above). This insertion of 'X' then enables the C–H functionalisation of 'Y' at the *ortho* position. Again, this Y could be a metal centre or the coupling partner installed (Y = R). This can be seen to carried out with or without 'X' still in places at the *ortho* position. Finally, cross coupling chemistry allows the functionalisation of this intermediate structure to give the *meta*-functionalised product.

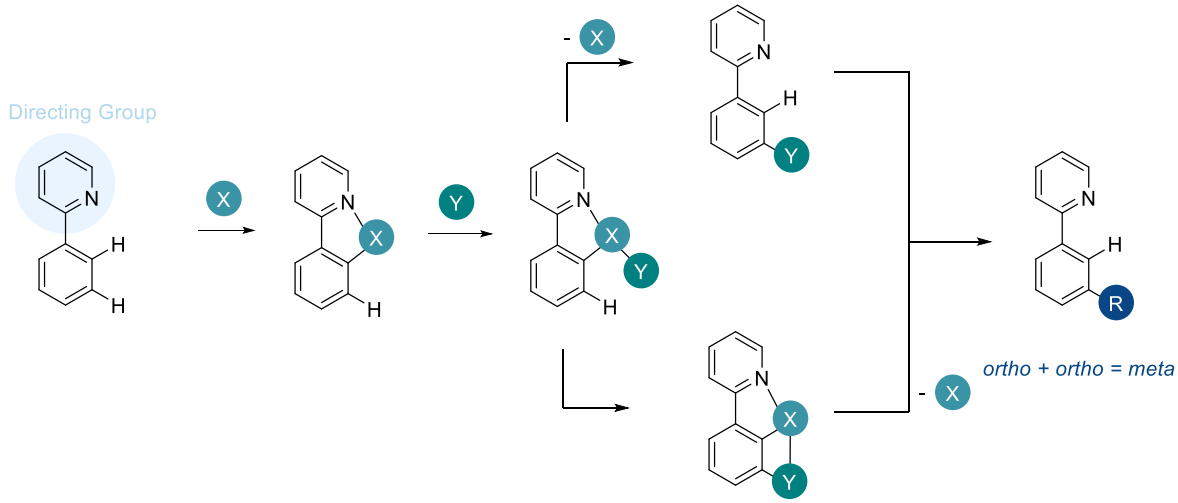

Scheme 1-21: Remote *meta*-Functionalisation *via* Transient Mediator Chemistry

Larrosa and co-workers described the use of the formal *meta*-selective arylation of arenes. Here they utilised the benzoic acid directing group neighbouring an 'R' group (Scheme 1-22). With respect to Scheme 1-11, the 'X' group is already furnished in place, then removed *in situ*. They carried out an *ortho*-C–H arylation of the acid and *in situ* protodecarboxylation to afford net *meta*-substituted arene.[57] Larrosa expanded on this in a report applying similar methodology using salicylic acids as readily available feedstocks.[58]

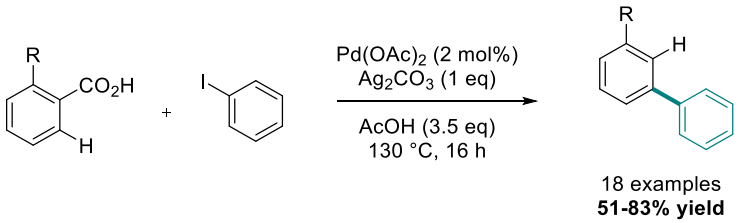

Scheme 1-22: Palladium-Catalysed *meta*-Arylation of Arenes

This concept has also been applied by Ackermann and co-workers, where they employ ruthenium-catalysed C–H alkenylation and hydroarylation reactions including an *in situ* decarboxylation to give *meta*-substituted arenes (Scheme 1-23).[59] In the case of unsymmetrical alkynes used in the hydroarylation methodology the larger substituent is located at R^4. In the hydroarylation work *para*-substituted benzoic acids were also employed which, again, gave *meta*-functionalised products however starting from a different synthetic feedstock.

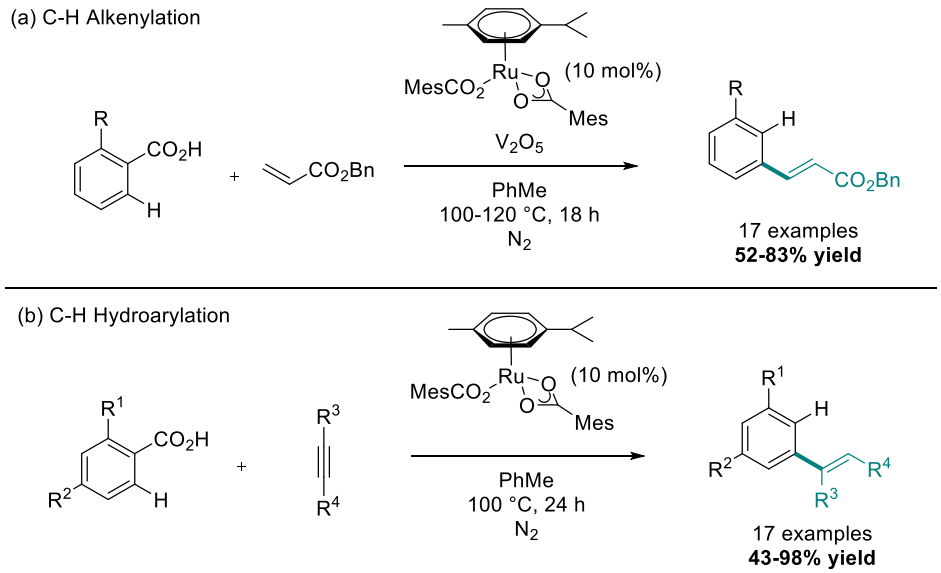

Scheme 1-23: Ruthenium-Catalysed *meta*-Alkenylation and Hydroarylation of Arenes

The drawbacks of the chemistry discussed above is necessity of a pre-installed acid in your structure to direct C–H functionalisation and then protodecarboxylate. Larrosa and co-workers provided a follow up to their previous report exploring the use of *in situ* methods to install, use and then remove the directing group in a “traceless directing group” strategy.[60] They employ phenol as a substrate for investigation in the hope to override the innate *ortho*-/*para*-directing nature of a phenol (Scheme 1-24). They showed that a one-pot process of *ortho*-carboxylation of phenol followed by a palladium-catalysed C–H arylation and subsequent decarboxylation gave the *meta*-arylated phenol. The reaction was shown to be widely tolerated with a vast scope of examples and in excellent yields for such a multistep process

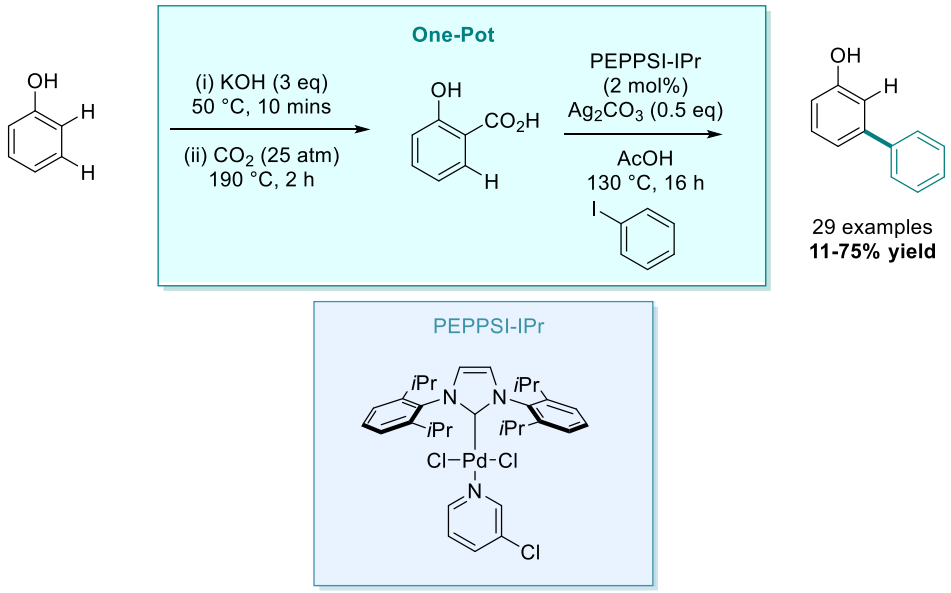

Scheme 1-24: Relay Palladium-Catalysed *meta*-C–H Arylation of Phenols

In 2015, Wang and co-workers reported the *meta*-functionalisation of *O*-naphthyl carbamates applying methodology similar to that proposed to Gaunt (Scheme 1-25). Here they employ palladium catalysis to enable C–H arylation at the *meta*-position.[61] Here they propose a carbopalladation taking place *via* an electrophilic palladium leaving a carbocation at the *meta*-position which is now free to interact with the coordinated aryl group.

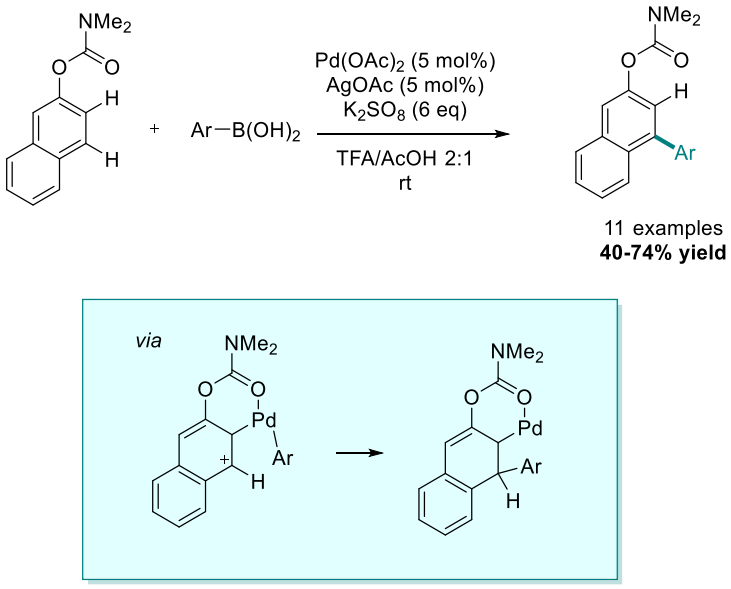

Scheme 1-25: Palladium-Catalysed *meta*-C–H Arylation of Naphthalene Derivatives

Njardarson and co-workers reported the *meta*-C–H alkylation of catechol ethers in 2016 by a careful study on dearomatisation, functionalisation and subsequent rearomatisation (Scheme 1-26).[62] Initially they carry out oxidative dearomatisation using lead tetra-acetate. Pinacol is then added to sequester the remaining lead in the mixture and forces it out of solution, therefore a filtration allows a telescoped process to the alkyl addition. Radical alkylation then takes place in a 1,4-type addition to the intermediate enone. On addition of TFA rearomatisation gives the *meta*-substituted catechol. This methodology was shown to primarily restricted by the availability of different boronic ethers as alkyl radical sources.

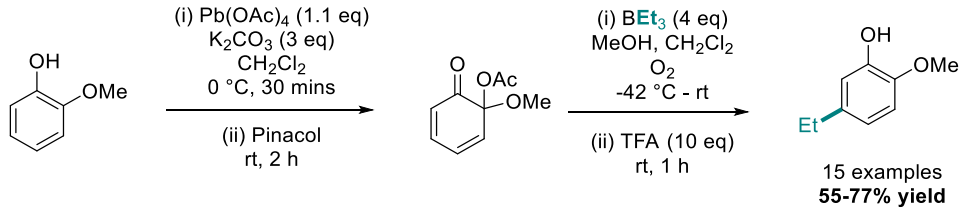

Scheme 1-26: Transition-Metal Free *meta*-C–H Alkylation of Catechols

In 2015, Yu and co-workers reported one of the pioneering contributions to this method of *meta*-functionalisation.[63] They took inspiration from one of the first ground-breaking pieces of transition metal C–H activation chemistry, the Catellani reaction (Scheme 1-27).[64] This methodology centres on the ability of cyclopalladated norbornene to 'walk' from one M-C bond to the neighbouring C–H bond. In this catalytic cycle norbornene is then reproduced in the cycle to reform the arene-palladium bond. This renders the reaction catalytic in both palladium and norbornene. The power of norbornene in transition metal catalysis has also been highlighted in a recent review.[65]

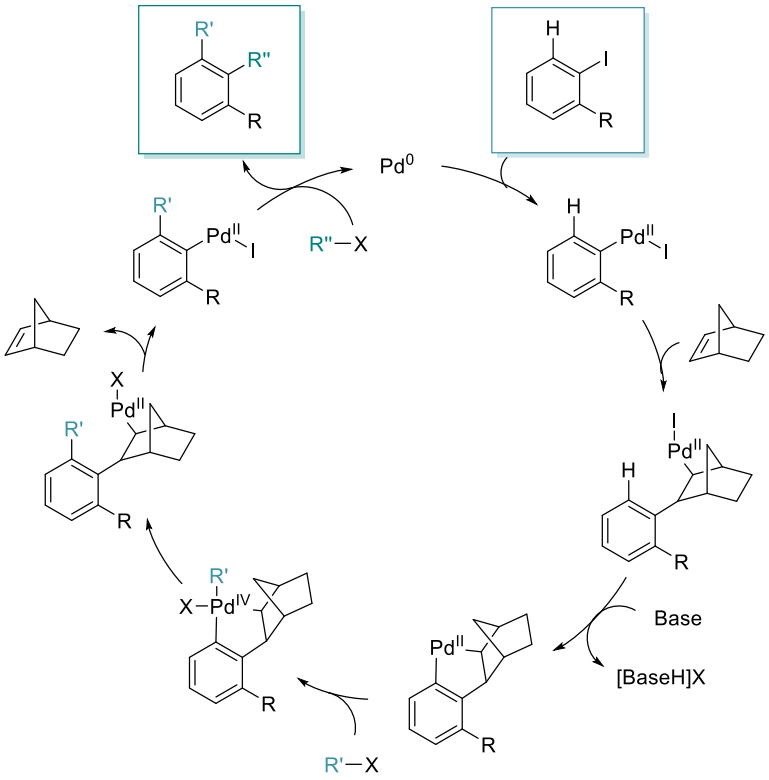

Scheme 1-27: Palladium Catalysed Catellani Reaction

Yu applied this to the *meta*-functionalisation of phenylacetic amides.[63] They demonstrated that both alkyl and aryl iodides were viable coupling partners enabling a wide scope of transformations (Scheme 1-28). With regards to mechanism they used directed cyclopalladation *ortho* to the acetamide directing group, which then allowed norbornene coordination and migratory insertion, to give the Catellani-type intermediate. This then enabled cyclopalladation in the *meta* C–H bond, and subsequent oxidative addition / reductive elimination gives the C–H functionalised intermediate. Instead of a further insertion (as in the Catellani) protodemetalation is suggested to take place to give the *meta* substituted structure. Even though the mechanism is catalytic in norbornene, they employ super-stoichiometric amounts in order to suppress competing pathways.

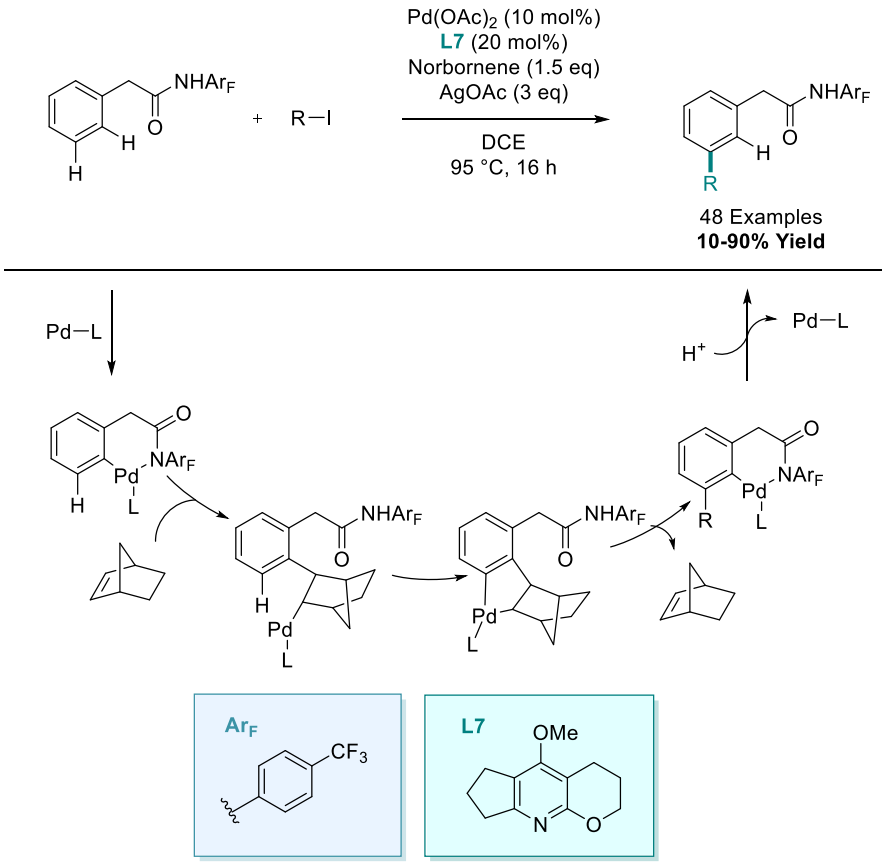

Scheme 1-28: Norbornene Mediated *meta*-Functionalisation of Phenylacetic Amides

Almost simultaneously with Yu's report, Dong and co-workers demonstrated the *meta* arylation of benzylamine derivatives using the same norbornene strategy. Here they made use of a triphenylarsine ligand and what they refer to as an 'acetate cocktail' to enable selective *meta*-C–H functionalisation (Scheme 1-29).[66] They also showed, like in Yu's report above, that aryl iodides containing coordinating groups *ortho* to the C-I bond were the most efficient by a significant margin.

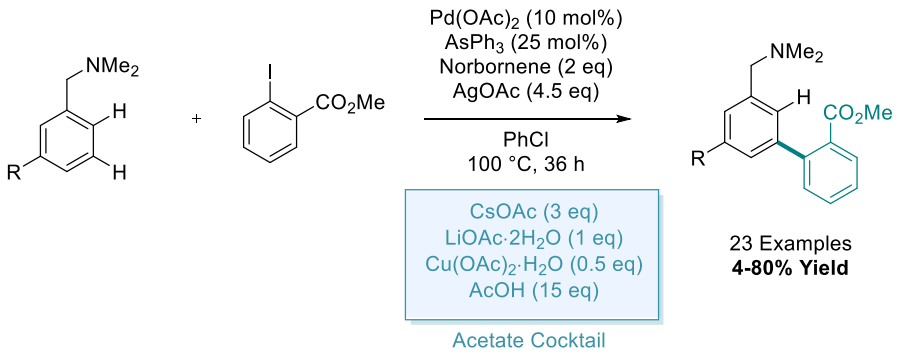

Scheme 1-29: Palladium Catalysed *meta*-Arylation of Benzylamines using Norbornene Chemistry

Since these first examples of using norbornene in this kind of chemistry, multiple developments have been made by the Yu group in order to expand the scope of C-C and C-X bond forming reactions available and structural templates amenable to this reaction methodology. These developments are summarised in Scheme 1-30. In the first of these, they investigated modification of the norbornene additive to improve the scope of coupling partners and versatility of their initial *meta*-arylation and alkylation methodology discussed above. These developments enabled the use of alkyl iodide substrates with more delicate functionality and also allowed arylation with aryl iodides without an *ortho*-coordinating substituent (Scheme 1-30b).[67] They then demonstrated the ligand-promoted *meta*-arylation of a vast array of aniline and phenol derivatives containing a multitude of different directing groups (in the interest of lack of generality and space this has not been included in Scheme 1-30)[68]. This was followed with the *meta*-amination and alkynylation of aniline derivatives (Scheme 1-30c)[69] and then the *meta*-chlorination of aniline derivatives (Scheme 1-30d).[70] They then reported the *meta*-arylation of nosyl protected phenethylamines, benzylamines, and 2-arylanilines. This was also the first demonstration of the use of catalytic norbornene in these kinds of transformations (Scheme 1-30e).[71] In 2017, they also reported the *meta*-arylation benzylamine derivatives,[72] the *meta*-arylation of auxiliary-free phenylacetic acids (Scheme 1-30f),[73] and the *meta*-arylation and alkylation of sulfonamide derivatives.[74] Amongst these contributions from Yu's laboratory, other groups have also entered the field.[75] Since the first report in 2015, there has been a continuous stream of publications using this concept and if there is a sustained influx of reaction systems this methodology could easily break into mainstream total synthesis, building block development and drug discovery.

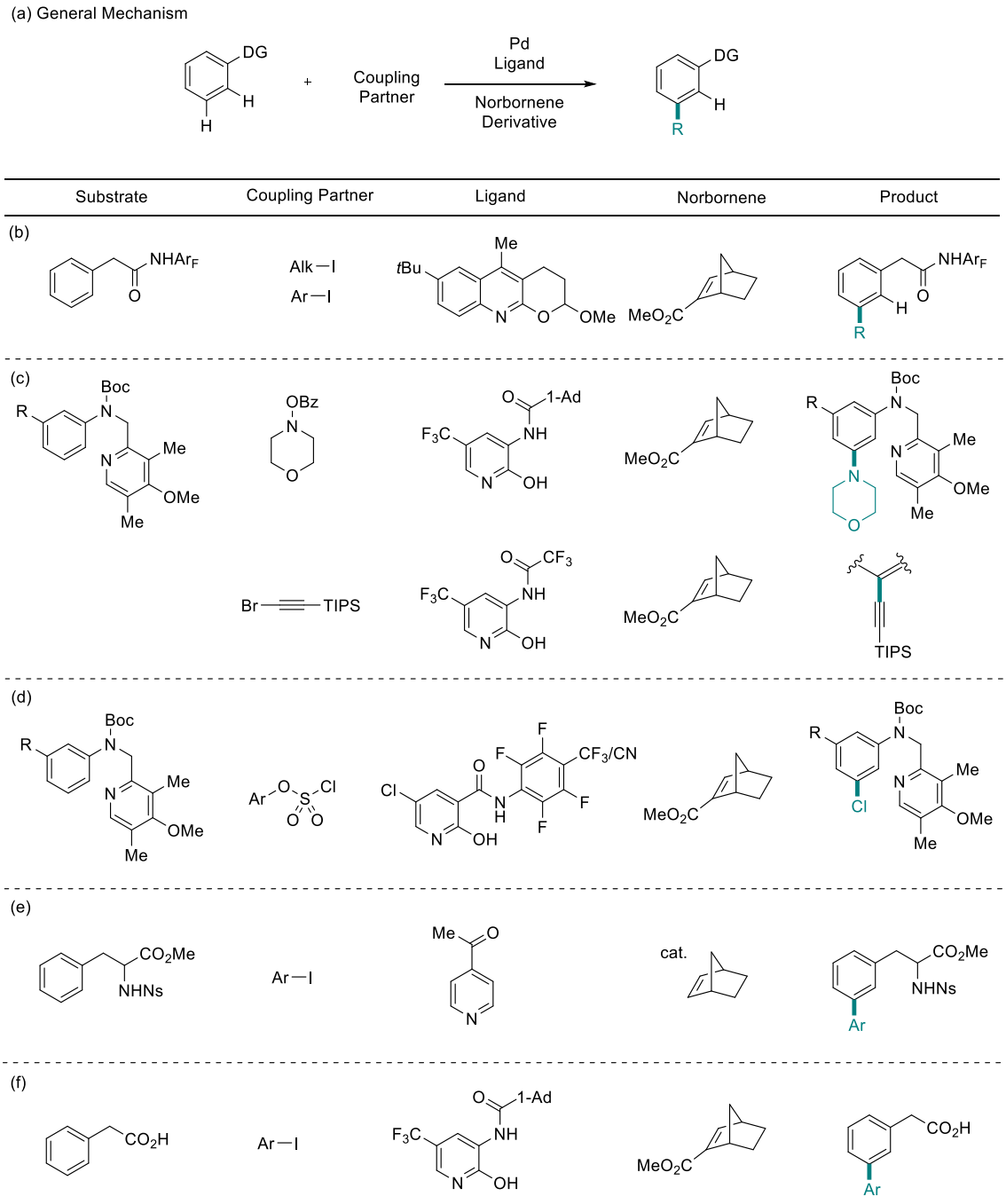

Scheme 1-30: Developments in Norbornene Mediate *meta*-C–H Functionalisation

1.2.4: Ruthenium Catalysed σ-Activation

1.2.4.1: Authorships and Permissions

This declaration concerns the article entitled									
Ruthenium Catalysed σ-Activation for Remote *meta*-Selective C–H Functionalisation									
Publication status (tick one)									
Draft manuscript		**Submitted**		**In review**		**Accepted**		**Published**	X
Publication details (reference)	J. A. Leitch and C. G. Frost, *Chem. Soc. Rev.*, 2017, **46**, 7145.								
Candidate's contribution to the paper (detailed, and also given as a percentage)	The candidate contributed to/ considerably contribute to/predominantly execute the: **Formulation of ideas (80%)**: JAL contributed the majority in discussion with CGF (20%) **Design of methodology:** N/A **Experimental work:** N/A **Presentation of data in journal format (85%)**: JAL wrote the manuscript and was edited by CGF (15%)								
Statement from Candidate	This paper reports on original research I conducted during the period of my Higher Degree by Research candidature								
Signed	Jamie A. Leitch						**Date**	06/12/17	

1.2.4.2: Manuscript for "Ruthenium Catalysed σ-Activation for Remote *meta*-Selective C–H Functionalisation."

Layout changes have been made for consistency for this thesis. Contents have not been changed. The references and scheme numbers in this section are self-contained within the manuscript as submitted and the references and scheme numbers for **Chapter 1** continue from above in "**1.3**: *para*: Beyond *meta*-Selectivity" from reference 76 and Scheme 1-31.

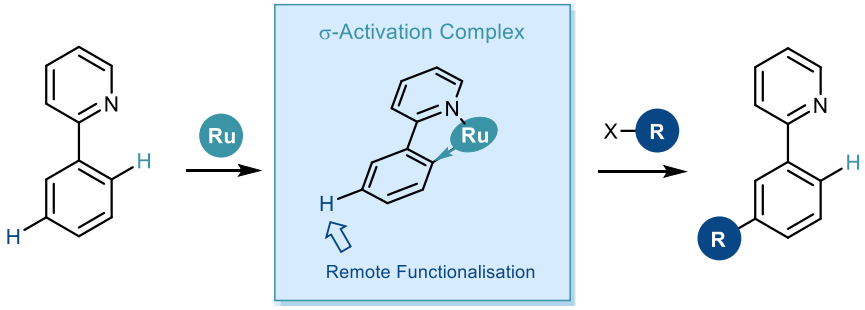

Ruthenium-Catalysed σ-Activation for Remote *meta*-Selective C–H Functionalisation

Jamie A. Leitch[a] and Christopher G. Frost[a]

[a] *Department of Chemistry. University of Bath, Claverton Down, Somerset, BA2 7AY, United Kingdom*

ABSTRACT: The search for selective C–H functionalisation has enabled some of the most elegant techniques in modern catalysis. Herein, we review the rapidly expanding field of Ruthenium Catalysed σ-activation as a tool in the selective *meta*-C–H functionalisation of arenes.

I: Introduction

The ability to transform inert C–H bonds into reactive functional groups has come to the forefront of modern synthetic developments in recent years. A range of elegant methods have been developed using a multitude of transition metal catalysts to enable the formation of a variety of C-X and C-C bonds.[1-2] One of the major assets of C–H functionalisation is in the potential it holds for late stage functionalisation of bioactive structures in *inter alia* drug discovery.[3]

The major challenge in C–H functionalisation is the ubiquity and similarity of many C–H bonds in a complex organic molecule vis-à-vis steric and electronic influences. To this end, the utilisation of a Lewis basic directing group has become commonplace in the C–H activation toolbox. Here a directing group (DG) coordinates a metal centre, which then facilitates C–H activation selectively in the *ortho* position to the directing group (Scheme 1a). This reduces the thermodynamic cost of C–H activation and enables the specific activation of certain C–H bonds and, most importantly, with predictability. This cyclometalated species can subsequently enable coordination of a coupling partner and reductive elimination to give the C–H functionalised product and regenerate the metal centre (Scheme 1b).

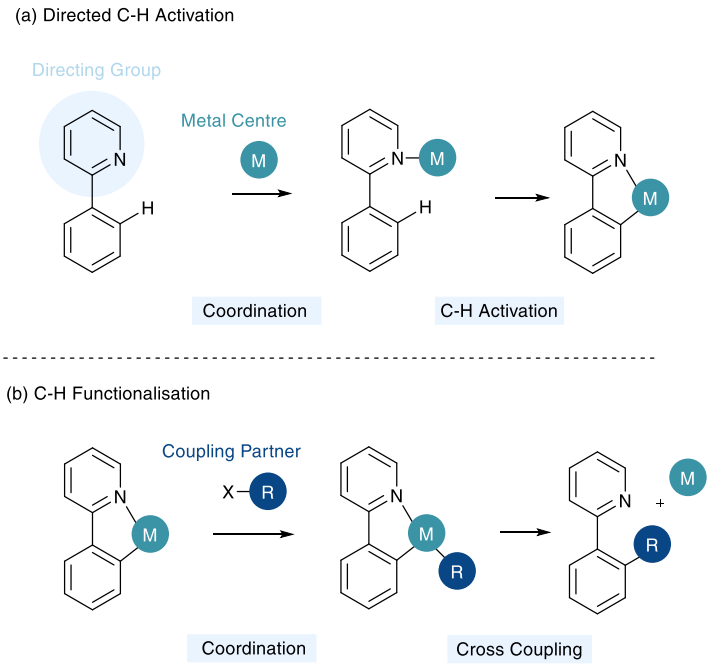

Scheme 1: Directed C–H Functionalisation Methodology

This has led to an influx of catalytic systems utilising a plethora of different Lewis basic directing groups, covered in depth in a recent review by Liu and Zhang.[4] However, in order to access more remote C–H bonds in an arene (*meta* and *para*-selective C–H functionalisation)[5-6] specialised techniques have been developed.[7-8] In the arena of *meta*-selective C–H functionalisation three primary techniques have been established. The first of these is the use of meticulously designed templated directing groups, pioneered by Yu (Scheme 2a).[9-10] Here an organic linker "template" places a directing group proximal to the *meta* C–H bond. Traditional metal coordination, cyclometalation and functionalisation then occurs at the *meta* position. The second is the use of a transient mediator (Scheme 2b) where an *ortho* / *ortho* functionalisation pattern where the first insertion is then removed *in situ*.[11-12] The final of these is ruthenium-catalysed σ-activation. σ-Activation benefits from the use of strong cyclometalated species as described in Scheme 1, however instead of partaking in standard oxidative addition / reductive elimination chemistry, it uses the cyclometalate to influence the ring electronically enabling *para* functionalisation to the metal centre. This *ortho* / *para* relationship gives a net *meta*-selective C–H functionalisation with respect to the directing group (Scheme 2c). This functionalization can only take place in an *ortho* / *ortho* fashion under sterically biased substrates, however the *meta*-substituted structure is still formed.

This tutorial review is based on the last of these techniques, and hopes to educate and excite readers about σ-activation, from its genesis at the stoichiometric organometallic level, the transfer to synthetically viable catalysis, and the possibilities available for the future of this chemistry in site-selective synthesis.

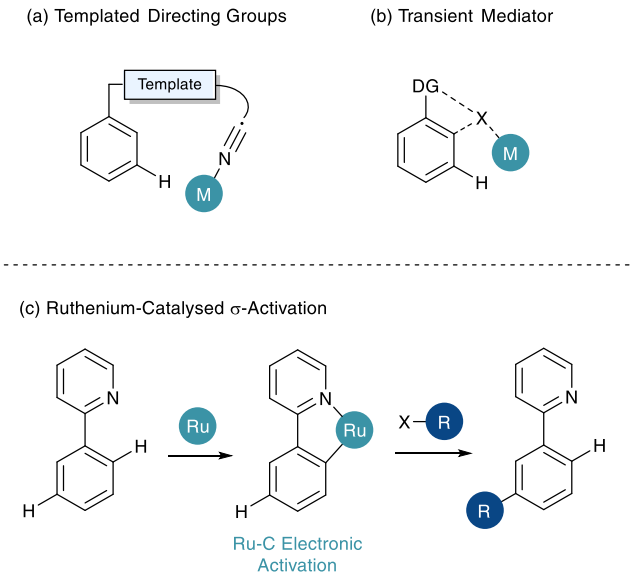

Scheme 2: Techniques for *meta*-Selective C–H Functionalization

II: Stoichiometric Work

The concept of utilising a ruthenium metal centre in this kind of methodology was first investigated by Roper in 1994, where benzene and toluene complexes of ruthenium were shown to undergo nitration *para* to the ruthenium centre (Scheme 3).[13] The reaction methodology was shown to give rise to multiple products based on the ruthenium core, however only the most relevant structure is shown. This shows that the location of the ruthenium centre was actively dictating the regioselectivity of C–H functionalisation via electronic influence on the aromatic ring.

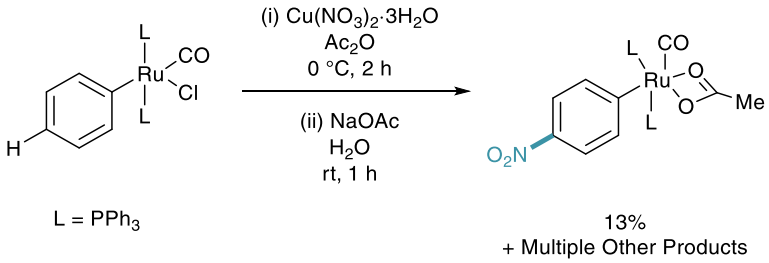

Scheme 3: C–H Halogenation of Cyclometalated Ruthenium Complexes

In 1998 Coudret reported that phenylpyridine complexes of ruthenium underwent electrophilic C–H halogenations at the *para* position to the metal-carbon σ-bond in impressive yields.[14] In this case *N*-bromosuccinimide (NBS) and iodine were used as the halogenating agents (Scheme 4).

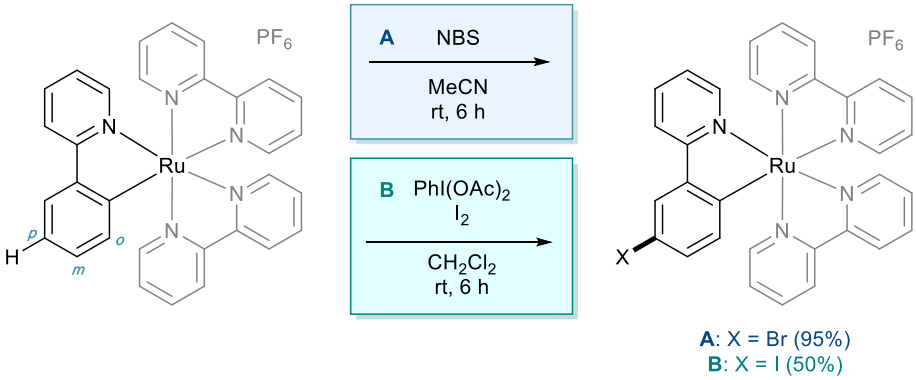

Scheme 4: C–H Halogenation of Cyclometalated Ruthenium Complexes

They then used these aryl halide structures in palladium catalysed cross coupling methodology. This was followed the subsequent year by the work carried out by Roper and Wright. Here they found, again, that cyclometalated phenylpyridine complexes of ruthenium (and osmium) underwent electrophilic aromatic substitution (S_EAr) on the phenylpyridine ligand (Scheme 5).[15] They showed that under nitration conditions that the di-nitrated substrate *ortho* and *para* to the metal centre was isolated in low yields (Scheme 4a). They also demonstrated that electrophilic bromination took place in much higher yields and with selectivity solely for the *para* position (Scheme 4b).

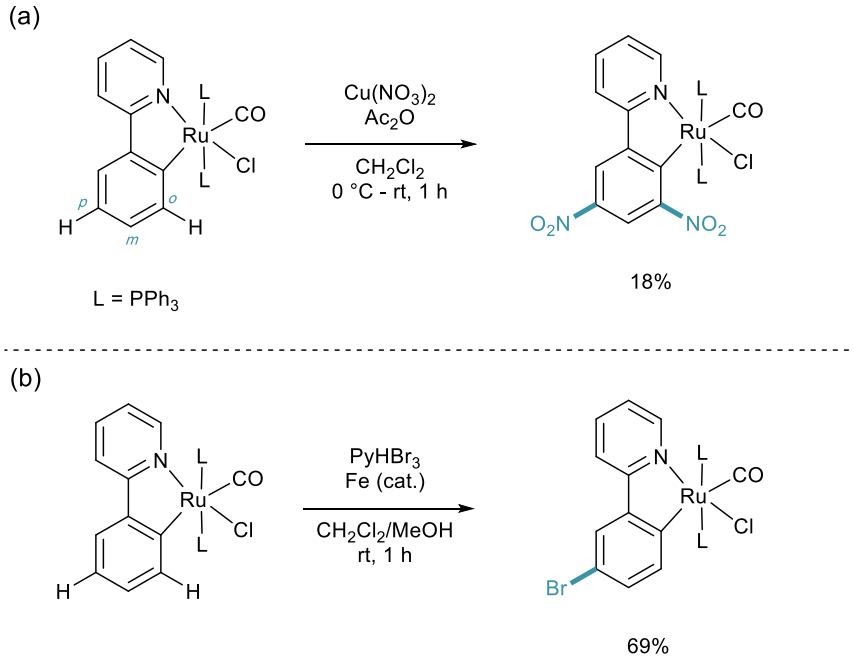

Scheme 5. Electrophilic Substitution of Cyclometalated Ruthenium Species

These two products indicate that the selectivity has been dictated by the metal centre acting as a Friedel-Crafts type *ortho* / *para* directing group, through the Ru-C σ-bond. It is this activation through a σ-bond which has since given its name to this field of catalysis.

III: From Organometallic to Catalytic

This initial organometallic work and concept that σ-activation could be used as a tool in selective synthesis then lay dormant until 2011. In a report on the *ortho*-C–H alkylation of ketimine derivatives using primary alkyl bromides as coupling partners, Ackermann disclosed *meta*-substituted by-products in yields up to 7% (Scheme 6). Whilst this was not ratified as σ-activation mechanistically at the time, it has been noted as the first example of this methodology reported in the literature.[16]

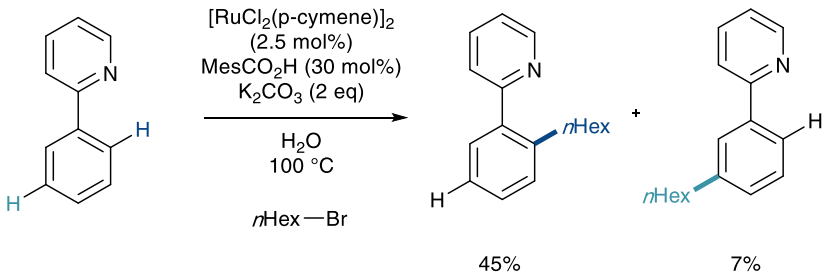

Scheme 6: First Observation of *meta*-C–H Functionalisation in a Catalytic Process

Later that year, Frost disclosed the first catalytic process to enable the selective ruthenium catalysed *meta*-sulfonation of phenylpyridine (Scheme 7a).[17] Here yields of up to 80% were reported with no *ortho*-selective impurities which would take place *via* traditional pathways. The report also contained key information about the potential mechanism at play. The *ortho*-cyclometalated phenylpyridine species was synthesised and submitted to the reaction conditions enabling quantitative access to the *meta*-sulfonated product (Scheme 7b). This ruthenacycle was also shown to be a catalytically competent organometallic in the reaction methodology. These findings, along with the initial stoichiometric work led the authors to propose that the cyclometalated species could direct S_EAr C–H sulfonation *para* to the metal centre giving the net *meta*-sulfonated phenylpyridine. This presented the first synthetically useful catalytic development in σ-activation and set the stage for further investigation.

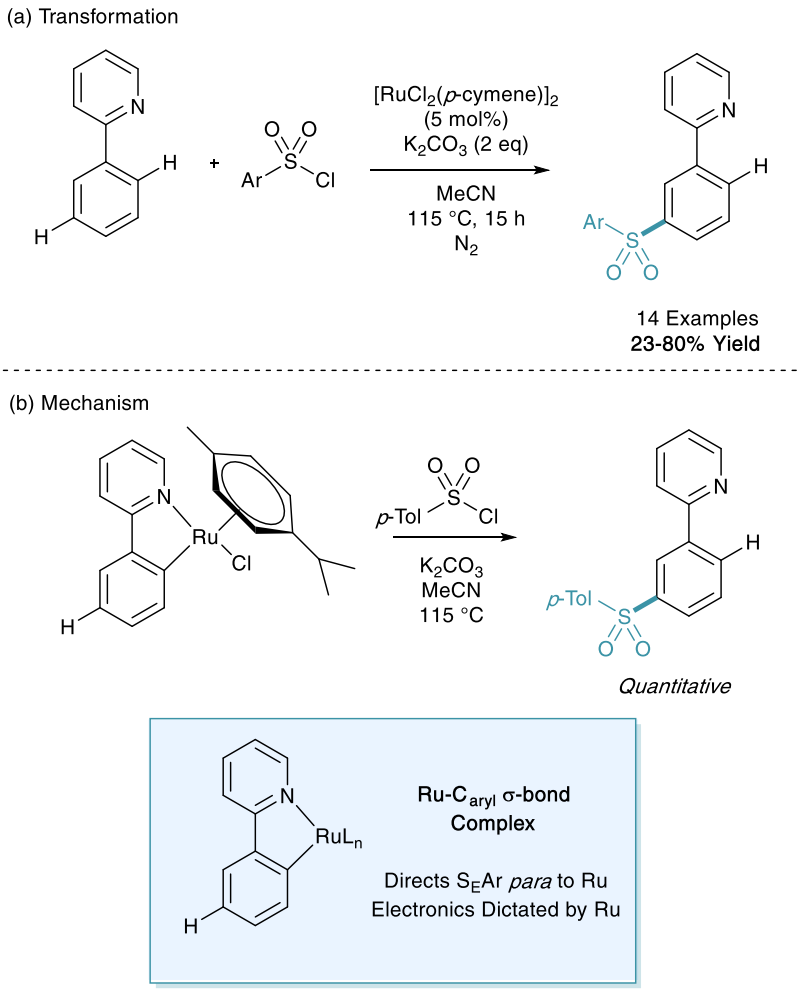

Scheme 7: Ruthenium Catalysed *meta*-Sulfonation of Phenylpyridine

This was followed in 2013 with a report from Ackermann on the *meta*-alkylation of phenylpyridine.[18] Moving on from his previous report (Scheme 6), here he established that employing secondary alkyl halides enabled solely *meta*-selective C–H functionalisation in synthetically useful yields (Scheme 8a). In this report, they detailed the vital use of the sterically demanding benzoic acid, 1,4,6-trimethyl (mesityl) benzoic acid ($MesCO_2H$). The authors also present a much wider scope of this methodology, using pyrazole, pyrimidine, benzimidazole and imidazole directing groups. This methodology was also reported to proceed *via* a cyclometalation, σ-activation, S_EAr-type pathway and a full plausible mechanism was proposed (Scheme 8b). They also observed complete racemization of a enantiomerically enriched coupling partner which reinforced up this electrophilic proposal. In a footnote, the authors did note that the interesting find that the addition of radical scavenger TEMPO supressed reactivity, which foreshadowed subsequent developments.

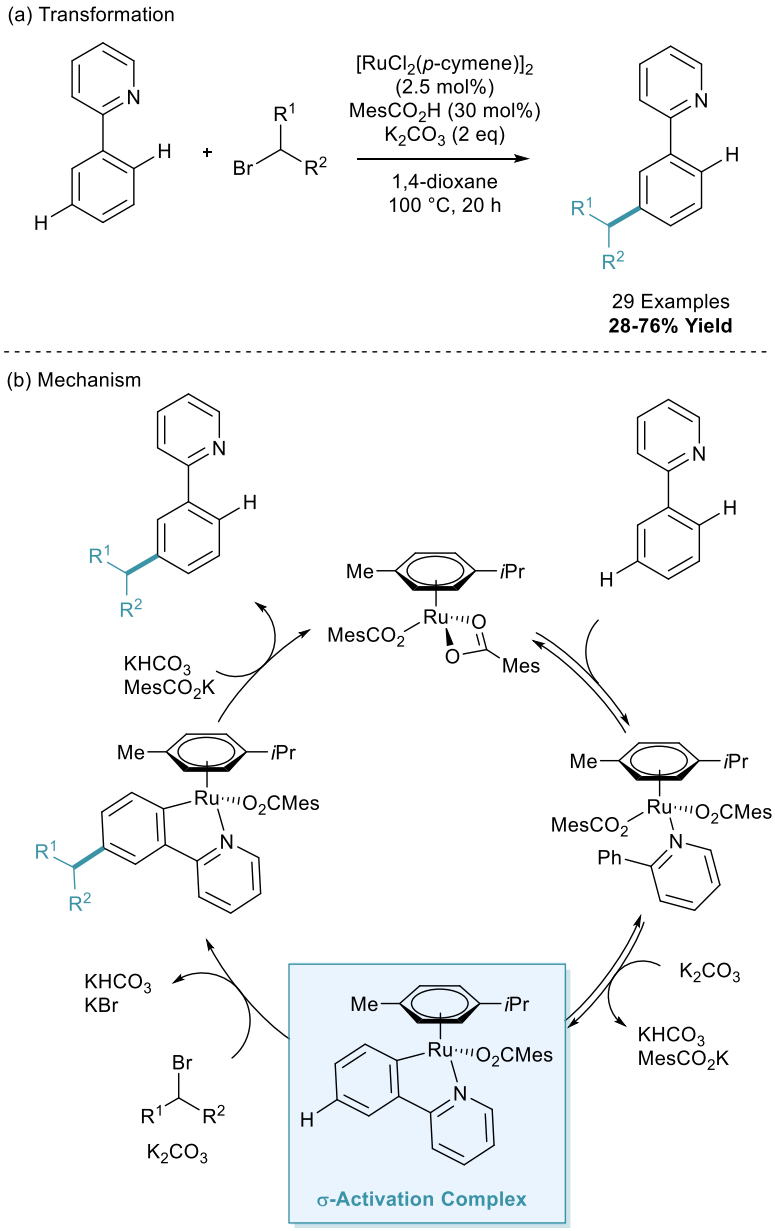

Scheme 8: Ruthenium Catalysed *meta*-Alkylation of Phenylpyridine using Secondary Alkyl Halides

IV: The Radical Revolution

The development of methodologies slowed as other classic electrophiles were explored with little success.[19] It wasn't until 2015 that a full alternative radical mechanism was proposed resulting in a flood of new methodologies to the area. The groups of Frost and Ackermann simultaneously reported the *meta*-selective alkylation using tertiary alkyl halides (Scheme 9a).[20-21] Whilst the transformation itself was inherently iterative of the *meta*-alkylation methodology above, the two new reports contained game-changing insights into the mechanistic nature of the functionalisation. The two groups suggested that the

coupling partner interaction with the cyclometalated arene were through a radical addition rather than S_EAr proposed beforehand (Scheme 9b).[22]

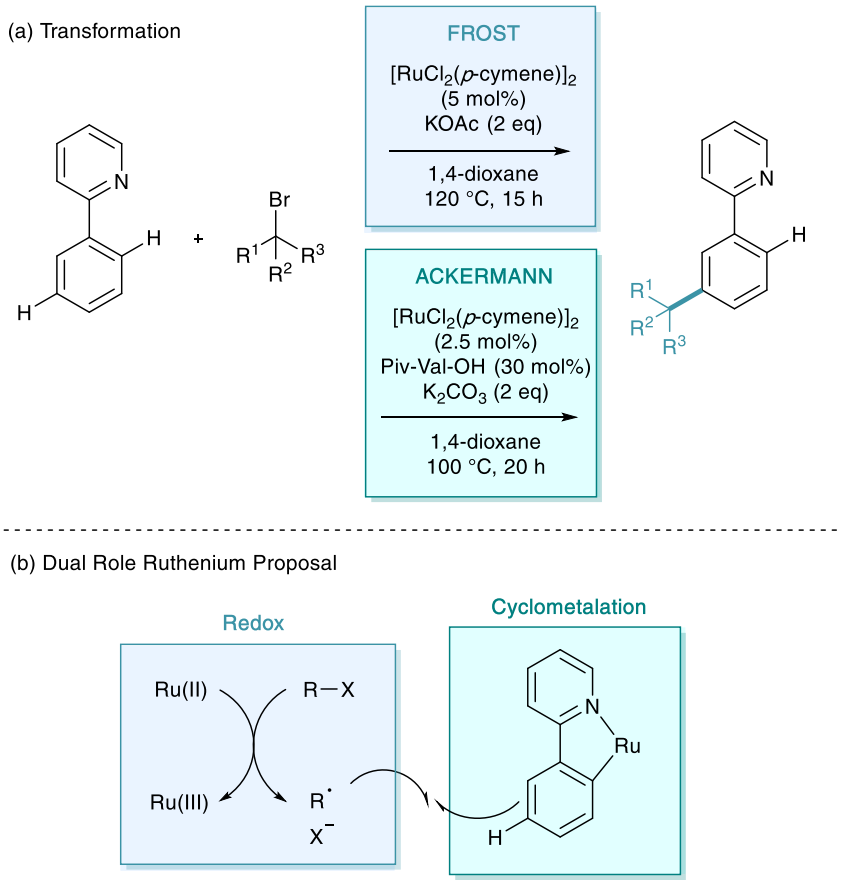

Scheme 9: Ruthenium Catalysed *meta*-Alkylation of Phenylpyridine using Tertiary Alkyl Halides and Radical Proposal

Frost evidenced this radical functionalisation using radical trapping experiments (TEMPO), by using coupling partners with a strongly disfavoured carbocation such as 1-bromoadamantane and tertiary α-halo carbonyls, and also by the isolation and characterisation of polymeric by-products. Ackermann explored radical clock experiments, racemisation, and S_EAr precursor studies. Between the two reports on the same transformation, one could argue there was now unequivocal proof of a radical functionalisation. Both of the mechanisms proposed suggest a dual role ruthenium which enables both the traditional cyclometalation but also as a redox catalyst (Scheme 10). This secondary role is capable of donating an electron to the coupling partner *via* single electron transfer (SET), facilitating homolytic cleavage, leaving the stabilised tertiary alkyl radical. This radical then interacts with the *para* position of the cyclometalate. Redox rearomatisation, proton abstraction and protodemetalation gives the *meta*-substituted product. Both groups did not specify the nature of this “Ru(II)” species, however kinetic

investigations by Ackermann suggest the reaction is second order in catalyst, suggesting a secondary outer sphere ruthenium species.[23]

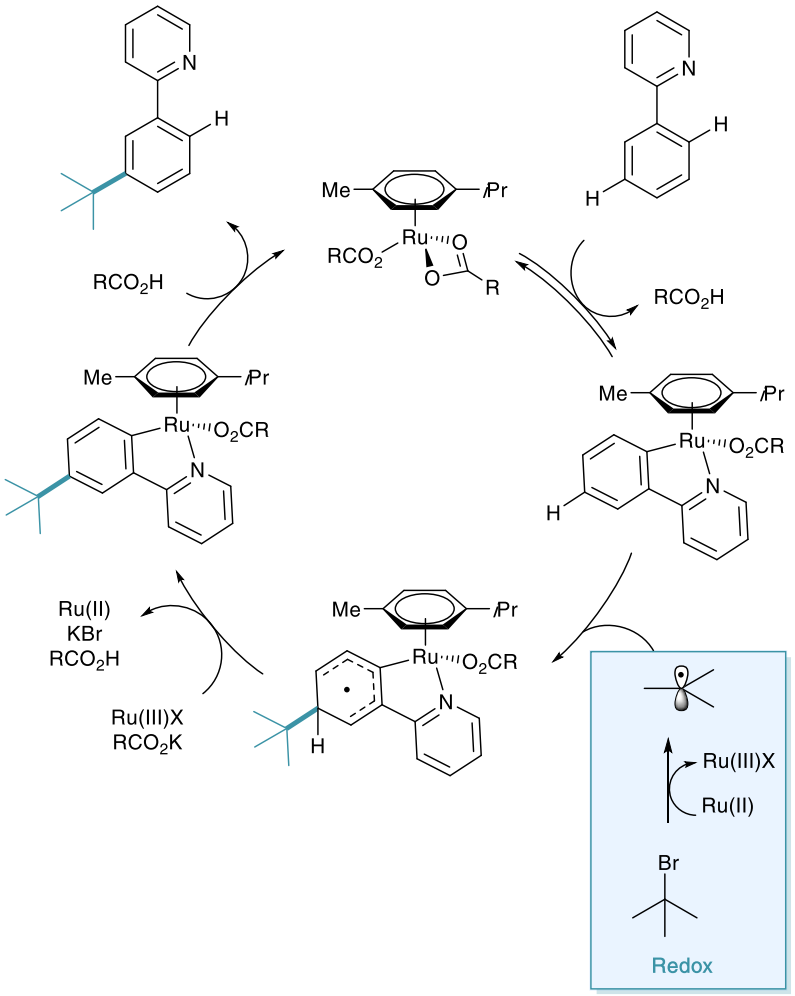

Scheme 10: Mechanism for *meta*-Alkylation of Phenylpyridine

Later in 2015, both the Greaney and Huang groups proposed, again almost simultaneously, the *meta*-bromination of phenylpyridine derivatives.[24-25] Greaney and Huang utilised tetrabutylammonium tribromide and *N*-bromosuccinimide as the bromine source respectively (Scheme 11). Huang suggested an SET process similar to those shown above. However, here involving a second C–H activation and with a defined inner sphere ruthenium catalyst generating bromine radicals. Despite the necessity for an air atmosphere (uncommon in σ-activation), this is not commented on with regards to the mechanism. Both reports made great use of the key benefit of installing aryl bromides, where subsequent palladium catalysed cross coupling enabled the formation of *meta*-arylated, borylated, alkenylated, alkylated and alkynylated arenes.

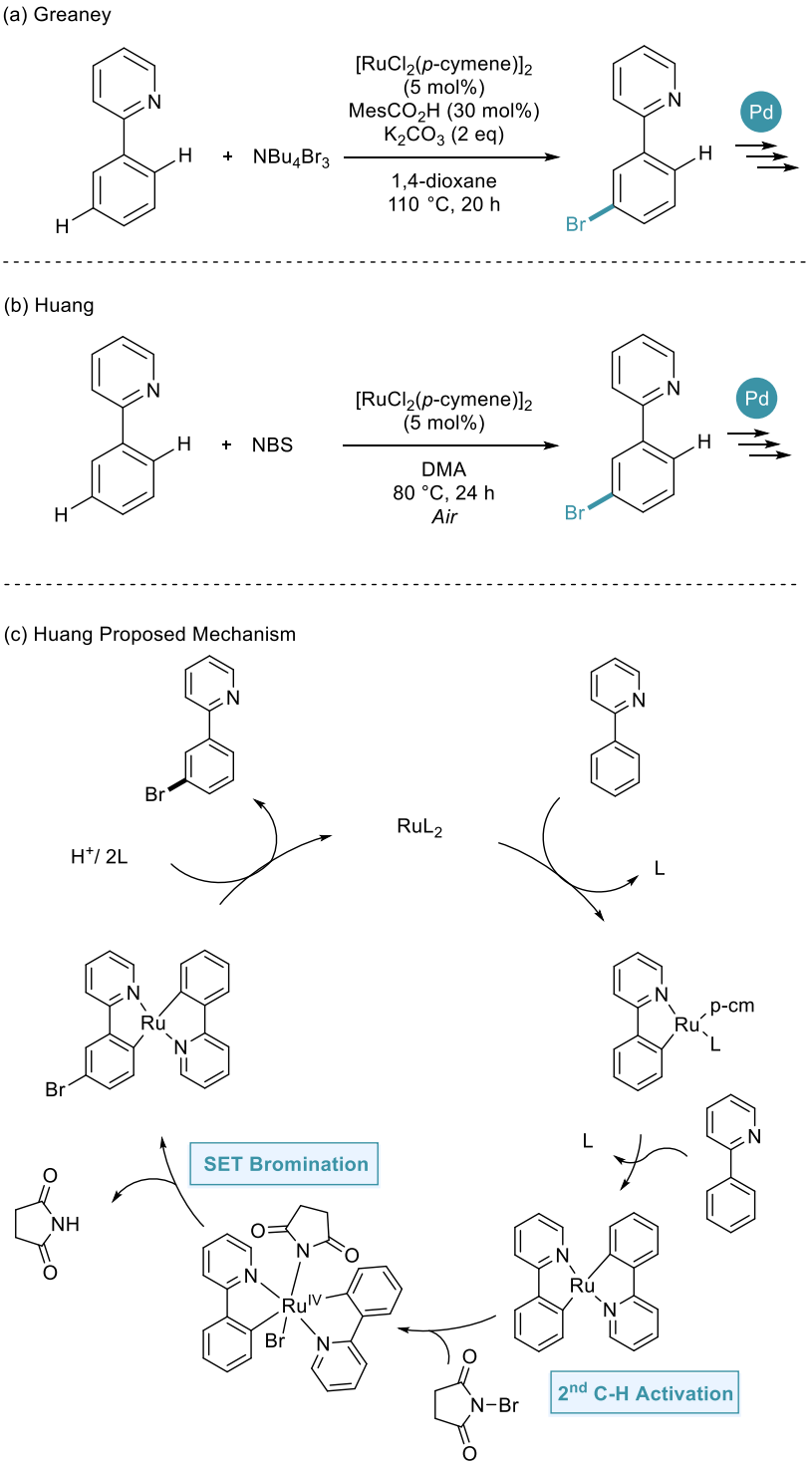

Scheme 11: Ruthenium Catalysed *meta*-Bromination of Phenylpyridine

Despite a C–H nitration reaction being the first example of stoichiometric ruthenium σ-activation, it took until 2016 for ruthenium catalysed *meta*-selective C–H nitration to be developed.[26] Here, Zhang employed $[Ru_3(CO)]_{12}$ as the ruthenium catalyst, as well as a silver salt (silver trifluoroacetate, AgTFA), oxidant (oxone), base (tetrabutylammonium acetate, NBu_4OAc), and nitro source (copper nitrate trihydrate). Despite the cocktail of

reagents, this has enabled efficient and selective *meta*-nitration of an array of arenes (Scheme 12). Zhang also proposed a mechanism involving two C–H activated phenylpyridine structures. In this instance this bi-pyridyl complex was isolated from the mixture, characterised *via* single crystal x-ray diffraction and proven to be catalytically competent in the reaction mixture. They also propose a dual copper/silver oxidation cascade which enables the formation of the nitro radical. The *meta*-nitrated arenes were also shown to be widely diversifiable in a variety of post-synthetic functional group interconversions (FGI).

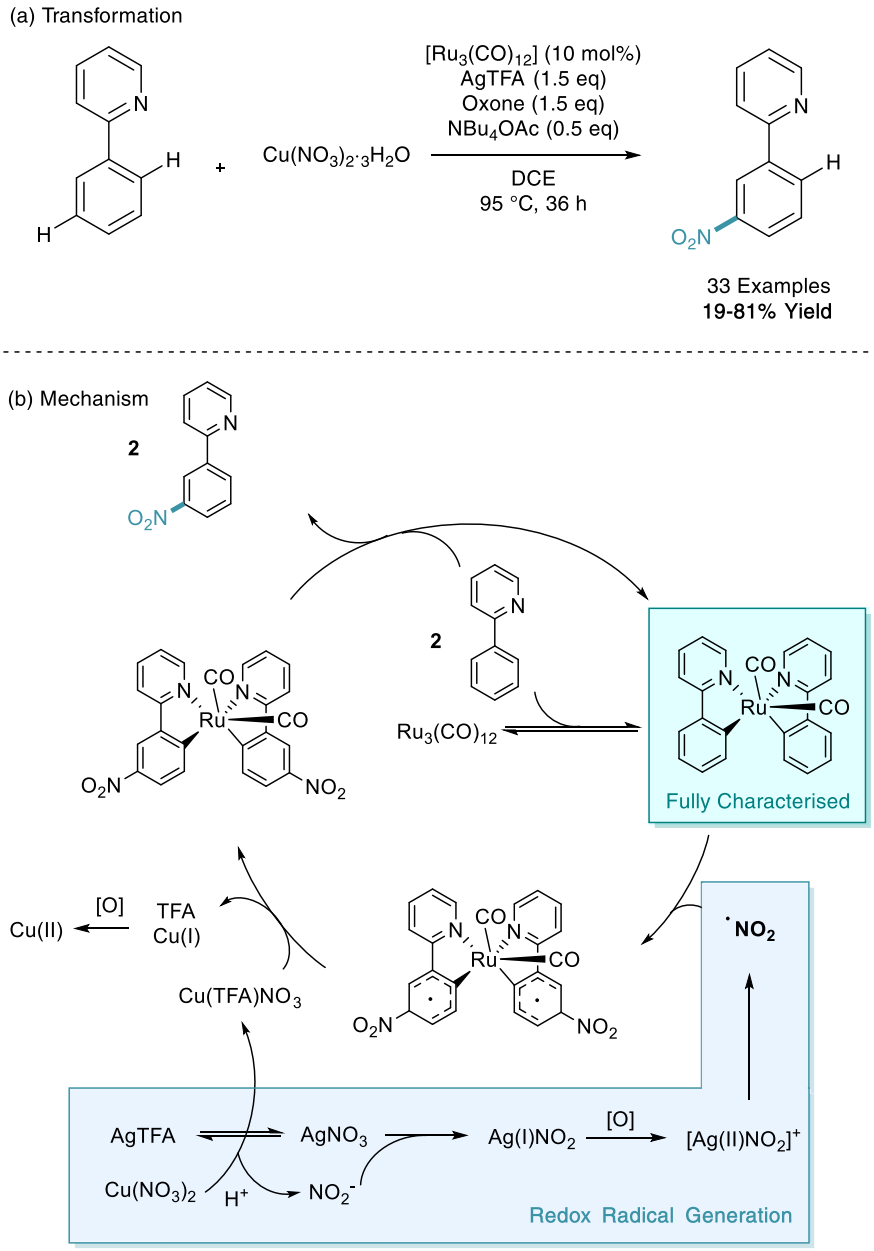

Scheme 12: Ruthenium(0)-Catalysed *meta*-Nitration of Phenylpyridine

Following these mechanistic insights, Frost also reported a revised radical mechanism in 2016 for the initial *meta*-sulfonation methodology. This was proposed to undergo a similar mechanism where SET enables formation of the tosyl radical, after similar mechanistic results were discovered with that methodology.[27]

V: Recent Advances

The mechanistic foundations had now been set for σ-activation methodology, and these insights inspired a catalogue of different applications building on the established transformations. The following part of this review is split into three subsections entailing the expansion of this technique: structural template expansion, new C-X bond formations, and catalyst development.

V.I: Structural Template Expansion

One of the key drawbacks in σ-activation, which the reader may have identified, is the over reliance on phenylpyridine. Despite being an excellent model substrate employed by multiple groups, phenylpyridine has limited biological activity and limited scope for further derivation. To expand the scope of this synthetic technique, an auxiliary approach can be used. Here one can furnish a motif with a directing group, carry out the remote functionalisation, and then cleave the directing group to reveal the more useful functionality.

This technique was first employed by Ackermann in his 2015 tertiary alkylation report. Here they use *N*-pyrimidinyl aniline as a model substrate in the *meta*-alkylation methodology (Scheme 13a).[21] After acidic cleavage of this directing group in aqueous media, this now led to the *meta*-functionalised aniline. It should be noted that the regioselectivity of functionalisation is complementary to the natural *ortho / para* directing selectivity of an aniline. The same group also expanded on this in a recent report using ketimine directing groups, which when treated with aqueous acid after functionalisation, reveals the acetophenone (Scheme 13b).[28] They reported a vast scope of 40 examples of different structures utilising both secondary and tertiary alkyl halide coupling partners. They also demonstrated a vast array of post-synthetic modifications of the ketimine group to give anilines, phenols, indoles and benzylamines, as well as *in situ ortho*-C–H functionalisation to give di-substituted arenes.

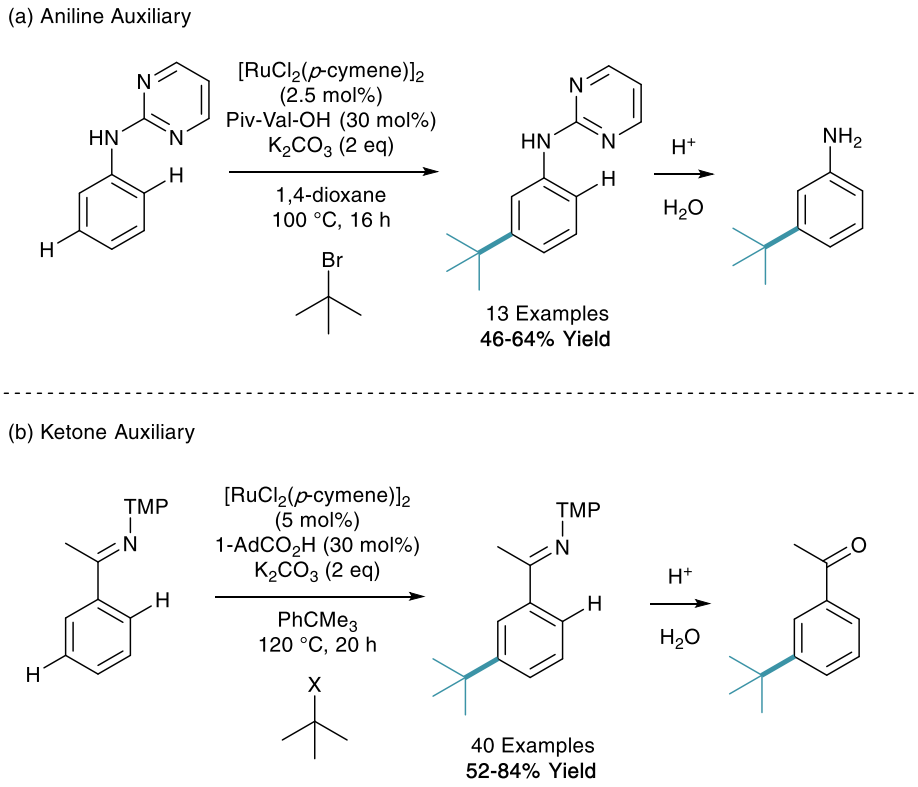

Scheme 13: Use of Cleavable Auxiliaries in *meta*- Selective C–H Functionalisation. TMP = 3,4,5-trimethoxyphenyl. X = Cl, Br or I

Following a similar concept of creating the *meta* substituted aniline building block, Li has reported the *meta*-alkylation and sulfonation of diazobenzenes (Scheme 14a).[29-30] Both methodologies were shown to be selective for functionalisation on only one of the aryl rings and using catalytic iron powder in acetic acid, the diazo could be transformed into the free aniline. The same group have also demonstrated the *meta*-alkylation of phenol furnished with a pyridine directing group (Scheme 14b). This can subsequently be removed under incredibly forcing conditions to give the *meta*-alkyl phenol.[31]

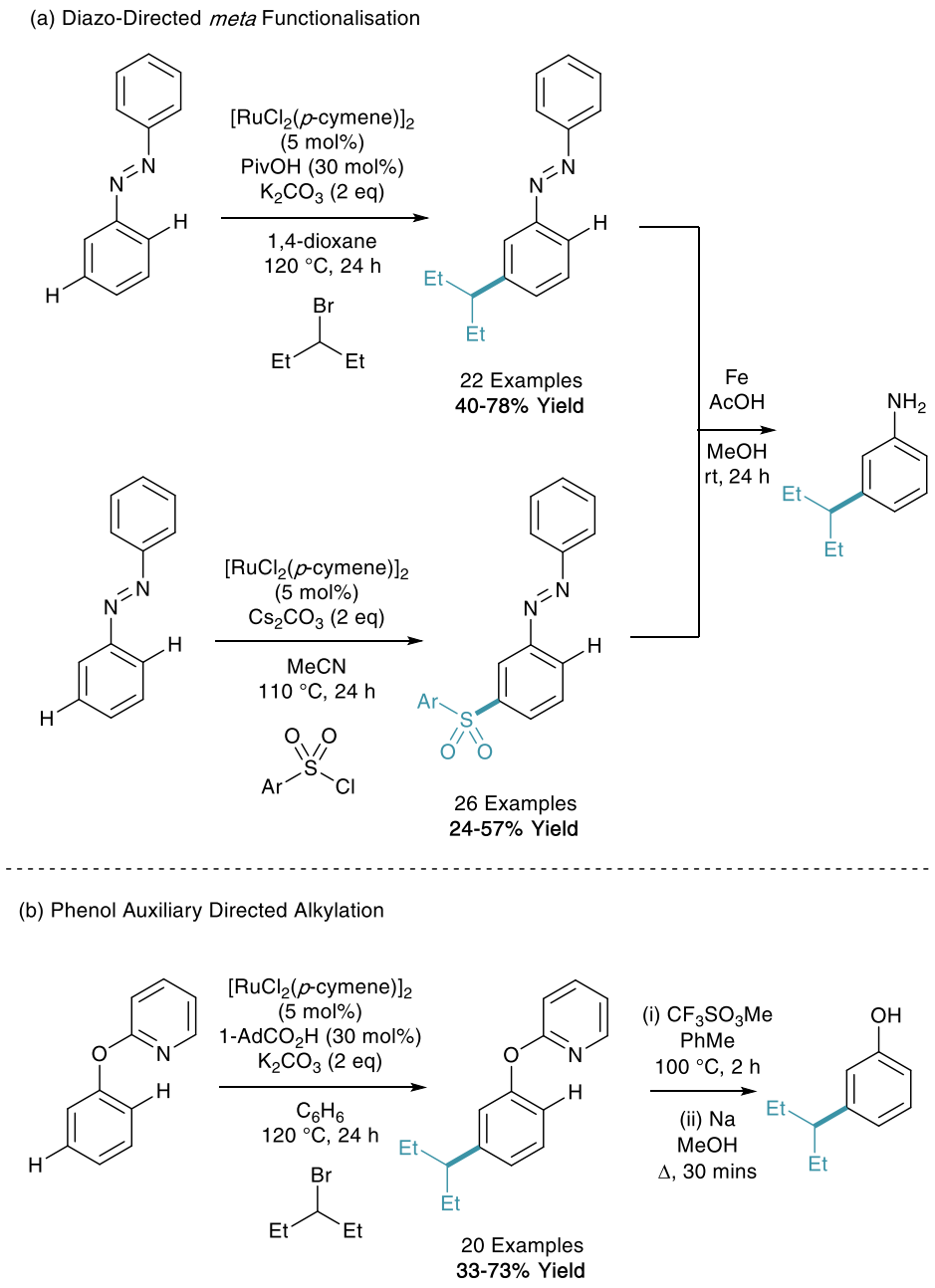

Scheme 14: Ruthenium Catalysed *meta*-Functionalisation of Aniline and Phenol Auxiliaries

C–H activation is a powerful tool that can be employed to derivatise biologically relevant structures[32] such as indoles. Frost reported the remote C–H alkylation of indole derivatives in 2017 (Scheme 15).[33] The difficulty of selectively accessing the benzenoid ring (C4-7) of an indole has been highlighted in a recent review.[34] This functionalisation was shown to utilise a primary directing group at N1 and an ancillary directing group at C3 to enable remote C6 alkylation on the benzenoid ring. This methodology also benefited from the first input from computational chemistry in σ-activation, where calculated Fukui indices on organic and inorganic structures helped elucidate that cyclometalation at C2 would in turn place electron density on the C6 position.

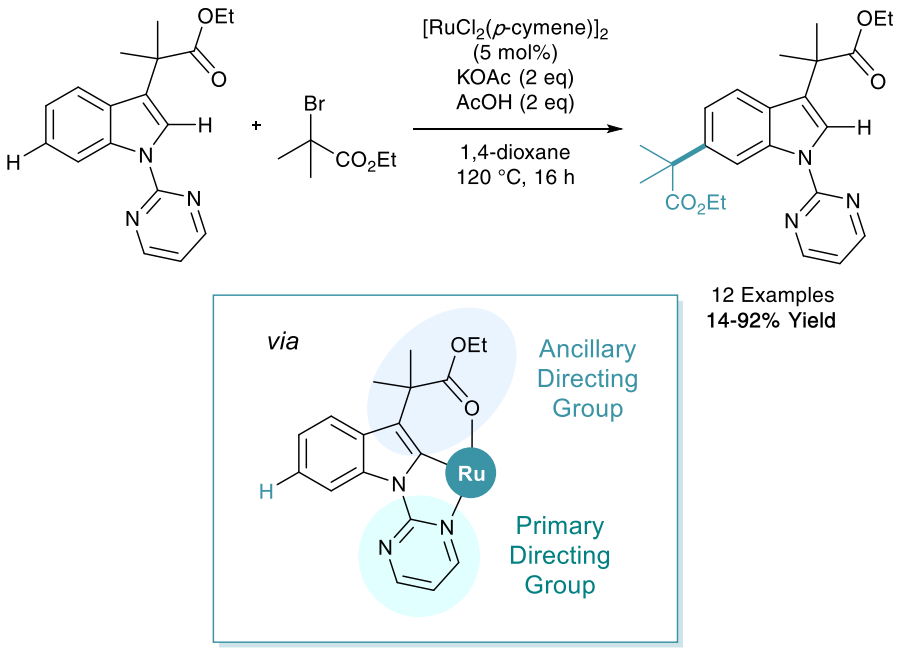

Scheme 15: Remote C6-Selective Ruthenium Catalysed C–H Alkylation of Indole Derivatives

As a follow up to their work on the *meta*-nitration of phenylpyridines (and related heteroaromatics), Zhang reported a further iteration of this methodology in 2017.[35] Here, they focused on the use of the oxime directing group as a removal auxiliary. In this process, they also reported a variation on their catalytic system to utilise silver nitrate as the nitro source and O_2 as a co-oxidant (Scheme 16).

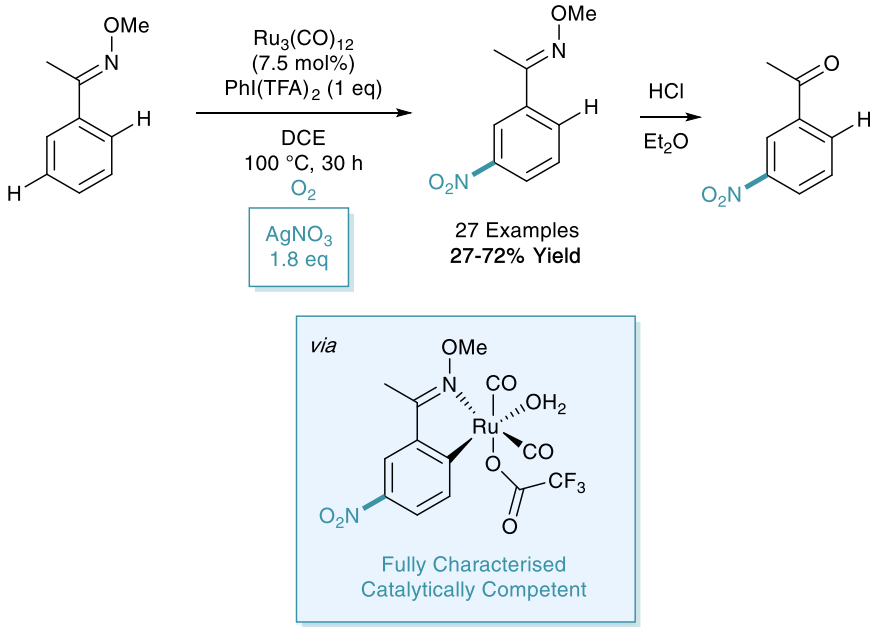

Scheme 16: Ruthenium(0) Catalysed *meta*-Nitration of Oximes

V.II: New C-X Bond Formations

One of the other avenues which is necessary to develop σ-activation is the search for new C-X or C-C bond formation reactions to expand the arsenal of transformations available. In early 2017, both Ackermann and Wang reported the *meta*-selective C–H difluoroalkylation and monofluoroalkylation of heteroarenes (Scheme 17).[36-37] Ackermann proposed a triarylphosphine additive as a co-catalyst, along with a wide scope of arenes, directed by pyridine, pyrimidine, pyrazole, and purine directing groups (Scheme 17a). A radical process was also suggested although the exact role of the nature of phosphine in the mechanism was not presented. Despite this, they did demonstrate both carboxylic acid ($MesCO_2H$) and phosphine co-catalysts were vital to catalysis. Wang's report employs a palladium(0) co-catalyst ($Pd(PPh_3)_4$) in the same transformation. They propose a Pd(0)/Pd(I) redox cycle for the generation of the difluoroalkyl radicals (Scheme 17b). Zhao has also since proposed a ruthenium catalysed *meta*-difluoroalkylation of similar substrates with an alternative additive of silver triflimide ($AgNTf_2$) and, surprisingly, in many cases without an additive at all.[38]

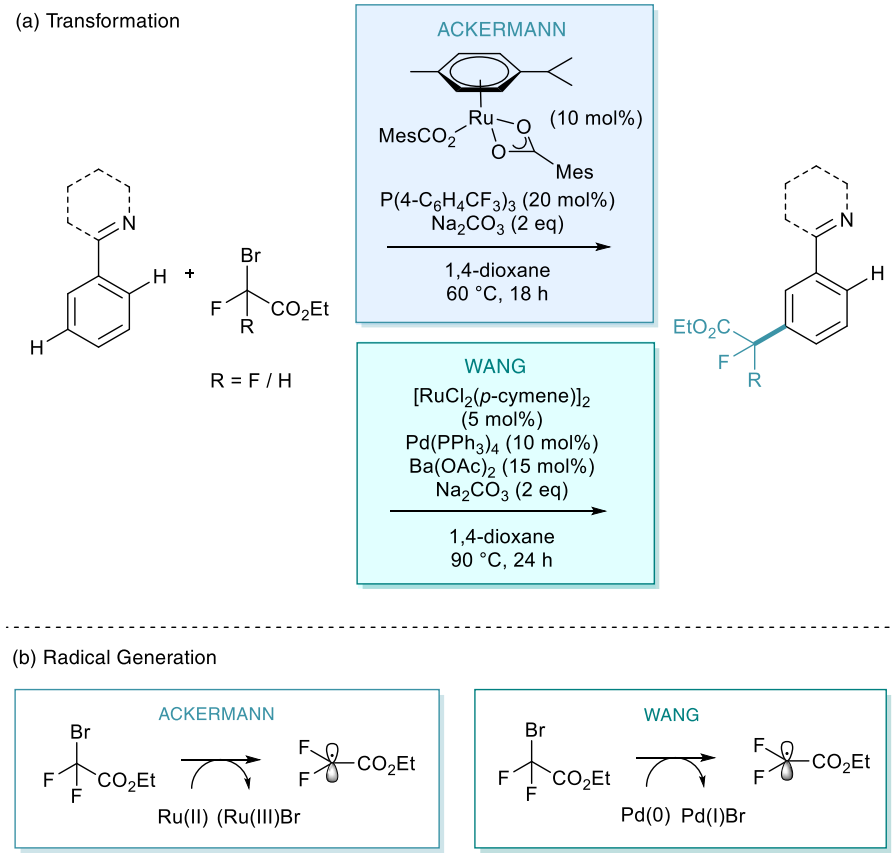

Scheme 17: Ruthenium Catalysed *meta* Difluoro- and Monofluoroalkylation of Heteroarenes

Since Ackermann's first observation of a *meta*-C–H alkylation using primary alkyl halides in small quantities, σ-activation methodology has utilised secondary and tertiary alkyl halides much more frequently as they are less likely to undergo tradition oxidative addition / reductive elimination pathways. In 2017, Frost reported the *meta*-alkylation of phenylpyridine derivatives utilising primary α-halocarbonyls. They found that similar co-catalysts as above (triarylphosphines and $Pd(PPh_3)_4$) drive the reaction towards *meta*-selectivity over competing *ortho*-selectivity (Scheme 18). A majority of the examples led to exclusive *meta*-selectivity, however with some substituted arenes some selectivity issues did remain.[39]

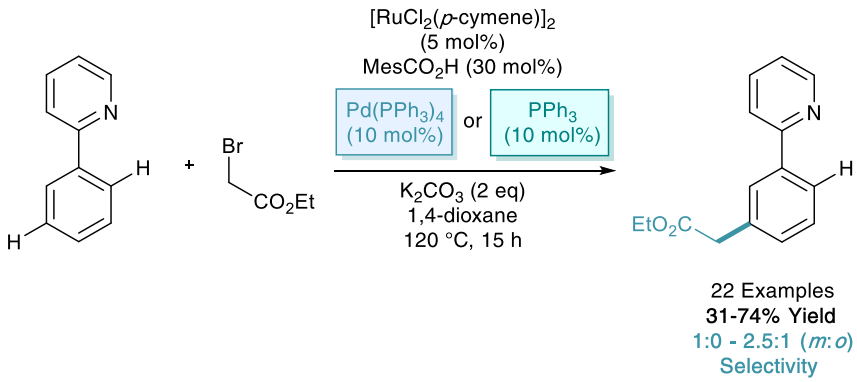

Scheme 18: Ruthenium Catalysed Alkylation of Phenylpyridine with Primary Alkyl Halides

In early 2017, Shi and Zhao reported the *meta*-benzylation of phenylpyridine.[40] This was achieved using $RuCl_3$ as the ruthenium source, ferrocene and ditertbutyl peroxide (DTBP) in radical generation, toluenes as benzyl precursors, and a binol derived phosphate ligand (L1, Scheme 19a). The use of bulky phosphate was shown to suppress competing *ortho*-functionalisation. Through in-depth investigation into the role of the additives they proposed a mechanism (Scheme 19b), they proposed the formation of a di-phenylpyridine structure similar to that reported by Zhang,[26] however with the bulky phosphate ligand bound. They then suggest that through SET from ferrocene and hydrogen abstraction from DTBP give the tolyl radical. This radical then interacts with the cyclometalated phenylpyridine at the *para* position to the metal, redox rearomatisation with Fe(III) and proton abstraction, and finally protodemetalation gives the *meta*-benzylated substrate.[41]
The methodologies described in this subsection not only permit the introduction of different C-C bonds but also allow the use of varying redox active metals, such as iron and silver, and more importantly show they are compatible with the σ-activation system. These developments set the stage for further investigation into redox partners.

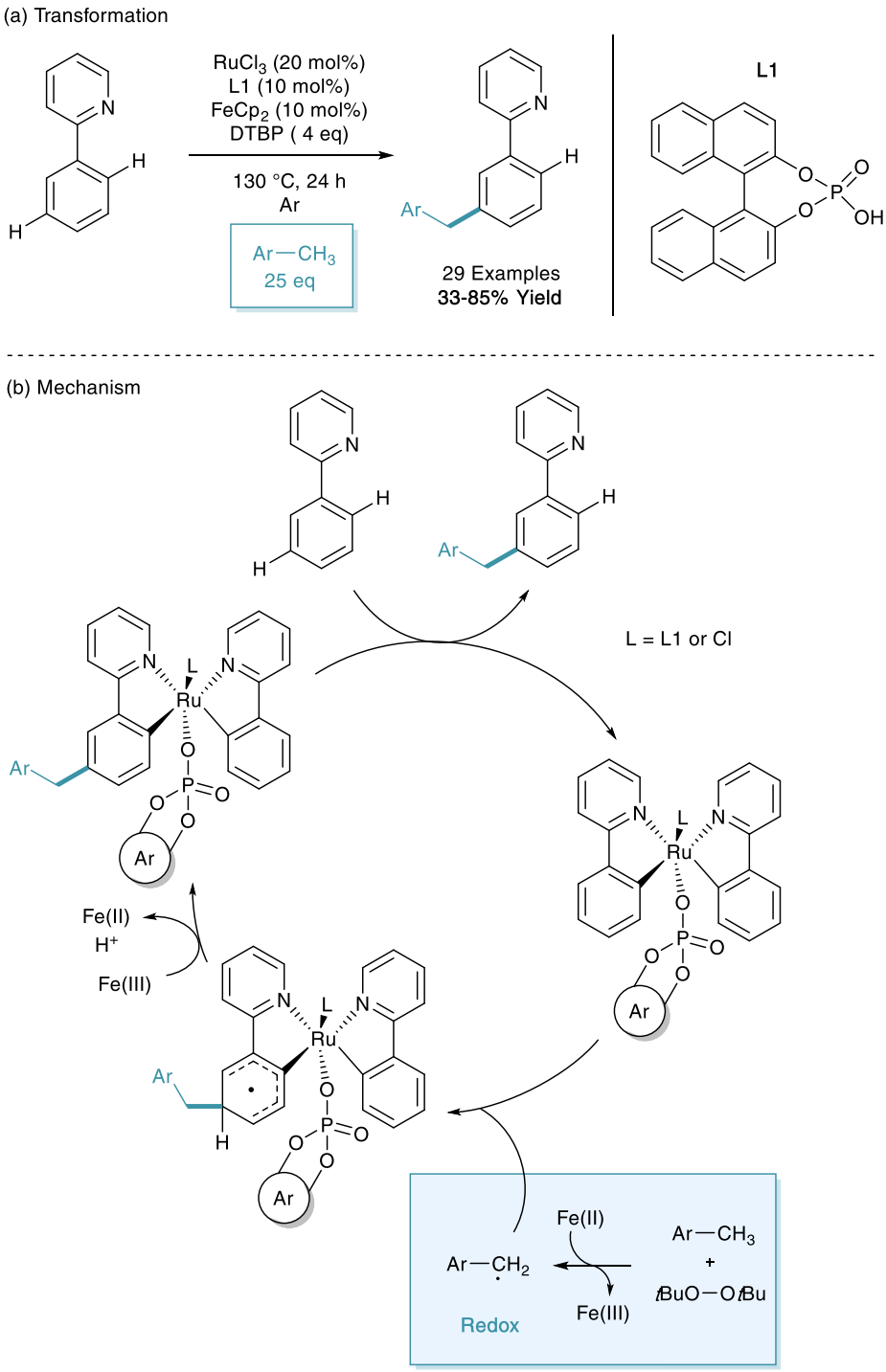

Scheme 19: Ruthenium Catalysed *meta* Benzylation of Phenylpyridine

V.III: Catalyst Development

As shown throughout this tutorial review, catalytic σ-activation relies on the use of the platinum-group transition metal, ruthenium. The use of high loadings (<30 mol% Ru by weight) is also a common feature of many processes. Due to this there will be should be a focus in the coming years on performing these methodologies in a more sustainable manner.

In early 2017, Ackermann was the first (and to date, only) to tackle this problem.[42] Here they adapted the *meta*-bromination methodology developed by Huang and set out to investigate the use of a recyclable heterogeneous ruthenium catalyst (Scheme 20). They showed that the use of a user-friendly silica-derived catalysts Ru@SiO_2 outperformed its homogeneous counterparts. The substrate of focus of this report also demonstrated the first use of a purine directing in σ-activation methodology. The catalyst was shown to be amenable to recycling, and was used as many as seven times with an impressive yield drop of less than 20%.

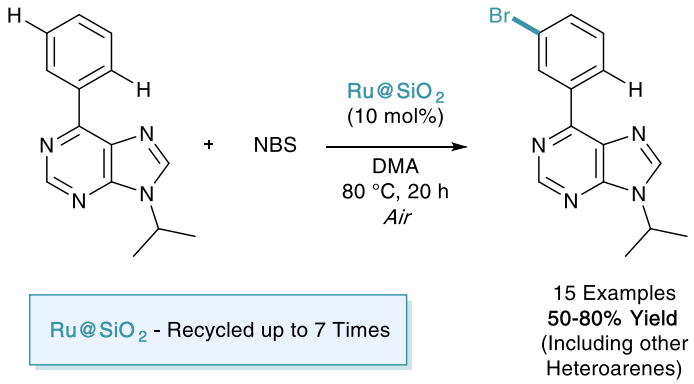

Scheme 20: *meta*-Bromination using a Recyclable Heterogeneous Ruthenium Catalyst

Conclusions

Ruthenium catalysed σ-activation has been shown as a key tool in accessing remote *meta*-selective functionalisation, moving from an organometallic to catalytic synthetic methodology. We have seen the radical revolution which has enabled the development of many new methodologies seen post-2015 in this field. We have seen that either sterically crowded coupling partners or ligand sets have suppressed traditional *ortho*-functionalization pathways and promoted complementary *meta*-functionalization. These insights will only lead to a stronger influx of reports in this field. As there have already been as many methodologies published in 2017 as the previous six years combined, the stage is now set for ruthenium-catalyzed σ-activation to move from proof of concept research to a broadly

applicable methodology in the synthetic toolbox. We now stare into the horizon of ruthenium catalysed σ-activation where we expect to see the continuing rapid expansion in scaffolds, new C-C/C-X bond forming processes and well-defined bespoke catalysts. These will no doubt be applied in the late stage functionalization of biologically relevant molecules, in drug development, and in the creation of novel building blocks.

Notes and references

(1) L. Ackermann, *Chem. Rev.*, 2011, **111**, 1315.

(2) P. B. Arockiam, C. Bruneau, and P. H. Dixneuf, *Chem. Rev.*, 2012, **112**, 5879.

(3) J. Wencel-Delord and F. Glorius, *Nat. Chem.*, 2013, **5**, 369.

(4) Z. Chen, B. wang, J. Zhang, W. Yu, Z. Liu, Y. Zhang, *Org. Chem. Front.*, 2015, **2**, 1107.

(5) A. Dey, S. Agasti, and D. Maiti, *Org. Biomol. Chem.*, 2016, **14**, 5440 and references therein.

(6) A. Dey, S. Maity, and D. Maiti, *Chem. Commun.*, 2016, **52**, 12398 and references therein.

(7) J. Schrank, A. Tlili, and M. Beller, *Angew. Chem. Int. Ed.*, 2014, **53**, 9426

(8) J. Li, S. De Sarkar, and L. Ackermann, *Top. Organomet. Chem.*, 2016, **55**, 217.

(9) D. Leow, G. Li, T.-S. Mei, and J.-Q. Yu, *Nature*, 2012, **416**, 518 and citing references.

(10) S. Das, C. D. Incarvito, R. H. Crabtree, and G. W. Brudwig, *Science*, 2006, **312**, 1941.

(11) X.-C. Wang, W. Gong, L.-Z. Fang, R.-Y. Zhu, S. Li, K. M. Engle, and J.-Q- Yu, *Nature*, 2015, **519**, 334 and citing references.

(12) Z. Dong, J. Wang, and G. Dong, *J. Am. Chem. Soc.*, 2015, **137**, 5887.

(13) G. R. Clark, C. E. L. Headford, W. R. Roper, L. J. Wright, and V. P. D. Yap, *Inorg. Chim. Acta*, 1994, **220**, 261.

(14) C. Coudret, S. Frayasse, and J.-P. Launay, *Chem. Commun.*, 1998, 663.

(15) A. M. Clark, C. E. F. Rickard, W. R. Roper, and L. J. Wright, *Organometallics,* 1999, **18**, 2813.

(16) L. Ackermann, N. Hofmann, and R. Vicente, *Org. Lett.*, 2011, **13**, 1875.

(17) O. Saidi, J. Marafie, A. E. W. Ledger, P. M. Liu, M. F. Mahon, G. Kociok-Kohn, M. K. Whittlesey, and C. G. Frost, *J. Am. Chem. Soc.*, 2011, **133**, 19298.

(18) N Hofmann and L. Ackermann, *J. Am. Chem. Soc.*, 2013, **135**, 5877.

(19) P. M. Liu and C. G. Frost, *Org. Lett.*, 2013, **15**, 5862.

(20) A. J. Paterson, S. St John-Campbell, M. F. Mahon, N. J. Press, and C. G. Frost, *Chem. Commun.*, 2015, **51**, 12807.

(21) J. Li, S. Warratz, D. Zell, S. De Sarkar, E. E. Ishikawa, and L. Ackermann, *J. Am. Chem. Soc.*, 2015, **137**, 13894.

(22) G. B. Boursalian, W. S. Ham, A. R. Mazzotti, and T. Ritter, *Nat. Chem.*, 2016, **8**, 810 and references therein.
(23) Ackermann and co-workers have since proposed a first order dependence on ruthenium catalyst in reference 28.
(24) C. J. Teskey, A. Y. W. Lui, and M. F. Greaney, *Angew. Chem. Int. Ed.*, 2015, *54*, 11677.
(25) Q. Yu, L. Hu, Y. Wang, S. Zheng, and J. Huang, *Angew. Chem. Int. Ed.*, 2015, **54**, 15284.
(26) Z. Fan, J. Ni, and A. Zhang, *J. Am. Chem. Soc.*, 2016, **138**, 8470.
(27) P. Marcé, A. J. Paterson, M. F. Mahon, and C. G. Frost, *Catal. Sci. Technol.*, 2016, **6**, 7068.
(28) J. Li, K. Korvorapun, S. De Sarkar, T. Rogge, D. J. Burns, S. Warratz, and L. Ackermann, *Nat. Commun.*, 2017, **8**, 15430.
(29) G. Li, X. Ma, C. Jia, Q. Han, Y. Wang, J. Wang, L. Yu, and S. Yang, *Chem. Commun*., 2017, **53**, 1261.
(30) G. Li, X. Lv, K. Gao, Y. Wang, S. Yang, L. Yu, Y. Yu, J. Wang, *Org. Chem. Front.*, 2017, **4**, 1145.
(31) G. Li, P. Gao, X. Lv, C. Qu, Q. Yan, Y. Wang, S. Yang, J. Wang, *Org. Lett.*, 2017, **19**, 2682.
(32) J. A. Leitch, P. B. Wilson, C. L. McMullin, M. F. Mahon, Y. Bhonoah, I. H. Williams, and C. G. Frost, *ACS Catal.*, 2016, **6**, 5520 and references therein.
(33) J. A. Leitch, C. L. McMullin, M. F. Mahon, Y. Bhonoah, and C. G. Frost, *ACS Catal.*, 2017, **7**, 2616.
(34) J. A. Leitch, Y. Bhonoah, and C. G. Frost, *ACS Catal.*, 2017, **7**, 5618.
(35) Z. Fan, J. Li, H. Lu, D.-Y. Wang, C. Wang, M. Uchiyama, and A. Zhang, 2017, **19**, 3199.
(36) Z. Ruan, S.-K. Zhang, C. Zhu, P. N. Ruth, D. Stalke, and L. Ackermann, *Angew. Chem. Int. Ed.*, 2017, **56**, 2045.
(37) Z.-Y. Li, L. Li, Q.-L. Li, K. Jing, H. Xu, and G.-W. Wang, *Chem. Eur. J.*, 2017, **23**, 3285.
C. C. Yuan, X. L. Chen, J. Y. Zhang, and Y. S. Zhao, *Org. Chem. Front.*, 2017, DOI: 10.1039/C7QO00449D
(38) A. J. Paterson, C. J. Heron, C. L. McMullin, M. F. Mahon, N. J. Press, and C. G. Frost, *Org. Biomol. Chem.*, 2017, **15**, 5993.
(39) G. Li, D. Li, J. Zhang, D.-Q. Shi, and Y. Zhao, *ACS Catal.*, 2017, **7**, 4138. Prior to submission of this manuscript, a second *meta*-benzylation was published: B. Li, S.-L. Fang,
(40) D.-Y. Huang, B.-F. Shi, *Org. Lett.*, 2017, **19**, 3950.
(41) S. Warratz, D. J. Burns, C. Zhu, K. Korvorapun, T. Rogge, J. Scholz, C. Jooss, D. Gelman, and L. Ackermann, *Angew. Chem. Int. Ed.*, 2017, **56**, 1557.

1.3: *para*: Beyond *meta*-Selectivity

The search for *para*-selective C–H functionalisation methodology has received a smaller influx of generality in their reaction systems cf. *meta*-selectivity. This is as the C–H bond lies even more remote from any functionality that can impart selectivity of functionalisation. This has led to these methodologies focusing less on the use of Lewis basic directing groups and more on utilising steric and electronic influences in direct C–H functionalisation.[76] Despite this, there have been methods that utilise the directing group strategies using expansions of the template chemistry above.

1.3.1: Template-Assisted *para*-C–H Functionalisation

In 2015, Maiti reported the development of a template that *via* appreciation of geometry and distance, they enabled selective *para*-C–H alkenylation reaction methodology (Scheme 1-31a).[77] They proposed that the template made use of the Thorpe-Ingold effect, and a longer chain length to enact selectivity for the *para* position over the *ortho* and *meta* positions. Despite this, regioselectivity of functionalisation were found to be between 5:1 and 20:1 for *para*:others. The same report also reported the *para*-acetoxylation of the same templated structure. As with the template chemistry discussed previously, the ability to remove and recover these templates is a vital concept to recover atom economy of this transformation. On treatment of the silyl linker with TBAF, the Si-C_{benzyl} bond is cleaved to leave access to the *para*-substituted toluene in excellent yields and with near quantitative recovery of the Si-O cleaved phenol derivative which can be used to reform the template (Scheme 1-31b).

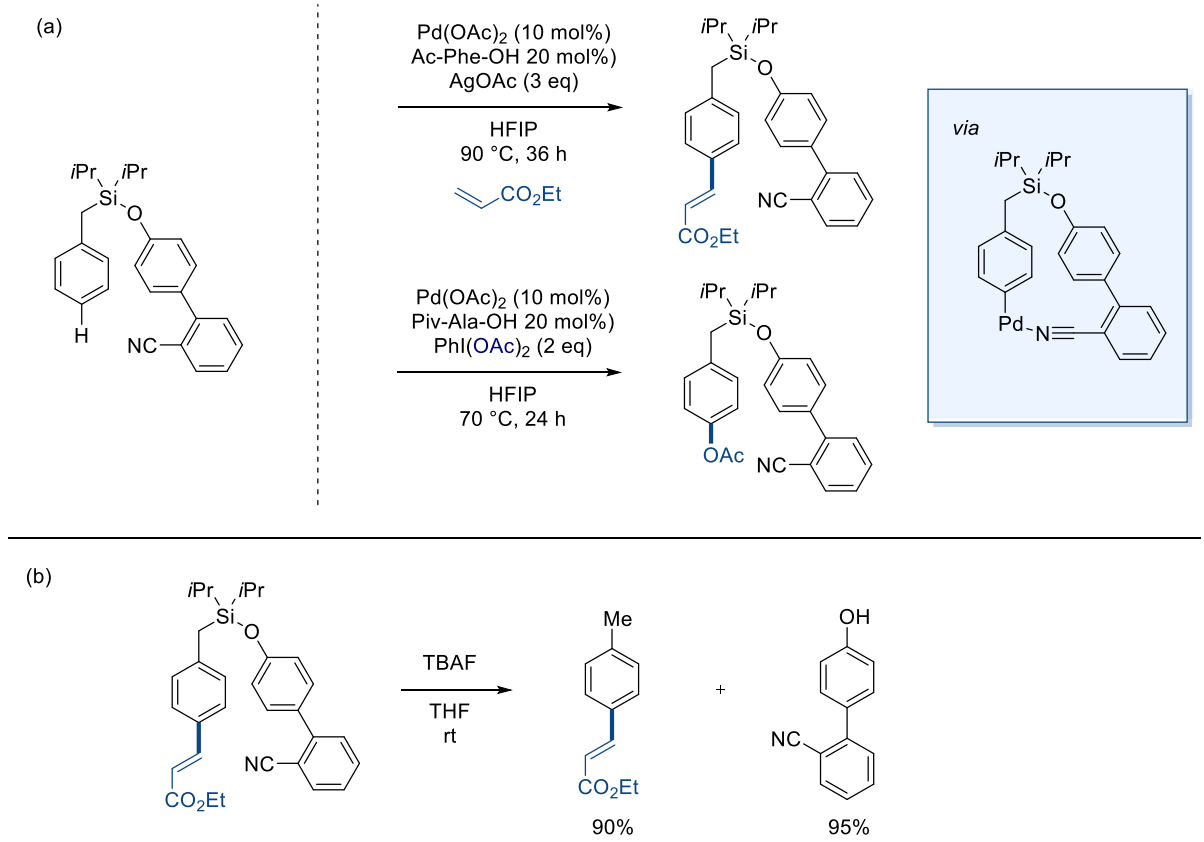

Scheme 1-31: *para*-C–H Functionalisation of Toluene Derivatives *via* Template Assistance

In 2016, the same group proposed the template-assisted *para*-C–H alkenylation of phenol derivatives (Scheme 1-32).[78] This methodology was realised *via* a switch in atom connectivity with their previous report.[77] They then demonstrated cleavage of this template using *p*-TSA which produced the *para*-substituted phenol and the silanol-based template which was shown to reform the templated substrate in great efficiency (Scheme 1-32b).

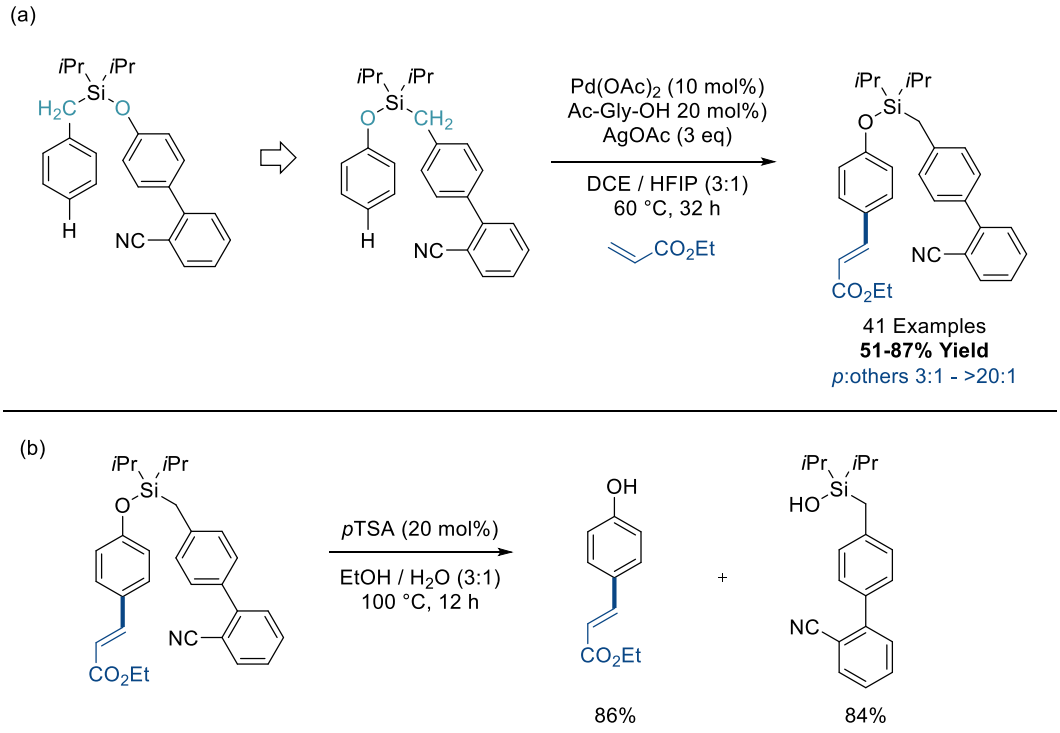

Scheme 1-32: *para*-C–H Alkenylation of Phenol Derivatives *via* Template Assistance

As discussed above, the use of catalytic non-covalent templates can be an incredibly powerful methodology in template-assisted remote C–H functionalisation. In 2017, Chattopadhyay reported the iridium catalysed *para*-C–H borylation of benzoates using a salt / Lewis basic chelate-type model to enact *para*-selectivity (Scheme 1-33).[79] This chemistry enabled highly selective C–H borylation with regioselectivities ranging from 9:1 to 99:1 with most results considerably higher than 20:1. They proposed this mechanism based on insights of using the preformed potassium alkoxide (OK) salt and comparing it to the OMe substituted ligand (cannot form the non-covalent interaction). Here, high conversions were observed in both cases however the salt gave selectivity of *para*:*meta* of 33:1, cf. 1.9:1 for OMe.

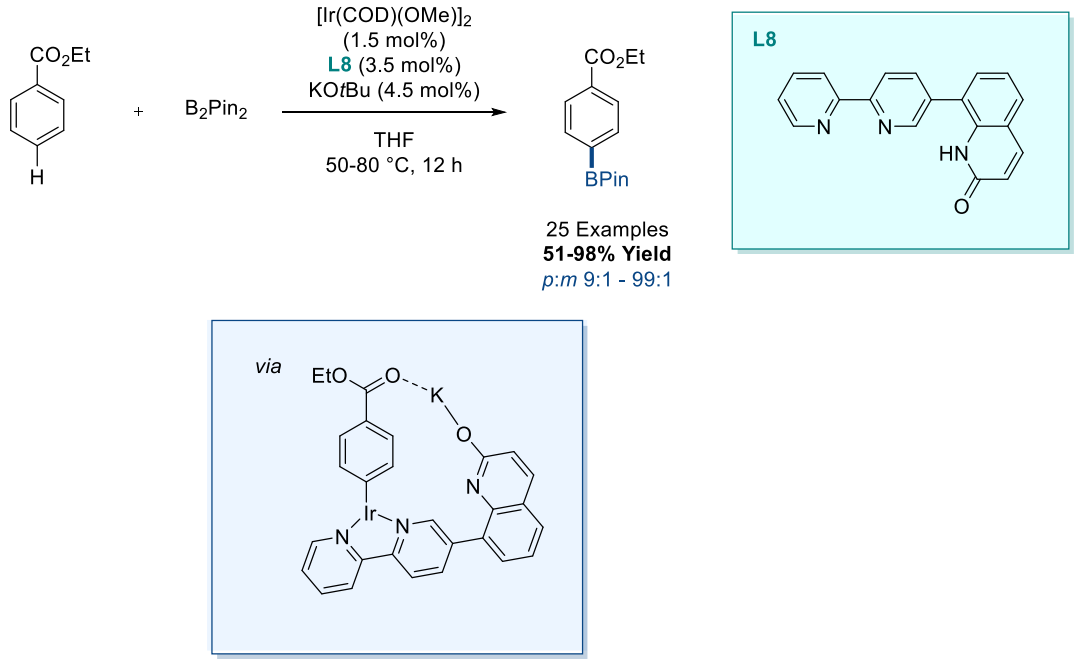

Scheme 1-33: Iridium Catalysed *para*-C–H Borylation of Benzoates using a Salt-Templated Non-Covalent Interaction

1.3.2: Sterics-Induced *para*-C–H Functionalisation

The use of sterics to influence the regioselectivity of C–H functionalisation tends to rely on pre-existing sterically demanding functionality, especially in the case of *para*-C–H functionalisation where the site of potential reactivity lies distal from those steric influences, which could lead to major regioselectivity issues.[80-81]

This has combatted in two ways in recent years, the first reported by Itami where the steric influence is enacted by the ligand on the metal (Figure 1-1), and the second pioneered by Nakao by using bulky Lewis acids to enable selective direct C–H functionalisation at the *para* position.

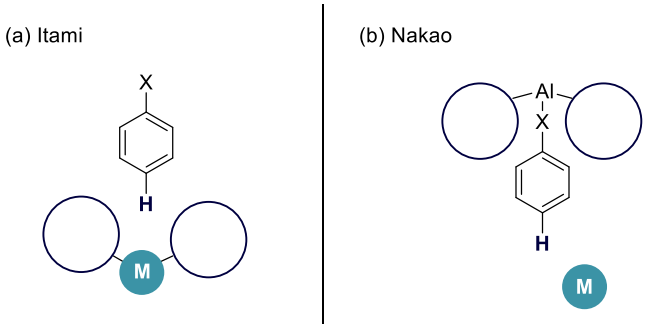

Figure 1-1: Techniques for Sterics-Induced *para*-Selective C–H Functionalisation

In 2015, Itami and co-workers reported the iridium catalysed *para*-C–H borylation of alkylbenzene and silylbenzene derivatives (Scheme 1-34).[82] Here they utilised an incredibly sterically demanding bidentate phosphine ligand (**L8**) to disfavour competing *meta*-functionalisation. This concept has also been studied computationally in modelling reactivity pocket of the ligand bound iridium complex.[83]

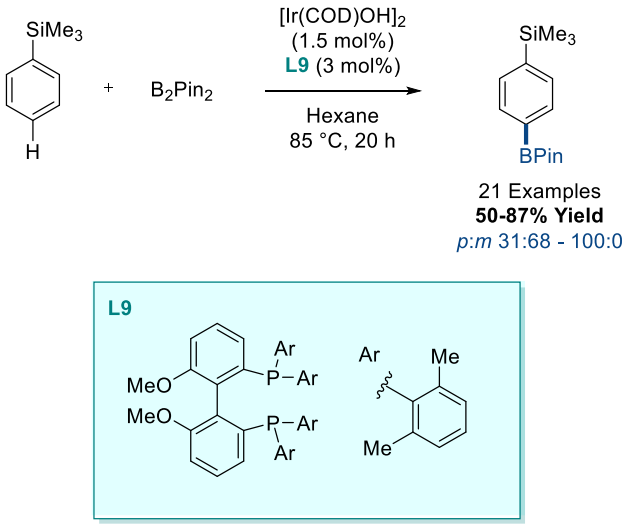

Scheme 1-34: Iridium Catalysed *para*-C–H Borylation using a Bulky Iridium Catalyst

After preliminary work on the selective C4-alkylation of pyridines using a bulky aluminium Lewis acid to enable site selective C4-metalation and functionalisation,[84] the Nakao group looked to apply this concept to the *para*-C–H functionalisation of arenes. Here they employed a dual aluminium / nickel system to enable the *para*-C–H alkylation of benzamides and aromatic ketones (Scheme 1-35).[85] The demonstrated that coordination of the carbonyl to a bulky Lewis acidic aluminium centre, coupled with a bulky nickel system enabled steric clash between the two, leading to selective *para*-selective C–H functionalisation. Following this the same group then reported the use of sulfones as substrates for the same reaction methodology.[86]

In 2017, the Nakao group coupled this chemistry to an iridium C–H borylation system to produce the *para*-C–H borylation of benzamides (Scheme 1-36).[87] Here they employed the same aluminium centre (**Al1**), however this time with an iridium precatalyst and bipyridyl based ligand. This concept led to a wide scope of *para*-borylation reactions, and it was also applied to C4-borylation of pyridines.

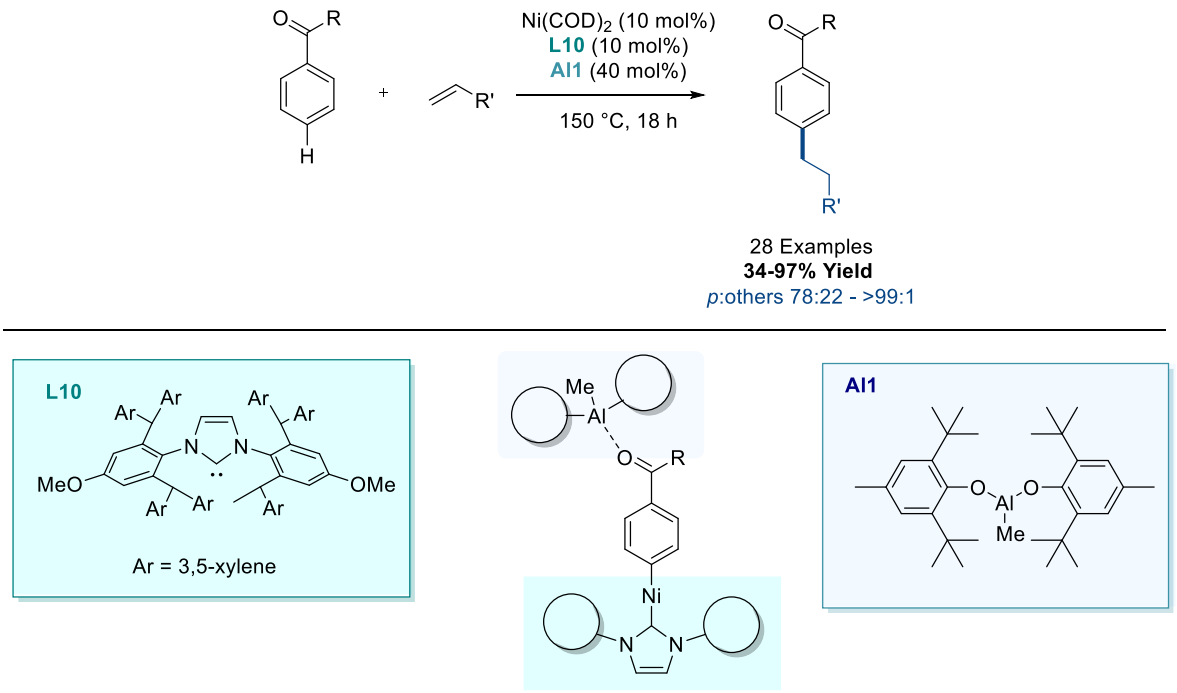

Scheme 1-35: Nickel / Aluminium Catalysed *para*-C–H Alkylation of Arenes

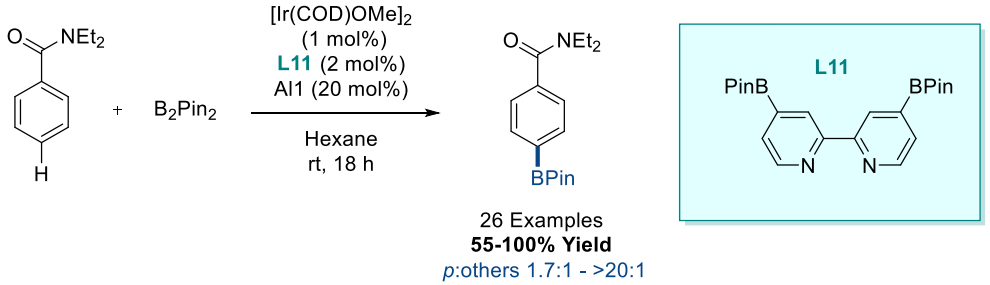

Scheme 1-36: Iridium / Aluminium Catalysed *para*-C–H Borylation of Arenes

1.3.3: Electronics-Defined *para*-C–H Functionalisation

A majority of the examples of *para*-C–H functionalisation to this date have electronics to thank for the selectivity dictated in the reaction methodology. Here, substituents which place electron density on the *para* position of an arene can enable interaction with electrophilic metal centres or substrates. With regards to modern transition metal catalysis, the first example of selective *para*-C–H functionalisation came from the Gaunt group in 2011. They adapted the reaction systems they'd developed for the copper catalysed C–H arylation of indoles[55] (and subsequently the *meta*-arylation of acetanilides)[56] to electron rich aromatics such as anisoles, anilines, and steroid derivatives (Scheme 1-37).[88] Selectivity issues were only shown to take place in arenes with one or more electron rich substituent (such as 2-methylanisole). Interestingly, they also demonstrated that, despite in lower yields, this reaction can proceed metal free.

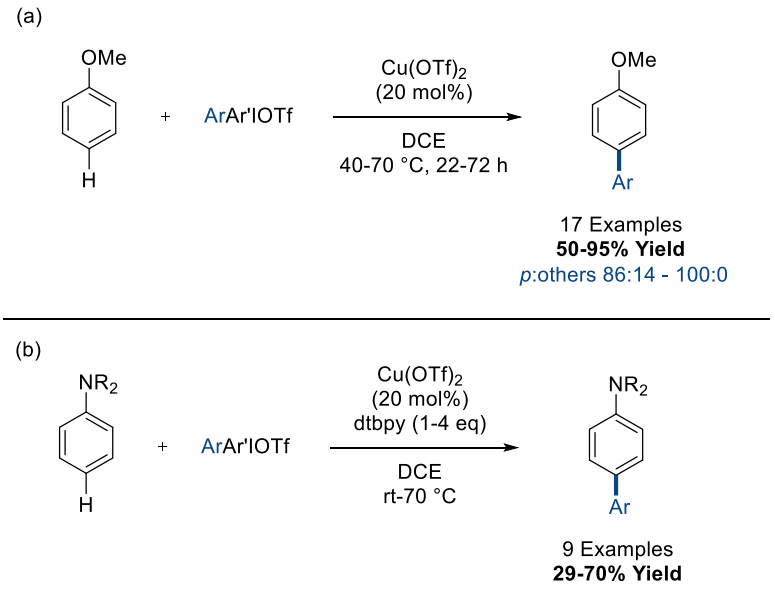

Scheme 1-37: Copper Catalysed *para*-C–H Arylation of Electron Rich Arenes

In 2011, Yu and co-workers reported the *para*-selective C–H arylation of mono-substituted arenes using palladium catalysis. They demonstrated that oxidative C–H/C–H cross coupling could take place between benzamides and *para*-directing arenes (alkyl, alkoxy and halo-substituted arenes) in great *para* selectivity (Scheme 1-38a).[89] In the same year, Cheng and co-workers also reported the *ortho*-arylation of *N*-methoxybenzamides where coupling partner functionalisation took place *para* to the directing functionality with no regioselectivity issues. They also showed that the benzamide then forms an *in situ* N-aryl bond to form the tricylic structure shown (Scheme 1-38b).[90]

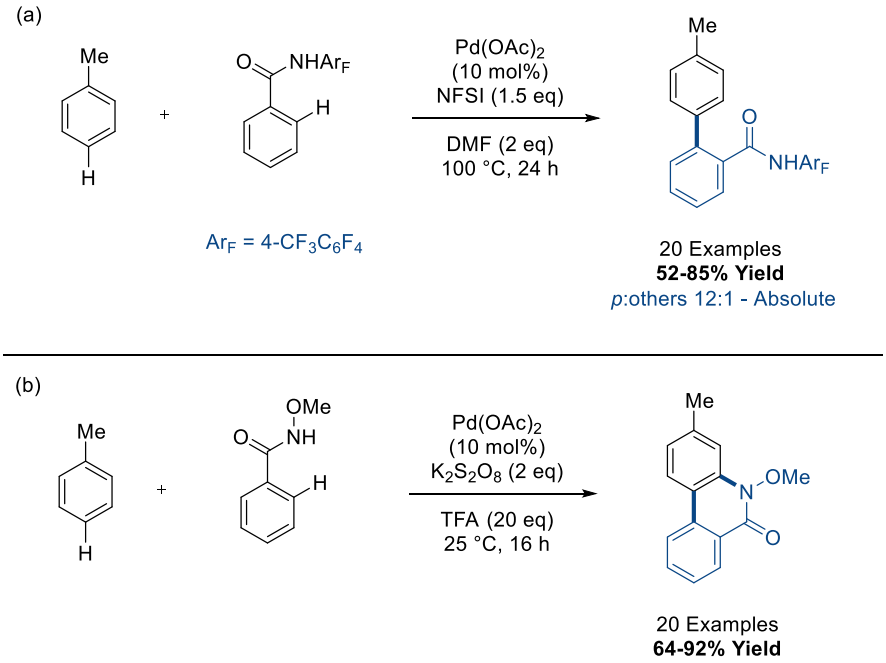

Scheme 1-38: Palladium Catalysed *para* Oxidative C–H Functionalisation of *para*-Directing Arenes

In 2012, Lloyd-Jones and Russell reported the gold-catalysed direct cross coupling between aryl silanes and electron rich arenes. They demonstrated that substrates such as anisole can be coupled at the *para* C–H bond to the alkoxy substituent. (Scheme 1-39).[91] The reaction was shown to be most efficient using 1,2-substitued arenes, and selectivity issues were only sparingly observed. A supplementary in depth kinetic and computational study dictated that the carboauration proceeded *via* an S_EAr type mechanism.[92]

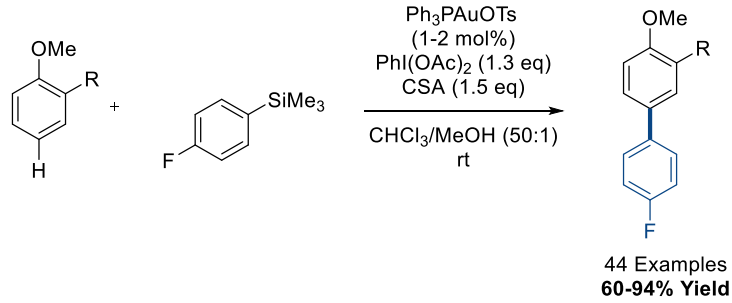

Scheme 1-39: Gold Catalysed *para*-C–H Arylation of Electron Rich Arenes

In 2013, Ackermann and co-workers demonstrated that under ruthenium catalysis, anisoles can be oxygenated at the *para* position with complete selectivity. Brief mechanistic studies detailed that radical scavengers such as TEMPO reduced reaction efficacy,

suggesting a single electron oxidation mechanism however a full catalytic cycle was not proposed. (Scheme 1-40).[93]

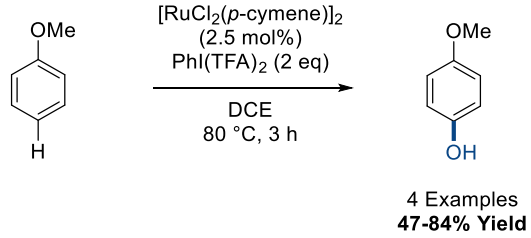

Scheme 1-40: Ruthenium Catalysed *para*-C–H Oxygenation of Anisoles

In 2015, Nicewicz reported a pioneering study in remote C–H functionalisation on the *para*-selective amination of electron rich arenes using photoredox catalysis. (Scheme 1-41a).[94] Here they employed an organic acridinium photocatalyst (**PC1**) and catalytic TEMPO in an oxygen atmosphere to facilitate the coupling of anisole and pyrazole. As with previous methodologies, regioselectivity issues with the *ortho* position were observed throughout (with exception). They also reported the late stage functionalisation of representative drug-like structures and investigated the use of ammonia equivalents to enable the free amination of anisole (Scheme 1-41b).

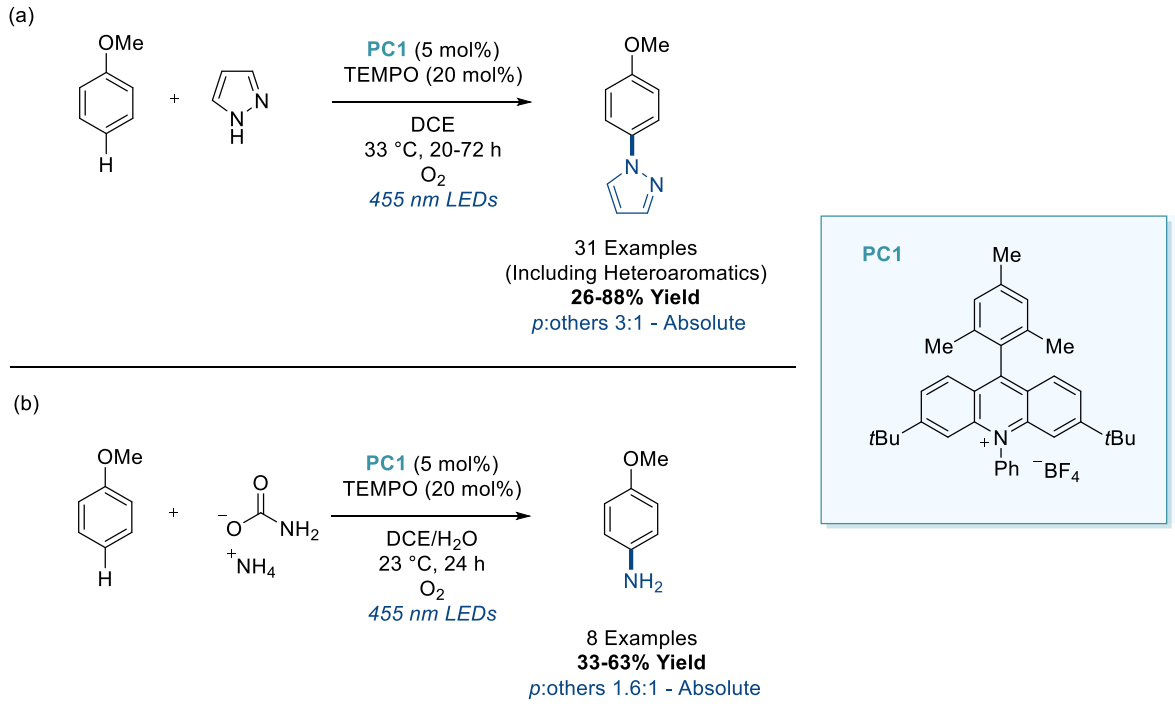

Scheme 1-41: Photoredox Catalysed *para*-C–H Amination of Electron Rich Arenes

In 2016, Ritter and co-workers disclosed the *para*-C–H amination using dual palladium and ruthenium catalysis. They used selectfluor as the aminating source which they demonstrated could be interconverted to the piperazine motif in aqueous sodium bisulfite. (Scheme 1-42).[95] They proposed that the selectivity was dictated by a "Charge-Transfer Radical Addition" where transition state interactions between the SOMO of the coupling partner and the LUMO of the arene enable electron shuttling.[96-97] They demonstrated that the greater electron affinity of the coupling partner (more positive), the higher selectivity of functionalisation. This was rationalised as the higher electron affinity, the more readily the coupling partner will accept an electron from the arene to enable the charge transfer complex, responsible for selective C–H functionalisation. The selectivity of different substrates was also predicted and then experimentally validated by the use of computationally calculated Fukui indices.

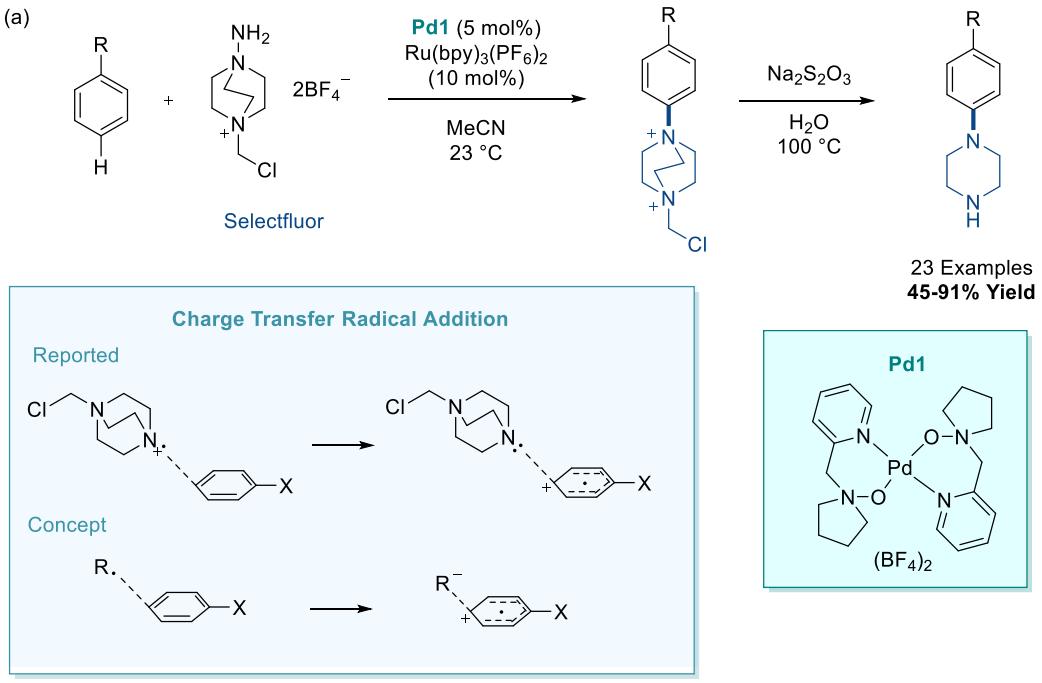

Scheme 1-42: Palladium / Ruthenium Catalysed *para*-C–H Amination of Electron Rich Arenes

In 2015, Suna and co-workers proposed the *para*-C–H amination of electron rich arenes. This was achieved by an electrophilic *para*-iodonation with a hypervalent iodine source, followed by a one-pot copper catalysed amination to give the *para*-aminated product (Scheme 1-43).[98] In 2016, this same methodology was applied to copper catalysed C-O bond formations by the same group.[99]

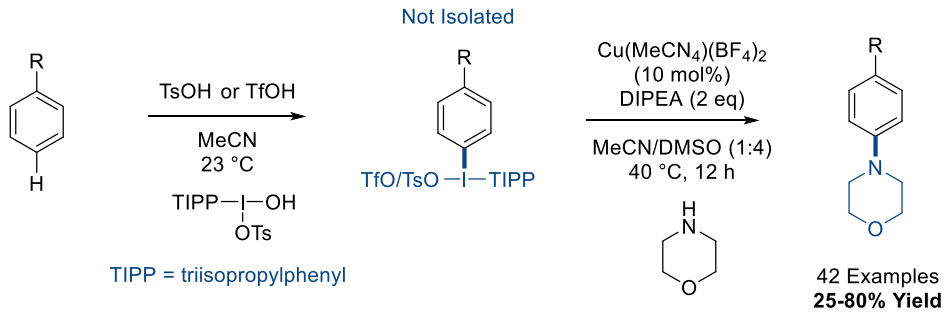

Scheme 1-43: Copper Catalysed *para*-C–H Amination of Electron Rich Arenes *via* Electrophilic Iodonation

Zhang and co-workers reported the gold catalysed *para*-C–H alkylation of electron rich arenes using activated diazo compounds as alkyl surrogates (Scheme 1-44).[100] This chemistry was demonstrated to be incredibly high yielding in as little as 3 minutes of reaction time. They also applied the reaction system to the late stage modification of biologically relevant steroid and menthol derivatives.

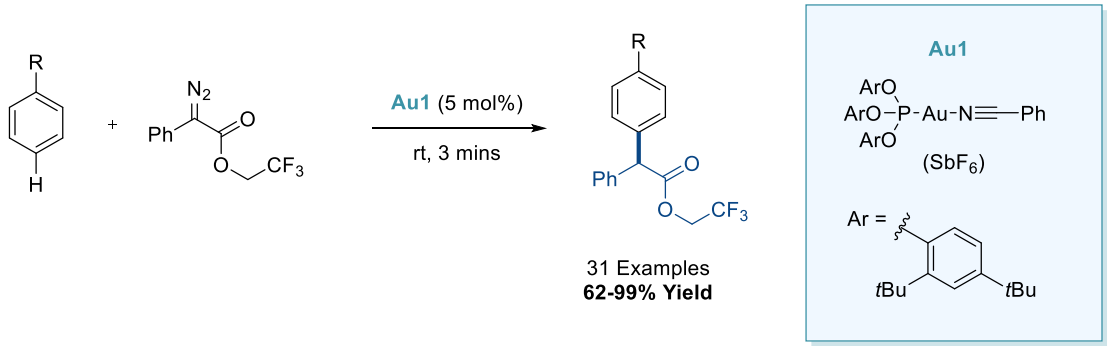

Scheme 1-44: Gold Catalysed *para*-C–H Alkylation of Electron Rich Arenes

In 2017 Ye demonstrated that using a palladium/NFSI system, one could access *para*-C–H arylation of simple arenes using aryl boronic acids. They disclosed that the use of dimethylformamide (DMF) as a ligand was critical to reactivity at the *para*-position (Scheme 1-45).[101] Like the gold catalysed *para*-C–H arylation proposed by Lloyd-Jones and Russell, Ye proposes that an electrophilic S_EAr-type carbopalladation dictates the *para*-selectivity.

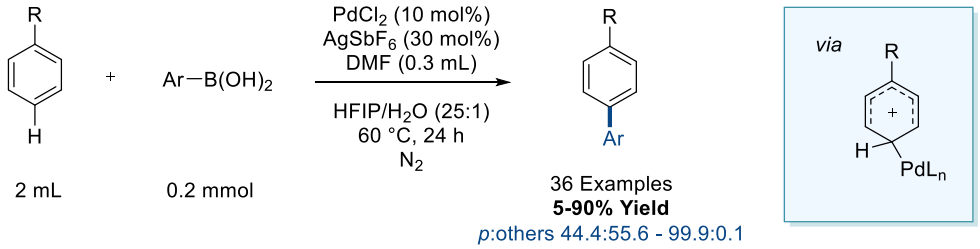

Scheme 1-45: Palladium Catalysed *para*-C–H Arylation of Arenes

Deng and co-workers reported the *para*-C–H acylation of aniline derivatives utilising copper redox catalysis (Scheme 1-46a).[102] They proposed that on removing a proton (*via* a Cu^{II} species generated *in situ*) and an electron from an aniline, one can access a highly activated anilino radical which can then couple to an enol (Scheme 1-46b). Single electron oxidation (using another equivalent of Cu^{II}) and loss of a proton then enables formation of the ketone. They then suggest that oxidation of the benzylic position using the copper enables formation of the 1,2-diketone structure. The oxygen is also proposed to continuously cycle Cu^{I} species to the catalytically competent Cu^{II}.

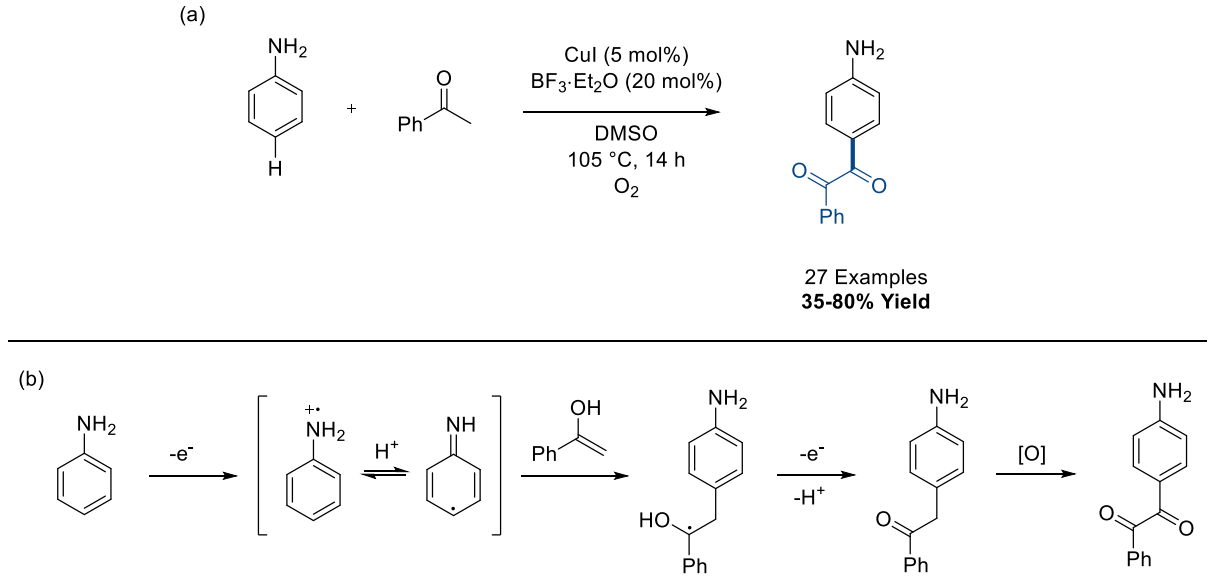

Scheme 1-46: Copper Catalysed *para*-C–H Acylation of Anilines

The aminoquinoline directing group (also known as ‘Q’ or ‘AQ’) has become a widely used directing group in C–H functionalisation methodology.[103] It can form an incredibly stable tridentate cyclometalate it can form with a metal centre, which has led to its use in more challenging base metal and sp^3 C–H functionalisation (Figure 1-2).

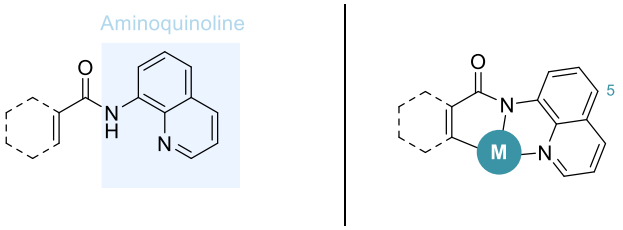

Figure 1-2: The 8-Aminoquinoline Directing Group in C–H Functionalisation

The cyclometalate above is most often formed and therefore enables C–H functionalisation of C(sp^2)/C(sp^3)-H bonds on a structure. However, if C–H activation does not take place (or even in small amounts in an equilibrium) competing functionalisation can take place on the aminoquinoline directing group itself. This has almost exclusively been shown to take place at the 5-position (Figure 1-2), which is the *para* position the amine.

The first attempt to render this a catalytic process in its own right, was achieved in 2015 by Wei, where the copper catalysed C5-sulfonation of aminoquinoline derivatives was reported (Scheme 1-47).[104] The same transformation using similar systems was then published later that year by Yang, Wu, and Wu,[105] and in 2016 by Lin and Zheng,[106] Xia and Zhang,[107] Manolikakes,[108] and (under metal-free conditions) Zhang and Lee.[109]

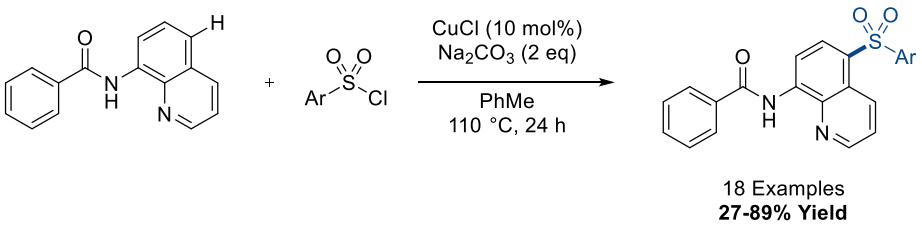

Scheme 1-47: Copper Catalysed C5-Sulfonation of 8-Aminoquinoline Derivatives

This concept was adapted *via* Manolikakes and co-workers in 2017, where the quinoline section (green, Scheme 1-48) of the structure was swapped with the aryl section (blue).[110] This then enabled a benzoylquinoline auxiliary to be furnished to an aniline structure, which could then enable *para*-C–H sulfonation in the same manner to above. Some selectivity issues were observed with arenes containing electron donating substituents.

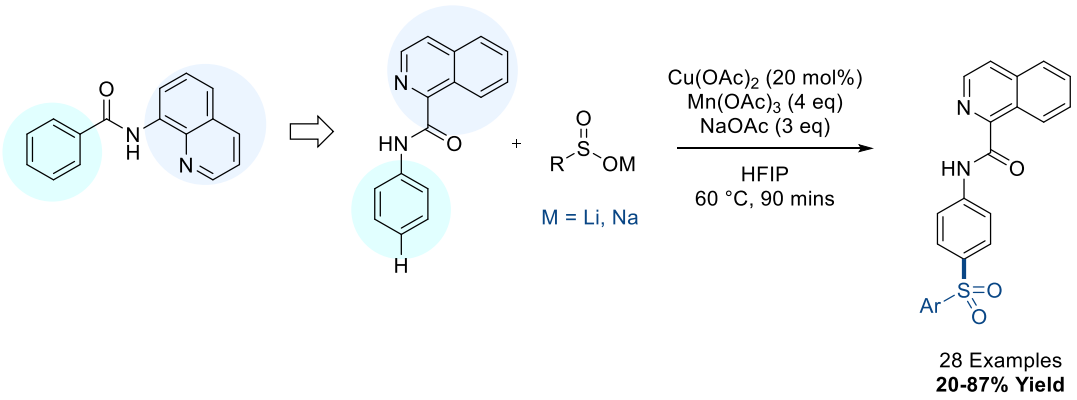

Scheme 1-48: Copper Catalysed *para*-C–H Sulfonation of Aniline Derivatives

This concept was also taken on by Weng and Lu, who instead of swapping the whole structure around, moved the basic nitrogen to the arene, creating a pyridine and a naphthalene (Scheme 1-49).[111] They then applied this structure to a copper catalysed *para*-C–H sulfonation reaction as a model, however in the report, they also show unoptimised conditions for the *para*-acetoxylation, halogenation, tifluoromethylation and amidation of the aminonaphthalene derivatives. More detail on the mechanism of this transformation will be given in Chapter 4.

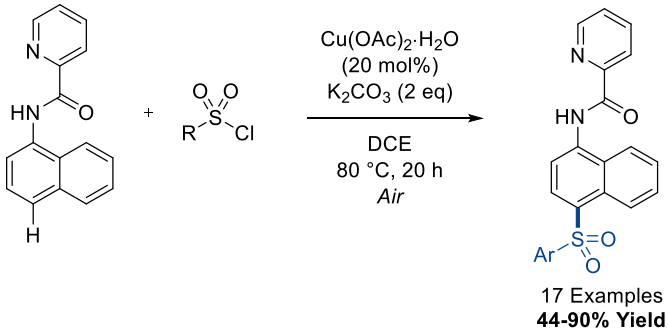

Scheme 1-49: Copper Catalysed *para*-C–H Sulfonation of Aminonaphthalene Derivatives

1.4: Aims and Objectives

At the outset of the following research, the major aims were to develop techniques which can enable the control of site selectivity in C–H functionalisation, with a large focus on the manipulation of ruthenium catalysis to enable this chemistry. To this end, this thesis will be split into three distinct chapters which will focus on the regioselectivity of the C–H functionalisation methodologies developed: *ortho*, *meta*, and *para*.

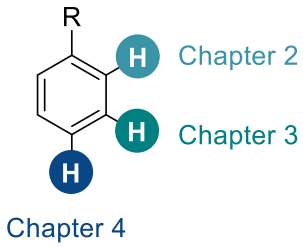

We planned to expand the ongoing project in our group on the synthesis and modification of biologically relevant heterocycles. This was to be done on using these heterocycles as weakly coordinating directing groups in C–H functionalisation.

We also planned to investigate and develop further our previous efforts into ruthenium catalysed σ-activation methodology. This was to be done with a primary focus to expand the structural template scope away from privileged motifs such as phenylpyridine, into more synthetically viable and biologically interesting structures.

1.5: References

(1) L. Ping, D. S. Chung, J. Bouffard, and S.-G. Lee, *Chem. Soc. Rev.*, 2017, **46**, 4299.

(2) W. R. Gutekunst and P. Baran, *Chem. Soc. Rev.*, 2011, **40**, 1976.

(3) T. Brucki, R. D. Baxter, Y. Ishihara, and P. Baran, *Acc. Chem. Res.*, 2012, **45**, 826.

(4) D. L. Davies, S. M. A. Donald, and S. A. Macgregor, *J. Am. Chem. Soc.*, 2005, **127**, 13754.

(5) (a) M. Lafrance and K. Fagnou, *J. Am. Chem. Soc.*, 2006, **128**, 16496. (b) S. I. Gorelsky, D. Lapointe, and K. Fagnou, *J. Am. Chem. Soc.*, 2008, **130**, 10848.

(6) I. Özdemir, S. Demir, B Çetinkaya, C. Gourlaouen, F. Maseras, C. Bruneau, and P. H. Dixneuf, *J. Am. Chem. Soc.*, 2008, **130**, 1156.

(7) L. Ackermann, R. Vicente, A. Althammer, *Org. Lett.*, 2008, **10**, 2299.

(8) X. Chen, K. M. Engle, D.-H. Wang, J.-Q. Yu, *Angew. Chem. Int. Ed.*, 2009, **48**, 5094.

(9) (a) Z. Chen, B. Wang, J. Zhang, W. Yu, Z. Liu, and Y. Zhang, *Org. Chem. Front.*, 2015, **2**, 1107. (b) T. W. Lyons and M. S. Sanford, *Chem. Rev.*, 2010, **110**, 1147

(10) S. R. Neufeldt and M. S. Sanford, *Acc. Chem. Res.*, 2012, **45**, 936.

(11) K. Godula and D. Sames, *Science*, 2006, **312**, 67.

(12) L. Ackermann, *Chem. Rev.*, 2011, **111**, 1315.

(13) M. Moselage, J. Li, and L. Ackermann, *ACS Catal.*, 2016, **6**, 498.

(14) W. Liu and L. Ackermann, *ACS Catal.*, 2016, **6**, 3743.

(15) G. Cera and L. Ackermann, *Top Curr. Chem.,* 2016, **374**, 57.

(16) K. M. Engle, T.-S. Mei, M. Wasa, and J.-Q. Yu, *Acc. Chem. Res.*, 2012, **45**, 788.

(17) S. De Sarkar, W. Liu, S. I. Kozhushkov, and L. Ackermann, *Adv. Synth. Catal.*, 2014, **356**, 1461.

(18) J. Yang, *Org. Biomol. Chem.*, 2015, **13**, 1930

(19) J.-Y. Cho, M. K. Tse, D. Holmes, R. E. Maleczka, and M. R. Smith, *Science*, 2002, **295**, 305.

(20) D. W. Robbins and J. F. Hartwig, *Angew. Chem. Int. Ed.*, 2013, **52**, 933.

(21) Y.-H. Zhang, B.-F. Shi, and J.-Q. Yu, *J. Am. Chem. Soc.*, 2009, **131**, 5072.

(22) X. Cong, H. Tang, C. Wu, and X. Zeng, *Organometallics,* 2013, **32**, 6565.

(23) M. H. Emmert, A. K. Cook, Y. J. Xie, and M. S. Sanford, *Angew. Chem. Int. Ed.*, 2011, **50**, 9409.

(24) G. B. Boursalian, M.-Y. Ngai, K. N. Hojczyk, and T. Ritter, *J. Am. Chem. Soc.*, 2013, **135**, 13278.

(25) A. Dey, S. Agasti, and D. Maiti, *Org. Biomol. Chem.*, 2016, **14**, 5440.

(26) D. Leow, G. Li, T.-S. Mei, and J.-Q. Yu, *Nature,* 2012, **486**, 518.

(27) Y.-F. Yang, G.-J. Cheng, P. Liu, D. Leow, T.-Y. Sun, P. Chen, X. Zhang, J.-Q. Yu, Y.-D. Wu, and K. N. Houk, *J. Am. Chem. Soc.*, 2014, **136**, 344.

(28) G.-J. Cheng, Y.-F. Yang, P. Liu, P. Chen, T.-Y. Sun, G. Li, Z. Zhang, K. N. Houk, J.-Q. Yu, and Y.-D. Wu, *J. Am. Chem. Soc.*, 2014, **136**, 894.

(29) L. Wan, N. Dastbaravardeh, G. Li, and J.-Q. Yu, *J. Am. Chem. Soc.*, 2013, **135**, 18056.

(30) H.-X. Dai, G. Li, X.-G. Zhang, A. F. Stepan, and J.-Q. Yu, *J. Am. Chem. Soc.*, 2013, **135**, 7567.

(31) S. Lee, H. Lee, and K. L. Tan, *J. Am. Chem. Soc.*, 2013, **135**, 18778.

(32) R.-Y. Tang, G. Li, and J.-Q. Yu, *Nature*, 2014, **507**, 215.

(33) G. Yang, P. Lindovska, D. Zhu, J. Kim, P. Wang, R.-Y. Tang, M. Movassaghi, and J.-Q. Yu, *J. Am. Chem. Soc.*, 2014, **136**, 10807.

(34) M. Bera, A. Modak, T. Patra, A. Maji, and D. Maiti, *Org. Lett.*, 2014, **16**, 5760.

(35) S. Li, H. Ji, L. Cai, and G. Li, *Chem. Sci.*, 2015, **6**, 5595.

(36) Y. Deng and J.-Q. Yu, *Angew. Chem. Int. Ed.*, 2015, **54**, 888.

(37) M. Bera, A. Maji, S. K. Sahoo, and D. Maiti, *Angew. Chem. Int. Ed.*, 2015, **54**, 8515.

(38) L. Chu, M. Shang, K. Tanaka, Q. Chen, N. Pissarnitski, E. Streckfuss, and J.-Q. Yu, *ACS Cent. Sci.*, 2015, **1**, 394.

(39) S. Li, L. Cai, H. Ji, L. Yang, and G. Li, *Nat. Commun.*, 2016, **7**, 10443.

(40) A. Maji, B. Bhaskararao, S. Singha, R. B. Sunoj, and D. Maiti, *Chem. Sci.*, 2016, **7**, 3147.

(41) A. Modak, A. Mondal, R. Watile, S. Mukherjee, and D. Maiti, *Chem. Commun.*, 2016, **52**, 13916.

(42) S. Maity, E. Hoque, U. Dhawa, and D. Maiti, *Chem. Commun.*, 2016, **52**, 14003.

(43) M. Bera, S. K. Sahoo, and D. Maiti, *ACS Catal.*, 2016, **6**, 3575.

(44) S. Bag, R. Jayarajan, R. Mondal, and D. Maiti, *Angew. Chem. Int. Ed.*, 2017, **56**, 3182.

(45) U. Dutta, A. Modak, B. Bhaskararao, M. Bera, S. Bag, A. Mondal, D. W. Lupton, R. B. Sunoj, and D. Maiti, *ACS Catal.*, 2017, **7**, 3162.

(46) H.-J- Xu, Y. Lu, M. E. Farmer, H.-W. Wang, D. Zhao, Y.-S. Kang, W.-Y. Sun, and J.-Q. Yu, *J. Am. Chem. Soc.*, 2017, **139**, 2200.

(47) M. Bera, S. Agasti, R. Chowdhury, R. Mondal, D. Pal, and D. Maiti, *Angew. Chem. Int. Ed.*, 2017, **56**, 5272.

(48) D. A. Colby, A. S. Tsai, R. G. Bergman, and J. A. Ellman, *Acc. Chem. Res.*, 2012, **45**, 814.

(49) H. J. Davis and R. J. Phipps, *Chem. Sci.*, 2017, **8**, 864.
(50) Y. Kuninobu, H. Ida, M. Nishi, and M. Kanai, *Nat. Chem.*, 2015, **7**, 712.
(51) R. Bisht and B. Chattopadhyay, *J. Am. Chem. Soc.*, 2016, **138**, 84.
(52) H. J. Davis, M. T. Mihai, and R. J. Phipps, *J. Am. Chem. Soc.*, 2016, **138**, 12759.
(53) Z. Zhang, K. Tanaka, and J.-Q. Yu, *Nature*, 2017, **543**, 538.
(54) R. J. Phipps and M. J. Gaunt, *Science*, 2009, **323**, 1593.
(55) R. J. Phipps, N. P. Grimster, and M. J. Gaunt, *J. Am. Chem. Soc.*, 2008, **130**, 8172.
(56) H. A. Duong, R. E. Gilligan, M. L. Cooke, R. J. Phipps, and M. J. Gaunt, *Angew. Chem. Int. Ed.*, 2011, **50**, 463.
(57) J. Cornella, M. Righi, and I. Larrosa, *Angew. Chem. Int. Ed.*, 2011, **50**, 9429.
(58) J. Luo, S. Preciado, and I. Larrosa, *Chem. Commun.*, 2015, **51**, 3127.
(59) N. Y. P. Kumar, A. Bechtoldt, K. Raghuvanshi, and L. Ackermann, *Angew. Chem. Int. Ed.*, 2016, **55**, 6929.
(60) J. Luo, S. Preciado, and I. Larrosa, *J. Am. Chem. Soc.*, 2014, **136**, 4109.
(61) J. Zhang, Q. Liu, X. Liu, S. Zhang, P. Jiang, Y. Wang, S. Luo, Y. Li, and Q. Wang, *Chem. Commun.*, 2015, **51**, 1297.
(62) E. Vitaku and J. T. Njardarson, *Eur. J. Org. Chem.*, 2016, **2016**, 3679.
(63) X.-C. Wang, W. Gong, L.-Z/ Fang, R.-Y. Zhu, S. Li, K. M. Engle, and J-Q. Yu, *Nature*, 2015, **519**, 334.
(64) M. Catellani, F. Frignani, and A. Rangoni, *Angew. Chem. Int. Ed.*, 1997, **36**, 119.
(65) J. Ye and M. Lautens, *Nat. Chem.*, 2015, **7**, 863.
(66) Z. Dong, J. Wang, and G. Dong, *J. Am. Chem. Soc.*, 2015, **137**, 5887.
(67) P.-X. Shen, X.-C. Wang, P. Wang, R.-Y. Zhu, and J.-Q. Yu, *J. Am. Chem. Soc.*, 2015, **137**, 11574.
(68) P. Wang, M. E. Farmer, X. Huo, P. Jain, P.-X. Shen, M. Ishoey, J. E. Bradner, S. R. Wisniewski, M. D. Eastgate, and J.-Q. Yu, *J. Am. Chem. Soc.*, 2016, **138**, 9269.
(69) P. Wang, G.-C. Li, P. Jain, M. E. Farmer, J. He, P.-X. Shen, and J.-Q. Yu, *J. Am. Chem. Soc.*, 2016, **138**, 14092.
(70) H. Shi, P. Wang, S. Suzuki, M. E. Farmer, and J.-Q. Yu, *J. Am. Chem. Soc.*, 2016, **138**, 14876.
(71) Q. Ding, S. Ye, G. Cheng, P. Wang, M. E. Farmer, and J.-Q. Yu, *J. Am. Chem. Soc.*, 2017, **139**, 417.
(72) P. Wang, M. E. Farmer, and J.-Q. Yu, *Angew. Chem. Int. Ed.*, 2017, **56**, 5125.
(73) G.-C. Li, P. Wang, M. E. Farmer, and J.-Q. Yu, *Angew. Chem. Int. Ed.*, 2017, **56**, 6874.
(74) G. Cheng, P. Wang, and J.-Q. Yu, *Angew. Chem. Int. Ed.*, 2017, **56**, 8183.

(75) P.-X. Ling, K. Chen, and B.-F. Shi, *Chem. Commun.*, 2017, **53**, 2166.
(76) A. Dey, S. Maity, and D. Maiti, *Chem. Commun.*, 2016, **52**, 12398.
(77) S. Bag, T. Patra, A. Modak, A. Deb, S. Maity, U. Dutta, A, Dey, R. Kancherla, A. Maji, A. Hazra, M. Bera, and D. Maiti, *J. Am. Chem. Soc.*, 2015, **137**, 11888.
(78) T. Patra, S. Bag, R. Kancherla, A. Mondal, A. Dey, S. Pimparka, S. Agasti, A. Modak, and D. Maiti, *Angew. Chem. Int. Ed.*, 2016, **55**, 7751.
(79) M. E. Hoque, R. Bisht, C. Haldar, and B. Chattopadhyay, *J. Am. Chem. Soc.*, 2017, **139**, 7745.
(80) N. Kuhl, M. N. Hopkinson, J. Wencel-Delord, and F. Glorius, *Angew. Chem., Int. Ed.*, 2012, **51**, 10236.
(81) C. Zheng and S.-L. You, *RSC Adv.*, 2014, **4**, 6173.
(82) Y. Saito, Y. Segawa, and K. Itami, *J. Am. Chem. Soc.*, 2015, **137**, 5193
(83) B. E. Haines, Y. Saito, Y. Segawa, K. Itami, and D. G. Musaev, *ACS Catal.*, 2016, **6**, 7536.
(84) Y. Nakao, Y. Yamada, N. Kashihira, and T. Hiyama, *J. Am. Chem. Soc.*, 2010, **132**, 13666.
(85) S. Okumura, S. Tang, T. Saito, K. Semba, S. Sakaki, Y. Nakao, *J. Am. Chem. Soc.*, 2016, **138**, 14699
(86) S. Okumura and Y. Nakao, *Org. Lett.*, 2017, **19**, 584.
(87) L. Yang, K. Semba, and Y. Nakao, *Angew. Chem. Int. Ed.*, 2017, **56**, 4853
(88) C.-L. Ciana, R. J. Phipps, J. R. Brandt, F.-M. Meyer, and M. J. Gaunt, *Angew. Chem. Int. Ed.*, 2011, **50**, 458.
(89) X. Wang, D. Leow, and J.-Q. Yu, *J. Am. Chem. Soc.*, **2011**, *133*, 13864.
(90) J. Karthikeyan and C.-H. Cheng, *Angew. Chem., Int. Ed.*, 2011, **50**, 9880.
(91) L. T. Ball, G. C. Lloyd-Jones, C. A. Russell, *Science,* 2012, **337**, 1644.
(92) L. T. Ball, G. C. Lloyd-Jones, C. A. Russell, *J. Am. Chem. Soc*, 2014, **136**, 254.
(93) W. Liu and L. Ackermann, *Org. Lett.*, 2013, **15**, 3484.
(94) N. A. Romero, K. A. Margrey, N. E. Tay, and D. A. Nicewicz, *Science*, 2015, **349**, 1326.
(95) G. B. Boursalian, W. S. Ham, A. R. Mazzotti, and T. Ritter, *Nat. Chem.*, 2016, **8**, 810.
(96) J. Zhao and S. Li, *J. Org. Chem.*, 2017, **82**, 2984.
(97) J. Lalevée, X. Allonas, S. Genet, and J.-P. Fouassier, *J. Am. Chem. Soc.*, 2003, **125**, 9377.
(98) B. Berzina, I. Sokolovs, and E. Suna, *ACS Catal.*, 2015, **5**, 7008.
(99) I. Sokolovs, and E. Suna, *J. Org. Chem.*, 2016, **81**, 371.

(100) B. Ma, Z. Chu, B. Huang, Z. Liu, L. Liu, and J. Zhang, *Angew. Chem. Int. Ed.*, 2017, **56**, 2749.

(101) Y.-X. Luan, T. Zhang, W.-W. Yao, K. Le, L.-Y. Kong, Y.-T. Lin, and M. Ye, *J. Am. Chem. Soc.*, 2017, **139**, 1786.

(102) X. Ji, D. Li, X. Zhou, H. Huang, and G.-J. Deng, *Green. Chem.*, 2017, **19**, 619.

(103) M. Corbet and F. De Campo, *Angew. Chem. Int. Ed.*, 2013, **52**, 9896.

(104) H.-W. Liang, K. Jiang, W. Ding, Y. Yuan, L. Shuai, Y.-C. Chen, and Y. Wei, *Chem. Commun.*, 2015, **51**, 16928.

(105) H. Qiao, S. Sun, F. Yang, Y. Zhu, W. Zhu, Y. Dong, Y. Wu, X. Kong, L. Jiang, and Y. Wu, *Org. Lett.*, 2015, **17**, 6086.

(106) J. Wei, J. Jiang, X. Xiao, D. Lin, Y. Deng, K. Ke, H. Jiang, and W. Zeng, *J. Org. Chem.*, 2016, **81**, 946.

(107) C. Xia, K. Wang, Z. Wei, Z. Shen, C. Shen, G. Duan, Q. Zhu, and P. Zhang, *RSC Adv.*, 2016, **6**, 37173.

(108) S. Liang and G. Manolikakes, *Adv. Synth. Catal.*, 2016, **358**, 2371.

(109) Y. Wang, Y. Wang, Q. Zhang, and D. Li, *Org. Chem. Front.*, 2017, **4**, 514.

(110) S. Liang, M. Bolte, and G. Manolikakes, *Chem. Eur. J.*, 2017, **23**, 96

(111) J.-M. Li, Y.-H. Wang, Y. Yu, R.-B. Wu, J. Weng, and G. Lu, *ACS Catal.*, 2017, **7**, 2661

Chapter 2: *ortho* - The Use of Biologically Relevant Directing Groups in Ruthenium-Catalysed C–H Functionalisation

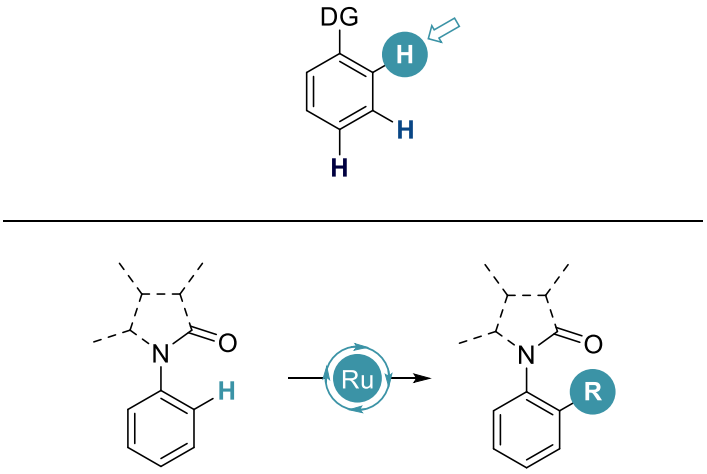

2.1: Chapter Introduction - Ruthenium-Catalysed *ortho*-C–H Alkenylation Reactions *via* Weak Assistance

The *ortho*-C–H alkenylation of an aromatic compound has been well documented with a wide number of weakly coordinating directing groups since Miura and co-workers reported the C–H alkenylation of benzothiophenes, indoles and benzofurans (Scheme 2-1).[1] This was reported to take place through chelation assisted cycloruthenation aided by the acetate additive. Following this alkene coordination, migratory insertion and β-hydride elimination afford the C–H alkenylated motif. Copper acetate is then used to re-oxidise the Ru(0) to Ru(II) to re-enter the cycle. The C–H alkenylated structures were isolated as the methyl esters to facilitate purification.

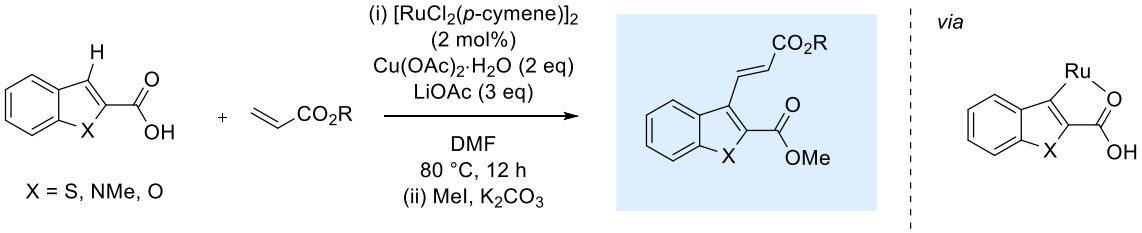

Scheme 2-1: Ruthenium-catalysed *ortho*-alkenylations of arenes

Since then, the methodology has been expanded primarily by the Jeganmohan and Ackermann groups to include benzoic acids,[2] ketones,[3] aldehydes,[4] esters,[5] anilides,[6] and carbamates.[7] (Scheme 2-2). Benzoic acids were shown to carry out an *in situ* intramolecular conjugate addition to afford the lactone product.

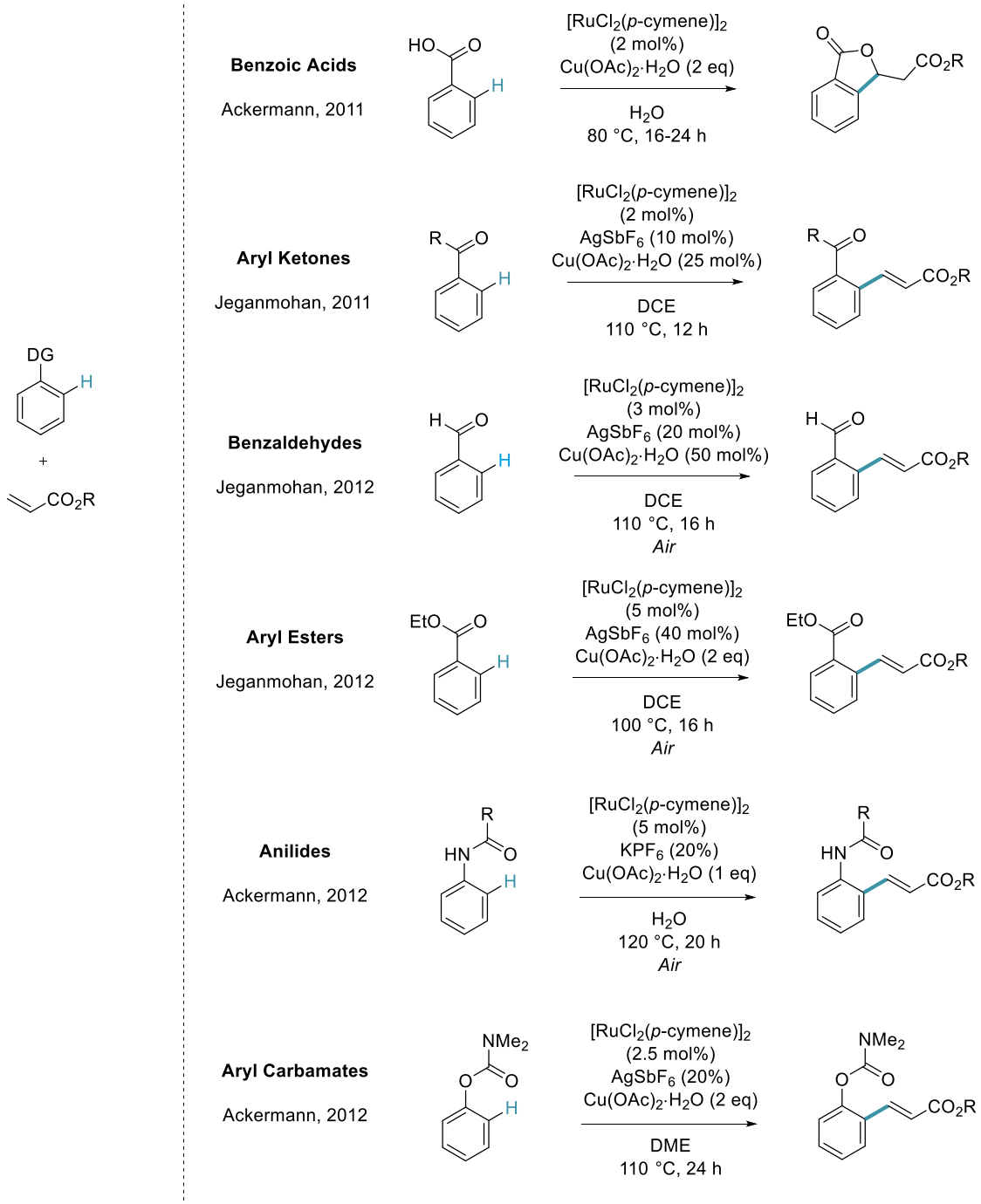

Scheme 2-2: Iterations of Ruthenium-Catalysed C–H alkenylation

The use of weakly coordinating groups in C–H functionalisation is becoming more and more well established and a multitude of techniques are now available to use oxygen directing groups in C-X and C-C bond forming reactions.[8] The ability to use these weakly coordinating directing groups is attractive as these functional groups are ubiquitous in organic molecules, unlike strongly coordinating directing groups.[9] These groups often possess potential for quick and simple further derivation as well (Figure 2-1).[10] The research described in this first chapter is based around the concept of using weakly coordinating directing groups with intrinsic biological relevance, not just a common functional group nor a tool for further derivation. This C–H alkenylation reaction was used as a model proof of concept of cycloruthenation and potential C–H functionalisation. Two families of biologically relevant structures were investigated in depth, the oxazolidinones and hydantoins.

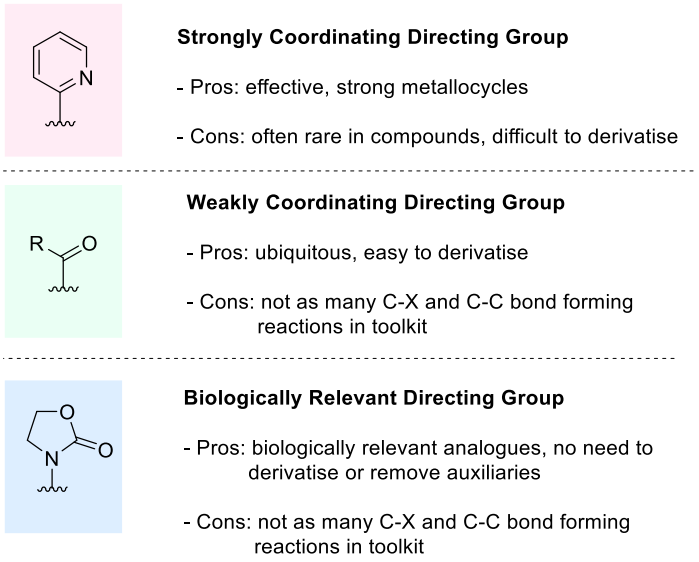

Figure 2-1: Pros and Cons of different types of directing groups

References

(1) T. Ueyama, S. Mochida, T. Fukutani, K. Hirano, T. Satoh, and M. Miura, *Org. Lett.*, 2011, **13**, 706

(2) L. Ackermann and J. Pospech, *Org. Lett.*, 2011, **13**, 4153

(3) K. Padala and M. Jeganmohan, *Org. Lett.*, 2011, **13**, 6144

(4) K. Padala and M. Jeganmohan, *Org. Lett.*, 2012, **14**, 1134

(5) K. Graczyk and W. Ma, L. Ackermann, *Org. Lett.*, 2012, **14**, 4110

(6) L. Ackermann, L. Wang, R. Wolfram, and A. V. Lygin, *Org. Lett.*, 2012, **14**, 728

(7) J. Li, C. Kornhaass, and L. Ackermann, *Chem. Commun.*, 2012, **48**, 11343
(8) S. De Sarkar, W. Liu, S. I. Kozhushkov, and L. Ackermann, *Adv. Synth. Catal.*, 2014, **356**, 1461
(9) Z. Chen, B. Wang, J. Zhang, W. Yu, Z. Li, and Y. Zhang, *Org. Chem. Front.*, 2015, **2**, 1107.

2.2: Ruthenium(II)-Catalyzed C–H Functionalization Using the Oxazolidinone Heterocycle as a Weakly Coordinating Directing Group: Experimental and Computational Insights

2.2.1: Introduction and Commentary

The oxazolidinones heterocycle is classically derived from amino alcohols (which in turn are derived from their corresponding amino acids) and a carbonyl equivalent. This has been shown to be introduced using diethyl carbonate, carbonyl diimidazole (CDI) and phosgene (Scheme). A bulk of the methods to produce *N*-aryloxazolidinones involve the arylation of the oxazolidinone heterocycle *via* transition metal-catalysed cross coupling (Scheme 2-3).

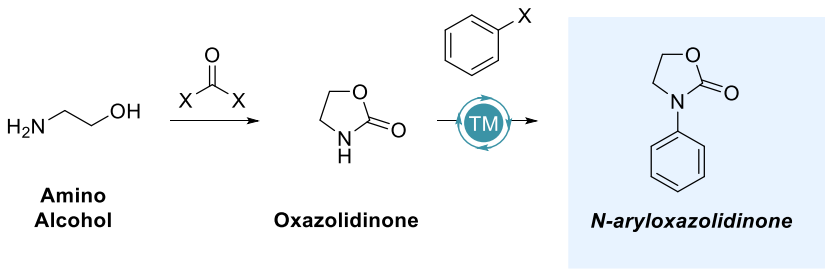

Scheme 2-3: Streamlined synthesis of *N*-aryloxazolidinones

A multitude of methods have been developed for this cross coupling, primarily using copper and palladium chemistry, a select few are displayed below (Scheme 2-4).[1] There is also literature precedent to access the *N*-aryloxazolidinone structure from the commercially available *N*-phenylethanolamine using phosgene,[2] through a carboxylation and *in situ* Mitsunobu reaction (Scheme 2-5)[3], or through organocatalysis using diethylcarbonate.[4]

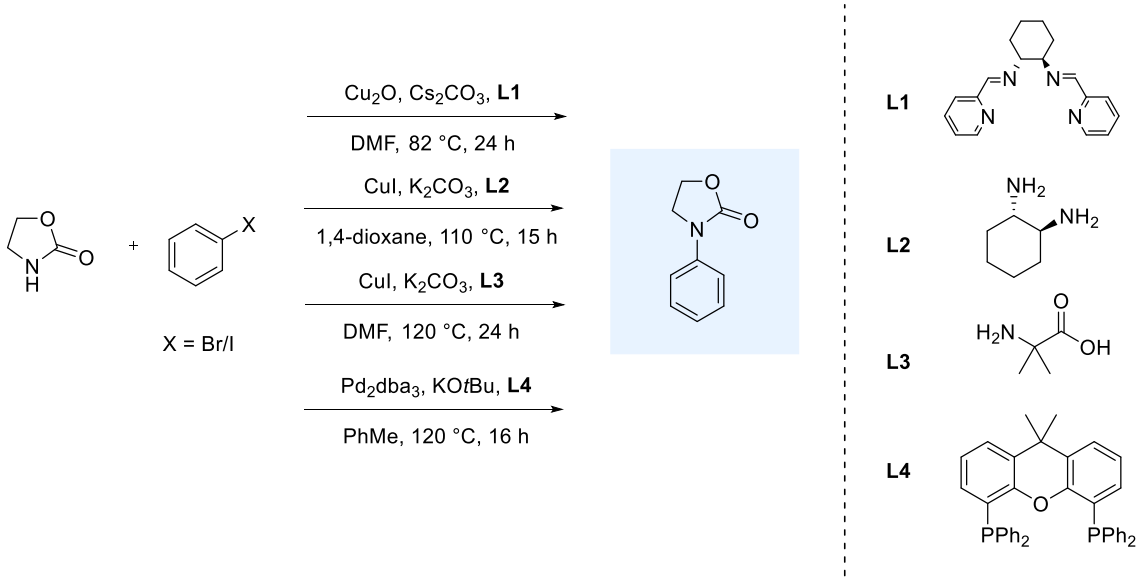

Scheme 2-4: Synthesis of *N*-aryloxazolidinones

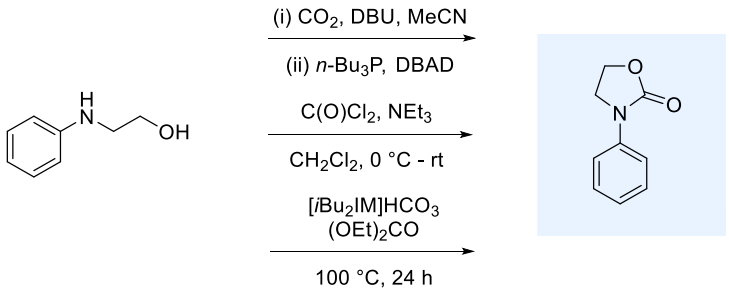

Scheme 2-5: Synthesis of *N*-aryloxazolidinones

The Frost group has been interested in the oxazolidinone heterocycle for a number of years. Due to this, expedient in–house methods for their synthesis have been developed, with emphasis on the ability create diverse oxazolidinones quickly and efficiently (Scheme 2-6).[5] A one-pot cyclisation-arylation methodology was reported in 2014, where the synthesis of decorated oxazolidinones was developed from readily available starting materials. This method has also been employed as the key step in the synthesis of three API structures: linezolid, tedizolid, and rivaroxaban.[6]

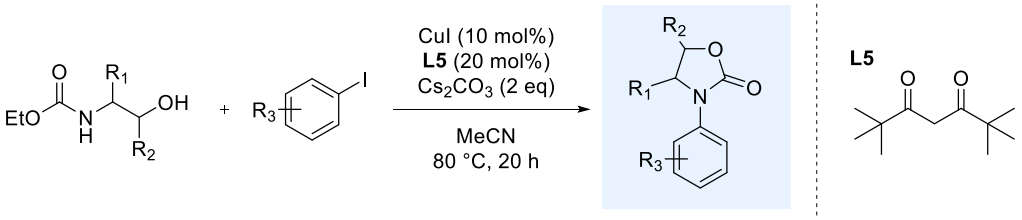

Scheme 2-6: Copper-catalysed one-pot cyclisation-arylation synthesis of *N*-aryloxazolidinones

The modification of *N*-aryloxazolidinones could provide a novel route into new biologically active molecules. The post-synthetic modification of biologically interesting compounds can be a vital tool to access untapped chemical space. This could lead to improved activity against wild or resistant strains, or hold a completely different biological activity. The Frost group has used this concept and developed a method to synthesise 2-thiazolidinones from oxazolidinones (Scheme 2-7).[7] The use of Lawesson's reagent creates the oxazolidinthione which then undergoes a pseudo-reversible Barton-McCombie type rearrangement to incorporate sulphur into the ring. This reaction was deduced to function *via* a radical mechanism through investigations into scrambling of enantiomeric purity and *in silico* calculations.

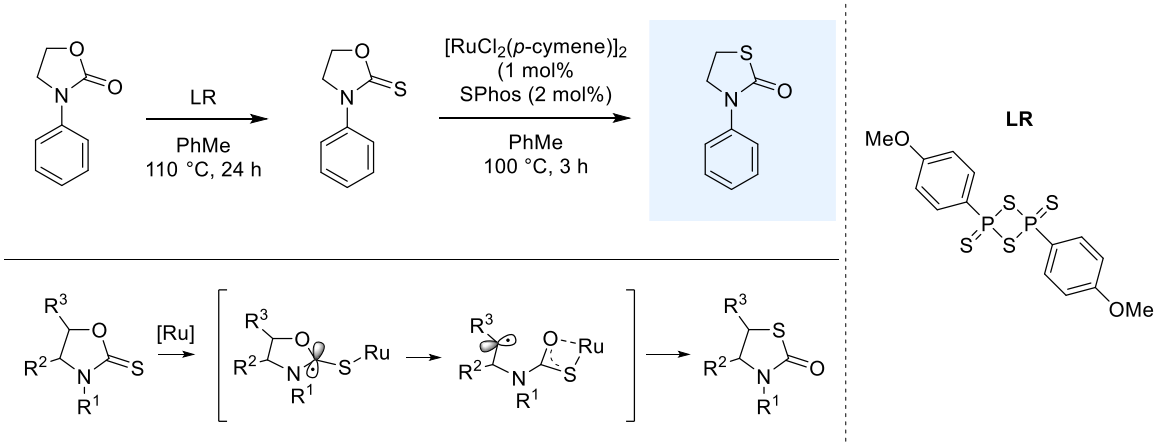

Scheme 2-7: Ruthenium-catalysed oxazolidinthione rearrangement

As mentioned previously C–H functionalisation is a powerful tool in the modification of arenes. The *N*-aryloxazolidinone motif has been subject to some investigation into its use as a C–H functionalisation template. In 2015, Suna and co-workers reported the *para*-C–H amination of electron rich arenes (Scheme 2-8).[8]

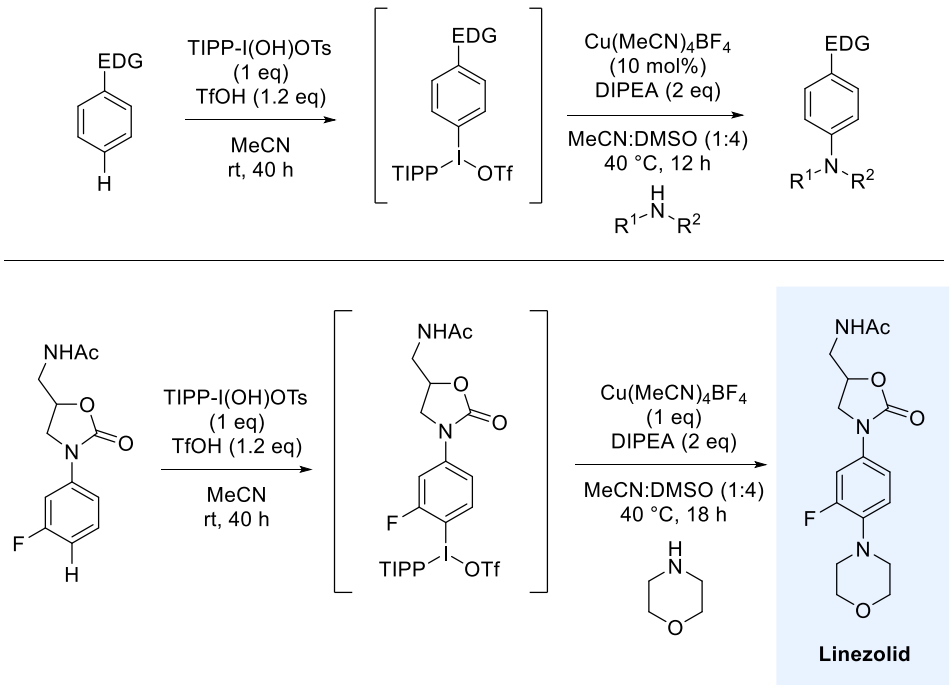

Scheme 2-8: Copper catalysed C–H amination of *N*-aryloxazolidinones

They achieved this by electronically installing the iodonium *para*- to the electron donating group and then using an *in situ* Ullman coupling to afford the *para*-C–H aminated product. They applied this methodology to the synthesis of linezolid using the oxazolidinone as the electron donating group.

As the *N*-aryloxazolidinone structure bears a Lewis basic site neighbouring an sp^2 carbon hydrogen bond, one could envisage the heterocycle could be utilised as a directing group in chelation assisted C–H functionalisation. This was first realised by Sanford utilising hypervalent iodine salts as the coupling partner (Scheme 2-9).[9] This methodology was expanded by Dong and co-workers to introduce cross dehydrogenative coupling of arenes to give the C–H arylated product.[10]

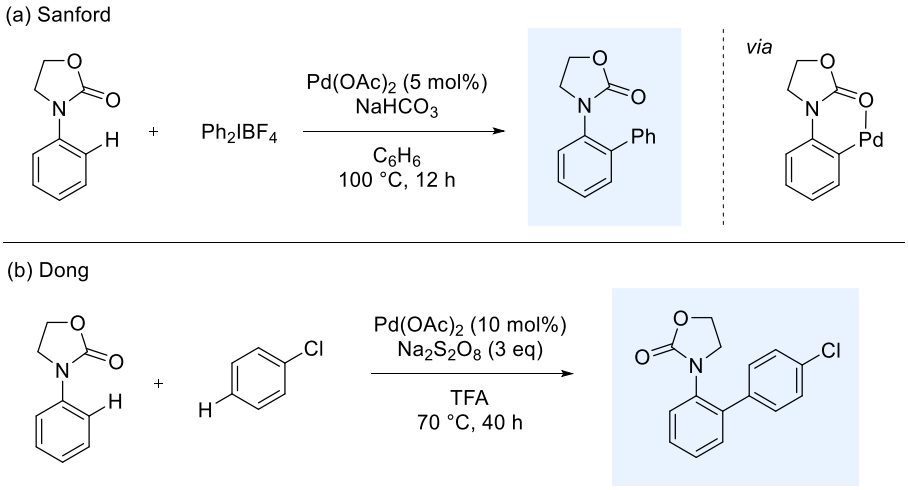

Scheme 2-9: Palladium-Catalysed *ortho*-arylation of *N*-aryloxazolidinones

The aim of the following project was to utilise ruthenium catalysis in the derivation of biologically relevant motifs using the oxazolidinone heterocycle as a weakly coordinating directing group. My results are herein reported as the article published in ACS Catalysis in 2016.

References

(1) (a) H. J. Cristau, P. P. Cellier, J. F. Spindler, and M. Taillefer, *Chem. Eur. J.*, 2004, **10**, 5607. (b) B. Mallesham, B. M. Rajesh, P. R. Reddy, D. Srinivas, and S. Trehan, *Org. Lett.*, 2003, **5**, 963. (c) J. Li, Y. Zhang, Y. Jiang, and D. Ma, *Tet. Lett.*, 2012, **53**, 3981. (d) S. Cacchi, G. Fabrizi, A. Goggiamani, and G. Zappia, *Org. Lett.*, 2001, **3**, 2539.

(2) J. A. Leitch, P. B. Wilson, C. L. McMullin, M. F. Mahon, Y. Bhonoah, I. H. Williams, and C. G. Frost, *ACS Catal.*, 2016, **6**, 5520.

(3) C. J. Dinsmore, and S. P. Mercer, *Org. Lett.*, 2004, **6**, 2885

(4) A. H. Fournier, G. de Robillard, C. H. Devilliers, L. Plasseraud, and J. Andrieu, *Eur. J. Org. Chem.*, 2016, **2016**, 3514

(5) W. Mahy, P. K. Plucinski, and C. G. Frost, *Org. Lett.*, 2014, **16**, 5020.

(6) W. Mahy, J. A. Leitch, and C. G. Frost, *Eur. J. Org. Chem.*, 2016, **2016**, 1305.

(7) W. Mahy, P. Plucinski, J. Jover, and C. G. Frost. *Angew. Chem. Int. Ed.*, 2015, **54**, 10944.

(8) B. Berzina, I. Sokolovs, and E. Suna, *ACS Catal.*, 2015, **5**, 7008.

(9) D. Kalyani, N. R. Deprez, L. V. Desai, and M. S. Sanford, *J. Am. Chem. Soc.*, 2005, **127**, 7330.

(10) C. S. Yeung and V. M. Dong, *Synlett*, 2011, **7**, 974.

2.2.2: Authorships and Permissions

This declaration concerns the article entitled									
Ruthenium(II)-Catalyzed C–H Functionalization Using the Oxazolidinone Heterocycle as a Weakly Coordinating Directing Group: Experimental and Computational Insights									
Publication status (tick one)									
Draft manuscript		**Submitted**		**In review**		**Accepted**		**Published**	X
Publication details (reference)	J. A. Leitch, P. B. Wilson, C. L. McMullin, M. F. Mahon, Y. Bhonoah, I. H. Williams, and C. G. Frost, *ACS Catal.*, 2016, **6**, 5520								
Candidate's contribution to the paper (detailed, and also given as a percentage)	The candidate contributed to/ considerably contribute to/predominantly execute the: **Formulation of ideas (20%)**: JAL, PBW, CLM, IHW and CGF contributed equally **Design of methodology (50%):** JAL contributed all the design of the synthetic work along with CGF (10%). CLM, PBW and IHW contributed the computational methodology design (combined remaining 40%) **Experimental work (50%):** JAL completed all the synthetic work. CLM (20%), PBW (20%) and IHW (5%) contributed to the computational methodology. MFM contributed crystallography (5%) **Presentation of data in journal format (45%)**: JAL wrote the introduction and synthetic results and discussion, MFM contributed crystallography discussion (5%). CLM wrote up the discussion for inorganic computational (20%). PBW and IHW jointly wrote the physical organic computational section (20%). CGF made edits to the manuscript before submission (8%). YB checked over the manuscript (2%).								
Statement from Candidate	This paper reports on original research I conducted during the period of my Higher Degree by Research candidature								
Signed	Jamie A. Leitch						**Date**	14/09/17	

2.2.3: Manuscript for Ruthenium(II)-Catalyzed C–H Functionalization Using the Oxazolidinone Heterocycle as a Weakly Coordinating Directing Group: Experimental and Computational Insights"

Complete manuscript given at point of corrections follows on the next page. Layout changes have been made to be consistent with the thesis. Contents remain unchanged.

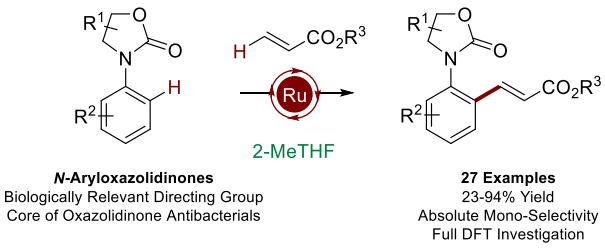

Ruthenium(II) Catalyzed C–H Functionalization Using the Oxazolidinone Heterocycle as a Weakly Coordinating Directing Group: Experimental and Computational Insights.

Jamie A. Leitch,[†] Philippe B. Wilson,[†] Claire L. McMullin,[*,†] Mary F. Mahon,[†] Yunas Bhonoah,[‡] Ian H. Williams[*,†] and Christopher G. Frost.[*,†]

[†]Department of Chemistry, University of Bath, Claverton Down, Bath, Somerset, BA2 7AY, United Kingdom

[‡]Syngenta, Jealott's Hill International Research Centre, Bracknell, Berkshire, RG42 6EY, United Kingdom

ABSTRACT: Herein reports the ruthenium-catalyzed *ortho*-C–H alkenylation of a wide range of *N*-aryloxazolidinone scaffolds. Alkenylation was achieved with complete mono-selectivity with a scope of 27 examples in 2-MeTHF. Yields ranged from 23-94% creating highly decorated oxazolidinone scaffolds. A kinetically relevant C–H cleavage was also observed with a KIE ~ 2. DFT calculations elucidated information on mechanism, detailing the β-hydride elimination as the most energetically challenging step of +13.5 kcalmol^{-1}. In-depth computational kinetic studies also predicted a KIE of 2.17 for C–H cleavage and an intrinsic KIE for the reaction of 2.22, in line with the experimentally observed value.

INTRODUCTION

The oxazolidinone heterocycle is prevalent in pharmaceutically active compounds with widespread bioactivity for example Linezolid[1], Tedizolid[2] (antibacterial, Figure 1), Rivaroxaban[3] (anti-coagulant) and Toloxatone[4] (antidepressant). For these reasons the synthesis of these heterocycles and their modification has received great attention in recent years.[5] These biologically active structures contain the oxazolidinone heterocycle neighboring an aromatic ring. This makes these structures prime for investigation as directing groups in C–H functionalization catalysis.

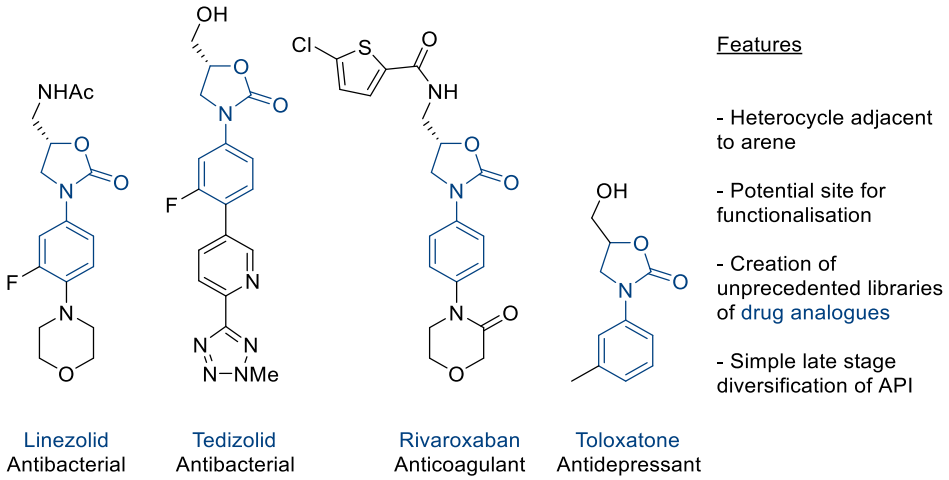

Figure 1: Pharmacologically active compounds containing the oxazolidinone heterocycle.

Transition metal catalyzed C–H functionalization has become a vital synthetic tool to facilitate the formation of useful C-C and C-X bonds.[6] This methodology transforms latent C–H bonds into potentially reactive functional groups. Harnessing this concept to allow derivatization of biologically active compounds such as the oxazolidinones is a very attractive strategy to enable the synthesis of drug analogues through expedient late-stage modification.[7]

Ruthenium catalyzed C–H bond functionalization has seen widespread application into the modern synthetic world due to pioneering developments from Oi and Inoue, Ackermann, and Bruneau and Dixneuf[8]. Methodology has evolved rapidly to utilize weakly coordinating carbonyl directing groups to install diverse functionality.[9] This functionality is often ubiquitous in chemical structures; however, if necessary, an auxiliary approach can be used which involves separate installation and removal steps.[9k] The presented study is focused on the utility of directing groups with intrinsic biological activity and how they facilitate C–H insertion via chelation assistance (Scheme 1). Despite early work reporting palladium catalyzed *ortho*-arylation of the 3-aryl-2-oxazolidinone structure, the motif has not been widely used as a directing group and there have been no such examples employing ruthenium catalysis.[10]

Scheme 1: Ruthenium Catalyzed Alkenylation of Arenes

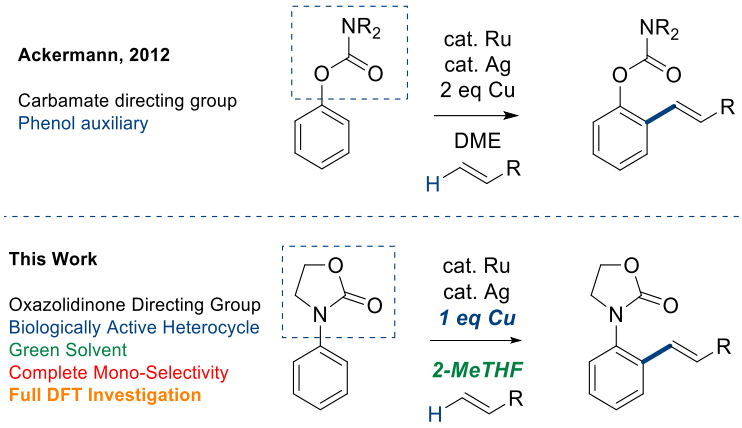

RESULTS & DISCUSSION

Optimization

The envisioned reaction methodology was probed using 3-phenyl-2-oxazolidinone (**1a**) and ethyl acrylate (**2a**). The electron deficient nature of acrylates has shown them to be excellent coupling partners in ruthenium, palladium and rhodium catalyzed C–H functionalization reactions.[9a,11] A summary of the optimization is displayed in Table 1.

Starting conditions were obtained from literature precedent for the use of ruthenium, silver and copper in cooperative catalysis for similar transformations (full optimization information is available in the supporting information).[9f,h,i,k] Alkenylation was observed in DCE in low conversions (entry 1). Much more substantial formation of product was observed with higher boiling polar aprotic etheric solvents (1,4-dioxane, DME and 2-MeTHF, entries 2-4). A 2-MeTHF/AcOH mixture was interestingly shown to completely nullify reactivity (entry 5) as AcOH is a proposed by-product in the reaction. 2-MeTHF was carried forward as solvent as choice as is a more sustainably sourced alternative to DME.[12] Multiple silver(I) oxidants were investigated with none showing superior activity to $Cu(OAc)_2$ (entries 6-9). However, the monO–Hydrate complex was not only tolerated but shown to accelerate catalysis (entry 10). Only oxidants containing carboxylate counter ions promoted the reaction. This is in line with literature precedent for a concerted metalation-deprotonation (CMD) or ambiphilic metal-ligand activation (AMLA) mechanism of C–H metalation.[6a,b]

Table 1: Optimization of Oxazolidinone Directed C–H Alkenylation[a]

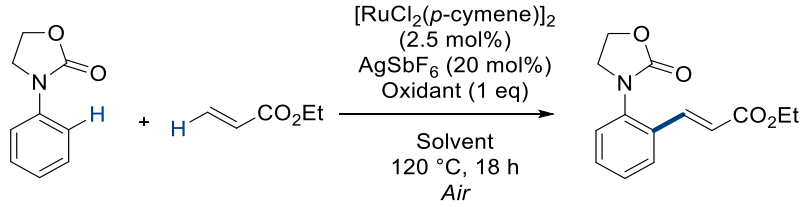

1a **2a** **3a**

Entry	Solvent	Oxidant	3a[b]
1	DCE	$Cu(OAc)_2$	15
2	1,4-dioxane	$Cu(OAc)_2$	56
3	DME	$Cu(OAc)_2$	72 (68)[c]
4	2-MeTHF	$Cu(OAc)_2$	70 (67)[c]
5	2-MeTHF/AcOH 3:1	$Cu(OAc)_2$	-
6	2-MeTHF	Ag_2CO_3	13
7	2-MeTHF	AgOAc	48
8	2-MeTHF	AgOAc[d]	64
9	2-MeTHF	AgO_2CCF_3	Trace
10	2-MeTHF	$Cu(OAc)_2{\cdot}H_2O$	77
11[e]	2-MeTHF	$Cu(OAc)_2{\cdot}H_2O$	-
12[f]	2-MeTHF	$Cu(OAc)_2{\cdot}H_2O$	-
13[g]	2-MeTHF	$Cu(OAc)_2{\cdot}H_2O$	68
14[h]	2-MeTHF	$Cu(OAc)_2{\cdot}H_2O$	78
15[h,i]	**2-MeTHF**	**$Cu(OAc)_2{\cdot}H_2O$**	**80 (76)[c]**

[a]General Reaction Conditions: **1a** – 1 mmol, **2a** – 3 mmol, $[RuCl_2(p\text{-cymene})]$ (2.5 mol%), $AgSbF_6$ (20 mol%), Solvent (4 mL). [b] ^1H NMR conversion. [c]Isolated Yields after purification. [d]AgOAc (2 eq). [e]Without $[RuCl_2(p\text{-cymene})]_2$. [f]Without $AgSbF_6$. [g]Reaction performed at 100 ° C [h]$AgSbF_6$ (10 mol%). [i]Solvent (1 mL)

It must be noted that reaction efficacy was not maintained in the absence of either ruthenium catalyst or silver co-catalyst (entries 11-12), however it was possible to decrease silver co-catalyst loading without detriment to the reaction (entry 14). Finally, the reaction was shown to proceed with equal if not superior reactivity at higher concentration and proceeding with excellent catalytic efficiency under air (entry 15). Here oxygen in the atmosphere aids oxidant recycling.[8a] Also noteworthy was that throughout this optimization there was no observation of *o-,o*-di-alkenylated product either by NMR or TLC. This high level of selectivity is an attractive feature.[6b, 8a]

Reaction Scope

With optimized conditions in hand, 3-phenyl-2-oxazolidinone (**1a**) was reacted with a variety of electron deficient and electron rich alkenes to explore the scope of this catalytic transformation (Scheme 2).

Scheme 2: Acrylate Scope of Oxazolidinone Directed C–H Alkenylation

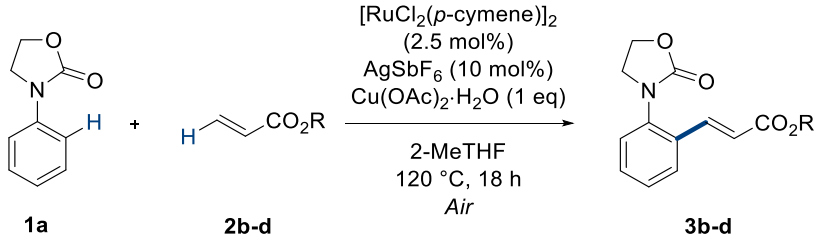

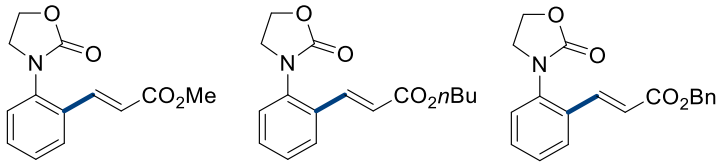

3b - 93% **3c** - 74% **3d** - 94%

Excellent catalytic activity was maintained using methyl, *n*-butyl and benzyl acrylates showing yields up to 94%. Unfortunately the reaction did not proceed with other electron deficient alkenes and electron rich alkenes due to lack of reactivity or high volatility of substrates in open atmosphere (see supporting information). Despite this, similar structures can be accessed from **3a-d** through functional group interconversions. The use of methyl acrylate enabled more facile purification *via* standard chromatographic methods (cf. benzyl) as well as superior isolated yields (cf. ethyl). Due to this, methyl acrylate was carried forward as the acrylate of choice for expansion of the scope with aryl oxazolidinones (Scheme 3).

The reaction was shown to tolerate a wide variety of functionality on the aryl ring including fluoro-, chloro-, bromo-, alkoxy-, aryl, and alkyl. Highest yields were achieved using electron rich substituents (**3ab**, **3ac**, **3ai**, **3aj**). Yields were reduced when using highly electron deficient arenes with substituents such as CF_3 or *m*-*p*-Cl (**3ag** & **3an**). These patterns in reaction efficiency are consistent with similar reported methodology.[8k] Unsymmetrical examples such as 3-methyl and 3-chloro (**3ai**-**3an**) gave major isomers based on the least sterically hindered site with excellent selectivity. An *ortho*-substituted example (**3ao**) was also tolerated however in reduced yield. Heteroaromatics could also be functionalized with excellent efficiency demonstrated with thiophene derivative (**3ap**).

Scheme 3: Arene Scope of Oxazolidinone Directed C–H Alkenylation

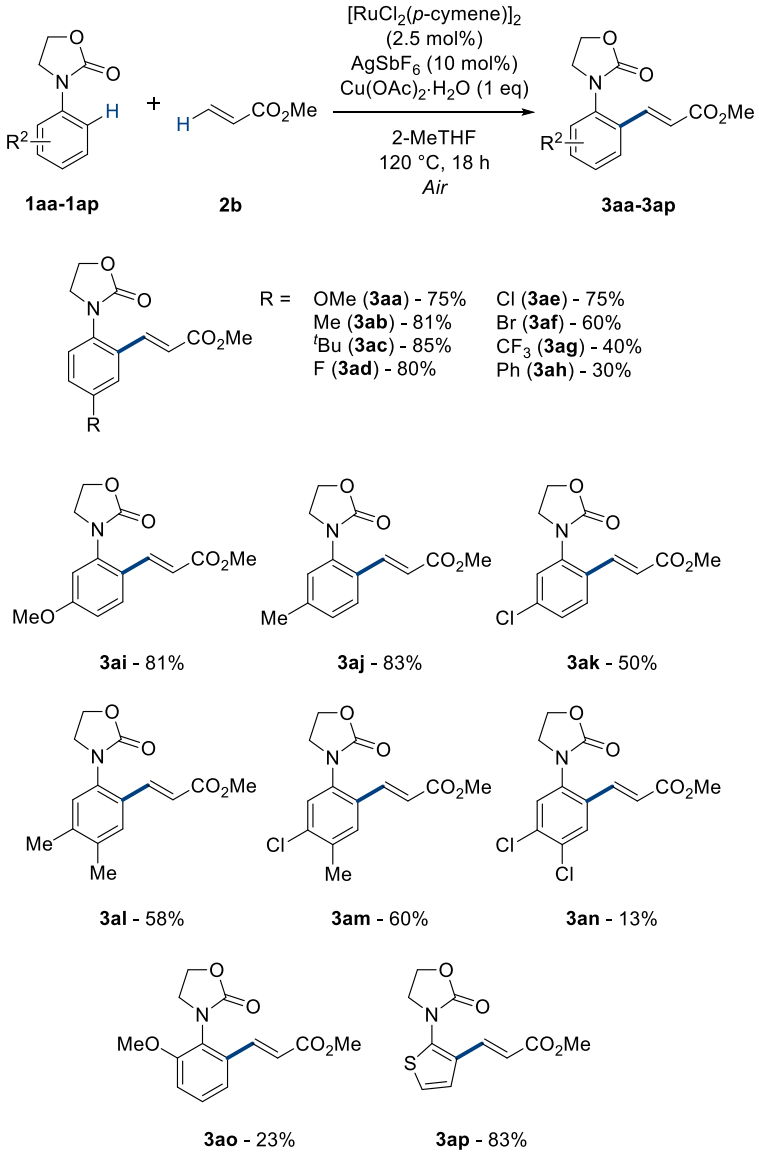

Structures bearing a fluoro substituent *meta*- to the oxazolidinone directing group (**3aq** & **3ar**) gave a mixture of regioisomers (Scheme 4), separable *via* column chromatography. Regioisomers of structure **3aq** gave an impressive combined yield of 91% and were further characterized by single crystal X-ray crystallography to confirm regiochemistry.[13] These validated that the electronics of the system dictate the selectivity in these structures. This insight in selectivity is mirrored in a previous report in a benzamide assisted C–H cyanation reaction.[14] **3ar** gave a similar distribution of C–H alkenylated products with comparable isomer ratios albeit in lower yield.

Scheme 4: Oxazolidinone Directed C–H Alkenylation of Structures Bearing *meta*-Fluoro Substituent

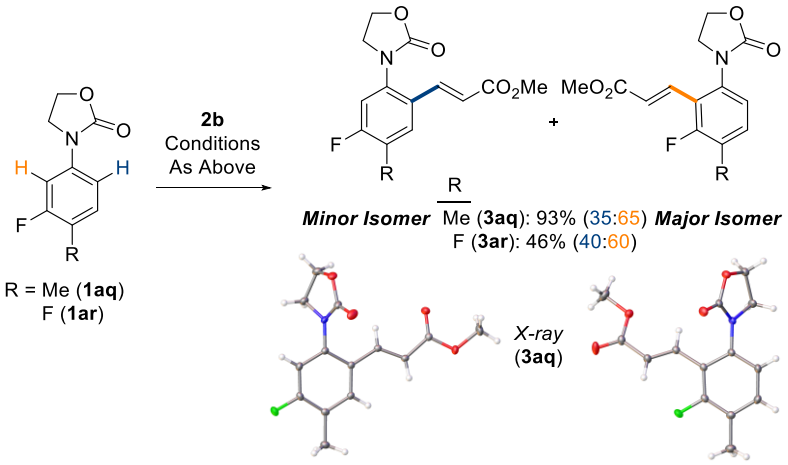

Functionalization of the heterocycle itself was then varied using structures synthesized from natural amino acids valine and leucine (Scheme 5a). These substrates performed with good efficiency for such highly functionalized motifs. Yields were reduced with larger alkyl derivatives due to potential disruption of directing group C–H alignment, highlighted with **3bd**.

Methanol derivative (**1ca**) bearing functionality in the 5-position was reacted under the catalytic conditions (Scheme 5b). The reaction conditions led to some undesired removal of the silyl protecting group. Due to this, the crude mixture was submitted to an *in situ* deprotection to afford the primary alcohol structure. One pot methodology was pleasingly shown to manifest comparable efficiency to sequential isolation and separate deprotection. This allows for more expedient synthesis and reduced waste from work-up and purification. This methodology now allowed the synthesis of highly decorated oxazolidinone structures.

Scheme 5: Heterocycle Scope of Oxazolidinone Directed C–H Alkenylation

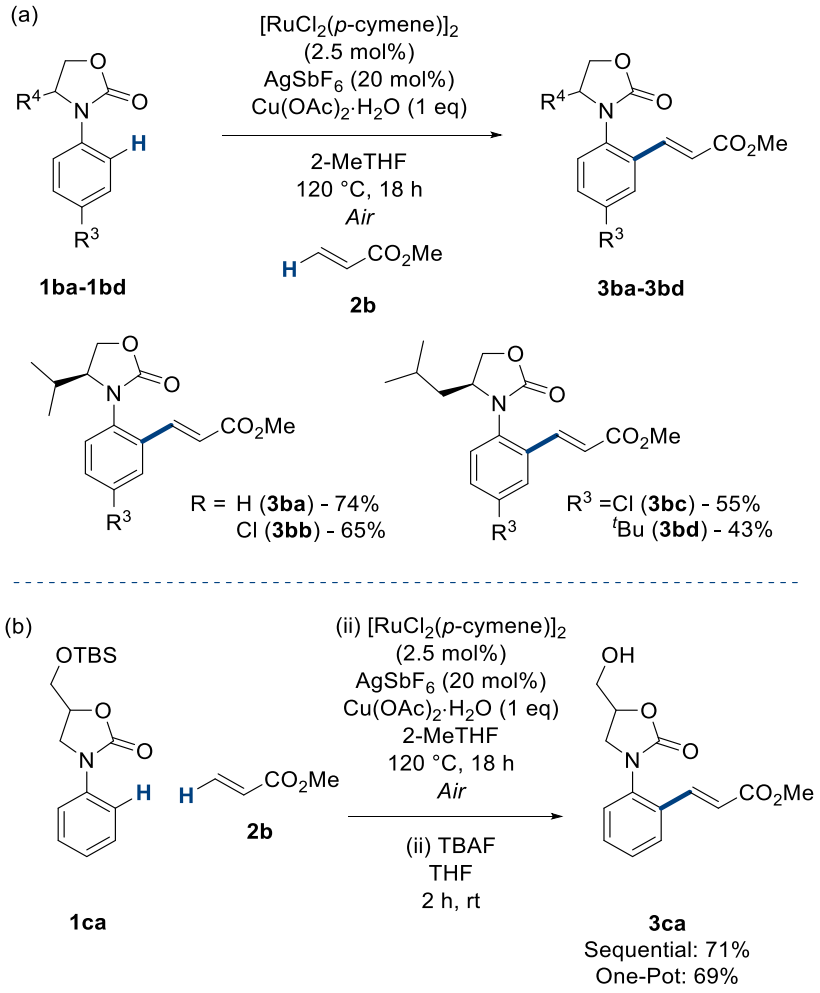

This methodology was shown to be scalable affording over 2 grams' worth of alkenylated product (Scheme 6). On a gram scale the lowering of ruthenium and silver loadings afforded a 77% yield along with a 22% yield of recovered starting material. Interestingly there was still no observed presence of a di-alkenylated structure, which was also not observed throughout the scope of the reaction. Complete mono-substitution selectivity in C–H functionalization methodology is highly sought after. To investigate this further, mono-alkenylated product **3b** was re-exposed to the optimized reaction conditions in an attempt to force formation of the di-alkenylated product $\mathbf{3b_{di}}$ (Scheme 7). Despite this, no sign of this product was observed via TLC or crude NMR where only starting material was present. This highlighted the absolute selectivity of the oxazolidinone directing group towards mono-functionalization.

Scheme 6: Gram Scale Ruthenium Catalyzed C–H Alkenylation

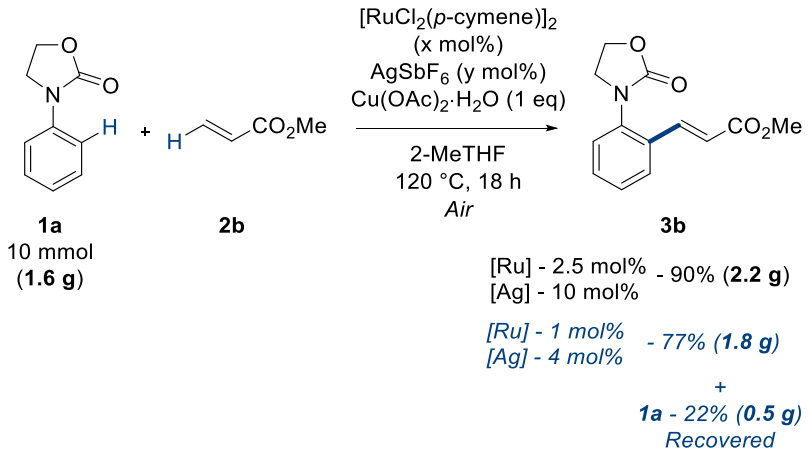

Scheme 7: Attempted Di-Alkenylation of Mono-Substituted Structure 3b

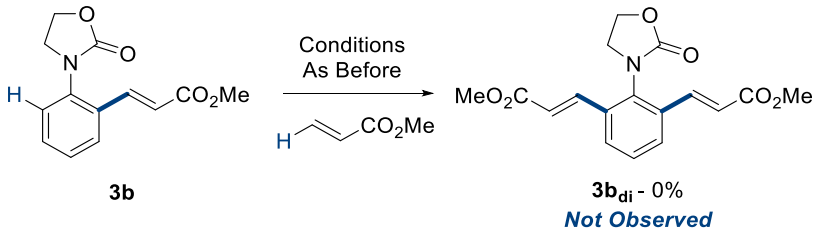

The introduction of ester and alkene functionality to the compound allows further derivation to form more complex and decorated structures. Heterogeneous hydrogenation allowed access to the *ortho*-alkylated motif in quantitative yield (**4a**, Scheme 8). Selective mild saponification allowed hydrolysis of the ester (**4b**) without interaction with the oxazolidinone heterocycle. Amidation conditions also afforded the amide in good yields (**4c**). These functional group interconversions allowed access to cinnamic acids and cinnanamide structures which are known to possess antimicrobial activity.[15]

The reaction conditions were now employed with analogous derivatives of the oxazolidinone heterocycle core to explore electronic effects on efficiency of catalysis (Scheme 9). The pyrrolidinone (**6a**), 2-thiazolidinone (**6b**) and 4-thiazolidinone (**6c**) structures gave modest-good yields in the C–H alkenylation reaction. These results manifest how subtle changes in heterocycle electronics can affect C–H functionalisation efficiency under the same reaction conditions.[10a,16]

Mechanistic Studies

There have been multiple other examples of weak directing groups directing C–H alkenylation reactions such as carboxylic acids[8c] ketones[8i], aldehydes[8f] and esters[8h]. As reported reaction conditions for these protocols are similar, it was of mechanistic interest to perform intermolecular competition experiments to create a reactivity order of directing groups. One equivalent of further weakly coordinating directing groups: ketone, acid, ester and aldehyde (**7a-d**) were reacted under the optimized conditions from this report with one equivalent of 3-phenyl-2-oxazolidinone (**1a**) to compete with one equivalent of methyl acrylate (**2b**) (Scheme 10).

Scheme 8: Further Derivation of Alkenylated 3-Phenyloxazolidinone 3b

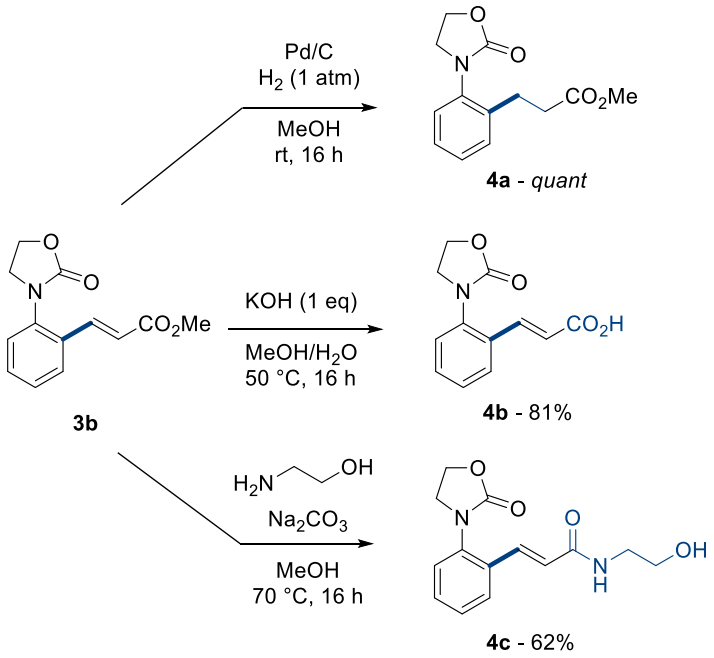

Scheme 9: Ruthenium Catalyzed Alkenylation of 5-Membered Heterocycles

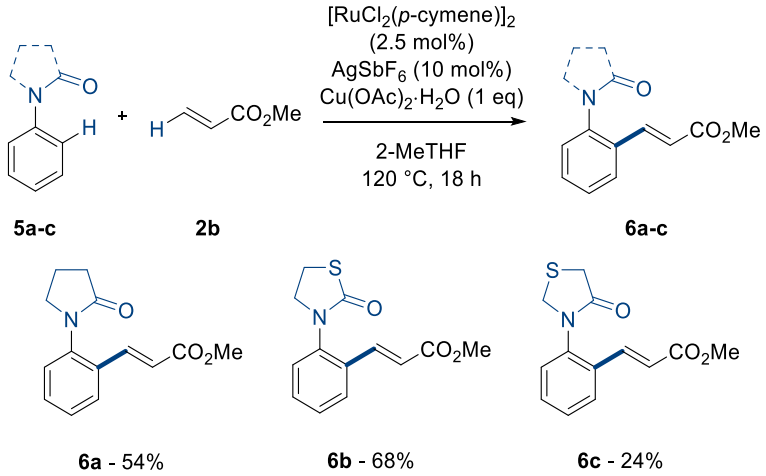

These experimental insights show that the ketone directing group (**7a**) competes preferentially over the oxazolidinone whereas acids, aldehydes and esters give rise to a larger majority of alkenylated aryloxazolidinone. This also allows understanding into potential functional group tolerance of this methodology, where aromatic acyl derivatives of the aryloxazolidinone would give rise to a large mixture of products which was observed experimentally when *para*-acetyl-*N*-aryloxazolidinone was submitted to the reaction conditions.

Silver hexafluoroantimonate ($AgSbF_6$) is a ubiquitous catalytic partner to ruthenium *para*-cymene dimer.[8c,8f] It was of interest to investigate whether it only acts as a catalyst activator or plays a further part in the reaction. Due to this, a proposed catalytically active monomeric species [Ru(*p*-cymene)$(OAc)_2$] was subjected to the reaction conditions with and without the co-catalyst (Scheme 11). Interestingly no conversion to product was observed without the additive, highlighting its further importance as a source of SbF_6 anion in the reaction.

Scheme 10: Intermolecular Competition Experiments with Weakly Coordinating Directing Groups 7a-d

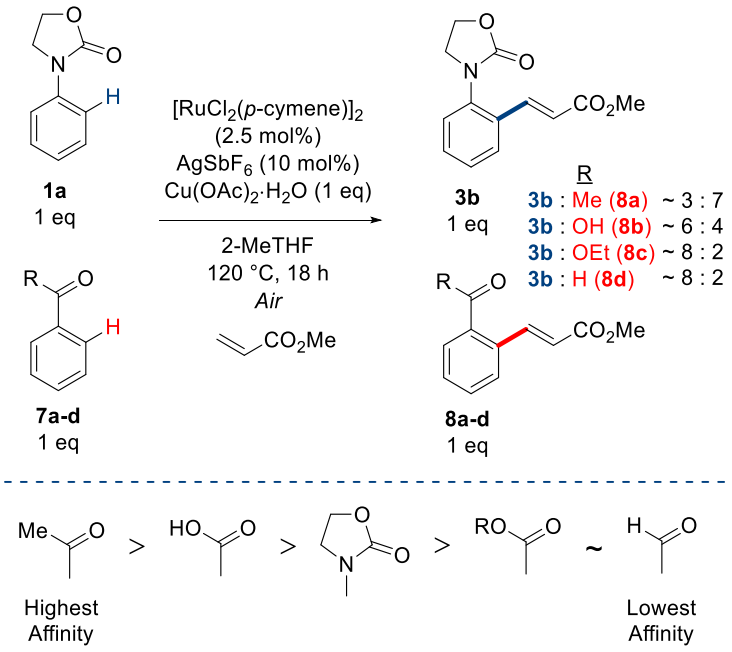

Scheme 11: Ru(II) Catalyzed C–H Alkenylation using a Defined Ruthenium Catalyst Monomer

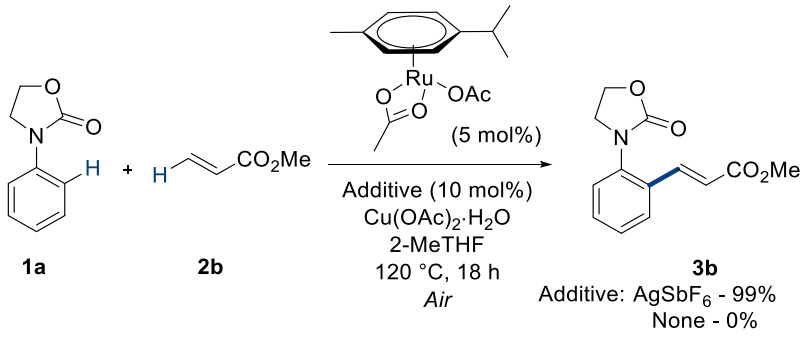

Replacement of the aromatic C–H bonds with deuterium atoms gave the isotopically labelled structure **[D]$_5$-1a**. This was submitted to the reaction conditions in order to investigate the potential hydrogen incorporation into the final product. This would be indicative of a reversible cyclometalation. The resulting reaction gave rise to an 8% hydrogen incorporation into the *ortho*-C-D bond (Scheme 12), also affording the isotopically labelled product in a reduced but still good yield of 69%.

Scheme 12: Ru(II)-Catalyzed Alkenylation of Isotopically Labelled Substrate

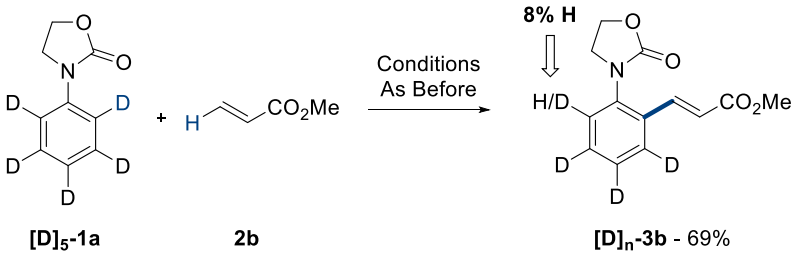

The kinetic isotope effect (KIE) of a substrate can give great insight into mechanism and give information about the rate limiting sections of the catalytic cycle (Scheme 13).

Scheme 13: Experimental Investigation of Kinetic Isotope Effect

(a) KIE by Initial Rates using Parallel Reactions

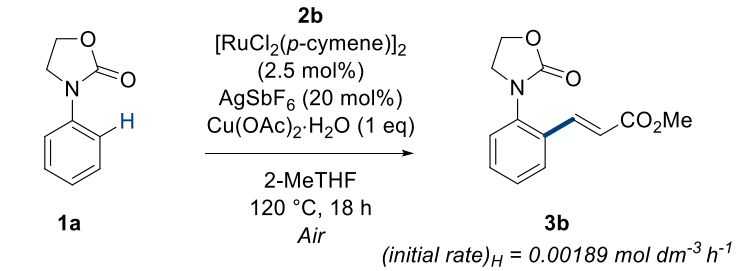

(b) KIE by Intermolecular Competition

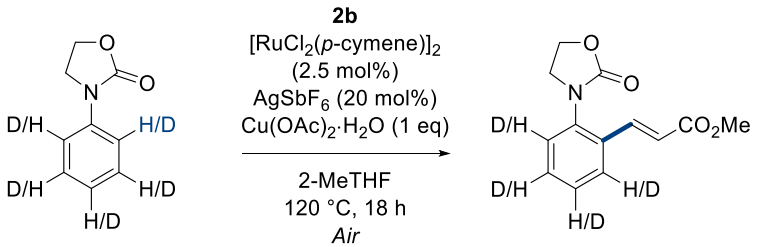

Run	H	D	KIE
1	0.73	0.27	2.7
2	0.72	0.28	2.5
Av.			**2.6**

This allows greater in-depth understanding of reaction tuning and optimization.[17] Kinetic isotope analysis was carried out experimentally using two methods: initial rates by parallel reactions (Scheme 13a) and through intermolecular competition between **1a** and **[D]$_5$-1a** (Scheme 13b). Both methods showed that the reaction had a kinetically relevant isotope effect, signifying that C–H cleavage is in or near the rate limiting step.

Computational Mechanistic Studies

Density functional theory (DFT) calculations were undertaken to establish the mechanism and energetics of the reaction for 3-phenyl-2-oxazolidinone **1a** and methyl acrylate **2b**.[18] Previous studies have shown the importance of using corrections for dispersion, solvation and extended basis sets when treating large organometallic reaction systems that involve charged species. A similar approach was adopted in this work, with geometries initially optimized in the gas phase with the BP86 functional and a medium sized basis set (SDD for Ru and 6-31G** on all other atoms). The resultant free energies were then corrected for solvation (2-Me-THF), dispersion (Grimme's D3-BJ parameter set) and an extended basis-set (cc-pVTZ for Ru and 6-311++G** for all other atoms) giving rise to composite free energy differences ΔG_{MeTHF} (1 atm, 25 °C) relative to complex **A** and separate species **1a** and **2b**.

Under the catalytic conditions, acetate from the copper complex ($Cu(OAc)_2 \cdot H_2O$) breaks up the dimer $[RuCl_2(p\text{-cymene})]_2$ to form the *in situ* catalytically active intermediate **A**, [Ru(*p*-cymene)(OAc)(**1a**)]$^+$, with the silver compound ($AgSbF_6$) removing chloride anions from the solution. The cationic complex **A** has the oxazolidinone coordinated through the carbonyl oxygen, one κ^2-acetate and an η^6 *para*-cymene ligand around the ruthenium center. Concerted metalation-deprotonation (CMD), also known as ambiphilic metal-ligand activation (AMLA), occurs as a two-step reversible process (see Figure 2). The first step, via **TS(A-B)1**, involves κ^2- κ^1 displacement of acetate, by the approaching *ortho* C–H bond of **1a**, to form an agostic intermediate **INT(A-B)**, where the pendant oxygen of the acetate is directed towards the *ortho* H (O···H = 1.686 Å), thereby elongating the C–H bond from 1.091 Å to 1.148 Å. The second step, via **TS(A-B)2**, involves endergonic C–H bond cleavage to form a six-membered cyclometalate **B** (+4.0 kcal mol^{-1}). Formation of the agostic intermediate, which involves breaking a strong Ru-O bond, determines the overall C–H activation barrier of 12.4 kcal mol^{-1}.

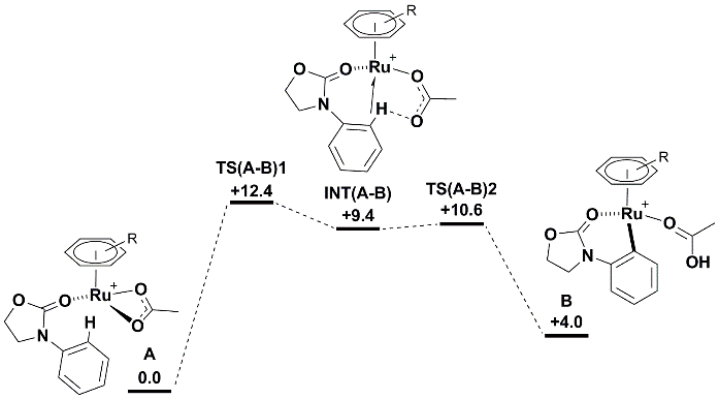

Figure 2: DFT calculated free energies (kcal mol^{-1}) relative to **A** for the C–H activation of *N*-aryloxazolidinone **1a** at [Ru(OAc)(*p*-cymene)]$^{+}$ in Me-THF.

Ligand substitution of acetic acid in **B** for methyl acrylate **2b** forms four isomers of **C**, which differ with respect to the orientation of the alkene at the ruthenium center. Despite the pre-1,2-insertion intermediates **C1**$_{1,2}$ and **C2**$_{1,2}$ being more stable than the equivalent pre-2,1-insertion intermediates, the free energy barriers for 1,2-insertion (**TS(C1-D1)**$_{1,2}$ and **TS(C2-D2)**$_{1,2}$) are respectively 20.0 and 19.9 kcal mol^{-1}, approximately 5 kcal mol^{-1} higher than 2,1-insertion (see Figure 3 and Figure S1 in the supporting information). Therefore, 2,1-insertion of **2b** into the Ru-C bond is regiosterically favored via **TS(C1-D1)**$_{2,1}$ (13.8 kcal mol^{-1}) and **TS(C2-D2)**$_{2,1}$ (14.9 kcal mol^{-1}), placing the methyl ester substituent next to the ruthenium in the exergonic eight-membered metallacycles either below (**D1**$_{2,1}$; -1.7 kcal mol^{-1}) or above (**D2**$_{2,1}$; -1.3 kcal mol^{-1}) the plane of the ruthenacycle (when looking at the complex from the position of the *para*-cymene ligand).

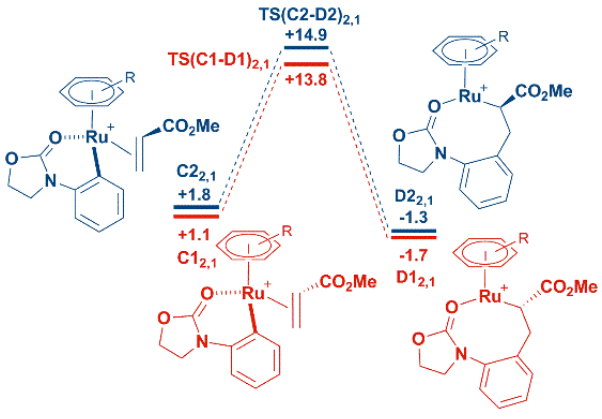

Figure 3: DFT calculated free energies (kcal mol^{-1}) relative to **A** and the free substrates, for the 2,1-insertion of methyl acrylate **2b** into adduct **C**.

Unlike in previous functionalization studies with methyl acrylate (by Davies and Macgregor[19], who used 3-phenyl-pyrazole to form a seven-membered rhodacycle) for this

2,1-insertion no interaction is observed between Ru and the ester substituent in the eight-membered ruthenacycle. In fact, the increased size of the metallacycle restricts its ability to interconvert between conformers **D1$_{2,1}$** and **D2$_{2,1}$**, as the preference for the boat-chair conformation reduces the flexibility of the metallacycle ring; this contrasts with the behavior that has been reported for similar, yet smaller, equivalent seven-membered intermediates.[19] The stereochemistry of the 1,2-disubstituted alkene product **3b** is determined exclusively by which β-hydrogen is transferred to the ruthenium center; from either above (H_a, Figure 4) or below (H_b) the plane of the ruthenacycle.

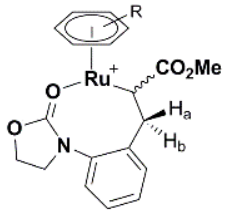

Figure 4: Ruthenacycle **D$_{2,1}$** showing the position of H_a (above) and H_b (below) the plane of the metallacycle. **D1$_{2,1}$** has the CO_2Me substituent *cis* to H_b whilst **D2$_{2,1}$** has the ester group *cis* to H_a

The β-hydrogen transfer process involves two steps: formation of an agostic intermediate followed by C–H cleavage, as the β-H moves to the Ru center. Figure 5 shows the transfer of H_a, which lies above the plane of the ruthenacycle, for both **D$_{2,1}$** isomers. In the case of **D1$_{2,1}$**, where the transferring hydrogen is *trans* to the ester group, formation of the agostic interaction between H_a and Ru proceeds via **TS(D1-E1)1$_a$** (19.1 kcal mol^{-1}) to give intermediate **INT(D1-E1)$_a$** (+13.1 kcal mol^{-1}), and C–H cleavage occurs via **TS(D1-E1)2$_a$** (13.9 kcal mol^{-1}) to form the *cis* product **E1$_{cis}$** (+10.4 kcal mol^{-1}). For **D2$_{2,1}$**, with H_a *cis* to the ester group, formation of the agostic interaction proceeds via **TS(D2-E2)1$_a$** (13.5 kcal mol^{-1}), decreasing the Ru···H_a distance from 3.701 to 2.716 Å in **INT(D2-E2)$_a$** (+5.8 kcal mol^{-1}) before C–H cleavage via **TS(D2-E2)2$_a$** (7.8 kcal mol^{-1}) and formation of the experimentally observed *trans* **3b** product [Ru(p-cymene)(**3b**)(H)]$^+$ (**E2$_{trans}$**; +4.9 kcalmol^{-1}).

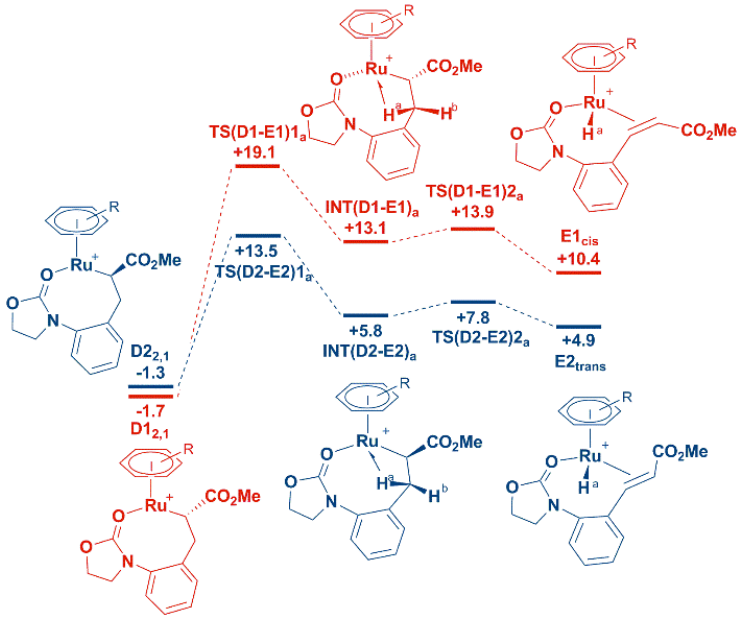

Figure 5: DFT calculated free energies (kcal mol^{-1}) relative to **A** and the free substrates, for the β-H_a transfer from 2,1-insertion ruthenacycles (**$D_{2,1}$**) in Me-THF.

The process of β-H transfer is more complicated for the "bottom" hydrogen, H_b shown in Figure 6, as the formation of the agostic interaction between H_b and Ru (Ru···H_b decreasing to 2.4 Å) forces dissociation of the oxazolidinone group at the ruthenium center (Ru···O increasing to 3.4 Å). This raises the barriers for the first step from **$D1_{2,1}$** via **TS(D1-E1)1_b** (17.5 kcal mol^{-1}) and from **$D2_{2,1}$** via **TS(D2-E2)1_b** (31.9 kcal mol^{-1})**.** The C–H_b bond is elongating by ~ 0.03 Å as the Ru-H_b distance decreases; this is a greater distortion than C–H_a (~ 0.01 Å) when the agostic intermediate is formed for the top β-H transfer. C–H_b cleavage occurs via **TS(D1-E1)2_b** (13.6 kcal mol^{-1}) and **TS(D2-E2)2_b** (20.4 kcal mol^{-1}) for **D1** and **D2** respectively to give intermediates **E1'$_{trans}$** (+9.7 kcal mol^{-1}) and **E2'$_{cis}$** (+14.1 kcal mol^{-1}). Reassociation of the oxazolidinone oxygen occurs via **TS(E1'-E1)$_{trans}$** (12.8 kcal mol^{-1}) and **TS(E2'-E2)$_{cis}$** (16.8 kcal mol^{-1}) to form the equivalent **E1$_{trans}$** (+11.3 kcal mol^{-1}) and **E2$_{cis}$** (+14.3 kcal mol^{-1}) complexes, which are less stable than the preceding **E'** complexes.

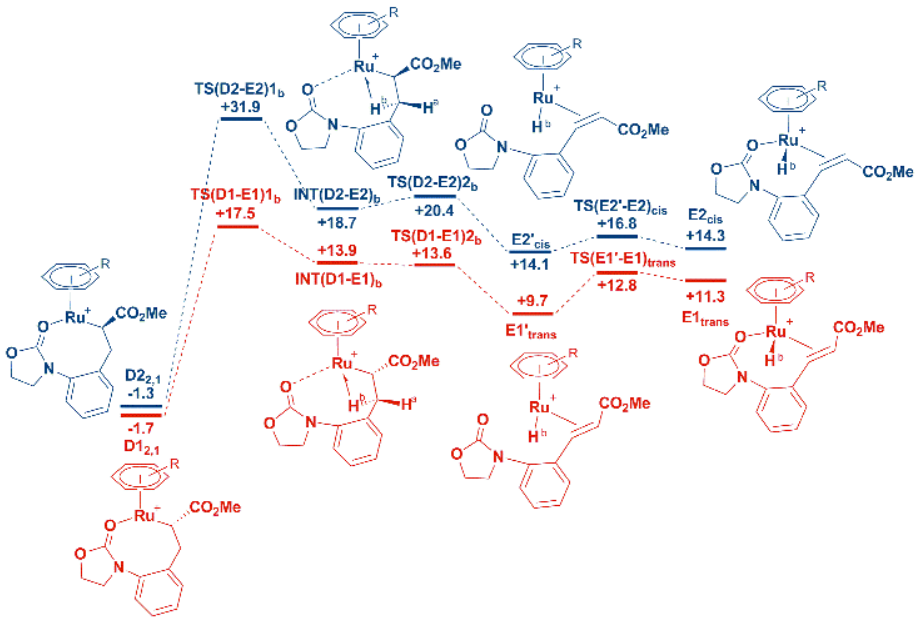

Figure 6: DFT calculated free energies (kcal mol^{-1}) relative to **A** and the free substrates, for the β-H_b transfer from 2,1-insertion ruthenacycles (**$D_{2,1}$**) in Me-THF.

Based on the assumption that the energy difference of 0.4 kcal mol^{-1} between the two 2,1-insertion ruthenacycle complexes (**$D1_{2,1}$** and **$D2_{2,1}$**) is small enough that both species are populated during the catalytic cycle, it is comforting to note that both ruthenacycle isomers preferentially form the *trans* 1,2-disubstituted alkene product over the *cis* stereoisomer. This agrees with experiment that only *trans* **3b** is observed, and is due to H transfer of different β-hydrogens (H_a or H_b). The free-energy difference between **TS(D1-E1)1_a** and **TS(D2-E2)1_a** suggests a preference of about 10^4 for formation of the *trans* product over the *cis* isomer.

The absence of a di-alkenylated product (**$3b_{di}$**) formed during the reaction was investigated, with the subsequent C–H activation of **3b** at the remaining *ortho* C–H position modelled. The barrier for this activation was 15.4 kcal mol^{-1} (see Supporting Information, Table S2), 3 kcal mol^{-1} higher than activation of the initial C–H site in substrate **1b** (**TS(A-B)1** = +12.4 kcal mol^{-1}), hence **3b** does not undergo a second C–H activation. The unusual isomeric preference **1ar** / **1aq** substrates were likewise studied. Here, the major and minor C–H activation pathways were modelled for **1ar** (see Supporting Information, Table S3) and unsurprisingly the barrier for the major isomer pathway was lower in free energy, by 0.9 kcal mol^{-1}. This small difference, and similar energies for ^{1ar}**A** and ^{1ar}**A′**, the major and minor isomers of [Ru(*p*-cymene)(OAc)(**1ar**)]$^+$ respectively, (ΔG = 0.4 kcal mol^{-1}) agree with the experimental observation of both isomers, showing a slight energetic preference for the formation of the major isomer.

In order to estimate the Gibbs energy change for the uncatalyzed coupling of **1a** to **2b** to give **3b**, the oxidation process also needs to be included (equation 1). The overall reaction may be considered as:

$$\mathbf{1a} + \mathbf{2b} + \tfrac{1}{2}O_2 \rightarrow \mathbf{3b} + H_2O \qquad (1)$$

for which the exergonic Gibbs energy change (at 25 °C) is -49 kcal mol^{-1}. This is the amount by which all the Gibbs energies relative to **A** must be reduced between one turnover of the catalytic cycle and the next. (Note that the reaction path for the conversion from $\mathbf{E2_{trans}}$ to **A** in the next cycle has not been investigated computationally.) The significance of this consideration is that it allows the turnover-dependent intermediate and the turnover-dependent transition state to be identified as $\mathbf{D2_{2,1}}$ and $\mathbf{TS(D2\text{-}E2)1_a}$, respectively, which occur sequentially within the same turnover cycle (Figure 7); the possibility of the turnover-dependent transition state occurring in the subsequent cycle can be discounted in this case.[20] Thus the computational modelling predicts the rate-determining step (as commonly understood) to be formation of the agostic intermediate immediately prior to β-hydride transfer. Under the experimental conditions the oxidation step is undoubtedly mediated by $Cu(OAc)_2$, although the detailed mechanism is unknown.[21] However, for the present purpose it is necessary only to consider overall stoichiometry and thermochemistry, not kinetics and mechanism for this stage of the turnover cycle. The calculated free energy changes ΔG_{MeTHF} reported above (Figures 2 – 6) refer to a standard state of 1 atm for all species, but detailed considerations of the rate-determining step (or, in general, of the turnover-dependent intermediate and transition state within a steady-state catalytic cycle)[20] depend upon actual concentrations under experimental conditions. The relative Gibbs energies shown in Figure 7 are corrected for the change from 1 atm (concentration c_1) to the standard reaction conditions (Table 1; concentration c_2) by the term $RT\ln(c_1/c_2)$ at temperature T = 120 °C. The ligand exchange step **B** → **C** (for which a transition structure has not been determined) becomes exergonic due to the larger relative concentration of alkene **2b**, with the consequence that the free energies of the transition structures for the alkene insertion and β-hydride transfer sections of the cycle are lowered with respect to those in the C–H activation section. The resulting profile (Figure 7) shows four transition structures (**TS(A-B)1**, **TS(A-B)2**, $\mathbf{TS(C2\text{-}D2)_{2,1}}$ and $\mathbf{TS(D2\text{-}E2)1_a}$) all with quite similar free energies.

Kinetic Isotope Effects

Relative to **A**, the computational modelling predicts an intrinsic KIE k_{H5}/k_{D5} = 2.2 for the C–H activation step. Since the preceding transition structure **TS(A-B)1** for formation of the agostic intermediate is calculated to be slightly higher in energy, the intrinsic KIE would be partially masked, leading to a reduced value for the observed isotope effect. The experimental KIE by direct comparison of initial reaction rates for **1a** and **[D]$_5$-1a** has a value of about 2, which seems to suggest that most of the intrinsic KIE is being expressed. The KIEs calculated for the individual agostic formation, migratory insertion, and β-hydride elimination steps are all essentially unity as expected (Scheme 14).

The KIE determined by the method of intermolecular competition expresses the isotopic discrimination up to the first irreversible step of the cycle, relative to free starting material. It is known that cyclometallation is reversible (Scheme 12), leading to loss of deuterium from the *ortho* position of **1a**. The product ratio determined in the competition experiment therefore reflects the isotope effect on cyclometallation. However, the interpretation of the experimental isotope effect is complicated by at least two factors.

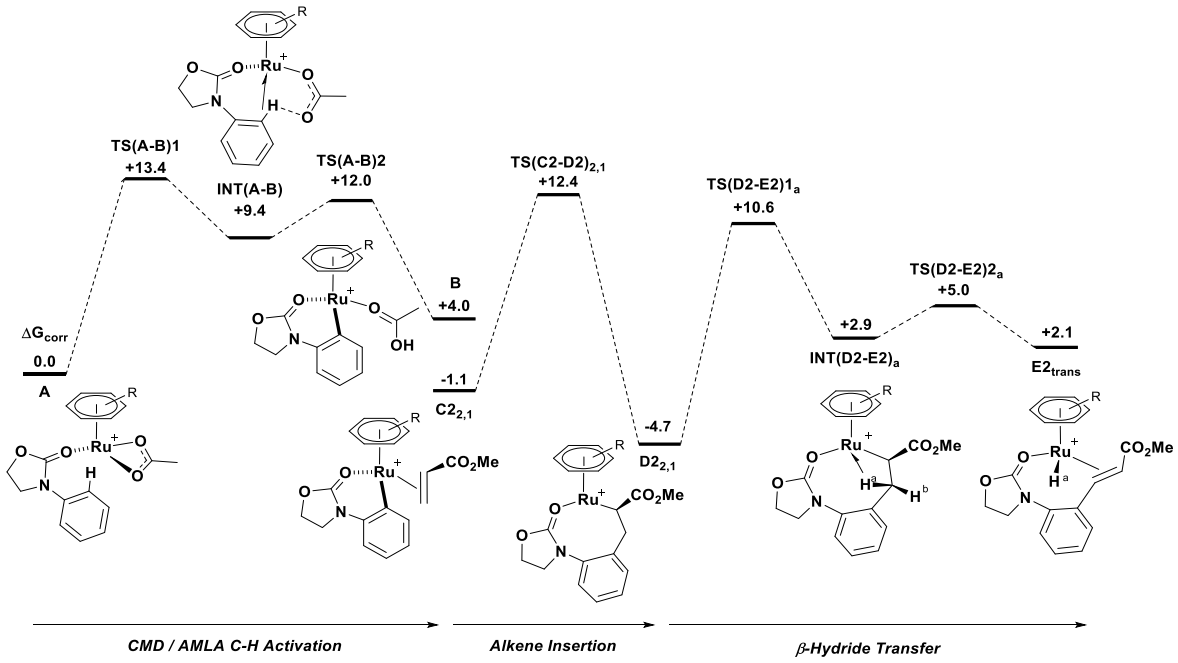

Figure 7: DFT calculated free energies (kcal mol^{-1} relative to **A**) for the coupling of **1a** and **2b** to form **3b** using a ruthenium catalyst at 120 °C in Me-THF and at concentrations corresponding to the standard experimental conditions (Table 1).

First, the isotopic product ratio observed depends upon the degree of conversion, since starting from a 1:1 mixture of isotopologues, a product ratio of 1:1 must be obtained for 100% conversion: the observed isotope effect should be corrected for the fractional degree

of conversion, which leads to a greater value for the KIE.[22] Second, the fact that isotopic exchange at the *ortho* position is seen to take place during cyclometallation means that the proportion of deuterated **1a** in the reaction mixture is reduced, leading to an increase in the apparent value of the KIE. Numerical simulation shows that only a small percentage of isotopic exchange due to **B** → **A** reversibility is required to account for an apparent KIE of about 2.6 as observed for the intermolecular competition experiment.

Scheme 14: Full Mechanism of Ruthenium-Catalyzed C–H Alkenylation including Kinetic and Energetic (kcal mol^{-1}) DFT Contributions

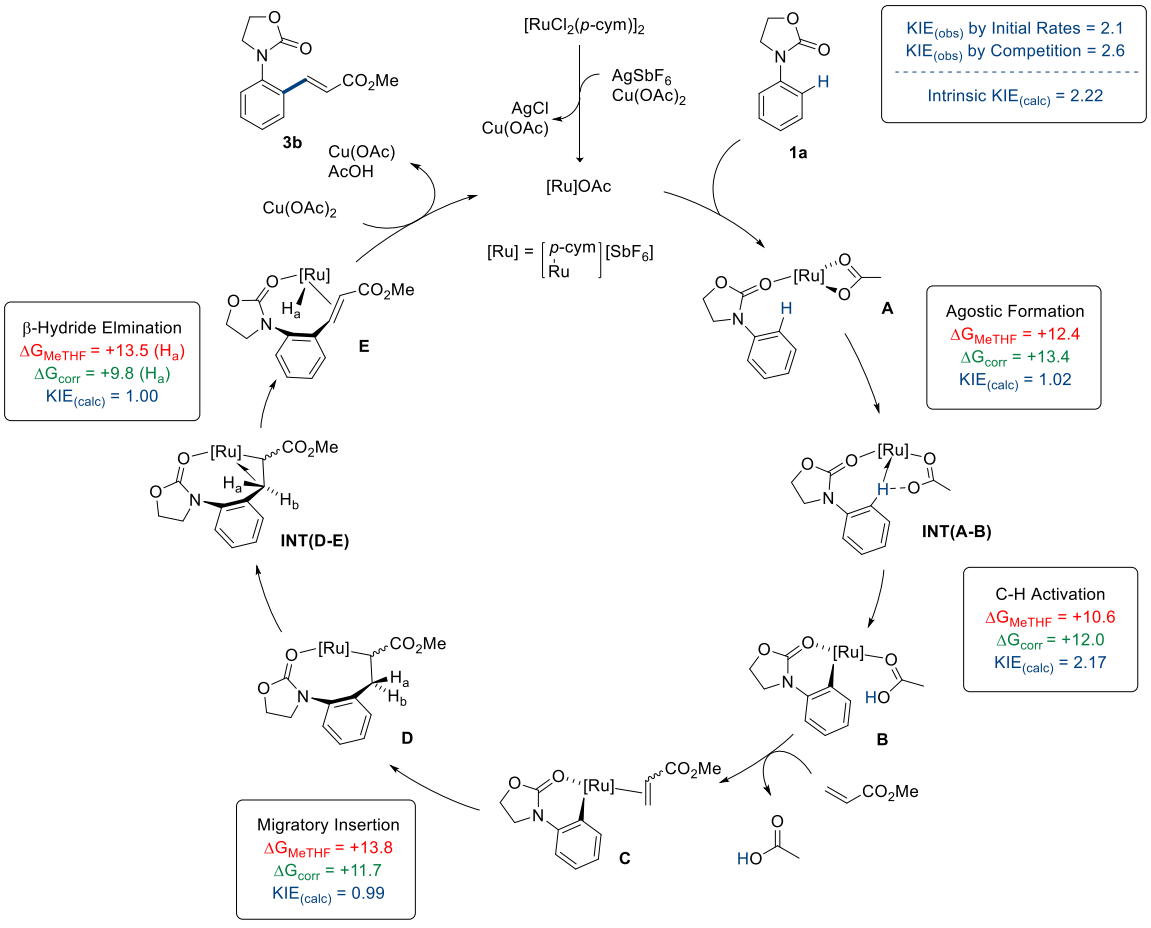

Conclusion

We have reported the first use of the oxazolidinone directing group in ruthenium catalyzed C–H functionalization. This proof of concept of cyclometalation and subsequent functionalization was modeled on an alkenylation reaction. This led to the synthesis of over 25 novel substituted *N*-aryloxazolidinone motifs with up to 94% yields with absolute mono-selectivity. This methodology granted access to biologically relevant derivatives of oxazolidinone pharmaceuticals and could be applied to late stage drug modification.

DFT calculations for most sections of the catalytic cycle suggest why ***trans*-3b** is the only product isomer obtained, but yield very similar free energies for the transition states of several steps in the proposed mechanism using relative concentrations corresponding to the experimental conditions. The C–H activation step involves a KIE of $k_H/k_{D5} \approx 2$ in apparent agreement with the observed value, but several reasons are noted why a direct comparison between calculation and experiment may not be warranted.

ASSOCIATED CONTENT

Supporting Information. Full characterization, NMR spectra, computational data and crystallographic information is attached. This material is available free of charge via the Internet at http://pubs.acs.org.

AUTHOR INFORMATION

Corresponding Author

* Christopher G. Frost: C.G.Frost@bath.ac.uk (Synthetic)

* Ian H. Williams: I.H.Williams@bath.ac.uk (Physical Organic Computational)

* Claire L. McMullin: C.McMullin@bath.ac.uk (Inorganic Computational)

Notes

The authors declare no competing financial interest.

ACKNOWLEDGMENT

The authors gratefully acknowledge the University of Bath, Syngenta (JL) and the EPSRC (PW) for financial support. JL would also like to thank Christina Gulacsy and Dr. David Carbery for use and help with HPLC work, and John Lowe for NMR expertise. We thank the University of Bath for access to its High Performance Computing Facility.

REFERENCES

(1) For reading on linezolid see: (a) Barbachyn, M. R.; Ford, C. W. *Angew. Chem*. Int. Ed., **2003**, *42*, 2010-2023. (b) Gregory, W, A.; D. Brittelli, R.; Wang, C. L. J.; Wuonola, M. A.; McRipley, R. J.; Eustice, D. C.; Eberly, V. S.; Bartholomew, P. T.; Slee, A. M.; Forbes, M. *J. Med. Chem*. **1989**, *32*, 1673-1681. (c) Brickner, S. J.; Hutchinson, D. K.; Barbachyn, M. R.; Manninen, P. R.; Ulanowicz, D. A.; Garmon S. A.; Grega, K. C.; Hendges, S. K.; Toops, D. S.; Ford, C. W.; Zurenko, G. E. *J. Med. Chem*. **1996**, *39*, 673-679. (d) Evans, D. A.; Seidel, D.; Rueping, M.; Lam, H. W.; Shaw, J. T.; Downey, C. W. *J. Am. Chem. Soc*. **2003**, *125*, 12692-12693.

(2) For reading on tedizolid see: (a) Locke, J. B.; Finn, J.; Hilgers, M.; Morales, G.; Rahawi, S.; Kedar, G. C.; Picazo, J. J.; Im, W. B.; Shaw, K. J., Stein, J. L. *Antimicrob*. *Agents Chemother*. **2010**, *54*, 5337-5343. (b) Im, W. B.; Choi, S. H., Park, J. Y.; Finn, J.; Yoon, S. H. Eur. *J. Med. Chem*. **2011**, *46*, 1027-1039

(3) For reading on rivaroxaban see: (a) Roehrig, S.; Straub, A.; Pohlmann, J.; Lampe, T.; Pernerstorfer, J.; Schlemmer, K. H.; Reinemer, P.; Perzborn, E. *J. Med. Chem*. **2005**, *48*, 5900-5908. (b) Perzborn, E.; Roehrig, S.; Straub, A.; Kubitza, D.; Misselwitz, F. *Nature Reviews Drug Discovery*. **2011**, *10*, 61-75. (c) Yuan, J.; Liu, K.; Li, L.; Yuan, Y.; Liu, X.; Li, Y. *Molecules*, **2014**, *19*, 14999-15004, d) Rafecas, J. L.; Comely, A. C.; Ferrali, A.; Amelia Cortes, C.; Pasto Aguila, M. WO2011080341A1, **2011**.

(4) Moureau, F.; Wouters, J.; Vercauteren, D. P.; Collin, S.; Evrard, G.; Durant, F.; Ducrey, F.; Koenig, J. J.; Jarreau, F. X. *Eur. J. Med. Chem.* **1992**, *27*, 939-948.

(5) For reading on the synthesis and modification of *N*-aryloxazolidinones see: (a) Ghosh, A.; Sieser, J. E.; Riou, M.; Cai, W.; Rivera-Ruiz, L. *Org. Lett.*, **2003**, *5*, 2207–2210. (b) Mahy, W.; Plucinski, P.; Frost, C. G. *Org. Lett.*, **2014**, *16*, 5020-5023. (c) Mallesham, B.; Rajesh, B. M.; Rajamohan Reddy, P.; Srinivas, D.; Trehan, S. *Org. Lett.,* **2003**, *5*, 963-965. (d) Mahy, W.; Plucinski, P.; Jover, J.; Frost, C. G. *Angew. Chem. Int. Ed.* **2015**, *127*, 11094-11098. (e) Mahy, W.; Leitch, J. A.; Frost, C. G. *Eur. J. Org. Chem.* **2016**, *7*, 1305-1313.

(6) For reviews on transition metal catalyzed C–H functionalization see: (a) Ackermann, L. *Chem. Rev.* **2011**, *13*, 3075-3078, (b) Arockiam, P. B.; Bruneau, C.; Dixneuf, P. *Chem. Rev*. **2012**, *112*, 5879−5918. (c) Chen, X.; Engle, K. M.; Wang, D-H.; Yu, J-Q. *Angew. Chem. Int. Ed.* **2009**, *48*, 5094–5115. (d) Engle, K. M., Mei, T-S.; Wasa, M.; Yu, J-Q. *Acc. Chem. Res.* **2012**, *45,* 788-802. (e) Rao, Y. Shan, G. Yang, X-L. *Sci. China Chem.* **2014**, *57*, 930-944. (f) Thirunavukkarasu, V. S.; Kozhushkov, S. I.; Ackermann, L. *Chem. Commun*, **2014**, *50*, 29-39.

(7) (a) Yamaguchi, J.; Yamaguchi, A. D.; Itami, K. *Angew. Chem. Int. Ed.* **2012**, *51*, 8960-9009 (b) Mahy, W.; Plucinski, P.; Jover, J.; Frost, C. G. *Angew. Chem. Int. Ed.* **2015**, *54*, 10944-10948. (c) Liu, P. M.; Frost, C. G. *Org. Lett.* **2013**, *15*, 5862-5865. (d) Brown, J. A.; Cochrane, A. R.; Irvine, S.; Kerr, W. J.; Mondal, B.; Parkinson, J. A.; Paterson, L. C.; Reid, M.; Tuttle, T.; Andersson, S.; Nilsson, G. N. *Adv. Synth. Catal.* **2014**, *356*, 3551-3562.

(8) For key seminal publications on directed ruthenium catalyzed C–H functionalization see: (a) Murai, S.; Kakiuchi, F. Sekine, S.; Tanaka, Y.; Kamatani, A.; Sonoda, M.; Chatani, N. *Nature*, **1993**, 366, 529-531 (b) Oi, S.; Fukita, S.; Hirata, N.; Watanuki, N.; Miyano, S.; Inoue, Y. *Org. Lett.* **2001**, *3*, 2579-2581. (c) Oi, S.; Ogino, Y.; Fukita, S.; Inoue, Y. *Org. Lett.* **2002**, *4*, 1783-1785. (d) Ackermann, L. *Org. Lett.* **2005**, *7* , 3123-3125. (e) Ackermann, L.; Althammer, A.; Born, R. *Angew. Chem. Int. Ed.* **2006**, *45*, 2619-2622, (f) Ackermann, L.; Vicente, R.; Althammer, A. *Org. Lett.* **2008**, *10*, 2299-2302. (g) Ozdemir, I.; Demir, S.;

Cetinkaya, B.; Gourlaouen, C.; Maseras, F.; Bruneau, C.; Dixneuf, P. H., *J. Am. Chem. Soc.* **2008**, *130*, 1156-1157.

(9) For key examples of ruthenium catalyzed C–H functionalization using weakly coordinating directing groups see: (a) De Sarkar S.; Liu, W.; Kozhushkov, S. I.; Ackermann, L. *Adv. Synth. Catal.* **2014**, *356*, 1461-1479. (b) Ueyama, T.; Mochida, S.; Fukutani, T.; Hirano, K.; Satoh, T.; Miura, M. *Org. Lett.* **2011**, *13*, 706-708. (c) Ackermann, L.; Pospech, J. *Org. Lett.* **2011**, *13*, 4153-4155. (d) Kakiuchi, F.; Kan, S.; Igi, K.; Chatani, N.; Murai, S. *J. Am. Chem. Soc.* **2003**, *125*, 1698-1699. (e) Bhanuchandra, M.; Yadav, M. R.; Rit, R. K.; Kuram, M. R.; Sahoo, A. K. *Chem. Commun.* **2013**, *49*, 5225-5227. (f) Padala, K.; Jeganmohan, M. *Org. Lett.* **2012**, *14*, 1134-1137. (g) Ackermann, L.; Lygin, A. V.; Hofmann, N. *Angew. Chem. Int. Ed.* **2011**, *50*, 6379-6382. (h) Graczyk, K.; Ma, W.; Ackermann, L. *Org. Lett.* **2012**, *14*, 4110-4113. (i) Padala, K.; Jeganmohan, M. *Org. Lett.* **2011**, *13*, 6144-6147. (j) Reddy, M. C.; Jeganmohan, M. *Chem. Commun.* **2014**, *51*, 10738-10741. (k) Li, J.; Kornhaass, C.; Ackermann, L. *Chem. Commun.*, **2012**, *48*, 11343-11345.

(10) (a) Kalyani, D.; Deprez, N. R.; Desai, L. V.; Sanford, M. S. *J. Am. Chem Soc.* **2005**, *127*, 7330-7331. (b) Yeung, C. S.; Dong, V. M. *Synlett,* **2011**, *7,* 974-978

(11) For palladium see: Leow, D.; Li, G.; Mei, T-S.; Yu, J-Q, *Nature*, **2012**, *486*, 518-522. For rhodium see: Colby, D. A.; Bergman, R. G.; Ellman, J. A. *Chem Rev*, **2010**, *110*, 624-655.

(12) (a) Pace, V.; Hoyos, Fernandez, M.; P.;Sinisterra, J. V.; Alcantara, A. R. *Green Chem.* **2010**, *12*, 1380-1382. (b) Pace, V.; Hoyos, P.; Castoldi, L.; De Maria, P. D.; Alcantara, A. R. *Chemsuschem*, **2012**, *5*, 1369-1379

(13) (a) **Crystal Data** for $C_{14}H_{14}FNO_4$ (compound **3aq$_1$**): M =279.26 g mol^{-1}, triclinic, space group P-1 (no. 2), a = 6.8220(2), b = 10.6058(3), c = 19.5239(7) Å, α = 105.484(3), β = 90.601(3), γ = 102.910(2)°, U = 1323.22(7) Å^3, Z = 4, T = 150.00(10) K, μ(Cu-Kα) = 0.954 mm^{-1}, D_c = 1.402 g cm^{-3}, 13114 reflections measured (8.9° ≤ 2θ ≤ 143.942°), 5164 unique (R_{int} = 0.0248, R_{sigma} = 0.0279) which were used in all calculations. The final R1 was 0.0379 (I > 2σ(I)) and wR_2 was 0.0994 (all data). (b) **Crystal Data** for $C_{14}H_{14}FNO_4$ (compound **3aq$_2$**): M =279.26 g mol^{-1}, tetragonal, space group $P4_32_12$, a = 9.43321(9), c = 29.5288(4) Å, U = 2627.64(6) Å^3, Z = 8, T = 150.00(10) K, μ(Cu-Kα) = 0.960 mm^{-1}, D_c = 1.412 g cm^{-3}, 23288 reflections measured (9.844° ≤ 2θ ≤ 143.71°), 2586 unique (R_{int} = 0.0317, R_{sigma} = 0.0148) which were used in all calculations. The final R1 was 0.0283 (I > 2σ(I)) and wR_2 was 0.0720 (all data). CCDC 1479666-1479667 (for 3aq$_1$ and 3aq$_2$, respectively) contain the supplementary crystallographic data for this paper. These data can be obtained free of charge via http://www.ccdc.cam.ac.uk/conts/retrieving.html, or from the Cambridge Crystallographic Data Centre, CCDC, 12 Union Road, Cambridge CB2 1EZ, UK.

(14) Liu, W.; Ackermann, L. *Chem. Commun.* **2014**, *50*, 1878-1881

(15) (a) Sova, M. *Mini. Rev. Mec. Chem.*, **2012**, *12*, 749-767 (b) Seelolla, G.; Cheera, P.; Ponneri, V. *Med. Chem.*, **2014**, *4*, 778-783

(16) For previous use of the pyrolidinone directing group in palladium catalyzed C–H functionalization see: (a) Giri, R.; Lam, J. K.; Yu, J-Q. *J. Am. Chem. Soc,* **2010**, *132*, 686-693. (b) Bedford, R. B.; Mitchell, C. J.; Webster, R. L. *Chem. Commun.* **2010**, *46*, 3095-3097. (c) Desai, L. V.; Malik, H. A.; Sanford, M. S. *Org. Lett.* **2006**, *8*, 1141-1144. (d) Prakash, G. K. S.; Mathew, T.; Hoole, D.; Esteves, P. M.; Wang, Q.; Rasul, G.; Olah, G. A. *J. Am. Chem. Soc*. **2004**, *126*, 15770-15776.

(17) Simmons, E. M.; Hartwig, J. F. *Angew. Chem. Int. Ed.*, **2012**, *51*, 3066-3072.

(18) DFT calculations were run with Gaussian 09 (Revision D.01). Ru centers were described with the Stuttgart RECPs and associated basis sets, and 6-31G** basis sets were used for all other atoms. Full details and references for all computational methods can be found in SI.

(19) Algarra, A. G.; Davies, D. L.; Khamker, Q.; Macgregor, S.; McMullin, C. L.; Singh, K.; Villa-Marcos, B. *Chem. Eur. J.*, **2015**, *21*, 3087-3096.

(20) (a) Kozuch, S.; Shaik, S. *Acc. Chem. Res*. **2010**, *44*, 101-110. (b) Kozuch, S.; Martin, J. M. L. *ACS Catal.* **2012**, *2*, 2787-2794.

(21) Funes-Ardoiz, A.; Maseras, F. *Angew. Chem. Int. Ed.*, **2016**, *55*, 2764-2767

(22) Melander, L.; Saunders, W. H. *Reaction Rates of Isotopic Molecules*, Wiley, New York, 1980, 56-129

2.3: Use of the Hydantoin Directing Group in Ruthenium(II)-Catalyzed C–H Functionalization

2.3.1: Introduction and Commentary

With the success of the oxazolidinone project, it was of interest to investigate further biologically relevant directing groups in ruthenium catalysed C–H activation. The hydantoin heterocycle bears both urea and amide functionality and has been used in a variety of biological applications. Hydantoins are classically synthesised by two methods. The first of these is the Bucherer-Bergs reaction which involves the condensation a ketone, potassium cyanide and ammonium carbonate (Scheme 2-10a).[1] This takes place *via* an isocyanate intermediate after reaction of the cyanohydrin with CO_2. The identical product will also be formed by submitting the cyanohydrin to ammonium carbonate. This reaction has since been applied to continuous flow synthesis, highlighting the robustness of this chemistry (Scheme 2-10b).[2]

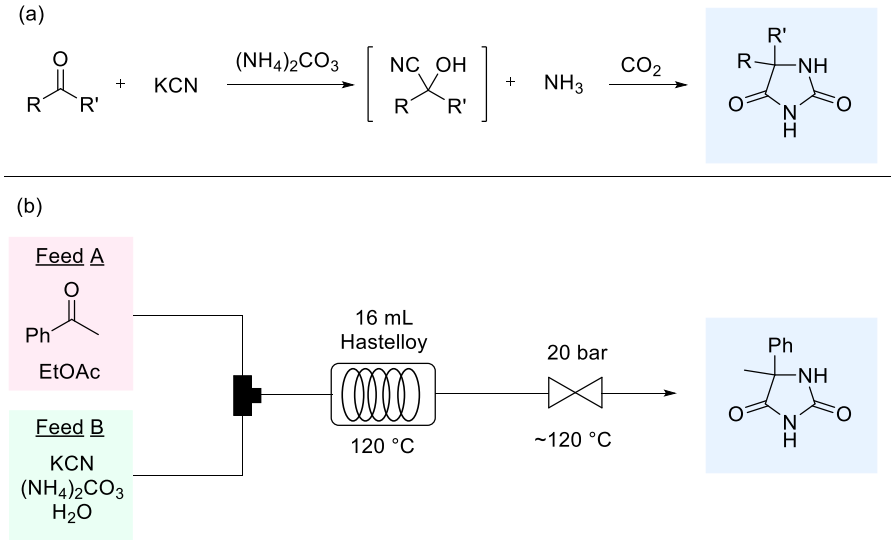

Scheme 2-10: Bucherer-Bergs Reaction in the Formation of Hydantoins

The second method is the treatment of isocyanates with amino acids followed by a cyclisation *via* condensation. This enables a wide range of readily available synthetic feedstocks. The glycine derivative can be synthesized using an aqueous protocol (Scheme 2-11a)[3] however other derivatives can be accessed using sequential addition and ring closure reactions (Scheme 2-11b).[4]

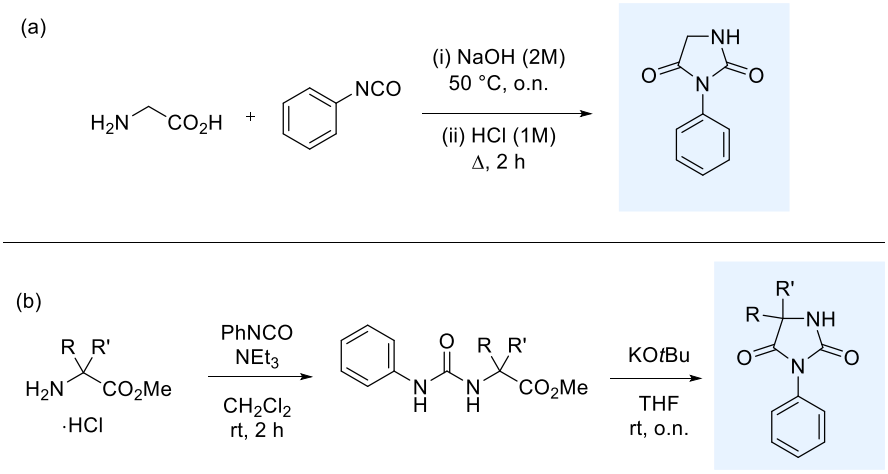

Scheme 2-11: Synthesis of *N*-arylhydantoins from Amino Acids

The arylation of dimethylhydantoin has also been reported using copper catalysis and aryl iodides. Forcing conditions are generally used in high boiling polar aprotic solvents such as DMF and DMA (Scheme 2-12).[5]

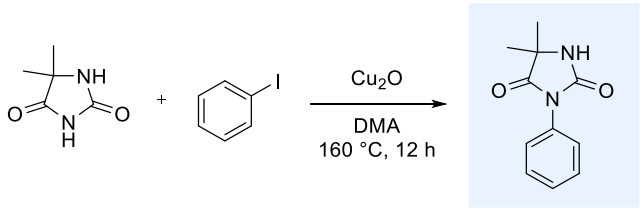

Scheme 2-12: Synthesis of *N*-arylhydantoin via Ullmann Condensation

In 2013, Krische and co-workers reported the ruthenium-catalysed prenylation of hydantoins (Scheme 2-13). This was shown to take place through a hydroaminoalkylation reaction which was initiated by a transfer hydrogenation to dehydrogenate the hydantoin starting material.[6]

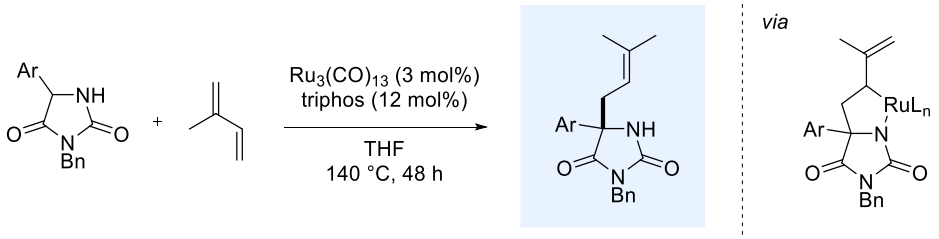

Scheme 2-13: Ruthenium-Catalysed Allylation of the Hydantoin Heterocycle

As shown above the hydantoin heterocycle can be formed from amino acids, they can also reform the corresponding amino acid. Due to this hydantoins have been used as intermediates in the synthesis of unnatural amino acids, and in the derivatisation of hydantoins themselves. In 2015, Clayden and co-workers reported the palladium catalysed C-arylation of hydantoins on the heterocycle itself (Scheme 2-14).[4]

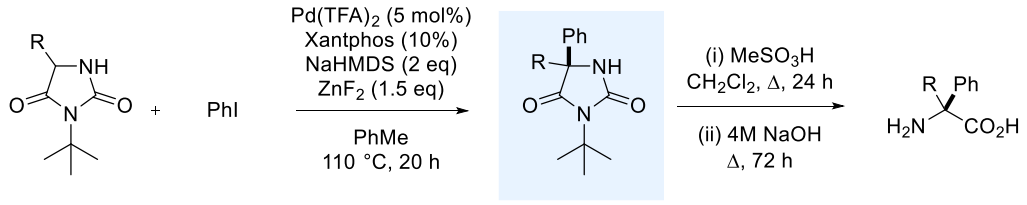

Scheme 2-14: Palladium-Catalysed C–H arylation of the Hydantoin Heterocycle

The hydantoin heterocycle has been used as a directing group in transition metal catalysed C–H activation. Kerr and co-workers elegantly employed iridium catalysis in the C–H deuteration of Nilutamide (Scheme 2-15) among other pharmaceutically active compounds.[7]

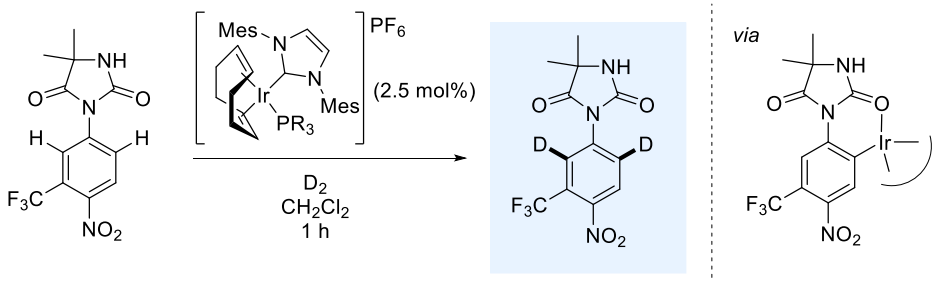

Scheme 2-15: Iridium-Catalysed *ortho*-Deuteration of Nilutamide

This acted as proof as concept that one could utilise the hydantoin heterocycle as a directing group to enable cyclometalation. The aim for this project was to apply previously developed methodology from the oxazolidinone project to this new scaffold. The results achieved in this project are presented in the form of the Note that was published in The Journal of Organic Chemistry in 2016.

References

(1) H. T. Bucherer and H. T. J. Fischbeck, *J. Prakt. Chem.*, 1934, **140**, 69.

(2) J. L. Monteiro, B. Pieber, A. G. Corrêa, and C. O. Kappe, *Synlett,* 2016, 27, 80

(3) L. Hrich, M. Hruskova, J. Schmitz, G. Schnakenburg, and M. Gutschow, *Synthesis*, 2012, **44**, 1907

(4) F. Fernandez-Nieto, J. M. Rosello, S. Lenoir, S. Hardy, and J. Clayden, *Org. Lett.*, 2015, **17**, 3838

(5) C. Wang, Q. Zhao, M. Vargas, J. O. Jones, K. L. White, D. M. Shackleford, G. Chen, J. Saunders, A. C. F. Ng, F. C. K. Chiu, Y. Dong, S. A. Charman, J. Keiser, and J. L. Vennerstrom, *J. Med. Chem.*, 2016, **59**, 10705.

(6) D. C. Schmitt, J. Lee, A.-M. Dechert-Schmitt, E. Yamaguchi, and M. J. Krische. *Chem. Commun.*, 2013, **49**, 6096.

(7) J. A. Brown, A. R. Cochrane, S. Irvine, W. J. Kerr, B. Mondal, J. A. Parkinson, L. C. Paterson, M. Reid, T. Tuttle, S. Andersson, and G. N. Nilsson, *Adv. Synth. Catal.*, 2014, **356**, 3551.

2.3.2: Authorships and Permissions

This declaration concerns the article entitled									
Use of the Hydantoin Directing Group in Ruthenium(II)-Catalyzed C–H Functionalization									
Publication status (tick one)									
Draft manuscript		**Submitted**		**In review**		**Accepted**		**Published**	X
Publication details (reference)	J. A. Leitch, H. P. Cook, Y. Bhonoah, and C. G. Frost, *J. Org. Chem.*, 2016, **81**, 10081								
Candidate's contribution to the paper (detailed, and also given as a percentage)	The candidate contributed to/ considerably contribute to/predominantly execute the: **Formulation of ideas (80%)**: JAL had the idea for the project and formulated the plan. Project discussions with CGF (20%). **Design of methodology (90%):** JAL designed the lab work for the project. Design discussions with CGF (10%) **Experimental work (80%):** JAL completed a majority of the synthetic work (*N*-arylhydantoins). HPC completed the remainder of the synthetic work (*N*-arylsuccinimides, 20%) **Presentation of data in journal format (75%)**: JAL wrote all of the paper and compiled the data for publication. CGF edited the manuscript (20%). YB and HPC looked over the manuscript (combined 5%)								
Statement from Candidate	This paper reports on original research I conducted during the period of my Higher Degree by Research candidature								
Signed	Jamie A. Leitch						**Date**	14/09/17	

2.3.3: Manuscript for "Use of the Hydantoin Directing Group in Ruthenium(II)-Catalyzed C–H Functionalization"

Modified manuscript given at point of corrections follows on the next page. Layout changes have also been made for consistency of thesis. Contents remains unchanged although this manuscript has been modified to move compound characterisation into the experimental section (6.2) for completeness and consistency of the thesis.

.

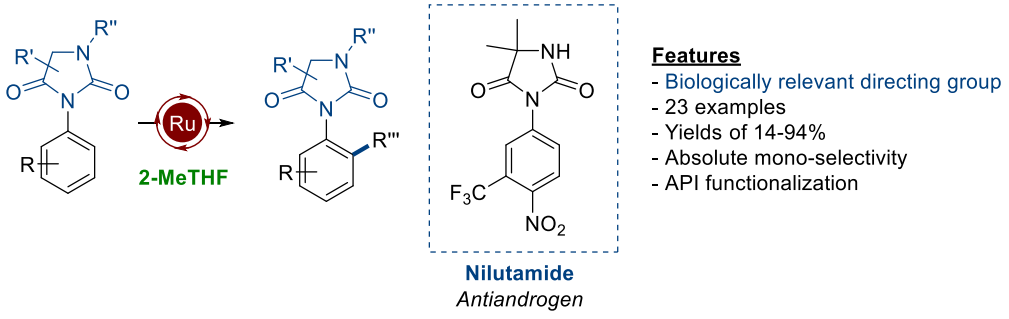

The Use of the Hydantoin Directing Group in Ruthenium(II)-Catalyzed C–H Functionalization

Jamie A. Leitch,† Hans P. Cook,† Yunas Bhonoah,‡ and Christopher G. Frost.*,†

†Department of Chemistry, University of Bath, Claverton Down, Bath, Somerset, BA2 7AY, United Kingdom

‡Jealott's Hill International Research Centre, Syngenta, Bracknell, Berkshire, RG42 6EY, United Kingdom

ABSTRACT: Ruthenium(II)-Catalyzed C–H Functionalization of *N*-arylhydantoins is herein described. The biologically relevant hydantoin (imidazolidinedione) heterocycle functions as a weakly coordinating directing group in a C–H alkenylation reaction. The reaction gave a wide scope of 23 examples with yields up to 94% in green solvent 2-MeTHF. Functionalization of API nilutamide (anti-androgen) is also reported. The use of the succinimide heterocycle as a directing group is also demonstrated in modest yields.

The hydantoin (imidazolidinedione) heterocycle (and sulfur anaologues) is prevalent in numerous medicinally and agrochemically active scaffolds. These include the hydantoin class of anticonvulsants (phenytoin, fosphenytoin, Figure 1), non-steroidal androgen antagonists (nilutamide, enzalutamide) and fungicides (iprodione).[1]

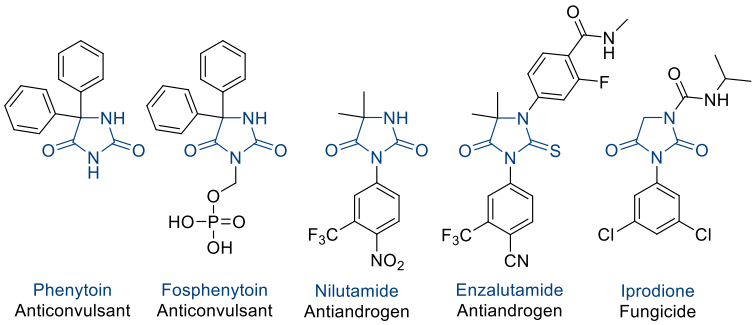

Figure 1: Biologically Relevant Compounds Containing the Hydantoin Heterocycle

Using biologically active heterocycles as directing groups in transition-metal catalyzed C–H functionalization is a powerful synthetic tool as this can grant access to a novel library of derivatives inaccessible through other synthetic methods.[2] Direct palladium-

catalyzed C–H arylation of the hydantoin heterocycle itself has been recently reported by Clayden and co-workers.[3] The hydantoin heterocycle has also been shown to form a six-membered metallacycle in elegant deuteration studies carried out by Kerr and co-workers (Scheme 1) using iridium catalysis on the anti-androgen nilutamide.[2d] This work acted as proof of concept that this heterocycle could potentially be utilized in transition metal catalyzed C–H functionalization, allowing the creation of novel analogues of biologically relevant motifs.

Scheme 1: C–H functionalization of *N*-arylhydantoins

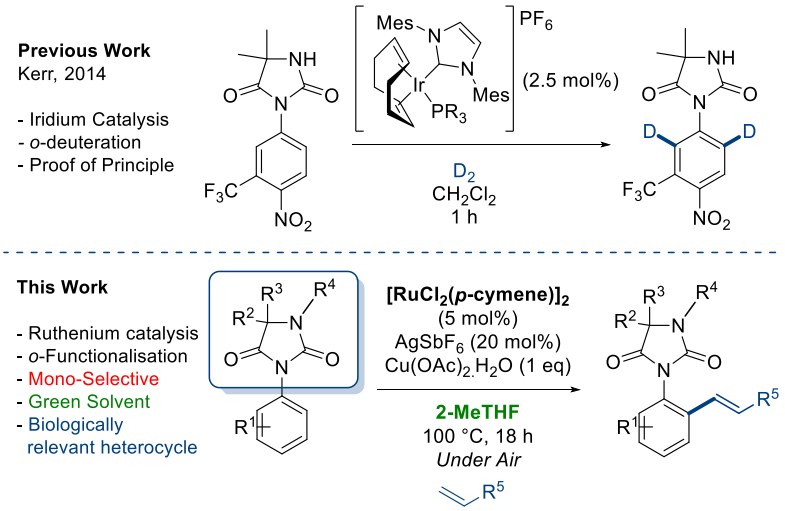

Ruthenium(II) catalysis has emerged as a powerful method of the formation of metallacycles and subsequent functionalization.[4] The ability of weakly coordinating directing groups to facilitate this functionalization has been brought to the forefront of C–H functionalization methodology through important contributions from Ackermann[5] and Jeganmohan[6] amongst others.

Preliminary reaction conditions were identified from previous work within the group and literature precedent on related alkenylation reactions.[2a,5,6] Electron deficient alkenes are commonly used coupling partners due to their high efficiency in cross dehydrogenative coupling reactions.[2a] Initial optimization was carried out using nilutamide test motif (**1a**) containing the gem-dimethyl substituent on the hydantoin heterocycle, methyl acrylate as the coupling partner (Table 1), $[RuCl_2(p\text{-cymene})]_2$ as the ruthenium source, $AgSbF_6$ as the co-catalyst and $Cu(OAc)_2.H_2O$ as the oxidant. Selected results will be discussed further.
The reaction was shown to not tolerate aqueous or acidic solvent media (entries 1-2) however polar aprotic etheric solvents afforded the alkenylated product in high conversions (entries 3-5). A number of silver(I) oxidants were employed in the reaction methodology

(entries 6-7) however none gave superior yields to $Cu(OAc)_2.H_2O$. Pleasingly the reaction performed more efficiently at lower temperatures (entry 8) giving a 95% conversion and 94% isolated yield. Despite this, when the catalyst and co-catalyst loadings were reduced the reaction conversions dropped (entry 9).

Table 1: Optimization of ruthenium(II)-catalyzed C–H alkenylation of *N*-arylhydantoin[a]

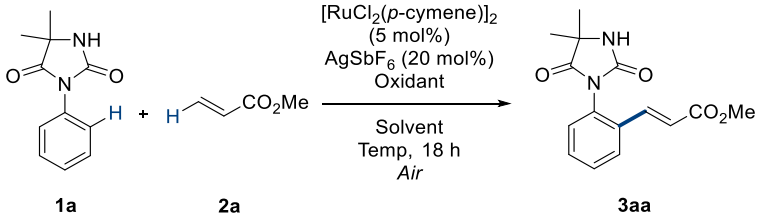

1a **2a** **3aa**

Entry	Solvent	Oxidant (1 eq)	Temp (°C)	3a (%)[b]
1	H_2O	$Cu(OAc)_2{\cdot}H_2O$	120	0
2	AcOH	$Cu(OAc)_2{\cdot}H_2O$	120	0
3	2-MeTHF	$Cu(OAc)_2{\cdot}H_2O$	120	85
4	THF	$Cu(OAc)_2{\cdot}H_2O$	120	74
5	DME	$Cu(OAc)_2{\cdot}H_2O$	120	81
6	2-MeTHF	AgOAc	120	39
7	2-MeTHF	AgO_2CCF_3	120	0
8[c]	**2-MeTHF**	**$Cu(OAc)_2{\cdot}H_2O$**	**100**	**95 (94)[d]**
9[c,e]	2-MeTHF	$Cu(OAc)_2{\cdot}H_2O$	100	70

[a]Standard Reaction Conditions: **1a** – 0.25 mmol, methyl acrylate – 0.75 mmol, $[RuCl_2(p\text{-cymene})]_2$ – 0.0125 mmol, $AgSbF_6$ – 0.05 mmol), Oxidant – 0.25 mmol, Solvent – 1 mL. [b] ^1H NMR Conversions taken after silica filtration compared to 1,1,2,2-tetrachloroethane as internal standard. [c]Reaction performed at 100 °C. [d] Isolated Yield. [e]Reaction performed using $[RuCl_2(p\text{-cymene})]_2$ – 2.5 mol% and $AgSbF_6$ – 10 mol%.

Armed with optimal C–H alkenylation conditions the scope of this methodology was expanded allowing access to a large number of potentially active pharmaceutical/agrochemical analogues. The nature of the coupling partners and of aromatic functionality was initially investigated (Scheme 2). Three different electron deficient alkenes were employed in the alkenylation reaction giving ethyl, *n*-butyl and benzyl derivatives (**3ab-ac**). Despite high yields, *n*-butyl example (**3ac**) was inseparable via standard chromatographic techniques from the starting material and was obtained in a yield of 94% as a 5:1 mixture giving a 78% NMR yield. Various aryl functionality was then introduced in order to examine electronic and steric effects on the efficiency and selectivity of the reaction. A wide range of alkoxy, alkyl and halogen functionality was tolerated (**3b-3f**) with highest yields obtained with electron rich aromatics. Trifluoromethyl derivative (**3g**) was synthesized in reduced yield, however allowed efficient functionalization of electron

poor aromatics. Compounds containing both *meta*- and *para*- functionality (**3h-i**) were obtained in high yields with excellent selectivity of functionalization in the least hindered *ortho*-position.

Scheme 2: Ruthenium(II) catalyzed C–H alkenylation of *N*-arylhydantoin derivatives

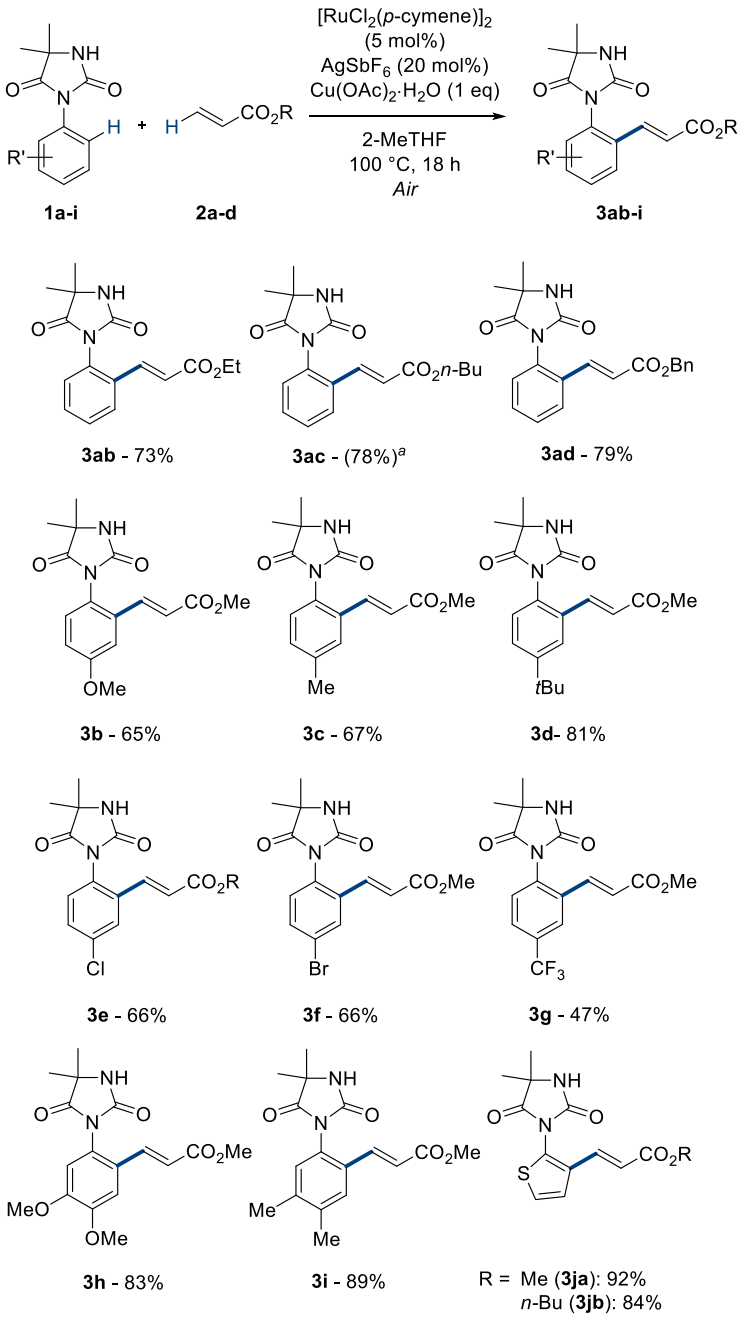

[a] = Isolated as an inseparable 5:1 mixture of **3ac**:**1a**. 78% depicts contribution from **3ac** (94% total yield)

A heteroaromatic variant was investigated under the conditions in order to expand the scope of sp^2 sites that are available for functionalization. Thiophene example (**1j**) was shown to

be alkenylated under the optimized conditions in excellent yields with both methyl and butyl acrylate coupling partners with no chromatographic separation issues.

The hydantoin heterocycle is commonly synthesized from naturally occurring amino acids which are a very attractive synthetic feedstock. Six examples were synthesized from natural and unnatural amino acids: glycine, valine, leucine, proline, homocycloleucine and sarcosine (Scheme 3).[3,7] This showed that multiple hydantoin heterocycles were tolerated as directing groups however the bare glycine derivative (**1k**) only afforded alkenylated product in reduced yields. Bicyclic and spirocyclic directing groups derived from proline (**1n**) and cyclohomoleucine (**1o**) gave rise to good to excellent yields of C–H alkenylated products (**3n**-**ob**), granting access to highly decorated structures. Sarcosine derived hydantoin (**1p**) showed that compounds containing NH-functionalization were also tolerated well.

Scheme 3: Ruthenium(II) Catalyzed C–H Alkenylation of Hydantoin Derivatives

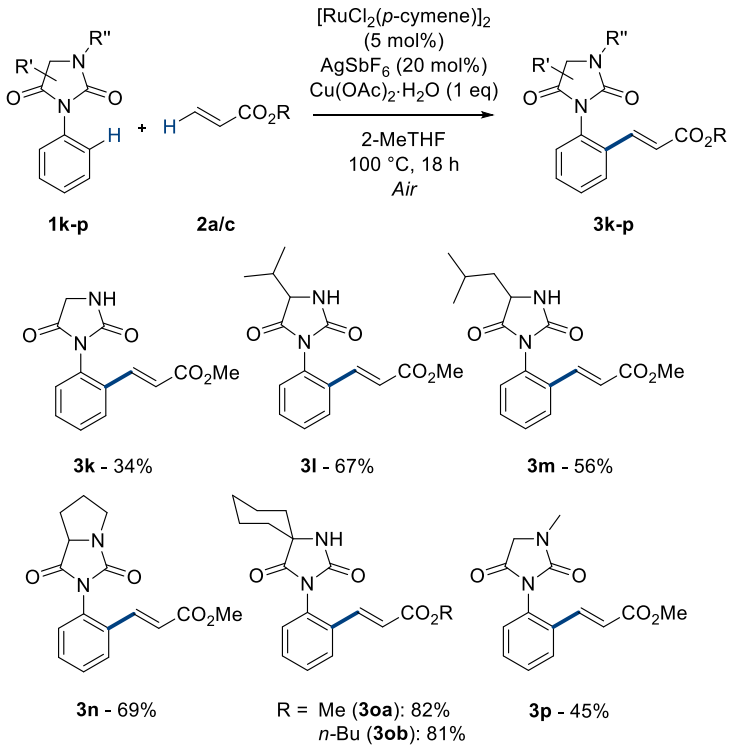

It was now of paramount interest to submit the drug structure nilutamide (Nilandron) to the reaction conditions in order to probe reactivity (Scheme 4). Despite the highly electron poor nature of the ring (containing both CF_3 and NO_2 substituents) formation of product was observed, albeit in low isolated yield. This manifests that this methodology can be used to create direct analogues of nilutamide itself as well as a selection of structural analogues.

Scheme 4: Nilutamide Functionalization

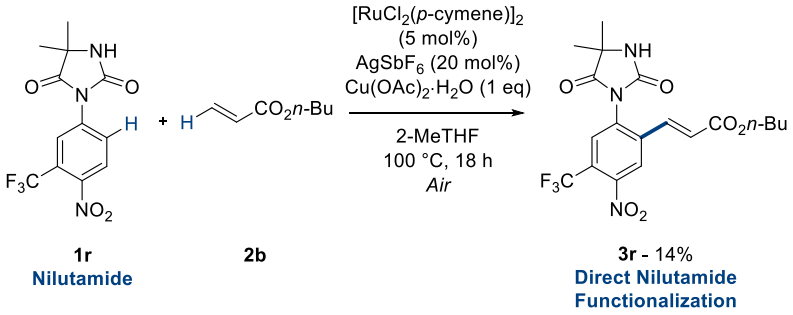

Intermolecular competition experiments were performed using electron-rich (**1b**) and an electron poor (**1e**) substrates. It was shown that the C–H alkenylation of electron rich substituents is preferred as a ratio of ~6:4 was observed (Scheme 5). This can be rationalized by the C–H activation occurring *via* an electrophilic-type activation mode by a cationic ruthenium catalyst. It is also proposed that the more electron rich and less sterically hindered urea directs the C–H functionalization (see supporting information, Scheme S1).[8]

Scheme 5: Intermolecular Competition Studies

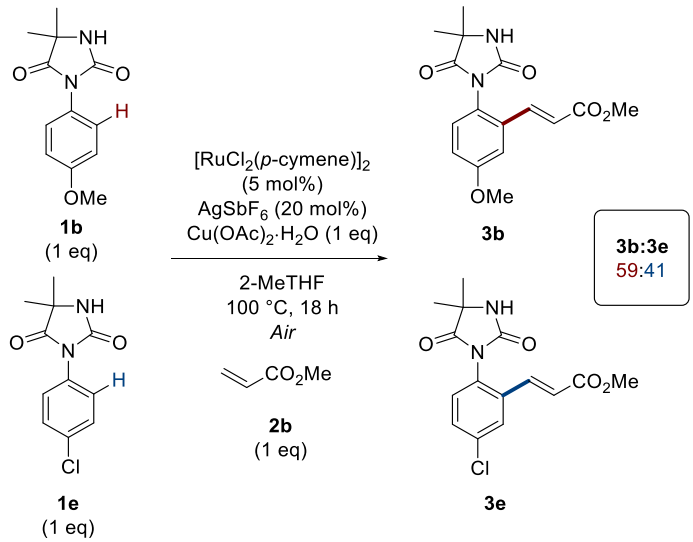

Our previous work depicts the functionalization of the biologically active oxazolidinone scaffold which bears a similar directing heterocyclic motif.[2a] Due to this, a competition experiment was carried out between the groups reacting them in equimolar quantities with one equivalent of methyl acrylate to probe how the directing groups compete for the coupling partner (Scheme 6). The investigation showed that the oxazolidinone

heterocycle competed more favorably for the acrylate as a 1:4 mixture of Hydantoin:Oxazolidinone was observed in NMR spectra.

Scheme 6: Competition Experiment with Oxazolidinone Directing Group

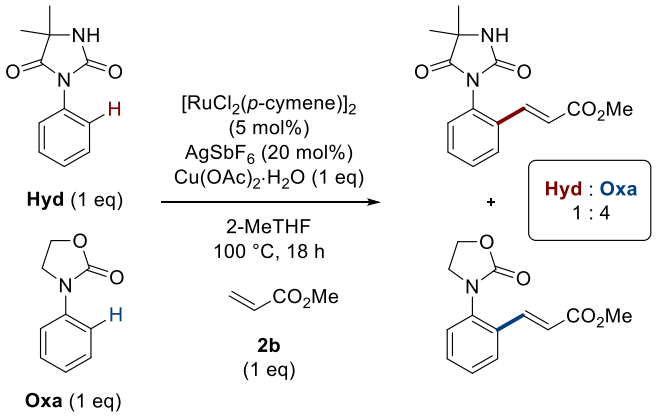

The succinimide group is also structurally similar to the hydantoin heterocycle. Due to this, it was of interest to explore whether this could also act as an efficient directing group in directed transition metal-catalyzed C–H functionalization, as to our knowledge its utility has not yet been investigated. Our previous reports have also indicated how such subtle electronic differences can strongly affect reaction efficiency.[2a]

Four *N*-arylsuccinimide derivatives were synthesized and submitted to the optimized reactions conditions (Scheme 7). However, in this case, it was found that slightly higher temperatures were necessary to allow the reaction to proceed efficiently. The yields are modest to poor, however this provides the first example of the use of the succinimide directing group, and is in the process of being explored further.

Scheme 7: Succinimide Directed Ruthenium-Catalyzed C–H Alkenylation

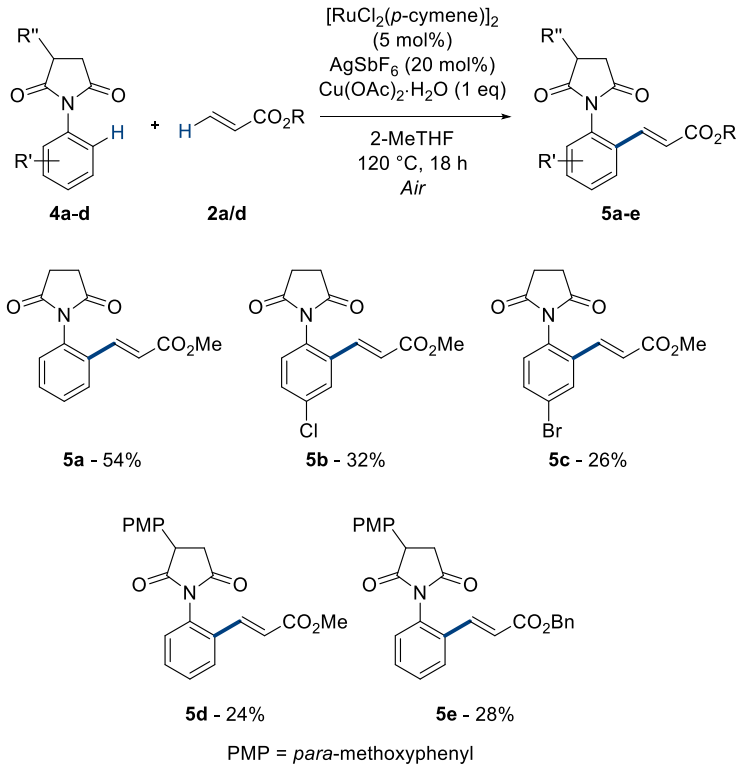

In conclusion we have utilized ruthenium(II)-catalyzed *ortho*-C–H alkenylation to derivate a large scope of biologically relevant *N*-arylhydantoins with yields of 14-94%. The reaction methodology also favorably takes place in the green solvent 2-MeTHF and absolute mono-selectivity was observed throughout the project. This report includes the application of this methodology to hydantoin directed C–H derivation of an anti-androgen API, nilutamide. We have also reported the first use of the succinimide directing group in directed C–H functionalization with limited but varied scope.

ASSOCIATED CONTENT

Supporting Information

NMR spectra for novel compounds and supporting spectra for competition experiments are included in the supporting information

AUTHOR INFORMATION

Corresponding Author

*C.G.Frost@bath.ac.uk

Notes

The authors declare no competing financial interests.

ACKNOWLEDGMENT

The authors would like to thank the University of Bath and Syngenta for funding and John Lowe for his NMR expertise.

REFERENCES

(1) For reading on biologically relevant hydantoin scaffolds see: (a) Labrie, F.; Dupont, A.; Belanger, A.; Lacoursiere, Y.; Raynaud, J. P.; Husson, J. M.; Gareau, J.; Fazekas, A. T. A.; Sandow, J.; Monfette, G.; Girar, J. G.; Emond, J.; Houle, J. G. *Prostate*, **1983**, *4*, 579-594. (b) Payen, O.; Top, S.; Vessières, Brulé, E.; Plamont, M-A.; McGlinchey, M. J.; Müller-Bunz, H.; Jaouen, G. *J. Med. Chem.* **2008**, *51*, 1791-1799. (c) Ivachtchenko, A. V.; Ivanenkov, Y. A.; Mitkin, O. D.; Vorobiev, A. A.; Kuznetsova, I. V.; Shevkun, N. A.; Koryakova, A. G.; Karapetian, R. N.; Trifelenkov, A. S.; Kravchenko, D. M.; Veselov, M. S.; Chufarova, N. V. *Eur. J. Med. Chem.* **2015**, *99*, 51-66. (d) Helsen, C.; Van den Broeck, T.; Voet, A.; Prekovic, S.; Van Poppel, H.; Joniau, S.; Claessens, F. *Endocr. Relat. Cancer*, **2014**, *T105-T118*. (e) Marton, J.; Enisz, J.; Hosztafi, S.; Timar, T. *J. Agric. Food Chem.* **1993**, *41*, 148-152. (f) Rogawski, M. A.; Löscher, W. *Nature Reviews Neuroscience,* **2004**, *5*, 553-564. (g) Cachet, N.; Genta-Jouve, G.; Regalado, E. L.; Mokrini, R.; Amade, P.; Culioli, G.; Thomas, O. P. *J. Nat. Prod.*, **2009**, *72*, 1612-1615.

(2) For reading on use of bioactive heterocycles as directing groups see: (a) Leitch, J. A.; Wilson, P. B.; McMullin, C. L.; Mahon, M. F.; Bhonoah, Y.; Williams, I. H.; Frost, C. G. *ACS Catal.*, **2016**, *6*, 5520-5529. (b) Yamaguchi, J.; Yamaguchi, A. D.; Itami, K. *Angew. Chem. Int. Ed*. **2012**, *51*, 8960-9009. (c) Liu, P. M.; Frost, C. G. *Org. Lett*. **2013**, *15*, 5862-5865. (d) Brown, J. A.; Cochrane, A. R.; Irvine, S.; Kerr, W. J.; Mondal, B.; Parkinson, J. A.; Paterson, L. C.; Reid, M.; Tuttle, T.; Andersson, S.; Nilsson, G. N. *Adv. Synth. Catal*. **2014**, *356*, 3551-3562. (e) Sunke, R.; Kumar, V.; Ramarao, E. V. V. S.; Bankala, R.; Parsa, K. V. L; Pal, M. *RSC Adv.* **2015**, *5*, 7064-70608.

(3) Fernández-Nieto, F.; Roselló, J. M.; Lenoir, S.; Hardy, S.; Clayden, J. *Org. Lett.*, **2015**, *17*, 3838-3841.

(4) For reading on ruthenium-catalyzed C–H functionalization see: (a) Ackermann, L. *Chem. Rev.* **2011**, *13*, 3075-3078, (b) Arockiam, P. B.; Bruneau, C.; Dixneuf, P. *Chem. Rev*. **2012**, *112*, 5879−5918. (c) Dixneuf, P. H.; Bruneau, C. *Ruthenium in Catalysis*; Topics in Organometallic Chemistry; Springer: New York, NY, 2014. (d) Ueyama, T.; Mochida, S.; Fukutani, T.; Hirano, K.; Satoh, T.; Miura, M. *Org. Lett.*, **2011**, *13*, 706-708. (e) Saidi, O.; Marafie, J.; Ledger, A. E. W.; Liu, P. M.; Mahon, M. F.; Kociok-Köhn, G.; Whittlesey, M. K.; Frost, C. G. *J. Am. Chem. Soc*. **2011**, *133*, 19298-19301. (f) Ackermann, L. *Acc. Chem. Res.* **2014**, *47*, 281-295.

(5) (a) De Sarkar S.; Liu, W.; Kozhushkov, S. I.; Ackermann, L. *Adv. Synth. Catal*. **2014**, *356*, 1461-1479. (b) Ackermann, L.; Pospech, J. *Org. Lett*. **2011**, *13*, 4153-4155. (c) Ackermann, L.; Lygin, A. V.; Hofmann, N. *Angew. Chem. Int. Ed*. **2011**, *50*, 6379-6382. (d) Li, J.; Kornhaass, C.; Ackermann, L. Chem. Commun., **2012**, *48*, 11343-11345.

(6) (a) Padala, K.; Jeganmohan, M. *Org. Lett*. **2012**, *14,* 1134-1137. (b) Padala, K.; Jeganmohan, M. *Org. Lett*. **2011**, *13*, 6144-6147. (c) Reddy, M. C.; Jeganmohan, M. *Chem. Commun*. **2014**, *51*, 10738-10741. (d) Manikandan, R.; Madasamy, P.; Jeganmohan, M. *ACS Catal.*, **2015**, *6*, 230-234.

(7) Liu, H.; Yang, Z.; Pan, S. *Org. Lett.*, **2014**, *16*, 5902-5905.

(8) For examples of urea directed transition metal catalyzed C–H functionalization see (a) Houlden, C. E.; Hutchby, M.; Bailey, C. D.; Ford, J. G.; Tylder, S. N. G.; Gagné, M. R.; Lloyd-Jones, G. C.; Brooker-Milburn, K. I. *Angew. Chem. Int. Ed.*, **2009**, *48*, 1830-1833. (b) Wang, L.; Liu, S.; Li, Z.; Yu, Y. *Org. Lett.*, **2011**, *13*, 6137-6139.

Chapter 3: *meta* – Ruthenium Catalysed Remote C–H Functionalisation of Heteroaromatics *via* σ-Activation

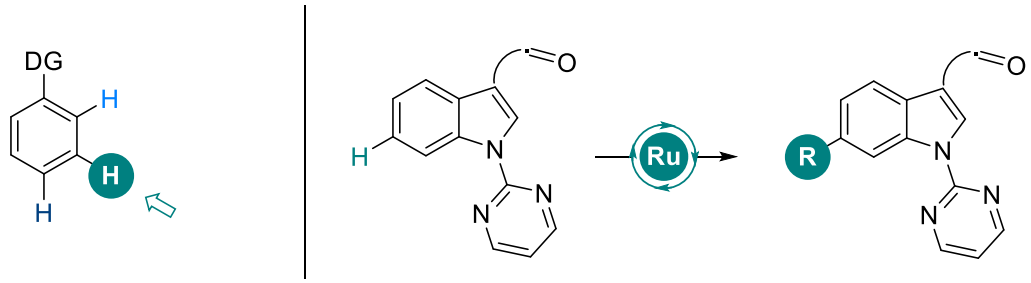

3.1: Chapter Introduction - Breaking the Phenylpyridine Monopoly

Still in its infancy, the technique of σ-activation for remote *meta*-functionalisation has relied heavily on the use of phenylpyridine as a template thus far. Phenylpyridine forms an incredibly strong and planar ruthenacycle making it the perfect candidate for investigation into these types of reactions. Unfortunately, the utility (and more importantly lack of utility) of the phenylpyridine structure has brought into question the broad synthetic value of this methodology. There has been effort towards expanding the scope of these transformations away from privileged motifs. Other strongly coordinating directing groups such as pyrazoles, benzimidazoles, imidazoles, pyrimidine, pyrazine, purines and ketimines have been employed in a few examples, although this is often at the expense of increased catalyst loading and/or lower yields. Ackermann and co-workers however have reported a large-scale investigation into the use of *N*-pyrimidinyl anilines as auxiliaries for *meta*-functionalisation (Scheme 3-1).[1]

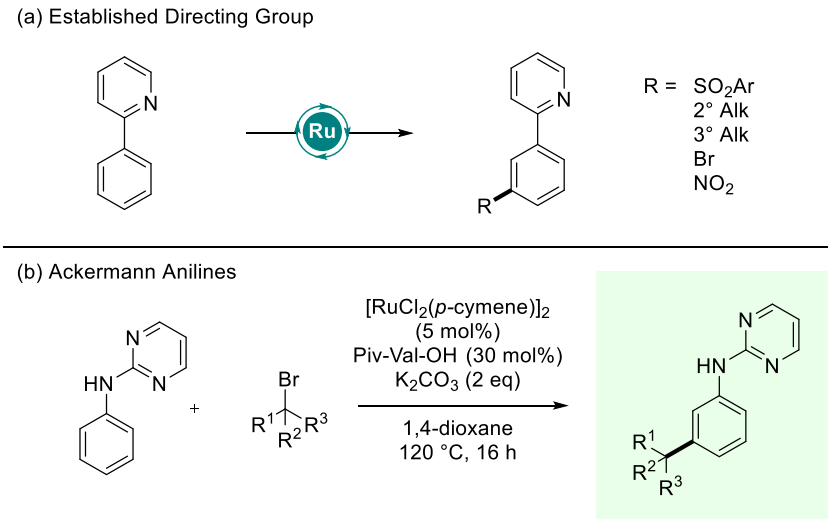

Scheme 3-1: *Meta*-Functionalisation of Heteroaromatics via α-Activation

At the start of this project, only Ackermann's report was present in the literature on removable auxiliaries however since then, as discussed in Chapter 1, there has been efforts to expand this methodology in diazo[2] and oxygen[3] bridged biaryls primarily by Li and co-workers (Scheme 3-2).

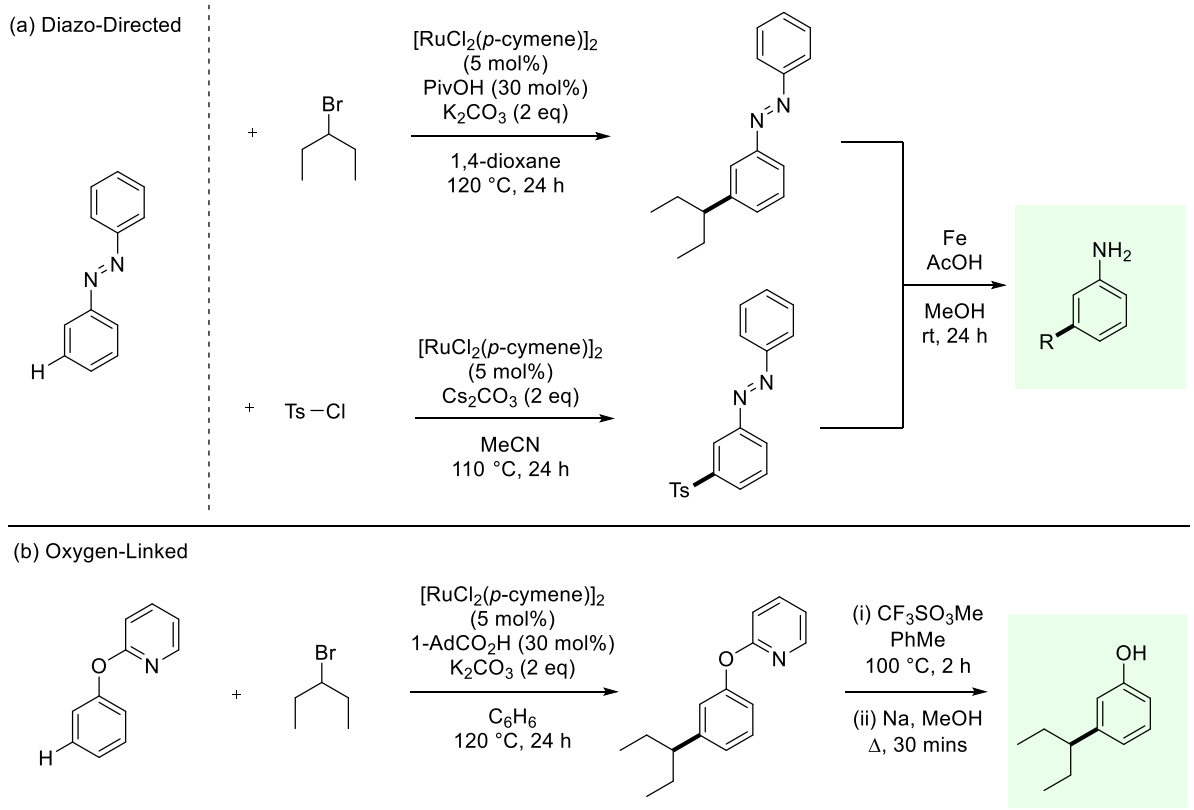

Scheme 3-2: Ruthenium-Catalysed *meta*-C–H Functionalisation of Cleavable Auxiliaries

The work carried out in this chapter revolves around the developments of scaffolds for remote σ-activation. This began with the investigation into different sulphur-linked biaryls and continued into the remote functionalisation of indole and carbazole derivatives. This chapter will initially be introduced using a perspective that was written for ACS Catalysis in 2017 on techniques for the C–H functionalisation of indole on the benzenoid ring. This review will underline the strategic importance and key developments in the synthetic toolkit for selective and effective C–H functionalisation of biologically relevant structures such as indoles and related heteroaromatics e.g. carbazoles.

References

(1) J. Li, S. Warratz, D. Zell, S. De Sarkar, E. E. Ishikawa, and L. Ackermann, *J. Am. Chem. Soc.*, 2015, **137**, 13894

(2) G. Li, X. Ma, C. Jia, Q. Hin, Y. Wang, J. Wang, L. Yu, and S. Yang, *Chem. Commun.*, 2017, **53**, 1261

(3) G. Li, X. Luv, K. Guo, Y. Wang, S. Yang, L. Yu, Y. Yu, and J. Wang, *Org. Chem. Front.*, 2017, **4**, 1145

(4) G. Li, P. Gao, X. Luv, C. Qu, Q. Yan, Y. Wang, S. Yang, J. Wang, *Org. Lett.*, 2017, **19**, 2682

3.2: Beyond C2 and C3: Transition-Metal-Catalyzed C–H Functionalization of Indole

3.2.1: Authorships and Permissions

This declaration concerns the article entitled									
Beyond C2 and C3: Transition-Metal-Catalyzed C–H Functionalization of Indole									
Publication status (tick one)									
Draft manuscript		**Submitted**		**In review**		**Accepted**		**Published**	X
Publication details (reference)	J. A. Leitch, Y. Bhonoah, and C. G. Frost, *ACS Catal.*, 2017, **7**, 5618.								
Candidate's contribution to the paper (detailed, and also given as a percentage)	The candidate contributed to/ considerably contribute to/predominantly execute the: **Formulation of ideas (80%)**: JAL had the idea for the review and was then discussed with CGF (20%) **Design of methodology**: N/A **Experimental work**: N/A **Presentation of data in journal format (80%)**: JAL wrote all of the manuscript. Manuscript was edited by CGF (15%) and looked over by YB (5%)								
Statement from Candidate	This paper reports on original research I conducted during the period of my Higher Degree by Research candidature								
Signed	Jamie A. Leitch						**Date**	14/09/17	

3.2.2: Manuscript for "Beyond C2 & C3: Transition Metal Catalyzed C–H Functionalization of Indole"

Complete manuscript given at point of corrections follows on the next page. Layout changes have been made for consistency for this thesis. Contents remain unchanged.

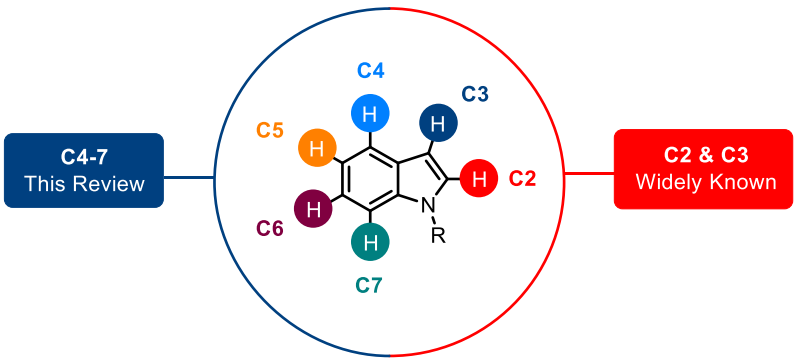

Beyond C2 & C3: Transition-Metal Catalyzed C–H Functionalization of Indole

Jamie A. Leitch,† Yunas Bhonoah,‡ and Christopher G. Frost*,†

†Department of Chemistry, University of Bath, Claverton Down, Bath, Somerset, BA2 7AY, United Kingdom

‡Syngenta, Jealott's Hill International Research Centre, Bracknell, Berkshire, RG42 6EY, United Kingdom

ABSTRACT: The indole scaffold will continue to play a vital part in the future of drug discovery and agrochemical development. Due to this the necessity for elegant techniques to enable the selective C–H functionalization is vast. Early developments have led to primarily C2 and C3 functionalization due to the inherent reactivity of the pyrrole ring. Despite this, elegant methods have been developed to enable selective C–H functionalization on the benzen moiety at C4, C5, C6 & C7. This review focuses on the contributions made in benzenoid C–H functionalization of indoles and other related heteroaromatics such as carbazoles.

INTRODUCTION

The indole heteroaromatic and has become one of the most widely studied organic templates over the past century.[1] This is due to their wide prevalence in the natural world and biologically active structures (Figure 1a).[2] The indole alkaloid motif itself is a bacterial intercellular signal molecule, and is also present in the natural amino acid tryptophan, the neurotransmitter serotonin, the plant growth hormone auxin, a number of marketed drugs sumatriptan (migraine), indomethacin (anti-inflammatory) and ondansetron (nausea) and bioactive hallucinogens such as dimethyltryptamine and LSD. From the review “Rings in Drugs” by Taylor, it is reported that the indole ring is present in 24 current marketed pharmaceuticals, where it lies as the 4th most prevalent heteroaromatic.[3]

The biological relevance of the indole scaffold has pushed it through to the forefront of synthetic developments. Classical syntheses such as the Fischer,[4] Bartoli,[5] and Larock[6] have become universally used, amongst a multitude of other synthetic protocols.[7] The

indole scaffold has also been a key substrate in the development of C–H functionalization methodologies for its synthesis and modification (Figure 1b).[8] Whilst these methods effectively grant access to the bicyclic system, they require the requisite functionality of the indole ring to be pre-installed on the organic reagents.

Transition metal-catalyzed C–H functionalization has emerged as a powerful tool for the late stage modification of biologically relevant structures such as indoles.[9] The synthetic toolbox has expanded to utilize a variety of metal catalysts using multiple different techniques to install a huge selection C-C and C-X bonds.[10] Effective C–H activation is achieved either via a reactive metal centre or through chelation assistance to a directing group.[11]

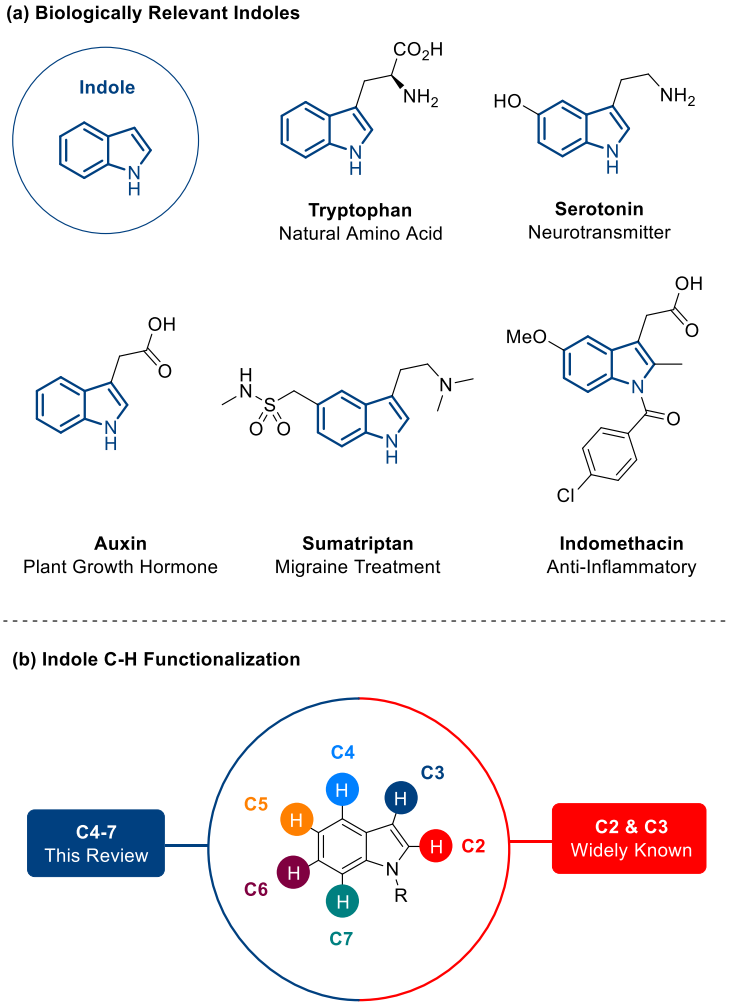

Figure 1: (a) Biologically Relevant Motifs Containing the Indole Heteroaromatic (b) Site Selective Indole C–H Functionalization

The indole scaffold has been widely used in both direct and directed C–H functionalization at C2 and C3, as covered in depth in an excellent review by Sandtorv.[12] There have also been a few elegant examples of systems that allow a reaction condition dependent switch between C2 and C3 functionalization.[12c-d,13]

Due to the inherent reactivity of the pyrrole-type ring, the development of methodologies to enable site selective C–H functionalization on the benzenoid ring has remained a great challenge in catalysis.[14] Despite this there have been a variety of elegant methods developed that will be discussed in detail herein, where this review will focus on accessing reactivity in less activated positions, at C4, C5, C6 & C7. These will be herein colour coded as in Figure 1b. The benzenoid C–H functionalization of related heteroaromatics such as carbazoles and benzothiophenes will also be discussed when relevant.

FUNCTIONALIZATION AT C4

The C4 position of an indole has been accessed almost exclusively through blocking the C3 position. This would then deem the C4 position the next most electron rich carbon centre on the indole structure. Jia and co-workers reported the direct C4 alkenylation of tryptophan derivatives employing palladium catalysis (Scheme 1). This reaction methodology gave complete selectivity for C4 however relatively high catalyst loadings and long reaction times were needed for more challenging substrates.[15]

Scheme 1. Palladium-Catalyzed C4 Alkenylation of Tryptophan Derivatives

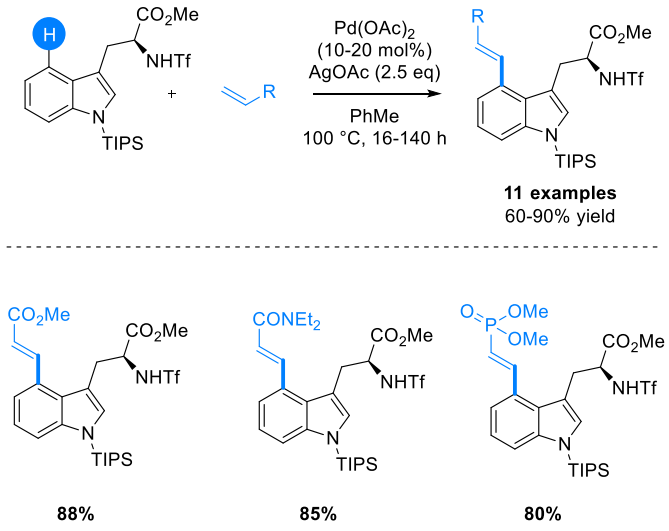

Following on from this seminal example of C4 functionalization, Prabhu and co-workers reported the complementary ruthenium-catalyzed alkenylation. This was proposed

to take place by the furnishing of C3 with an aldehyde directing group. It was shown that this directing group favoured forming a 6-membered transition state at C4 over a five membered metalacycle at C2 (Scheme 2). This alkenylation reaction was shown to be tolerant of a wide range of alkene coupling partners including acrylates, acrylonitrile, styrenes, and vinyl ketones.[16]

Scheme 2. Ruthenium-Catalyzed C4 Selective C–H Alkenylation of Indole-3-carboxaldehydes

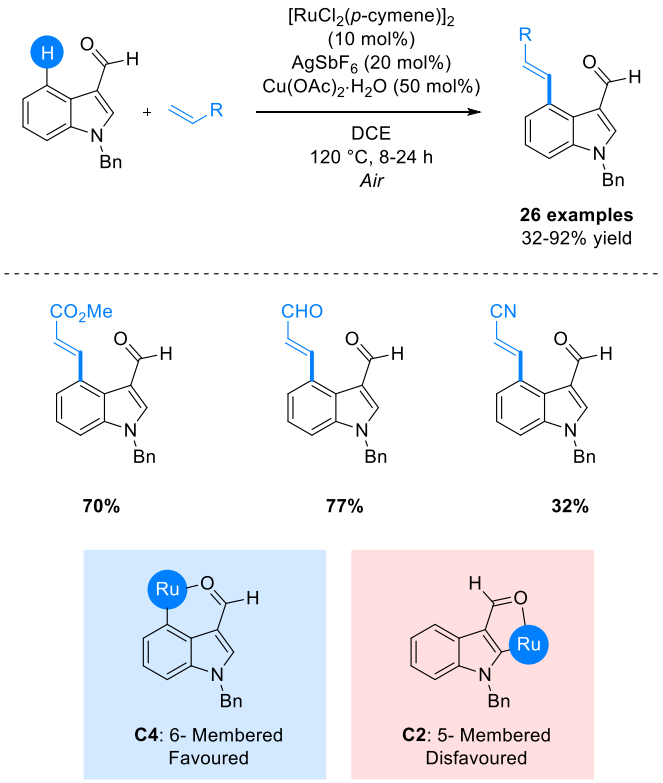

In 2017, Prabhu reported the use of a C3-aldehyde directing group in selective C4 amidation of free indoles. This reinforces the concept that the aldehyde directing group preferentially assist in C4 metalation (Scheme 3). This methodology permitted access to C4-substituted sulfonamides which were shown to be deprotected to give the corresponding aminoindole.[17]

Scheme 3. Iridium-Catalyzed C4-Sulfonamidation of Indole Derivatives

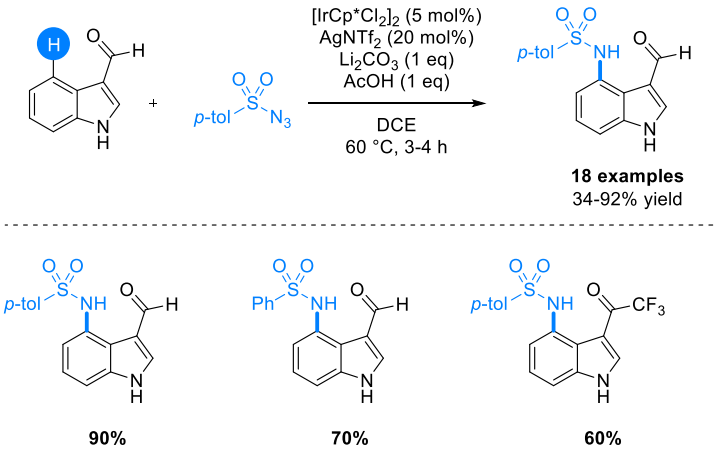

Prabhu and co-workers succeeded this with further insight into C4 vs C2 selectivity by developing complementary ketone directing groups at C3 where the methyl derivative selectively facilitated C–H functionalization at C2 under ruthenium catalysis, where the trifluoromethyl derivative exclusively gave C4 selectivity under complementary rhodium catalysis (Scheme 4). This along with the above investigation allowed the elucidation that stronger directing groups (COMe) carry out directed C–H insertion, giving C2 selectivity, and weaker directing groups (CHO, $COCF_3$) assist in the stabilisation of direct electrophilic metalation.[18]

Scheme 4. Directing Group/Metal Dependent C4 vs C2 C–H Functionalisation of 3-acylindole Derivatives

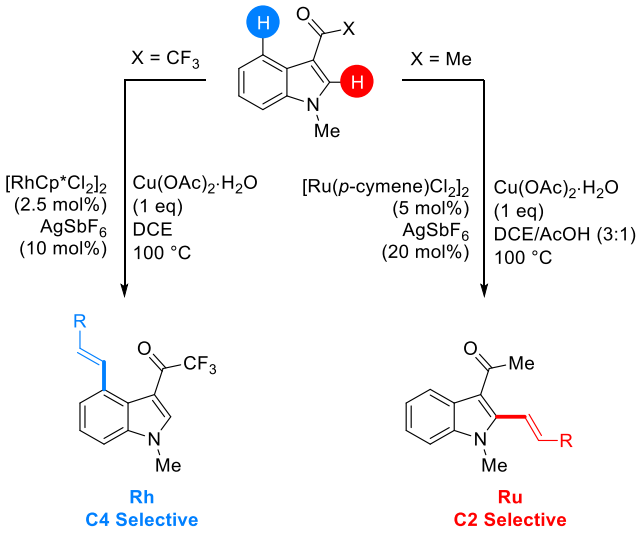

This work has been expanded upon by Zhang and co-workers where a carboxylic acid directing groups enables double C2 and C4 alkenylation using rhodium catalysis. This

di-alkenylated product then undergoes an *in-situ* decarboxylation to afford a free C3 position (Scheme 5).[19]

Scheme 5. Rhodium-Catalyzed C4 and C2 Di-alkenylation and *in situ* Decarboxylation

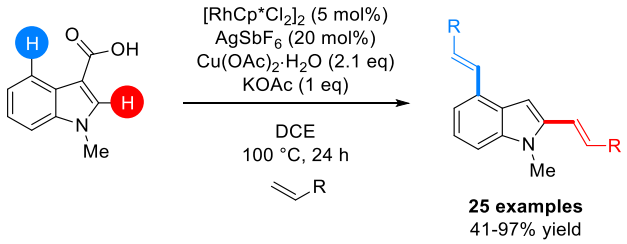

In 2017, Shi and co-workers have utilized this directing group strategy to enable the palladium catalyzed C4 selective C–H arylation of indole derivatives. Here the bulky pivaloyl directing group preferentially cyclopalladates at C4 and subsequent oxidative addition of the aryl iodide and reductive elimination gives the C4-arylated indole (Scheme 6). The pivalate directing group can also be readily cleaved to the proton using glycolic acid.[20]

Scheme 6. Palladium Catalyzed C4 Arylation of Indole Derivatives

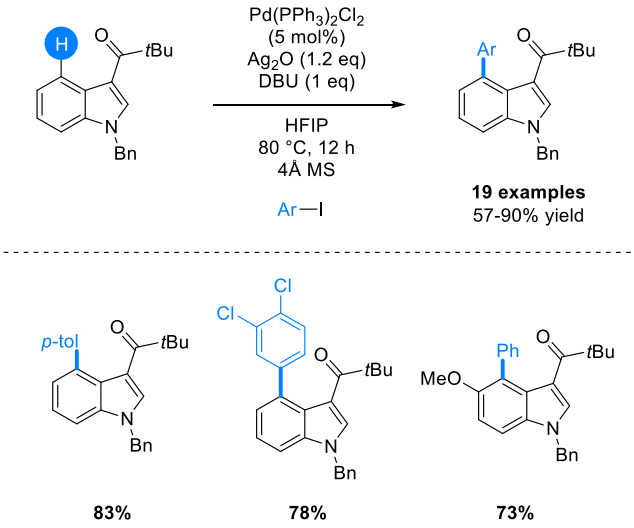

The same group also published the C4 alkylation of indoles in 2017, using hypervalent fluoroalkyl iodine reagents as coupling partners. Here, complementary to Prabhu's work,[18] they employed acetyl assistance to afford the relevant palladacycle to give the C4-substituted product (Scheme 7). The methodology was shown to be incredibly functional group tolerant, including boronate esters and benzothiophene. The directing group was again shown to be readily cleaved.[21]

Scheme 7. Palladium-Catalyzed C4 Alkylation of Indole Derivatives

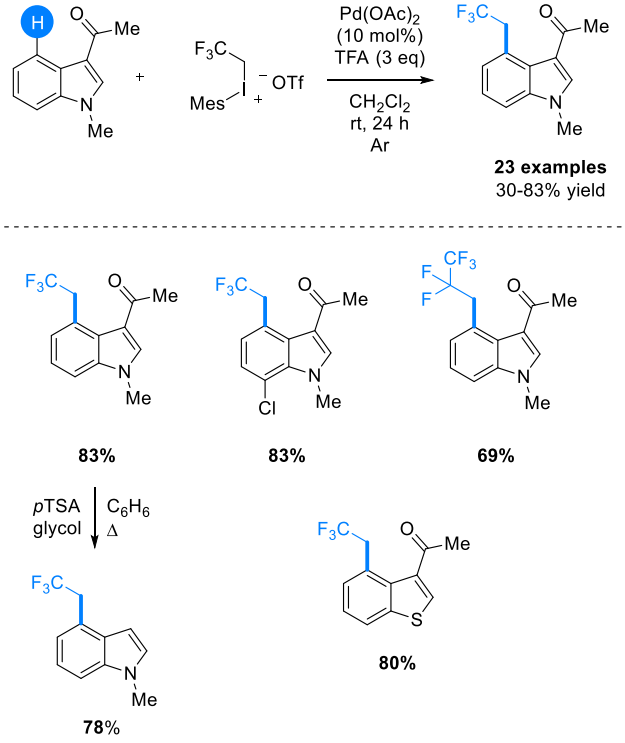

FUNCTIONALIZATION AT C7

The first report to access the C7 position came from Iwao and co-workers in 1999. Here they employed a specialized sterically demanding directing group to facilitate directed *ortho*-lithiation at the C7 position. they then showed they could quench this organolithium species with a variety of electrophiles including silanes, CO_2, DMF and alkyl groups (Scheme 8). Despite preferential selectivity for C7, C2 by-products were still observed in yields up to 13%.[22] This work was improved on in 2003 by Snieckus and co-workers. Here they detailed the use of a phosphonate directing group which was proposed to enact regioselectivity in a similar manner to above, however here the directing group was completely selective for C7.[23]

Scheme 8. C7 C–H Functionalisation of Indoles *via* Directed *ortho*-Lithiation

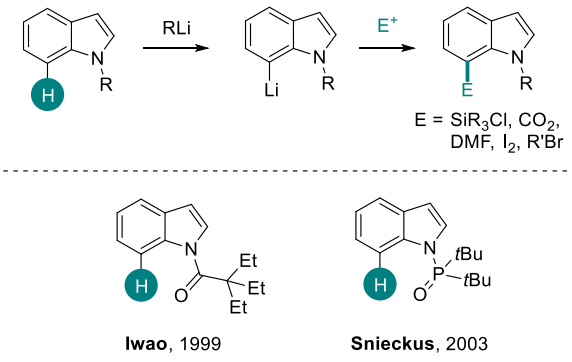

Shi and co-workers have recently devised a manner in which to apply Snieckus' directing group to transition metal catalysed C–H functionalization rather than directed *ortho*-lithiation. Here they use a pyridine ligand to enable palladium-catalyzed selective C–H arylation at C7 (Scheme 9). In this methodology competing direct C3 arylation was the main by-product observed although consistently in low quantities (with exception).[24]

Scheme 9. Palladium-Catalyzed C7 Arylation of Indoles

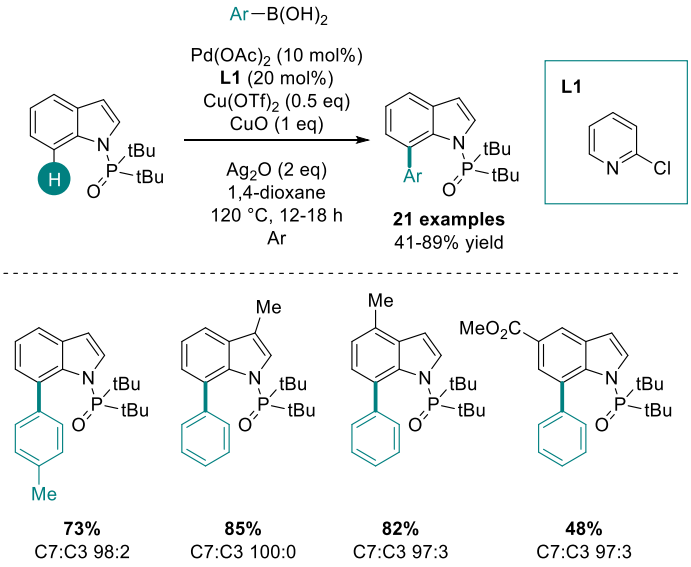

Ma and co-workers have also applied to the use of a sterically demanding directing group at N1 to afford C7 selectivity. Here the pivaloyl (CO*t*Bu) group acts as a weakly coordinating directing group for rhodium catalysis allowing C–H alkenylation (Scheme 10). The reaction methodology was shown to be widespread with 30 examples and yields up to 98%. Despite this the catalysis was not tolerant of C6 substitution and occasional competing C2 alkenylation was also observed in substantial quantities.[25]

Scheme 10. Piv Directed C7 Selective Rhodium-Catalyzed C–H Alkenylation of Indoles

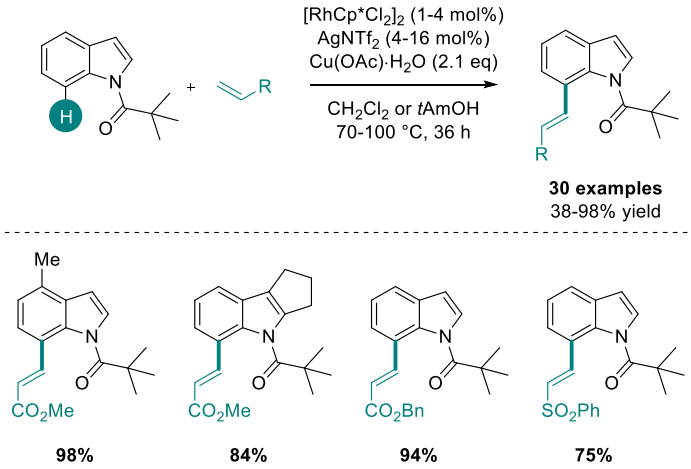

Pan and co-workers have also described the C7-selective rhodium catalyzed C–H alkenylation of indazole derivatives. Here a urea directing group is employed in the reaction methodology (Scheme 11). The catalysis was also shown to be amenable to both electron poor (acrylate) and electron rich (styrene) coupling partners.[26]

Scheme 11. Rhodium-Catalyzed C7-Selective C–H Alkenylation of Indole Derivatives

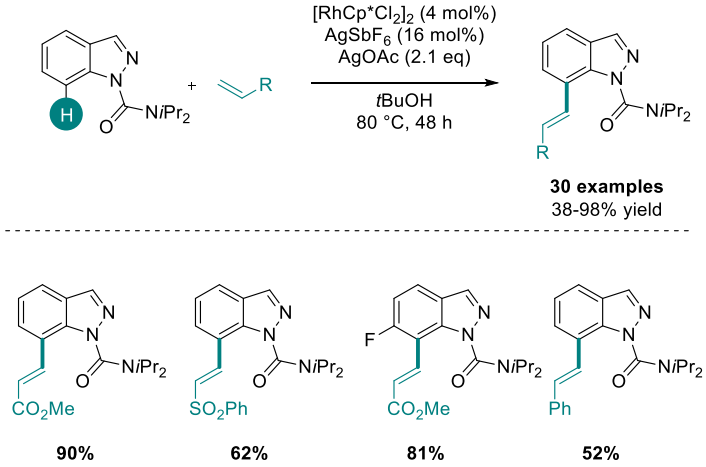

Shortly after the work from Ma, Antonchick applied the pivaloyl directing group to the C7 selective C–H sulfonamidation on indoles, this time employing iridium catalysis (Scheme 12). This methodology was shown to be applicable to aryl, heteroaryl and alkyl sulfonylazides and to be tolerant of C6 functionalization. Indole structures synthesized in this report were also shown to inhibit HeLa cell proliferation. This manifests the biological relevance of indole derivatives.[27]

Scheme 12. Piv Directed Iridium Catalyzed C–H Sulfonamidation of Indoles

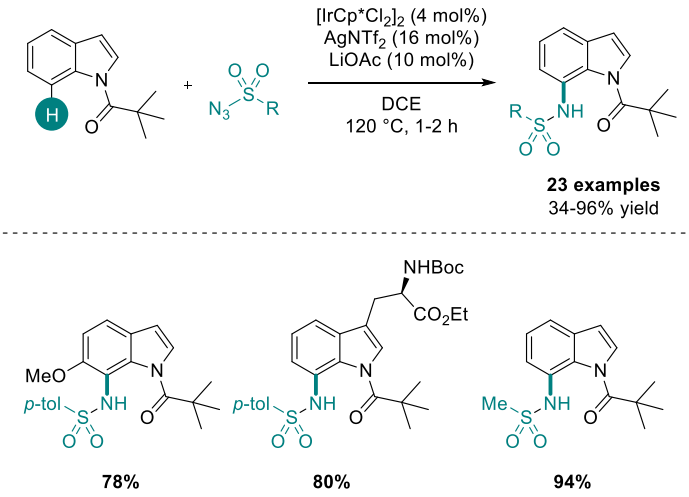

C7 functionalized indoles have been shown by multiple groups to be accessed *via* the indoline intermediate (Scheme 13). Here reduction of indoles, followed be directed C–H functionalisation and subsequent re-oxidation to the indole structure gave the desired product (Scheme 13). The C7 functionalization of indolines has been widely explored and has been applied to alkenylation,[28] alkylation,[29] arylation,[30] amidation,[31] acylation,[32] cyanation,[33] and chalcogenation[34] reactions using a variety of metal systems.

Scheme 13. C7 Functionalisation of Indolines to Access Indoles

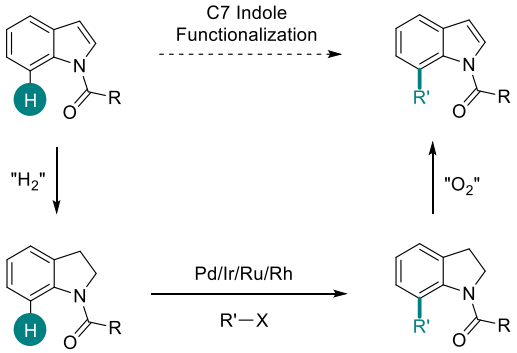

The above methodology functions *via* nullifying the reactivity of the C2 position towards directed metalation. This has also been used successfully by Smith and co-workers by using C2-substituted indoles in a C7 selective C–H borylation reaction (Scheme 14). Here the N–H is proposed to act as the directing group by coordinating the boronate ligand to enable site selective C–H iridation.[35] Interestingly the same group have also reported the selected protodeboronation of polyborylated indole derivatives using catalytic $Bi(OAc)_3$.[36]

Scheme 14. C7 Iridium Catalysed C–H Borylation of 2-Substituted Indoles

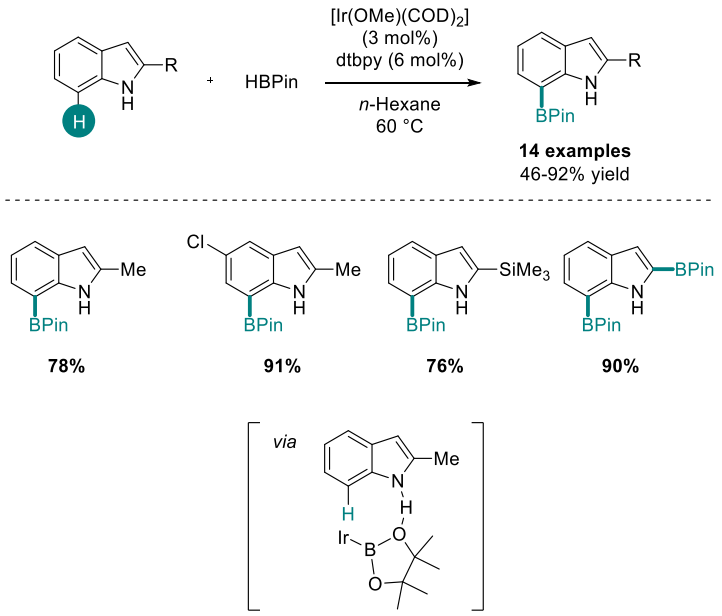

Movassaghi and co-workers expanded on this methodology by using Smith's reaction conditions on C2 free substrates, allowing C2 and C7 diborylation followed by a C2 selective acid promoted deborylation, affording solely the C7 borylated structure.[37] This methodology has also been applied under forcing conditions to afford the C2/5/7 triborylated indole.[38]

One of the most important examples of C7 C–H functionalisation of free indole came from the Hartwig group in 2010. They reported the iridium-catalysed C–H borylation on free indole with no other tricks to give the C7 functionalized product. Here they used a transient bulky silyl directing group to direct cycloiridation at C7 (Scheme 15). This methodology was shown to be incredibly selective and applicable to various substituted indoles as well as carbazoles and tetrahydroquinolines.[39]

Scheme 15. Iridium-Catalysed Silyl-Directed C–H Borylation at C7

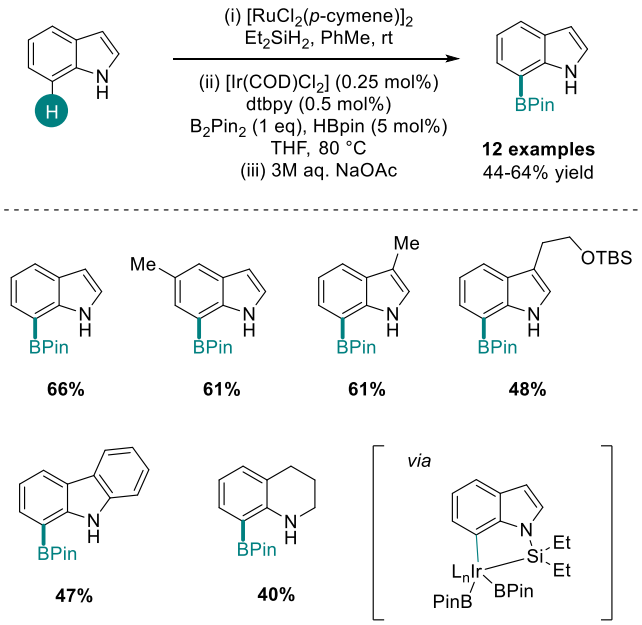

The C1-selective C–H functionalization of Carbazoles has also been explored *via* the furnishing of the NH with a directing group. A summary of the transformations, transition metal used and references is displayed in Scheme 16. This selectivity has been achieved in a wide number of systems as there is no competing direct selectivity observed at C2/C3 such as in indole.[40]

Scheme 16. Transition-Metal Catalyzed C–H Functionalization of Carbazole Derivatives

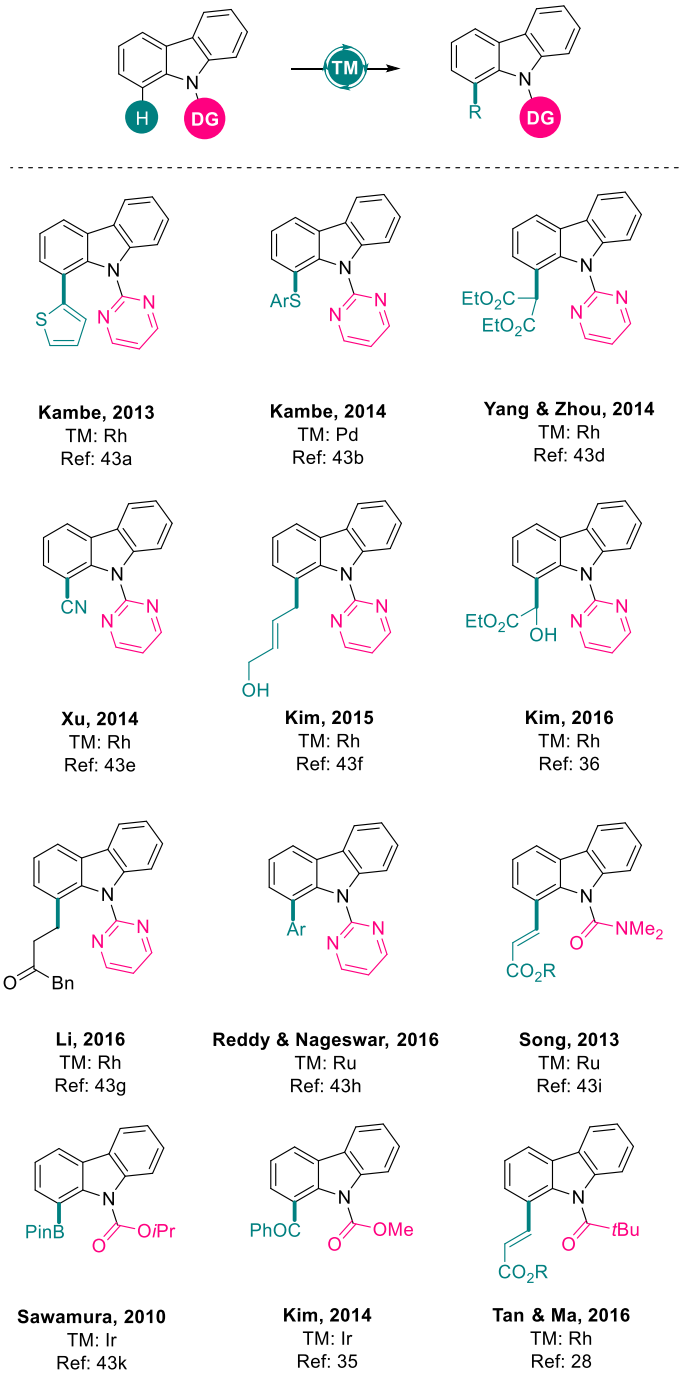

Kambe, 2013
TM: Rh
Ref: 43a

Kambe, 2014
TM: Pd
Ref: 43b

Yang & Zhou, 2014
TM: Rh
Ref: 43d

Xu, 2014
TM: Rh
Ref: 43e

Kim, 2015
TM: Rh
Ref: 43f

Kim, 2016
TM: Rh
Ref: 36

Li, 2016
TM: Rh
Ref: 43g

Reddy & Nageswar, 2016
TM: Ru
Ref: 43h

Song, 2013
TM: Ru
Ref: 43i

Sawamura, 2010
TM: Ir
Ref: 43k

Kim, 2014
TM: Ir
Ref: 35

Tan & Ma, 2016
TM: Rh
Ref: 28

FUNCTIONALIZATION AT C6

It has been demonstrated that the use of carefully tailored directing groups or reaction systems allow functionalization at C7. Unfortunately, the C6 position lies even more remote from a directing group, therefore other strategies have been employed to access this regioselectivity. These strategies have been more sparingly observed and more closely mimic those used for remote *meta*-functionalization.

The first to be discussed is the work by Baran and co-workers in 2015. They reported the remote C6 selective C–H borylation of tryptophan derivatives utilizing iridium chemistry. This selectivity was controlled by a bulky ligand to access the less hindered C–H bonds and selectivity issues were observed between C6 and C5 C–H borylation (Scheme 17). This was developed as the key step in the total synthesis of Verruculogen and Fumitremorgin natural products.[41]

Scheme 17. Iridium-Catalysed Ligand-Controlled C6 C–H Borylation

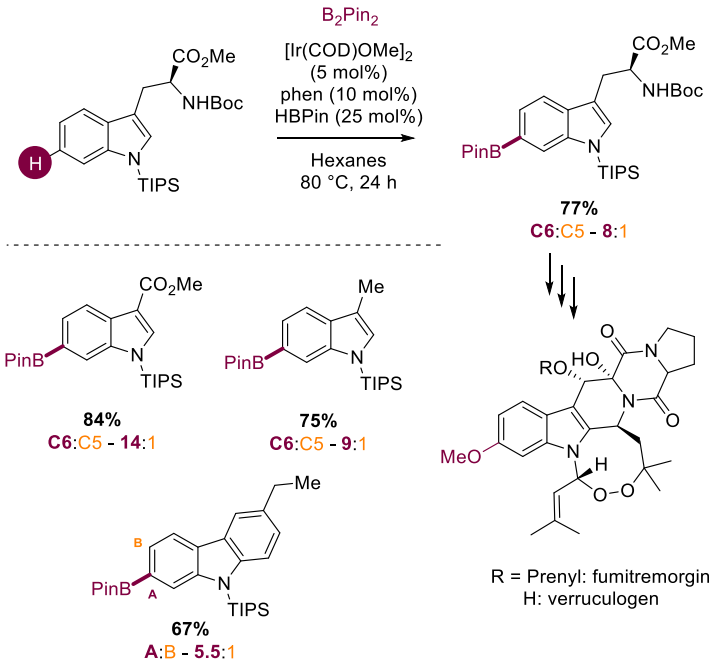

Yu and co-workers have pioneered the developments in remote functionalization *via* the use of a meticulously designed templated directing group.[42] From this, they have developed the remote C6 olefination, arylation and acetoxylation of indolines. Among the scope of this reaction there were two indole motifs which were functionalised in a C–H alkenylation reaction in good selectivity at C6 (Scheme 18). In both examples C2 and C3 are already functionalised. The template has been shown to be removable on the indole structures albeit under forcing conditions.[43]

Scheme 18. Template Controlled Palladium-Catalysed C–H Alkenylation of Indole Derivatives

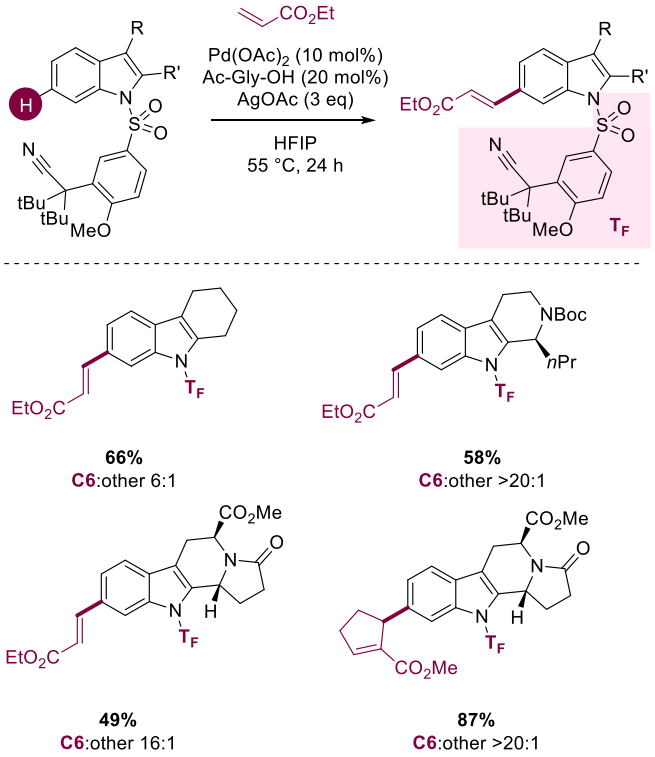

Shi and co-workers now applied established *meta*-selective C–H functionalization techniques to this *N*-phosphonate substituted indole. They successfully developed Gaunt's copper-catalyzed *meta*-arylation technique on this structure to afford C6 functionalized material in absolute selectivity, a feature which the previous two techniques have not provided (Scheme 19).[14h] A very wide scope with varying indole and coupling partner functionality was shown to be amenable to the reaction conditions. The reported mechanism entails coordination of a copper(III) species to the phosphonate directing group which on steric grounds preferentially positions itself towards the C7 proton. Here Cu-Ph across the double bond, followed by rearomatization gives the C6-arylated indole. The group also reported the C6-alkenylation using the corresponding hypervalent iodine salt.[44]

Scheme 19. Copper Catalyzed C6 Selective C–H Arylation of Indoles

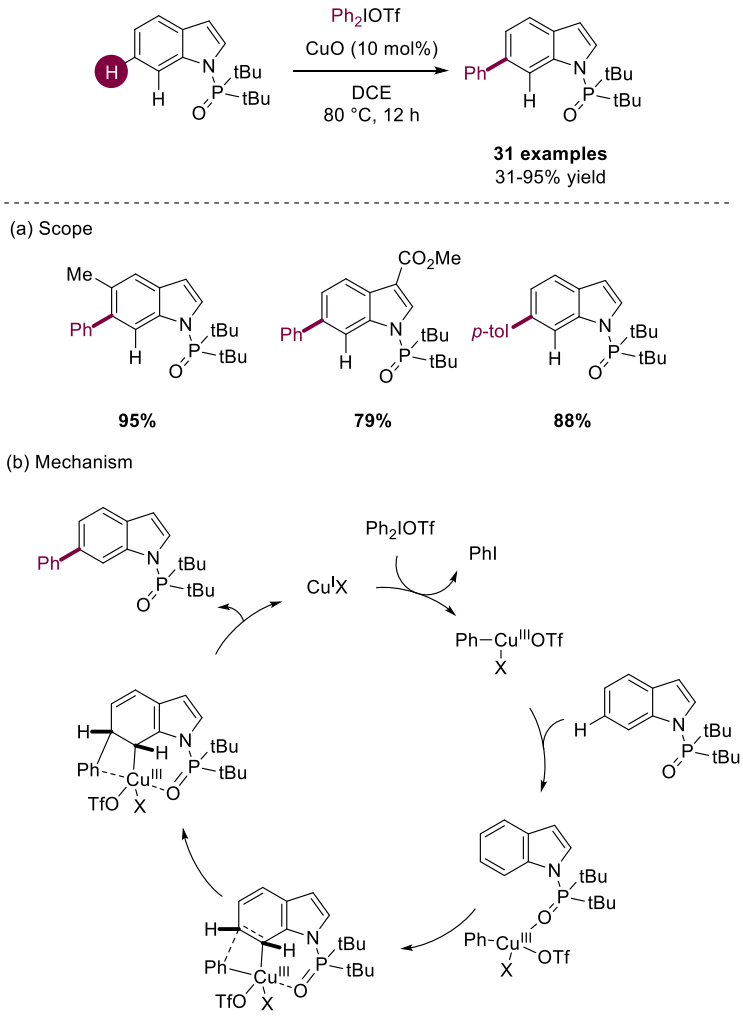

In 2014 You and Zheng developed the catalytic C6 functionalization C2/C3-disubstituted indoles using scandium triflate as catalyst. The reaction showed the indoles reacting with an aziridine in ring opening chemistry to afford C6 alkylated indoles after a reversible [3+2] annulation at the C2/C3 bridge (Scheme 20). DFT calculations elucidated a reversible annulation process that allowed the formation of the more thermodynamically stable C6 alkylated product. Again, with some of the above methods issues with C5 selectivity were also observed.[45]

Scheme 20. Scandium Triflate Catalysed C6 Alkylation of Indoles

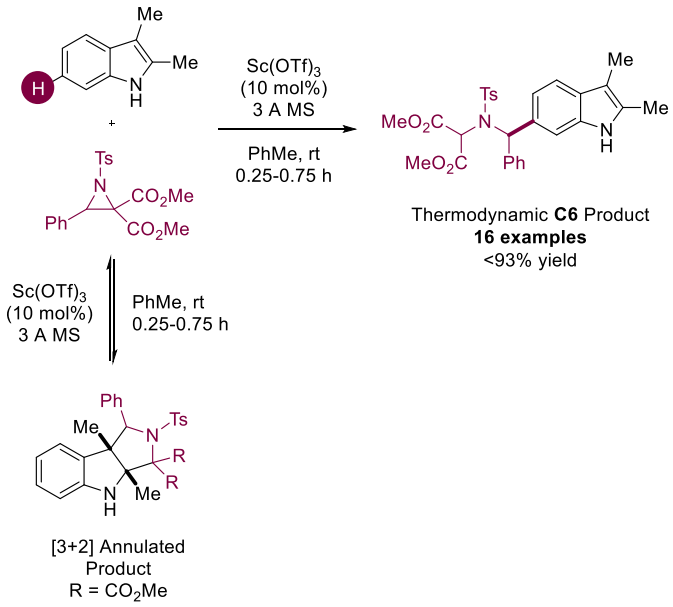

Ruthenium-catalyzed σ-activation has become a more widely used technique for the *meta*-functionalization of arenes.[14j-k,46] Here a strong metalacycle enables radical functionalization *para*-to the cyclometalation. This concept was applied to the indole structure by Frost and co-workers in 2017 (Scheme 21). This methodology used a strongly coordinating directing group at N1 and a weakly coordinating directing group at C3 to enable remote C6 selectivity. The reported mechanism shows a C–H activation at C2 with interaction from both N1 (strong) and C3 (weak) directing groups. Redox radical generation from a ruthenium centre then enables remote radical addition to the most electronically activated benzenoid position. Computational Fukui indices were shown to validate the shift in electron density in the proposed cyclometalation at C2 to the remote C6 position.[47]

Scheme 21. Remote C6 Selective C–H Alkylation of Indole Derivatives *via* σ-Activation

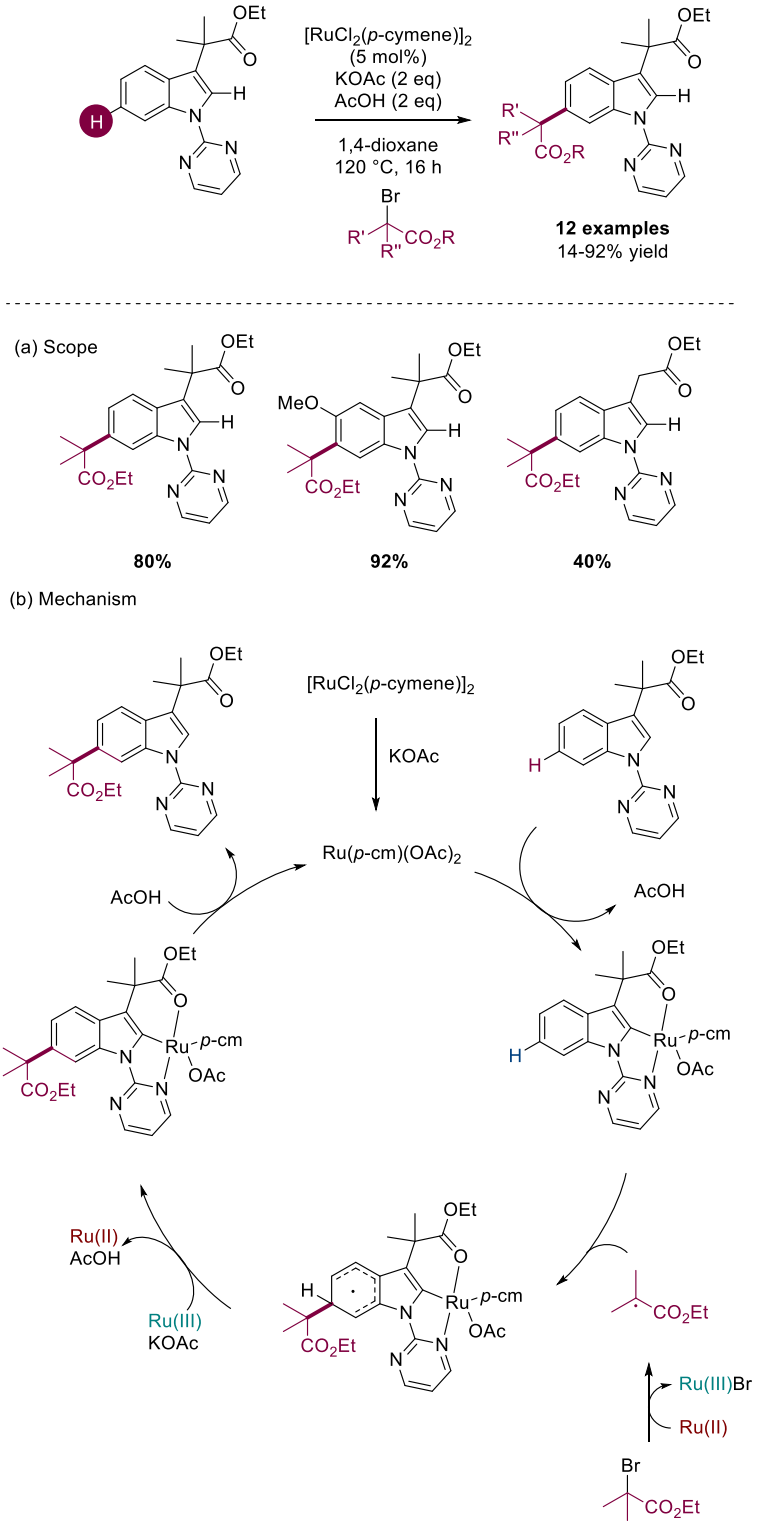

In 2016, Morandi reported the iron-catalyzed C–H amination of arenes. Here they employ the protonated hydroxylamine as a new amination reagent and iron sulphate as catalyst. Electronic bias and sterics were shown to affect the regioselectivity of functionalization in non-biased substrates. In the case of indoles (Scheme 22) the major C–

H aminated product observed was with functionalization taking place at the C6. The methodology was also applied to dibenzofurans where a higher yield was observed although the selectivity issues remained.[48]

Scheme 22. Iron Catalyzed C–H Amination of Indole and Dibenzofuran

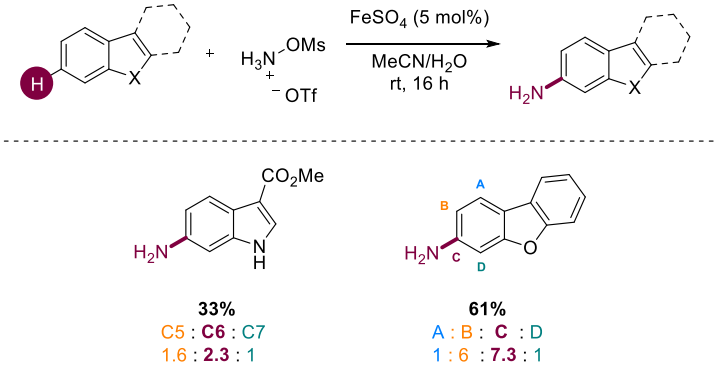

FUNCTIONALIZATION AT C5

The most sparingly observed selectivity in direct indole functionalization has been accessing chemistry at C5. Despite selectivity issues in some methods discussed above between C6 and C5 there have been incredibly limited reports showing conditions that preferentially go for the C5 position.

There have been reports of non-catalyzed Friedel-Crafts type acylation of the free indole structure using $AlCl_3$ as a Lewis acid by Demopoulos. This was shown to lead to a mixture of C5 and C6 substituted indoles with ratios of generally ~3:1 in favour of C5 (Scheme 23).[49] The product was also shown to undergo heterogeneous palladium catalysed deformylation to give the solely C5 substituted product mixtures.

Scheme 23. Aluminium trichloride mediated C5 acylation of indole derivatives

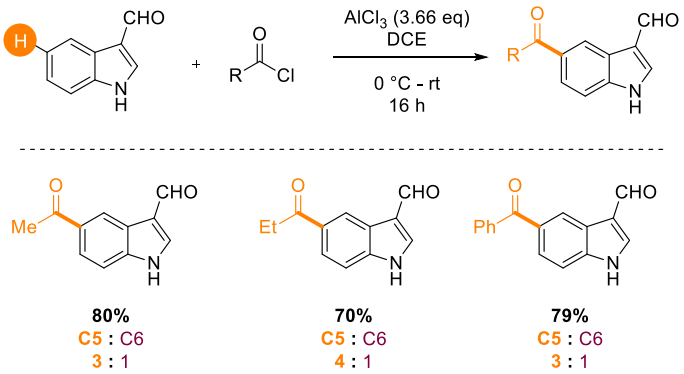

The sole example of selective transition-metal catalyzed direct C5 functionalization of the indole benzenoid ring came out from the Shi lab in 2017. Here they used a combination of the pivaloyl directing group at C3 (which directs to C4) and the remote copper catalysed process (which enabled C6 functionalization) to permit access to the C5 C–H bond (Scheme 24). The reaction pathway was proposed to follow the same mechanism as their work with the C6 arylation. As with the above methodology, the functionality at C3 (in this case the directing group) can be removed to give solely the C5 substituted indole. In this case the directing group is removed cleanly using *p*TSA in glycol.[20] This report also completed Shi's clean sweep of benzenoid indole functionalization having developed methods to access C4,5,6 & 7.

Scheme 24. Copper-Catalyzed C5 Arylation of Indole Derivatives

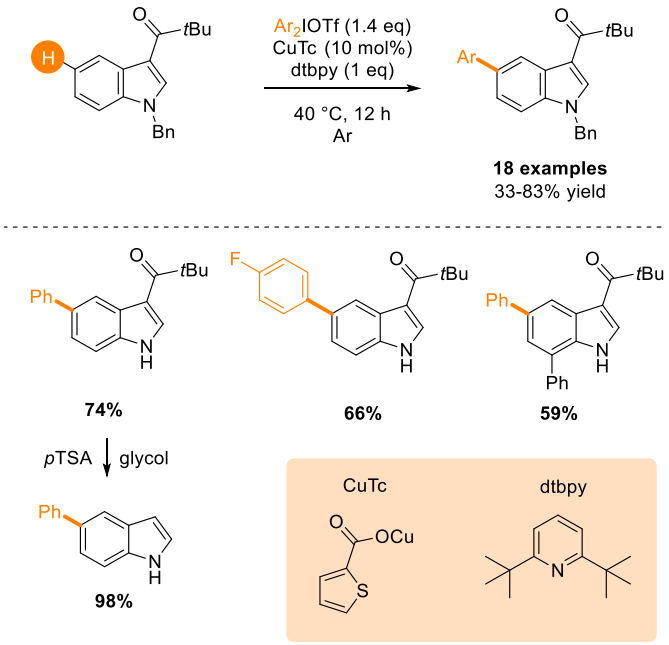

A clear majority of the examples that have been discussed above utilise a directing group on the pyrrole-type ring to enable positional selective catalysis on the benzenoid ring. However, there have been examples where a directing group on the benzene ring enables indole functionalization without reactivity at C2 or C3. The position of these directing groups enables a wide breadth of potential products.

In 2017, Larrosa and co-workers reported the regioselective C–H functionalization of indole-carboxylic acids. When using indole-7-carboxylic acids, C6 arylation was the only product observed (Scheme 25).[50]

Scheme 25. Ruthenium-Catalyzed C–H arylation of indole derivatives.

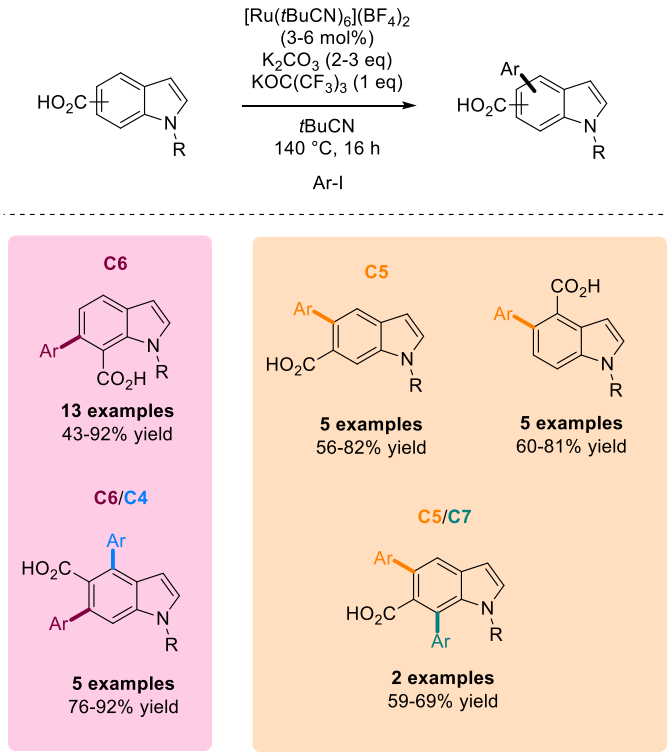

When using indole-5-carboxylic acid the C6/C4 disubstituted structure was observed on using heightened catalyst loading. When using indole-6-carboxylic acid or 4-carboxy derivative C5 arylation was observed. On increasing the catalyst loading using certain substrates the C5/C7 difunctionalized motif is also observed. This showed that depending on the functionality present on the benzenoid ring, any regiochemistry could be accessed using their ruthenium catalysis.[50]

Pedro and co-workers have also reported the organocatalyzed enantioselective Friedel-Crafts aminoalkylation of indoles on the carbocyclic ring directed by a hydroxy group already present on the benzenoid moiety of the indole heteroaromatic.[51]

CONCLUSION

The indole scaffold has become one of the most widely studied organic structure due to its prevalence throughout the natural product, pharmaceutical and agrochemical worlds. The ability to access site selective C–H functionalization on the benzenoid ring has remained a challenge due to the inherent reactivity of C2 and C3. In spite of this, elegant methods have come to the forefront of modern transition-metal catalysis. This review has covered the techniques to access the C4, C5, C6 and C7 positions of the benzenoid ring utilizing a vast number of remote functionalization techniques and selective directing group

chemistry. The development of site selective C–H functionalization will continue to be an integral part to synthetic development in the derivation of biologically relevant structures and these early methods set the stage for a full-frontal assault on everyday synthesis.

AUTHOR INFORMATION

Corresponding Author

*Christopher G. Frost: c.g.frost@bath.ac.uk

ACKNOWLEDGMENT

J. A. L. would like to thank the University of Bath and Syngenta for funding

REFERENCES

(1) (a) Van Order, R. B.; Lindwall, H. G. *Chem. Rev.*, **1942**, *30*, 69-96. (b) Taber, D. F.; Tirunahari, P. K. *Tetrahedron*, **2011**, *67*, 7195-7210.

(2) (a) Sharma, V.; Kumar, P.; Pathak, D. *J. Heterocyclic Chem.*, **2010**, *47*, 491-502. (b) Biswal, S.; Sahoo, U.; Sethy, S.; Kumar, H. K. S.; Banerjee, M. *Asian J. Pharm. Clin. Res.*, **2011**, *5*, 1-6. (c) Zhang, M.-Z.; Chen, Q.; Yang, G.-F. *Eur. J. Med. Chem.*, **2015**, *89*, 421-441. (d) Woodward, A. W.; Bartel, B. *Ann. Bot.*, **2005**, *95*, 707-735. (e) Galliford, C. V.; Sheidt, K. A. *Angew. Chem. Int. Ed.*, **2007**, *46*, 8748-8758. (f) Trost, B.; Brennan, M. K. *Synthesis*, **2009**, *2009*, 3003-3025 (g) Kochanowska-Karamyan, A. J.; Hamann, M. T. *Chem. Rev.*, **2010**, *110*, 4489-4497. (h) Taylor, R. D.; MacCoss, M.; Lawson, A. D. G. *J. Med. Chem.*, **2014**, *57*, 5845-5859.

(3) Taylor, R. D.; MacCoss, M.; Lawson, A. D. G. *J. Med. Chem.*, **2014**, *57*, 5845-5859

(4) (a) Fischer, E.; Jourdan, F. *Ber. Dtsch. Chem. Ges.*, **1883**, *16*, 2241-2245. (b) Robinson, B. *Chem. Rev.*, **1963**, *63*, 373-401. (c) Robinson, B. *Chem. Rev.*, **1969**, *69*, 227-250. (d) Allen, C. F. H.; Wilson, C. V. *J. Am. Chem. Soc.*, **1943**, *65*, 611-612.

(5) (a) Bartoli, G.; Palmieri, G. *Tet. Lett.*, **1989**, *30*, 2129-2132. (b) Bartoli, G.; Dalpozzo, R.; Nardi, M. *Chem. Soc. Rev.*, **2014**, *43*, 4728-4750.

(6) (a) Larock, R. C.; Yum, E. K. *J. Am. Chem. Soc.*, **1991**, *113*, 6689-6690. (b) Larock, R. C.; Yum, E. K.; Refvik, M. D. *J. Org. Chem.*, **1998**, *63*, 7652-7662.

(7) (a) Vicente, R. *Org. Biomol. Chem.*, **2011**, *9*, 6469-6480. (b) Gribble, G. W. *J. Chem. Soc., Perkin Trans. 1*, **2000**, 1045-1075. (c) Cacchi, S.; Fabrizi, G. *Chem. Rev*., **2005**, *105*, 2873-2920. (d) Humphrey, G. R.; Kuethe, J. T. *Chem. Rev.*, **2006**, *106*, 2875-2911.

(8) (a) Guo, T.; Huang, F.; Yu, L.; Yu, Z. *Tet. Lett.*, **2015**, *56*, 296-302. (b) Song, W.; Ackermann, L. *Chem. Commun.*, **2013**, *49*, 6638-6640. (c) Wang, H.; Moselage, M.; González, M. J.; Ackermann, L. *ACS Catal.*, **2016**, *6*, 2705-2709. (d) Ackermann, L.; Lygin, A. V. *Org. Lett.*, **2012**, *14*, 764-767. (e) Ackermann, L.; Barfüßer, S.; Potukuchi, H. K. *Adv.*

Synth. Catal., **2009**, *351*, 1064-1072. (f) Mei, T.-S.; Kou, L.; Ma, S.; Engle, K. M.; Yu, J.-Q. *Synthesis*, **2012**, *44*, 1778-1791.

(9) For reading on transition metal-catalyzed C–H functionalization see: (a) Ackermann, L. *Chem. Rev.* **2011**, *13*, 3075-3078, (b) Arockiam, P. B.; Bruneau, C.; Dixneuf, P. *Chem. Rev*. **2012**, *112*, 5879−5918. (c) Chen, X.; Engle, K. M.; Wang, D-H.; Yu, J-Q. *Angew. Chem. Int. Ed.* **2009**, *48*, 5094–5115. (d) Engle, K. M., Mei, T-S.; Wasa, M.; Yu, J-Q. *Acc. Chem. Res.* **2012**, *45,* 788-802. (e) Davies, H. M. L.; Morton, D., *J. Org. Chem.*, **2016**, *81*, 343-350. (f) Yoshino, T.; Matsunaga, S. *Adv. Synth. Catal.*, **2017**, *359*, 1245-1262. For reading on the modification of biologically active molecules see: (g) Leitch, J. A.; Wilson, P. B.; McMullin, C. L.; Mahon, M. F.; Bhonoah, Y.; Williams, I. H.; Frost, C. G. *ACS Catal.*, **2016**, *6*, 5520-5529. (h) Leitch, J. A.; Cook, H. P.; Bhonoah, Y.; Frost, C. G. *J. Org. Chem.*, **2016**, *81*, 10081-10087. (i) Ma, W.; Dong, H.; Wang, D.; Ackermann, L. *Adv. Synth. Catal.*, **2017**, *359*, 966-973. (j) Yamaguchi, J.; Yamaguchi, A. D.; Itami, K. *Angew. Chem., Int. Ed.* **2012**, *51*, 8960−9009. (k) Brown, J. A.; Cochrane, A. R.; Irvine, S.; Kerr, W. J.; Mondal, B.; Parkinson, J. A.; Paterson, L. C.; Reid, M.; Tuttle, T.; Andersson, S.; Nilsson, G. N. *Adv. Synth. Catal*. **2014**, *356*, 3551−3562.

(10) (a) Gensch, T.; Hopkinson, M. N.; Glorius, F.; Wencel-Delord, J. *Chem. Soc. Rev.*, **2016**, *45*, 2900-2936. (b) Gulías, Moisés.; Mascareñas, J. L. *Angew. Chem. Int. Ed.*, **2016**, *55*, 11000-11019.

(11) (a) Chen, Z.; Wang, B.; Zhang, J.; Yu, W.; Liu, Z.; Zhang, Y. *Org. Chem. Front.*, **2015**, *2*, 1107-1295 (b) De Sarakar, S.; Liu, W.; Kozhushkov, S. I.; Ackermann, L. *Adv. Synth. Catal.* **2014**, *356*, 1461-1479.

(12) For review see (a) Sandtorv, A. H. *Adv. Synth. Catal.*, **2015**, *357*, 2403-2435. For key seminal publications see: (b) Wang, X.; Lane, B. S.; Sames, D. *J. Am. Chem. Soc*. **2005**, *127*, 4996–4997. (c) Stuart, D. R.; Villemure, E.; Fagnou, K. *J. Am. Chem. Soc.* **2007**, *129*, 12072–12073. (c) Grimster, N. P.; Gauntlett, C.; Godfrey, C. R. A.; Gaunt, M. J. *Angew. Chem. Int. Ed.*, **2005**, *44*, 3125-3129. (d) Phipps, R. J.; Grimster, N. P.; Gaunt, M. J. *J. Am. Chem. Soc.*, **2008**, *130*, 8172-8174. (e) Deprez, N. R.; Kalyani, D.; Krause, A.; Sanford, M. S. *J. Am. Chem. Soc.*, **2006**, *128*, 4972-4973. (f) Lebrasseur, N.; Larrosa, I. *J. Am. Chem. Soc.*, **2008**, *130*, 2926-2927.

(13) (a) Lane, B. S.; Brown, M. A.; Sames, D. *J. Am. Chem. Soc.*, **2005**, *127*, 8050-8057. (b) Kirchberg, S.; Fröhlich, R.; Studer, A. *Angew. Chem. Int. Ed.*, **2009**, *48*, 4235-4238.

(14) For reviews on remote functionalization techniques of arenes see: (a) Yang, J. *Org. Biomol. Chem.*, **2015**, *13*, 1930-1941. (b) Sharma, R.; Thakur, K.; Kumar, R.; Kumar, I.; Sharma, U. *Cat. Rev.*, **2015**, *57*, 345-405. (c) Dey, A.; Agasti, S.; Maiti, D. *Org. Biomol. Chem.*, **2016**, *14*, 5440-5453. (d) Dey, A.; Maity, S.; Maiti, D. *Chem. Commun.*, **2016**, *52*, 12398-12414. (e) Frost, C. G.; Paterson, A. J. *ACS Cent. Sci.*, **2015**, *1*, 418-419. (f)

Ackermann, L.; Li, J. *Nat. Chem.*, **2015**, *7*, 686-687. For key seminal publications in remote arene C–H functionalization see: (g) Cho, J.-Y.; Tse, M. K.; Holmes, D.; Maleczka, R. E.; Smith, M. R. *Science*, **2002**, *295*, 305-308. (h) Phipps, R. J.; Gaunt, M. J. *Science*, **2009**, *323*, 1593-1597. (i) Leow, D.; Li, G.; Mei, T.-S.; Yu, J.-Q. *Nature*, **2012**, *486*, 518-522. (j) Saidi, O.; Marafie, J.; Ledger, A. E. W.; Liu, P. M.; Mahon, M. F.; Kociok-Köhn, G.; Whittlesey, M. K.; Frost, C. G. *J. Am. Chem. Soc.*, **2011**, *133*, 19298-19301. (k) Hofmann, N.; Ackermann, L. *J. Am. Chem. Soc*., **2013**, *135*, 5877-5884. (l) Wang, X.-C.; Gong, W.; Fang, L.-Z.; Zhu, R.-Y.; Li, S.; Engle, K. M.; Yu, J.-Q. *Nature*, **2015**, *519*, 334-338.

(15) Liu, Q.; Li, Q.; Ma, Y.; Jia, Y. *Org. Lett.*, **2013**, *15*, 4528-4531

(16) Lanke, V.; Prabhu, K. R. *Org. Lett.*, **2013**, *15*, 6262-6265

(17) (a) Lanke, V.; Prabhu, K. R. *Chem. Commun.*, **2017**, *53*, 5117-5120. (b) Chen, S.; Feng, B.; Zheng, X.; Yin, J.; Yang, S.; You, J. *Org. Lett.*, **2017**, *19*, 2502-2505.

(18) Lanke, V.; Bettadapur, K. R.; Prabhu, K. R. *Org. Lett.*, **2016**, *18*, 5496-5499

(19) Chen, H.; Lin, C.; Xiong, C.; Liu, Z.; Zhang, Y. *Org. Chem. Front.*, **2017**, *4*, 455-459

(20) Yang, Y.; Gao, P.; Zhao, Y.; Shi, Z. *Angew. Chem. Int. Ed.*, **2017**, *56*, 3966-3971

(21) Borah, A. J.; Shi, Z. *Chem. Commun.*, **2017**, *53*, 3945-3948

(22) Fukuda, T.; Maeda, R.; Iwao M. *Tetrahedron*, **1999**, *55*, 9151-9162

(23) Hartung, C. G.; Fecher, A.; Chapell, B.; Snieckus, V. *Org. Lett.*, **2003**, *5*, 1899-1902

(24) Yang, Y.; Qiu, X.; Zhao, Y.; Mu, Y.; Shi, Z. *J. Am. Chem. Soc.*, **2016**, *138*, 495-498

(25) Xu, L.; Zhang, C.; He, Y.; Tan, L.; Ma, D. *Angew. Chem. Int. Ed.*, **2016**, *55*, 321-325

(26) Guo, L.; Chen, Y.; Zahng, R.; Peng, Q.; Xu, L.; Pan, X. *Chem. Asian J.*, **2017**, *12*, 289-292

(27) Song, Z.; Antonchick, A. P. *Org. Biomol. Chem.*, **2016**, *14*, 4804-4808

(28) (a) Jiao, L.-Y.; Oestreich, M. *Org. Lett.*, **2013**, *15*, 5374-5377. (b) Song, Z.; Samanta, R.; Antonchick, A. P. *Org. Lett.*, **2013**, *15*, 5662-5665

(29) Neufeldt, S. R.; Seigerman, C. K.; Sanford, M. S. *Org. Lett.*, **2013**, *15*, 2302-2305

(30) (a) Luo, H.; Liu, H.; Zhang, Z.; Xiao, Y.; Wang, S.; Luo, X.; Wang, K. *RSC Adv.*, **2016**, *6*, 39292-39295. (b) Shi, Z.; Li, B.; Wan, X.; Cheng, J.; Fang, Z.; Cao, B.; Qin, C.; Wang, Y. *Angew. Chem. Int. Ed.*, **2007**, *46*, 5554-5558 (c) Nishikata, T.; Abela, A. R.; Huang, S.; Lipshutz, B. H. *J. Am. Chem. Soc.*, **2010**, *132*, 4978-4979. (d) Jiao, L.-Y.; Oestreich, M. *Chem. Eur. J.*, **2013**, *19*, 10845-10848

(31) Pan, C.; Abdukader, A.; Han, J.; Cheng, Y.; Zhu, C. *Chem. Eur. J.*, **2014**, *20*, 3606-3609

(32) Kim, M.; Mishra, N. K.; Park, J.; Han, S.; Shin, Y.; Sharma, S.; Lee, Y.; Lee, E.-K.; Kwak, J. H.; Kim, I. S. *Chem. Commun.*, **2014**, *50*, 14249-14252

(33) Mishra, N. K.; Jeong, T.; Sharma, S.; Shin, Y.; Han, S.; Park, J.; Oh. J. S.; Kwak, J. H.; Jung, Y. H.; Ki, I. S. *Adv. Synth. Catal.*, **2015**, *357*, 1293-1298

(34) Gandeepan, P.; Koeller, J.; Ackermann, L. *ACS Catal.*, **2017**, *7*, 1030-1034.
(35) Paul, S.; Chotana, G. A.; Holmes, D.; Reichle, R. C.; Maleczka, R. E.; Smith, M. R. *J. Am. Chem. Soc.*, **2006**, *128*, 15552-15553
(36) Shen, F.; Tyagarajan, S.; Perera, D.; Krska, S. W.; Maligres, P. E.; Smith, M. J.; Maleczka, R. E. *Org. Lett.*, **2016**, *18*, 1554-1557
(37) Loach, R. P.; Fenton, O. S.; Amaike, K.; Siegel, D. S.; Ozkal, E.; Movassaghi, M. *J. Org. Chem.*, **2014**, *79*, 11254-11263
(38) Eastabrook, A. S.; Sperry, J. *Aus. J. Chem.*, **2015**, *68*, 1810
(39) Robbins, D. W.; Boebel, T. A.; Hartwig, J. F. *J. Am. Chem. Soc.*, **2010**, *132*, 4068-4069
(40) (a) Reddy, V. P.; Qiu, R.; Iwasaki, T.; Kambe, N. *Org. Lett.*, **2013**, *15*, 1290-1293. (b) Qiu, R.; Reddy, V. P.; Iwasaki, T.; Kambe, N. *J. Org. Chem.*, **2015**, *80*, 367-374. (c) Zhu, L.; Cao, X.; Iwasaki, T.; Reddy, V. P.; Xu, X.; Yin, S.-F.; Kambe, N. *RSC Adv.*, **2015**, *5*, 39358-39365. (d) Ai, W.; Yang, X.; Wu, Y.; Wang, X.; Li, Y.; Yang, Y.; Zhou, B. *Chem. Eur. J.*, **2014**, *20*, 17653-17657. (e) Hong, X.; Wang, H.; Qian, G.; Tan, Q.; Xu, B. *J. Org. Chem.*, **2014**, *79*, 3228–3237. (f) Sharma, S.; Shin, Y.; Mishra, N. K.; Park, J.; Han, S.; Jeong, T.; Oh, Y.; Lee, Y.; Choi, M.; Kim, I. S. *Tetrahedron*, **2015**, *71*, 245-2441. (g) Zhou, X.; Yu, S.; Qi, Z.; Kong, L.; Li, X. *J. Org. Chem.*, **2016**, *81*, 4869-4875. (h) Reddy, K. H. V.; Kumar, R. U.; Reddy, V. P.; Satish, G.; Nanubolu, J. B.; Nageswar, Y. V. D. *RSC Adv.*, **2016**, *6*, 54431-54434. (i) Zhang, L.-Q.; Yang, S.; Huang, X.; You, J.; Song, F. *Chem. Commun.*, **2013**, *49*, 8830-8832. (k) Kawamorita, S.; Ohmiya, H.; Sawamura, M. *J. Org. Chem.*, **2010**, *75*, 3855-3858.
(41) Feng, Y.; Holte, D.; Zoller, J.; Umemiya, S.; Simke, L. R.; Baran, P. S. *J. Am. Chem. Soc.*, **2015**, *137*, 10160-10163
(42) (a) Leow, D.; Li, G.; Mei, T.-S.; Yu, J.-Q. *Nature*, **2012**, *486*, 518-522. (b) Tang, R.-Y.; Li, G.; Yu, J.-Q. *Nature*, **2014**, *507*, 215-220. (c) Chu, L.; Shang, M.; Tanaka, K.; Chen, Q.; Pissarnitski, N.; Streckfuss, E.; Yu, J.-Q. *ACS Cent. Sci*. **2015**, *1*, 394−399. (d) Das, S.; Incarvito, C. D.; Crabtree, R. H.; Brudwig, G. W. *Science*, **2006**, *312*, 1941-1943.
(43) Yang, G.; Lindovska, P.; Zhu, D.; Kim, J.; Wang, P.; Tang, R.-Y.; Movassaghi, M.; Yu, J.-Q. *J. Am. Chem. Soc.*, **2014**, *136*, 10807-10813
(44) Yang, Y.; Li, R.; Zhao, Y.; Zhao, D.; Shi, Z. *J. Am. Chem. Soc.*, **2016**, *138*, 8734-8737
(45) Liu, H.; Zheng, C.; You, S.-L.; *J. Org. Chem.*, **2014**, *79*, 1047-1054
(46) For further reading on σ-activation see: (a) Paterson, A. J.; St John Campbell, S.; Mahon, M. F.; Press, N. J.; Frost, C. G. *Chem. Commun.*, **2015**, *51*, 12807-12810. (b) Li, J.; Warratz, S.; Zell, D.; De Sarkar, S.; Ishikawa, E. E.; Ackermann, L. *J. Am. Chem. Soc.*, **2015**, *137*, 13894-13901. (c) Teskey, C. J.; Lui, Y. W.; Greaney, M. F. *Angew. Chem. Int. Ed.*, **2015**, *54*, 11677-11680. (d) Yu, Q.; Hu, L.; Wang, Y.; Zheng, S.; Huang, J. *Angew. Chem. Int. Ed.*, **2015**, *54*, 15284-15288. (e) Fan, Z.; Ni, J.; Zhang, A. *J. Am. Chem. Soc.*,

2016, *138*, 8470-8475. (f) Marcé, P.; Paterson, A. J.; Mahon, M. F.; Frost, C. G., *Catal. Sci. Technol.*, **2016**, *6*, 7068-7076. (g) Li, G.; Ma, X.; Jia, C.; Han, Q.; Wang, Y.; Wang, J.; Yu, L.; Yang, S. *Chem. Commun.*, **2017**, *53*, 1261-1264. (h) Warratz, S.; Burns, D. J.; Zhu, C.; Korvorapun, K.; Rogge, T.; Scholz, J.; Jooss, C.; Gelman, D.; Ackermann, L. *Angew. Chem. Int. Ed.*, **2017**, *56*, 1557-1560. (i) Ruan, Z.; Zhang, S.-K.; Zhu, C.; Ruth, P. N.; Stalke, D.; Ackermann, L. *Angew. Chem. Int. Ed.*, **2017**, *129*, 2077-2081. (j) Li, Z.-Y.; Li, L.; Li, Q.-L.; Jing, K.; Xu, H.; Wang, G.-W. *Chem. Eur. J.*, **2017**, *23*, 3285-3290. (k) Li, G.; Lv, X.; Guo, K.; Wang, Y.; Yang, S.; Yu, L.; Yu, Y.; Wang, J. *Org. Chem. Front.*, **2017**, *4*, 1145-1148. (l) Li, J.; Korvorapun, K.; De Sarkar, S.; Rogge, T.; Burns, D. J.; Warratz, S.; Ackermann, L. *Nat. Commun.*, **2017**, *8*, 15430. (m) Paterson, A. J.; Heron, C. J.; McMullin, C. L.; Mahon, M. F.; Press, N. J.; Frost, C. G. *Org. Biomol. Chem.*, **2017**, DOI: 10.1039/C7OB01192J.

(47) Leitch, J. A.; McMullin, C. L.; Mahon, M. F.; Bhonoah, Y.; Frost, C. G. *ACS Catal.*, **2017**, *7*, 2616-2623

(48) Legnani, L.; Cerai, G. P.; Morandi, B. *ACS Catal.*, **2016**, *6*, 8162-8165

(49) Demopoulos, V. J.; Nicolaou, I. *Synthesis*, **1998**, *1998*, 1519-1522

(50) Simonetti, M.; Cannas, D. M.; Panigrahi, A.; Kujawa, S.; Kryjewski, M.; Xie, P.; Larrosa, I. *Chem. Eur. J.*, **2017**, *23*, 549-543.

(51) (a) Montesinos-Magraner, M.; Vila, C.; Rendón-Patiño, A.; Blay, G.; Fernández, I.; Muñoz, M. C.; Pedro, J. R. *ACS Catal.*, **2016**, *6*, 2689-2693. (b) Montesinos-Magraner, M.; Vila, C.; Blay, G.; Fernández, I.; Muñoz, M. C.; Pedro, J. R. *Org. Lett.*, **2017**, *19*, 1546-1549

3.3: Remote C6-Selective Ruthenium-Catalyzed C–H Alkylation of Indoles via σ-Activation

3.3.1: Introduction, Commentary and Preliminary Results

The use of cleavable auxiliaries in *meta*-functionalisation is very attractive as one can install the strongly coordinating directing group onto a useful motif and then remove it to reveal the functionalised structure/building block.[1] The goal of this project was to diversify the structures amenable to σ-activation by investigating different auxiliary templates and exploring the known *meta*-functionalisation reactions with these structures. The review perspective above will serve as the introduction to this chapter however preliminary results will be discussed herein.

The investigation was initiated by synthesising a variety of S-linked arylpyrimidines, in the sulfide, sulfoxide and sulfone oxidation states and applying them to σ-activation methodology. Four test reactions were chosen for each oxidation state: Frost sulfonation,[2] Frost 3° alkylation,[3] Ackermann 3° alkylation,[1] and Huang bromination (Scheme 3-3).[4]

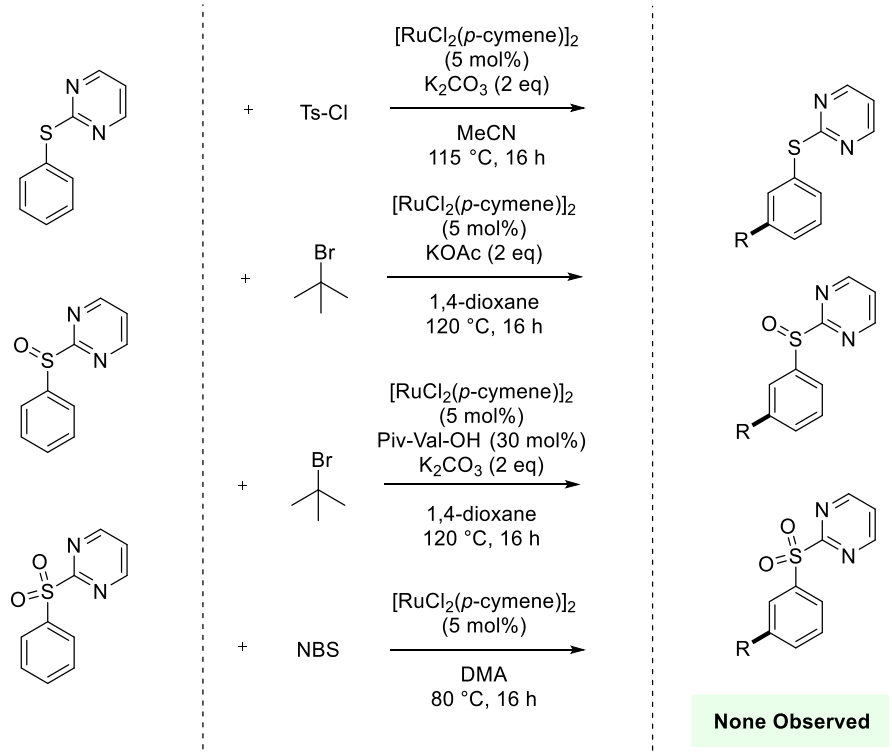

Scheme 3-3: Remote *meta*-Functionalisation of Sulphur Linked Arylpyrimidines

Unfortunately, no *meta*-functionalisation was observed for any starting material. Only the sulfoxide showed conversion in sulfonation and *tert*-alkylation reactions, although this was only to the sulfide. This was proposed to take place through *O*-tosylation/alkylation on the charge separated sulfoxide and subsequent loss to form the naked sulfide.

Following this, it was decided to investigate the use of *N*-substituted indoles in σ-activation reactions. *N*-pyrimidinylindole was synthesized and submitted to the Frost 3° alkylation conditions using *tert*-butyl bromide as coupling partner. Interestingly *tert*-butylation at C3 was observed, albeit in low yields (Scheme 3-4).

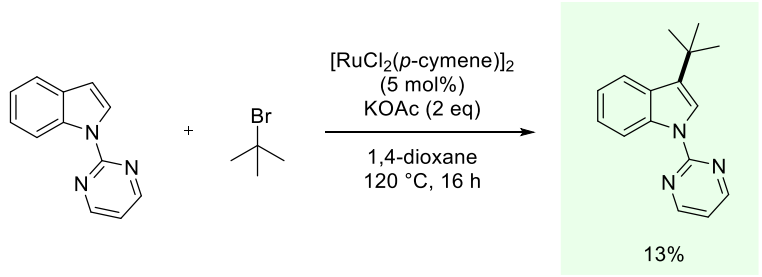

Scheme 3-4: Ruthenium-Catalysed Functionalisation of *N*-pyrimidinylindole

This is proposed have taken place through a radical functionalisation or through a Friedel-Crafts-type mechanism. This suggested that a redox catalyst with an appropriate oxidation potential to form these tertiary radicals could have been formed using the reagents present. Our previous reports highlight the use of tertiary α-halocarbonyls as more efficient and reliable coupling partners in remote *meta*-functionalisation than *tert*-butyl bromide. Due to this, ethyl α-bromoisobutyrate was reacted with *N*-pyrimidinylindole under the alkylation conditions (Scheme 3-5). Under these conditions the C3 functionalised material was again observed, however the C3/C6 di-functionalised material was also isolated from the reaction mixture. Pleasingly the addition of acetic acid to create a “pH buffer” with the potassium acetate led to quantitative conversion of the *N*-pyrimidinylindole starting material.

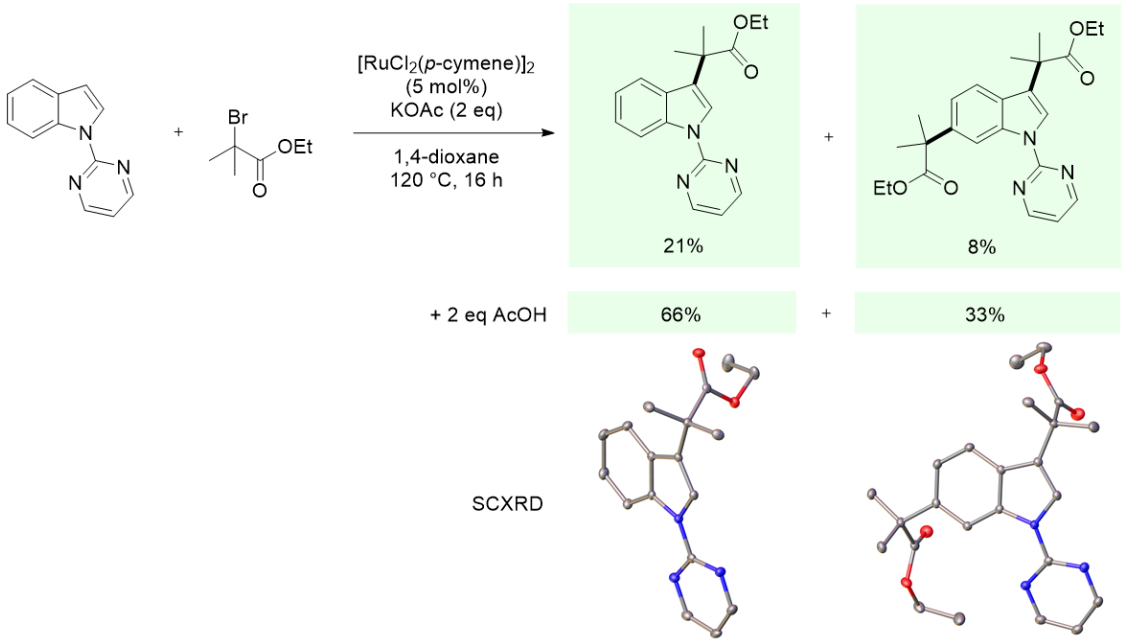

Scheme 3-5: Ruthenium-Catalysed C3/C6 C–H Alkylation of *N*-pyrimidinylindole

These two structures were further characterised by SCXRD to confirm regioselectivity of functionalisation. Both of these structures show functionalisation remote from the directing group, both in the equivalent "*meta*" positions of an indole. Despite this observation, it is well documented that the most inherent reactivity of an indole takes place at the 3 position, however the 6-position is notoriously unreactive.

As discussed above the ability to access C6 functionalised indoles is not readily observed.[5] Due to this we moved our investigation forward by other *N*-substituted indoles in this reaction, with strongly coordinating directing groups, weakly coordinating directing groups and non-coordinating (Scheme 3-6). Surprisingly the only substitution pattern that worked here was the structurally similar pyridyl unit, and boc, acyl, tosyl and benzyl derivatives were not tolerated in this reaction to either C3 or C6. The results from this point on will be presented herein using the Article that was published in ACS Catalysis in 2017.

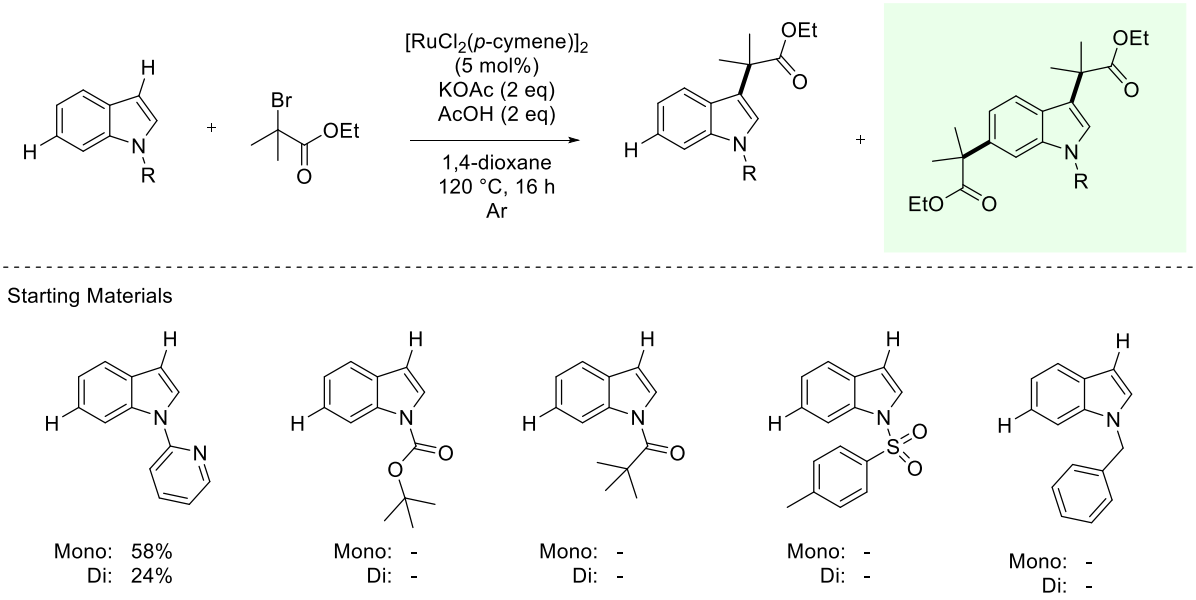

Scheme 3-6: C3/C6 Functionalisation of Indole Derivatives

References

(1) J. Li, S. Warratz, D. Zell, S. De Sarkar, E. E. Ishikawa, and L. Ackermann, *J. Am. Chem. Soc.*, 2015, **137**, 13894

(2) O. Saidi, J. Marafie, A. E. W. Ledger, P. M. Liu, M. F. Mahon, G. Kociok-Köhn, M. K. Whittlesey, and C. G. Frost, *J. Am. Chem. Soc.*, 2011, **133**, 19298.

(3) A. J. Paterson, S. St John Campbell, M. F. Mahon, N. J. Press, and C. G. Frost, *Chem. Commun.*, 2015, **51**, 12807.

(4) Q. Yu, L. Hu, Y. Wang, S. Zheng, and J. Huang, *Angew. Chem. Int. Ed.*, 2015, **54**, 15284

(5) J. A. Leitch, Y. Bhonoah, and C. G. Frost, *ACS Catal.*, 2017, **7**, 5618.

3.3.2: Authorships and Permissions

This declaration concerns the article entitled									
Remote C6-Selective Ruthenium-Catalyzed C–H Alkylation of Indole Derivatives *via* σ-Activation									
Publication status (tick one)									
Draft manuscript		**Submitted**		**In review**		**Accepted**		**Published**	X
Publication details (reference)	J. A. Leitch, C. L. McMullin, M. F. Mahon, Y. Bhonoah, and C. G. Frost, *ACS Catal.*, 2017, **7**, 2616								
Candidate's contribution to the paper (detailed, and also given as a percentage)	The candidate contributed to/ considerably contribute to/predominantly execute the: **Formulation of ideas (60%):** Ideas circulated in meetings between JAL and CGF (40%) **Design of methodology (70%)**: Plan for synthetic work done by JAL, with input from CGF (10%) and computational design carried out by CLM (20%) **Experimental work (70%)**: JAL carried out all the synthetic work and CLM carried out all computational work (25%). MFM provided the crystallography (5%) **Presentation of data in journal format (65%)**: JAL wrote the majority of the paper for publication. CLM provided discussion on computational work (20%). CGF (10%) and MFM (3%) edited the manuscript and YB looked over the manuscript (2%).								
Statement from Candidate	This paper reports on original research I conducted during the period of my Higher Degree by Research candidature								
Signed	Jamie A. Leitch						**Date**	14/09/17	

3.3.3: Manuscript for "Remote C6-Selective Ruthenium-Catalyzed C–H Alkylation of Indoles via σ-Activation"

Complete manuscript given at point of corrections follows on the next page. Layout changes have been made for consistency for this thesis. Contents remain unchanged.

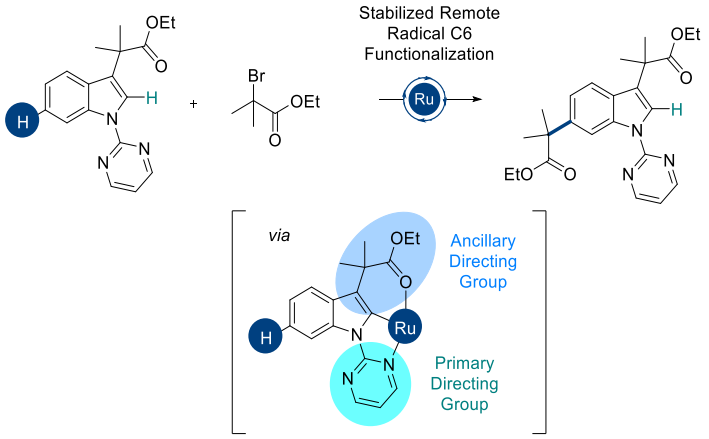

Remote C6 Selective Ruthenium-Catalyzed C–H Alkylation of Indole Derivatives *via* σ-Activation

Jamie A. Leitch,[†] Claire L. McMullin,[†] Mary F. Mahon,[†] Yunas Bhonoah,[‡] and Christopher G. Frost[*,†]

[†]Department of Chemistry, University of Bath, Claverton Down, Bath, Somerset, BA2 7AY, United Kingdom

[‡]Syngenta, Jealott's Hill International Research Centre, Bracknell, Berkshire, RG42 6EY, United Kingdom

ABSTRACT: The site-selective functionalization of an indole template offers exciting possibilities for the derivatization of molecules with useful biological properties. Herein, we report the remote C6 selective C–H alkylation of indole derivatives enabled by ruthenium(II) catalysis. Remote alkylation was achieved using *N*-pyrimidinyl indoles with an ancillary ester directing group at the C3 position. This ancillary directing group proved pivotal to reactivity at C6, with yields up to 92% achieved. A one-pot procedure to install this directing group followed by remote C6 functionalization has also been reported, both shown to proceed *via* ruthenium redox catalysis. Computationally calculated Fukui indices elucidated that the C6 position to be the most reactive vacant C–H site towards potential functionalization. When coupled with deuterium incorporation studies, a C2 cyclometalation/remote σ-activation pathway was deduced.

INTRODUCTION

The development of transition metal catalyzed C–H functionalization has emerged as a very powerful tool to synthesize and derivate biologically interesting molecules.[1] The indole heteroaromatic has received great attention over the past century due to their prevalence in a large number of natural products, pharmaceuticals and agrochemicals.[2] Because of this, the development of elegant methods for the synthesis of highly decorated indoles has received huge efforts in recent years.[3] Due to the high potential of these motifs, indoles have been widely used as C–H activation templates. The C3 position has been shown to be the C–H bond with the most intrinsic reactivity in direct transition metal catalyzed C–H functionalization (Figure 1).[4] C2 functionalization has been achieved using a variety of metal systems, primarily through functionalization of the NH bond with a

directing group. Here cyclometalation is facilitated *via* chelation assistance to afford C–H insertion and subsequent functionalization at C2.[5]

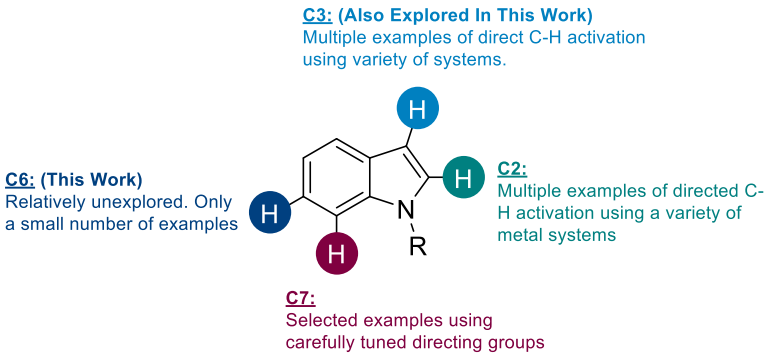

Figure 1: Current sites of C–H functionalization of indoles.

Additionally, carefully designed phosphonate directing groups have also granted access to C7 functionalized indoles in selected examples.[6]

Remote reactivity at C6 of an indole has only been sparingly observed. Selected examples include the use of ligand controlled iridium catalysis by Baran,[7] templated C–H insertion by Yu,[8] and elegant studies by Shi and co-workers combining the phosphonate directing group and other remote functionalization techniques (Scheme 1).[9] The ability to access remote unreactive C–H bonds has been a great challenge to catalytic chemists in recent years.[10] Despite this, a few methods have prevailed: meticulous template design,[11] metal-directed σ-activation,[12] the use of a transient mediator,[13] and the careful manipulation of steric/electronic effects (albeit sparingly). [14] The use of σ-activation lends itself as the most atom-economical versus the other two methods which often lead to high quantities of waste product streams. This is especially the case in the templated work where often templates are pre-synthesized, installed and then removed.[11]

Our previous work in the area depicts the remote *meta*-alkylation of 2-phenylpyridine using the α-bromo ester coupling partner.[12c] This was postulated to proceed *via* an *ortho*-cyclometalation which promotes a remote σ-activation *para*- to metal insertion to afford net *meta*-substituted products. Herein, we report the expansion of this methodology away from privileged structures such as 2-phenylpyridine to biologically relevant structures such as indoles. Ackermann and co-workers have recently explored the use of pyrimidinyl-substituted anilines in *meta*-functionalization[12d] and the expansion of motifs for remote activation is pivotal in moving towards broadly useful synthetic methodology. Here we have developed the remote C6 selective ruthenium-catalyzed C–H alkylation of pyrimidinyl-indole

derivatives. It is proposed to proceed *via* a C2 cyclometalation σ-activation pathway utilizing an ancillary directing group present at the C3 position

Scheme 1. Previous work on remote transition metal catalyzed C–H functionalization of indoles

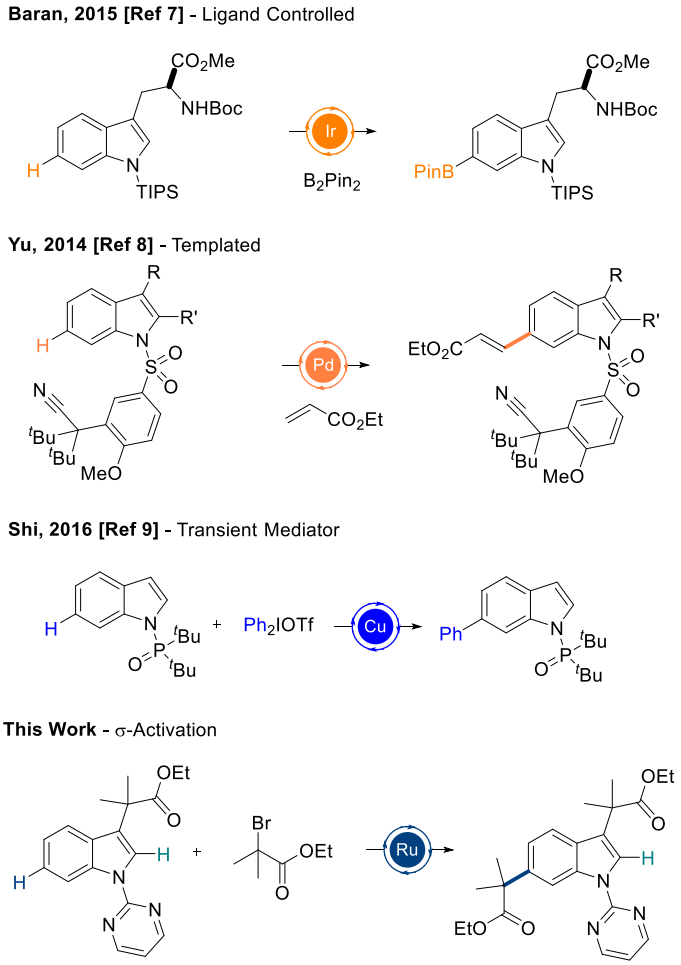

RESULTS & DISCUSSION

The investigation into the remote functionalization of indole derivatives began by applying our previous *meta*-alkylation conditions with 1-(pyrimidin-2-yl)-indole (**1a**, Scheme 2a).[12c] This gave rise to two products, primarily C3 alkylated indole motif (**3a**) and interestingly the C3/C6 di-alkylated structure was also observed (**4a**). Pleasingly, quantitative conversion of starting material **1a** to **3a** and **4a** was observed on addition of acetic acid to the reaction mixture. The regioselectivity of functionalization was further confirmed *via* single crystal X-ray crystallography (Figure 2).[15]

In the absence of the ruthenium catalyst no reactivity to either **3a** nor **4a** was maintained, despite the innate reactivity of the C3 position. The use of 1*H*-indole (**1b**,

Scheme 2b) in the reaction gave solely the C3 functionalized motif (**3b**) in excellent yields, however showed no selectivity to the C6 position (**4b**). This was also shown not to require the addition of AcOH, however still proceeded by a ruthenium-catalyzed mechanistic pathway. Interestingly, neither *tert*-butoxycarbonyl nor benzyl *N*-substituted indoles gave conversion to either product. This showed that an aromatic nitrogen or NH were vital to any catalytic functionalization, and a strongly coordinating directing group was key to granting access to C6 functionalized motifs. It should be noted that this initial C3 selectivity is complementary to the C2 selectivity that Stephenson and co-workers observed using ruthenium photocatalysis with similar coupling partners.[16]

Scheme 2. Ruthenium(II)-catalyzed C–H alkylation of indoles[a]

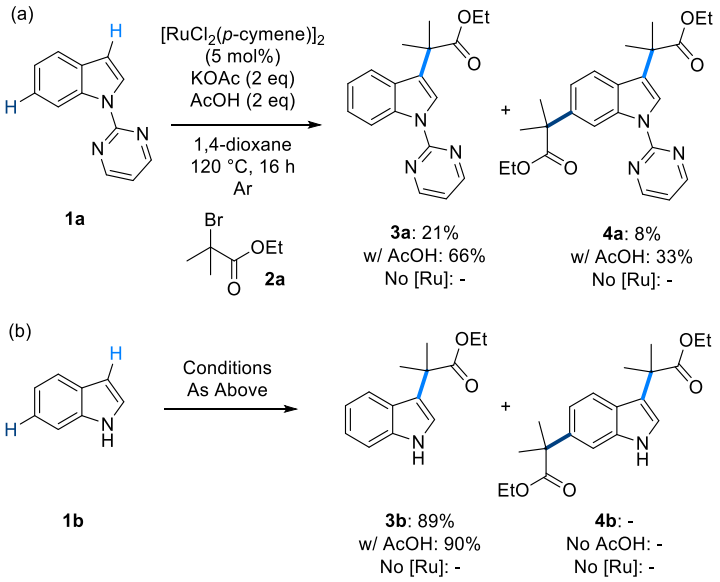

[a] Isolated yields after silica gel column chromatography

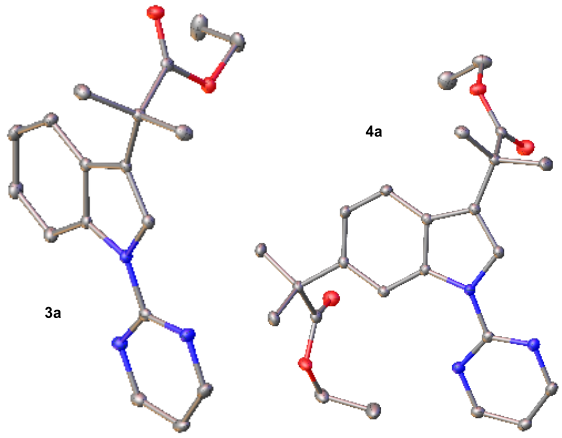

Figure 2: X-ray crystallographic structures of **3a** and **4a** which confirm the functionalization regioselectivity. Ellipsoids as depicted at 30% probability and hydrogen atoms have been omitted for clarity. Atom colors: N, blue; O, red; C, grey.

As there was no observation of indole structures solely functionalized in the C6 position, it was postulated that the C3 structure was an intermediate. This was investigated by resubmitting the C3 product (**3a**) to the reaction conditions. Pleasingly high conversions to di-substituted structure (**4a**) were observed *via* crude NMR analysis (entry 1, Table 1), leading to excellent isolated yields for remote σ-activation reactions.[12] Reaction efficiency was maintained when using THF and 2-MeTHF as solvent (entries 2-3). The reaction was also shown to proceed with modest efficiency without AcOH (entry 5). It is proposed that the added AcOH facilitates protodemetalation at the end of the reaction cycle. However, it's is not vital to reactivity as 2 equivalents are formed in the reaction mixture. Removal of KOAc nullified reactivity (entry 6) however increased loading (4 eq, entry 7) of potassium acetate showed some increased reactivity cf. without AcOH (entry 5). The reaction did not proceed in the absence of ruthenium catalyst (entry 8). This indicates that both C3 and C6 functionalizations are driven by ruthenium catalysis. The synthesis of **3a** was shown to be scalable, affording up to two grams of material (see Scheme S1 in supporting information).

Table 1. Remote ruthenium(II)-catalyzed C6 C–H alkylation of indole derivative

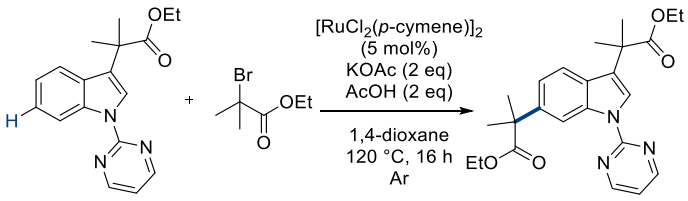

3a **2a** **4a**

Entry	Alteration from Standard Conditions[a]	4a (%)[b]
1	None	96 (80)[c]
2	THF used as solvent	95
3	2-MeTHF used as solvent	89
4	DME used as solvent	56
5	No AcOH	60
6	No KOAc	-
7	4 eq KOAc, No AcOH	70
8	No $[RuCl_2(p\text{-cymene})]_2$	-
9	Reaction carried out under air	9

[a] Standard Conditions: **3a** (0.25 mmol), **2a** (0.75 mmol), $[RuCl_2(p\text{-cymene})]_2$ (0.0125 mmol), KOAc (0.5 mmol), AcOH (0.5 mmol), 1,4-dioxane (1 mL), at 120 °C for 16 h under an argon atmosphere. [b] Direct conversion between **3a** and **4a** observed *via* crude NMR analysis. [c] Isolated Yield.

To investigate whether the C3 functionalization solely functioned as a positional block, permitting access to C6 functionalization on steric grounds as the next most reactive site or if the ester group had some ancillary directing group effect, a pyrimidinyl indole bearing a methyl group in the C3 position was submitted to the reaction conditions (**1c**,

Scheme 3a). No conversion to any product was observed, which signifies the importance of the nature of the C3 functionality in activating the remote C6 position. A C2-Me blocked substrate was also submitted to the reaction conditions (**1d**, Scheme 3b), giving rise to neither the C3 mono-functionalized nor C3/C6 di-functionalized products. This shows that the C2 cyclometalation site is also necessary for the reaction to proceed.

Scheme 3. Remote C6 functionalization of C3-Me and C2-Me indole derivatives

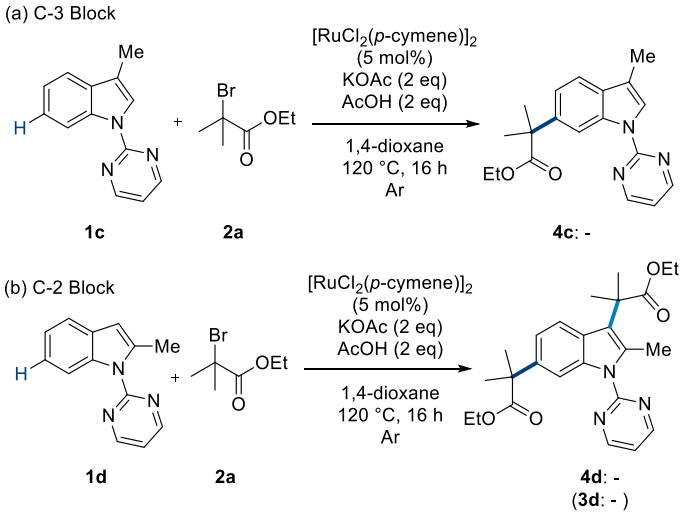

Using this knowledge further indole derivatives with proposed ancillary directing groups (A) were synthesized (Scheme 4a). Firstly, an auxin derivative, without the gem-dimethyl substituents, was shown to lead to conversion to product (**4e**) albeit in lower quantities. An inseparable, uncharacterisable polymeric byproduct was also obtained with this example, this could be due to the potential radical formed on the benzylic position of the ancillary directing group. Neither acetoxy (**4f**) nor formyl (**4g**) derivatives gave formation of C-6 alkylated product.

Scheme 4. Ancillary (A) and primary (P) directing group effects of remote C6 functionalization

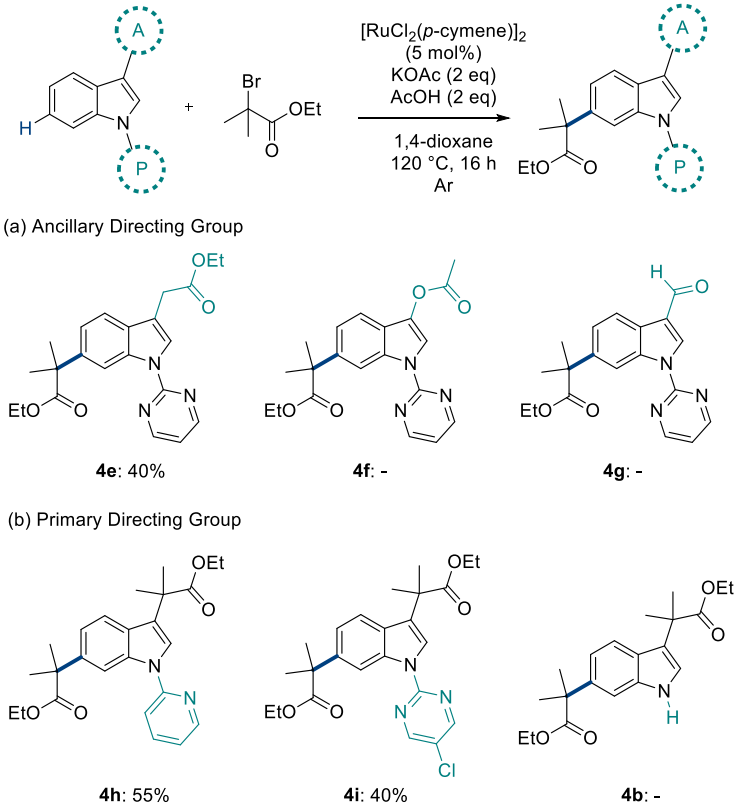

Further to this, a small screen of primary directing groups (P, Scheme 4b) was investigated. Pyridine (**4h**) and chloro-pyrimidine (**4i**) derivatives gave rise to good yields and the lack of primary directing group (**4b**) gave no conversion to product. This, along with the previous results, highlight the necessity for both the primary and ancillary directing groups for effective catalysis at C6 to take place. Various tertiary alkyl halides were submitted to the reaction conditions in order to create highly decorated indole structures (Scheme 5). The use of methyl α-bromoisobutyrate granted access to orthogonally functionalized positions with difficult to construct quaternary centers (**4j**). α-Bromo ketones have previously been used in ruthenium redox catalysis[17] and were also shown to be amenable to this reaction methodology (**4k**). Fluorinated and cyclohexyl variants of the esters were tolerated (**4l-m**), although in poor yields Unfortunately, secondary esters were shown to give trace formation of C6 alkylated product (**4n**). Primary esters, tertiary acids, tertiary amides and tertiary nitriles were not tolerated in this methodology under these reaction conditions (see supporting information).

Scheme 5. Remote C6 functionalization of indole derivatives

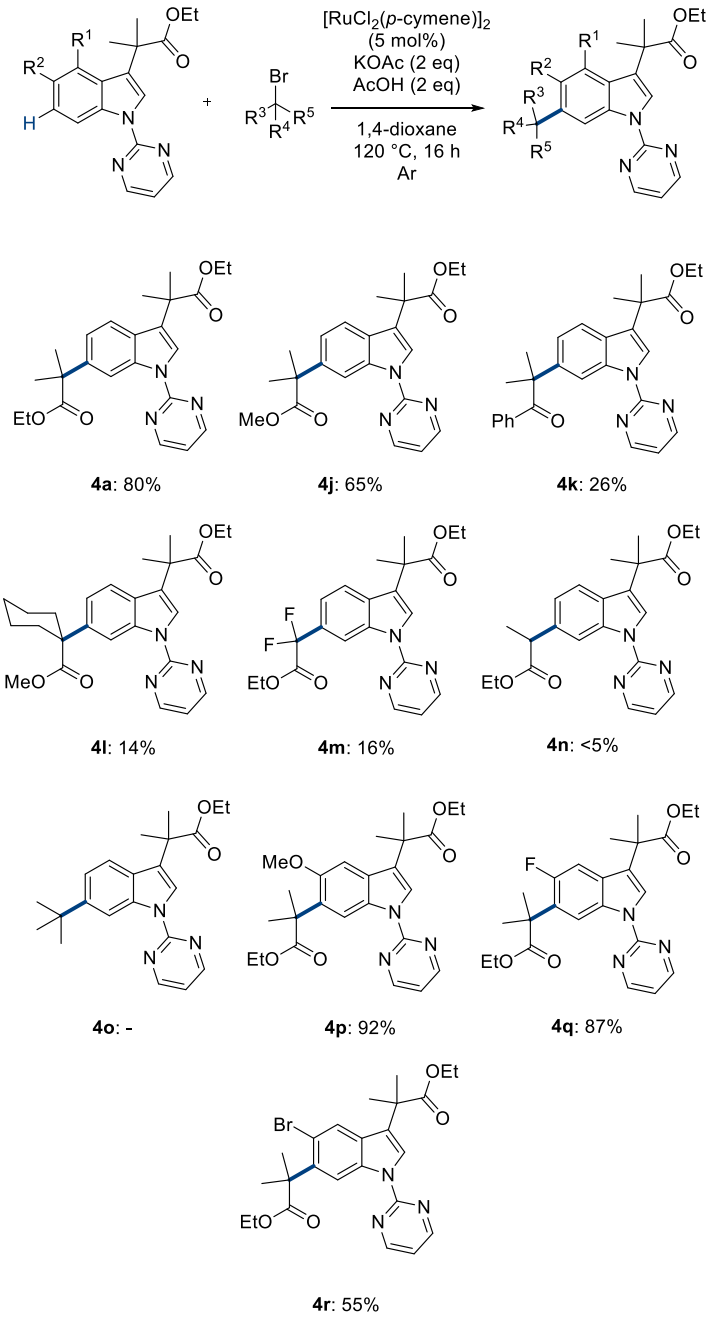

Despite its use in previous remote functionalizations,[12c.d] the use of *tert*-butyl bromide as coupling partner also afforded no C6 alkylated motif (**4o**) under these conditions.[18] This shows the unique reactivity of these α-ester radicals through captodative stabilization.[19] Indole structures bearing electron donating groups gave excellent yields (**4p**), whereas electron poor arenes gave poorer yields (**4r**), consistent with our previous reports.[12c] The *ortho*-/*para*- directing character of alkoxy and halogen substituents could have contributed to the improved yields observed by further activation of the C6 position towards radical attack. C4-F substituted indole was shown to react in poor yields, exclusively at C7 (*para*-

to the fluorine see supporting information, Scheme S3). This was interpreted to take place *via* radical attack to the organic non-cyclometalated species which was also confirmed *in silico* to be the most reactive vacant site (Figure S1).

It is possible to access the C3/C6 di functionalized motif (**4a**) directly from the unsubstituted indole derivative (**1a**). This allows one-pot ruthenium(II)-catalyzed C3 C–H alkylation and subsequent C3 enabled remote C6 selective C–H alkylation. Conditions were explored to drive the reaction methodology to the di-substituted motif (**4a**, Table 2).

Table 2. Optimization of ruthenium(II)-catalyzed C3 C–H alkylation of indole derivatives

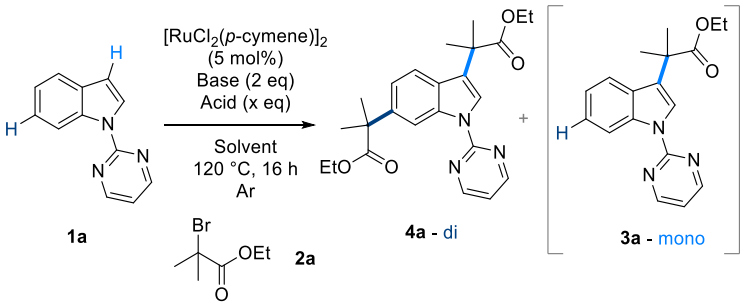

Entry	Solvent	Base	Acid	Acid Eq	4a (%)[b]	3a (%)[b]
1[c]	1,4-dioxane	KOAc	-	-	8	21
2[c]	1,4-dioxane	KOAc	AcOH	2	33	66
3	2-MeTHF	KOAc	AcOH	2	34	62
4	DME	KOAc	AcOH	2	45	48
5	**THF**	**KOAc**	**AcOH**	**2**	**57**	**39**
6	THF	-	AcOH	2	0	26
7	THF	NaOAc	AcOH	2	9	35
8	THF	K_2CO_3	AcOH	2	3	6
9	THF	K_2CO_3[d]	AcOH	2	43	46
10	THF	KOPiv	AcOH	2	9	17
11	THF	KOAc	PivOH	2	32	65
12	THF	KOAc	TFA	2	3	31
13	THF	KOAc	AcOH	3	46	56
14	THF	KOAc	AcOH	10	31	69
15	THF	KOAc	AcOH	33[e]	5	91

[a] General Conditions: 1-(pyrimin-2-yl)-1*H*-indole (**1a**, 0.25 mmol), ethyl α-bromoisobutyrate (0.75 mmol), $[RuCl^2(p\text{-cymene})]_2$ (0.0125 mmol, 5 mol%), Base (2 eq), Additive (x eq), Solvent (1 mL), 120 °C, 16 h under argon atmosphere. [b] Direct ^{1}H NMR conversion. [c] From Scheme 2 for comparison. [d] + KOAc (30 mol%). [e] AcOH used as solvent instead of THF.

A solvent screen showed that the use of THF led to more favorable formation of di-functionalized product (entry 5). Several different bases (entries 7 -10) and acids (entries 11-12) were used in the reaction however none gave superior conversion to the

KOAc/AcOH couple. The reaction system using K_2CO_3 as base (entry 8) was however shown to be reactivated on addition of catalytic quantities of KOAc (entry 9). This clearly demonstrates the need for a carboxylate partner for C–H metalation to take place at start the reaction.[1a] Interestingly it was shown increasing addition of AcOH correlated to increased selectivity towards mono-functionalized product **3a**. This was exemplified by use of AcOH as solvent (entry 15) which led to almost exclusive formation of **3a**. This highlights the importance of AcOH in the C3 functionalization of the pyrimidinyl substituted indole (**1a**), but is then detrimental to C6 functionalization in high quantities. This demonstrates that it is a careful balance of acid and base that drives to di-functionalization (**4a**).

The scope of the one-pot C3 and subsequent C6 functionalization was then explored (Scheme 6). 5-substituted indoles (**4n-p**) gave one-pot reactivity parallel to the C6 functionalization shown previously with the electron rich structure performing most efficiently. The pyridine directing group (**4h**) was shown to be amenable to this reaction albeit in slightly lower yields with respect to the pyrimidine counterpart. The use of the 5-chloropyrimidine directing group (**4i**) led to the highest yield of one-pot C3 and subsequent C6 alkylation. This ability to carry out this double C–H functionalization allows simple quick diversification to create highly decorated complex structures.[20] The mono-functionalized structures have also been shown to be amenable to resubmission to the reaction conditions to drive formation of the di-functionalized motif or reacted with a different coupling partner to give orthogonal C–H functionalization.

Scheme 6. One-Pot C3/C6 functionalization of indole derivatives

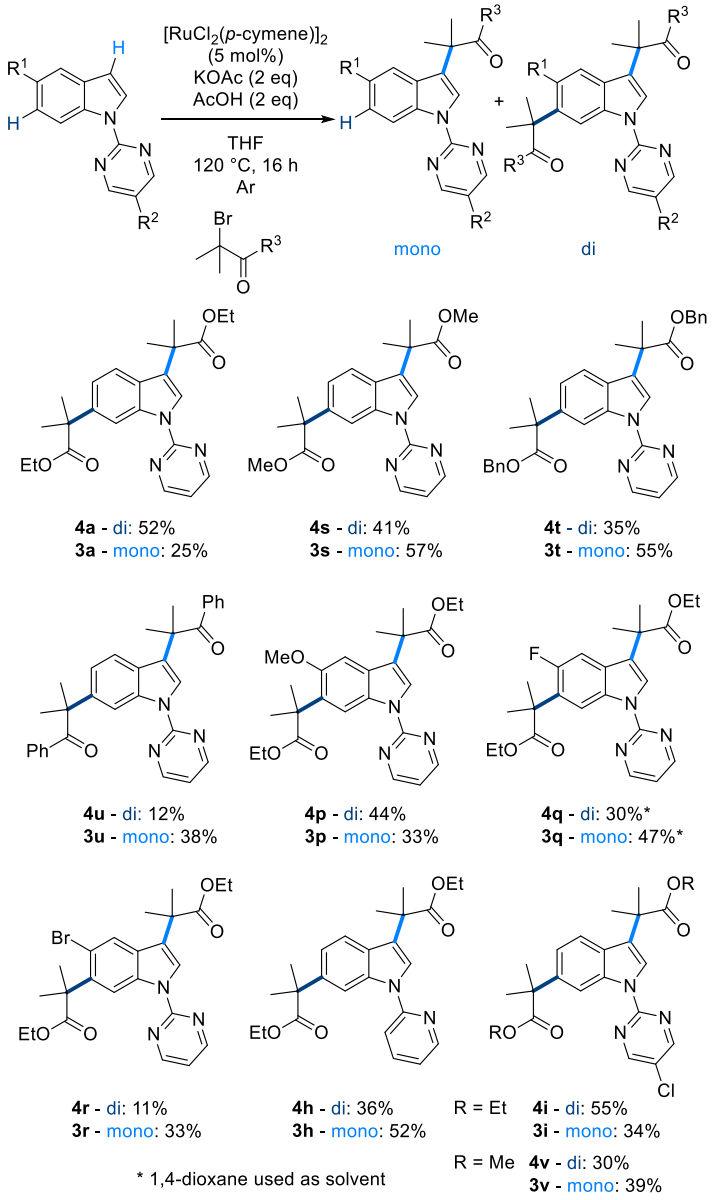

Mechanistic Studies

In order to determine reaction mechanism, experimental and computational mechanistic studies were undertaken. Our previous investigations in remote σ-activation methodology proposed a dual cyclometalation and radical pathway.[12c] Here, the presence of a radical mechanism was investigated by the use of a radical trapping agent (Scheme 7). Neither remote C6 functionalization nor one-pot C3/C6 di-functionalization were observed in the presence of stoichiometric TEMPO. One catalytic turnover was also observed using catalytic quantities of TEMPO, suggesting that a redox catalyst is unable to turn over in the presence of the radical trapping agent. As both reactions (Scheme 7a & 7b) were affected

by these investigations, it can be postulated that both C3 and C6 alkylation proceed *via* a radical pathway.[21]

Scheme 7. TEMPO studies on remote alkylation of indole derivatives

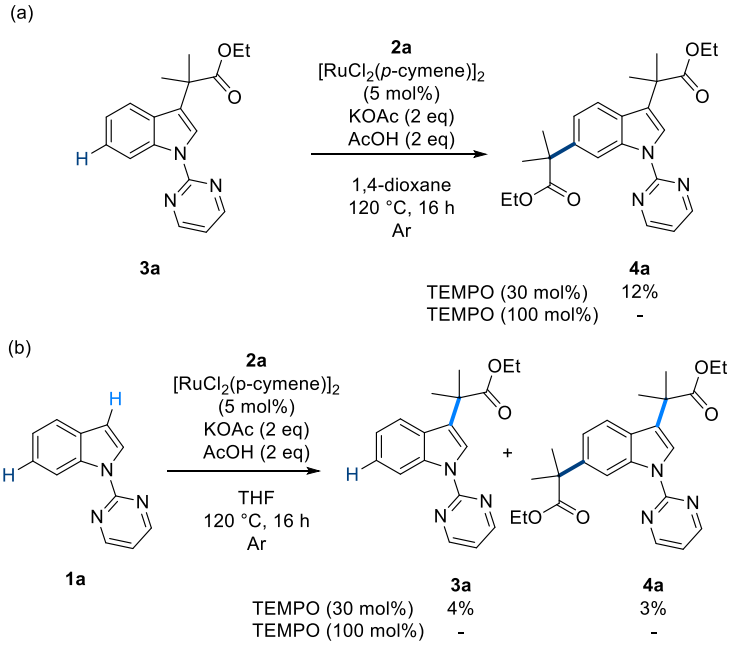

Deuterium incorporation studies using isotopically labelled AcOD were then performed to determine whether formation of C6 and C3 functionalized products are obtained *via* C2 insertion or C7 insertion (Scheme 8).

Scheme 8. Deuterium incorporation investigations

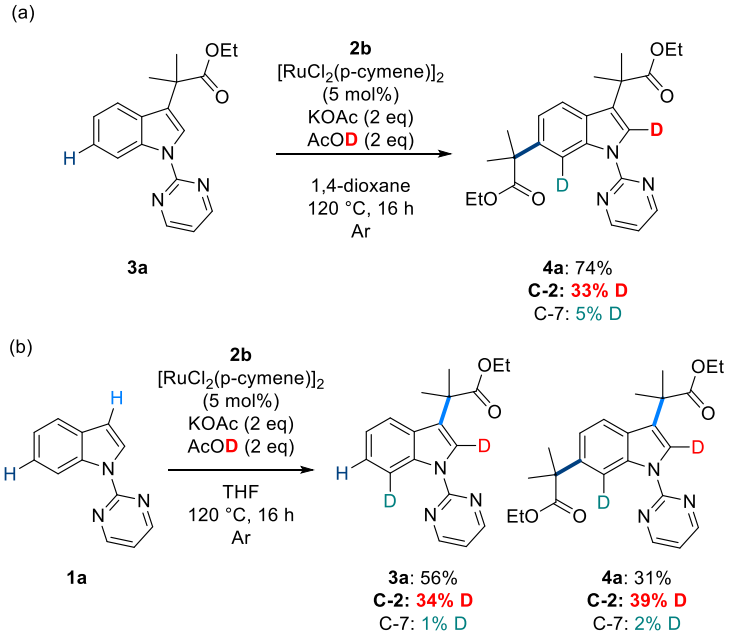

Deuterium was incorporated into the C2 position in significant quantities (33%, Scheme 8a) and only in negligible amounts at C7 (<5%). This highlights that the C6 functionalization is most likely not accessed through C7 insertion as observed in Shi's work but through a C2 cyclometalation σ-activation pathway.[9] Also seeing that similar D-incorporation is observed in **3a** and **4a** in the one-pot methodology (Scheme 9b), it could be suggested that these are formed through the same linear mechanistic pathway.

The cyclometalated complex of **1a** was synthesized and exposed to the reaction conditions (Scheme 9).[5e] Comparable efficiency to both mono and di-functionalization found previously was observed. This implies that such a cyclometalated species could be part of the catalytic cycle, either as a redox catalyst in radical generation or through a *ortho*-σ-activation catalyst, activating the C3 position for initial radical attack.[22]

Scheme 9. Remote functionalization using a well-define cyclometalated monomer

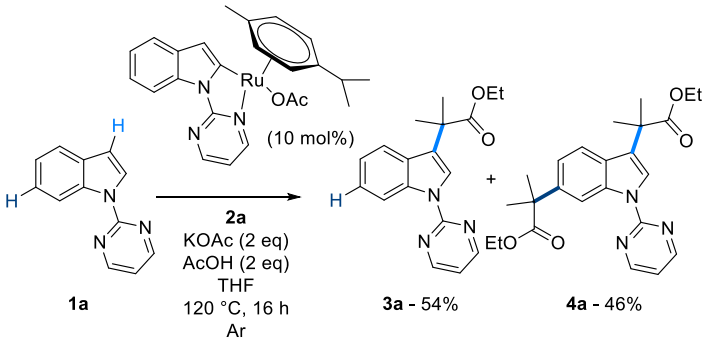

In order to elucidate the reasoning behind the exclusive C6 functionalization we employed computational methods. Ritter and co-workers used nucleophilic Fukui indices as a simple method to predict selectivity in aromatic radical reactions in a recent report.[23] We looked to apply this computational approach to the organic structures synthesized in this study as well as the equivalent cyclometalated complexes. In order to do this, the relative Fukui indices were calculated from NBO calculations for carbon atoms in both the organic (non-cyclometalated substrates) and a range of inorganic (cyclometalated at either the C2 or C7 position) structures, shown in Figure 3 (additional structures in the SI).[24] Our relative Fukui indices show the reactivity of carbons towards electrophilic attack with the most reactive carbon site for functionalization highlighted in red.[24]

The inherent reactivity of the organic indole reagent, **1a**, is unsurprisingly held at the C3 position according to the relative Fukui indices. Cyclometalation at C2 (**^{1a}B-C2**) shows that C3 is still the most reactive carbon, however, an increase in relative reactivity of the C6

position is observed. As both these organic and inorganic structures are shown to activate the C3 position, it is still possible for initial C3 radical addition (to form **3a**) to be achieved through an inner sphere or outer sphere mechanism. Cyclometalation at C7 (**^{1a}B-C7**) shows a huge increase in reactivity at the C4 position. As this regioselectivity is not observed experimentally, alongside deuterium incorporation experiment results, it is concluded that this cyclometalated species is not involved in the formation of the C-6 functionalized product (**4a**). A computed free energy difference of 6.3 kcal mol^{-1} between the more stable **^{1a}B-C2** and **^{1a}B-C7**, also confirms the experimental regioselectivity.

Relative Fukui indices were also calculated for the C3 functionalized material (**3a**), again cyclometalated at either the C2 or C7 position. Values for the organic **3a** show that the most reactive site for C–H functionalization is the C4 position. Therefore, a radical addition mechanism to a non-cyclometalated species can be dismissed and consequently this demonstrates that the metal center and cyclometalation are directly responsible for the observed regioselectivity of the reaction. Two conformers of the C2 cyclometalated structure, **^{3a}B-C2** have been optimized and are shown in Figure 4. The most stable conformer, **^{3a}B-C2***, involves coordination of the ester group to the Ru center through the carbonyl oxygen, forcing ring-slippage of the *para*-cymene to η^2 to accommodate this additional binding to **3a**, whilst the acetate coordinates through both oxygen atoms (κ^2). This additional binding of the ester group at the C3 position to the ruthenium stabilizes the organometallic structure by 3.4 kcal mol^{-1}, when compared to **^{3a}B-C2**.

The ability of **3a** to access this more stable planar tridentate binding motif through the ester group could explain the improved remote functionalization *via* σ-activation observed for this substrate. Previously, remote functionalization *via* this method has been primarily limited primarily to 2-phenylpyridine due to its strong planar ruthenacycle. Identification of this ancillary stabilization provided by the ester group at C3 presents the opportunity to explore similar structural motifs with this methodology.

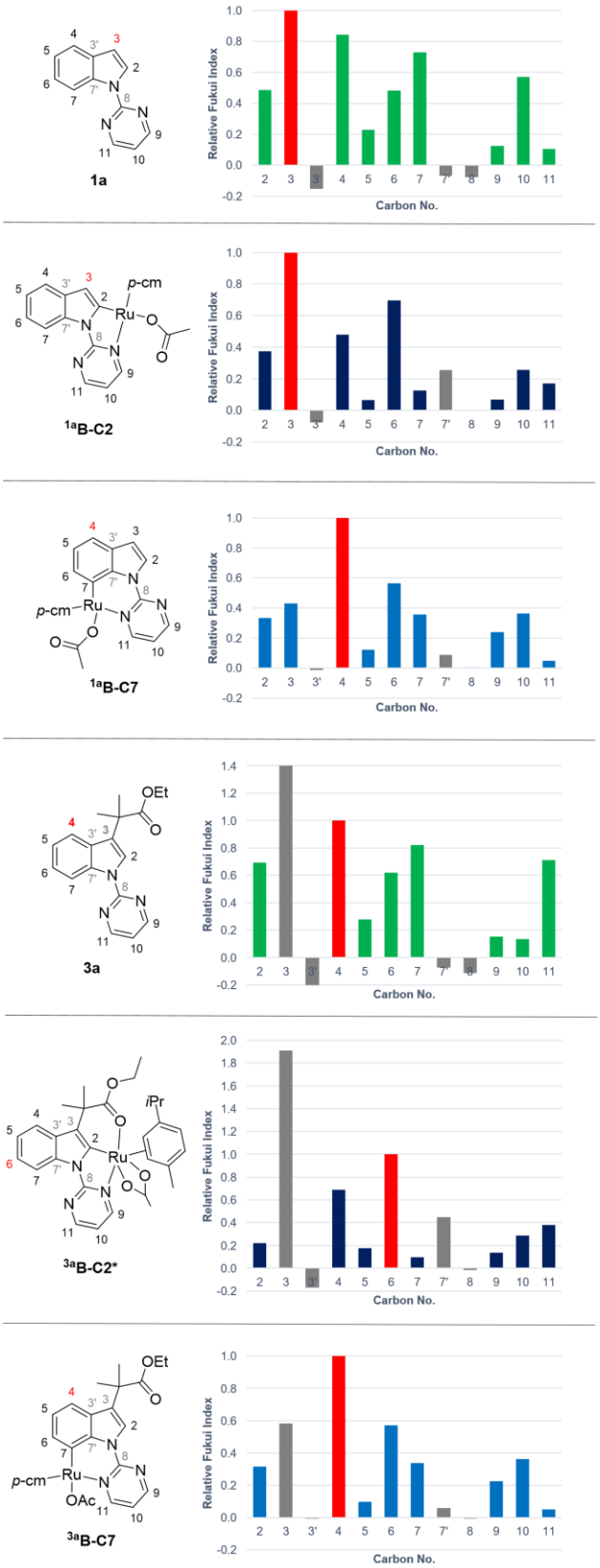

Figure 3. Relative nucleophilicity Fukui indices for organic and inorganic computed structures. Calculations were performed at the BP86/6-31G**&SDD(Ru) level of theory. Fukui indices were calculated with NBO total atomic charges from the optimized neutral structure. Most reactive vacant C–H position is highlighted in red.

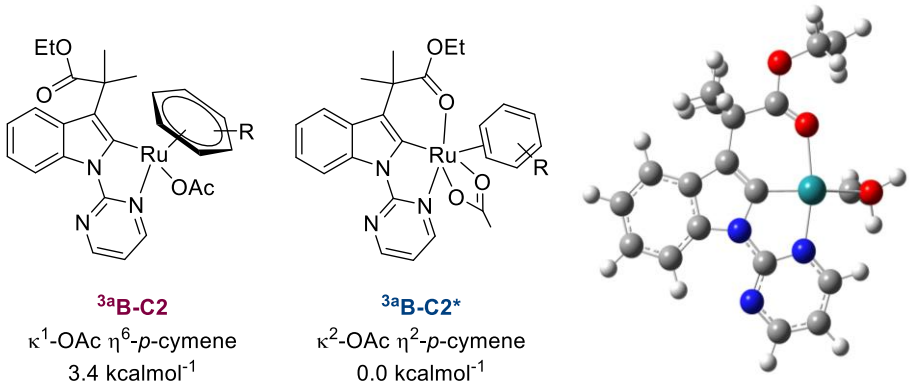

^{3a}B-C2
κ^1-OAc η^6-*p*-cymene
3.4 kcalmol^{-1}

^{3a}B-C2*
κ^2-OAc η^2-*p*-cymene
0.0 kcalmol^{-1}

Figure 4. Free energies of optimized conformers **^{3a}B-C2** and **^{3a}B-C2*** using BP86/6-31G**&SDD(Ru) in kcal mol^{-1} showing the impact of ester binding. The ball-and-stick structure is of **^{3a}B-C2*** with the η^2-*para*-cymene omitted for clarity.

Based on results from both computational and experimental investigations, a plausible mechanism is proposed for the remote radical functionalization of **3a** (Scheme 10). The $[RuCl_2(p\text{-cymene})]_2$ dimer is first broken apart using KOAc to form the proposed catalytically active monomer $[Ru(OAc)_2(p\text{-cymene})]$ (which is competent in the reaction, see supporting information Scheme S2). Carboxylate assisted cyclometalation at C2 then occurs, including a proposed ring slip of the *para*-cymene to accommodate the primary and ancillary directing groups. A ruthenium(II) catalyst then most likely creates the tertiary alkyl radical *via* single electron transfer.[12c] The alkyl radical then attacks the cyclometalated species at the most activated vacant position, confirmed to be C6 *in silico*. Redox rearomatization then takes place using the ruthenium(III) generated previously and an equivalent of potassium acetate. Protodemetalation then occurs using AcOH to give the C6 C–H alkylated product (**4a**) and reforms the catalytically active monomer.

Conclusion

In conclusion we have developed the first remote functionalization of indole derivatives *via* σ-activation. This was achieved using a cyclometalated ruthenium species at the C2 position of the indole. It has been reported that an ester ancillary directing group at C3 was essential for remote C–H alkylation at C6 to occur and yields of up to 92% were achieved applying this methodology. We also reported the one-pot installation of the ester at C3 *via* ruthenium catalysis followed by ruthenium-catalyzed remote C6 functionalization. Initial C3 functionalisation has been shown to proceed *via* a redox ruthenium-catalyzed pathway, as well as remote C6 functionalization *via* radical trapping experiments. Computed Fukui indices were applied to organic and cyclometallated inorganic structures to explain

the C6 position as the most reactive C–H site for functionalization. Work is ongoing to apply this template to other remote *meta*-functionalization reactions.

Scheme 10. Plausible mechanism for remote C6 C–H alkylation of 3a

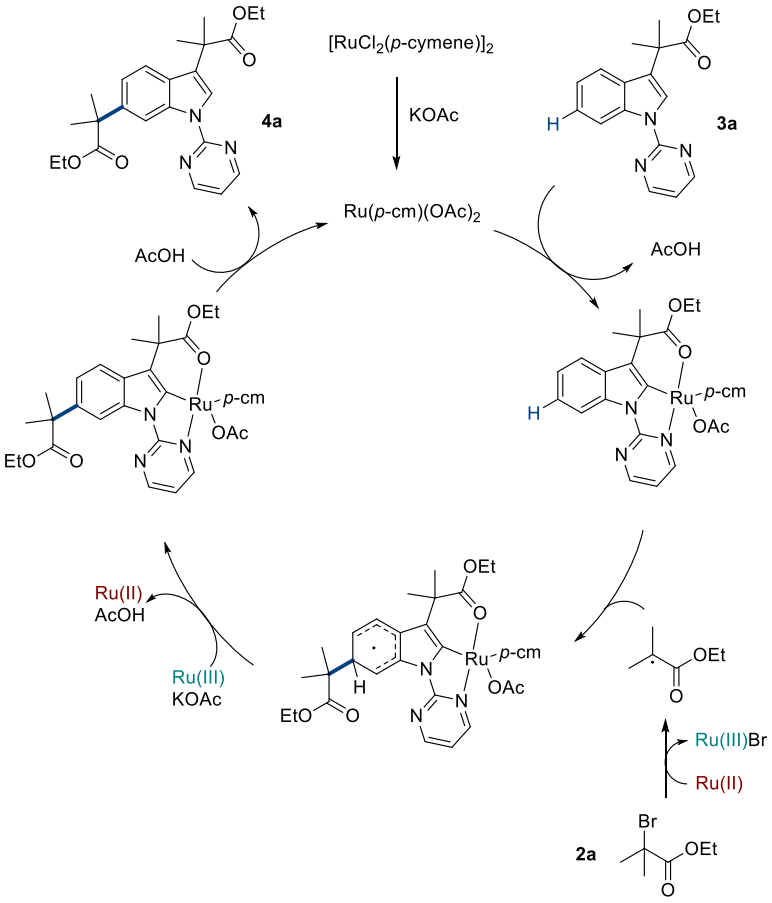

ASSOCIATED CONTENT

Supporting Information

Synthetic procedures and full characterization of compounds is available in the supporting information. Full crystallography data is available *via* the CIF files attached as supporting information.

The Supporting Information is available free of charge on the ACS Publications website.

AUTHOR INFORMATION

Corresponding Author

* Christopher G. Frost: c.g.frost@bath.ac.uk

ACKNOWLEDGMENT

JAL would like to thank the University of Bath and Syngenta for funding as well as Sam Spring for analytical help.

NOTES AND REFERENCES

(1) For reading on transition-metal catalyzed C–H functionalization see: (a) Ackermann, L. *Chem. Rev.* **2011**, *111*, 1315-1345. (b) Arockiam, P. B.; Bruneau, C.; Dixneuf, P. *Chem. Rev.* **2012**, *112*, 5879-5918. (c) Chen, X.; Engle, K. M.; Wang, D-H.; Yu, J-Q. *Angew. Chem. Int. Ed.* **2009**, *48*, 5094-5115. (d) Engle, K. M., Mei, T-S.; Wasa, M.; Yu, J-Q. *Acc. Chem. Res.* **2012**, *45*, 788-802. For reading on derivation of biologically active structures by C–H activation see: (a) Leitch, J. A.; Wilson, P. B.; McMullin, C. L.; Mahon, M. F.; Bhonoah, Y.; Williams, I. H.; Frost, C. G. *ACS Catal.*, **2016**, *6*, 5520-5529. (b) Yamaguchi, J.; Yamaguchi, A. D.; Itami, K. *Angew. Chem. Int. Ed.* **2012**, *51*, 8960-9009. (c) Brown, J. A.; Cochrane, A. R.; Irvine, S.; Kerr, W. J.; Mondal, B.; Parkinson, J. A.; Paterson, L. C.; Reid, M.; Tuttle, T.; Andersson, S.; Nilsson, G. N. *Adv. Synth. Catal.* **2014**, *356*, 3551-3562. (d) Leitch, J. A.; Cook, H. P.; Bhonoah, Y.; Frost, C. G. *J. Org. Chem.*, **2016**, *81*, 10081-10087.

(2) For reading on indoles in biologically relevant molecules see: (a) Zhang, M.-Z.; Chen, Q.; Yang, G.-F.; *Eur. J. Med. Chem*., **2015**, *89*, 421-441. (b) Woodward, A. W.; Bartel, B. *Ann. Bot*., **2005**, *95*, 707-735. (c) Galliford, C. V.; Sheidt, K. A. *Angew. Chem. Int. Ed*., **2007**, *46*, 8748-8758. (d) Trost, B. M.; Brennan, M. K. *Synthesis-Stuttgart*, **2009**, *18*, 3003-3025. (e) Kochanowska-Karamyan, A. J.; Hamann, M. T. *Chem. Rev.*, **2010**, *8*, 4489-4497. (f) Kaushik, N. K.; Kaushik, N.; Attri, P.; Kumar, N.; Kim, C. H.; Verma, A. K.; Choi, E. H. *Molecules*, **2013**, *18*, 6620-6662. (g) Taylor, R. D.; MacCoss, M.; Lawson, A. D. G. *J. Med. Chem.*, **2014**, *57*, 5845-5859.

(3) For reading on the synthesis of decorated indoles (a) Humphrey, G. R.; Kuethe, J. T. *Chem. Rev.*, **2006**, *106*, 2875-2911. (b) Bandini, M.; Eichholzer, A. *Angew. Chem. Int. Ed.*, **2009**, *48*, 9608-9644. (c) Larock, R. C.; Yum, E. K. *J. Am. Chem. Soc.*, **1991**, *113*, 6689-6690. (d) Beck, E. M.; Gaunt, M. J. *Top Curr. Chem.*, **2010**, *292*, 85-121. (e) Austin, J. F.; MacMillan, D. W. C. *J. Am. Chem. Soc.*, **2002**, *124*, 1172-1173. (f) Antilla, J. C.; Klapars, K.; Buchwald, S. L. *J. Am. Chem. Soc.*, **2002**, *124*, 11684-11688. (g) Ackermann, L. *Acc. Chem. Res.*, **2014**, *47*, 281-295. (h) Cacchi, S.; Fabrizi, G. *Chem. Rev.*, **2005**, *105*, 2873-2920. (i) Lebrasseur, N.; Larrosa, I. *Advances in Heterocyclic Chemistry, Vol. 105*, **2012**, 309-351.

(4) (a) Seregin, I. V.; Gevorgyan, V. *Chem. Soc. Rev.*, **2007**, *36*, 1173-1193. (b) Phipps, R. J.; Grimster, N. P.; Gaunt, M. J. *J. Am. Chem. Soc.*, **2008**, *130*, 8172-8174. (c) Brand, J. P.; Charpentier, J.; Waser, J. *Angew. Chem. Int. Ed.*, **2009**, *48*, 9346-9349. (d) Zhu, Y.; Rawal,

V. H. *J. Am. Chem. Soc.* **2012**, *134*, 111-114. (e) Grimster, N. P.; Gauntlett, C.; Godfrey, C. R. A.; Gaunt, M. J. *Angew. Chem. Int. Ed.*, **2005**, *44*, 3125-3129. (f) Jia, C.; Lu, W.; Kitamura, T.; Fujiwara, Y. *Org. Lett.*, **1999**, *1*, 2097-2100. (g) Phipps, R. J.; Grimster, N. P.; Gaunt, M. J. *J. Am. Chem. Soc.*, **2008**, *130*, 8172-8174.

(5) (a) Yan, Z.-B.; Shen, Y.-W.; Chen, D.-Q.; Gao, P.; Li, Y.-X.; Song, X.-R.; Liu, Z.-Y.; Liang, Y.-M. *Tetrahedron*, **2014**, *70*, 7490-7495. (b) Kumar, G. S.; Kapur, M. *Org. Lett.*, **2016**, *18*, 1112-1115 (c) Mei, R.; Loup, J.; Ackermann, L. *ACS Catal.*, **2016**, *6*, 793-797. (d) Xie, F.; Zisong, Yu, S.; Li, X. *J. Am. Chem. Soc.*, **2014**, *136*, 4780-4787. (e) Sollert, C.; Devaraj, K.; Orthaber, A.; Gates, P. J.; Pilarski, L. T. *Chem. Eur. J.*, **2015**, *21*, 5380-5386. (f) Capito, E.; Brown, J. M.; Ricci, A. *Chem. Commun.*, **2005**, 1854-1856. (g) Deprez, N. R.; Kalyani, D.; Krause, A.; Sanford, M. S. *J. Am. Chem. Soc.*, **2006**, *128*, 4972-4973. (h) Islam, S.; Larrosa. *Chem. Eur. J.*, **2013**, *19*, 15093-15096. (i) Lebrasseur, N.; Larrosa, I. *J. Am. Chem. Soc.*, **2008**, *130*, 2926-2927.

(6) (a) Yang, Y.; Qiu, X.; Zhao, Y.; Mu, Y.; Shi, Z. *J. Am. Chem. Soc.*, **2016**, *138*, 495-498. (b) Hartung, C. G.; Fecher, A.; Chapell, B.; Snieckus, V. *Org. Lett.*, **2003**, *5*, 1899-1902.

(7) Feng, Y.; Holte, D.; Zoller, J.; Umemiya, S.; Simke, L. R.; Baran, P. S*. J. Am. Chem. Soc.* **2015**, *137*, 10160-10163.

(8) Yang, G.; Lindovska, P.; Zhu, D.; Kim, J.; Wang, P.; Tang, R.- Y.; Movassaghi, M.; Yu, J.-Q. *J. Am. Chem. Soc.* **2014**, *136*, 10807-10813.

(9) (a) Yang, Y.; Li, R.; Zhao, Y.; Zhao, D.; Shi, Z. *J. Am. Chem. Soc.*, **2016**, *138*, 8734-8737. (b) Liu, H.; Zheng, C.; You, S.-L. *J. Org. Chem.*, **2014**, *79*, 1047-1054. (c) A recent report by Larrosa also gives C-6 arylation through the presence of a directing group at C-5 or C-7: Simonetti, M.; Cannas, D. M.; Panigrahi, A.; Kujawa, S.; Kryjewski, M.; Xie, P.; Larrosa, I. *Chem. Eur. J*., **2017**, 23, 549-553.

(10) (a) Yang. J. *Org. Biomol. Chem.*, **2015**, *13*, 1930-1941. (b) Phipps, R. J.; Gaunt, M. J. *Science*, **2009**, *323*, 1593-1597. (c) Frost, C. G.; Paterson, A. P. *ACS Cent. Sci.*, **2015**, *1*, 418-419. (d) Ackermann, L.; Li, J. *Nat. Chem.*, **2015**, *7*, 686-687.

(11) (a) Leow, D.; Li, G.; Mei, T-S.; Yu, J-Q. *Nature*, **2012**, *486*, 518-522. (b) Tang, R-Y.; Li, G.; Yu, J-Q. *Nature*, **2014**, *507*, 215-220. (c) Chu, L.; Shang, M.; Tanaka, K.; Chen, Q.; Pissarnitski, N.; Streckfuss, E.; Yu, J-Q. *ACS Cent. Sci.*, **2015**, *1*, 394-399. (d) Bera, M.; Sahoo, S. K.; Maiti, D. *ACS Catal.*, **2016**, *6*, 3575-3579. (e) Bera, M.; Modak, A.; Patra, T.; Maji, A.; Maiti, D. *Org. Lett.*, **2014**, *16*, 5760-5763. (f) Dey, A.; Agasti, S.; Maiti, D. *Org. Biomol. Chem.*, **2016**, *14*, 5440-5453. (g) Davis, H. J.; Mihai, M. T.; Phipps, R. J. *J. Am. Chem. Soc.*, **2016**, *138*, 12759-12762.

(12) (a) Saidi, O.; Marafie, J.; Ledger, A. E. W.; Liu, P. M.; Mahon, M. F.; Kociok-Köhn, G.; Whittlesey, M. K.; Frost, C. G. *J. Am. Chem. Soc.*, **2011**, *133*, 19298-19301. (b) Hofmann, N.; Ackermann, L. *J. Am. Chem. Soc.*, **2013**, *135*, 5877-5884. (c) Paterson, A. J.; St. John

Campbell, S.; Mahon, M. F.; Press, N. J.; Frost, C. G. *Chem. Commun.*, **2015**, *51*, 12807-12810. (d) Li, J.; Warratz, S.; Zell, D.; De Sarkar, S.; Ishikawa, E. E.; Ackermann, L. *J. Am. Chem. Soc.*, **2015**, *137*, 13894-13901. (e) Teskey, C. J.; Lui, Y. W.; Greaney, M. F. *Angew. Chem. Int. Ed.*, **2015**, *54*, 11677-11680. (f) Yu, Q.; Hu, L.; Wang, Y.; Zheng, S.; Huang, J. *Angew. Chem. Int. Ed.*, **2015**, *54*, 15284-15288. (g) Fan, Z.; Ni, J.; Zhang, A. *J. Am. Chem. Soc.*, **2016**, *138*, 8470-8475. (h) Warratz, S.; Burns, D. J.; Zhu, C.; Korvorapun, K.; Rogge, T.; Scholz, J.; Jooss, C.; Gelman, D.; Ackermann, L. *Angew. Chem. Int. Ed.*, **2017**, *56*, 1557-1560. (i) Ruan, Z.; Zhang, S.-K.; Zhu, C.; Ruth, P. N.; Stalke, D.; Ackermann, L. *Angew. Chem. Int. Ed.*, **2017**, DOI: 10.1002/anie.201611595. (j) Li, G.; Ma, X.; Jia, C.; Han, Q.; Wang, Y.; Wang, J.; Yu, L.; Yang, S. *Chem. Commun.*, **2017**, *53*, 1261-1264.

(13) (a) Luo, J.; Preciado, S.; Larrosa, I. *J. Am. Chem. Soc*., **2014**, *136*, 4109-4112. (b) Kuninobu, Y.; Ida, H.; Nishi, M.; Kanai, M. *Nat. Chem.*, **2015**, *7*, 712-717. (c) Wang, X-C.; Gong, W.; Fang, L-Z.; Zhu, R-Y.; Li, S.; Engle, K. M.; Yu, J-Q. *Nature*, **2015**, *519*, 334-338. (d) Dong, Z.; Wang, J.; Dong, G. *J. Am. Chem. Soc.*, **2015**, *137*, 5887-5890. (e) Shi, H. S.; Wang, P.; Suzuki, S.; Farmer, M. E.; Yu, J.-Q. *J. Am. Chem. Soc.*, **2016**, *138*, 14876-14879. (f) Ding, Q.; Ye, S.; Cheng, G.; Wang, P.; Farmer, M. E.; Yu, J.-Q. *J. Am. Chem. Soc.*, **2017**, *139*, 417-425.

(14) (a) Mkhalid, I. A. I.; Barnard, J. H.; Marder, T. B.; Murphy, J. M.; Hartwig, J. F., *Chem. Rev.*, **2010**, *110*, 890-931. (b) Cho, J.-Y.; Tse, M. K.; Holmes, D.; Maleczka, R. E.; Smith, M. R. *Science*, **2002**, *295*, 305-308. (c) Zhang, Y.-H.; Shi, B.-F.; Yu, J.-Q., *J. Am. Chem. Soc.*, **2009**, *131*, 5072-5074.

(15) (a) Crystal Data for $C_{18}H_{19}N_3O_2$ (compound **3a**): *M* =309.36 g/mol: monoclinic, space group $P2_1/n$ (no. 14), *a* = 8.2446(3) Å, *b* = 18.1585(6) Å, *c* = 10.6143(5) Å, *β* = 99.541(4)°, *V* = 1567.09(11) Å^3, *Z* = 4, *T* = 293(2) K, μ(MoKα) = 0.087 mm^{-1}, *Dcalc* = 1.311 g/cm^3, 13314 reflections measured (6.728° ≤ 2Θ ≤ 54.966°), 3591 unique (R_{int} = 0.0347, R_{sigma} = 0.0373) which were used in all calculations. The final R_1 was 0.0465 (I > 2σ(I)) and wR_2 was 0.1082 (all data). (b) Crystal Data for $C_{24}H_{29}N_3O_4$ (compound **4a**): *M* =423.50 g/mol: triclinic, space group P-1 (no. 2), *a* = 7.2094(3) Å, *b* = 12.0942(5) Å, *c* = 13.0064(6) Å, *α* = 106.921(4)°, *β* = 90.760(4)°, *γ* = 95.278(3)°, *V* = 1079.40(8) Å3, *Z* = 2, *T* = 293(2) K, μ(CuKα) = 0.725 mm^{-1}, *Dcalc* = 1.303 g/cm^3, 10342 reflections measured (7.11° ≤ 2Θ ≤ 146.734°), 4306 unique (R_{int} = 0.0223, R_{sigma} = 0.0252) which were used in all calculations. The final R_1 was 0.0383 (I > 2σ(I)) and wR_2 was 0.1011 (all data).

(16) Furst, L.; Matsuura, B. S.; Narayanam, J. M. R.; Tucker, J. W.; Stephenson, C. R. J. *Org. Lett.,* **2010**, *12*, 3104-3107.

(17) Cheng, J.; Deng, X.; Wang, G.; Li, Y.; Cheng, X.; Li, G. *Org. Lett*., **2016**, *18*, 4538-4541.

(18) **4m** was observed using conditions from references 12c and 12d in 0% and 8% conversions respectively

(19) Viehe, H. G.; Janousek, Z.; Merenyi, R.; Stella, L. *Acc. Chem. Res.*, **1985**, *18*, 148-154.

(20) Ghosh, K.; Rit, R. K.; Ramesh, E.; Sahoo, A. K. *Angew. Chem. Int. Ed.*, **2016**, *55*, 7821.

(21) Vogler, T.; Studer, A. *Synthesis*, **2008**, *13*, 1979-1993

(22) We were unable to isolate the cyclometalated complex of **3a** despite multiple efforts

(23) Boursalian, G. B.; Ham, W. S.; Mazzotti, A. R.; Ritter, T. *Nat. Chem.*, **2016**, *8*, 810-815.

(24) DFT calculations (BP86) were run with Gaussian 09 (Revision D.01). The Ru center was described with the Stuttgart RECP and associated basis set, whilst 6-31G** basis set was used for all other atoms. Full details and references for all computational methods can be found in SI.

3.4: Ruthenium-Catalyzed Remote C4-Selective C–H Functionalization of Carbazoles via σ-Activation

3.4.1: Introduction and Commentary

On the back of the success of the indole project, we were intrigued to see whether blocking the C2 and C3 positions of an indole could in turn enable selective cyclometalation at C7. This proposed cyclometalate (Scheme 3-7) could then potentially activate the remote C4 positions of the indole structure. This would grant access to a substrate-dependent complementary selectivity which could be an attractive strategy for accessing new chemical space for *inter alia* drug discovery and development.

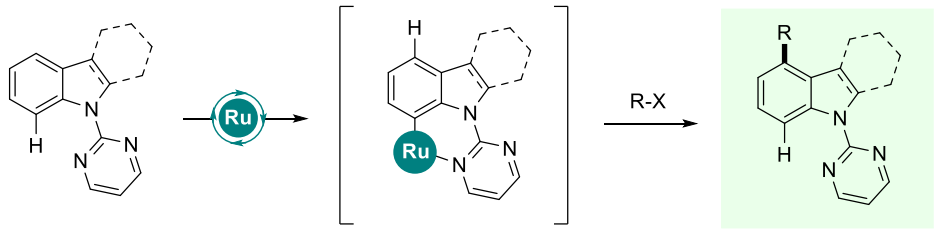

Scheme 3-7: Proposal for C4-Selective C–H Functionalisation of Indole Structures

In order to investigate this theory, three test motifs based on the indole structure were synthesised. These substrates were the indoline, 2,3-diethylindole and carbazole heteroaromatics furnished with a pyrimidinyl directing group. All three substrates would not permit cyclometalation at C2, hopefully prompting the regioselectivity switch. These test motifs were submitted to the indole conditions to probe potential reactivity (Scheme 3-8).

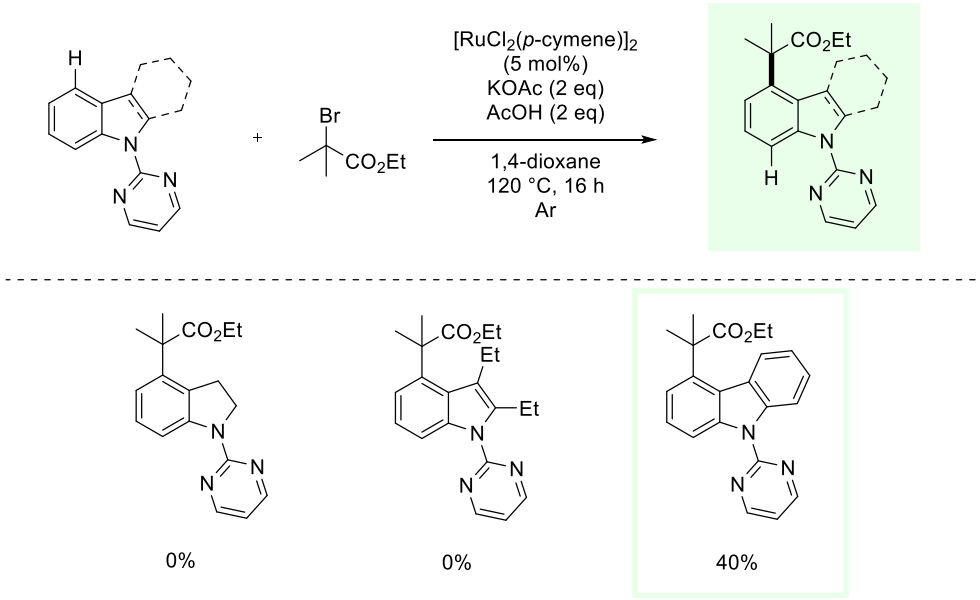

Scheme 3-8: Ruthenium-Catalysed C–H Alkylation of Indole-Cored Variants

These initial studies showed one of the structures was by far the most amenable to this remote functionalisation methodology, the carbazole derivative. The success of this derivative could be rationalised by looking at factors which have been previously suggested to be vital the reactivity of a σ-activation complex: stability and planarity.[1] Whilst the carbazole motif may not necessarily provide a more stable metallocycle than the other structures, it does however possess planarity across the whole arene system. This could be crucial to its proposed reactivity. As discussed previously, there have been multiple systems that enable the selective C1 cyclometalation and subsequent functionalisation of carbazoles at C1.[2] To this date there have been no reported methods to selective functionalise the C4 position. As carbazoles found widespread application in sensing[3] and OLED[4] applications, the ability to derivate these positions could prove to be a transformation of synthetic utility. From this point, it was decided to carry forward this project on C4 carbazole derivation in reaction optimisation and development. The results from this point will be displayed as the communication currently under peer review.

References

(1) J. A. Leitch, C. L. McMullin, M. F. Mahon, Y. Bhonoah, and C. G. Frost, *ACS Catal.*, 2017, **7**, 2616

(2) J. A. Leitch, Y. Bhonoah, and C. G. Frost, *ACS Catal.*, 2017, **7**, 5618.

(3) X. Zhang, L. Chi, S. Ji, Y. Wu, P. Song, K. Han, H. Guo, T. D. James, J. Zhao, *J. Am. Chem. Soc.*, 2009, **131**, 17452.

(4) Y. Tao, Q. Wang, C. Yang, Q. Wang, Z. Zhang, T. Zou, J. Qin, and D. Ma, *Angew. Chem. Int. Ed.*, 2008, **120**, 8224

3.4.2: Authorships and Permissions

This declaration concerns the article entitled									
Ruthenium-Catalyzed Remote C4-Selective C–H Functionalization of Carbazoles via σ-Activation									
Publication status (tick one)									
Draft manuscript		**Submitted**		**In review**		**Accepted**		**Published**	X
Publication details (reference)	J. A. Leitch, C. J. Heron, J. McKnight, G. Kociok-Kohn, and C. G. Frost, *Chem. Commun.,* 2017, **53**, 13039.								
Candidate's contribution to the paper (detailed, and also given as a percentage)	The candidate contributed to/ considerably contribute to/predominantly execute the: **Formulation of ideas (80%):** Project proposed and designed by JAL in discussion with CGF (20%) **Design of methodology (60%)**: Methodology designed by JAL and CJH (30%) in discussion with CGF (10%) **Experimental work (45%)**: JAL and CJH (35%) contributed the majority of synthetic work. JAL covered the synthesis of carbazole starting materials and half of the scope. CJH covered the optimisation and the rest of the scope. JM contributed preliminary results (15%) and GKK provided crystallography (5%). **Presentation of data in journal format (75%)**: JAL wrote the majority of the manuscript in preparation for submission. Edited by CJH (10%) and CGF (10%). Looked over by JM (2.5%) and YB (2.5%).								
Statement from Candidate	This paper reports on original research I conducted during the period of my Higher Degree by Research candidature								
Signed	Jamie A. Leitch						**Date**	06/12/17	

3.4.3: Manuscript for "Ruthenium-Catalyzed Remote C4-Selective C–H Functionalization of Carbazoles via σ-Activation"

Complete manuscript given at point of corrections follows on the next page. Layout changes have been made for consistency for this thesis. Scheme 6 has been included from the SI in the paper for ease of reading.

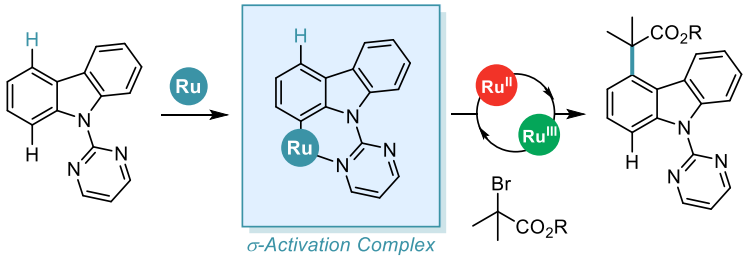

Ruthenium Catalyzed Remote C4-Selective C–H Functionalization of Carbazoles *via* σ-Activation

Jamie A. Leitch,[†] Callum J. Heron, [†,‡] Janette McKnight,[†] Gabriele Kociok-Köhn,[+] Yunas Bhonoah,[¥] and Christopher G. Frost.*[,†]

[†]Department of Chemistry, University of Bath, Claverton Down, Bath, Somerset, BA2 7AY, United Kingdom

[‡]Centre for Sustainable Chemical Technologies, University of Bath, Bath, Somerset, BA2 7AY, United Kingdom

[+]Chemical Characterisation and Analysis Facility, University of Bath, Bath, Somerset, BA2 7AY, United Kingdom

[¥] Syngenta, Jealott's Hill International Research Centre, Bracknell, Berkshire, RG42 6EY, United Kingdom

ABSTRACT: The selective C–H functionalization of the carbazole heteroaromatic offers potential utility in drug discovery, sensing, and in organic electronics chemistry. Herein, we report the C4-selective C–H alkylation of carbazole derivatives furnished with a pyrimidine directing group at N9. This was realized using ruthenium σ-activation methodology, whereby C–H activation at C1 enables the interaction of this ruthenacycle, at the *para* position to the metal center, with tertiary alkyl radicals. This transformation was shown to be tolerant of a variety of α-halocarbonyl coupling partners and aryl substitution patterns with yields up to 92% with complete selectivity for the C4 position of the carbazole structure.

Transition metal catalyzed C–H functionalization has emerged as a powerful asset to the synthetic toolkit in the synthesis and derivation of organic structures, especially biologically relevant motifs.[1] The inherent challenge in C–H functionalization of arenes is the differentiation of electronically similar C–H bonds. To overcome this, a directing group (DG) strategy is often employed to enable site selective cyclometalation *via* chelation assistance.[2] Subsequent coordination of a coupling partner and reductive elimination pathways lead to *ortho*-C–H functionalized products. To move away from *ortho*-selectivity, elegant remote C–H functionalization techniques have come to the forefront of modern catalytic progress.[3] This has enabled sophisticated routes to *meta*[4] and *para*[5]-substituted arenes.

Carbazoles are a fused tricylic heteroaromatic with important applications in drug discovery,[6] sensing,[7] and organic functional materials such as OLEDs.[8] For these reasons, studies into the modification of this heterocycle have allowed selective C–H functionalization of carbazoles and their derivatives. A majority of these techniques have been applied through furnishing the NH with a directing group. This enables directed C–H functionalization at the C1 position (Scheme 1a). This research has permitted the formation of a number of C-C and C-X bonds utilizing a multitude of catalytic systems.[9] Limited remote functionalization techniques studied on the related indole heteroaromatic have also granted access to C2 substituted carbazoles, with notable contributions from Baran.[10] C3-substitution has been widely studied due to the nucleophilic nature of this carbon enabling S_EAr chemistry.[11] To our knowledge, selective C–H functionalization of the C4 position has yet to be reported.

Ruthenium-catalyzed σ-activation has become a vital technique in the *meta*-functionalization of arenes,[12] enabling the sulfonation,[12,13] alkylation,[14] bromination,[15] nitration,[16] and benzylation[17] of aromatic systems. In this methodology, formation of a strong and stable ruthenacycle, allows *para*-functionalization to the metal center, *via* the electronic influence of the Ru-C σ-bond, instead of traditional oxidative addition/reductive elimination pathways. This gives net *meta*-C–H functionalization to the directing group. The ruthenium center has also been shown to act as a dual role catalyst, facilitating the redox formation of a radical which interacts with the *para* position of the arene. After our success in applying this technique to indole structures to enable selective C6 functionalization,[18] we sought to use this methodology on carbazole structures to give complementary C4 C–H functionalization (Scheme 1b).

Scheme 1. Selective C–H Functionalization of Carbazoles and the Context of this Work

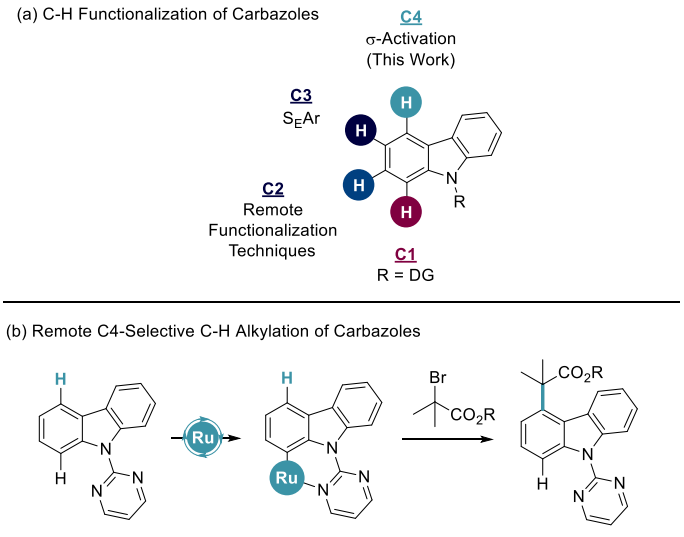

From ours and others previous contributions to *meta*-alkylation methodology,[14,18] we began our investigations by applying previously reported conditions for catalytic σ-activation to *N*-pyriminidylcarbazole (**1a**), using ethyl α-bromoisobutyrate as a coupling partner (**2a**) (Table 1, entries 1-4). To our delight we found that when using potassium acetate as base (entries 1-2), efficient C–H functionalization was shown to take place. As with our previous report, the addition of acetic acid into the reaction mixture was also shown to be beneficial (entry 2).[18]

Table 1. Ruthenium-Catalyzed C4 Selective C–H Alkylation of Carbazole Derivatives[a]

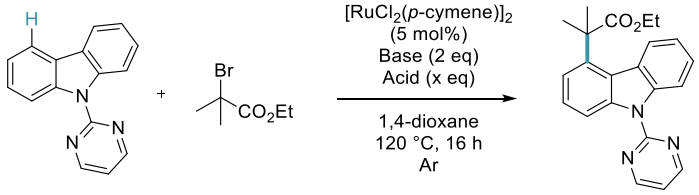

1a **2a** **3a**

Entry	Base	Acid	Acid (eq)	**3a** %[b]
1	KOAc	-	-	53
2	KOAc	AcOH	2	68 (48)[c]
3	K_2CO_3 (+$MesCO_2H$ 30 mol%)	-	-	7
4	K_2CO_3 (+ Piv-Val-OH 30 mol%)	-	-	7
5	K_2CO_3	-	-	-
6	K_3Citrate	AcOH	2	45
7	K_2Tartrate	AcOH	2	56
8	$AdCO_2Na$	AcOH	2	58
9	$MesCO_2K$	AcOH	2	80 (61)[c]
10	$MesCO_2K$	$MesCO_2H$	2	64
11	$MesCO_2K$	$AdCO_2H$	2	66
12	$MesCO_2K$	TFA	2	15
13	$MesCO_2K$	AcOH	0.5	80
14	**$MesCO_2K$**	**AcOH**	**1**	**84 (68)**
15	$MesCO_2K$	AcOH	4	68
16[d]	$MesCO_2K$	AcOH	1	61
17[e]	$MesCO_2K$	AcOH	1	-
18[f]	**$MesCO_2K$**	**AcOH**	**1**	**90 (76)**

[a] General Conditions: 9-(pyrimidin-2-yl)-9H-carbazole (1a, 0.25 mmol), ethyl α-bromoisobutyrate (2a, 0.75 mmol), $[RuCl_2(p\text{-cymene})]_2$ (5 mol%, 0.0125 mmol), Base (2 eq), Acid (x eq), 1,4-dioxane, 120 °C, 16 h, under argon atmosphere. [b] Direct conversion between starting material and product, as dictated by crude ^{1}H NMR. [c] Isolated yields given in brackets. [d] Reaction carried out at 100 °C. [e] Reaction carried out without $[RuCl_2(p\text{-cymene})]_2$. [f] $[Ru(O_2CMes)_2(p\text{-cymene})]$ (10 mol%) used as catalyst.

On screening different bases, we found that the sterically demanding potassium 2,4,6-trimethylbenzoate ($MesCO_2K$) was the most amenable to these reaction conditions (entries 6-9). $MesCO_2H$ and $AdCO_2H$ were shown to be reactive acids in this methodology however neither superior to AcOH (entries 10-11). We then found that reducing the quantity of acid to 1 equivalent led to the highest formation of product (entries 13-15). Reaction efficiency

was also shown to reduce in an air atmosphere (entry 16) and was completely nullified in the absence of ruthenium catalyst (entry 17). The use of the pre-synthesized [Ru(O_2CMes)(*p*-cymene)] monomer was shown to lead to the highest formation of product thus far (entry 18) In order to confirm regioselectivity, **3a** was characterized *via* single crystal X-ray diffraction (Figure 1).[19]

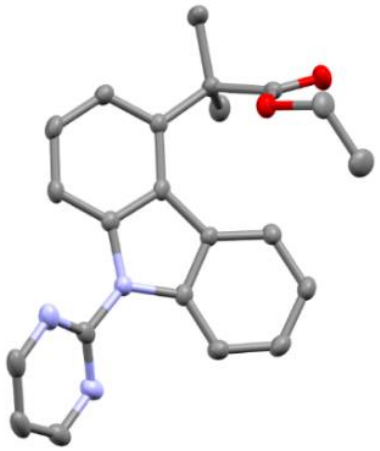

Figure 1. SCXRD Structure of **3a** confirming regioselectivity of functionalization.[19] CCDC 1574475.

With optimal conditions in hand to enable efficient and selective C4 alkylation, we were intrigued to employ a number of coupling partners to the reaction conditions to explore their respective reactivity in this chemistry (Scheme 2). The reaction methodology was explored using both the commercially available dimer (Conditions **A**) and the pre-synthesized monomer (Conditions **B**). A variety of ester substituents were shown to be very well tolerated in the remote functionalization methodology (**3aa-3ad**) with impressive yields up to 92% for the *tert*-butyl ester variant. It is noteworthy to find that *tert*-butyl bromide was not amenable to this methodology (**3ae**) despite its use in several previous reports in σ-activation methodology.[13] When the difluoro ester was reacted under the optimized conditions (**3ag**), unfortunately no product was observed, even with the addition of triarylphosphine co-catalysts, which has been shown to be vital in *meta*-difluoroalkylation strategies.[14e-f] Perfluorobenzyl ester derivative (**3ah**) was also tolerated in the chemistry. It has been demonstrated that generally the preformed monomer outperforms the dimer however in not all cases.

Scheme 2. Ruthenium-Catalyzed C4 Selective C–H Alkylation of Carbazole – Coupling Partner Scope

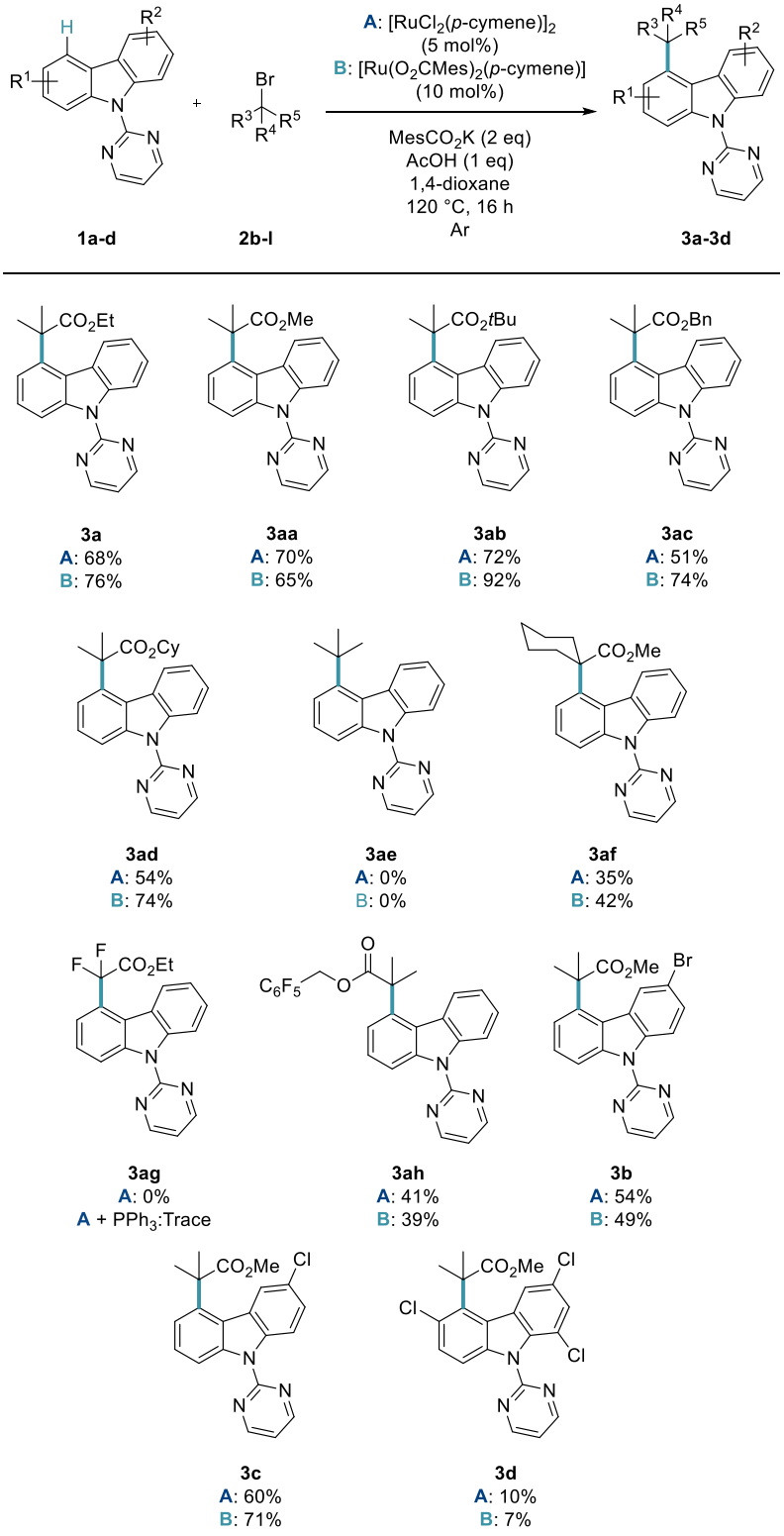

Following this, the variation of the aryl functionality was then studied. Mono-substituted bromo (**3b**) and chloro (**3c**) carbazole derivatives were shown to effective substrates for this

chemistry with exclusive selectivity for the non-substituted ring.[18] Trichloro-substituted structure (**3d**) was shown to proceed in reduced yields but exclusively at C4, truly highlighting the remote nature of the functionalization, as this enables the C–H derivation between two substitution patterns. For further experiments and further unsuccessful coupling partners, see supporting information.

At this point, we were intrigued to see how the influence of the *N*-substitution pattern affected the efficiency of C4-functionalisation (Scheme 3a). To this end, we investigated non-coordinating (**1e**) and weakly metal-coordinating (**1f**) substituents. Unfortunately, neither of these structures were shown to give conversion to any regioselectivity of product. Interestingly, when we submitted unsubstituted carbazole (**1g**) to the reaction conditions we observed selective C3-alkylation in low yields (Scheme 3b). This manifests that without the directing group the C3 position is the most activated to interact with a radical. This shows that this σ-activation methodology not only produces a highly selective and efficient C–H functionalization of carbazole, we also observe a complete switch in regioselectivity to the innate reactivity. It is also noteworthy that cf. **1f-g** (Scheme 3a), the presence of the NH is critical to any reactivity. We then looked to apply this methodology to two other substrates to expand the scope beyond carbazole structures. To this end, 2,3-diethylindole and indoline derivatives were synthesized and submitted to the reaction conditions (Scheme 3c).

Scheme 3. Remote Ruthenium-Catalyzed Functionalization of Carbazoles

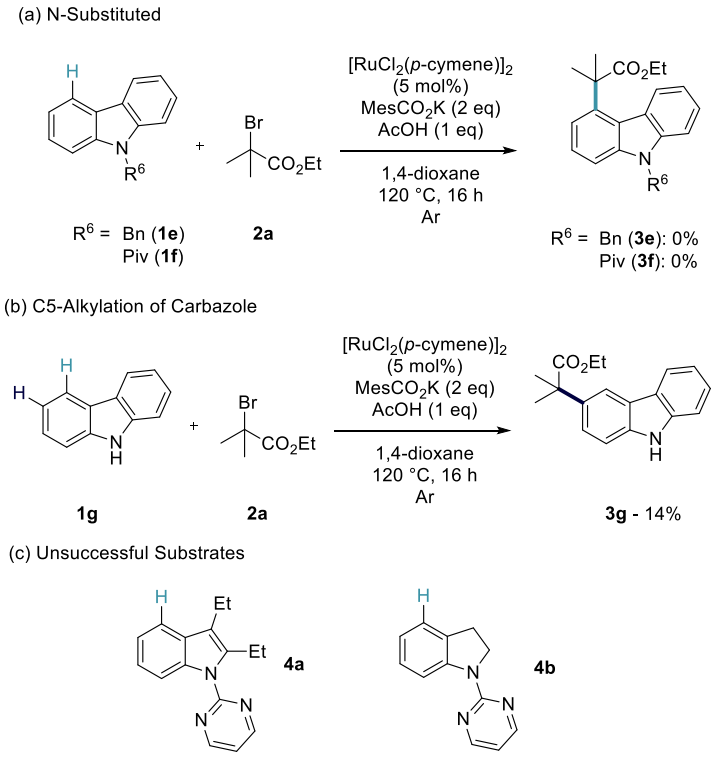

To our surprise neither substrate showed any reactivity towards the remote functionalization methodology (**5a-b**). This could be due to the indole substituent at C2 interfering with stable and planar cyclometalation or the ethyl at C3 blocking *tert*-alkylation on steric grounds (**4a**). In the case of the indoline, the cyclometalate formed on the benzenoid section of the structure may not be stable enough to permit remote σ-activation (**4b**).

We were intrigued to run radical trapping experiments to inform whether this reaction followed previous trends in σ-activation. We employed TEMPO trapping studies, where catalytic quantities (30 mol%) of the radical trapping agent gave a reduced conversion of 66% to product, and the use of stoichiometric quantities of TEMPO (1 eq) led to a sharp drop to 15% conversion. These findings suggest that a radical single electron transfer mechanism may be at play. It was then of interest to run H/D scrambling experiments using isotopically labelled acetic acid. This showed that there is deuterium incorporation in the C1 and C8 positions in both the starting material (10% each, see supporting information) and product (19% each). This suggests a reversible C–H activation at the *ortho*-positions. It must be noted that lack of scrambling at C5 in the product and at C4/C5 in the starting material rules out a readily reversible direct C–H metalation at these positions and lends itself to a C1 σ-activation protocol.

From these mechanistic investigations and from previous insights into this methodology, a plausible mechanism for the remote C4-alkylation of carbazole derivatives is proposed (Scheme 4). It is suggested that the ruthenium *para*-cymene dimer is broken apart using the $MesCO_2K$ base to form the catalytically active ruthenium bis-mesitylcarboxylate monomer ([Ru(*p*-cm)$(O_2CMes)_2$]). This monomer can then facilitate C–H activation at the C1 position *ortho* to the pyrimidine directing group. A single electron transfer process with an inner sphere or outer sphere ruthenium complex can then form the *tertiary* α-halocarbonyl radical. This radical then interacts with the sterically encumbered ruthenacycle at the *para* position to the metal center *via* a σ-activation process (likely due to a shift in electron density to the C4 position). Redox electron shuttling and proton abstraction enables rearomatization of the arene. Protodemetalation using either the $MesCO_2H$ formed previously or the stoichiometric AcOH releases the C4-alkylated structure and reforms the catalytically active monomer.

Scheme 6. Plausible Mechanism for the Remote C4-Alkylation of Carbazole Derivatives *via* σ-Activation

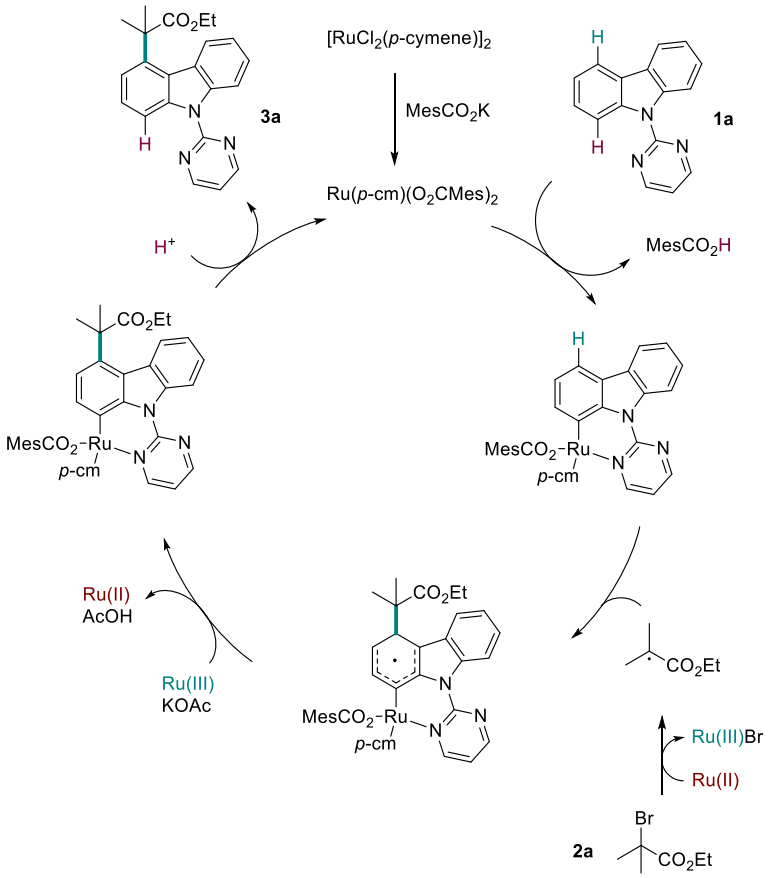

In conclusion, we have presented the remote C4-selective C–H alkylation of carbazole derivatives. As far as we are aware, there are no known selective methods to directly functionalize the carbazole at this position. We have demonstrated that furnishing the carbazole heteroaromatic with a pyrimidine directing group enabled a σ-activation process whereby a stable and planar ruthenacycle at C1 enabled interaction of the *para* position (C4) with a *tertiary* alkyl radical. We also demonstrate the unique reactivity of α-halocarbonyl coupling partners cf. aliphatic alkyl halides.

ASSOCIATED CONTENT

Supporting Information

Synthetic procedures and full characterization data of compounds (PDF)

The crystallographic data in CIF format has been deposited with CCDC (CCDC deposition number is **1574475**). This data can be obtained free of charge at www.ccdc.cam.ac.uk/conts/retrieving.html [or from the Cambridge Crystallographic Data

Centre, 12, Union Road, Cambridge CB2 1EZ, UK; fax: (internet.) +44-1223/336-033; E-mail: deposit@ccdc.cam.ac.uk].

AUTHOR INFORMATION

Corresponding Author

* Christopher G. Frost: C.G.Frost@bath.ac.uk

ACKNOWLEDGMENT

J. A. L. would like to thank the University of Bath and Syngenta for funding. C. J. H. would like to thank the EPSRC CDT in Sustainable Chemical Technologies for funding.

NOTES AND REFERENCES

(1) For reading on transition metal catalyzed C–H activation see: (a) (a) L. Ackermann, *Chem. Rev.*, 2011, **113**, 1315. (b) P. B. Arockiam, C. Bruneau, P. Dixneuf, *Chem. Rev.,* 2012, **112**, 5879. (c) X. Chen, K. M. Engle, D-H. Wang, J. Q. Yu, *Angew. Chem. Int. Ed.*, 2009, **48**, 5094. (d) K. M. Engle, T. S. Mei, M. Wasa, J. Q. Yu, *Acc. Chem. Res.*, 2012, **45***,* 788. (e) H. M. L. Davies, D. Morton, *J. Org. Chem.*, 2016, **81**, 343. (f) T. Yoshino, S. Matsunaga, *Adv. Synth. Catal.*, 2017, **359**, 1245. For reading on the modification of biologically active molecules see: (g) J. A. Leitch, P. B. Wilson, C. L. McMullin, M. F. Mahon, Y. Bhonoah, I. H. Williams, C. G. Frost, *ACS Catal.*, 2016, **6**, 5520. (h) J. A. Leitch, H. P. Cook, Y. Bhonoah, C. G. Frost, *J. Org. Chem.*, 2016, **81**, 10081. (i) W. Ma, H. Dong, D. Wang, L. Ackermann, *Adv. Synth. Catal.*, 2017, **359**, 966.

(2) (a) K. M. Engle, T. S. Mei, M. Wasa, J. Q. Yu, *Acc. Chem. Res.*, 2012, **45**, 788. (b) Z. Chen, B. Wang, J. Zhang, W. Yu, Z. Liu, Y. Zhang, *Org. Chem. Front.*, 2015, **2**, 1107.

(3) J. Li, S. De Sarkar, L. Ackermann, *Top Organomet. Chem.*, 2015, **55**, 217.

(4) For reviews see: (a) J. Yang, *Org. Biomol. Chem.*, 2015, **13**, 1930. (b) A. Dey, S. Agasti, D. Maiti, *Org. Biomol. Chem.*, 2016, **14**, 5440. For seminal publications see: (c) R. J. Phipps, M. J. Gaunt, *Science*, 2009, **323**, 1593. (d) D. Leow, G. Li, T. S. Mei, J. Q. Yu, *Nature*, 2012, **486**, 518. (e) X. C. Wang, W. Gong, L. Z. Fang, R. Y. Zhu, S. Li, K. M. Engle, J. Q. Yu, *Nature*, 2015, **519**, 334. (f) Y. Kuninobu, H. Ida, M. Nishi, M. Kanai, *Nat. Chem.*, 2015, **7**, 712. (g) J. Y. Cho, M. K. Tse, D. Holmes, R. E. Maleczka, M. R. Smith, *Science*, 2002, **295**, 305.

(5) For review see: A. Dey, S. Maity, D. Maiti, *Chem. Commun.*, 2016, **52**, 12398.

(6) (a) F. F. Zhang, L. L. Gan, C. H. Zhou, *Bioorg. Med. Chem. Lett.*, 2010, **20**, 1881. (b) C. C. Chang, L. C. Kuo, J. J. Lin, Y. C. Lu, C. T. Chen, H. T. Back, P. J. Lou, T. C. Chang, *Chem. Biodiversity*, 2004, **1**, 1377. (c) M. H. Block, S. Boyer, W. Brailsford, D. R. Brittain, D. Carroll, S. Chapman, D. S. Clarke, C. S. Donald, K. M. Foote, L. Godfrey, A. Ladner, P.

R. Marsham, D. J. Masters, C. D. Mee, M. R. O'Donovan, J. E. Pease, A. G. Pickup, J. W. Rayner, A. Robers, P. Schofield, A. Suleman, A. V. Turnbull, *J. Med. Chem.*, 2002, **45**, 3509.

(7) (a) C. C. Chang, I. C. Kuo, I. F. Ling, C. T. Chen, H. C. Chen, P. J. Lou, J. J. Lin, T. C. Chang, *Anal. Chem.*, 2004, **76**, 4490. (b) C. C. Chang, J. Y. Wu, C. W. Chien, W. S. Wu, H. Liu, C. C. Kang, L. J. Yu, T. C. Chang, *Anal. Chem.*, 2003, **75**, 6177.

(8) (a) K. Brunner, A. van Dijken, H. Borner, J. J. Am M. Bastiaansen, N. M. M. Kiggen, B. M. W. Langeweld, *J. Am. Chem. Soc.*, 2004, **126**, 6035. (b) J. Ding, J. Gao, Y. Cheng, Z. Xie, L. Wang, D. Ma, X. Jing, F. Wang, *Adv. Funct. Mater.*, 2006, **16**, 575.

(9) For review see: (a) J. A. Leitch, Y. Bhonoah, C. G. Frost, *ACS Catal.*, 2017, **7**, 5618. For selected examples see: (b) V. P. Reddy, R. Qiu, T. Iwasaki, N. Kambe, *Org. Lett.*, 2013, **15**, 1290. (c) R. Qiu, V. P. Reddy, T. Iwasaki, N. J. Kambe, *Org. Chem.*, 2015, **80**, 367. (d) L. Zhu, X. Cao, T. Iwasaki, V. P. Reddy, X. Xu, S. F. Yin, N. Kambe, *RSC Adv.*, 2015, **5**, 39358. (e) W. Ai, X. Yang, Y. Wu, X. Wang, Y. Li, Y. Yang, B. Zhou, *Chem. Eur. J.*, 2014, **20**, 17653. (f) X. Hong, H. Wang, G. Qian, Q. Tan, B. Xu, *J. Org. Chem.*, 2014, **79**, 3228. (g) S. Sharma, Y. Shin, N. K. Mishra, J. Park, S. Han, T. Jeong, Y. Oh, Y. Lee, M. Choi, I. S. Kim, *Tetrahedron*, 2015, **71**, 245.

(10) Y. Feng, D. Holte, J. Zoller S. Umemiya, L. R. Simke, P. S. Baran, *J. Am. Chem. Soc.*, 2015, **137**, 10160.

(11) M. Majchrzak, M. Grzelak, B. Marciniec, *Org. Biomol. Chem.*, 2016, **14**, 9406.

(12) J. A. Leitch and C. G. Frost, *Chem. Soc. Rev.*, 2017, DOI: 10.1039/C7CS00496F

(13) (a) O. Saidi, J. Marafie, A. E. W. Ledger, P. M. Liu, M. F. Mahon, G. Kociok-Kohn, M. K. Whittlesey, C. G. Frost, *J. Am. Chem. Soc.*, 2011, **133**, 19298. (b) P. Marcé, A. J. Paterson, M. F. Mahon, C. G. Frost, *Catal. Sci. Technol.*, 2016, **6**, 7068. (b) G. Li, X. Lv, K. Guo, Y. Wang, S. Yang, L. Yu, Y. Yu, Wang, J. *Org. Chem. Front.*, 2017, **4**, 1145.

(14) (a) N. Hofmann, L. Ackermann, *J. Am. Chem. Soc.*, 2013, **135**, 5877. (b) A. J. Paterson, S. St John Campbell, M. F. Mahon, N. J. Press, C. G. Frost, *Chem. Commun.*, 2015, **51**, 12807. (c) J. Li, S. Warratz, D. Zell, S. De Sarkar, E. E. Ishikawa, L. Ackermann, *J. Am. Chem. Soc.*, 2015, **137**, 13894. (d) G. Li, X. Ma, C. Jia, Q. Han, Y. Wang, J. Wang, L. Yu, S. Yang, *Chem. Commun.*, 2017, **53**, 1261. (e) Z. Ruan, S. K. Zhang, C. Zhu, P. N. Ruth, D. Stalke, L. Ackermann, *Angew. Chem. Int. Ed.*, 2017, **129**, 2077. (f) Z. Y. Li, L. Li, Q. L. Li, K. Jing, H. Xu, G. W. Wang, *Chem. Eur. J.*, 2017, **23**, 3285. (g) J. Li, K. Korvorapun, S. De Sarkar, T. Rogge, D. J. Burns, S. Warratz, L. Ackermann, *Nat. Commun.*, 2017, **8**, 15430. (h) A. J. Paterson, C. J. Heron, C. L. McMullin, M. F. Mahon, N. J. Press, C. G. Frost, *Org. Biomol. Chem.*, 2017, **15**, 5993.

(15) (a) C. J. Teskey, Y. W. Lui, M. F. Greaney, *Angew. Chem. Int. Ed.*, 2015, **54**, 11677. (b) Q. Yu, L. Hu, Y. Wang, S. Zheng, J. Huang, *Angew. Chem. Int. Ed.*, 2015, **54**, 15284.

(c) S. Warratz, D. J. Burns, C. Zhu, K. Korvorapun, T. Rogge,J. Scholz, C. Jooss, D. Gelman, L. Ackermann, *Angew. Chem. Int. Ed.*, 2017, **56**, 1557.

(16) (a) Z. Fan, J. Ni, A. Zhang, *J. Am. Chem. Soc.*, 2016, **138**, 8470. (b) Z. Fan, J. Li, H. Lu, D. Y. Wang, C. Wang, M. Uchiyama, A. Zhang, *Org. Lett.*, 2017, **19**, 3199.

(17) (a) G. Li, D. Li, J. Zhang, D. Q. Shi, Y. Zhao, *ACS Catal*., 2017, **7**, 4138. (b) B. Li, S. L. Fang, D. Y. Huang, B.F. Shi, *Org. Lett.*, 2017, **19**, 3950.

(18) J. A. Leitch, C. L. McMullin, M. F. Mahon, Y. Bhonoah, C. G. Frost, *ACS Catal.*, 2017, **7**, 2616.

(19) **Crystallographic data.** Intensity data were collected at 150 K on a RIGAKU Xcalibur EosS2 diffractometer, using graphite monochromated MoKα radiation (□□= 0.71073 Å). **(3a)** $C_{22}H_{21}N_3O_2$, M = 359.42, P-1, *a* = 8.3732(5) Å, *b* = 9.5046(5) Å, *c* = 11.9276(4) Å, α = 69.880(4)°, β = 88.812(4)°, γ = 84.255(4)° *V* = 886.74(8) $Å^3$, *Z* = 2, □ = 0.088 mm^{-1}, unique reflections = 4064 [R(int) = 0.0571], R_1 = 0.061, wR_2 = 0.1490 [I>2σ(I)], R_1 = 0.0735, wR_2 = 0.1576 (all data). **CCDC 1574475**.

(20) Unfortunately, 3,6-dihalocarbazole derivatives were not amenable to this methodology due to perceived lack of solubility in the reaction medium (see supporting information)

Chapter 4: *para* – Ruthenium Catalyzed *para*-Selective C–H Functionalisation

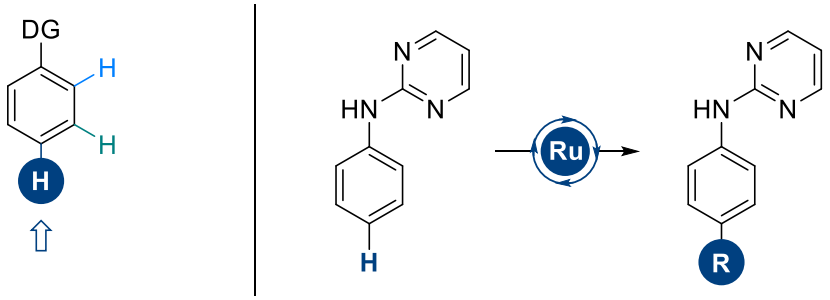

4.1: Ruthenium-Catalyzed *para*-Selective C–H Alkylation of Aniline Derivatives

4.1.1: Introduction and Commentary

Covered in depth in the excellent and aptly named review “Reaching the South” by Maiti,[1] the search for *para*-selective C–H functionalisation entails accessing an even more remote position on an aromatic ring vis-à-vis *ortho*- and *meta*-selective C–H functionalisation. For these reasons, as discussed in Chapter 1, most of the techniques do not utilize chelation assistance and rely more heavily on electronic and steric influences to enable selective C–H functionalisation.

For a number of years, we have been incredibly interested in the complete control of site selectivity in C–H functionalisation. Over the course of previous investigations of *meta*-alkylation methodology, we had observed *para*-substituted motifs as by-products (Scheme 4-1). Under conditions from our previous report,[2] using aniline furnished with a pyrimidine directing group and an α-halocarbonyl as a coupling partner, despite repetition of the reaction to reaffirm our findings, we only observed exclusively the *para*-C–H alkylated product in low yields.

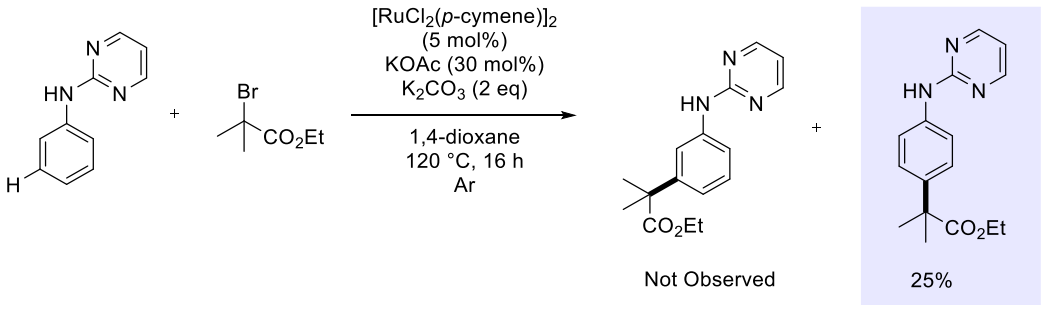

Scheme 4-1: Ruthenium-Catalysed C–H Alkylation of *N*-pyrimidinylaniline

Due to Ackermann's report on the *meta*-selective C–H alkylation of the same aniline substrate, under very similar conditions,[3] expanding this methodology could provide a complementary selectivity, and potentially a complementary mechanism, to that already known. (Scheme 4-2). This stark contrast of selectivity under almost identical conditions demonstrates the unique reactivity of α-halo carbonyls vs. regular alkyl halides.

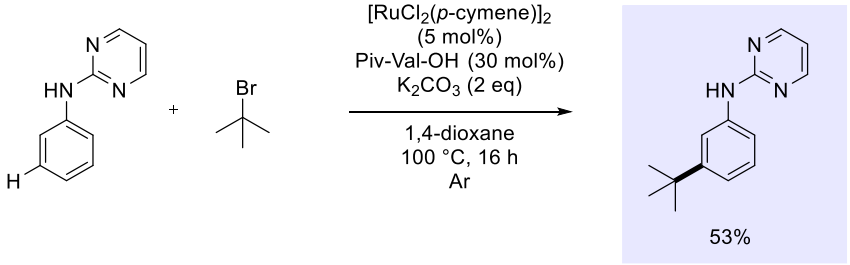

Scheme 4-2: Ruthenium-Catalysed *meta*-Alkylation of *N*-pyrimidinylaniline

During the investigation into this work, two papers were published which eluded to a potential mechanism at work here. The first from Weng and Lu[4] displayed the copper catalysed C–H sulfonation of aminonaphthalene derivatives, and the second from Manolikakes[5] again depicts the C–H sulfonation of aniline derivatives, here utilising manganese acetate as a stoichiometric oxidant for radical generation (Scheme 4-3).

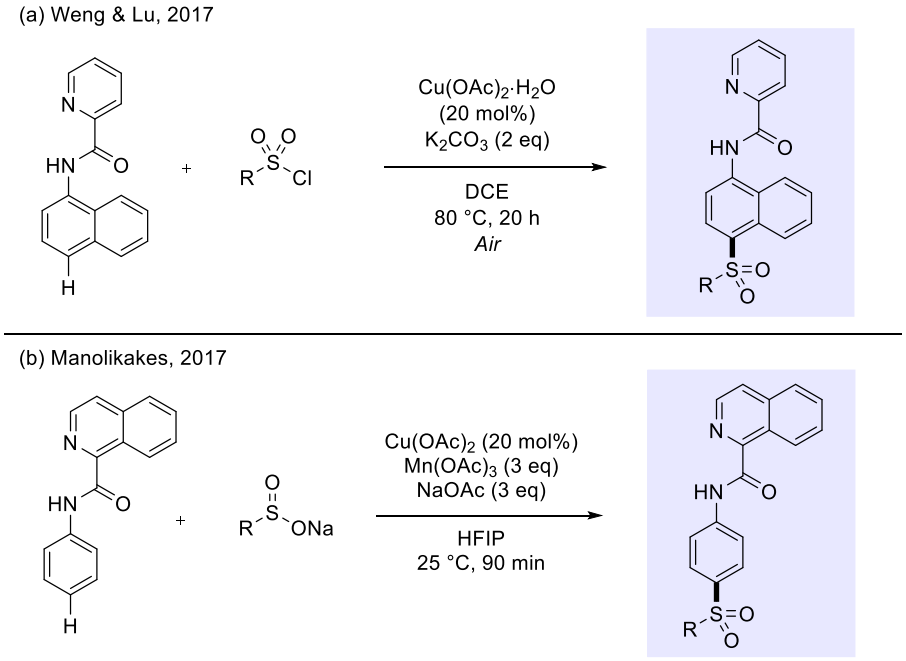

Scheme 4-3: Copper Catalysed *para*-C–H Sulfonation of Arenes

The mechanism proposed by Weng & Lu was of incredible interest to us as it presents a fundamentally similar process to σ-activation, where the copper metal centre is capable of cyclometalation (in this case at N–H) and redox radical generation (Scheme 4-4).[4]

From this point, these mechanistic insights were combined with our knowledge on ruthenium-catalysed σ-activation, to optimise and develop our *para*-selective C–H functionalisation into a useful synthetic methodology. The results herein are presented from the report under peer review at the point of thesis submission.

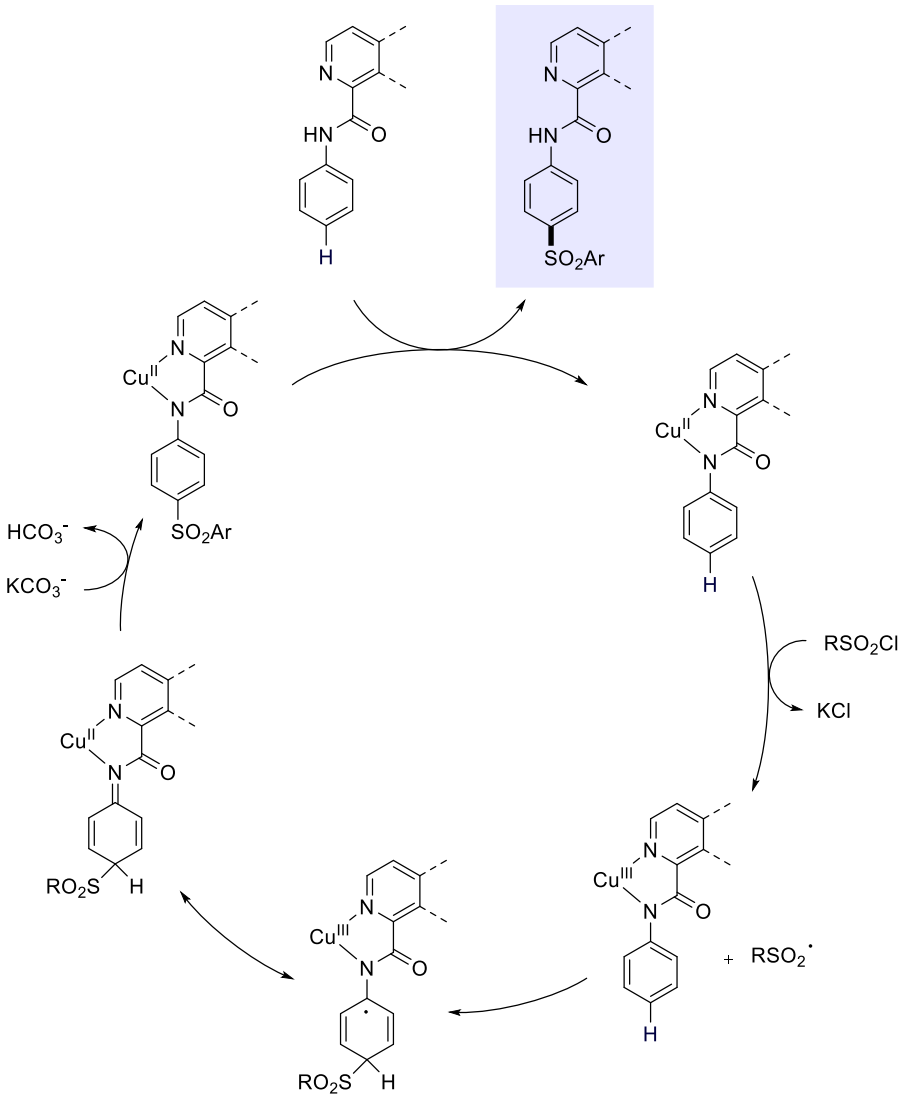

Scheme 4-4: Proposed Mechanism for Copper Catalysed *para*-C–H Sulfonation of Aniline Derivatives

---

References

(1) A. Dey, S. Maity, and D. Maiti, *Chem. Commun.*, 2016, **52**, 12398.

(2) A. J. Paterson, S. St John-Campbell, M. F. Mahon, N. J. Press, and C. G. Frost, *Chem. Commun.*, 2015, **51**, 12807.

(3) J. Li, S. Warratz, D. Zell, S. De Sarkar, E. E. Ishikawa, and L. Ackermann, *J. Am. Chem. Soc.*, 2015, **137**, 13984.

(4) J.-M. Li, Y.-H. Wang, Y. Yu, R.-B. Wu, J. Weng, and G. Lu, *ACS Catal.*, 2017, **7**, 2661

(5) S. Liang, M. Bolte, G. Manolikakes, *Chem. Eur. J.*, 2017, **23**, 96.

4.1.2: Authorships and Permissions

This declaration concerns the article entitled									
Ruthenium-Catalyzed *para*-Selective C–H Alkylation of Aniline Derivatives *via* Ru-N σ-Activation									
Publication status (tick one)									
Draft manuscript		**Submitted**		**In review**		**Accepted**		**Published**	X
Publication details (reference)	J. A. Leitch, C. L. McMullin, A. J. Paterson, M. F. Mahon, Y. Bhonoah, C. G. Frost, *Angew. Chem. Int. Ed.*, 2017, **129**, 15327								
Candidate's contribution to the paper (detailed, and also given as a percentage)	The candidate contributed to/ considerably contribute to/predominantly execute the: **Formulation of ideas (60%)**: JAL formulated plan and literature searching. CGF (20%) and AJP (20%) contributed to early discussions on project. **Design of methodology (50%):** JAL contributed primarily. CGF (25%) and CLM (25%, computational) **Experimental work**: **(60%)**: JAL contributed reaction optimization, scope and experimental mechanistic studies. CLM contributed computational mechanistic work (30%). AJP contributed initial observation of by-product (5%). MFM contributed X-ray crystallography (5%). **Presentation of data in journal format (70%)**: JAL wrote the introduction, results and discussion, conclusion and most of the supporting information. CLM contributed computational discussions and supporting information material (18%). Manuscript was edited by CGF (5%) and MFM (5%) and looked over by YB (2%)								
Statement from Candidate	This paper reports on original research I conducted during the period of my Higher Degree by Research candidature								
Signed	Jamie A. Leitch						**Date**	06/12/17	

4.1.3: Manuscript for "Ruthenium-Catalyzed *para*-Selective C–H Alkylation of Aniline Derivatives via Ru-N σ-Activation"

Complete manuscript given at point of submission follows on the next page. Layout changes have been made for consistency. Contents remain unchanged. Further experiments and information given in the experimental section (6.5).

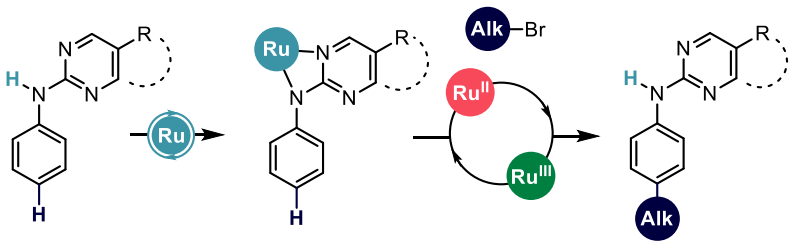

Ruthenium-Catalyzed *para*-Selective C–H Alkylation of Aniline Derivatives

Jamie A. Leitch,[a] Claire L. McMullin,[a] Andrew J. Paterson,[a], Mary F. Mahon,[a] Yunas Bhonoah,[b] and Christopher G. Frost*[a]

[a] Department of Chemistry, University of Bath, Claverton Down, Bath, Somerset, BA2 7AY, United Kingdom

[b] Syngenta, Jealott's Hill International Research Centre, Bracknell, Berkshire, RG42 6EY, United Kingdom

ABSTRACT: The *para*-selective C–H alkylation of aniline derivatives furnished with a pyrimidine auxiliary is herein reported. This is proposed to take place *via* a N–H activated cyclometalate formed *in situ*. Experimental and DFT mechanistic studies elucidate a dual role ruthenium catalyst. Here the ruthenium catalyst can undergo cyclometalation *via* N–H metalation (as opposed to C–H metalation in *meta*-selective processes) and form a redox active ruthenium species, to enable site selective radical addition at the *para* position.

Transition-metal catalyzed C–H functionalization has evolved into a widespread and effective technique to derivate (hetero)arenes and especially biologically relevant motifs.[1] The innate hurdle in C–H functionalization is the differentiation of electronically and sterically similar C–H bonds in an organic structure. To overcome this, a directing group strategy is often employed to enable selective *ortho*-C–H functionalization *via* chelation assistance with respect to the directing group.[2] Recent developments have allowed carefully tailored catalytic systems to permit *meta*-selective C–H functionalization.[3] These methods utilize three primary techniques; templated directing group design,[4] the use of a transient mediator,[5] and σ-activation by a metal center.[6] Accessing complementary *para*-selective methodologies typically takes advantage of electronic effects to permit C–H functionalization at the *para* position of an electron rich arene, with pioneering reports from Gaunt,[7] Nicewicz,[8] and Ritter[9] (Scheme 1a). There have been examples of the use of extended templates by Maiti,[10] and the careful manipulation of steric effects by Itami[11] and Nakao.[12],[13] In a recent report Weng and Lu described the use of 5-membered aminopyridine-based bidentate cyclometalates in the *para*-C–H functionalization of aminonaphthalene derivatives.[14] ,[15]

Herein, we demonstrate that certain aniline derivatives can undergo *para*-selective C–H alkylation reactions catalyzed by ruthenium complexes. σ-Activation focuses on the use of strongly bound ruthenacycles which can activate remote positions *via* electronic effects.[6] Ackermann applied this concept to aniline derivatives furnished with a pyrimidine directing groups to enable *meta*-selective alkylations (Scheme 1b).

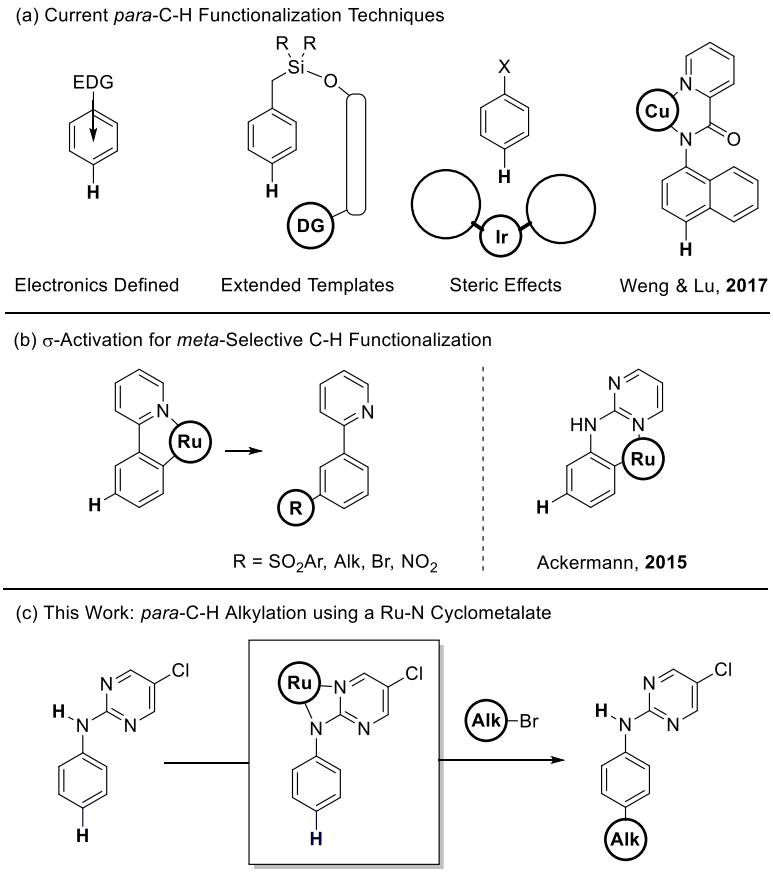

Scheme 1. Previous Reports on Site Selective Catalytic C–H Functionalization in the Context of this Work.

We were intrigued to investigate whether complementary Ru-N cyclometalation of anilines (as opposed to Ru-C in in *meta*-selective sigma activation strategies), could lead to an active catalyst which may permit complementary *para*-C–H functionalization (Scheme 1c). Anilines have been widely used as templates for C–H functionalization development,[16] due to their ubiquity in active pharmaceuticals[17] and agrochemicals.[18] This concept was initially investigated by submitting aniline to slightly modified conditions from our previous work on *meta*-alkylation methodology (Scheme 2).[6c]

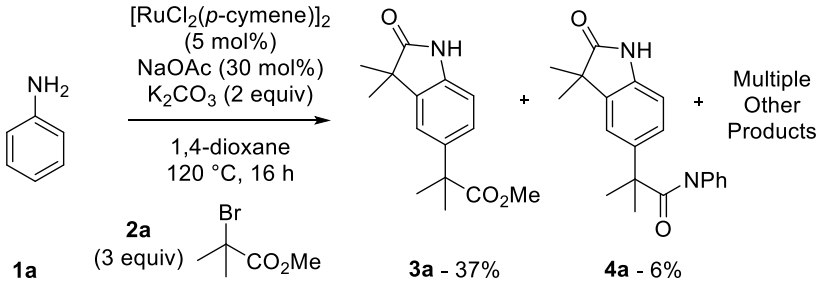

Scheme 2. Ruthenium Catalysed *para*-C–H Alkylation of Aniline

This led to primarily the *ortho*/*para*-substituted aniline (**3a**), whereby an *in situ* lactamization can take place on at the *ortho* position, amongst multiple other products. No C–H alkylation products were observed in the absence of ruthenium catalyst or in the presence of radical scavenger TEMPO. This suggests a redox catalyst is formed *in situ* enabling radical arene functionalization. Encouraged by this, we endeavored to promote a solely *para*-selective transformation by using a bespoke *N*-substituted auxiliary (Table 1).

Despite its use in other *meta*-alkylation methodologies a pyrimidine auxiliary (**1b**) gave the *para*-substituted structure in modest conversions (entry 1).[6d],[19] No *meta*-functionalization was observed, however competing di-C–H alkylation occurred on the auxiliary (**4b**), albeit in low amounts. It is worth noting throughout the auxiliary optimization, there was no observation of the *ortho*/*para*-disubstituted structure. Pleasingly the use of 5-chloropyrimidine as the auxiliary (**1c**) led to completely selective *para*-functionalization (entry 2). Pyridyl (**1e**) and Acetanilide (**1f**) did not lead to any C–H functionalized products (entries 4-5), and pyridoyl derivative (**1g**) was also unsuccessful (entry 6). A screen of solvents identified TBME (*tert*-butyl methyl ether) as the optimal reaction medium (entries 6-8). A ligand screen manifested that removal of the ligand entirely was of benefit to the reaction (entries 10-13), and could be due to a reduction in undesired *ortho*-cyclometalation. Unfortunately, isolated yields in this methodology were found to be substantially lower than NMR yields, primarily due to polymeric byproducts formed which were indistinguishable *via* proton NMR (see ESI, Scheme S3). Interestingly on increasing the temperature to 140 °C, we observed formation of competing *meta*-selectivity (entry 13), and importantly no reactivity was observed in the absence of the ruthenium catalyst (entry 16).

Table 1. Ruthenium-Catalyzed *para* C–H Alkylation of Aniline Derivatives

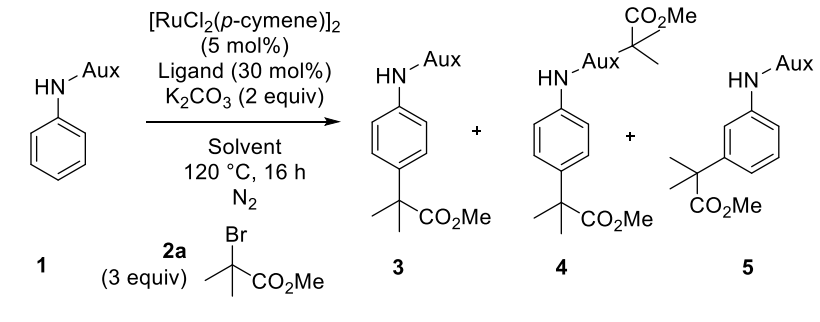

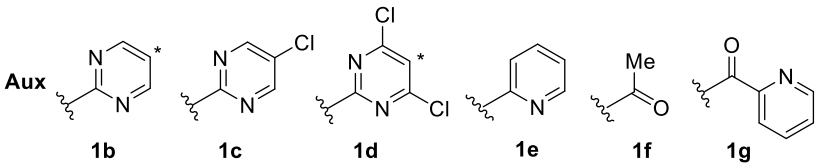

Entry[a]	Aux	Ligand	Solvent	**3** %[b]	**4** %[b]	**5** %[b]
1	**1b**	NaOAc	1,4-dioxane	35	6[c]	-
2	**1c**	NaOAc	1,4-dioxane	39	-	-
3	**1d**	NaOAc	1,4-dioxane	16	10[c]	-
4	**1e**	NaOAc	1,4-dioxane	-	-	-
5	**1f**	NaOAc	1,4-dioxane	-	-	-
6	**1g**	NaOAc	1,4-dioxane	-	-	-
7	**1c**	NaOAc	PhMe	56	-	-
8	**1c**	NaOAc	DCE	56	-	-
9	**1c**	NaOAc	TBME	81	-	-
10	**1c**	$MesCO_2H$	TBME	77	-	-
11	**1c**	Piv-Val-OH	TBME	70	-	-
12	**1c**	DMEDA	TBME	85	-	-
13	**1c**	**-**	**TBME**	**86 (55)[d]**	**-**	**-**
14[e]	**1c**	-	TBME	55	-	38
15[f]	**1c**	-	TBME	71		
16[g]	**1c**	-	TBME	-	-	-

Aux = auxiliary [a] Standard Conditions: aniline derivative (0.25 mmol), methyl α-bromoisobutyrate (0.75 mmol), $[RuCl_2(p\text{-cymene})]_2$ (0.0125 mmol), ligand (0.075 mmol), K_2CO_3 (0.5 mmol), solvent (1 mL) under a N_2 atmosphere. [b] ^1H NMR Yield. [c] * denotes position of di-functionalization. [d] isolated yield. [e] at 140 °C. [f] under an air atmosphere. [g] no ruthenium catalyst

With suitable conditions in hand to access *para*-substituted structures, we applied this methodology to a range of coupling partners and substituted arenes (Scheme 3).[20]

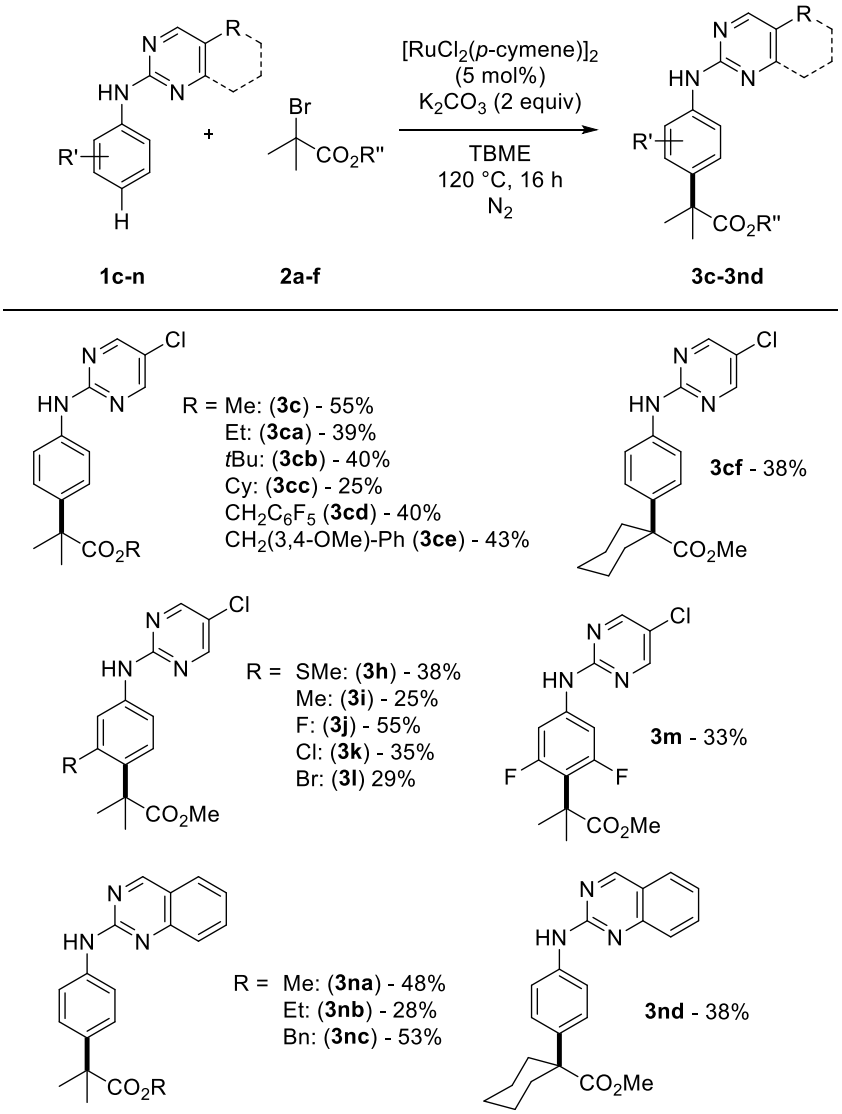

Scheme 3. Scope of Ruthenium-Catalyzed *para*-Selective C–H Alkylation of Aniline Derivatives

This scope showed that a variety of tertiary alkyl esters could be applied in modest yields (**3c**-**3ce**). A cyclohexyl derivative was also shown to be amenable to the reaction (**3cf**), and must be noted that all of these examples proceeded with absolute selectivity for the *para* position. On varying the ring electronics, it was found that 3-substitution was tolerated well (**3h-m**) and that the none of the electronic influences of these substituents overrode the selectivity dictated by the *N*-substitution pattern. The quinazoline heterocycle was also shown to be applicable to this methodology, again in modest yields (**3na**-**3nd**).

We anticipated that under certain conditions, the regioselectivity of functionalization could be switched to a *meta*-selective protocol using identical an starting material and coupling partner (Scheme 4).[21] With carboxylate assistance as well as a change of solvent from 1,4-dioxane to DME, the *meta*-selective reaction was strongly favored and led to

corresponding *meta*-C–H alkylated product with very high selectivity (99:1 *m*/*p*) (Scheme 4). It must be noted removal of the AcOH still favors meta-selectivity, however is less pronounced. This suggests that in a proposed equilibrium between N–H and C–H cyclometalated complexes, the use of a carbonate base (K_2CO_3) could favor an N–H cyclometalation to form *para*-substituted products, whereas acetate bases (KOAc) could favor an *ortho*-C–H cyclometalation to form *meta*-substituted products.

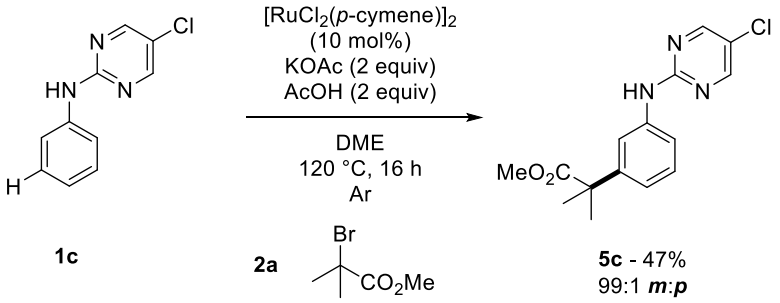

Scheme 4. Ruthenium-Catalyzed *meta*-C–H Alkylation of Aniline Derivative

As we were observing a definitive shift in selectivity from *meta* to *para*, it was of interest to perform experimental and computational mechanistic studies to provide rationale to a proposed Ru-N cyclometalation/activation pathway. Initially we carried out radical scavenger studies using TEMPO where the use of stoichiometric amounts led to complete suppression of reactivity. The isolation of polymeric byproducts, and the unique reactivity of α-halocarbonyls are also indicative of a radical mechanism.

The proposed mechanism for the remote *para* C–H alkylation does not involve cyclometalation on the aromatic ring *via ortho*-C–H cyclometalation. In order to explore this an isotopically labelled derivative **1c-*d*$_5$** was submitted to the reaction conditions (Scheme 5a). This showed that under the *para* conditions there was negligible H/D scrambling (~2%) in either the unreacted starting material or the product. This suggests readily reversible *ortho*-C–H cyclometalation is not possible. The complementary *meta*-selective conditions did however give rise to substantial scrambling in both recovered starting material and *meta*-alkylated product. Despite this, Huang and co-workers did not observe deuterium scrambling in their report.[6f] It must be noted there was no substantial hydrogen incorporation at either *meta* or *para* positions in either investigation, which demonstrates there is no reversible direct C–H metalation responsible for the selectivity observed.

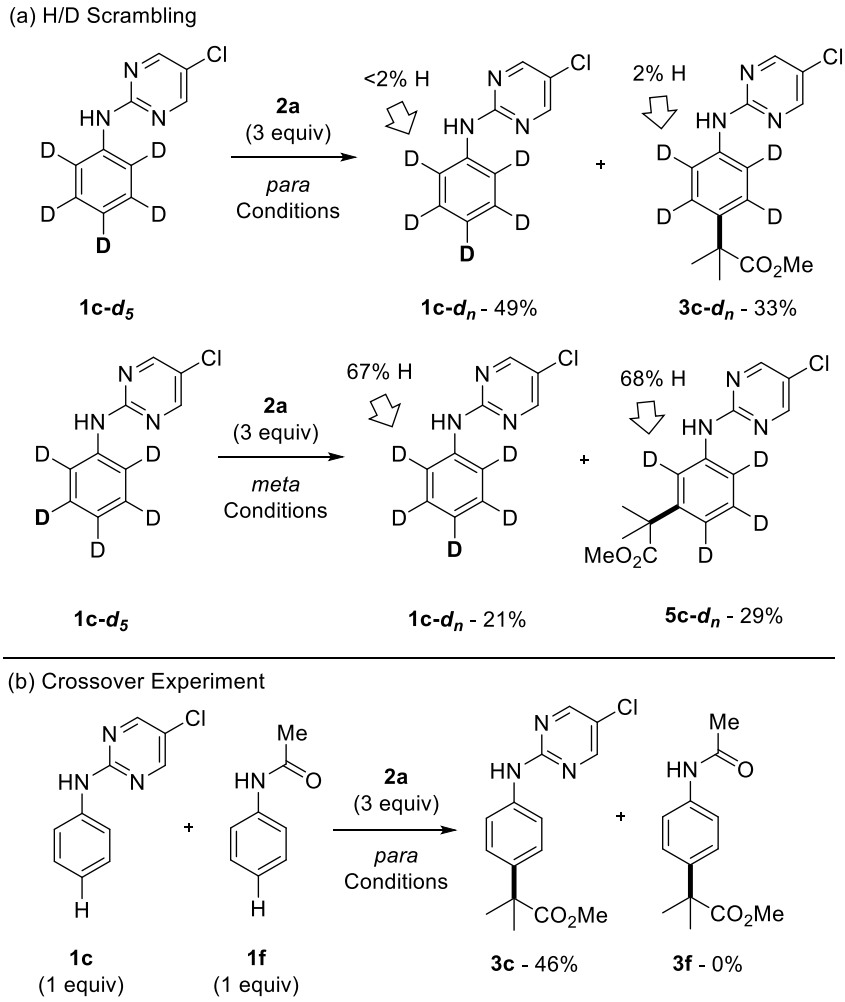

Scheme 5. Mechanistic Studies on *para* Alkylation Methodology

Acetanilide was chosen as a model comparison for a crossover study due to similar electronic influence on the ring, pK_a of the N–H, and that it contains a metal coordinating group (Scheme 5b). If the pyrimidine is only generating a redox active species capable of forming the tertiary radicals, which can then interact with an electron rich organic structure, one would expect to see a mixture of *para*-C–H alkylated pyrimidine (**3c**) and acetanilide (**3f**). No presence of **3f** was observed and **3c** was isolated in equable yields. This strongly suggests that the C–H functionalization taking place at the *para* position is directly influenced by electronic effects of a coordinated ruthenium species. This result along with the previous insights suggest a σ-activation/redox pathway analogous to previous *meta*-selective methodology,[6] however in this case unlocking the complementary *para*-selective chemistry.

Density Functional Theory (DFT) calculations of the competing N–H and C–H activation of

1c have been computed for acetate or carbonate as the base (see Figure 1 and ESI for discussion).[22] A change in preferred activation and hence mechanism occurs, with acetate favoring C–H activation and hence a meta-selective mechanism, whilst carbonate has a lower barrier to N–H activation and a para-selective product.

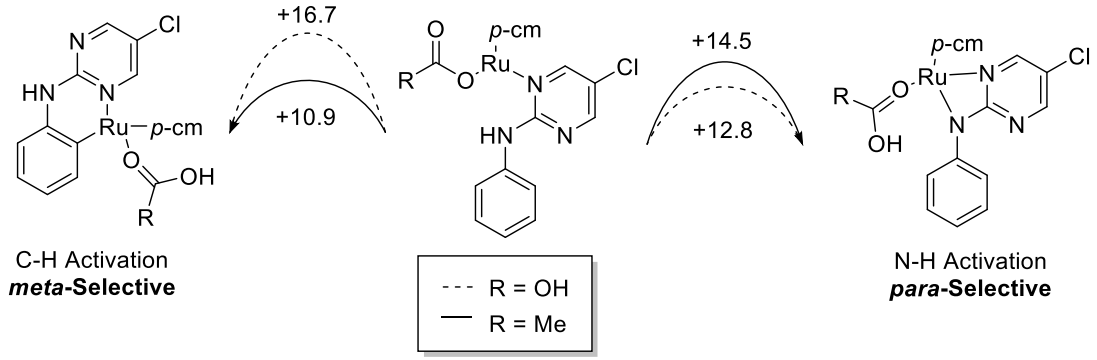

Figure 1: Summary of DFT calculated free energies (kcal mol^{-1}) relative to the most stable intermediate, for the competing C–H and N–H activations of **1c** at [Ru(*p*-cymene)(O_2CR)]$^+$ in dioxane, when R = Me (acetate) or OH (carbonate).[22]

In summary, we have reported the selective *para*-C–H alkylation of aniline derivatives, making use of pyrimidine and quinazoline auxiliaries. Experimental and computational mechanistic studies suggest that the addition takes place *via* a radical process to a ruthenium species cyclometalated at N–H rather than C–H (previously seen). This positional cyclometalation has been proposed to dictate the selectivity, which permits functionalization *para* to the metal center which in this case is *para* to the *N*-substituted auxiliary.

Acknowledgements

J. A. L. would like to thank the University of Bath and Syngenta for funding. This research made use of the Balena High Performance Computing (HPC) Service at the University of Bath.

[1] For reading on transition metal catalyzed C–H functionalization see: a) L. Ackermann, *Chem. Rev.* **2011**, *111*, 1315. b) P.B. Arockiam, C. Bruneau, P. Dixneuf, P. *Chem. Rev*. **2012**, *112*, 5879. c) X. Chen, K. M. Engle, D.-H. Wang, J.-Q. Yu, *Angew. Chem. Int. Ed.* **2009**, *48*, 5094. d) K. M. Engle, T.-S. Mei, M. Wasa, J.-Q. Yu, *Acc. Chem. Res.* **2012**, *45,* 788. e) H. M. L. Davies, D. Morton, *J. Org. Chem.*, **2016**, *81*, 343. f) S. De Sarakar,

W. Liu, S. I. Kozhushkov, L. Ackermann, *Adv. Synth. Catal.* **2014**, *356*, 1461. g) J. A. Leitch, Y. Bhonoah, C. G. Frost, *ACS Catal.*, **2017**, *7*, 5618-5627. For reading on the modification of biologically active molecules see: h) J. A. Leitch, P. B. Wilson, C. L. McMullin, M. F. Mahon, Y. Bhonoah, I. H. Williams, C. G. Frost, *ACS Catal.*, **2016**, *6*, 5520. i) J. A. Leitch, H. P. Cook, Y. Bhonoah, C. G. Frost, *J. Org. Chem.*, **2016**, *81*, 10081. j) W. Ma, H. Dong, D. Wang, L. Ackermann, *Adv. Synth. Catal.*, **2017**, *359*, 966.

[2] a) J.-Q. Yu, *Adv. Synth. Catal.*, **2014**, *356*, 1393. b) M. Zhing, Y. Zahng, X. Jie, H. Zhao, G. Li, W. Su, *Org. Chem. Front.*, **2014**, *1*, 843. c) T. W. Lyons, M. S. Sanford, *Chem. Rev.*, **2010**, *110*, 1147. d) W. Ma, P. Gandeepan, J. Li, L. Ackermann, *Org. Chem. Front.*, **2017**, *4*, 1435. e) L. Ping, D. S. Chung, J. Bouffard, S.-G. Lee, *Chem. Soc. Rev.*, **2017**, *46*, 4299. f) Z. Chen, B. Wang, J Zhang, W. Yu, Y. Zhang, *Org. Chem. Front,* , **2015**, *2*, 1107.

[3] a) J.-Y. Cho, M. K. Tse, D. Holmes, R. E. Maleczka, M. R. Smith, *Science*, **2002**, *295*, 305. b) D. W. Robbins, J. F. Hartwig, *Angew. Chem. Int. Ed.*, **2013**, *52*, 933. c) Y.-H. Zhang, B-F. Shi, J.-Q. Yu, *J. Am. Chem. Soc.*, **2009**, *131*, 5072. d) J. Yang, *Org. Biomol. Chem.*, **2015**, *13*, 1930. e) R. J. Phipps, M. J. Gaunt, *Science*, **2009**, *323*, 1593.

[4] For selected contributions see: a) D. Leow, G. Li, T.S. Mei, J.-Q. Yu, *Nature*, **2012**, *486*, 518. b) R.-Y. Tang, G. Li, J.-Q. Yu, *Nature*, **2014**, *507*, 215. c) A. Dey, S. Agasti, D. Maiti, *Org. Biomol. Chem.*, **2016**, *14*, 5440. d) Y. Kuninobu, H. Ida, M. Nishi, M. Kanai, *Nat. Chem.* **2015**, *7*, 712. e) H. J. Davis, M. T. Mihai, R. J. Phipps, *J. Am. Chem. Soc.*, **2016**, *138*, 12759. f) Z. Zhang, K. Tanaka, J.-Q. Yu, *Nature*, **2017**, *543*, 538.

[5] For selected contributions see: a) J. Luo, S. Preciado, I. Larrosa, *J. Am. Chem. Soc.*, **2014**, *136*, 4109. b) X.-C. Wang, W. Gong, L.-Z. Fang, R.-Y. Zhu, S. Li, K. M. Engle, J.-Q. Yu, *Nature*, **2015**, *519*, 334. c) Z. Dong, J. Wang, G. Dong, *J. Am. Chem. Soc.*, **2015**, *137*, 5887. d) H. S. Shi, P. Wang, S. Suzuki, M. E. Farmer, J.-Q. Yu, *J. Am. Chem. Soc*. **2016**, *138*, 14876. e) Q.-L. Zhang, B.-L. Wan, B. Sun, S. Yeung, F.-L. Zhang, J.-Q. Yu. *J. Am. Chem. Soc.*, **2017**, *139*, 888.

[6] For selected contributions see: a) O. Saidi, J. Marafie, A. E. W. Ledger, P. M. Liu, M. F. Mahon, G. Kociok-Köhn, M. K. Whittlesey, C. G. Frost, *J. Am. Chem. Soc.*, **2011**, *133*, 19298. b) N. Hofmann, L. Ackermann, *J. Am. Chem. Soc*., **2013**, *135*, 5877. c) A. J. Paterson, S. St John Campbell, M. F. Mahon, N. J. Press, C. G. Frost, *Chem. Commun.*, **2015**, *51*, 12807. d) J. Li, S. Warratz, D. Zell, S. De Sarkar, E. E. Ishikawa, L. Ackermann, *J. Am. Chem. Soc.*, **2015**, *137*, 13894. e) C. J. Teskey, Y. W. Lui, M. F. Greaney, *Angew. Chem. Int. Ed.*, **2015**, *54*, 11677. f) Q. Yu, L. Hu, Y. Wang, S. Zheng, J. Huang, *Angew. Chem. Int. Ed.*, **2015**, *54*, 15284. g) Z. Fan, J. Ni, A. Zhang, *J. Am. Chem. Soc.*, **2016**, *138*, 8470. h) Z. Ruan, S.-K. Zhang, C. Zhu, P. N. Ruth, D. Stalke, L. Ackermann, *Angew. Chem. Int. Ed.*, **2017**, *129*, 2077. i) J. A. Leitch, C. L. McMullin, M. F. Mahon, Y. Bhonoah, C. G. Frost, *ACS Catal.* **2017**, *7*, 2616. j) J. Li, K. Korvorapun, S. De Sarkar, T. Rogge, D. J.

Burns, S. Warratz, L. Ackermann, *Nat. Commun.*, **2017**, *8*, 15430. k) A. J. Paterson, C. J. Heron, C. L. McMullin, M. F. Mahon, N. J. Press, C. G. Frost, *Org. Biomol. Chem.*, **2017**, *15*, 5993.

[7] C.-L. Ciana, R. J. Phipps, J. R.; Brandt, F.-M.; Meyer, M. J. Gaunt, *Angew. Chem. Int. Ed.*, **2011**, *50*, 458.

[8] N. A. Romero, K. A. Margery, N. E. Tay, D. A. Nicewicz, *Science*, **2015**, *349*, 1326.

[9] G. B. Boursalian, W. S. Ham, A. R. Mazzotti, T. Ritter, *Nat. Chem.*, **2016**, *8*, 810.

[10] a) S. Bag, T. Patra, A. Modak, A. Deb, S. Maity, U. Dutta, A. Dey, R. Kancherla, A. Maji, A. Hazra, M. Bera, D. Maiti, *J. Am. Chem. Soc.*, **2015**, *137*, 11888. b) T. Patra, S. Bag, R. Kancherla, A. Mondal, A. Dey, S. Pimparka, S. Agasti, A. Modak, D. Maiti, *Angew. Chem. Int. Ed.*, **2016**, *55*, 7751. c) M. E. Hoque, R. Bisht, C. Haldar, B. Chattopadhyay, *J. Am. Chem. Soc.*, **2017**, *139*, 7745.

[11] a) Y. Saito, Y. Segawa, K. Itami, *J. Am. Chem. Soc.*, **2015**, *137*, 5193. b) B. E. Haines, Y. Saito, Y. Segawa, K. Itami, D. G. Musaev, *ACS Catal.*, **2016**, *6*, 7536.

[12] a) S. Okumura, S. Tang, T. Saito, K. Semba, S. Sakaki, Y. Nakao, *J. Am. Chem. Soc.*, **2016**, *138*, 14699. b) S. Okumura, Y. Nakao, *Org. Lett.*, **2017**, *19*, 584. c) L. Yang, K. Semba, Y. Nakao, *Angew. Chem. Int. Ed.*, **2017**, *56*, 4853.

[13] For selected contribution on remote aminoquinoline functionalization seeL: H. Qiao, S. Sun, F. Yang, Y. Zhu, W. Zhu, Y. Dong, Y. Wu, X. Kong, L. Jiang, Y. Wu, *Org. Lett.*, **2015**, *17*, 6086.

[14] a) J.-M. Li, Y.-H. Wang, Y. Yu, R.-B. Weng, G. Lu, *ACS Catal.*, **2017**, *7*, 2661. b) S. Liang, M. Bolte, G. Manolikakes, *Chem. Eur. J.*, **2017**, *23*, 96.

[15] Other examples of *para*-selective C–H functionalisation include: a) W. Liu, L. Ackermann, *Org. Lett.*, **2013**, *15*, 3484. b) X. Wang, D. Leow, J.-Q. Yu, *J. Am. Chem. Soc.*, **2011**, *133*, 13864. c) B. Ma, Z. Chu, B. Huang, Z. Liu, L. Liu, J. Zhang, *Angew. Chem. Int. Ed.*, **2017**, *56*, 2749. d) Y. X. Luan, T. Zhang, W.-W. Yao, K. Lu, L.-Y. Kong, Y.-T. Lin, M. Ye, *J. Am. Chem. Soc.*, **2017**, *139*, 1786. e) B. Berzina, I. Sokolovs, E. Suna, *ACS Catal.*, **2015**, *5*, 7008. f) L. T. Ball, G. C. Lloyd-Jones, C. A. Russell, *Science*, **2012**, *337*, 1644.

[16] For selected contributions see: a) Z. Ruan, S. Lackner, L. Ackermann, *Angew. Cem. Int. Ed.*, **2016**, *55*, 3153. b) C. E. Houlden, M. Hutchby, C. D. Bailey, J. G. Ford, S. Tyler, M. Gagné, G. C. Lloyd-Jones, *Angew. Chem. Int. Ed.*, **2009**, *48*, 1830. c) S. P. Midya, M. K. Sahoo, V. G. Landge, P. P. Rajamohanan, E. Balaraman, *Nat. Commun.*, **2015**, *6*, 8591.

[17] a) E. Weisberg, P. Manley, J. Mestan, S. Cowan-Jacob, A. Ray, J. D. B. Griffin, *Cancer*, **2006**, *94*, 1765. b) M. Baccarani, J. Cortes, F. Pane, D. Niederwieser, G. Saglio, J. Apperley, F. Cervantes, M. Deininger, A. Gratwohl, F. Guilhot, A. Hochhaus, M. Horowitz, T. Hughes, H. Kantarjian, R. Larson, J. Radich, B. Simonsson, R. T. Silver, J. Goldman, R. Hehlmann, *J. Clin. Oncol.*, **2009**, *27*, 6041.

[18] Rappoport, Z. The Chemistry of Anilines; Wiley: New York, **2007**

[19] Crystallographic data for **3b**. Crystal Data for $C_{15}H_{17}N_3O_2$ (**3b**): M =271.32 g mol^{-1}, triclinic, space group P-1 (no. 2), a = 6.0353(3), b = 7.4947(3), c = 16.2821(8) Å, α = 98.032(4), β = 90.419(4), γ = 111.856(4)°, U = 675.43(6) Å^3, Z = 2, T = 150 K, μ(Cu$K\alpha$) = 0.736 mm^{-1}, D_{calc} = 1.334 g cm^{-3}, 5703 reflections measured (10.998° ≤ 2Θ ≤ 146.772°), 2713 unique (R_{int} = 0.0251 which were used in all calculations. The final R1 was 0.0389 (I > 2σ(I)) and wR2 was 0.1047 (all data). Crystallographic data for 3 have been deposited with Cambridge Crystallographic Data Centre: Deposition number CCDC 1555867. Copies of these data can be obtained free of charge via http://www.ccdc.cam.ac.uk/conts/retrieving.html (or from the Cambridge Crystallographic Data Centre, 12, Union Road, Cambridge, CB2 1EZ, UK; Fax: +44 1223 336033; e-mail: deposit@ccdc.cam.ac.uk).

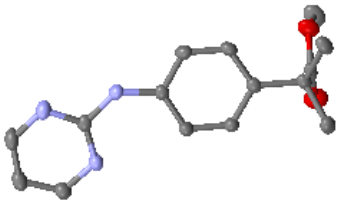

[20] Unreactive and low yielding coupling partners are given in the ESI.

[21] Under Ackermann's conditions from references 6b or 6d only *para*-substituted products were formed.

[22] Full details and references for computational methods can be found in the ESI.

4.1.4: Post-Commentary

The following work has been moved from the supporting information. A proposed viable mechanism based on experimental and computational mechanistic findings (see **6.1.9**: DFT Discussion), is proposed as below. The ruthenium dimer is broken apart using potassium carbonate and solvent to produce a catalytically active monomer. This monomer then forms a 4-membered cyclometalate as a bidentate aminopyrimidine ligand, shown to be a feasible *in silico*. Redox radical generation via single electron transfer (SET) from a ruthenium(II) species (which could be the inner sphere or outer sphere catalytic species) gives the tertiary alkyl radical. This radical then interacts *para* to the location of the metal centre, at the para position of the aniline. Redox rearomatization and proton abstraction gives the C–H alkylated arene and subsequent protodemetalation with potassium bicarbonate or from the coupling partner gives the product and reforms the ruthenium monomer. Despite these understandings a mechanism involving a coordinated ruthenium-assisted deprotonation (without formal formation of a Ru-N bond) cannot be ruled out. This anionic nitrogen could then interact at the *para*-position with a radical formed exogenously.

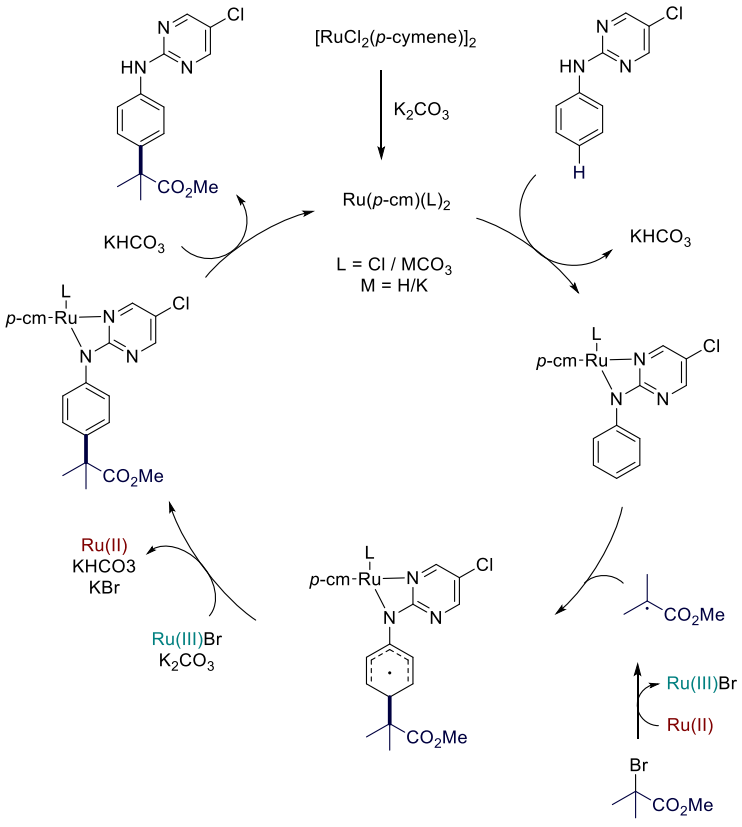

Scheme 4-5: Proposed Mechanism for the *para*-C–H Alkylation of Aniline Derivatives

Chapter 5: Site Selective Catalytic C–H Functionalisation – Conclusions and Outlooks

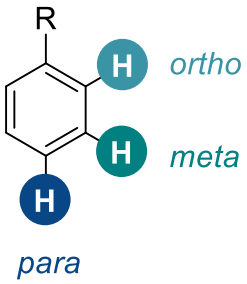

The development of catalytic C–H functionalisation chemistry will continue to see a rapid influx of reaction systems in years to come. The ability of this technique to bypass pre-functionalisation necessary in traditional cross coupling methodology will make it a major player in discovery and, in time, industrial kilo scale processes.

One of the key problems in C–H functionalisation is the differentiation of sterically and electronically similar C–H bonds in a chemical structure. The use of metal-chelating directing groups has enabled pioneering developments in selective *ortho*-functionalisation of arenes. This chemistry was rapidly evolved to enable the use of weakly coordinating directing groups and base metals to facilitate catalysis.

Chapter 2 of this thesis focused on the use of biologically relevant weakly coordinating directing groups in *ortho*-C–H functionalisation. At the outset of this work, this area had focused on ubiquitous functional groups, which could be further transformed or removed, rather than utilizing directing groups with intrinsic biological relevance. We sought to use the oxazolidinone heterocycle as a proof of concept of this methodology. As *N*-aryloxazolidinones are the core of a family of antibacterials and anticoagulants, the ability to access untapped chemical space on these structures could lead to biologically interesting structures. We developed the *ortho*-C–H alkenylation of *N*-phenyloxazolidinone as a model reaction, and expanded it into using heterocyclic variants derives from amino acids as well as a variety of arenes. We were then intrigued to apply this to other heterocycles, which led to the C–H alkenylation of *N*-arylhydantoins (the core of antiandrogens). Both methodologies were shown to be tolerant of widespread functionality and both were shown to proceed in excellent efficiency in the green solvent 2-MeTHF.

Moving beyond *ortho*-selective C–H functionalisation has seen elegant catalytic methods to enable *meta*-selective chemistries. These have relied on a variety of techniques including meticulously designed templates, using a transient mediator at the *ortho*-position, and ruthenium-catalysed σ-activation. The latter of these entails the use of strongly bound *ortho* cyclometalates which can electronically activate the remote *para* position to the metal. This brings about a net *meta*-functionalisation protocol. σ-Activation also forms the basis of Chapter 3.

At the outset of this project, ruthenium-catalysed σ-activation had relied heavily on the use of model substrates such as 2-phenylpyridine. Here, an incredibly strongly bound, planar, ruthenacycle creates an excellent σ-activation complex. The focus of my endeavours in this catalysis was in expanding the scope of structural templates amenable to this chemistry. This led to the use of indole derivatives in the remote C6-functionalisation of indoles furnished with a strongly coordinating directing group at N1 and a weakly coordinating directing group at C3. This enabled the first use of indoles in σ-activation, and also accessed a notoriously benign position to C–H functionalisation (C6). This concept was also applied to carbazole derivatives where a shift in the site of cyclometalation to the benzenoid ring (cf. pyrrole type ring in indole) led to a shift in the regioselectivity of functionalisation to C4.

Moving further beyond *meta* into *para*-C–H functionalisation, we are more-so at the mercy of steric and electronic control, rather than proximal chelating groups. Due to our interest in radical reactions, stemming from our previous work on σ-activation, we were intrigued to see whether altering a position of cyclometalation to N–H instead of C–H could still generate a redox active ruthenium catalyst, and still enable selective C–H functionalisation. However, in this case on using aniline derivatives the site of functionalisation would be shifted to a *para*-selective methodology. This was achieved using anilines furnished with a 5-chloropyrimidine auxiliary, whereby a complementary N–H cyclometalation promoted selective *para*-C–H functionalisation.

The revolution of replacing platinum group metals with base metals has already begun. The synthetic toolkit has already expanded to enable almost pretty much any C-C and C-X bond forming transformation imaginable.

With regards to the future of σ-activation, despite a rapid increase in the number of reaction methodologies available, structural templates amenable, and now potential shifts in regioselectivity in C–H functionalisation, one section of the process is still ambiguous. Since

the discovery in 2015 that in fact radicals are the primary active functionalisation reagent, an influx of systems based on this knowledge has come through to the forefront of catalytic development. However, there has been limited information on the true nature of the radical formation, the redox potential of these redox active co-catalysts, and there is even less knowledge on the nature of the interaction of the radical and the arene. Is the ruthenium dictating selectivity *via* induction of electron density to the aromatic ring? Is this a charge-transfer radical addition? Is there direct interaction of the molecular orbitals on the ruthenium and incoming radical? Is there a second inner sphere metal centre?

We have begun to utilise computational methods in aiding our understanding of this chemistry. Thus far, this has mostly focused on the use of Fukui indices, which demonstrate that the ruthenium centre places most electron density at a certain position of an arene with respect to the location of cyclometalation and, to this date, this computational method has not failed us in predicting/validating regioselectivities. Despite this, more *in silico* and electrochemical understanding is absolutely paramount to the development of this technique, to take us from elegant proof of concept methodology to a broadly synthetically useful technique, in the *meta*-functionalisation of arenes *via* rapid and rational catalyst design and reaction development.

Chapter 6: Experimental

6.1: Data and Supporting Information for "Ruthenium(II)-Catalyzed C–H Functionalization using the Oxazolidinone Directing Group as a Weakly Coordinating Directing Group: Experimental and Computational Insights"

In the interest of presentation in a thesis, NMR spectra, crystallography data and computational data have not been included. However, in the interest of the reader these are available online at:
http://pubs.acs.org/doi/suppl/10.1021/acscatal.6b01370/suppl_file/cs6b01370_si_001.pdf
The supporting information has also been submitted to formatting and colour changes, however no changes in the data have been made.

6.1.1: General

Proton, carbon and fluorine NMR spectra were recorded on Bruker 300 MHz or Agilent Technologies 500 MHz spectrometer (^{1}H NMR at 300 MHz or 500 MHz, ^{13}C{^{1}H} NMR at 126 MHz or 75 MHz and ^{19}F NMR at 470 MHz). Chemical shifts for protons are reported in parts per million downfield from $Si(CH_3)_4$ and are referenced to residual protium in the deuterated solvent ($CHCl_3$ at 7.26 ppm, D_2O at 4.79 and CD_3OD at 3.31). Chemical shifts for fluorines are reported in parts per million downfield from $CFCl_3$. NMR data are presented in the following format: chemical shift (number of equivalent nuclei by integration, multiplicity [app = apparent, br = broad, d = doublet, t = triplet, q = quartet, dd = doublet of doublets, dt = doublet of triplets, dq = doublet of quartets, ddd = doublet of doublet of doublets, m = multiplet], coupling constant [in Hz], assignment). Electrospray ionisation ultrahigh resolution time-of-flight mass spectrometry (ESI–UHR–TOF–MS) was performed on a Bruker maXis mass spectrometer. Electrospray ionisation high resolution time-of-flight mass spectrometry (ESI–HR–TOF–MS) was performed on a Bruker micrOTOF spectrometer. Infrared (IR) spectra were recorded on a Perkin–Elmer 1600 FT (Fourier transform) IR spectrophotometer, with absorbencies quoted as wavelength (v [in cm^{-1}]). Melting points were obtained on a Bibby Sterilin SMP10 melting point machine and are uncorrected.

Analytical thin-layer chromatography (TLC) was performed on aluminium-backed plates coated with Alugram® SIL G/UV254 purchased from Macherey–Nagel and visualised with UV light (254 or 365 nm) and/or KMnO4, 2,4-DNPH or I_2/Silica staining. Silica gel column

chromatography was performed using 60 Å, 200-400 mesh particle size silica gel purchased from Sigma–Aldrich. Samples were loaded as saturated solutions in an appropriate solvent system.

All reactions were performed using reagents obtained from Sigma-Aldrich, Acros Organics, Alfa Aesar, Fluorochem chemicals without further purification unless stated. $[RuCl_2(p\text{-cymene})]_2$ was purchased from STREM chemicals. All water used was purified through a Merck Millipore reverse osmosis purification system prior to use. Anhydrous acetonitrile (MeCN), anhydrous dichloromethane (CH_2Cl_2), anhydrous tetrahydrofuran (THF) and anhydrous toluene (PhMe) were dried and degassed by passing through anhydrous alumina columns using an Innovative Technology Inc. PS-400-7 solvent purification system (SPS) and stored under an atmosphere of N_2 prior to use.

Reactions were performed in oven-dried glassware and under a blanket of N_2 if not stated. Temperatures quoted are external. Solvents were removed under reduced pressure using Büchi-Rotorvapor apparatus.

6.1.2: Optimisation of Ruthenium Catalysed C–H Alkenylation

Proton NMR conversions were taken from the labelled diagnostic protons. Only one product formed from reaction (complete mono-selectivity) and no observed starting material decomposition lead to ^{1}H NMR conversions being indicative of yield of alkenylated product.

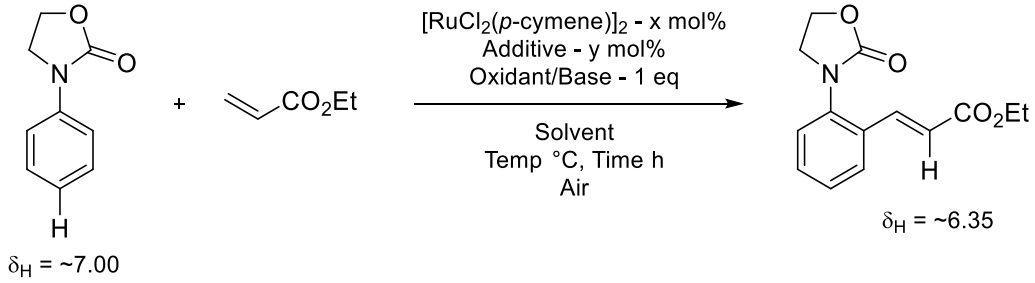

General Optimisation Conditions

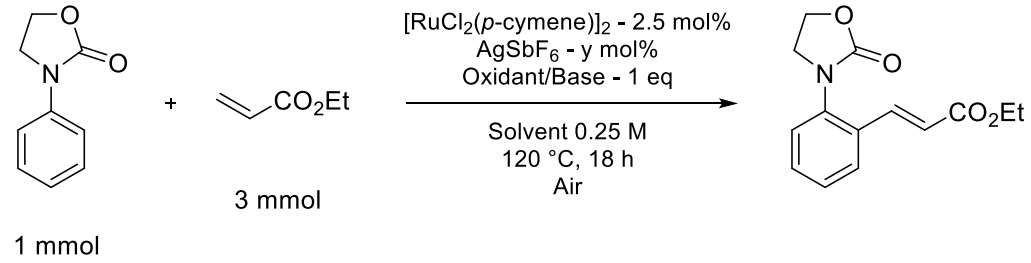

Solvent Screen

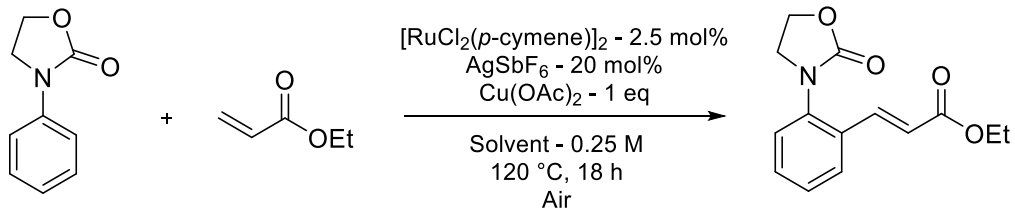

Entry	Solvent	Conversion (Yield)
1	Xylene	0
2	Trifluorotoluene	0
3	Dioxane	56
4	THF	30
5	NMP	0
6	CH_3CN	15
7	DMF	0
8	No Solvent	47
9	Ethyl Acrylate	36
10	H_2O	0
11	DME	72 (68)
12	AcOH	Trace
13	2-MeTHF	70 (66)
14	^{t}BuOMe	36
15	CPME	30
16	Diglyme	46
17	2-MeTHF:AcOH (3:1)	Trace

Exclusion Screen

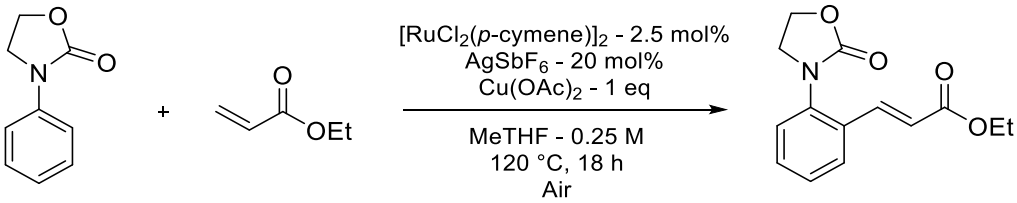

Entry	Component Excluded	Conversion
1	$[RuCl_2(p\text{-cymene})]_2$	0
2	$AgSbF_6$	0
3	$Cu(OAc)_2$	0
4	$CuCl_2$ (No Acetate)	0
5	KOAc – 2 eq (No Cu^{2+})	11

Additive Screen

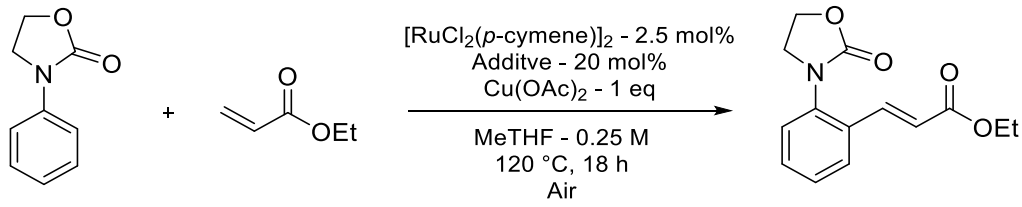

Entry	Additive - 20 mol%	Conversion
1	KPF_6	10
2	$AgPF_6$	28
3	$KSbF_6$	45

Screen of Bifunctional Oxidant/Bases

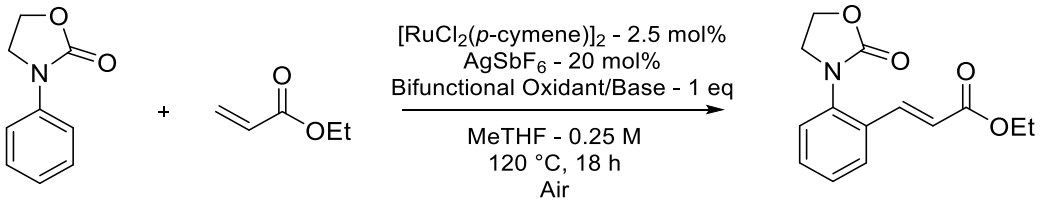

Entry	Bifunctional Oxidant/Base	Conversion
1	$Cu(OAc)_2.H_2O$	77
2	Ag_2CO_3	13
3	AgOAc	48
4	AgOAc – 2 eq	64
5	AgTFA	Trace

Screen of sole oxidants

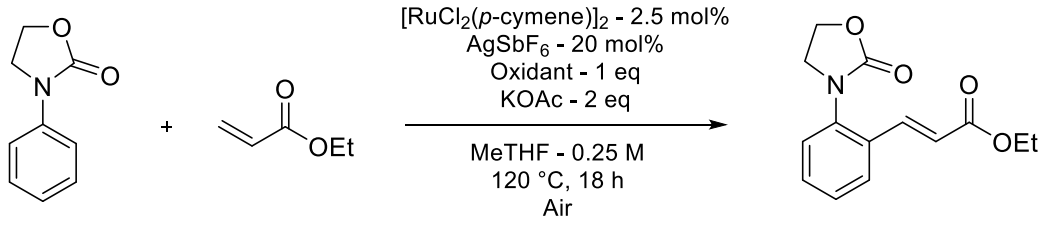

Entry	Oxidant – 1 eq	Conversion
1	$K_2S_2O_8$	0
2	Oxone	0
3	Ag_xO	0
4	TBHP	0
5	$Cu(OAc)_2.H_2O$[a]	Trace

[a] = K_2CO_3 used instead of KOAc

Catalytic $Cu(OAc)_2.H_2O$ with Stoichiometric Oxidant Screen

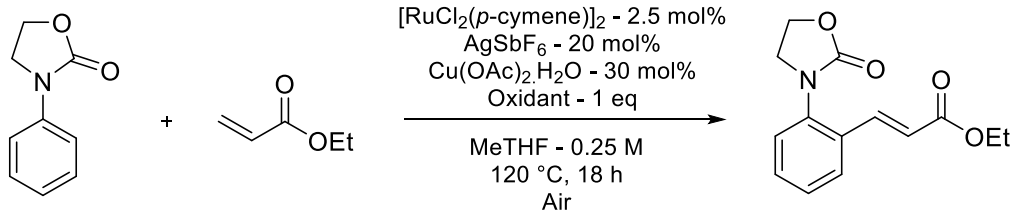

Entry	Oxidant	Conversion
1	-	38
2	$Cu(OAc)_2.H_2O$[a]	56
3	$FeCl_3$	14
4	Benzoquinone	39
5	$Na_2S_2O_8$	32
6	O_2 – 1 atm	56

[a] = Therefore 1.3 eq $Cu(OAc)_2H_2O$

Temperature Screen

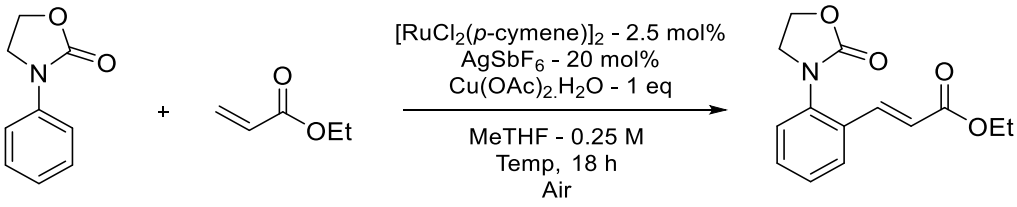

Entry	Temperature / °C	Conversion
1	80	15
2	100	68
3	140	60

Atmosphere Screen

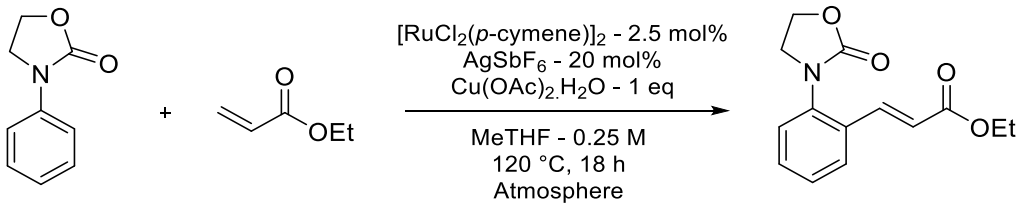

Entry	Atmosphere	Conversion
1	Closed[a]	72
2	Argon	66
3	Oxygen	72

[a] = Teflon cap closed over course of reaction, still under air atmosphere

Time Screen

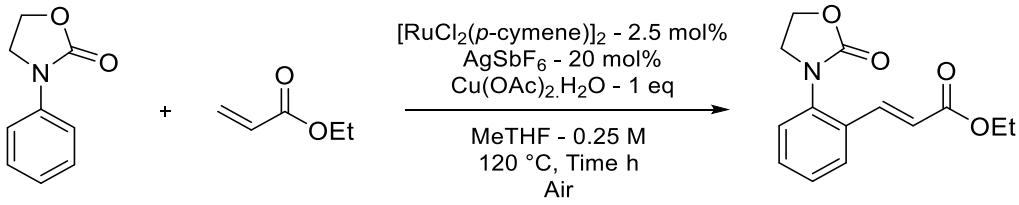

Entry	Time / h	Conversion
1	4	40
2	8	64
3	12	71
4	24	78

Equivalencies Screen

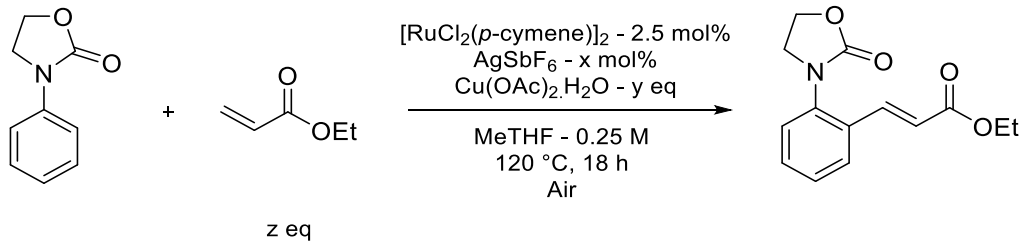

Entry	$AgSbF_6$ mol%	$Cu(OAc)_2.H_2O$ eq	Acrylate eq	Conversion
1	5	1	3	65
2	10	1	3	78
3	10	2	3	70
4	10	3	3	68
5	10	1	1	71
6	10	1	2	64

Reaction Concentration Screen

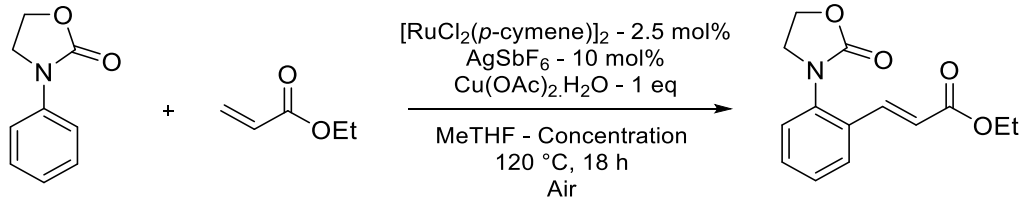

Entry	Solvent / mL	Solvent / M	Conversion (Yield)
1	1	1 M	80 (76)
2	2	0.5 M	75
3	8	0.125 M	65

From this optimum conditions as below were achieved:

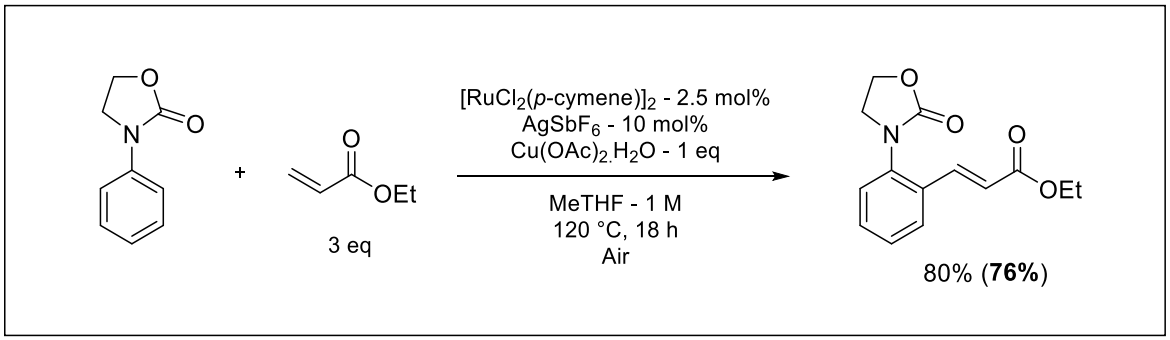

Previous work in the field has been shown to use two equivalents of $Cu(OAc)_2.H_2O$ in similar transformations. Despite only using one equivalent in this work, it is still necessary to attempt to reduce this loading and instead use air as the environmentally benign terminal oxidant. The reaction was run with co-catalytic $Cu(OAc)_2.H_2O$ which was shown to afford the C–H alkenylated scaffold in moderate isolated yield (Scheme 7). This allows only the two reactants to be use in stoichiometric quantities, an incredibly attractive feature in catalysis.

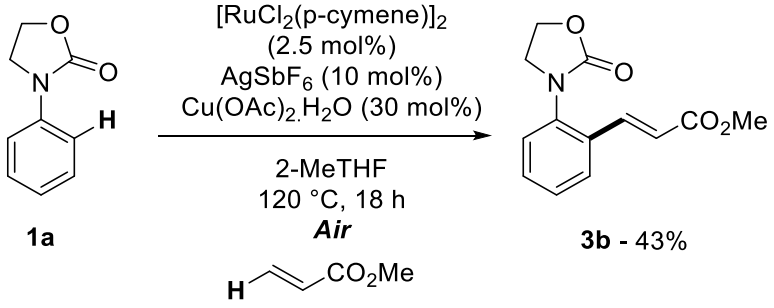

6.1.3: Synthesis of Starting Materials

Synthesis of 3-phenyl-1,3-oxazolidnone (**1a**)

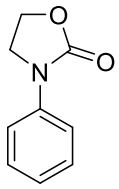

To a solution of *N*-(2-hydroxyethyl)aniline (6.27 mL, 6.86 g, 50 mmol), triethylamine (13.95 mL, 10.12 g, 100 mmol) and CH_2Cl_2 (100 mL) at 0 °C was slowly added phosgene (20% wt in toluene) (24.73 mL, 4.95 g, 50 mmol) in CH_2Cl_2 (50 mL) using a dropping funnel. After addition was complete the mixture was stirred at room temperature for 1 hour. To the mixture was added 150 mL saturated $NaHCO_3$ solution at 0 °C and was left to stir for a further 15 mins. The organic layer was removed and the aqueous layer was extracted with 2 x 150 mL EtOAc. The combined organics were washed with 3 x 150 mL 1M HCl solution then 1 x 150 mL brine. The organic layer was dried over $MgSO_4$ and concentrated *in vacuo*. The crude mixture was recrystallized from hot EtOH to give white crystalline solid, **1a**, 67% (4.58 g). **^{1}H NMR** (500 MHz, $CDCl_3$) δ 7.54 (2H, d, *J* = 8.7 Hz, Ar*H*), 7.40–7.35 (2H, m, Ar*H*), 7.14 (1H, td, *J* = 7.4, 1.1 Hz, Ar*H*), 4.50–4.44 (2H, m, OCH_2), 4.08–4.02 (2H, m, NCH_2). **^{13}C NMR** (126 MHz, $CDCl_3$) δ 155.42 (N*C*(O)O), 138.42 (Ar*C*), 129.21 (Ar*C*), 124.23 (Ar*C*), 118.40 (Ar*C*), 61.44 (O*C*H_2), 45.35 (N*C*H_2). Data is in line with literature precedent.[1]

Synthesis of ethylcarbamate protected amino alcohols

Synthesis of ethyl 2-hydroxy-ethylcarbamate

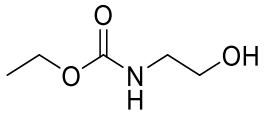

To a solution of ethanolamine (3.02 mL, 3.05 g, 50 mmol), triethylamine (8.32 mL, 6.07 g, 60 mmol) in CH_2Cl_2 (100 mL) at 0 °C was added dropwise ethyl chloroformate (5.71 mL, 6.51 g, 60 mmol). The solution was allowed to stir for 30 mins before allowing the solution to return to room temperature and allowed to stir overnight. The solvent was removed *in vacuo* and re-diluted in EtOAc. The resulting slurry was filtered using a silica plug eluting with EtOAc. The solvent was again removed *in vacuo* and the crude oil was purified using silica gel chromatography (EtOAc:Hexanes 90:10) to give pure compound, isolated as a clear off-white oil, 70% (4.65 g). **^{1}H NMR** (500 MHz, $CDCl_3$) δ 5.52 (1H, s, N*H*), 4.04 (2H, q, *J* = 7.1 Hz, NC*H*$_2$), 3.64–3.58 (2H, m, OC*H*$_2$), 3.26–3.21 (2H, m, OC*H*$_2$), 1.17 (3H, t, *J* = 7.1 Hz, OCH_2CH_3). **^{13}C NMR** (126 MHz, $CDCl_3$) δ 157.55 (N*C*(O)O), 61.79 (O*C*H_2), 61.08 (O*C*H_2), 43.46 (N*C*H_2), 14.59 (OCH_2CH_3). Data is in line with literature precedent[1]

Synthesis of (S)-ethyl (1-hydroxy-3-methylbutan-2-yl)carbamate

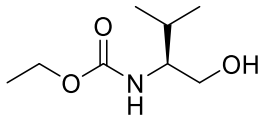

To a solution of valine (4.68 g, 40 mmol) in MeOH (100 mL) at 0 °C was added dropwise thionyl chloride (4.3 mL, 60 mmol). The mixture was then heated to reflux overnight. The resulting solution was concentrated *in vacuo*. This material was re-dissolved in dry THF (150 mL) and at -5 °C was added lithium aluminium hydride (4.56 g, 120 mmol) in four portions. The resulting mixture was stirred for 30 mins and then allowed to return to room temperature and stir for a further 1 hour. The reaction mixture was cooled to 0 °C and in subsequent portions was added, 4.56 mL H_2O, 4.56 mL NaOH (15% in H_2O) and 13.68 mL H_2O. The reaction was left to stir for 1 hour at room temperature. The resulting slurry was filtered and the filtrate was dried over $MgSO_4$ and concentrated *in vacuo* to give a crude amorphous solid (3.2 g, 31 mmol). This solid was suspended in H_2O (30 mL) and was added sodium bicarbonate (5.21 g, 62 mmol) and CH_2Cl_2 (90 mL) to form a biphasic mixture. Ethyl chloroformate (3.23 mL, 3.68 g, 34.1 mmol) in CH_2Cl_2 (5 mL) was added dropwise and after addition was complete the reaction was allowed to stir at room temperature overnight. The reaction mixture was concentrated *in vacuo* to give a slurry which was re-diluted in EtOAc and filtered using a silica plug eluting with EtOAc. The solvent was again removed *in vacuo* and the crude oil was purified using column chromatography (EtOAc:Hexanes 80:20) to give clear off-white oil, 20% (1.37 g). **^{1}H NMR** (500 MHz, $CDCl_3$) δ 5.02 (1H, s, N*H*), 4.08 (2H, q, *J* = 7.0 Hz, OC*H*$_2$), 3.69–3.55 (2H, m, OC*H*$_2$), 3.43 (1H, app s, NC*H*), 3.08 (1H, s, O*H*), 1.82 (1H, td, *J* = 13.3, 6.6 Hz, C*H*$(CH_3)_2$, 1.21 (3H, t, *J* = 7.1 Hz, OCH_2CH_3), 0.95–0.87 (6H, m, $CH(CH_3)_2$). **^{13}C NMR** (126 MHz, $CDCl_3$) δ 157.62 (N*C*(O)O), 63.76 (OCH_2), 61.10 (OCH_2), 58.54 (N*C*H), 29.36 (*C*H$(CH_3)_2$), 19.62 (CH(*C*$H_3)_2$), 18.61 (CH(*C*$H_3)_2$), 14.68 (OCH_2CH_3). Data is in line with literature precedent[1]

Synthesis of (S)-ethyl (1-hydroxy-4-methylpentan-2-yl)carbamate

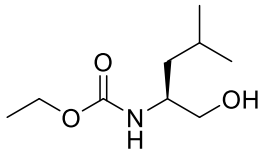

To a solution of leucine (5.25 g, 40 mmol) in MeOH (100 mL) at 0 °C was added dropwise thionyl chloride (4.3 mL, 60 mmol). The mixture was then heated to reflux overnight. The resulting solution was concentrated *in vacuo*. This material was re-dissolved in dry THF (150 mL) and at -5 °C was added lithium aluminium hydride (4.56 g, 120 mmol) in four portions. The resulting mixture was stirred for 30 mins and then allowed to return to room temperature and stir for a further 1 hour. The reaction mixture was cooled to 0 °C and in subsequent portions was added, 4.56 mL H_2O, 4.56 mL NaOH (15% in H_2O) and 13.68 mL H_2O. The reaction was left to stir for 1 hour at room temperature. The resulting slurry was filtered and the filtrate was dried over $MgSO_4$ and concentrated *in vacuo* to give a crude amorphous solid (3.8 g, 32 mmol). This solid was suspended in H_2O (30 mL) and was added sodium bicarbonate (5.38 g, 64 mmol) and CH_2Cl_2 (90 mL) to form a biphasic mixture. Ethyl chloroformate (3.33 mL, 3.80 g, 35.2 mmol) in CH_2Cl_2 (5 mL) was added dropwise and after addition was complete the reaction was allowed to stir at room temperature overnight. The reaction mixture was concentrated *in vacuo* to give a slurry which was re-diluted in EtOAc and filtered using a silica plug eluting with EtOAc. The solvent was again removed *in vacuo* and the crude oil was purified using column chromatography (EtOAc:Hexanes 80:20) to give clear off-white oil, 27% (2.05 g). **FT-IR** (thin film): ν_{max} (cm^{-1}) = 3329.4, 2956.2, 1688.4, 1581.6. **^{1}H NMR** (500 MHz, $CDCl_3$) δ 5.17 (1H, s, N*H*), 4.11–3.95 (2H, m, OC*H*$_2$), 3.66 (1H, s, O*H*), 3.54 (1H, dd, *J* = 11.0, 2.9 Hz, NC*H*), 3.43 (2H, d, *J* = 3.8 Hz, OC*H*$_2$), 1.66–1.52 (1H, m, C*H*$(CH_3)_2$), 1.34–1.20 (3H, m, OCH_2CH_3), 1.21–1.03 (2H, m, C*H*$_2$), 0.84 (6H, d, *J* = 6.6 Hz, $CH(CH_3)_2$). **^{13}C NMR** (126 MHz, $CDCl_3$) δ 157.15 (N*C*(O)O), 65.56 (OCH_2), 60.83 (OCH_2), 51.16 (N*C*H), 40.54, 24.76 (*C*H$_2$), 23.08 (*C*H$(CH_3)_2$), 22.17 (*C*H$(CH_3)_2$), 14.56 (OCH_2CH_3). **HRMS** (ESI): m/z calculated for $C_9H_{19}N_1O_3$ requires 190.1443 for $[M+H]^+$, found 190.1444.

Synthesis of ethyl(2,3-dihydroxypropyl) carbamate

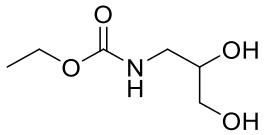

3-Amino-2-hydroxypropanol (3.101 mL, 40 mmol) was suspended in CH_2Cl_2 (110 mL) and H_2O (35 mL). To the biphasic mixture was added sodium bicarbonate (6.72 g, 80 mmol) followed by dropwise addition of ethyl chloroformate (4.00 mL, 42 mmol) at 0 °C. The reaction was left to return to room temperature and stir overnight. The solvent was removed *in vacuo*. The resulting slurry was dissolved in EtOAc and was filtered using a silica plug eluting with EtOAc. The solvent was again removed *in vacuo* to give a thick pale yellow oil, 91% (5.943 g). **^{1}H NMR** (300MHz, $CDCl_3$): δ 5.43 (1H, s, N*H*), 4.11 (2H, q, *J* = 7.9 Hz (OC*H*$_2$), 3.77 (1H, app dt, *J* = 10.2, 5.2 Hz, C*H*OH), 3.58 (2H, ddd, *J* = 17.2, 11.6, 4.8 Hz, OC*H*$_2$), 3.38 (2H, m, NC*H*$_2$), 3.31 (1H, s, O*H*), 3.26 (1H, s, O*H*), 1.24 (3H, t, *J* = 7.1 Hz, OCH_2CH_3). **^{13}C NMR** (75MHz, $CDCl_3$): δ 158.2 (N*C*(O)O), 71.4 (OC*H*$_2$), 64.0 (*C*HOH), 61.6 (O*C*H_2), 43.4 (N*C*H_2), 14.8 (OCH_2CH_3). Data is in line with literature precedent[1]

Synthesis of ethyl(2-hydroxy 3-(dimethyl-tert-butyl siloxy)propyl) carbamate

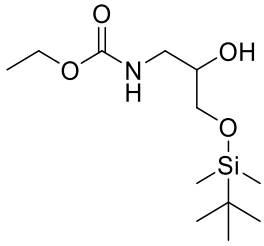

To a solution of the above compound (3.26 g, 20 mmol), triethylamine (1.12 mL, 0.81 g, 11 mmol), dimethylaminopyridine (4.48 g, 36.7 mmol) in 50 mL CH_2Cl_2 was added tert-butyl-dimethylsilyl chloride (3.014 g, 20 mmol),. The reaction was stirred overnight at room temperature. The solvent was then removed *in vacuo*. The crude mixture was purified using column chromatography (EtOAc:Hexanes 70:30) to yield a thick pale yellow oil, 3.155g, 57%. **^{1}H NMR** (300MHz, $CDCl_3$): δ 5.17 (1H, s, N*H*), 4.10 (2H, q, *J* = 7.1 Hz, OC*H*$_2$), 3.73 (1H, m, C*H*OH), 3.67-3.34 (4H, m, OC*H*$_2$ + NC*H*$_2$), 2.95 (1H, s, O*H*), 1.22 (3H, t, *J* = 7.1 Hz, OCH_2CH_3), 0.88 (9H, s, $SiC(CH_3)_3$), 0.06 (6H, s, $SiCH_3$). **^{13}C NMR** (75MHz, $CDCl_3$): δ 157.6 (N*C*(O)O), 71.4 (O*C*H_2), 65.0 (*C*HOH), 61.3 (O*C*H_2), 43.9 (N*C*H_2), 18.5 (OCH_2CH_3), 14.9 ($SiC(CH_3)_3$, 5.16 (Si*C*), 4.46 (Si*C*). Data is in line with literature precedent[1]

Synthesis of *N*-phenyloxazolidinones **1aa-ca**

General Procedure **A** for formation of *N*-phenyloxazolidinones

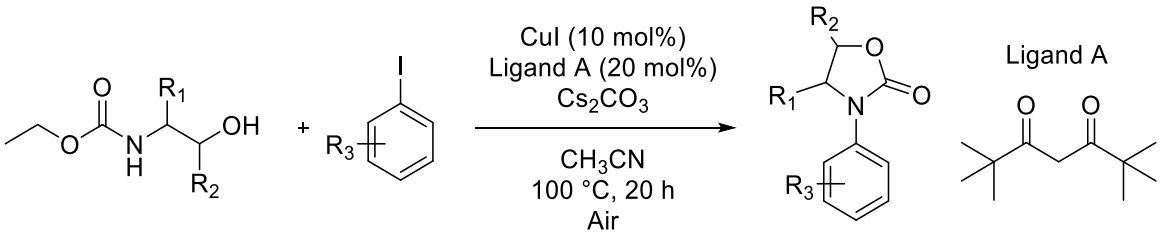

The procedure was adapted from literature method.[1] In an oven dried carousel tube, to a solution of ethyl carbamate protected amino alcohol (1 eq), 2,2,6,6-tetramethyl-3,5-heptanedione (Ligand A, 20 mol%) and aryl iodide (2 eq) in CH_3CN (0.25-0.5 M) was added caesium carbonate (2 eq) and copper iodide (10 mol%). The carousel tube was sealed with a Teflon cap closing the tap. The reaction was heated to 100 °C for 20 h. The mixture was diluted in EtOAc and filtered using a silica plug, eluting with EtOAc. The solvent was removed *in vacuo* and the crude mixture was purified using column chromatography (EtOAc:Hexanes 50:50 unless otherwise stated) to yield *N*-aryloxazolidinone.

General Procedure **B** for formation of *N*-phenyloxazolidinones

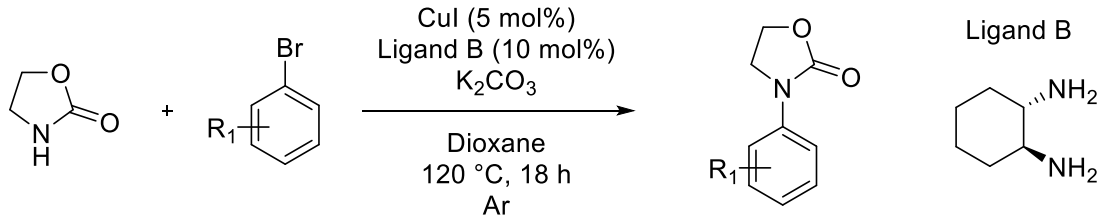

The procedure was adapted from a literature method.[2] In an oven dried carousel tube, to a solution of 2-oxazolidinone (1 eq), (±)-trans-1,2-diaminocyclohexane (Ligand B, 10 mol%) and aryl bromide in 1,4-dioxane (2 M) was added potassium carbonate (2 eq) and copper iodide (5 mol%). The carousel tube was sealed with a Teflon cap and the tube was purged with Argon for 10 minutes before closing the tap. The reaction mixture was heated to 120 °C for 18 h. The mixture was diluted in EtOAc and filtered using a celite plug, eluting with EtOAc. The solvent was removed *in vacuo* and the crude mixture was purified using column chromatography (EtOAc:Hexanes 50:50 unless otherwise stated) or via recrystallization from hot EtOH to yield *N*-aryloxazolidinone.

Synthesis of **1aa**

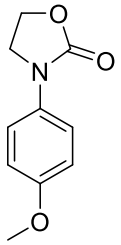

General Procedure **A** was followed using the following compounds: ethyl 2-hydroxyethylcarbamate (0.67 g, 5 mmol), copper iodide (0.095 g, 0.5 mmol), 2,2,6,6-tetramethyl-3,5-heptanedione (0.21 mL, 0.18 g, 1 mmol), caesium carbonate (3.26 g, 10 mmol), 4-iodoanisole (2.34 g, 10 mmol) and CH_3CN (20 mL). Column chromatography gave an off-white solid, **1aa**, 21% (0.20 g). **^{1}H NMR** (500 MHz, $CDCl_3$): δ 7.44 (2H, d, *J* = 8.9 Hz, Ar*H*), 6.91 (2H, d, *J* = 8.9 Hz, Ar*H*), 4.47 (2H, t, *J* = 7.9 Hz, OC*H*$_2$), 4.05–4.00 (2H, m, NC*H*$_2$), 3.80 (3H, s, ArOC*H*$_3$). **^{13}C NMR** (126 MHz, $CDCl_3$) δ 156.41 (N*C*(O)O), 131.53 (Ar*C*), 120.32 (Ar*C*), 114.31 (Ar*C*), 61.38 (O*C*H$_2$), 55.56 (ArO*C*H$_3$), 45.75 (N*C*H$_2$). Data is in line with literature precedent[1]

Synthesis of **1ab**

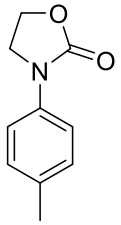

General Procedure **A** was followed using the following compounds: ethyl 2-hydroxyethylcarbamate (0.13 g, 1 mmol), copper iodide (0.019 g, 0.1 mmol), 2,2,6,6-tetramethyl-3,5-heptanedione (0.042 mL, 0.037 g, 0.2 mmol), caesium carbonate (0.65 g, 2 mmol), 4-iodotoluene (0.44 g, 2 mmol) and CH_3CN (4 mL). Column chromatography gave an off-white solid, **1ab**, 81% (0.14 g). **^{1}H NMR** (500 MHz, $CDCl_3$) δ 7.43–7.38 (2H, m, Ar*H*), 7.16 (2H, d, *J* = 8.2 Hz, Ar*H*), 4.43 (2H, dd, *J* = 8.8, 7.2 Hz, OC*H*$_2$), 4.00 (2H, dd, *J* = 8.8, 7.2 Hz, NC*H*$_2$), 2.32 (3H, s, ArC*H*$_3$). **^{13}C NMR** (126 MHz, $CDCl_3$) δ 155.49 (N*C*(O)O), 135.88 (Ar*C*), 133.84 (Ar*C*), 129.67 (Ar*C*), 118.47 (Ar*C*), 61.41 (O*C*H$_2$), 45.45 (N*C*H$_2$), 20.85 (Ar*C*H$_3$). Data is in line with literature precedent[1]

Synthesis of **1ac**

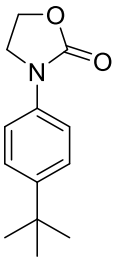

General Procedure **B** was followed using the following compounds: 2-oxazolidinone (0.17 g, 2 mmol), copper iodide (0.019 g, 0.1 mmol), (±)-trans-1,2-diaminocyclohexane (0.024 mL, 0.023 g, 0.2 mmol), potassium carbonate (0.55 g, 4 mmol), 1-bromo-4-*tert*-butylbenzene (0.35 mL, 0.43 g, 2 mmol) and dioxane (1 mL) Column chromatography gave a white crystalline solid, **1ac**, 60%, (0.26 g). **^{1}H NMR** (500 MHz, $CDCl_3$) δ 7.48–7.43 (2H, m, Ar*H*), 7.41–7.37 (2H, m, Ar*H*), 4.50–4.41 (2H, m, OCH_2), 4.07–4.00 (2H, m, NCH_2), 1.31 (9H, s, *J* = 2.1 Hz, C(CH_3)$_3$). **^{13}C NMR** (126 MHz, $CDCl_3$) δ 155.58 (N*C*(O)O), 147.32 (Ar*C*), 135.86 (Ar*C*), 126.10 (Ar*C*), 118.35 (Ar*C*), 61.51 (O*C*H$_2$), 45.52 (N*C*H$_2$), 34.52 (*C*(CH$_3$)$_3$), 31.52 (C(*C*H$_3$)$_3$. Data is in line with literature precedent.[3]

Synthesis of **1ad**

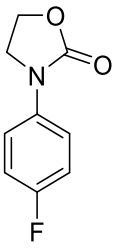

General Procedure **B** was followed using the following compounds: 2-oxazolidinone (0.17 g, 2 mmol), copper iodide (0.019 g, 0.1 mmol), (±)-trans-1,2-diaminocyclohexane (0.024 mL, 0.023 g, 0.2 mmol), potassium carbonate (0.55 g, 4 mmol), 1-fluoro-4-iodobenzene (0.12 mL, 0.22 g, 2 mmol) and dioxane (1 mL) Column chromatography gave an off-white solid, **1ad**, 34%, (0.12 g). **^{1}H NMR** (500 MHz, $CDCl_3$) δ 7.52–7.44 (2H, m, Ar*H*), 7.09–7.00 (2H, m, Ar*H*), 4.46 (2H, dd, *J* = 8.7, 7.3 Hz, OCH_2), 4.02 (2H, dd, *J* = 8.7, 7.3 Hz, NCH_2). **^{13}C NMR** (126 MHz, $CDCl_3$) δ 159.40 (d, *J* = 243.8 Hz, Ar*C*F), 155.50 (N*C*(O)O), 134.51 (d, *J* = 2.8 Hz, Ar*C*), 120.18 (d, *J* = 7.9 Hz, Ar*C*), 115.86 (d, *J* = 22.5 Hz, Ar*C*), 61.40 (O*C*H$_2$), 45.59 (N*C*H$_2$). Data is in line with literature precedent.[3]

Synthesis of **1ae**

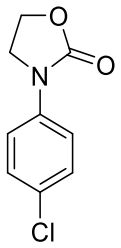

General Procedure **B** was followed using the following compounds: 2-oxazolidinone (0.17 g, 2 mmol), copper iodide (0.019 g, 0.1 mmol), (±)-trans-1,2-diaminocyclohexane (0.024 mL, 0.023 g, 0.2 mmol), potassium carbonate (0.55 g, 4 mmol), 1-fluoro-4-iodobenzene (0.12 mL, 0.22 g, 2 mmol) and dioxane (1 mL) Column chromatography gave an off-white solid, **1ae**, 34%, (0.12 g). **^{1}H NMR** (500 MHz, $CDCl_3$) δ 7.52–7.44 (2H, m, Ar*H*), 7.09–7.00 (2H, m, Ar*H*), 4.46 (2H, dd, *J* = 8.7, 7.3 Hz, OC*H*$_2$), 4.02 (2H, dd, *J* = 8.7, 7.3 Hz, NC*H*$_2$). **^{13}C NMR** (126 MHz, $CDCl_3$) δ 159.40 (d, *J* = 243.8 Hz, Ar*C*F), 155.50 (N*C*(O)O), 134.51 (d, *J* = 2.8 Hz, Ar*C*), 120.18 (d, *J* = 7.9 Hz, Ar*C*), 115.86 (d, *J* = 22.5 Hz, Ar*C*), 61.40 (O*C*H$_2$), 45.59 (N*C*H$_2$). Data is in line with literature precedent.[3]

Synthesis of **1af**

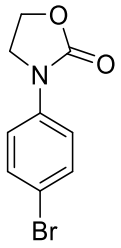

General Procedure **A** was followed using the following compounds: ethyl 2-hydroxy-ethylcarbamate (0.13 g, 1 mmol), copper iodide (0.019 g, 0.1 mmol), 2,2,6,6-tetramethyl-3,5-heptanedione (0.042 mL, 0.037 g, 0.2 mmol), caesium carbonate (0.65 g, 2 mmol), 1-bromo-4-iodobenzene (0.57 g, 2 mmol) and CH_3CN (4 mL). Column chromatography gave an off-white solid, **1af**, 71% (0.17 g). **^{1}H NMR** (500 MHz, $CDCl_3$) δ 7.46 (2H, app d, *J* = 8.0, 0.9 Hz, Ar*H*), 7.42 (2H, app d, *J* = 7.3, 1.7 Hz, Ar*H*), 4.46 (2H, t, *J* = 7.5 Hz, OC*H*$_2$), 4.06–3.96 (2H, m, NC*H*$_2$). **^{13}C NMR** (126 MHz, $CDCl_3$) δ 155.14 (N*C*(O)O), 137.50 (Ar*C*), 132.07 (Ar*C*), 119.76 (Ar*C*), 116.93 (Ar*C*), 61.40 (O*C*H$_2$), 45.12 (N*C*H$_2$). Data is in line with literature precedent[1]

Synthesis of **1ag**

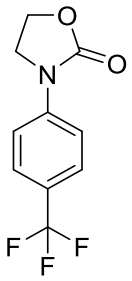

General Procedure **A** was followed using the following compounds: ethyl 2-hydroxy-ethylcarbamate (0.67 g, 5 mmol), copper iodide (0.095 g, 0.5 mmol), 2,2,6,6-tetramethyl-3,5-heptanedione (0.21 mL, 0.18 g, 1 mmol), caesium carbonate (3.26 g, 10 mmol), 4-iodobenzotrifluoride (1.47 mL, 2.72 g, 10 mmol) and CH_3CN (20 mL). Column chromatography gave a white solid, **1ag**, 55% (0.63 g). **^{1}H NMR** (500 MHz, $CDCl_3$) δ 7.62 (2H, d, *J* = 7.4 Hz, Ar*H*), 7.56 (2H, d, *J* = 7.2 Hz, Ar*H*), 4.46 (2H, t, *J* = 7.1 Hz, OC*H*$_2$), 4.07–3.96 (2H, m, NC*H*$_2$). **^{13}C NMR** (126 MHz, CDCl3) δ 155.02 (N*C*(O)O), 141.34 (Ar*C*), 126.16 (q, *J* = 3.8 Hz, Ar*C*), 125.49 (d, *J* = 32.8 Hz Ar*C*), 124.14 (app d, *J* = 271.4 Hz, Ar*C*F$_3$), 117.63 (Ar*C*), 61.47 (O*C*H$_2$), 44.86 (N*C*H$_2$). Data is in line with literature precedent[1]

Synthesis of **1ah**

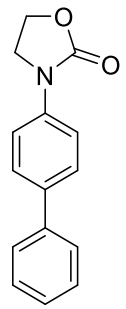

General Procedure **B** was followed using the following compounds: 2-oxazolidinone (0.17 g, 2 mmol), copper iodide (0.019 g, 0.1 mmol), (±)-trans-1,2-diaminocyclohexane (0.024 mL, 0.023 g, 0.2 mmol), potassium carbonate (0.55 g, 4 mmol), 4-bromobiphenyl (0.47 g, 2 mmol) and dioxane (1 mL) Column chromatography (EtOAc:Hexanes 30:70) gave an off-white solid, **1ah**, 34%, (0.16 g). **^{1}H NMR** (500 MHz, $CDCl_3$) δ 7.62 (4H, s, Ar*H*), 7.58 (2H, dt, *J* = 7.9, 1.5 Hz, Ar*H*), 7.46–7.42 (2H, m, Ar*H*), 7.36–7.32 (1H, m, Ar*H*), 4.53–4.48 (2H, m, OC*H*$_2$), 4.13–4.08 (2H, m, NC*H*$_2$). **^{13}C NMR** (126 MHz, $CDCl_3$) δ 155.44 (N*C*(O)O),

140.48 (Ar*C*), 137.73 (Ar*C*), 137.16 (Ar*C*), 129.04 (Ar*C*), 127.88 (Ar*C*), 127.44 (Ar*C*), 127.07 (Ar*C*), 118.72 (Ar*C*), 61.53 (O*C*H_2), 45.45 (N*C*H_2). Data is in line with literature precedent[4]

Synthesis of **1ai**

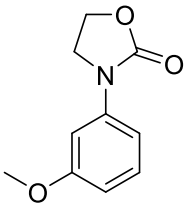

General Procedure **A** was followed using the following compounds: ethyl 2-hydroxyethylcarbamate (0.27 g, 2 mmol), copper iodide (0.038 g, 0.2 mmol), 2,2,6,6-tetramethyl-3,5-heptanedione (0.083 mL, 0.074 g, 0.4 mmol), caesium carbonate (1.30 g, 4 mmol), 3-iodoanisole (0.48 mL, 0.94 g, 4 mmol) and CH_3CN (4 mL). Column chromatography gave a white solid, **1ai**, 75% (0.29 g). **^{1}H NMR** (500 MHz, $CDCl_3$) δ 7.28–7.20 (2H, m, Ar*H*), 7.01 (1H, ddd, *J* = 8.1, 2.2, 0.8 Hz, Ar*H*), 6.67 (1H, ddd, *J* = 8.3, 2.5, 0.8 Hz, Ar*H*), 4.45–4.38 (2H, m, OCH_2), 4.01–3.96 (2H, m, NCH_2), 3.79 (3H, s, ArOCH_3). **^{13}C NMR** (126 MHz, $CDCl_3$) δ 160.23 (Ar*C*), 155.23 (N*C*(O)O), 139.59 (Ar*C*), 129.78 (Ar*C*), 110.35 (Ar*C*), 109.51 (Ar*C*), 104.53 (Ar*C*), 61.34 (O*C*H_2), 55.40 (ArO*C*H_3), 45.31 (N*C*H_2). Data is in line with literature precedent[1]

Synthesis of **1aj**

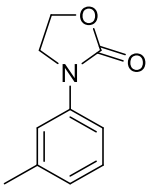

General Procedure **A** was followed using the following compounds: ethyl 2-hydroxyethylcarbamate (0.67 g, 5 mmol), copper iodide (0.095 g, 0.5 mmol), 2,2,6,6-tetramethyl-3,5-heptanedione (0.21 mL, 0.18 g, 1 mmol), caesium carbonate (3.26 g, 10 mmol), 3-iodotoluene (1.28 mL, 2.18 g, 10 mmol) and CH_3CN (20 mL). Column chromatography gave an off-white solid, **1aj**, 48% (0.43 g). **^{1}H NMR** (500 MHz, $CDCl_3$) δ 7.36 (1H, s, Ar*H*), 7.29 (1H, d, *J* = 8.4 Hz, Ar*H*), 7.27–7.21 (m, Ar*H*), 6.94 (1H, d, *J* = 7.4 Hz, Ar*H*), 4.41 (2H, dd, *J* = 8.7, 7.3 Hz, OCH_2), 3.99 (2H, dd, *J* = 8.7, 7.3 Hz, NCH_2), 2.35 (3H, s, ArCH_3). **^{13}C NMR** (126 MHz, $CDCl_3$) δ 155.36 (N*C*(O)O), 139.02 (Ar*C*), 138.28 (Ar*C*), 128.88 (Ar*C*), 124.93

(Ar*C*), 119.04 (Ar*C*), 115.43 (Ar*C*), 61.37 (O*C*H_2), 45.34 (N*C*H_2), 21.67 (Ar*C*H_3). Data is in line with literature precedent[1]

Synthesis of **1ak**

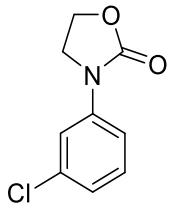

General Procedure **B** was followed using the following compounds: 2-oxazolidinone (0.17 g, 2 mmol), copper iodide (0.019 g, 0.1 mmol), (±)-trans-1,2-diaminocyclohexane (0.024 mL, 0.023 g, 0.2 mmol), potassium carbonate (0.55 g, 4 mmol), 1-bromo-3-chorobenzene (0.23 mL, 0.38 g, 2 mmol) and dioxane (1 mL). Column chromatography gave an off-white powdery solid, **1ak**, 98%, (0.39 g). **^{1}H NMR** (500 MHz, $CDCl_3$) δ 7.54 (1H, t, *J* = 2.1 Hz, Ar*H*), 7.28 (1H, ddd, *J* = 8.3, 2.2, 0.9 Hz, Ar*H*), 7.20 (1H, t, *J* = 8.1 Hz, Ar*H*), 7.01 (1H, ddd, *J* = 8.0, 1.9, 0.9 Hz, Ar*H*), 4.40–4.35 (2H, m, OC*H*$_2$), 3.91 (2H, dd, *J* = 8.8, 7.2 Hz, NC*H*$_2$). **^{13}C NMR** (126 MHz, $CDCl_3$) δ 154.92 (N*C*(O)O), 139.38 (Ar*C*), 134.51 (Ar*C*), 129.95 (Ar*C*), 123.69 (Ar*C*), 117.95 (Ar*C*), 115.84 (Ar*C*), 61.37 (O*C*H_2), 44.86 (N*C*H_2). Data is in line with literature precedent[5]

Synthesis of **1al**

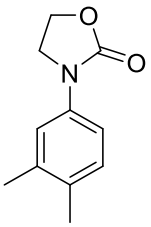

General Procedure **B** was followed using the following compounds: 2-oxazolidinone (0.17 g, 2 mmol), copper iodide (0.019 g, 0.1 mmol), (±)-trans-1,2-diaminocyclohexane (0.024 mL, 0.023 g, 0.2 mmol), potassium carbonate (0.55 g, 4 mmol), 4-bromo-1,2-dimethylbenzene (0.27 mL, 0.37 g, 2 mmol) and dioxane (1 mL) Recrystallization from EtOH/Water gave a white crystalline solid, **1al**, 39%, (0.147 g) **^{1}H NMR** (500 MHz, $CDCl_3$) δ 7.28 (1H, d, *J* = 2.4 Hz, Ar*H*), 7.19 (1H, dd, *J* = 8.2, 2.5 Hz, Ar*H*), 7.07 (1H, d, *J* = 8.3 Hz, Ar*H*), 4.37–4.32 (2H, m, OC*H*$_2$), 3.93–3.88 (2H, m, NC*H*$_2$), 2.23 (3H, s, ArC*H*$_3$), 2.20 (3H,

s, ArC*H*$_3$). **^{13}C NMR** (126 MHz, $CDCl_3$) δ 155.31 (N*C*(O)O), 137.15 (Ar*C*), 135.98 (Ar*C*), 132.22 (Ar*C*), 129.83 (Ar*C*), 119.56 (Ar*C*), 115.71 (Ar*C*), 61.26 (O*C*H$_2$), 45.23 (N*C*H$_2$), 19.90 (Ar*C*H$_3$), 18.94 (Ar*C*H$_3$). Data is in line with literature precedent[6]

Synthesis of **1am**

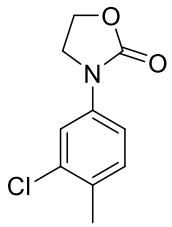

General Procedure **B** was followed using the following compounds: 2-oxazolidinone (0.17 g, 2 mmol), copper iodide (0.019 g, 0.1 mmol), (±)-trans-1,2-diaminocyclohexane (0.024 mL, 0.023 g, 0.2 mmol), potassium carbonate (0.55 g, 4 mmol), 4-bromo-2-chlorotoluene (0.27 mL, 0.41 g, 2 mmol) and dioxane (1 mL) Column chromatography gave an off-white powdery solid, **1am**, 72%, (0.32 g). **mp** (from $CHCl_3$) = 86-88 °C. **FT-IR** (thin film): ν_{max} (cm^{-1}) = 1742.3. **^{1}H NMR** (500 MHz, $CDCl_3$) δ 7.53 (1H, d, *J* = 2.4 Hz, Ar*H*), 7.35 (1H, dd, *J* = 8.4, 2.4 Hz, Ar*H*), 7.20 (1H, d, *J* = 8.3 Hz, Ar*H*), 4.50–4.44 (2H, m, OC*H*$_2$), 4.03–3.97 (2H, m, N*C*H$_2$), 2.33 (3H, s, ArC*H*$_3$). **^{13}C NMR** (126 MHz, $CDCl_3$) δ 155.21 (N*C*(O)O), 137.28 (Ar*C*), 134.85 (Ar*C*), 131.77 (Ar*C*), 131.27 (Ar*C*), 118.85 (Ar*C*), 116.59 (Ar*C*), 61.47 (O*C*H$_2$), 45.30 (N*C*H$_2$), 19.52 (Ar*C*H$_3$). **HRMS** (ESI): m/z calculated for $C_{10}H_{10}N_1O_2Cl_1$ requires 234.0400 for $[M+Na]^+$, found 234.0300.

Synthesis of **1an**

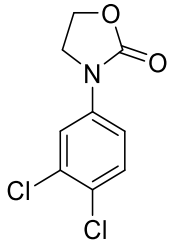

General Procedure **B** was followed using the following compounds: 2-oxazolidinone (0.17 g, 2 mmol), copper iodide (0.019 g, 0.1 mmol), (±)-trans-1,2-diaminocyclohexane (0.024 mL, 0.023 g, 0.2 mmol), potassium carbonate (0.55 g, 4 mmol), 4-bromo-1,2-dichlorobenzenee (0.26 mL, 0.45 g, 2 mmol) and dioxane (1 mL) Recrystallization from

EtOH/Water gave an amorphous solid, **1an**, 32%, (0.15 g). **FTIR** (thin film): ν_{max} (cm^{-1}) = 1738.7. **^{1}H NMR** (500 MHz, $CDCl_3$) δ 7.63 (1H, d, *J* = 2.4 Hz, Ar*H*), 7.35–7.27 (2H, m, Ar*H*), 4.44 (2H, dd, *J* = 8.7, 7.3 Hz, OC*H*$_2$), 3.99–3.94 (2H, m, NC*H*$_2$). **^{13}C NMR** (126 MHz, $CDCl_3$) δ 154.95 (N*C*(O)O), 137.78 (Ar*C*), 132.80 (Ar*C*), 130.50 (Ar*C*), 127.21 (Ar*C*), 119.62 (Ar*C*), 117.21 (Ar*C*), 61.45 (O*C*H$_2$), 44.96 (N*C*H$_2$). **HRMS** (ESI): m/z calculated for $C_9H_7N_1O_2Cl_2$ requires 253.9900 for $[M+Na]^+$, found 253.9720

Synthesis of **1ao**

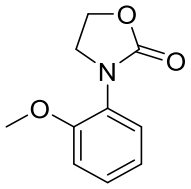

General Procedure **B** was followed using the following compounds: 2-oxazolidinone (0.17 g, 2 mmol), copper iodide (0.019 g, 0.1 mmol), (±)-trans-1,2-diaminocyclohexane (0.024 mL, 0.023 g, 0.2 mmol), potassium carbonate (0.55 g, 4 mmol), 2-bromoanisole (0.25 mL, 0.37 g, 2 mmol) and dioxane (1 mL) Column chromatography gave a white powdery solid, **1ao**, 95%, (0.37 g). **^{1}H NMR** (500 MHz, $CDCl_3$) δ 7.32 (1H, dd, *J* = 7.7, 1.7 Hz, Ar*H*), 7.28–7.22 (1H, m, Ar*H*), 6.98–6.91 (2H, m, Ar*H*), 4.44–4.40 (2H, m, OC*H*$_2$), 3.96–3.90 (2H, m, NC*H*$_2$), 3.82 (3H, s, ArOC*H*$_3$). **^{13}C NMR** (126 MHz, $CDCl_3$) δ 157.40 (Ar*C*), 154.90 (N*C*(O)O), 128.81 (Ar*C*), 128.32 (Ar*C*), 126.04 (Ar*C*), 120.85 (Ar*C*), 112.00 (Ar*C*), 62.46 (O*C*H$_2$), 55.60 (ArO*C*H$_3$), 46.94 (N*C*H$_2$). Data is in line with literature precedent[2]

Synthesis of **1ap**

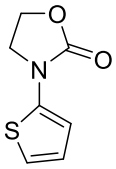

General Procedure **A** was followed using the following compounds: ethyl 2-hydroxy-ethylcarbamate (0.27 g, 2 mmol), copper iodide (0.038 g, 0.2 mmol), 2,2,6,6-tetramethyl-3,5-heptanedione (0.083 mL, 0.074 g, 0.4 mmol), caesium carbonate (1.30 g, 4 mmol), 2-iodothiophene (0.44 mL, 0.84 g, 4 mmol) and CH_3CN (4 mL). Column chromatography gave a yellow solid, **1ap**, 73% (0.25 g). **^{1}H NMR** (500 MHz, $CDCl_3$) δ 6.88 (1H, dd, *J* = 5.5, 1.4 Hz, Ar*H*), 6.83 (1H, dd, *J* = 5.5, 3.7 Hz, Ar*H*), 6.44 (1H, dd, *J* = 3.8, 1.4 Hz, Ar*H*), 4.51–4.46

(2H, m, OC*H*$_2$), 4.05–3.95 (2H, m, NC*H*$_2$). **^{13}C NMR** (126 MHz, $CDCl_3$j) δ 154.67 (N*C*(O)O), 140.30 (Ar*C*), 124.69 (Ar*C*), 117.98 (Ar*C*), 110.91 (Ar*C*), 62.34 (O*C*H$_2$), 46.01 (N*C*H$_2$). Data is in line with literature precedent[1]

Synthesis of **1aq**

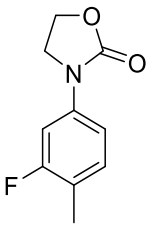

General Procedure **B** was followed using the following compounds: 2-oxazolidinone (0.17 g, 2 mmol), copper iodide (0.019 g, 0.1 mmol), (±)-trans-1,2-diaminocyclohexane (0.024 mL, 0.023 g, 0.2 mmol), potassium carbonate (0.55 g, 4 mmol), 4-bromo-2-fluorotoluene (0.25 mL, 0.38 g, 2 mmol) and dioxane (1 mL) Column chromatography gave a white crystalline solid, **1aq**, 58%, (0.21 g). **mp** (from $CHCl_3$) = 116-117 °C. **FT-IR** (thin film): ν_{max} (cm^{-1}) = 1730.6. **^{1}H NMR** (500 MHz, $CDCl_3$) δ 7.36 (1H, dd, *J* = 11.9, 2.1 Hz, Ar*H*), 7.19–7.09 (2H, m, Ar*H*), 4.50–4.45 (2H, m, OC*H*$_2$), 4.05–3.99 (2H, m, NC*H*$_2$), 2.24 (3H, d, *J* = 1.8 Hz, ArC*H*$_3$). **^{13}C NMR** (126 MHz, $CDCl_3$) δ 161.44 (d, *J* = 244.1 Hz, Ar*C*F), 155.21 (N*C*(O)O), 131.68 (d, *J* = 6.3 Hz, Ar*C*), 120.51 (d, *J* = 17.6 Hz, Ar*C*), 113.37 (d, *J* = 3.4 Hz, Ar*C*), 105.82 (d, *J* = 27.9 Hz, *Ar*C), 61.43 (O*C*H$_2$), 45.38 (N*C*H$_2$), 14.18 (d, *J* = 3.1 Hz Ar*C*H$_3$). **^{19}F NMR** (470 MHz, $CDCl_3$) δ -114.96– -115.07 (m, Ar*F*). **HRMS** (ESI): m/z calculated for $C_{10}H_{10}N_1O_2F_1$ requires 196.0774 for $[M+H]^+$, found 196.0784

Synthesis of **1ar**

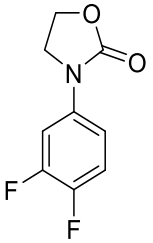

General Procedure **B** was followed using the following compounds: 2-oxazolidinone (0.17 g, 2 mmol), copper iodide (0.019 g, 0.1 mmol), (±)-trans-1,2-diaminocyclohexane (0.024 mL, 0.023 g, 0.2 mmol), potassium carbonate (0.55 g, 4 mmol), 4-bromo-1,2-

difluorobenzene (0.23 mL, 0.38 g, 2 mmol) and dioxane (1 mL) Recrystallization from EtOH/Water gave a white crystalline solid, **1ar**, 58%, (0.21 g). **FT-IR** (thin film): ν_{max} (cm^{-1}) = 1733.3. **^{1}H NMR** (500 MHz, $CDCl_3$) δ 7.61–7.54 (1H, m, Ar*H*), 7.16–7.06 (2H, m, Ar*H*), 4.50–4.44 (2H, m, OCH_2), 4.03–3.99 (2H, m, NCH_2). **^{13}C NMR** (126 MHz, $CDCl_3$) δ 155.17 (N*C*(O)O), 150.29 (dd, *J* = 247.3, 13.3 Hz, Ar*C*F), 146.93 (dd, *J* = 245.6, 12.8 Hz, Ar*C*F), 135.02 (dd, *J* = 8.6, 2.9 Hz, Ar*C*), 117.41 (dd, *J* = 18.2, 1.4 Hz, Ar*C*), 113.67 (dd, *J* = 5.9, 3.7 Hz, Ar*C*), 108.15 (d, *J* = 22.3 Hz, Ar*C*), 61.39 (O*C*H_2), 45.32 (N*C*H_2). **^{19}F NMR** (470 MHz, $CDCl_3$) δ -135.22 (ddd, *J* = 20.3, 12.4, 7.4 Hz, Ar*F*), -143.28 (dddd, *J* = 10.8, 9.6, 7.2, 4.3 Hz, Ar*F*). **HRMS** (ESI): m/z calculated for $C_9H_7N_1O_2F_2$ requires 200.0523 for $[M+H]^+$, found 200.0532

Synthesis of **1ba**

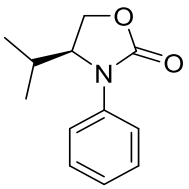

General Procedure **A** was followed using the following compounds: (S)-ethyl (1-hydroxy-3-methylbutan-2-yl)carbamate (0.35 g, 2 mmol), copper iodide (0.038 g, 0.2 mmol), 2,2,6,6-tetramethyl-3,5-heptanedione (0.083 mL, 0.074 g, 0.4 mmol), caesium carbonate (1.30 g, 4 mmol), iodobenzene (0.45 mL, 0.82 g, 4 mmol) and CH_3CN (4 mL). Column chromatography (EtOAc:Hexanes 30:70) gave an off-white solid, **1ba**, 19% (0.077 g). **^{1}H NMR** (500 MHz, $CDCl_3$) δ 7.44 (2H, ddd, *J* = 4.1, 3.2, 1.6 Hz, Ar*H*), 7.40–7.35 (2H, m, Ar*H*), 7.17 (1H, ddd, *J* = 7.6, 2.4, 1.2 Hz, Ar*H*), 4.48–4.36 (2H, m, OCH_2), 4.25–4.19 (1H, m, NC*H*), 2.17–2.05 (1H, m, C*H*(CH_3)$_2$), 0.89 (3H, app d, *J* = 7.1 Hz, CH(CH_3)$_2$), 0.83 (3H, app d, J = 6.8 Hz, CH(CH_3)$_2$). **^{13}C NMR** (126 MHz, $CDCl_3$) δ 156.15 (N*C*(O)O), 136.89 (Ar*C*), 129.27 (Ar*C*), 125.39 (Ar*C*), 122.38 (Ar*C*), 62.61 (O*C*H_2), 60.62 (NCH), 27.73 (*C*H(CH_3)$_2$), 17.80 (CH(*C*H_3)$_2$), 14.35 (CH(*C*H_3)$_2$). Data is in line with literature precedent[1]

Synthesis of **1bb**

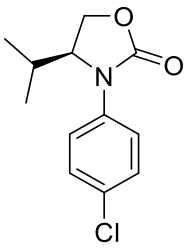

General Procedure **A** was followed using the following compounds: (S)-ethyl (1-hydroxy-3-methylbutan-2-yl)carbamate (0.35 g, 2 mmol), copper iodide (0.038 g, 0.2 mmol), 2,2,6,6-tetramethyl-3,5-heptanedione (0.083 mL, 0.074 g, 0.4 mmol), caesium carbonate (1.30 g, 4 mmol), 1-chloro-4-iodobenzene (0.96 g, 4 mmol) and CH_3CN (4 mL). Column chromatography (EtOAc:Hexanes 30:70) gave an off-white solid, **1bb**, 94% (0.44 g). **FT-IR** (thin film): vmax (cm^{-1}) = 2964.1, 1740.6. **^{1}H NMR** (500 MHz, $CDCl_3$) δ 7.45–7.38 (2H, m, Ar*H*), 7.37–7.33 (2H, m, Ar*H*), 4.46–4.36 (2H, m, O*C*H_2), 4.27–4.21 (1H, m, N*C*H), 2.11 (1H, dtd, *J* = 13.9, 6.9, 3.2 Hz, C*H*(CH_3)$_2$), 0.91 (3H, d, *J* = 7.1 Hz, CH(CH_3)$_2$), 0.83 (3H, d, *J* = 6.8 Hz, CH(CH_3)$_2$). **^{13}C NMR** (126 MHz, $CDCl_3$) δ 156.01 (N*C*(O)O), 135.64 (Ar*C*), 130.78 (Ar*C*), 129.51 (Ar*C*), 123.48 (Ar*C*), 62.73 (O*C*H_2), 60.66 (N*C*H), 27.81 (*C*H(CH_3)$_2$, 17.91 (CH(*C*H_3)$_2$), 14.45 (CH(*C*H_3)$_2$). **HRMS** (ESI): m/z calculated for $C_{12}H_{14}N_1O_2Cl_1$ for [M+H]+ requires 240.0791, found 240.0803.

Synthesis of **1bc**

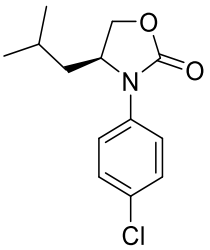

General Procedure **A** was followed using the following compounds: (S)-ethyl (1-hydroxy-4-methylpentan-2-yl)carbamate (0.38 g, 2 mmol), copper iodide (0.038 g, 0.2 mmol), 2,2,6,6-tetramethyl-3,5-heptanedione (0.083 mL, 0.074 g, 0.4 mmol), caesium carbonate (1.30 g, 4 mmol), 1-chloro-4-iodobenzene (0.96 g, 4 mmol) and CH_3CN (4 mL). Column chromatography (EtOAc:Hexanes 30:70) gave an off-white solid, **1bc**, 42% (0.23 g). **[α]$_D$**: (c 1, $CHCl_3$) = +45. **mp** (from $CHCl_3$) = 99-102 °C. **FT-IR** (thin film): vmax (cm^{-1}) = 2959.6,

1753.9. **^{1}H NMR** (500 MHz, $CDCl_3$) δ 7.35–7.28 (4H, m, Ar*H*), 4.51 (1H, t, *J* = 8.3 Hz, OCH_2), 4.37 (1H, dddd, *J* = 10.9, 8.2, 5.4, 2.6 Hz, OCH_2), 4.08 (1H, dd, *J* = 8.5, 5.4 Hz, NC*H*), 1.64–1.52 (2H, m, CH_2), 1.46–1.37 (1H, m, C*H*(CH_3)$_2$), 0.91 (3H, dd, *J* = 9.8, 3.9 Hz, CH(CH_3)$_2$), 0.87 (3H, d, *J* = 6.4 Hz, CH(CH_3)$_2$). **^{13}C NMR** (126 MHz, $CDCl_3$) δ 155.51 (N*C*(O)O), 135.48 (Ar*C*), 130.33 (Ar*C*), 129.22 (Ar*C*), 122.95 (Ar*C*), 67.64 (OCH_2), 54.96 (N*C*H), 41.02 (*C*H_2), 24.64 (*C*H(CH_3)$_2$), 23.51 (CH(*C*H_3)$_2$), 21.72 (CH(*C*H_3)$_2$). **HRMS** (ESI): m/z calculated for $C_{13}H_{16}N_1O_2Cl_1$ requires 254.0948 for $[M+H]^+$, found 254.0932

Synthesis of **1bd**

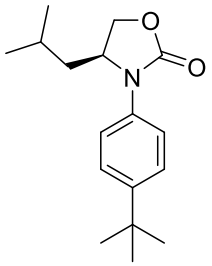

General Procedure **A** was followed using the following compounds: (S)-ethyl (1-hydroxy-4-methylpentan-2-yl)carbamate (0.38 g, 2 mmol), copper iodide (0.038 g, 0.2 mmol), 2,2,6,6-tetramethyl-3,5-heptanedione (0.083 mL, 0.074 g, 0.4 mmol), caesium carbonate (1.30 g, 4 mmol), 4-*tert*-butyliodobenzene (0.71 mL, 1.04 g, 4 mmol) and CH_3CN (4 mL). Column chromatography (EtOAc:Hexanes 30:70) gave an off-white solid, **1bd**, 15% (0.08 g). **$[\alpha]_D$:** (*c* 1, $CHCl_3$) = +23. **FT-IR** (thin film): ν_{max} (cm^{-1}) = 1749.2. **^{1}H NMR** (500 MHz, $CDCl_3$) δ 7.41–7.37 (2H, m, Ar*H*), 7.32–7.29 (2H, m, Ar*H*), 4.53 (1H, t, *J* = 8.3 Hz, OCH_2), 4.43–4.36 (1H, m, OCH_2), 4.12–4.07 (1H, m, OCH_2), 1.71–1.64 (1H, m, CH_2), 1.63–1.55 (1H, m, CH_2), 1.48–1.40 (1H, m, C*H*(CH_3)$_2$), 1.30 (9H, s, C(CH_3)$_3$), 0.93 (3h, d, *J* = 6.5 Hz, CH(CH_3)$_2$), 0.91 (2H, d, *J* = 6.6 Hz, CH(CH_3)$_2$). **^{13}C NMR** (126 MHz, $CDCl_3$) δ 156.06 (N*C*(O)O), 148.32 (Ar*C*), 134.15 (Ar*C*), 126.19 (Ar*C*), 121.83 (Ar*C*), 67.82 (OCH_2), 55.29 (N*C*H), 41.36 (CH_2), 34.56, 31.46 (AlkylC*H*), 26.48 (AlkylC*H*), 24.83 (AlkylC*H*), 23.72 (AlkylC*H*), 21.79 (AlkylC*H*). **HRMS** (ESI): m/z calculated for $C_{17}H_{25}N_1O_2$ requires 276.1964 for $[M+H]^+$, found 276.1947

Synthesis of **1ca**

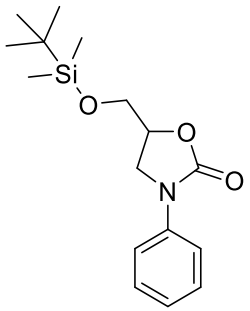

General Procedure **A** was followed using the following compounds: ethyl(2-hydroxy 3-(dimethyl-tert-butyl siloxy)propyl) carbamate (0.55 g, 2 mmol), copper iodide (0.038 g, 0.2 mmol), 2,2,6,6-tetramethyl-3,5-heptanedione (0.083 mL, 0.074 g, 0.4 mmol), caesium carbonate (1.30 g, 4 mmol), iodobenzene (0.45 mL, 0.82 g, 4 mmol) and CH_3CN (4 mL). Column chromatography (EtOAc:Hexanes 40:60) gave an off-white solid, **75**, 86% (0.53 g). **^{1}H NMR** (500 MHz, $CDCl_3$) δ 7.58–7.54 (2H, m, Ar*H*), 7.39–7.35 (2H, m, Ar*H*), 7.15–7.10 (1H, m, Ar*H*), 4.70–4.63 (1H, m, OC*H*), 4.04 (1H, t, *J* = 8.7 Hz, OCH_2), 3.99–3.93 (1H, m, OCH_2), 3.89 (1H, dd, *J* = 11.2, 4.5 Hz, NCH_2), 3.81 (1H, dd, *J* = 11.2, 3.5 Hz, NCH_2), 0.86 (9H, s, SiC(CH_3)$_3$), 0.09 (6H, s, SiCH_3). **^{13}C NMR** (126 MHz, $CDCl_3$) δ 154.74 (N*C*(O)O), 138.36 (Ar*C*), 128.99 (Ar*C*), 123.85 (Ar*C*), 118.17 (Ar*C*), 72.36 (O*C*H), 63.52 (O*C*H_2), 46.75 (N*C*H_2), 25.70 (SiC(*C*H_3)$_3$), 18.17 (Si*C*), -5.40 (Si*C*). Data is in line with literature precedent.[1]

6.1.4: Synthesis of Directing Group Analogues

Synthesis of *3*-phenyl-2-thiazolidinone

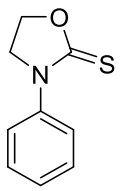

The procedure was adapted from a literature method.[7] To a solution of *N*-(2-Hydroxyethyl)aniline (1.25 mL, 1.37 g, 10 mmol), triethylamine (2.79 mL, 2.02 g, 20 mmol) and CH_2Cl_2 (30 mL) at 0 °C was slowly added thiophosgene (0.77 mL, 1.15 g, 10 mmol) in CH_2Cl_2 (10 mL) using a dropping funnel. After addition was complete the mixture was stirred at room temperature for 1 hour. The reaction mixture was concentrated *in vacuo*. The crude mixture was diluted in EtOAc and filtered using a silica plug, eluting with EtOAc. The solvent was again removed *in vacuo* and the crude mixture was purified using column chromatography (CH_2Cl_2:Hexanes 60:40) to yield off-white solid, 77% (1.38 g). **^{1}H NMR** (500 MHz, $CDCl_3$) δ 7.58–7.52 (2H, m, Ar*H*), 7.43–7.38 (2H, m, Ar*H*), 7.31–7.25 (1H, m, Ar*H*), 4.64–4.57 (2H, m, OCH_2), 4.23–4.16 (2H, m, NCH_2). **^{13}C NMR** (126 MHz, $CDCl_3$) δ 186.99 (N*C*(S)O), 138.54 (Ar*C*), 129.13 (Ar*C*), 127.46 (Ar*C*), 124.40 (Ar*C*), 66.33 (OCH_2), 51.63 (NCH_2). Data is line with literature precedent.[7]

Synthesis of 3-phenylthioxazolidin-2-one (**5b**)

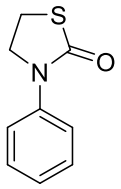

The procedure was adapted from a literature method.[7] To a solution of the compound above (0.72 g, 4 mmol) in toluene (16 mL) was added $[RuCl_2(p\text{-cymene})]_2$ (0.024 g, 0.04 mmol) and 2-dicyclohexylphosphino-2′,6′-dimethoxybiphenyl (SPhos, 0.033 g, 0.08 mmol). The reaction was heated to 120 °C for 4 h. After the reaction was deemed complete by TLC the solvent was removed *in vacuo* and the crude mixture was purified using column chromatography (EtOAc:Hexanes 50:50) to yield an off-white solid, **5b**, 66% (0.47 g). **^{1}H NMR** (500 MHz, $CDCl_3$) δ 7.41–7.35 (4H, m, Ar*H*), 7.21–7.17 (1H, m, Ar*H*), 4.13 (2H, t, *J* = 7.2 Hz, NCH_2), 3.39 (2H, t, *J* = 7.1 Hz, SCH_2). **^{13}C NMR** (126 MHz, $CDCl_3$) δ 171.26 (N*C*(O)S), 139.20 (Ar*C*), 129.18 (Ar*C*), 125.63 (Ar*C*), 122.05 (Ar*C*), 50.95 (NCH_2), 25.80 (SCH_2). Data is line with literature precedent.[7]

Synthesis of 3-phenylthiazolidin-4-one (**5c**)

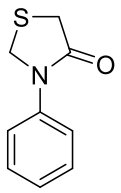

To a solution of aniline (1.83 mL, 1.86 g, 20 mmol) in anhydrous toluene (100 mL) was added paraformaldehyde (0.60 g, 20 mmol) and the mixture was allowed to stir for 5 minutes. Following this mercaptoacetic acid (1.39 mL, 1.84 g, 20 mmol) was added portionwise followed by *para*-toluenesulfonic acid (0.034 g, 1 mol%) and the mixture was heated to reflux overnight. The mixture was diluted in 100 mL EtOAc and washed with saturated $NaHCO_3$ solution (3 x 100 mL) and 1M HCl (3 x 100 mL). The organic layer was dried over $MgSO_4$ and concentrated *in vacuo*. The crude mixture was diluted in hot EtOH and the remaining precipitate was filtered and collected to give title compound, 28% (1.00 g). **^{1}H NMR** (500 MHz, $CDCl_3$) δ 7.46–7.38 (4H, m, Ar*H*), 7.29–7.24 (1H, m, Ar*H*), 4.83 (2H, t, *J* = 1.1 Hz, NC*H*$_2$S), 3.75 (2H, t, *J* = 1.0 Hz, SC*H*$_2$C=O). **^{13}C NMR** (126 MHz, $CDCl_3$) δ 170.58 (N*C*(O)CH$_2$), 138.74 (Ar*C*), 129.40 (Ar*C*), 126.74 (Ar*C*), 123.07 (Ar*C*), 49.65 (N*C*H$_2$S), 33.42 (S*C*H$_2$C=O). Data is in line with literature precedent.[8]

6.1.5: Synthesis of C–H Alkenylated Products

General Procedure **C** for Ruthenium-Catalysed C–H Alkenylation

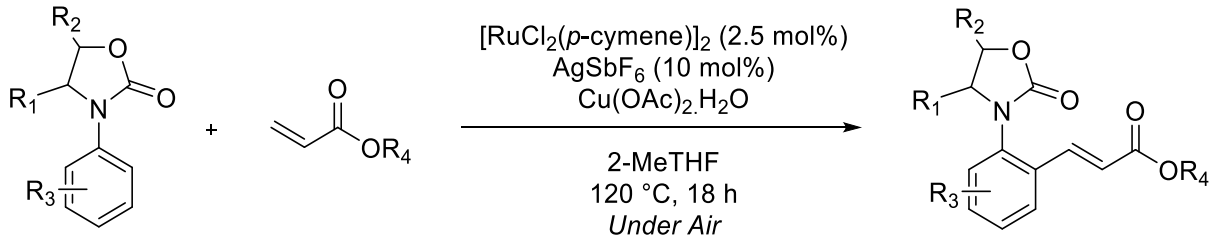

In an oven dried carousel tube, to a solution of aryloxazolidinone (1 eq), acrylate (3 eq) in 2-MeTHF (1 mL) was added the combined solids: $[RuCl_2(p\text{-cymene})]_2$ (2.5 mol%), $AgSbF_6$ (10 mol%) and $Cu(OAc)_2.H_2O$ (1 eq). The carousel tube was sealed with a Teflon cap leaving the tap open and was heated to 120 °C for 18 h. The reaction mixture was diluted in EtOAc and filtered using a silica plug, eluting with EtOAc. The solvent was removed *in vacuo* and the crude mixture was purified using column chromatography (EtOAc:Hexanes 50:50 to 60:40 unless otherwise stated) to give C–H alkenylated products.

Synthesis of **3a**

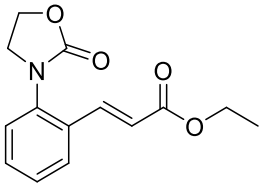

General Procedure **C** was followed using the following compounds: 3-phenyl-2-oxazolidinone, **1a**, (0.16 g, 1 mmol), ethyl acrylate (0.33 mL, 0.30 g, 3 mmol), $[RuCl_2(p\text{-cymene})]_2$ (0.016 g, 0.025 mmol), $AgSbF_6$ (0.035 g, 0.1 mmol), $Cu(OAc)_2.H_2O$ (0.20 g, 1 mmol). Column chromatography gave amorphous solid, **3a**, 76% (0.20 g). **FT-IR** (thin film): ν_{max} (cm^{-1}) = 1754.8, 1709.3. **mp** (from $CHCl_3$) = 68-71 °C. **^{1}H NMR** (500 MHz, $CDCl_3$) δ 7.77 (1H, d, *J* = 16.0 Hz, ArC*H*=CHR), 7.66 (1H, dd, *J* = 7.8, 1.5 Hz, Ar*H*), 7.44 (1H, td, *J* = 7.7, 1.5 Hz, Ar*H*), 7.38–7.32 (2H, m, Ar*H*), 6.44 (1H, d, *J* = 16.0 Hz, ArCH=C*H*R), 4.61–4.49 (2H, m, OCH_2), 4.25 (2H, q, *J* = 7.1 Hz, OCH_2CH$_3$), 3.96–3.91 (2H, m, NCH_2), 1.32 (3H, t, *J* = 7.1 Hz, OCH$_2$CH_3). **^{13}C NMR** (126 MHz, $CDCl_3$) δ 166.68 (*C*(O)O), 157.17 (N*C*(O)O), 139.35 (Ar*C*H=CHR), 137.12 (Ar*C*), 132.36 (Ar*C*), 131.26 (Ar*C*), 128.52 (Ar*C*), 127.77 (Ar*C*), 127.09 (Ar*C*), 120.96 (ArCH=*C*HR), 62.48 (O*C*H$_2$), 60.83 (O*C*H$_2$CH$_3$), 48.87 (NCH$_2$),

14.43 (OCH_2CH_3). **HRMS** (ESI): m/z calculated for $C_{14}H_{15}N_1O_4$ requires 284.0899 for $[M+Na]^+$, found 284.0867

Synthesis of **3b**

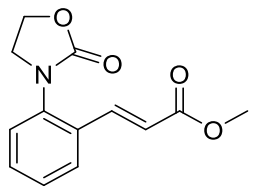

General Procedure **C** was followed using the following compounds: 3-phenyloxazolidinone, **1a**, (0.16 g, 1 mmol), methyl acrylate (0.27 mL, 0.26 g, 3 mmol), $[RuCl_2(p\text{-cymene})]_2$ (0.016 g, 0.025 mmol), $AgSbF_6$ (0.035 g, 0.1 mmol), $Cu(OAc)_2.H_2O$ (0.20 g, 1 mmol). Column chromatography gave amorphous solid, **3b**, 93% (0.23 g). **mp** (from $CHCl_3$) = 81-84 °C. **FT-IR** (thin film): ν_{max} (cm^{-1}) = 1746.1, 1708.7. **^{1}H NMR** (500 MHz, $CDCl_3$) δ 7.76 (1H, d, *J* = 16.0 Hz, ArC*H*=CHR), 7.65 (1H, dd, *J* = 7.8, 1.5 Hz, Ar*H*), 7.43 (1H, td, *J* = 7.7, 1.5 Hz, Ar*H*), 7.37–7.31 (2H, m, Ar*H*), 6.44 (1H, d, *J* = 16.0 Hz, ArCH=C*H*R), 4.57–4.51 (2H, m, OCH_2), 3.96–3.91 (2H, m, NCH_2), 3.79 (3H, s, OCH_3). **13C NMR** (126 MHz, CDCl3) δ 167.07 (*C*(O)O), 157.12 (N*C*(O)O), 139.59 (Ar*C*H=CHR), 137.12 (Ar*C*), 132.22 (Ar*C*), 131.29 (Ar*C*), 128.48 (Ar*C*), 127.73 (Ar*C*), 126.95 (Ar*C*), 120.43 (ArCH=*C*HR), 62.47 (O*C*H_2), 51.95 (OCH_3), 48.78 (NCH_2). **HRMS** (ESI): m/z calculated for $C_{13}H_{13}N_1O_4$ requires 270.0742 for $[M+Na]^+$, found 270.0762

Synthesis of **3c**

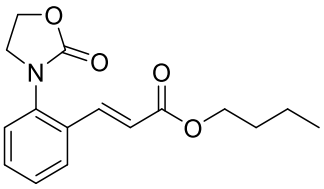

General Procedure **C** was followed using the following compounds: 3-phenyl-2-oxazolidinone, **1a**, (0.16 g, 1 mmol), butyl acrylate (0.43 mL, 0.38 g, 3 mmol), $[RuCl_2(p\text{-cymene})]_2$ (0.016 g, 0.025 mmol), $AgSbF_6$ (0.035 g, 0.1 mmol), $Cu(OAc)_2.H_2O$ (0.20 g, 1 mmol). Column chromatography gave amorphous solid (EtOAc:Hexanes 40:60 to 50:50), **3c**, 74% (0.21 g). **FT-IR** (thin film): ν_{max} (cm^{-1}) = 2959.7, 1749.1, 1706.2 **^{1}H NMR** (500 MHz, $CDCl_3$) δ 7.72 (1H, d, *J* = 16.0 Hz, ArC*H*=CHR), 7.62 (1H, dd, *J* = 7.8, 1.4 Hz, Ar*H*), 7.38

(1H, td, *J* = 7.6, 1.5 Hz, Ar*H*), 7.32–7.27 (2H, m, Ar*H*), 6.40 (1H, d, *J* = 16.0 Hz, ArCH=C*H*R), 4.50–4.43 (2H, m, OCH_2), 4.15 (2H, t, *J* = 6.7 Hz, OCH_2R), 3.88 (2H, dd, *J* = 8.5, 7.2 Hz, NCH_2), 1.63 (2H, dt, *J* = 14.5, 6.7 Hz, OCH_2CH_2R), 1.38 (2H, dq, *J* = 14.8, 7.4 Hz, $OCH_2CH_2CH_2$R), 0.91 (3H, t, *J* = 7.4 Hz, $OCH_2CH_2CH_2CH_3$). **13C NMR** (126 MHz, $CDCl_3$) δ 166.55 (*C*(O)O), 157.00 (N*C*(O)O), 139.18 (Ar*C*H=CHR), 136.98 (Ar*C*), 132.08 (Ar*C*), 131.04 (Ar*C*), 128.26 (Ar*C*), 127.48 (Ar*C*), 126.84 (Ar*C*), 120.61 (ArCH=*C*HR), 64.48 (OCH_2), 62.37 (OCH_2R), 48.60 (NCH_2), 30.63 (OCH_2CH_2R), 19.12 ($OCH_2CH_2CH_2$R), 13.67 ($OCH_2CH_2CH_2CH_3$). **HRMS** (ESI): m/z calculated for $C_{16}H_{19}N_1O_4$ requires 290.1392 for $[M+H]^+$, found 290.1369

Synthesis of **3d**

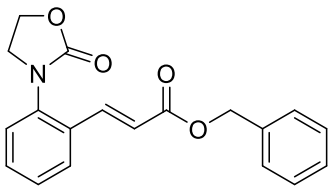

General Procedure **C** was followed using the following compounds: 3-phenyl-2-oxazolidinone, **1a**, (0.16 g, 1 mmol), benzyl acrylate (0.46 mL, 3 mmol), $[RuCl_2(p\text{-cymene})]_2$ (0.016 g, 0.025 mmol), $AgSbF_6$ (0.035 g, 0.1 mmol), $Cu(OAc)_2.H_2O$ (0.20 g, 1 mmol). Column chromatography (EtOAc:Hexanes 40:60 to 50:50) gave amorphous solid, **3d**, 94% (0.303 g). **FTIR** (thin film): ν_{max} (cm^{-1}) = 1749.3, 1709.9. **^{1}H NMR** (500 MHz, $CDCl_3$) δ 7.83 (1H, d, *J* = 16.0 Hz, ArC*H*=CHR), 7.65 (1H, app dd, Ar*H*), 7.47–7.31 (8H, m, Ar*H*), 6.50 (1H, d, *J* = 16.0 Hz, ArCH=C*H*R), 5.25 (2H, s, OCH_2Ph), 4.52–4.47 (2H, m, OCH_2), 3.94–3.88 (2H, m, NCH_2). **^{13}C NMR** (126 MHz, $CDCl_3$) δ 166.41 (*C*(O)O), 157.10 (N*C*(O)O), 139.95 (Ar*C*H=CHR), 137.18 (Ar*C*), 136.01 (Ar*C*), 132.09 (Ar*C*), 131.32 (Ar*C*), 128.67 (Ar*C*), 128.42 (Ar*C*), 128.36 (Ar*C*), 128.28 (Ar*C*), 127.66 (Ar*C*), 126.93 (Ar*C*), 120.32 (ArCH=*C*HR), 66.54 (OCH_2Ph), 62.44 (OCH_2), 48.75 (NCH_2). **HRMS** (ESI): m/z calculated for $C_{19}H_{17}N_1O_4$ requires 324.1236 for $[M+H]^+$, found 324.1220

Synthesis of **3aa**

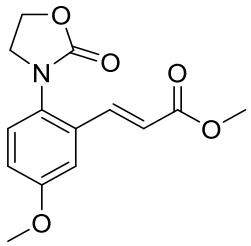

General Procedure **C** was followed using the following compounds: **1aa**, (0.19 g, 1 mmol), methyl acrylate (0.27 mL, 0.26 g, 3 mmol), $[RuCl_2(p\text{-cymene})]_2$ (0.016 g, 0.025 mmol), $AgSbF_6$ (0.035 g, 0.1 mmol), $Cu(OAc)_2.H_2O$ (0.20 g, 1 mmol). Column chromatography gave a white solid, **3aa**, 75% (0.21 g). **mp** (from $CHCl_3$) = 150-157 °C. **FT-IR** (thin film): ν_{max} (cm^{-1}) = 1743.9, 1702.7. **^{1}H NMR** (500 MHz, $CDCl_3$) δ 7.73 (1H, d, *J* = 16.0 Hz, ArC*H*=CHR), 7.25 (1H, d, *J* = 8.4 Hz, Ar*H*), 7.13 (1H, d, *J* = 2.9 Hz, Ar*H*), 6.98 (1H, dd, *J* = 8.8, 2.9 Hz, Ar*H*), 6.43 (1H, d, *J* = 16.0 Hz, ArCH=C*H*R), 4.54 (2H, dd, *J* = 8.5, 7.3 Hz, OCH_2), 3.89 (2H, dd, *J* = 8.5, 7.3 Hz, OCH_2), 3.83 (3H, s, OCH_3), 3.80 (3H, s, OCH_3). **^{13}C NMR** (126 MHz, $CDCl_3$) δ 167.04 (*C*(O)O), 159.40 (N*C*(O)O), 157.53 (Ar*C*H=CHR), 139.50 (Ar*C*), 133.59 (Ar*C*), 130.06 (Ar*C*), 128.70 (Ar*C*), 120.80 (Ar*C*), 117.37 (Ar*C*), 112.08 (ArCH=*C*HR), 62.41 (O*C*H_2), 55.80 (ArO*C*H_3), 52.05 (O*C*H_3), 49.17 (N*C*H_2). **HRMS** (ESI): m/z calculated for $C_{14}H_{15}N_1O_5$ requires 278.1028 for $[M+H]^+$, found 278.1006

Synthesis of **3ab**

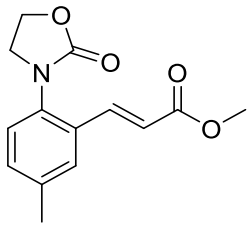

General Procedure **C** was followed using the following compounds: **1ab**, (0.16 g, 0.9 mmol), methyl acrylate (0.24 mL, 0.23 g, 2.7 mmol), $[RuCl_2(p\text{-cymene})]_2$ (0.014 g, 0.023 mmol), $AgSbF_6$ (0.032 g, 0.09 mmol), $Cu(OAc)_2.H_2O$ (0.18 g, 0.9 mmol). Column chromatography a gave white solid, **3ab**, 81% (0.19 g). **mp** (from $CHCl_3$) = 128-130 °C. **FT-IR** (thin film): ν_{max} (cm^{-1}) = 1746.9, 1711.7. **^{1}H NMR** (500 MHz, $CDCl_3$) δ 7.75 (1H, d, *J* = 16.1 Hz, ArC*H*=CHR), 7.50–7.45 (1H, m, Ar*H*), 7.30–7.19 (2H, m, Ar*H*), 6.44 (1H, d, *J* = 16.0 Hz, ArCH=C*H*R), 4.54 (2H, dd, *J* = 8.3, 7.5 Hz, OCH_2), 3.91 (2H, dd, *J* = 8.3, 7.5 Hz, NCH_2),

3.80 (3H, s, OC*H*$_3$), 2.37 (3H, s, ArC*H*$_3$). **^{13}C NMR** (126 MHz, $CDCl_3$) δ 167.20 (*C*(O)O), 157.35 (N*C*(O)O), 139.74 (Ar*C*H=CHR), 138.61 (Ar*C*), 134.68 (Ar*C*), 132.20 (Ar*C*), 132.06 (Ar*C*), 128.20 (Ar*C*), 127.02 (Ar*C*), 120.31 (ArCH=*C*HR), 62.45 (O*C*H$_2$), 51.99 (O*C*H$_3$), 48.98 (N*C*H$_2$), 21.28 (Ar*C*H$_3$). **HRMS** (ESI): m/z calculated for $C_{14}H_{15}N_1O_4$ requires 284.0899 for $[M+Na]^+$, found 284.0901

Synthesis of **3ac**

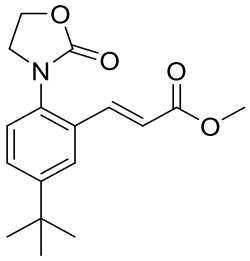

General Procedure **C** was followed using the following compounds: **1ac**, (0.22 g, 1 mmol), methyl acrylate (0.27 mL, 0.26 g, 3 mmol), $[RuCl_2(p\text{-cymene})]_2$ (0.016 g, 0.025 mmol), $AgSbF_6$ (0.035 g, 0.1 mmol), $Cu(OAc)_2.H_2O$ (0.20 g, 1 mmol). Column chromatography gave a white solid, **3ac**, 85% (0.26 g). **mp** (from $CHCl_3$) = 145-147 °C. **FT-IR** (thin film): ν_{max} (cm^{-1}) = 1750.0, 1713.3. **^{1}H NMR** (500 MHz, $CDCl_3$) δ 7.73 (1H, d, *J* = 16.1 Hz, ArC*H*=CHR), 7.60 (1H, d, *J* = 2.3 Hz, Ar*H*), 7.42 (1H, dd, *J* = 8.4, 2.3 Hz, Ar*H*), 7.21 (1H, d, *J* = 8.4 Hz, Ar*H*), 6.42 (1H, d, *J* = 16.0 Hz, ArCH=C*H*R), 4.48–4.44 (2H, m, OC*H*$_2$), 3.89 – 3.85 (2H, m, NC*H*$_2$), 3.73 (3H, s, OC*H*$_3$), 1.27 (9H, s, C(C*H*$_3$)$_3$). **^{13}C NMR** (126 MHz, $CDCl_3$) δ 166.91 (*C*(O)O), 157.13 (N*C*(O)O), 151.26 (Ar*C*H=CHR), 140.01 (Ar*C*), 134.41 (Ar*C*), 131.31 (Ar*C*), 128.51 (Ar*C*), 126.41 (Ar*C*), 124.25 (Ar*C*), 119.76 (ArCH=*C*HR), 62.34 (O*C*H$_2$), 51.66 (O*C*H$_3$), 48.56 (N*C*H$_2$), 34.64 (*C*(CH$_3$)$_3$), 31.07 (C(*C*H$_3$)$_3$). **HRMS** (ESI): m/z calculated for $C_{17}H_{21}N_1O_4$ requires 304.1549 for $[M+H]^+$, found 304.1518

Synthesis of **3ad**

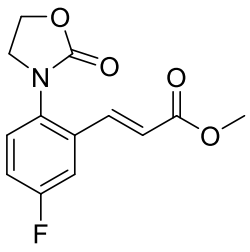

General Procedure **C** was followed using the following compounds: **1ad**, (0.18 g, 1 mmol), methyl acrylate (0.27 mL, 0.26 g, 3 mmol), $[RuCl_2(p\text{-cymene})]_2$ (0.016 g, 0.025 mmol), $AgSbF_6$ (0.035 g, 0.1 mmol), $Cu(OAc)_2.H_2O$ (0.20 g, 1 mmol). Column chromatography gave a white solid, **3ad**, 80% (0.21 g). **mp** (from $CHCl_3$) = 130-133 °C. **FT-IR** (thin film): v_{max} (cm^{-1}) = 1746.3, 1713.1. **^{1}H NMR** (500 MHz, $CDCl_3$) δ 7.70 (1H, dd, *J* = 16.0, 1.4 Hz, ArC*H*=CHR), 7.33 (2H, dt, *J* = 8.6, 4.4 Hz, Ar*H*), 7.14 (1H, ddd, J = 8.8, 7.6, 2.9 Hz, Ar*H*), 6.43 (1H, d, *J* = 16.0 Hz, ArCH=C*H*R), 4.59–4.52 (2H, m, OCH_2), 3.94–3.88 (2H, m, NCH_2), 3.80 (3H, s, OCH_3). **13C NMR** (126 MHz, $CDCl_3$) δ 166.78 (*C*(O)O), 162.04 (d, *J* = 248.9 Hz, Ar*C*F), 157.33 (N*C*(O)O), 138.47 (d, *J* = 2.2 Hz, Ar*C*H=CHR), 134.59 (d, *J* = 8.3 Hz, Ar*C*), 133.21 (d, *J* = 3.0 Hz, Ar*C*), 129.23 (d, *J* = 9.0 Hz, Ar*C*), 121.84 (ArCH=*C*HR), 118.39 (d, *J* = 23.0 Hz, Ar*C*), 114.17 (d, *J* = 23.6 Hz, Ar*C*), 62.53 (O*C*H_2), 52.16 (O*C*H_3), 48.98 (O*C*H_2). **^{19}F NMR** (470 MHz, $CDCl_3$) δ -112.14 (dd, *J* = 13.0, 8.1 Hz). **HRMS** (ESI): m/z calculated for $C_{13}H_{12}N_1O_4F_1$ requires 266.0829 for $[M+H]^+$, found 266.0800

Synthesis of **3ae**

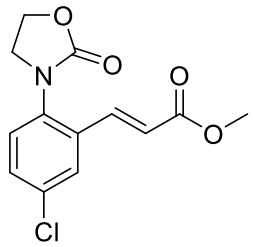

General Procedure **C** was followed using the following compounds: **1ae**, (0.20 g, 1 mmol), methyl acrylate (0.27 mL, 0.26 g, 3 mmol), $[RuCl_2(p\text{-cymene})]_2$ (0.016 g, 0.025 mmol), $AgSbF_6$ (0.035 g, 0.1 mmol), $Cu(OAc)_2.H_2O$ (0.20 g, 1 mmol). Column chromatography gave a white solid, **3ae**, 75% (0.21 g). **mp** (from $CHCl_3$) = 156-160 °C. FT-**IR** (thin film): v_{max} (cm^{-1}) = 1747.1, 1705.3. **^{1}H NMR** (500 MHz, $CDCl_3$) δ 7.68 (1H, d, *J* = 16.0 Hz, ArC*H*=CHR), 7.62 (1H, d, *J* = 2.4 Hz, Ar*H*), 7.40 (1H, dd, *J* = 8.5, 2.4 Hz, Ar*H*), 7.29 (1H, d, *J* = 8.6 Hz, Ar*H*), 6.44 (1H, d, *J* = 16.0 Hz, ArCH=C*H*R), 4.56 (2H, dd, *J* = 8.5, 7.2 Hz, OCH_2), 3.92 (2H, dd, *J* = 8.4, 7.2 Hz, NCH_2), 3.80 (3H, s, *J* = 2.7 Hz, OCH_3). **^{13}C NMR** (126 MHz, $CDCl_3$) δ 166.74 (*C*(O)O), 156.97 (N*C*(O)O), 138.37 (Ar*C*H=CHR), 135.62 (Ar*C*), 134.32 (Ar*C*), 133.92 (Ar*C*), 131.17 (Ar*C*), 128.31 (Ar*C*), 127.69 (Ar*C*), 121.73 (ArCH=*C*HR), 62.53 (O*C*H_2), 52.16 (O*C*H_3), 48.70 (N*C*H_2). **HRMS** (ESI): m/z calculated for $C_{13}H_{12}N_1O_4Cl_1$ requires 282.0533 for $[M+H]^+$, found 282.0515.

Synthesis of **3af**

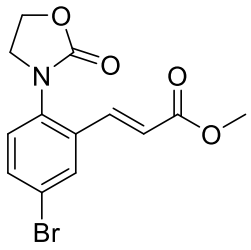

General Procedure **C** was followed using the following compounds: **1af**, (0.24 g, 1 mmol), methyl acrylate (0.27 mL, 0.26 g, 3 mmol), $[RuCl_2(p\text{-cymene})]_2$ (0.016 g, 0.025 mmol), $AgSbF_6$ (0.035 g, 0.1 mmol), $Cu(OAc)_2.H_2O$ (0.20 g, 1 mmol). Column chromatography gave a white solid, **3af**, 60% (0.20 g). **mp** (from $CHCl_3$) = 174-176 °C. **FT-IR** (thin film): ν_{max} (cm^{-1}) = 1747.7, 1713.0. **^{1}H NMR** (500 MHz, $CDCl_3$) δ 7.78 (1H, d, *J* = 2.3 Hz, ArC*H*=CHR), 7.68 (1H, d, *J* = 16.0 Hz, Ar*H*), 7.55 (1H, dd, *J* = 8.5, 2.3 Hz, Ar*H*), 7.23 (1H, d, *J* = 8.5 Hz, Ar*H*), 6.44 (1H, d, *J* = 16.0 Hz, ArCH=C*H*R), 4.59–4.52 (2H, m, OC*H*$_2$), 3.95–3.90 (2H, m, NC*H*$_2$), 3.81 (3H, s, OC*H*$_3$). **^{13}C NMR** (126 MHz, $CDCl_3$) δ 166.74 (*C*(O)O), 156.92 (N*C*(O)O), 138.32 (Ar*C*H=CHR), 136.15 (Ar*C*), 134.25 (Ar*C*), 134.12 (Ar*C*), 130.74 (Ar*C*), 128.52 (Ar*C*), 122.21 (Ar*C*), 121.79 (ArCH=*C*HR), 62.55 (O*C*H$_2$), 52.16 (O*C*H$_3$), 48.66 (N*C*H$_2$). **HRMS** (ESI): m/z calculated for $C_{13}H_{12}N_1O_4Br_1$ requires 326.0028 for $[M+H]^+$, found 326.0016

Synthesis of **3ag**

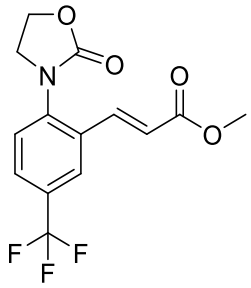

General Procedure **C** was followed using the following compounds: **1ag**, (0.23 g, 1 mmol), methyl acrylate (0.27 mL, 0.26 g, 3 mmol), $[RuCl_2(p\text{-cymene})]_2$ (0.016 g, 0.025 mmol), $AgSbF_6$ (0.035 g, 0.1 mmol), $Cu(OAc)_2.H_2O$ (0.20 g, 1 mmol). Column chromatography gave a white solid, **3ag**, 40% (0.13 g). **mp** (from $CHCl_3$) = 158-161 °C. **FT-IR** (thin film): ν_{max} (cm^{-1}) = 1751.3, 1706.1. **^{1}H NMR** (500 MHz, $CDCl_3$) δ 7.89 (1H, d, *J* = 1.5 Hz, ArC*H*=CHR), 7.75 (1H, d, *J* = 16.0 Hz, Ar*H*), 7.69 (1H, dd, *J* = 8.4, 1.8 Hz, Ar*H*), 7.49 (1H, d, *J* = 8.3 Hz,

Ar*H*), 6.52 (1H, d, *J* = 16.0 Hz, ArCH=C*H*R), 4.59 (2H, dd, *J* = 8.4, 7.2 Hz, OCH_2), 3.99 (2H, dd, *J* = 8.4, 7.2 Hz, NCH_2), 3.82 (3H, s, *J* = 3.5 Hz, OCH_3). **^{13}C NMR** (126 MHz, $CDCl_3$) δ 166.67 (*C*(O)O), 156.64 (N*C*(O)O), 140.34–139.70 (m, Ar*C*), 138.52 (Ar*C*), 132.80 (Ar*C*), 130.40 (Ar*C*), 127.69 (q, *J* = 3.1 Hz, Ar*C*), 127.04 (Ar*C*), 125.09 (q, *J* = 3.8 Hz, Ar*C*), 122.10 (s, *J* = 20.4 Hz, Ar*C*), 121.78 (app dd, Ar*C*F_3), 62.60 ($CO_2C$$H_3$), 52.19 (O*C*$H_2$), 48.40 (N*C*$H_2$). **^{19}F NMR** (470 MHz, $CDCl_3$) δ -62.89 (s, CF_3). **HRMS** (ESI): m/z calculated for $C_{14}H_{12}N_1O_4F_3$ requires 338.0616 for $[M+Na]^+$, found 338.0579

Synthesis of **3ah**

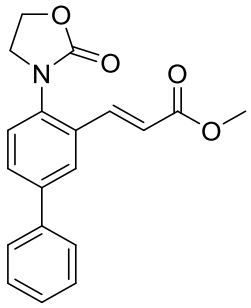

General Procedure **C** was followed using the following compounds: **1ah**, (0.12 g, 0.5 mmol), methyl acrylate (0.14 mL, 0.13 g, 1.5 mmol), $[RuCl_2(p\text{-cymene})]_2$ (0.008 g, 0.013 mmol), $AgSbF_6$ (0.018 g, 0.05 mmol), $Cu(OAc)_2.H_2O$ (0.10 g, 0.5 mmol). Column chromatography (EtOAc:Hexanes 40:60 to 50:50) gave a white solid, **3ah**, 31% (0.050 g). **mp** (from $CHCl_3$) = 167-169 °C**. FT-IR** (thin film): ν_{max} (cm^{-1}) = 1750.3, 1701.8. **^{1}H NMR** (500 MHz, $CDCl_3$) δ 7.83 (2H, dd, *J* = 9.0, 6.8 Hz, Ar*H*), 7.65 (1H, dd, *J* = 8.2, 2.1 Hz, Ar*H*), 7.57–7.54 (2H, m, ArC*H*=CHR + Ar*H*), 7.48–7.43 (2H, m, Ar*H*), 7.43–7.37 (2H, m, Ar*H*), 6.53 (1H, d, *J* = 16.0 Hz, ArCH=C*H*R), 4.61–4.55 (2H, m, OCH_2), 4.01–3.96 (2H, m, NCH_2), 3.81 (3H, s, OCH_3). **^{13}C NMR** (126 MHz, $CDCl_3$) δ 167.11 (*C*(O)O), 157.24 (N*C*(O)O), 141.68 (Ar*C*H=CHR), 139.80 (Ar*C*), 139.74 (Ar*C*), 136.23 (Ar*C*), 132.54 (Ar*C*), 130.06 (Ar*C*), 129.14 (Ar*C*), 128.17 (Ar*C*), 127.36 (Ar*C*), 127.29 (Ar*C*), 126.50 (Ar*C*), 120.79 (ArCH=*C*HR), 62.57 (O*C*H_2), 52.06 (O*C*H_3), 48.86 (N*C*H_2). **HRMS** (ESI): m/z calculated for $C_{19}H_{17}N_1O_4$ requires 324.1200 for $[M+H]^+$, found 324.1223

Synthesis of **3ai**

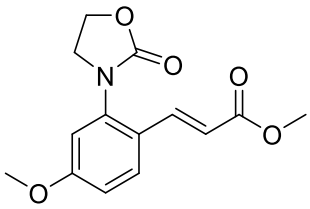

General Procedure **C** was followed using the following compounds: **1ai**, (0.19 g, 1 mmol), methyl acrylate (0.27 mL, 0.26 g, 3 mmol), $[RuCl_2(p\text{-cymene})]_2$ (0.016 g, 0.025 mmol), $AgSbF_6$ (0.035 g, 0.1 mmol), $Cu(OAc)_2.H_2O$ (0.20 g, 1 mmol). Column chromatography gave a white solid, **3ai**, 81% (0.22 g). **mp** (from $CHCl_3$) = 120-123 °C. **FT-IR** (thin film): ν_{max} (cm^{-1}) = 1751.6, 1704.3. **^{1}H NMR** (500 MHz, $CDCl_3$) δ 7.67 (1H, d, *J* = 16.0 Hz, ArC*H*=CHR), 7.57 (1H, d, *J* = 8.8 Hz, Ar*H*), 6.87 (1H, dd, *J* = 8.8, 1.6 Hz, Ar*H*), 6.82 (1H, d, *J* = 1.9 Hz, Ar*H*), 6.31 (1H, d, *J* = 15.9 Hz, ArCH=C*H*R), 4.51 (2H, t, *J* = 7.3 Hz, OC*H*$_2$), 3.91 (2H, t, *J* = 7.7 H, NC*H*$_2$), 3.78 (3H, s, OC*H*$_3$), 3.75 (3H, s, OC*H*$_3$). **^{13}C NMR** (126 MHz, $CDCl_3$) δ 167.35 (*C*(O)O), 161.95 (N*C*(O)O), 157.03 (Ar*C*H=CHR), 139.15 (Ar*C*), 138.48 (Ar*C*), 128.81 (Ar*C*), 124.44 (Ar*C*), 117.75 (Ar*C*), 114.76 (Ar*C*), 112.06 (ArCH=*C*HR), 62.51 (O*C*H$_2$), 55.71 (O*C*H$_3$), 51.73 (O*C*H$_3$), 48.82 (N*C*H$_2$). **HRMS** (ESI): m/z calculated for $C_{14}H_{15}N_1O_5$ requires 278.1.028 for $[M+H]^+$, found 278.1000

Synthesis of **3aj**

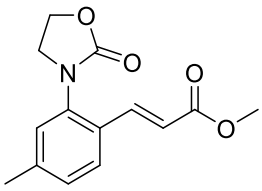

General Procedure **C** was followed using the following compounds: **1aj**, (0.18 g, 1 mmol), methyl acrylate (0.27 mL, 0.26 g, 3 mmol), $[RuCl_2(p\text{-cymene})]_2$ (0.016 g, 0.025 mmol), $AgSbF_6$ (0.035 g, 0.1 mmol), $Cu(OAc)_2.H_2O$ (0.20 g, 1 mmol). Column chromatography gave a light brown solid, **3aj**, 83% (0.22 g). **mp** (from $CHCl_3$) = 103-105 °C. **FT-IR** (thin film): ν_{max} (cm^{-1}) = 1746.0, 1709.3. **^{1}H NMR** (500 MHz, $CDCl_3$) δ 7.74 (1H, d, *J* = 16.0 Hz, ArC*H*=CHR), 7.55 (1H, d, *J* = 7.9 Hz, Ar*H*), 7.20–7.10 (2H, m, Ar*H*), 6.41 (1H, d, *J* = 16.0 Hz, ArCH=C*H*R), 4.54 (2H, dd, *J* = 8.5, 7.2 Hz, OC*H*$_2$), 3.92 (2H, dd, *J* = 8.5, 7.3 Hz, NC*H*$_2$), 3.78 (3H, s, OC*H*$_3$), 2.36 (3H, s, ArC*H*$_3$). **^{13}C NMR** (126 MHz, $CDCl_3$) δ 167.29 (*C*(O)O), 157.25 (N*C*(O)O), 142.15 (Ar*C*H=CHR), 139.50 (Ar*C*), 137.03 (Ar*C*), 129.51 (Ar*C*), 129.35

(Ar*C*), 127.65 (Ar*C*), 127.57 (Ar*C*), 119.42 (ArCH=*C*HR), 62.47 (O*C*H_2), 51.92 (O*C*H_3), 48.95 (N*C*H_2), 21.43 (Ar*C*H_3). **HRMS** (ESI): m/z calculated for $C_{14}H_{15}N_1O_4$ requires 262.1079 for $[M+H]^+$, found 262.1059

Synthesis of **3ak**

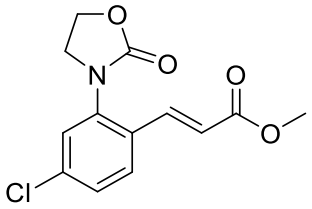

General Procedure **C** was followed using the following compounds: **1ak**, (0.25 g, 1 mmol), methyl acrylate (0.27 mL, 0.26 g, 3 mmol), $[RuCl_2(p\text{-cymene})]_2$ (0.016 g, 0.025 mmol), $AgSbF_6$ (0.035 g, 0.1 mmol), $Cu(OAc)_2.H_2O$ (0.20 g, 1 mmol). Column chromatography gave a light brown amorphous solid, **3ak**, 50% (0.14 g). **FTIR** (thin film): ν_{max} (cm^{-1}) = 1749.8, 1713.4. **^{1}H NMR** (500 MHz, $CDCl_3$) δ 7.67 (1H, d, J = 16.0 Hz, ArC*H*=CHR), 7.57 (1H, d, *J* = 8.5 Hz, Ar*H*), 7.34 (1H, d, *J* = 2.1 Hz, Ar*H*), 7.31 (1H, ddd, *J* = 8.5, 2.2, 0.5 Hz, Ar*H*), 6.41 (1H, d, *J* = 16.0 Hz, ArCH=C*H*R), 4.58–4.50 (2H, m, OC*H*$_2$), 3.96–3.91 (2H, m, NC*H*$_2$), 3.77 (3H, s, OC*H*$_3$). **^{13}C NMR** (126 MHz, $CDCl_3$) δ 166.87 (*C*(O)O), 156.77 (N*C*(O)O), 138.54 (Ar*C*H=CHR), 138.07 (Ar*C*), 136.57 (Ar*C*), 130.71 (Ar*C*), 128.77 (Ar*C*), 128.69 (Ar*C*), 126.99 (Ar*C*), 120.72 (ArCH=*C*HR), 62.59 (O*C*H_2), 52.01 (O*C*H_3), 48.51 (N*C*H_2). **HRMS** (ESI): m/z calculated for $C_{13}H_{12}N_1O_4Cl_1$ requires 304.0500 for $[M+Na]^+$, found 304.0342

Synthesis of **3al**

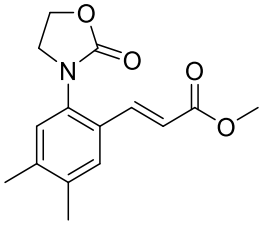

General Procedure **C** was followed using the following compounds: **1al**, (0.096 g, 0.5 mmol), methyl acrylate (0.14 mL, 0.13 g, 1.5 mmol), $[RuCl_2(p\text{-cymene})]_2$ (0.008 g, 0.013 mmol), $AgSbF_6$ (0.018 g, 0.05 mmol), $Cu(OAc)_2.H_2O$ (0.10 g, 0.5 mmol). Column chromatography gave a brown amorphous solid, **3al**, 58% (0.080 g). **FTIR** (thin film): ν_{max} (cm^{-1}) = 1745.7, 1709.3. **^{1}H NMR** (500 MHz, $CDCl_3$) δ 7.72 (1H, d, *J* = 16.0 Hz, ArC*H*=CHR),

7.42 (1H, s, Ar*H*), 7.10 (1H, s, Ar*H*), 6.40 (1H, d, *J* = 16.0 Hz, ArCH=C*H*R), 4.53 (2H, dd, *J* = 8.5, 7.3 Hz, OCH_2), 3.90 (2H, dd, *J* = 8.4, 7.3 Hz, NCH_2), 3.78 (3H, s, OCH_3), 2.27 (6H, s, ArCH_3). **^{13}C NMR** (126 MHz, $CDCl_3$) δ 167.36 (*C*(O)O), 157.44 (N*C*(O)O), 140.91 (Ar*C*), 139.59 (Ar*C*), 137.45 (Ar*C*), 134.84 (Ar*C*), 129.61 (Ar*C*), 128.56 (Ar*C*), 128.23 (Ar*C*), 119.26 (ArCH=*C*HR), 62.46 (O*C*H_2), 51.90 (O*C*H_3), 49.10 (N*C*H_2), 19.96 (Ar*C*H_3), 19.65 (Ar*C*H_3). **HRMS** (ESI): m/z calculated for $C_{15}H_{17}N_1O_4$ requires 276.1236 for $[M+H]^+$, found 276.1221

Synthesis of **3am**

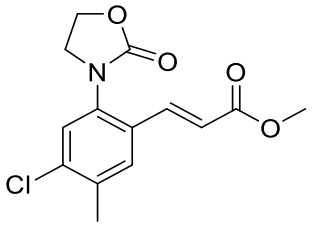

General Procedure **C** was followed using the following compounds: **1am**, (0.21 g, 1 mmol), methyl acrylate (0.27 mL, 0.26 g, 3 mmol), $[RuCl_2(p\text{-cymene})]_2$ (0.016 g, 0.025 mmol), $AgSbF_6$ (0.035 g, 0.1 mmol), $Cu(OAc)_2.H_2O$ (0.20 g, 1 mmol). Column chromatography gave an off-white powdery solid, **3am**, 60% (0.18 g). **mp** (from $CHCl_3$) = 154-155 °C. **FT-IR** (thin film): ν_{max} (cm^{-1}) = 1752.5, 1711.4. **^{1}H NMR** (500 MHz, $CDCl_3$) δ 7.62 (1H, d, *J* = 16.0 Hz, ArC*H*=CHR), 7.47 (1H, s, Ar*H*), 7.30 (1H, s, Ar*H*), 6.37 (1H, d, *J* = 16.0 Hz, ArCH=C*H*R), 4.52–4.46 (2H, m, OCH_2), 3.88 (2H, dd, *J* = 8.5, 7.2 Hz, NCH_2), 3.74 (3H, s, OCH_3), 2.33 (3H, s, ArCH_3). **^{13}C NMR** (126 MHz, $CDCl_3$) δ 166.80 (*C*(O)O), 156.87 (N*C*(O)O), 138.54 (Ar*C*H=CHR), 136.55 (Ar*C*), 136.49 (Ar*C*), 135.59 (Ar*C*), 130.52 (Ar*C*), 129.41 (Ar*C*), 127.26 (Ar*C*), 120.29 (ArCH=*C*HR), 62.48 (O*C*H_2), 51.83 (O*C*H_3), 48.49 (N*C*H_2), 19.75 (Ar*C*H_3). **HRMS** (ESI): m/z calculated for $C_{14}H_{14}N_1O_4Cl_1$ requires 318.0509 for $[M+Na]^+$, found 318.0498

Synthesis of **3an**

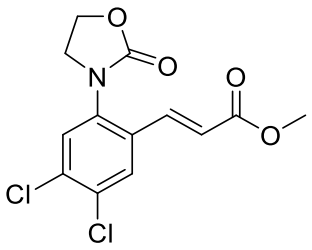

General Procedure **C** was followed using the following compounds: **1an**, (0.12 g, 0.5 mmol), methyl acrylate (0.14 mL, 0.13 g, 1.5 mmol), $[RuCl_2(p\text{-cymene})]_2$ (0.008 g, 0.013 mmol), $AgSbF_6$ (0.018 g, 0.05 mmol), $Cu(OAc)_2.H_2O$ (0.10 g, 0.5 mmol). Column chromatography gave off-white solid **3an**, 13% (0.021 g). **mp** (from $CHCl_3$) = 124-128 °C. **FT-IR** (thin film): ν_{max} (cm^{-1}) = 1749.6, 1714.1. **^{1}H NMR** (500 MHz, $CDCl_3$) δ 7.72 (1H, s, Ar*H*), 7.63 (1H, d, *J* = 16.1 Hz, ArC*H*=CHR), 7.47 (1H, s, Ar*H*), 6.43 (1H, d, *J* = 16.0 Hz, ArCH=C*H*R), 4.57 (2H, dd, *J* = 8.1, 7.5 Hz, OCH_2), 3.93 (2H, dd, *J* = 8.1, 7.5 Hz, NCH_2), 3.81 (3H, s, OCH_3). **^{13}C NMR** (126 MHz, $CDCl_3$) δ 166.64 (*C*(O)O), 156.71 (N*C*(O)O), 137.59 (Ar*C*H=CHR), 136.27 (Ar*C*), 134.86 (Ar*C*), 132.86 (Ar*C*), 132.27 (Ar*C*), 129.17 (Ar*C*), 128.81 (Ar*C*), 121.95 (ArCH=*C*HR), 62.65 (O*C*H_2), 52.24 (O*C*H_3), 48.57 (N*C*H_2). **HRMS** (ESI): m/z calculated for $C_{13}H_{11}N_1O_4Cl_2$ requires 316.0143 for $[M+H]^+$, found 316.0129

Synthesis of **3ao**

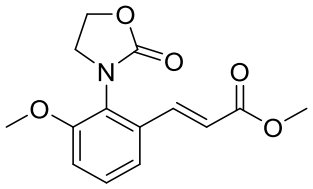

General Procedure **C** was followed using the following compounds: **1ao**, (0.19 g, 1 mmol), methyl acrylate (0.27 mL, 0.26 g, 3 mmol), $[RuCl_2(p\text{-cymene})]_2$ (0.016 g, 0.025 mmol), $AgSbF_6$ (0.035 g, 0.1 mmol), $Cu(OAc)_2.H_2O$ (0.20 g, 1 mmol). Column chromatography gave an off-white powdery solid, **3ao**, 23% (0.064 g). **mp** (from $CHCl_3$) = 104-108 °C. **FTIR** (thin film): ν_{max} (cm^{-1}) = 1747.2, 1712.6. **^{1}H NMR** (500 MHz, $CDCl_3$) δ 7.80 (1H, d, *J* = 16.0 Hz, ArC*H*=CHR), 7.34 (1H, t, *J* = 8.0 Hz, Ar*H*), 7.26–7.23 (1H, m, Ar*H*), 7.00 (1H, dd, *J* = 8.2, 1.0 Hz, Ar*H*), 6.45 (1H, d, *J* = 16.0 Hz, ArCH=C*H*R), 4.60–4.51 (2H, m, OCH_2), 4.06–3.96 (1H, m, NCH_2), 3.86 (3H, s, OCH_3), 3.79 (3H, s, OCH_3), 3.71–3.66 (1H, m, NCH_2). **^{13}C NMR** (126 MHz, $CDCl_3$) δ 167.12 (*C*(O)O), 156.50 (N*C*(O)O), 139.45 (Ar*C*H=CHR), 135.09 (Ar*C*), 129.85 (Ar*C*), 129.02 (Ar*C*), 128.56 (Ar*C*), 125.63 (Ar*C*), 121.21 (Ar*C*), 118.95 (ArCH=*C*HR), 113.52 (Ar*C*), 62.98 (O*C*H_2), 56.23 (O*C*H_3), 51.98 (O*C*H_3), 47.27 (N*C*H_2). **HRMS** (ESI): m/z calculated for $C_{14}H_{15}N_1O_5$ requires 278.1028 for $[M+H]^+$, found 278.1008

Synthesis of **3ap**

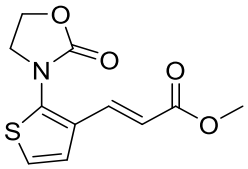

General Procedure **C** was followed using the following compounds: **1ap**, (0.17 g, 1 mmol), methyl acrylate (0.27 mL, 0.26 g, 3 mmol), $[RuCl_2(p\text{-cymene})]_2$ (0.016 g, 0.025 mmol), $AgSbF_6$ (0.035 g, 0.1 mmol), $Cu(OAc)_2.H_2O$ (0.20 g, 1 mmol). Column chromatography gave an off-white solid, **3ap**, 83% (0.21 g). **mp** (from $CHCl_3$) = 120-123 °C. **FT-IR** (thin film): ν_{max} (cm^{-1}) = 1746.9, 1707.6. **^{1}H NMR** (500 MHz, $CDCl_3$) δ 7.53 (1H, d, *J* = 15.9 Hz, ArC*H*=CHR), 7.17 (1H, dd, *J* = 5.8, 0.6 Hz, Ar*H*), 7.15–7.12 (1H, m, Ar*H*), 6.25 (1H, d, *J* = 15.9 Hz, ArCH=C*H*R), 4.57–4.52 (2H, m, OCH_2), 4.02–3.96 (2H, m, NCH_2), 3.77 (3H, s, OCH_3). **^{13}C NMR** (126 MHz, $CDCl_3$) δ 167.41 (*C*(O)O), 156.44 (N*C*(O)O), 140.25 (Ar*C*H=CHR), 134.63 (Ar*C*), 132.06 (Ar*C*), 124.18 (Ar*C*), 123.61 (Ar*C*), 119.07 (ArCH=*C*HR), 62.62 (O*C*H_2), 51.88 (O*C*H_3), 49.72 (N*C*H_2). **HRMS** (ESI): m/z calculated for $C_{11}H_{11}N_1O_4S_1$ requires 254.0487 for $[M+H]^+$, found 254.0464

Synthesis of **3aq$_1$** and **3aq$_2$**

General Procedure **C** was followed using the following compounds: **1aq**, (0.20 g, 1 mmol), methyl acrylate (0.27 mL, 0.26 g, 3 mmol), $[RuCl_2(p\text{-cymene})]_2$ (0.016 g, 0.025 mmol), $AgSbF_6$ (0.035 g, 0.1 mmol), $Cu(OAc)_2.H_2O$ (0.20 g, 1 mmol). Column chromatography (EtOAc:Hexanes 30:70 to 40:60) gave two separable regioisomers **3aq$_1$** and **3aq$_2$** (ratio of 36:64)**,** combined yield 91% (0.25 g)

3aq$_1$, 33% individual yield (0.90 g)

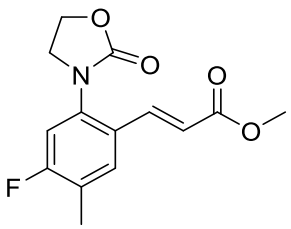

mp (from $CHCl_3$) = 128-130 °C. **FT-IR** (thin film): ν_{max} (cm^{-1}) = 1757.6, 1716.0. **^{1}H NMR** (500 MHz, $CDCl_3$) δ 7.67 (1H, d, *J* = 16.0 Hz, ArC*H*=CHR), 7.48 (1H, d, *J* = 8.1 Hz, Ar*H*), 7.01 (1H, d, *J* = 9.7 Hz, Ar*H*), 6.37 (1H, d, *J* = 16.0 Hz, ArCH=C*H*R), 4.54 (2H, t, *J* = 7.7 Hz,

OC*H*$_2$), 3.94–3.88 (2H, m, NC*H*$_2$), 3.78 (3H, s, OC*H*$_3$), 2.28 (3H, d, *J* = 1.5 Hz, ArC*H*$_3$). **^{13}C NMR** (126 MHz, $CDCl_3$) δ 167.02 (*C*(O)O), 162.28 (d, *J* = 252.0 Hz, Ar*C*F), 156.93 (N*C*(O)O), 138.75 (d, *J* = 1.2 Hz, Ar*C*), 136.17 (d, *J* = 9.7 Hz, Ar*C*), 130.39 (d, *J* = 6.5 Hz, Ar*C*), 128.05 (d, *J* = 3.8 Hz, Ar*C*), 125.79 (d, *J* = 17.7 Hz, Ar*C*), 119.70 (ArCH=*C*HR), 113.63 (d, *J* = 24.0 Hz, Ar*C*), 62.50 (O*C*H$_2$), 51.88 (O*C*H$_3$), 48.62 (N*C*H$_2$), 14.44 (d, *J* = 2.9 Hz, Ar*C*H$_3$). **^{19}F NMR** (470 MHz, $CDCl_3$) δ -111.38 – -111.44 (app t, Ar*F*). **HRMS** (ESI): m/z calculated for $C_{14}H_{14}N_1O_4F_1$ requires 302.0985 for $[M+Na]^+$, found 302.0817

3aq$_2$, 58% individual yield (0.16 g)

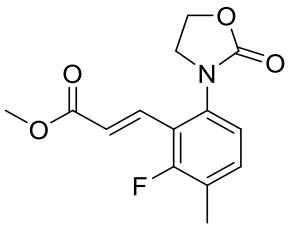

mp (from $CHCl_3$) = 125-127 °C. **FT-IR** (thin film): ν_{max} (cm^{-1}) = 1749.4, 1714.0. **^{1}H NMR** (500 MHz, $CDCl_3$) δ 7.56 (1H, d, *J* = 16.4 Hz, ArC*H*=CHR), 7.21 (1H, t, *J* = 8.2 Hz, Ar*H*), 7.04 (1H, d, *J* = 8.1 Hz, Ar*H*), 6.65 (1H, d, *J* = 16.8 Hz, ArCH=C*H*R), 4.51 (2H, dd, *J* = 8.5, 7.3 Hz, OC*H*$_2$), 3.89 (2H, dd, *J* = 8.4, 7.3 Hz, NC*H*$_2$), 3.77 (3H, s, OC*H*$_3$), 2.27 (3H, d, *J* = 2.2 Hz, ArC*H*$_3$). **^{13}C NMR** (126 MHz, $CDCl_3$) δ 167.41 (*C*(O)O), 160.15 (d, *J* = 253.9 Hz, Ar*C*F), 157.09 (N*C*(O)O), 136.22 (d, *J* = 5.3 Hz, Ar*C*), 134.10 (Ar*C*H=CHR), 132.80 (d, *J* = 7.2 Hz, Ar*C*), 125.79 (d, *J* = 18.5 Hz, Ar*C*), 124.35 (d, *J* = 13.8 Hz, Ar*C*), 122.40 (d, *J* = 3.7 Hz, ArCH=*C*HR), 120.51 (d, *J* = 13.4 Hz, Ar*C*), 62.52 (O*C*H$_2$), 51.94 (O*C*H$_3$), 48.68 (N*C*H$_2$), 14.60 (d, *J* = 4.7 Hz, Ar*C*H$_3$). **^{19}F NMR** (470 MHz, $CDCl_3$) δ -112.40 (app d, Ar*F*). **HRMS**: (ESI): m/z calculated for $C_{14}H_{14}N_1O_4F_1$ requires 280.0985 for $[M+H]^+$, found 280.0964

Synthesis of **3ar$_1$** and **3ar$_2$**

General Procedure **C** was followed using the following compounds: **1ar**, (0.10 g, 0.5 mmol), methyl acrylate (0.14 mL, 0.13 g, 1.5 mmol), $[RuCl_2(p\text{-cymene})]_2$ (0.008 g, 0.013 mmol), $AgSbF_6$ (0.018 g, 0.05 mmol), $Cu(OAc)_2.H_2O$ (0.10 g, 0.5 mmol). Column chromatography (EtOAc:Hexanes 30:70 to 40:60) gave two separable regioisomers **3ar$_1$** and **3ar$_2$** (ratio of 39:61)**,** combined yield 46% (0.046 g)

3ar$_1$, 18% individual yield (0.018 g)

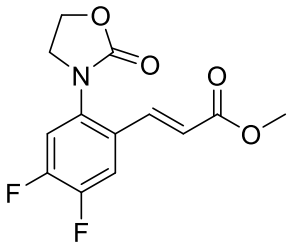

mp (from $CHCl_3$) = 123-125 °C. **FTIR** (thin film): ν_{max} (cm^{-1}) = 1749.8, 1712.2. **^{1}H NMR** (500 MHz, $CDCl_3$) δ 7.65 (1H, dd, *J* = 16.0, 1.2 Hz, ArC*H*=CHR), 7.45 (1H, dd, J = 10.8, 8.4 Hz, Ar*H*), 7.21 (1H, dd, *J* = 10.3, 7.2 Hz, Ar*H*), 6.37 (1H, d, *J* = 16.0 Hz, ArCH=C*H*R), 4.60–4.54 (2H, m, OCH_2), 3.92 (2H, dd, *J* = 8.4, 7.2 Hz, NC_{H2}), 3.80 (3H, s, OCH_3). **^{13}C NMR** (126 MHz, $CDCl_3$) δ 166.69 (*C*(O)O), 156.91 (N*C*(O)O), 151.79 (dd, *J* = 170.5, 13.5 Hz, Ar*C*), 149.77 (dd, *J* = 166.0, 13.4 Hz, Ar*C*), 137.67 (Ar*C*), 121.50 (ArCH=*C*HR), 116.53 (d, *J* = 18.5 Hz, Ar*C*), 115.98 (d, *J* = 19.0 Hz, Ar*C*), 62.60 (O*C*H_2), 52.21 (O*C*H_3), 48.79 (N*C*H_2). **^{19}F NMR** (470 MHz, cdcl3) δ -131.22 (ddd, *J* = 21.7, 10.1, 8.8 Hz, Ar*F*), -135.71–-136.03 (m, Ar*F*). **HRMS** (ESI): m/z calculated for $C_{13}H_{11}N_1O_4F_2$ requires 284.0734 for $[M+H]^+$, found 284.0712

3ar$_1$, 28% individual yield (0.028 g)

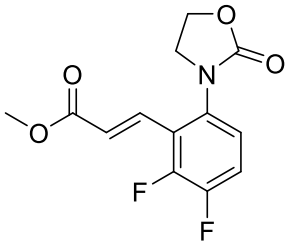

mp (from $CHCl_3$) = 128-130 °C. **FTIR** (thin film): ν_{max} (cm^{-1}) = 1748.8, 1717.1. **^{1}H NMR** (500 MHz, $CDCl_3$) δ 7.52 (1H, d, *J* = 16.4 Hz, ArC*H*=CHR), 7.25–7.20 (1H, m, Ar*H*), 7.14 (1H, ddd, *J* = 8.9, 4.4, 1.9 Hz, Ar*H*), 6.70 (1H, dd, *J* = 16.4, 0.6 Hz, ArCH=C*H*R), 4.57–4.54 (2H, m, OCH_2), 3.93–3.89 (2H, m, NCH_2), 3.82 (3H, s, OCH_3). **^{13}C NMR** (126 MHz, $CDCl_3$) δ 167.02 (*C*(O)O), 157.02 (N*C*(O)O), 151.14 (dd, *J* = 48.3, 13.9 Hz, Ar*C*F), 149.12 (dd, *J* = 54.0, 13.8 Hz, Ar*C*F), 133.69 (Ar*C*H=CHR), 133.03 (ArCH=*C*HR), 125.99 (d, *J* = 12.9 Hz, Ar*C*), 123.26 (dd, *J* = 6.9, 4.0 Hz, Ar*C*), 118.49 (d, *J* = 18.5 Hz, Ar*C*), 62.60 (O*C*H_2), 52.24 (O*C*H_3), 48.76 (N*C*H_2). **^{19}F NMR** (470 MHz, $CDCl_3$) δ -133.86–-134.19 (m, Ar*F*), -135.90 (ddd, *J* = 20.4, 9.3, 4.4 Hz, Ar*F*). **HRMS** (ESI): M/z calculated for $C_{13}H_{11}N_1O_4F_2$ requires 284.0700 for $[M+H]^+$, found 284.0718

Synthesis of **3ba**

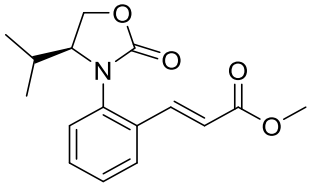

General Procedure **C** was followed using the following compounds: **1ba**, (0.077 g, 0.38 mmol), methyl acrylate (0.10 mL, 0.098 g, 1.14 mmol), $[RuCl_2(p\text{-cymene})]_2$ (0.006 g, 0.0095 mmol), $AgSbF_6$ (0.013 g, 0.014 mmol), $Cu(OAc)_2.H_2O$ (0.076 g, 0.38 mmol). Column chromatography (EtOAc:Hexanes 40:60 to 50:50) gave a an off-white solid, **3ba**, 74% (0.081 g). **$[\alpha]_D$:** (*c* 1, $CHCl_3$) = +25. **mp** (from $CHCl_3$) = 89-92 °C. **FT-IR** (thin film): ν_{max} (cm^{-1}) = 2962.7, 1749.5, 1712.9. **^{1}H NMR** (500 MHz, $CDCl_3$) δ 7.81 (1H, d, *J* = 16.0 Hz, ArC*H*=CHR), 7.65 (1H, d, *J* = 7.9 Hz, Ar*H*), 7.43 (1H, td, *J* = 7.6, 1.5 Hz, Ar*H*), 7.34 (2H, t, *J* = 7.6 Hz, Ar*H*), 6.43 (1H, d, *J* = 16.0 Hz, ArCH=C*H*R), 4.52 (1H, t, *J* = 8.8 Hz, OCH_2), 4.27 (1H, dd, *J* = 8.9, 5.8 Hz, OCH_2), 4.20–4.12 (1H, m, NC*H*), 3.79 (3H, s, OCH_3), 1.80 (1H, dtd, *J* = 13.8, 6.9, 3.9 Hz, C*H*(CH_3)$_2$), 0.89 (3H, d, *J* = 6.8 Hz, CH(CH_3)$_2$), 0.80 (3H, d, *J* = 7.0 Hz, CH(CH_3)$_2$). **^{13}C NMR** (126 MHz, $CDCl_3$) δ 167.05 (*C*(O)O), 157.06 (N*C*(O)O), 139.93 (Ar*C*H=CHR), 136.13 (Ar*C*), 132.46 (Ar*C*), 131.03 (Ar*C*), 128.33 (Ar*C*), 127.89 (Ar*C*), 120.41 (ArCH=*C*HR), 64.00 (O*C*H_2), 63.43 (O*C*H_3), 51.97 (N*C*H), 29.04 (*C*H(CH_3)$_2$), 18.22 (CH(*C*H_3)$_2$), 15.40 (CH(*C*H_3)$_2$). **HRMS** (ESI): m/z calculated for $C_{16}H_{19}N_1O_4$ requires 290.1392 for $[M+H]^+$, found 290.1366

Synthesis of **3bb**

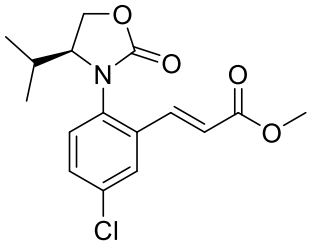

General Procedure **C** was followed using the following compounds: **1bb**, (0.24 g, 1 mmol), methyl acrylate (0.27 mL, 0.26 g, 3 mmol), $[RuCl_2(p\text{-cymene})]_2$ (0.016 g, 0.025 mmol), $AgSbF_6$ (0.035 g, 0.1 mmol), $Cu(OAc)_2.H_2O$ (0.20 g, 1 mmol). Column chromatography (EtOAc:Hexanes 40:60 to 50:50) gave a pale orange solid, **3bb**, 65% (0.21 g). **$[\alpha]_D$:** (*c* 1, $CHCl_3$) = +8. **mp** (from $CHCl_3$) = 108-114 °C. **FT-IR** (thin film): ν_{max} (cm^{-1}) = 2964.1, 1749.9, 1715.4. **^{1}H NMR** (500 MHz, $CDCl_3$) δ 7.71 (1H, d, *J* = 16.0 Hz, ArC*H*=CHR), 7.60 (1H, d, *J*

= 2.4 Hz, Ar*H*), 7.37 (1H, dd, *J* = 8.5, 2.4 Hz, Ar*H*), 7.26 (1H, d, *J* = 8.5 Hz, Ar*H*), 6.41 (1H, d, *J* = 16.0 Hz, ArCH=C*H*R), 4.50 (1H, t, *J* = 8.8 Hz, OCH_2), 4.24 (1H, dd, *J* = 9.0, 6.0 Hz, OCH_2), 4.17–4.10 (1H, m, NC*H*), 3.78 (3H, s, OCH_3), 1.82–1.73 (1H, m, C*H*(CH_3)$_2$), 0.86 (3H, d, *J* = 6.8 Hz, CH(CH_3)$_2$), 0.79 (3H, d, *J* = 7.0 Hz, CH(CH_3)$_2$). **^{13}C NMR** (126 MHz, $CDCl_3$) δ 166.58 (*C*(O)O), 156.81 (N*C*(O)O), 138.59 (Ar*C*H=CHR), 134.63 (Ar*C*), 134.03 (Ar*C*), 133.98 (Ar*C*), 130.81 (Ar*C*), 128.87 (Ar*C*), 127.68 (Ar*C*), 121.53 (ArCH=*C*HR), 64.06 (O*C*H_2), 63.23 (O*C*H_3), 52.03 (N*C*H), 29.03 (*C*H(CH_3)$_2$), 18.13 (CH(*C*H_3)$_2$), 15.39 (CH(*C*H_3)$_2$). **HRMS** (ESI): m/z calculated for $C_{16}H_{18}N_1O_4Cl_1$ requires 324.1003 for $[M+H]^+$, found 324.0973

Synthesis of **3bc**

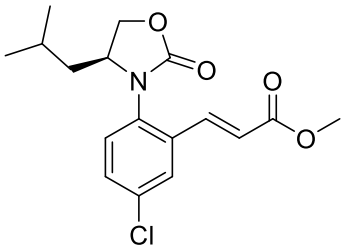

General Procedure **C** was followed using the following compounds: **1bc**, (0.16 g, 0.63 mmol), methyl acrylate (0.17 mL, 0.16 g, 1.89 mmol), $[RuCl_2(p\text{-cymene})]_2$ (0.0098 g, 0.0016 mmol), $AgSbF_6$ (0.022 g, 0.063 mmol), $Cu(OAc)_2.H_2O$ (0.13 g, 0.63 mmol). Column chromatography (EtOAc:Hexanes 40:60 to 50:50) gave a pale orange solid, **3bc**, 55% (0.12 g). **$[\alpha]_D$:** (*c* 1, $CHCl_3$) = +14. **mp** (from $CHCl_3$) = 147-149 °C. **FT-IR** (thin film): ν_{max} (cm^{-1}) = 2957.4, 1756.4, 1718.4. **^{1}H NMR** (500 MHz, $CDCl_3$) δ 7.69 (1H, d, *J* = 16.0 Hz, ArC*H*=CHR), 7.64 (1H, d, *J* = 2.4 Hz, Ar*H*), 7.41 (1H, dd, J = 8.5, 2.4 Hz, Ar*H*), 7.22 (1H, d, *J* = 8.5 Hz, Ar*H*), 6.43 (1H, d, *J* = 16.0 Hz, ArCH=C*H*R), 4.66 (1H, t, *J* = 8.1 Hz, OCH_2), 4.27–4.19 (1H, m, OCH_2), 4.18–4.13 (1H, m, NC*H*), 3.81 (3H, s, OCH_3), 1.50–1.43 (1H, m, C*H*(CH_3)$_2$), 1.43–1.36 (2H, m, CH_2), 0.84 (3H, d, *J* = 6.4 Hz, CH(CH_3)$_2$), 0.80 (3H, d, *J* = 6.4 Hz, CH(CH_3)$_2$). **^{13}C NMR** (126 MHz, $CDCl_3$) δ 166.71 (*C*(O)O), 156.66 (N*C*(O)O), 138.51 (Ar*C*H=CHR), 134.47 (Ar*C*), 131.10 (Ar*C*), 127.75 (Ar*C*), 121.77 (ArCH=*C*HR), 68.93 (O*C*H_2), 57.78 (O*C*H_3), 52.15 (N*C*H), 42.01 (*C*H_2), 24.79 (*C*H(CH_3)$_2$), 23.42 (CH(*C*H_3)$_2$), 21.99 (CH(*C*H_3)$_2$). **HRMS** (ESI): m/z calculated for $C_{17}H_{20}N_1O_4Cl_1$ requires 338.1159 for $[M+H]^+$, found 338.1134

Synthesis of **3bd**

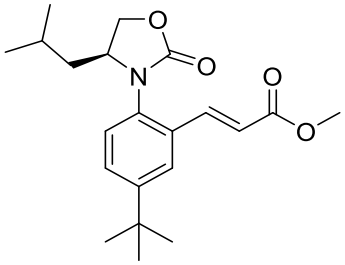

General Procedure **C** was followed using the following compounds: **1bd**, (0.056 g, 0.2 mmol), methyl acrylate (0.054 mL, 0.052 g, 0.6 mmol), $[RuCl_2(p\text{-cymene})]_2$ (0.0031 g, 0.005 mmol), $AgSbF_6$ (0.007 g, 0.02 mmol), $Cu(OAc)_2.H_2O$ (0.04 g, 0.2 mmol). Column chromatography (EtOAc:Hexanes 40:60 to 50:50) gave a brown amorphous solid, **3bd**, 43% (0.073 g). **$[\alpha]_D$:** (*c* 1, $CHCl_3$) = +19. **FT-IR** (thin film): ν_{max} (cm^{-1}) = 2957.8, 1757.9, 1718.9. **^{1}H NMR** (500 MHz, $CDCl_3$) δ 7.78 (1H, d, *J* = 16.0 Hz, ArC*H*=CHR), 7.66 (1H, d, *J* = 2.3 Hz, Ar*H*), 7.47 (1H, dd, *J* = 8.4, 2.3 Hz, Ar*H*), 7.17 (1H, d, *J* = 8.4 Hz, Ar*H*), 6.45 (1H, d, *J* = 16.0 Hz, ArCH=C*H*R), 4.65 (1H, t, *J* = 8.1 Hz, OC*H*$_2$), 4.23 (1H, dt, *J* = 14.7, 7.5 Hz, OC*H*$_2$), 4.15 (1H, dd, *J* = 8.4, 7.4 Hz, NC*H*), 3.81 (3H, s, OC*H*$_3$), 1.52–1.45 (1H, m, C*H*$(CH_3)_2$), 1.44–1.39 (2H, m, C*H*$_2$), 1.34 (9H, s, C$(CH_3)_3$), 0.85 (3H, d, *J* = 6.4 Hz, CH$(CH_3)_2$), 0.80 (3H, d, J = 6.3 Hz, CH$(CH_3)_2$). **^{13}C NMR** (126 MHz, $CDCl_3$) δ 167.23 (*C*(O)O), 157.05 (N*C*(O)O), 151.60 (Ar*C*H=CHR), 140.43 (Ar*C*), 133.21 (Ar*C*), 132.46 (Ar*C*), 128.67 (Ar*C*), 124.58 (Ar*C*), 120.03 (ArCH=*C*HR), 68.87 (O*C*H$_2$), 57.90 (O*C*H$_3$), 51.98 (N*C*H), 41.95 (*C*H$_2$), 34.96 (*C*$(CH_3)_3$), 31.37 (C$(CH_3)_3$), 24.82 (*C*H$(CH_3)_2$), 23.54 (CH$(CH_3)_2$), 21.95 (CH$(CH_3)_2$). **HRMS** (ESI): m/z calculated for $C_{21}H_{29}N_1O_4$ requires 360.2174 for $[M+H]^+$, found 360.2162

Synthesis of **3ca**

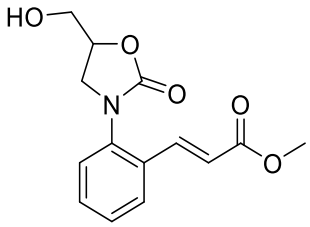

In an oven dried carousel tube, to a solution of **1ca** (0.15 g, 0.5 mmol), methyl acrylate (0.14 mL, 0.13 g, 1.5 mmol) in 2-MeTHF (1 mL) was added the combined solids: $[RuCl_2(p\text{-cymene})]_2$ (0.08 g, 0.013 mmol), $AgSbF_6$ (0.018 g, 0.05 mmol) and $Cu(OAc)_2.H_2O$ (0.10 g,

0.5 mmol). The carousel tube was sealed with a Teflon cap leaving the tap open and was heated to 120 °C for 18 h. The reaction mixture was allowed to return to room temperature and was added tetrabutylammonium fluoride – 1 M solution in THF (2 mL) and was left to stir for 2 hours at room temperature. The reaction mixture was diluted in EtOAc and filtered using a silica plug, eluting with EtOAc. The solvent was removed *in vacuo* and the crude mixture was purified using column chromatography (EtOAc:Hexanes 60:40 to 80:20) to yield an amorphous solid, **3ca**, 69% (0.095 g). **mp** (from $CHCl_3$) = 114-116 °C. **FT-IR** (thin film): ν_{max} (cm^{-1}) = 3440.3, 1710.8 **. ^{1}H NMR** (500 MHz, $CDCl_3$) δ 7.82 (1H, d, *J* = 16.0 Hz, ArC*H*=CHR), 7.69–7.61 (1H, m, Ar*H*), 7.45–7.38 (1H, m, Ar*H*), 7.37–7.32 (2H, m, Ar*H*), 6.44 (1H, d, *J* = 16.0 Hz, ArCH=C*H*R), 4.78 (1H, td, *J* = 5.9, 3.0 Hz, OC*H*), 4.02–3.93 (2H, m, CH_2OH), 3.92–3.87 (1H, m, NCH_2), 3.77 (3H, s, OCH_3), 3.70 (1H, dd, *J* = 12.6, 3.2 Hz, NCH_2), 3.24 (1H, s, CH_2O*H*). **^{13}C NMR** (126 MHz, CD_3OD) δ 167.50 (*C*(O)O), 157.03 (N*C*(O)O), 139.99 (Ar*C*H=CHR), 137.01 (Ar*C*), 132.42 (Ar*C*), 131.37 (Ar*C*), 128.66 (Ar*C*), 127.57 (Ar*C*), 127.54 (ArC), 120.24 (ArCH=*C*HR), 74.31 (O*C*H), 62.81 (*C*H_2OH), 52.07 (O*C*H_3), 49.84 (N*C*H_2). **HRMS** (ESI): m/z calculated for $C_{14}H_{15}N_1O_5$ requires 278.1028 for $[M+H]^+$, found 278.1000

Coupling partners shown below were not tolerated in the alkenylation reaction due to either low volatility or low reactivity.

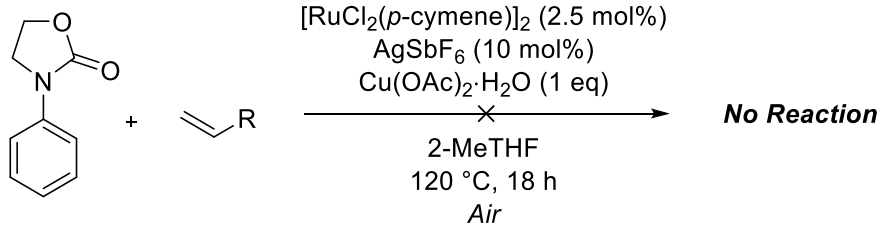

R = C(O)Me, CO_2H, $CO_2{}^t$Bu, C(O)Cl, $C(O)NMe_2$, CN, OAc, C_6H_6, 2-pyridine

Compounds below were not tolerated under the alkenylation conditions discussed in the report. The nitrile example could be either electron deficient deactivation of the ring or nitrile catalyst binding and poisoning, or a combination of both. Pyridines are well documented directing groups in ruthenium catalysis[9] therefore it is unsurprising that these motifs were not tolerated due to potential catalyst poisoning. Napthalene example was not tolerated due to most likely unfavourable steric interactions between $C–H_{oxazolidinone}$ and $C–H_{napthalene}$

preventing the oxazolidinone heterocycle to align with the aromatic C–H bond for chelation assisted insertion.

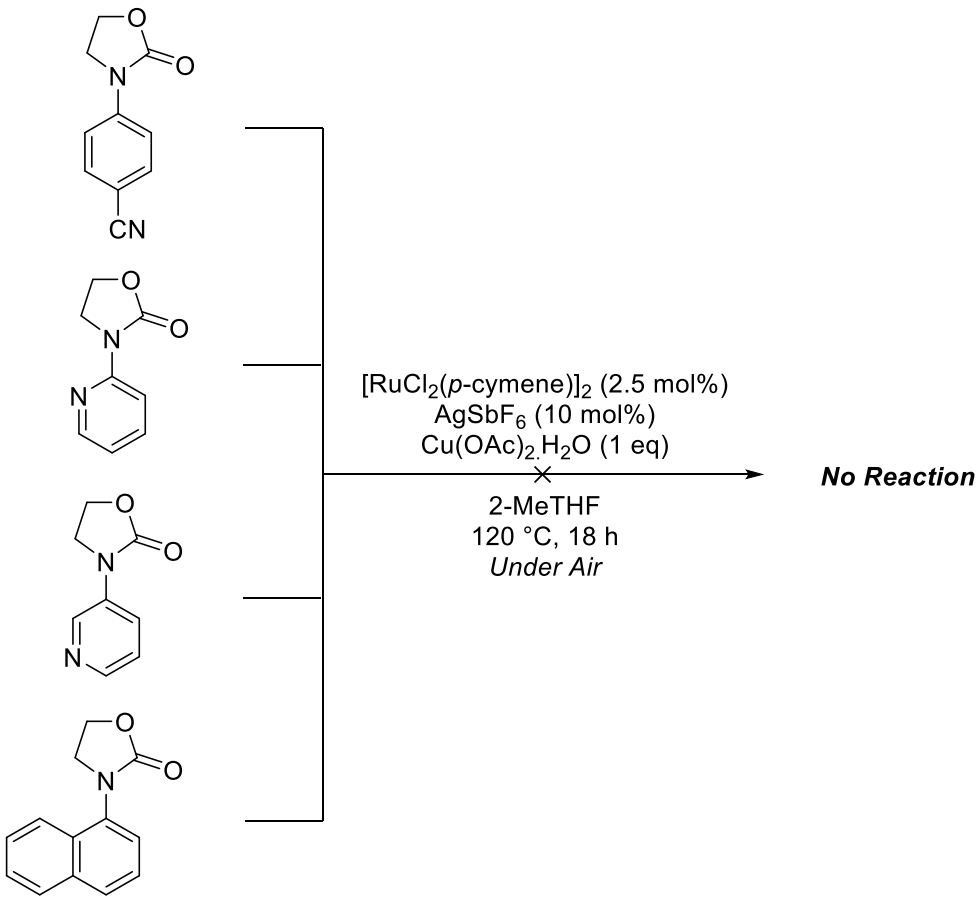

Synthesis of **6a**

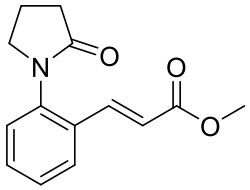

In an oven dried carousel tube, to a solution of 1-phenyl-2-pyrrolidinone (0.16 g, 1 mmol), methyl acrylate (0.27 mL, 0.26 g, 3 mmol) in 2-MeTHF (1 mL) was added the combined solids: $[RuCl_2(p\text{-cymene})]_2$ (0.016 g, 0.025 mmol), $AgSbF_6$ (0.035 g, 0.1 mmol) and $Cu(OAc)_2.H_2O$ (0.20 g, 1 mmol). The carousel tube was sealed with a Teflon cap leaving the tap open and was heated to 120 °C for 18 h. The reaction mixture was diluted in EtOAc and filtered using a silica plug, eluting with EtOAc. The solvent was removed *in vacuo* and the crude mixture was purified using column chromatography (EtOAc:Hexanes 50:50) to yield an amorphous solid, **6a**, 54% (0.13 g). **FT-IR** (thin film): ν_{max} (cm^{-1}) = 2951.1, 1691.2, 1633.4. **^{1}H NMR** (500 MHz, $CDCl_3$) δ 7.67–7.57 (2H, m, ArC*H*=CHR + Ar*H*), 7.40 (1H, t, *J* = 7.0 Hz, Ar*H*), 7.30 (1H, t, *J* = 7.6 Hz, Ar*H*), 7.21 (1H, d, *J* = 7.8 Hz, Ar*H*), 6.40 (1H, d, *J* = 16.0 Hz, ArCH=C*H*R), 3.75 (3H, s, *J* = 3.8 Hz, OC*H*$_3$), 3.71 (2H, t, *J* = 6.9 Hz, NC*H*$_2$), 2.58 (2H, t, *J* = 8.0 Hz, C*H*$_2$C=O), 2.22 (2H, m, $CH_2CH_2CH_2$). **^{13}C NMR** (126 MHz, $CDCl_3$) δ 175.27 (*C*(O)O), 167.13 (N*C*(O)C), 139.99 (Ar*C*H=CHR), 138.36 (Ar*C*), 131.83 (Ar*C*), 131.11 (Ar*C*), 128.15 (Ar*C*), 127.46 (Ar*C*), 127.36 (Ar*C*), 119.78 (ArCH=*C*HR), 51.79 (O*C*H$_3$), 51.60 (N*C*H$_2$), 31.27 (*C*H$_2$C=O), 19.05 ($CH_2CH_2CH_2$). **HRMS** (ESI): m/z calculated for $C_{14}H_{16}N_1O_3$ requires 246.1130 for $[M+H]^+$, found 246.1124

Synthesis of **6b**

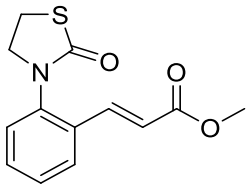

In an oven dried carousel tube, to a solution of 3-phenylthiazolidin-2-one, **5b**, (0.18 g, 1 mmol), methyl acrylate (0.27 mL, 0.26 g, 3 mmol) in 2-MeTHF (1 mL) was added the combined solids: $[RuCl_2(p\text{-cymene})]_2$ (0.016 g, 0.025 mmol), $AgSbF_6$ (0.035 g, 0.1 mmol) and $Cu(OAc)_2.H_2O$ (0.20 g, 1 mmol). The carousel tube was sealed with a Teflon cap leaving the tap open and was heated to 120 °C for 18 h. The reaction mixture was diluted in EtOAc and filtered using a silica plug, eluting with EtOAc. The solvent was removed *in vacuo* and the crude mixture was purified using column chromatography (EtOAc:Hexanes 40:60 to 50:50) to yield a white solid, **6b**, 68% (0.1 g). **mp** (from $CHCl_3$) = 108-109 °C. **FT-IR** (thin film): ν_{max} (cm^{-1}) = 1710.6, 1667.9, 1634.9**.** **^{1}H NMR** (500 MHz, $CDCl_3$) δ 7.74 (1H, d, *J* = 16.0 Hz, ArC*H*=CHR), 7.67 (1H, dd, *J* = 7.8, 1.5 Hz, Ar*H*), 7.45 (1H, td, *J* = 7.7, 1.5 Hz, Ar*H*), 7.37 (1H, td, *J* = 7.5, 0.8 Hz, Ar*H*), 7.29 (1H, d, *J* = 1.2 Hz, Ar*H*), 6.46 (1H, d, *J* = 16.0 Hz, ArCH=C*H*R), 3.95 (2H, t, *J* = 7.1 Hz, NCH_2), 3.81 (3H, s, OCH_3), 3.49 (2H, t, *J* = 7.1 Hz, SCH_2). **^{13}C NMR** (126 MHz, $CDCl_3$) δ 172.26 (*C*(O)O), 167.14 (N*C*(O)S), 139.62 (Ar*C*H=CHR), 138.43 (Ar*C*), 132.44 (Ar*C*), 131.37 (Ar*C*), 128.70 (Ar*C*), 127.79 (Ar*C*), 127.61 (Ar*C*), 120.57 (ArCH=*C*HR), 52.48 (O*C*H_3), 52.02 (N*C*H_2), 26.77 (S*C*H_2). **HRMS** (ESI): m/z calculated for $C_{13}H_{13}N_1O_3S_1$ requires 264.0694 for $[M+H]^+$, found 264.0671

Synthesis of **6c**

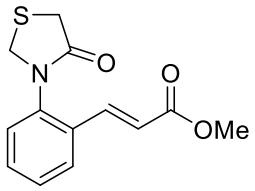

In an oven dried carousel tube, to a solution of 3-phenyl-1,3-thiazolidin-4-one (0.18 g, 1 mmol), methyl acrylate (0.27 mL, 0.26 g, 3 mmol) in 2-MeTHF (1 mL) was added the combined solids: $[RuCl_2(p\text{-cymene})]_2$ (0.016 g, 0.025 mmol), $AgSbF_6$ (0.035 g, 0.1 mmol) and $Cu(OAc)_2.H_2O$ (0.20 g, 1 mmol). The carousel tube was sealed with a Teflon cap leaving the tap open and was heated to 120 °C for 18 h. The reaction mixture was diluted in EtOAc and filtered using a silica plug, eluting with EtOAc. The solvent was removed *in vacuo* and the crude mixture was purified using column chromatography (EtOAc:Hexanes 50:50 to 60:40) to yield a cream powdery solid, **6c**, 24% (0.063 g). **mp** (from $CHCl_3$) = 122-123 °C. **FT-IR** (thin film) ν_{max} (cm^{-1}) = 1710.9, 1683.7. **^{1}H NMR** (500 MHz, $CDCl_3$) δ 7.69 (1H, dd, *J* = 7.8, 1.0 Hz, Ar*H*), 7.63 (1H, d, J = 16.0 Hz, ArC*H*=CHR), 7.46 (1H, td, *J* = 7.6, 1.4 Hz, Ar*H*), 7.40 (1H, t, *J* = 7.3 Hz, Ar*H*), 7.26 (1H, dd, *J* = 7.9, 1.0 Hz, Ar*H*), 6.46 (1H, d, *J* = 16.0 Hz, ArCH=C*H*R), 4.63 (2H, s, NCH_2S), 3.80 (3H, s, OCH_3), 3.76 (2H, s, SCH_2C=O).**^{13}C NMR** (126 MHz, $CDCl_3$) δ 171.51 (*C*(O)O), 166.94 (N*C*(O)C), 139.08 (Ar*C*H=CHR), 137.63 (Ar*C*), 132.46 (Ar*C*), 131.48 (Ar*C*), 129.27 (Ar*C*), 128.20 (Ar*C*), 127.95 (Ar*C*), 120.98 (ArCH=*C*HR), 51.99 (O*C*H_3), 50.49 (N*C*H_2S), 32.49 (S*C*H_2C=O). **HRMS** (ESI): m/z calculated for $C_{13}H_{13}N_1O_3S_1$ requires 264.0694 for $[M+H]^+$, found 264.0672

6.1.6: Further Derivations

Synthesis of **4a**

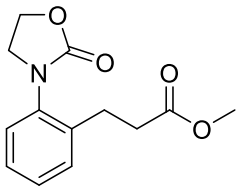

To an oven dried carousel tube was added **3b** (0.247 g, 1 mmol), palladium 10% on activated carbon (0.050 g) and MeOH (4 mL). Through the reaction mixture was bubbled hydrogen gas using a balloon. This was repeated twice before carousel tube was sealed and a balloon of hydrogen gas was placed through the septum. The reaction was left to stir overnight at room temperature. After TLC had deemed the reaction complete, the mixture was diluted in EtOAc and filtered through a plug of celite, eluting with EtOAc. The filtrate was concentrate *in vacuo* to give an amorphous solid, **4a**, quantitative yield (0.248 g). **FTIR** (thin film): ν_{max} (cm^{-1}) = 1739.4. **^{1}H NMR** (500 MHz, $CDCl_3$) δ 7.24–7.14 (4H, m, Ar*H*), 4.42 (2H, m, OCH_2), 3.87 (2H, m, NCH_2), 3.57 (3H, s, OCH_3), 2.88 (2H, m, ArCH_2), 2.60 (2H, m, CH_2CO_2Me). **^{13}C NMR** (126 MHz, $CDCl_3$) δ 173.08 (*C*(O)O), 157.14 (N*C*(O)O), 138.46 (Ar*C*), 135.89 (Ar*C*), 129.65 (Ar*C*), 128.39 (Ar*C*), 127.51 (Ar*C*), 126.83 (Ar*C*), 62.38 (OCH_2), 51.48 (OCH_3), 48.35 (NCH_2), 34.13 (ArCH_2), 25.97 (*C*H_2CO_2Me). **HRMS** (ESI): m/z calculated for $C_{13}H_{15}N_1O_4$ for $[M+H]^+$ requires 250.1079, found 250.1084

Synthesis of **4b**

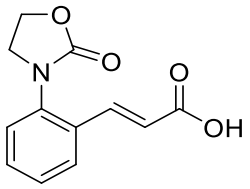

To a solution of **3b** (0.247 g, 1 mmol) in H_2O (2 mL) and MeOH (2 mL) was added KOH (1.1 mmol, 0.074 g) and the reaction mixture was stirred at 50°C overnight. The mixture was brought to pH 1 and then extracted with 3 x 10 mL CH_2Cl_2. The organic phase was then washed with 1 x 30 mL brine and was dried over $MgSO_4$. The resulting mixture was concentrated *in vacuo* to give a crude solid. This solid was triturated with 3 x 1 mL Et_2O to give a crystalline solid, **4b**, 81%. (0.19 g). **mp** (from $CHCl_3$) = 172-174 °C. **FT-IR** (thin film): ν_{max} (cm^{-1}) = 2988.7, 1715.0. **^{1}H NMR** (500 MHz, CD_3OD) δ 7.82 (1H, d, J = 7.9 Hz, Ar*H*), 7.78 (1H, d, *J* = 16.0 Hz, ArC*H*=CHR), 7.53–7.47 (1H, m, Ar*H*), 7.42 (2H, dd, *J* = 11.7, 4.1 Hz, Ar*H*), 6.53 (1H, d, *J* = 16.0 Hz, ArCH=C*H*R), 4.59 (2H, dd, *J* = 8.6, 7.3 Hz, OCH_2), 4.06–3.99 (2H, m, NCH_2). **^{13}C NMR** (126 MHz, CD_3OD) δ 168.58 (*C*O_2H), 158.18 (N*C*(O)O), 139.50 (Ar*C*H=CHR), 136.93 (Ar*C*), 132.14 (Ar*C*), 130.89 (Ar*C*), 128.24 (Ar*C*), 127.18 (Ar*C*), 126.65 (Ar*C*), 120.30 (ArCH=*C*HR), 62.94 (O*C*H_2), 48.41 (N*C*H_2). **HRMS** (ESI): m/z calculated for $C_{12}H_{11}N_1O_4$ requires 234.0766 for $[M+H]^+$, found 234.0753

Synthesis of **4c**

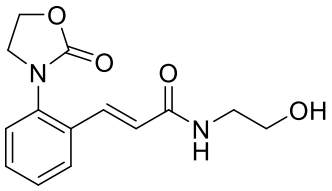

To a mixture of **3a** (0.247 g, 1 mmol) and Na_2CO_3 (0.106 g, 1 mmol) in MeOH (1 mL) was added ethanolamine (0.301 mL, 5 mmol) portionwise. The reaction mixture was heated to reflux overnight before being allowed to return to room temperature. The reaction mixture was diluted with 10 mL MeOH and the remaining solids were filtered. The filtrate was concentrated and then purified using silica gel chromatography (EtOAc:Hexanes 60:40 to 80:20) to give an amorphous white solid, **4c**, 62% (0.171 g). **FT-IR** (thin film): ν_{max} (cm^{-1}) = 3318.1, 1736.0, 1659.5. **^{1}H NMR** (500 MHz, $CDCl_3$) δ 7.54 (1H, d, *J* = 15.7 Hz, ArC*H*=CHR), 7.42 (1H, d, *J* = 7.5 Hz, Ar*H*), 7.31 (1H, t, *J* = 7.5 Hz, Ar*H*), 7.23 (1H, d, *J* = 7.9 Hz, Ar*H*), 7.14 (1H, t, *J* = 7.5 Hz, 1H), 6.42 (1H, d, *J* = 15.7 Hz, ArCH=C*H*R), 4.50 (2H, t, *J* = 7.7 Hz, OC*H*$_2$), 4.45 (1H, s, N*H*), 3.89 (2H, t, *J* = 7.7 Hz, NC*H*$_2$), 3.64 (2H, s, OC*H*$_2$), 3.39–3.34 (2H, m, NC*H*$_2$), 2.93 (1H, s, O*H*). ^{13}C NMR (126 MHz, cdcl$_3$) δ 166.90 (*C*(O)N), 158.00 (N*C*(O)O), 136.47 (Ar*C*H=CHR), 134.75 (Ar*C*), 132.84 (Ar*C*), 130.48 (Ar*C*), 128.59 (Ar*C*), 127.56 (Ar*C*), 126.77 (Ar*C*), 123.78 (ArCH=*C*HR), 62.94 (O*C*H$_2$), 61.24 (O*C*H$_2$), 48.61 (N*C*H$_2$), 42.76 (N*C*H$_2$). **HRMS** (ESI): m/z calculated $C_{14}H_{16}N_2O_4$ requires 275.1032 for $[M-H]^+$, found 275.1024.

6.1.7: Deuterium Labelling and Kinetics Data

Synthesis of **[D]$_5$-1a**

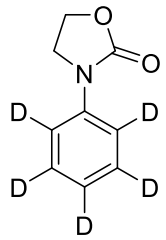

Deuterated Analogue of 3-phenyl-2-oxazolidinone was synthesised using General Procedure **B** using the following compounds: 2-oxazolidinone (0.17 g, 2 mmol), copper iodide (0.019 g, 0.1 mmol), (±)-trans-1,2-diaminocyclohexane (0.024 mL, 0.023 g, 0.2 mmol), potassium carbonate (0.55 g, 4 mmol), bromobenzene-d_5 (0.21 mL, 0.32 g, 2 mmol) and dioxane (1 mL) Column chromatography gave an off-white solid, **[D]$_5$-1a**, 70%, (0.24 g). **FT-IR** (thin film): ν_{max} (cm^{-1}) = 1734.4 cm^{-1}. **^{1}H NMR** (500 MHz, $CDCl_3$) δ 4.50–4.45 (2H, m, OC*H*$_2$), 4.08–4.03 (2H, m, NC*H*$_2$). **^{13}C NMR** (126 MHz, $CDCl_3$) δ 155.44 (N*C*(O)O), 138.33 (Ar*C*), 129.07–128.41 (Ar*C*D), 124.11–123.36 (Ar*C*D), 118.45–117.63 (Ar*C*D), 61.48 (O*C*H$_2$), 45.38 (N*C*H$_2$). **HRMS** (ESI): m/z calculated for $C_9H_4N_1O_2D_5$ requires 191.0845 for $[M+Na]^+$, found 191.0867.

Reaction of deuterated analogue under the reaction conditions (Scheme 12)

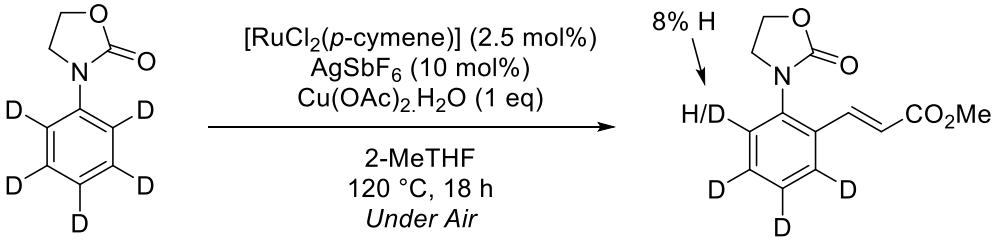

[D]$_5$-1a **2b** **[D]$_n$-3b** - 69%

General Procedure **C** was followed using the following compounds: **[D]$_5$-1a**, (0.168 g, 1 mmol), methyl acrylate (0.27 mL, 0.26 g, 3 mmol), $[RuCl_2(p\text{-cymene})]_2$ (0.016 g, 0.025 mmol), $AgSbF_6$ (0.035 g, 0.1 mmol), $Cu(OAc)_2.H_2O$ (0.20 g, 1 mmol). Column chromatography (EtOAc:Hexanes) gave an amorphous white solid, **[D]$_n$-3b**, 69% (0.17 g). **FT-IR** (thin film): ν_{max} (cm^{-1}) = 1745.2, 1710.4. **^{1}H NMR** (500 MHz, $CDCl_3$) δ 7.73 (1H, d, *J* = 16.0 Hz, ArC*H*=CHR), 7.29 (1H, s, *J* = 7.3 Hz, Ar*H*), 6.41 (1H, d, *J* = 16.0 Hz, ArCH=C*H*R),

4.52–4.46 (2H, m, OC*H*$_2$), 3.93–3.87 (2H, m, NC*H*$_2$), 3.75 (3H, s, CO_2C*H*$_3$). **^{13}C NMR** (126 MHz, $CDCl_3$) δ 167.01 (*C*(O)O), 157.10 (N*C*(O)O), 139.53 (Ar*C*H=CHR), 136.99 (Ar*C*), 132.00 (Ar*C*), 131.17–130.35 (m, Ar*C*), 128.27–126.01 (Ar*C*), 120.25 (ArCH=*C*HR), 62.45 (O*C*H$_2$), 51.84 (CO_2CH$_3$), 48.66 (N*C*H$_2$). **HRMS** (ESI): m/z calculated for $C_{13}H_9N_1O_4D_4$ requires 252.1174 for $[M+H]^+$, found 252.1147.

Kinetic Isotope Effect (KIE) Studies

Parallel Reactions (Scheme 13a)

Two parallel reactions were run using General Procedure **C** using the following compounds: **1a** (0.163 g, 1 mmol) or **[D]$_5$-1a**, (0.168 g, 1 mmol), methyl acrylate (0.27 mL, 0.26 g, 3 mmol), $[RuCl_2(p\text{-cymene})]_2$ (0.016 g, 0.025 mmol), $AgSbF_6$ (0.035 g, 0.1 mmol), $Cu(OAc)_2.H_2O$ (0.20 g, 1 mmol) and Naphthalene (0.128 g, 1 mmol). Column chromatography (EtOAc:Hexanes) gave an amorphous white solid, **[D]$_n$-3b**, 69% (0.17 g). Aliquots were taken periodically and analysed via HPLC to provide the following conversions. A representative HPLC trace is also given.

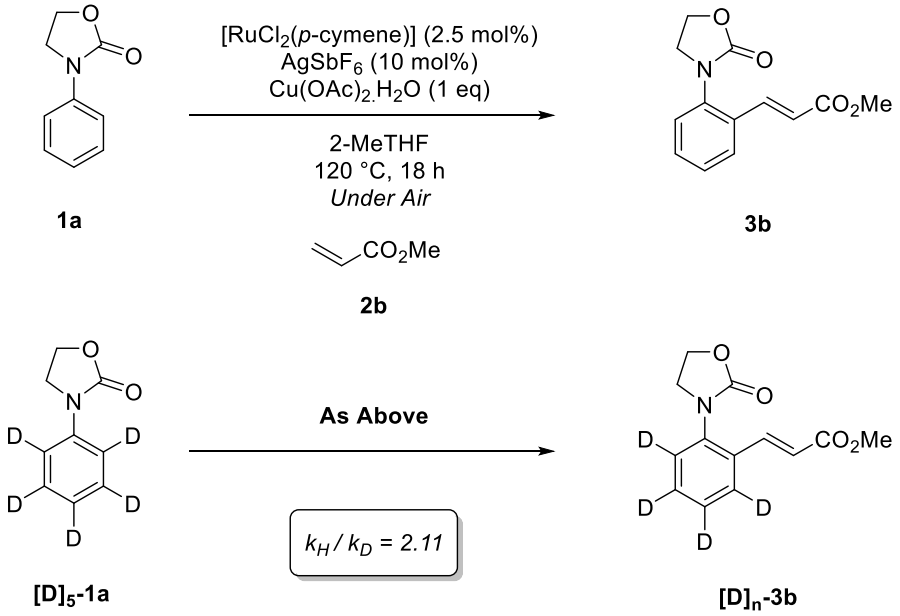

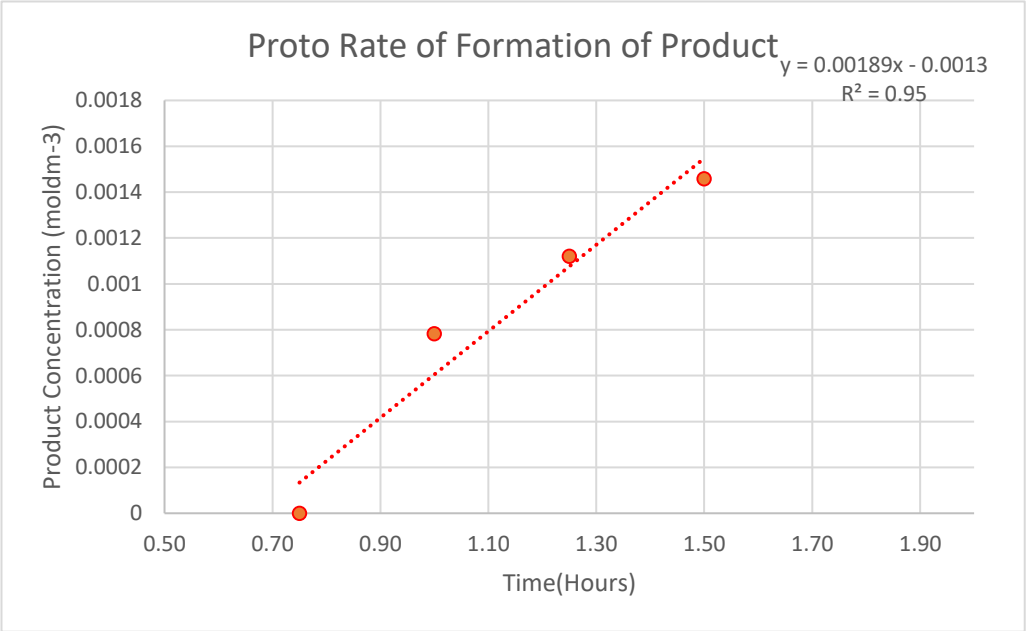
Proto Rate of Formation of Product
y = 0.00189x - 0.0013
R² = 0.95
Product Concentration (moldm-3)
0.0018
0.0016
0.0014
0.0012
0.001
0.0008
0.0006
0.0004
0.0002
0
0.50
0.70
0.90
1.10
1.30
1.50
1.70
1.90
Time(Hours)

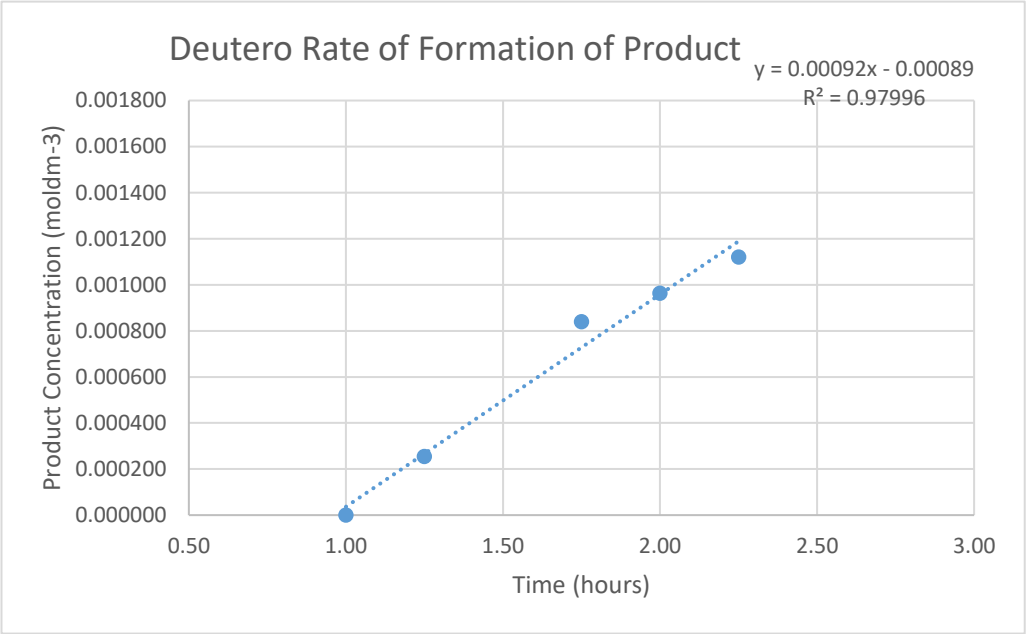
Deutero Rate of Formation of Product
y = 0.00092x - 0.00089
R² = 0.97996
Product Concentration (moldm-3)
0.001800
0.001600
0.001400
0.001200
0.001000
0.000800
0.000600
0.000400
0.000200
0.000000
0.50
1.00
1.50
2.00
2.50
3.00
Time (hours)

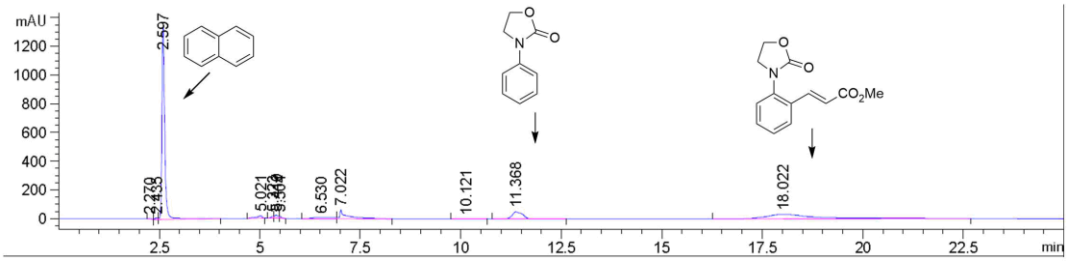
mAU
1200
1000
800
600
400
200
0
2.597
6.530
7.022
10.121
11.368
18.022
CO2Me
2.5
5
7.5
10
12.5
15
17.5
20
22.5
min

Intermolecular Competition (Scheme 13b)

Two parallel reactions were run (Run **1** & Run **2**) using General Procedure **C** using the following compounds: **1a** (0.81 g, 0.5 mmol) and **[D]$_5$-1a**, (0.84 g, 0.5 mmol), methyl acrylate (0.27 mL, 0.26 g, 3 mmol), [RuCl$_2$(*p*-cymene)]$_2$ (0.016 g, 0.025 mmol), AgSbF$_6$ (0.035 g, 0.1 mmol), Cu(OAc)$_2$.H$_2$O (0.20 g, 1 mmol). Column chromatography (EtOAc:Hexanes) gave a mixture of **3b** and **[D]$_n$-3b**, (average for 2 runs: 60% yield). The distribution was then measured via ^{1}H NMR spectroscopy.

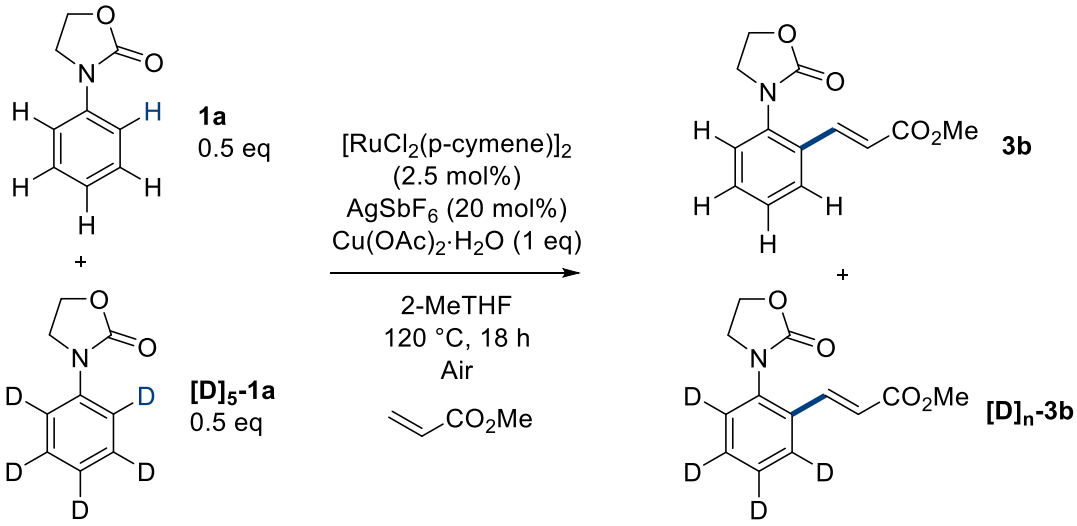

Run 1 – H = 0.73. D = 0.27. KIE = 2.7

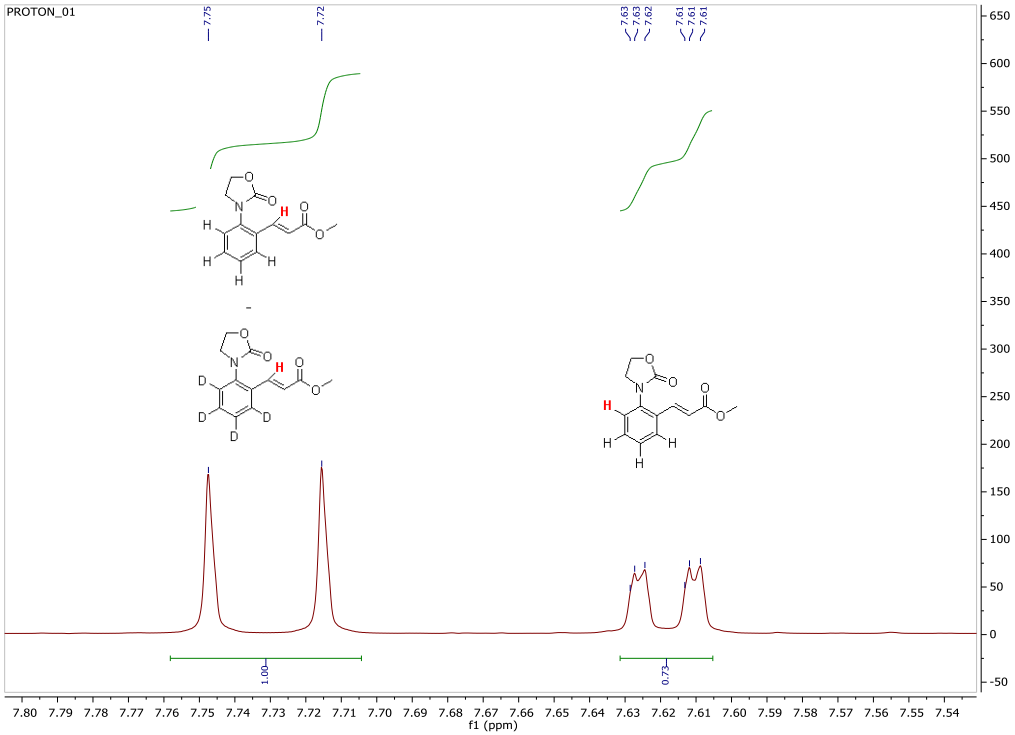

Run 2 – H = 0.72. D = 0.28. KIE = 2.5

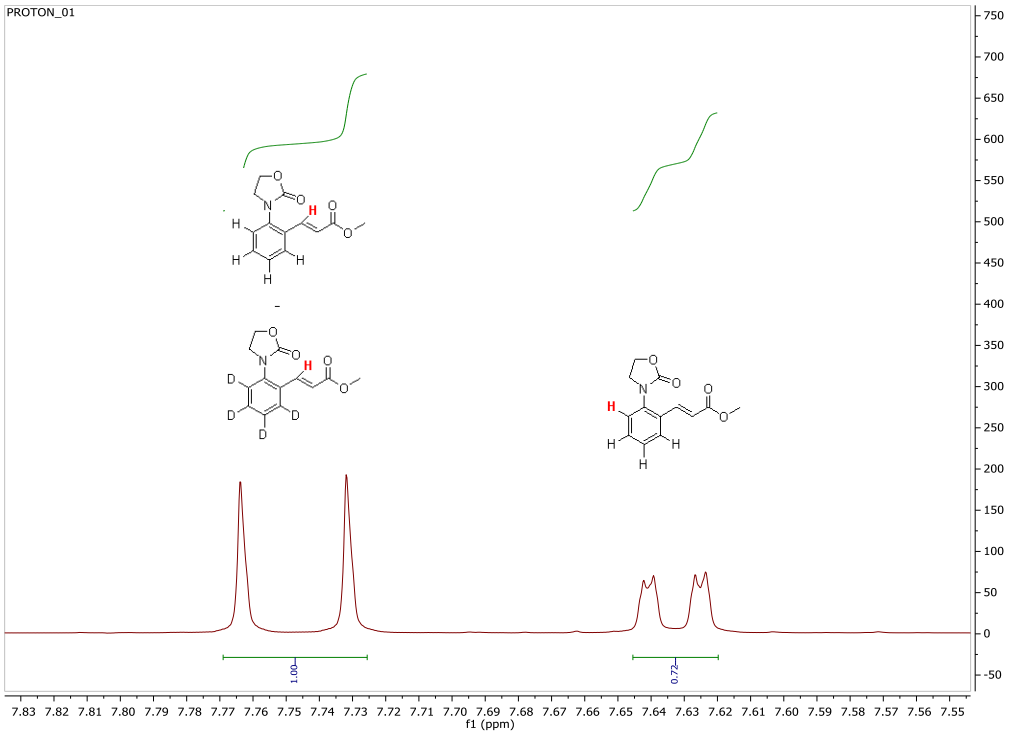

6.1.8: Competition Experiments

Crude ^{1}H NMR spectra were taken after silica plug work-up and diagnostic peaks were taken versus literature precedent of exact/similar structures in references given in titles

Acetophenone[10]

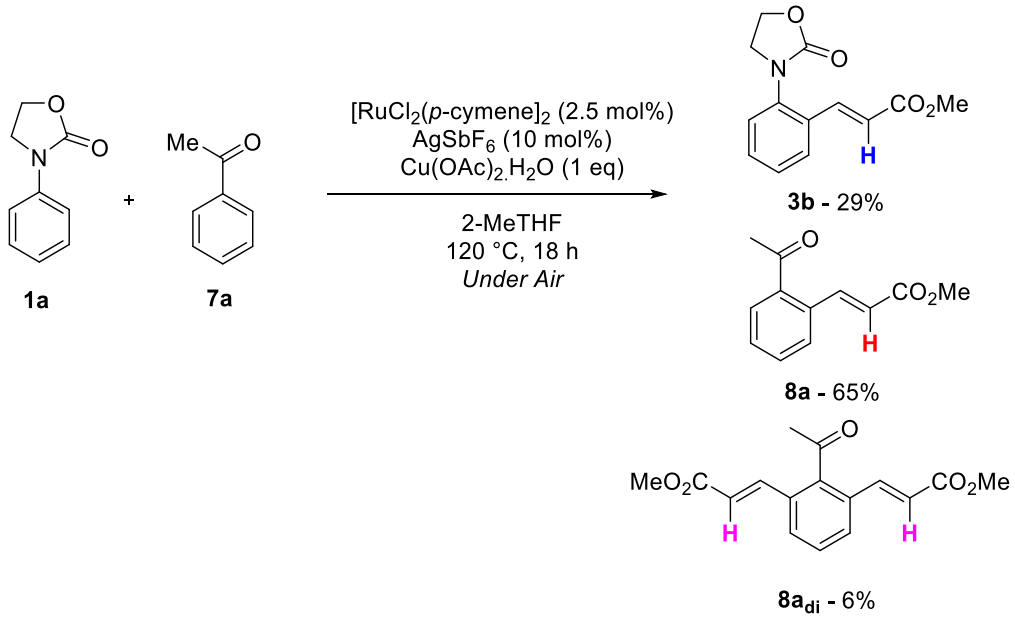

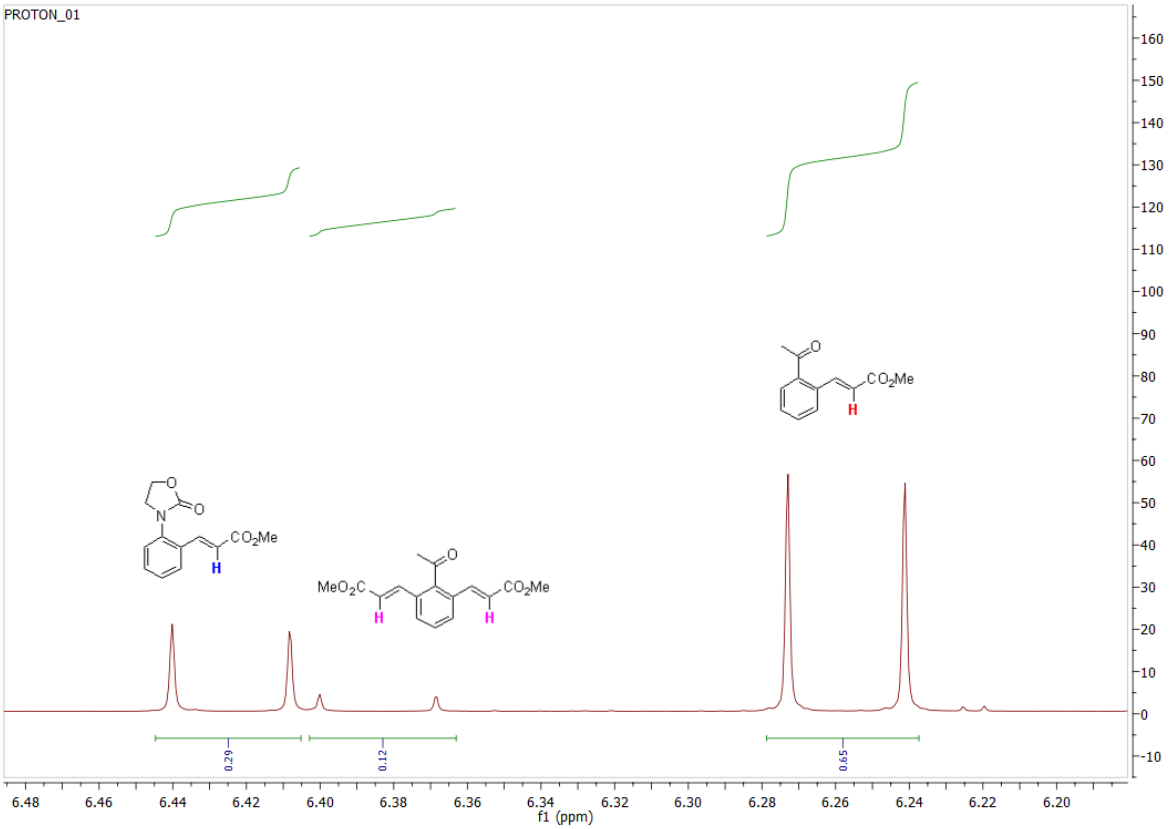

Benzoic Acid[10]

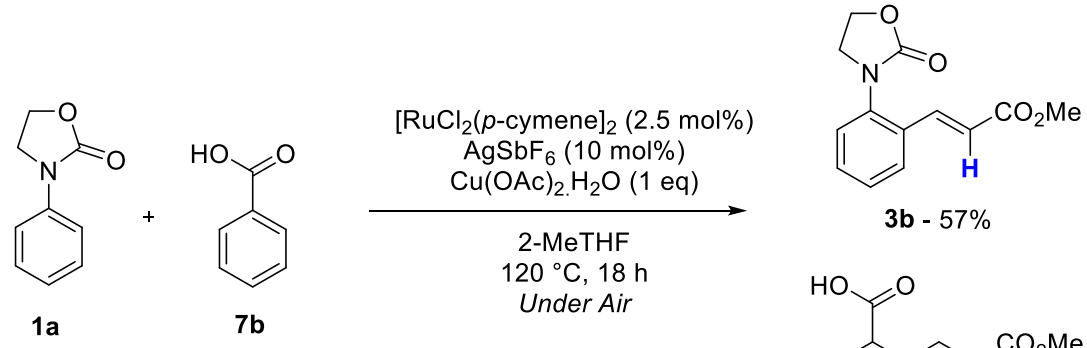

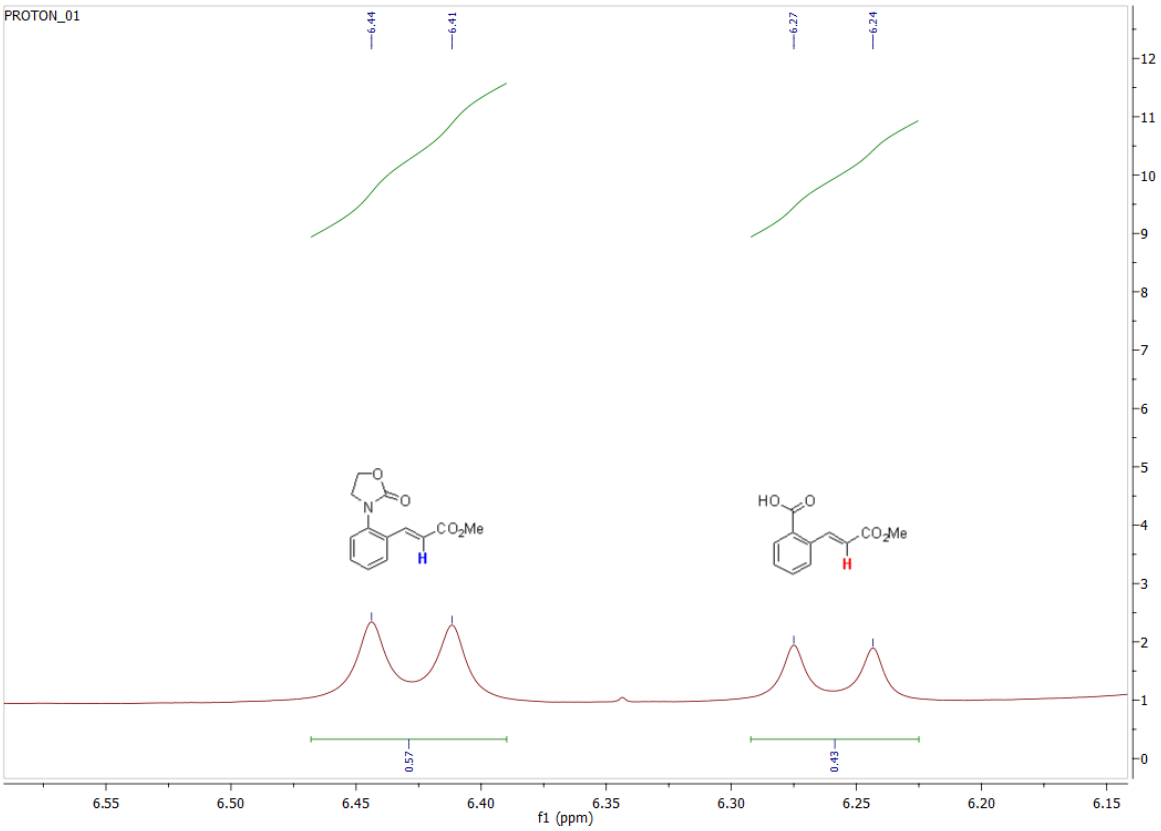

Ethyl Benzoate[11]

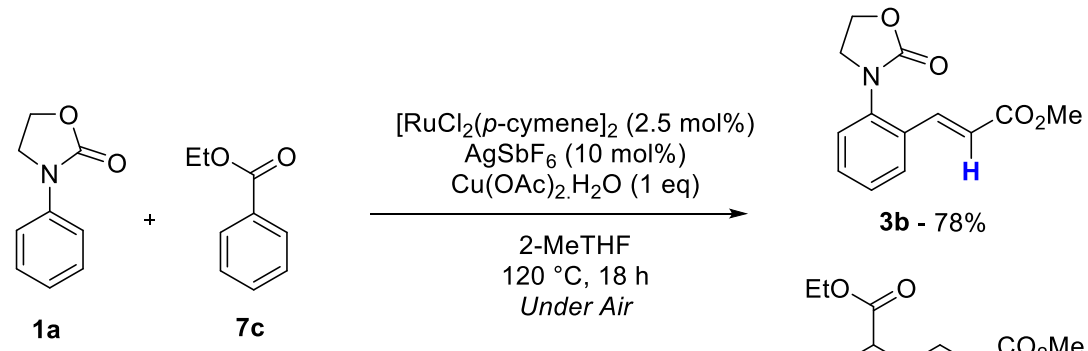

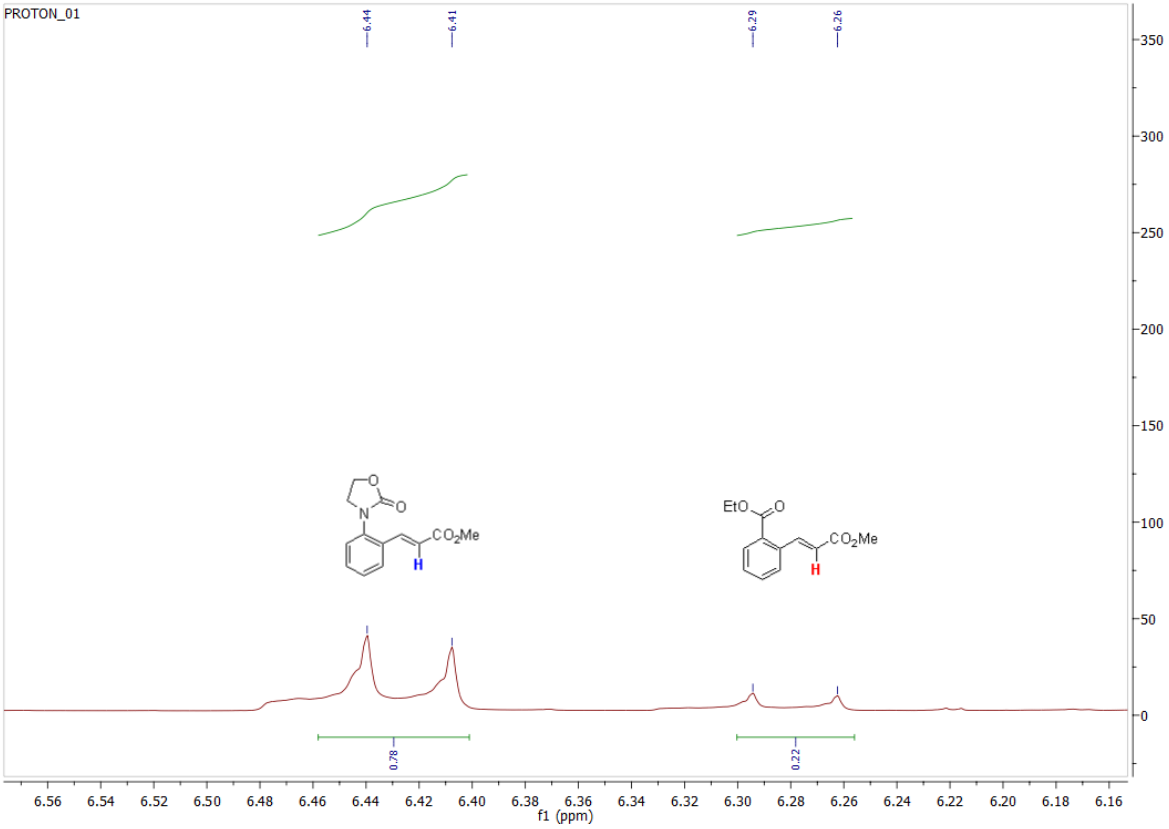

Benzaldehyde[12,13]

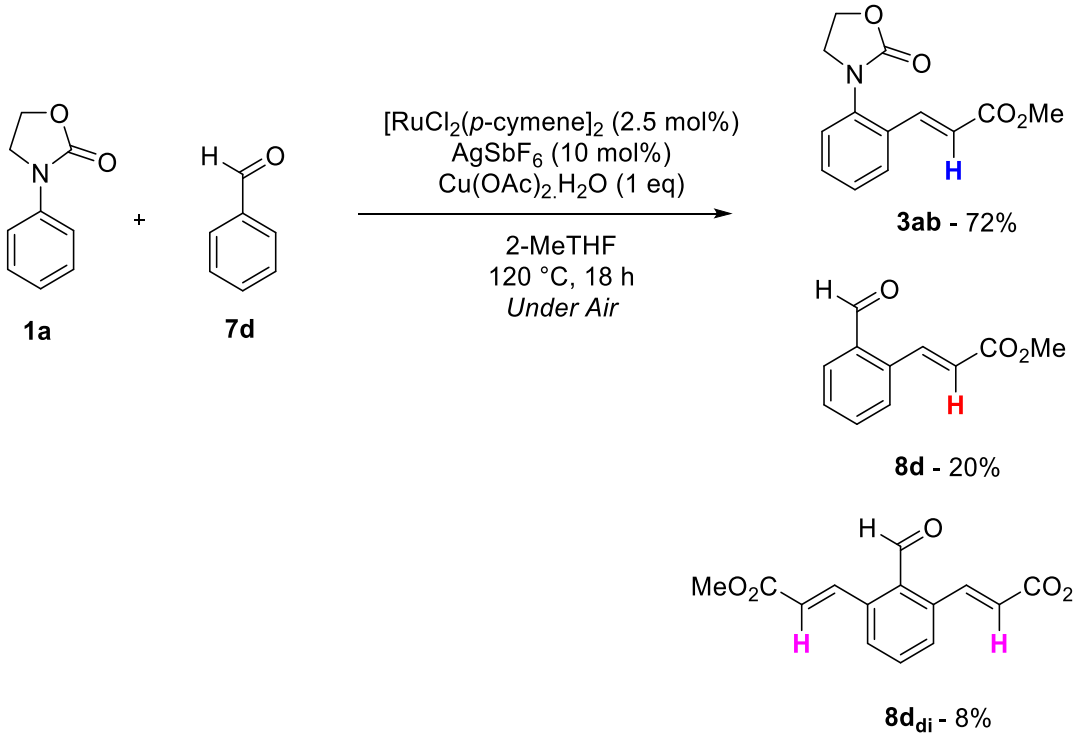

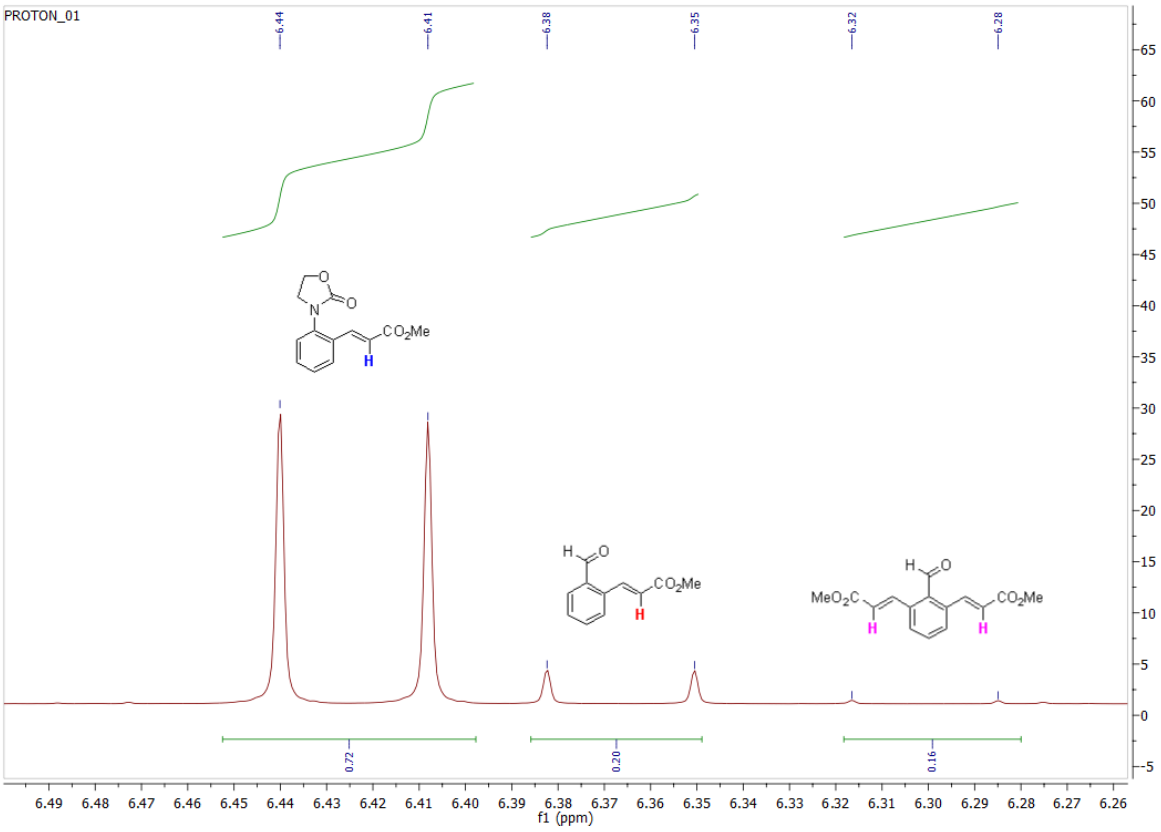

6.1.9: References

(1) Mahy, W.; Plucinski, P.; Frost, C. G. *Org. Lett.*, **2014**, *16*, 5020-5023

(2) Mallesham, B.; Rajesh, B. M.; Reddy, P. R.; Srinivas, D.; Trehan, S. *Org. Lett.*, **2003**, *5*, 963-965

(3) Ramussen, L. K.; Begtrup, M.; Ruhland, T. *J. Org. Chem.*, **2004**, *69*, 6890-6893

(4) Cacchi, S.; Fabrizi, G.; Goggiamani, A.; Zappia, G. *Org Lett.*, **2001**, *3*, 2539-2541

(5) Wang, B.; Elageed, E. H. M.; Zhang, D.; Yang, S.; Wu, S.; Zhang, G.; Gao, G. *ChemCatChem*, **2014**, *6*, 278-283

(6) Yeung, C. S.; Dong, V. M.; Synlett, **2011**, 974-978

(7) Mahy, W.; Plucinski, P.; Jover, J.; Frost, C. G. *Angew. Chem. Int. Ed.*, **2015**, *127*, 11094-11098

(8) Haecker, H. G.; Elsinghorst, P. W.; Michels, S.; Daniels, J.; Schnakenburg, G.; Guetschow, M. *Synthesis*, **2009**, 1195-1203

(9) Ackermann, L. *Chem. Rev.*, **2011**, *111*, 1315-1345

(10) Nalivela, K. S.; Tilley, M.; McGuire, M. A.; Organ, M. G. *Chem. Eur. J.*, **2014**, *20*, 6603-6607

(11) Diebold, C.; Schweizer, S.; Becht, J. M.; Le Drian, C. *Org. Biomol. Chem.*, **2010**, *8*, 4834-4836

(12) Zhang, T.; Wu, L.; Li, X. *Org. Lett.*, **2013**, *15*, 6294-6297

(13) Peacock, L. R.; Chapman, R. S. L.; Sedgwick, A. C.; Mahon, M. F.; Amans, D.; Bull, S. D. *Org. Lett.*, **2015**, *17*, 994-997.

6.2: Data and Supporting Information for “Use of the Hydantoin Directing Group in Ruthenium(II)-Catalyzed C–H Functionalization

In the interest of presentation in a thesis, NMR spectra have not been included. However, in the interest of the reader these are available online at:
http://pubs.acs.org/doi/suppl/10.1021/acs.joc.6b02073/suppl_file/jo6b02073_si_001.pdf
The supporting information has also been submitted to formatting and colour changes however no changes in the data have been made.

6.2.1: General

Proton, carbon and fluorine NMR spectra were recorded on Bruker 300 MHz or Agilent Technologies 500 MHz spectrometer (^{1}H NMR at 300 MHz or 500 MHz, ^{13}C{^{1}H} NMR at 126 MHz or 75 MHz and ^{19}F NMR at 470 MHz). Chemical shifts for protons are reported in parts per million downfield from $Si(CH_3)_4$ and are referenced to residual protium in the deuterated solvent ($CHCl_3$ at 7.26 ppm, D_2O at 4.79 and CD_3OD at 3.31). Chemical shifts for fluorine s are reported in parts per million downfield from $CFCl_3$. NMR data are presented in the following format: chemical shift (number of equivalent nuclei by integration, multiplicity [app = apparent, br = broad, d = doublet, t = triplet, q = quartet, dd = doublet of doublets, dt = doublet of triplets, dq = doublet of quartets, ddd = doublet of doublet of doublets, m = multiplet], coupling constant [in Hz], assignment). Electrospray ionisation ultrahigh resolution time-of-flight mass spectrometry (ESI–UHR–TOF–MS) was performed on a Bruker maXis mass spectrometer. Electrospray ionisation high resolution time-of-flight mass spectrometry (ESI–HR–TOF–MS) was performed on a Bruker micrOTOF spectrometer. Infrared (IR) spectra were recorded on a Perkin–Elmer 1600 FT (Fourier transform) IR spectrophotometer, with absorbencies quoted as wavelength (v [in cm^{-1}]). Melting points were obtained on a Bibby Sterilin SMP10 melting point machine and are uncorrected.

Analytical thin-layer chromatography (TLC) was performed on aluminium-backed plates coated with Alugram® SIL G/UV254 purchased from Macherey–Nagel and visualised with UV light (254 or 365 nm) and/or KMnO4, 2,4-DNPH or I_2/Silica staining. Silica gel column chromatography was performed using 60 Å, 200-400 mesh particle size silica gel purchased from Sigma–Aldrich. Samples were loaded as saturated solutions in an appropriate solvent system.

All reactions were performed using reagents obtained from Sigma-Aldrich, Acros Organics, Alfa Aesar, Fluorochem chemicals without further purification unless stated. $[RuCl_2(p\text{-cymene})]_2$ was purchased from STREM chemicals. All water used was purified through a Merck Millipore reverse osmosis purification system prior to use. Anhydrous acetonitrile (MeCN), anhydrous dichloromethane (CH_2Cl_2), anhydrous tetrahydrofuran (THF) and anhydrous toluene (PhMe) were dried and degassed by passing through anhydrous alumina columns using an Innovative Technology Inc. PS-400-7 solvent purification system (SPS) and stored under an atmosphere of N_2 prior to use.

Reactions were performed in oven-dried glassware and under a blanket of N_2 if not stated. Temperatures quoted are external. Solvents were removed under reduced pressure using Büchi-Rotorvapor apparatus.

6.2.2: Optimization

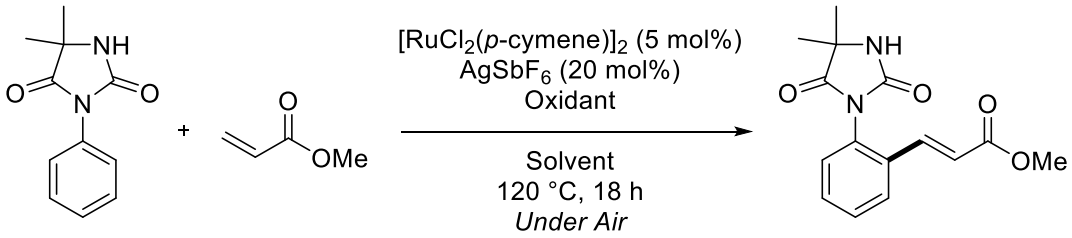

Entry	Solvent	Oxidant	NMR Yield
1	Dioxane	$Cu(OAc)_2.H_2O$	35
2	Bu_2O	$Cu(OAc)_2.H_2O$	19
3	CPME	$Cu(OAc)_2.H_2O$	59
4	DME	$Cu(OAc)_2.H_2O$	81
5	DCE	$Cu(OAc)_2.H_2O$	53
6	DMA	$Cu(OAc)_2.H_2O$	0
7	*t*AmOH	$Cu(OAc)_2.H_2O$	33
8	2-Butanone	$Cu(OAc)_2.H_2O$	38
9	NMP	$Cu(OAc)_2.H_2O$	0
10	DMF	$Cu(OAc)_2.H_2O$	0
11	H_2O	$Cu(OAc)_2.H_2O$	0
12	PhMe	$Cu(OAc)_2.H_2O$	17
13	$PhCF_3$	$Cu(OAc)_2.H_2O$	46
14	2-MeTHF (Repeat)	$Cu(OAc)_2.H_2O$	85
15	THF	$Cu(OAc)_2.H_2O$	74
16	AcOH	$Cu(OAc)_2.H_2O$	0
20	2-MeTHF	AgOAc	39
21	2-MeTHF	Ag_2CO_3	8
22	2-MeTHF	AgTFA	0
23	2-MeTHF	AgOTf	0
24	2-MeTHF	$Cu(OTf)_2$	0
25	2-MeTHF	$Zn(OTf)_2$	0
26[b]	2-MeTHF	$Cu(OAc)_2.H_2O$	30
27[c]	2-MeTHF	$Cu(OAc)_2.H_2O$	95 (94)
28[c,d]	2-MeTHF	$Cu(OAc)_2.H_2O$	70

Reaction general conditions. *N*-phenylhydantoin (0.25 mmol), methyl acrylate (0.75 mmol), $[RuCl_2(p\text{-cymene})]_2$ (0.0125 mmol), $AbSbF_6$ (0.05 mmol) oxidant (1 eq) solvent (1 mL). 1,1,2,2-tetrachloroethane (0.25 mmol) as internal standard.

[b] = Reaction performed at 80 °C

[c] = Reaction performed at 100 °C

[d] = Reaction performed using $[RuCl_2(p\text{-cymene})]_2$ (2.5 mol%) and $AgSbF_6$ (10 mol%)

6.2.3: Synthesis of Hydantoin Starting Materials

Synthesis of **1a**

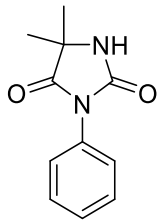

To a solution of 2-aminoisobutyric acid (4.12 g, 40 mmol) in MeOH (200 mL) was added thionyl chloride (3.20 mL, 5.30 g, 44 mmol) dropwise. The reaction mixture was heated to reflux and left to stir overnight. The resulting mixture was concentrated *in vacuo* affording a crystalline solid. This solid was re-dissolved in 160 mL anhydrous dichloromethane and triethylamine (6.12 mL, 4.44 g, 44 mmol). The flask was cooled to 0 °C and was added dropwise phenyl isocyanate (4.78 mL, 5.24 g, 44 mmol). After addition was complete the reaction mixture was allowed to return to room temperature and was stirred for two hours. The crude mixture was quenched with HCl (1M, 100 mL) and the organic phase extracted. The organic phase then washed with HCl (1M, 2 x 100 mL). The combined aqueous phases were re-extracted with 150 mL CH_2Cl_2. The organic phases were combined and dried over $MgSO_4$ then concentrated *in vacuo*. The crude reaction mixture was then recrystallized from boiling ethanol to give pure urea intermediate. **^{1}H NMR** (500 MHz, $CDCl_3$) δ 7.34–7.24 (4H, m, Ar*H*), 7.10–7.00 (1H, m, Ar*H*), 6.79 (1H, s, N*H*), 3.80–3.70 (3H, m, OCH_3), 1.56 (6H, s, C(CH_3)$_2$). **^{13}C NMR** (126 MHz, $CDCl_3$) δ 176.18 (N*C*(O)C), 155.03 (N*C*(O)N), 138.71 (Ar*C*), 129.40 (Ar*C*), 123.93 (Ar*C*), 121.04 (Ar*C*), 56.61 (O*C*H_3), 52.90 (*C*(CH$_3$)$_2$), 25.73 (C(*C*H_3)$_2$). To a solution of the urea (6.74 g, 29 mmol) in THF (116 mL) was added potassium *tert*-butoxide (3.58 g, 32 mmol). The reaction mixture was allowed to stir overnight at room temperature. The mixture was concentrated *in vacuo* and the crude residue was partitioned between EtOAc (100 mL) and Water (100 mL). The organic layer was separated and the aqueous layer was extracted with two further portions of EtOAc (2 x 100 mL). The combined organics were dried over $MgSO_4$ and concentrated *in vacuo* to give a white crystalline solid, **1a**, 71% (4.21 g). **^{1}H NMR** (500 MHz, $CDCl_3$) δ 7.50–7.33 (5H, m, Ar*H*), 6.87 (1H, s, N*H*), 1.49 (6H, s, C(CH_3)$_2$). **^{13}C NMR** (126 MHz, $CDCl_3$) δ 176.43 (N*C*(O)C), 155.85 (N*C*(O)N), 131.80 (Ar*C*), 129.26 (Ar*C*), 128.38 (Ar*C*), 126.36 (Ar*C*) 58.82 (*C*(CH$_3$)$_2$, 25.38 (C(*C*H_3)$_2$. Data is in line with literature precedent.[1]

General Procedure **A** for the Synthesis of Acyl Azides

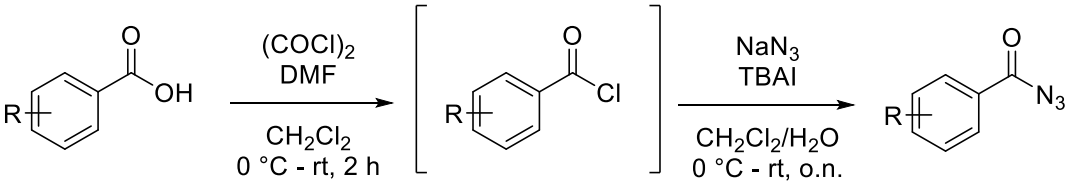

To a solution of benzoic acid (10 mmol) in anhydrous CH_2Cl_2 (40 mL) was added DMF (0.1 mL) and oxalyl chloride (15 mmol) dropwise at 0 °C. After addition was complete the reaction mixture was allowed to return to room temperature and stir for two hours. The mixture concentrated *in vacuo*. The mixture was re-dispersed in CH_2Cl_2 and was added tetrabutylammonium iodide (0.01 mmol). The mixture was cooled to 0 °C and was added sodium azide (15 mmol) solution in water (8 mL) portionwise. After addition was complete the reaction mixture was allowed to return to room temperature and stir overnight. The reaction mixture was diluted in water (32 mL) and the organic phase extracted. The aqueous phase was further extracted with dichloromethane (2 x 40 mL) and the combined organic phases were dried over $MgSO_4$ and concentrated *in vacuo*. The crude mixture was purified using column chromatography (EtOAc:Petroleum Ether 40-60 °C) to give aryl acyl azide.

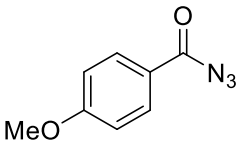

81%

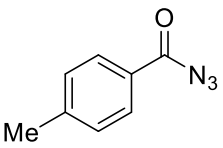

90%

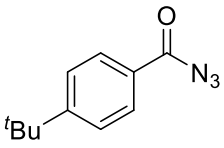

82%

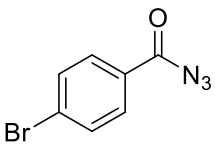

67%

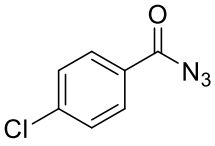

82%

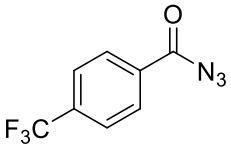

85%

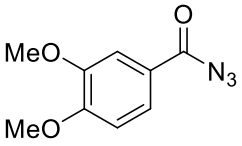

53%

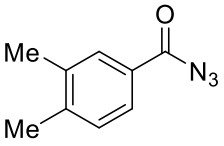

78%

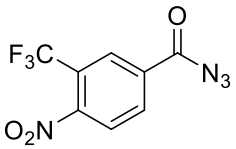

75%

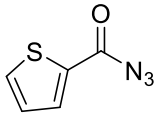

88%

General Procedure **B** for the Synthesis of *N*-arylhydantoins from acyl amino acids

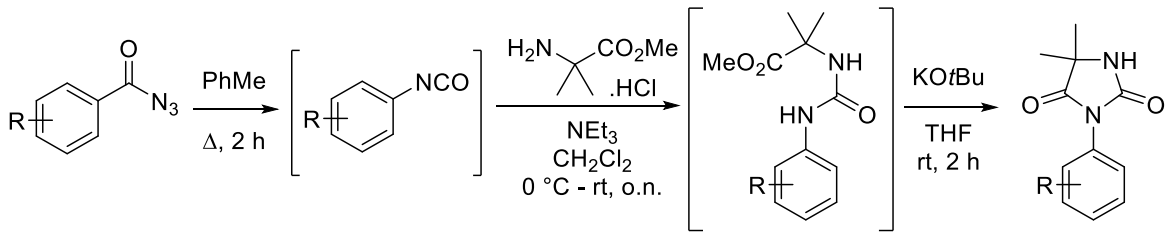

Aryl acyl azide was dissolved in anhydrous toluene (8 mL) and heated to reflux for two hours. The reaction mixture was allowed to cool and concentrated *in vacuo*. The reaction mixture was then diluted in anhydrous CH_2Cl_2 (5 mL). In a separate flask, H-Aib-OMe hydrochloride salt (1 eq wrt. acyl azide) was diluted in anhydrous CH_2Cl_2 and was added triethylamine (1.1 eq) at 0 °C. The isocyanate mixture was then syringed into the amino acid mixture dropwise at 0 °C, allowing for mild effervescence. After the mixtures were completely combined the reaction mixture was allowed to return to room temperature and stir overnight. The reaction mixture was diluted with HCl (1M, 40 mL) and the organic phase was extracted. The organic phase was further washed with HCl (1M, 2 x 40 mL) and the organic phase was dried over $MgSO_4$ and concentrated *in vacuo*. The crude residue was diluted in THF (40 mL) and was added potassium *tert*-butoxide (1.1 eq) and the reaction mixture was allowed to stir for two hours at room temperature. The mixture was concentrated *in vacuo* and dispersed in a mixture of CH_2Cl_2 (40 mL) and water (40 mL). The organic phase was extracted and the aqueous phase was further extracted with CH_2Cl_2 (2 x 40 mL). The combined organic phases were dried with $MgSO_4$ (if possible, often the hydantoin falls out of solution) and concentrated *in vacuo* to give *N*-arylhydantoin. The crude mixture was purified by silica gel column chromatography (EtOAc:Petroleum Ether 40-60°C) or recrystallization from boiling ethanol.

Synthesis of **1b**

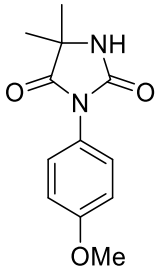

The above compound was obtained from the appropriate acyl azide synthesized previously following General Procedure **B** using the following reagents: acyl azide (1.4 g, 8 mmol), H-Aib-OMe.HCl (1.22 g, 8 mmol), triethylamine (1.22 mL, 8.8 mmol), potassium *tert*-butoxide (0.98 g, 8.8 mmol). The resulting crude mixture was purified via recrystallization using boiling ethanol to give a crystalline white solid, **1b**, 64% from acyl azide, 52% from acid (1.19 g). **mp** (from $CHCl_3$): 147-149 °C. **FT-IR** (thin film): ν_{max} (cm^{-1}) = 3224.8, 1780.5, 1714.9. **^{1}H NMR** (500 MHz, $CDCl_3$) δ 7.32–7.27 (2H, m, Ar*H*), 7.00–6.94 (2H, m, Ar*H*), 6.71 (1H, s, N*H*), 3.82 (3H, s, ArOCH_3), 1.50 (6H, s, C(CH_3)$_2$). **^{13}C NMR** (75 MHz, $CDCl_3$) δ 176.62 (N*C*(O)C), 159.39 (N*C*(O)N), 156.11 (Ar*C*OCH$_3$), 127.71 (Ar*C*), 124.22 (Ar*C*), 114.54 (Ar*C*), 58.74 (*C*(CH$_3$)$_2$), 55.61 (ArO*C*H$_3$), 25.28 (C(*C*H$_3$)$_2$). **HRMS** (ESI): m/z calculated for $C_{12}H_{14}N_2O_3$ requires 257.0902 for $[M+Na]^+$, found 257.0893.

Synthesis of **1c**

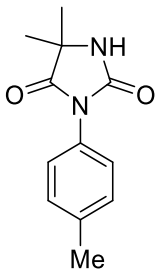

The above compound was obtained from the appropriate acyl azide synthesized previously following General Procedure **B** using the following reagents: acyl azide (1.45 g, 9 mmol), H-Aib-OMe.HCl (1.38 g, 9 mmol), triethylamine (1.38 mL, 9.9 mmol), potassium *tert*-butoxide (1.01 g, 9.9 mmol). The resulting crude mixture did not require further purification as an off-white solid, **1c**, 50% from acyl azide, 56% from acid (1.10 g). **mp** (from $CHCl_3$): 175-177 °C. **FT-IR** (thin film): ν_{max} (cm^{-1}) = 3385.3, 2979.9, 1773.8, 1714.6. **^{1}H NMR** (300 MHz, $CDCl_3$) δ 7.27 (4H, s, Ar*H*), 2.38 (3H, s, ArCH_3), 1.53 (6H, s, C(CH_3)$_2$). **^{13}C NMR** (75

MHz, $CDCl_3$) δ 176.50 (N*C*(O)C), 156.00 (N*C*(O)N), 138.39 (Ar*C*), 129.84 (Ar*C*), 129.04 (Ar*C*), 126.22 (Ar*C*), 58.75 (*C*(CH_3)$_2$), 25.28 (C(*C*H_3)$_2$), 21.29 (Ar*C*H_3). **HRMS** (ESI): m/z calculated for $C_{12}H_{14}N_2O_2$ requires 241.0955 for $[M+Na]^+$, found 241.0973.

Synthesis of **1d**

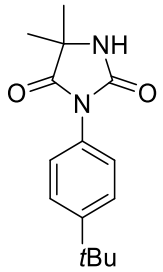

The above compound was obtained from the appropriate acyl azide synthesized previously following General Procedure **B** using the following reagents: acyl azide (1.26 g, 8.2 mmol), H-Aib-OMe.HCl (1.26 g, 9 mmol), triethylamine (1.25 mL, 9 mmol), potassium *tert*-butoxide (0.92 g, 9 mmol). The resulting crude mixture was purified via silica gel chromatography to give a crystalline white solid, **1d**, 38% from acyl azide, 31% from acid (0.82 g). **mp** (from $CHCl_3$): 188-189 °C. **FTIR** (thin film): ν_{max} (cm^{-1}) = 2956.3, 1780.9, 1717.7. **^{1}H NMR** (500 MHz, $CDCl_3$) δ 7.50–7.45 (2H, m, Ar*H*), 7.34–7.30 (2H, m, Ar*H*), 5.77 (1H, s, N*H*), 1.54 (6H, s, C(C*H*$_3$)$_2$), 1.33 (9H, s, C(C*H*$_3$)$_3$). **^{13}C NMR** (126 MHz, $CDCl_3$) δ 176.34 (N*C*(O)C), 151.44 (N*C*(O)N), 129.03 (Ar*C*), 128.80 (Ar*C*), 126.33 (Ar*C*), 125.82 (Ar*C*), 58.80 (*C*(CH_3)$_2$), 34.92 (*C*(CH_3)$_3$), 31.49 (C(*C*H_3)$_3$), 25.56 (C(*C*H_3)$_2$). **HRMS** (ESI): m/z calculated for $C_{15}H_{20}N_2O_2$ requires 283.1422 for $[M+Na]^+$, found 283.1390.

Synthesis of **1e**

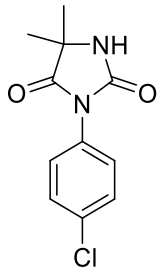

The above compound was obtained from the appropriate acyl azide synthesized previously following General Procedure **B** using the following reagents: acyl azide (1.49 g, 8 mmol), H-Aib-OMe.HCl (1.22 g, 8 mmol), triethylamine (1.22 mL, 8.8 mmol), potassium *tert*-

butoxide (0.98 g, 8.8 mmol). The resulting crude mixture was purified via recrystallization using boiling ethanol to give a crystalline white solid, 59% from acyl azide, 48% from acid (1.13 g). **mp** (from $CHCl_3$): 139-141 °C. **FT-IR** (thin film): ν_{max} (cm^{-1}) = 3297.0, 2981.0, 1780.0, 1707.3. **^{1}H NMR** (300 MHz, $CDCl_3$) δ 7.48–7.35 (4H, m, Ar*H*), 6.52 (1H, s, N*H*), 1.53 (6H, s, C(CH_3)$_2$). **^{13}C NMR** (75 MHz, $CDCl_3$) δ 176.11 (N*C*(O)C), 155.36 (N*C*(O)N), 134.07 (Ar*C*), 130.25 (Ar*C*), 129.45 (Ar*C*), 127.46 (Ar*C*), 58.90 (*C*(CH_3), 25.42 (C(*C*H_3)$_2$). **HRMS** (ESI): m/z calculated for $C_{11}H_{11}N_2O_2Cl_1$ requires 21.0407 for $[M+Na]^+$, found 261.0385.

Synthesis of **1f**

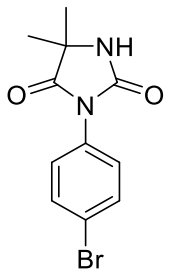

The above compound was obtained from the appropriate acyl azide synthesized previously following General Procedure **B** using the following reagents: acyl azide (1.51 g, 6.7 mmol), H-Aib-OMe.HCl (1.03 g, 6.7 mmol), triethylamine (1.03 mL, 7.4 mmol), potassium *tert*-butoxide (0.83 g, 7.4 mmol). The resulting crude mixture was purified via recrystallization using boiling ethanol to give a crystalline white solid, 63% from acyl azide, 42% from acid (1.20 g). **mp** (from $CHCl_3$): 176-177 °C. **FT-IR** (thin film): ν_{max} (cm^{-1}) = 3295.7, 2979.9, 1780.8 1708.4. **^{1}H NMR** (300 MHz, $CDCl_3$) δ 7.59 (2H, d, *J* = 8.6 Hz, Ar*H*), 7.33 (2H, d, *J* = 8.6 Hz, Ar*H*), 6.27 (1H, s, N*H*), 1.54 (6H, s, C(CH_3)$_2$). **^{13}C NMR** (75 MHz, $CDCl_3$) δ 175.97 (N*C*(O)C), 155.15 (N*C*(O)N), 132.43 (Ar*C*), 130.82 (Ar*C*), 127.71 (Ar*C*), 122.09 (Ar*C*), 58.90 (*C*(CH_3)$_2$), 25.47 (C(*C*H_3)$_2$). **HRMS** (ESI): m/z calculated for $C_{11}H_{11}N_2O_2Br_1$ requires 304.9902 for $[M+Na]^+$, found 304.9876.

Synthesis of **1g**

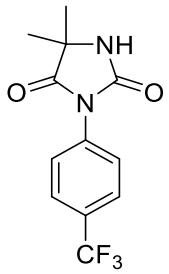

The above compound was obtained from the appropriate acyl azide synthesized previously following General Procedure **B** using the following reagents: acyl azide (1.82 g, 8.5 mmol), H-Aib-OMe.HCl (1.31 g, 8.5 mmol), triethylamine (1.30 mL, 9.4 mmol), potassium *tert*-butoxide (0.95 g, 9.4 mmol). The resulting crude mixture was purified via recrystallization using boiling ethanol to give a crystalline white solid, 66% from acyl azide, 56% from acid (1.53 g). **FT-IR** (thin film): ν_{max} (cm^{-1}) = 3328.1, 1779.8, 1719.2. **^{1}H NMR** (300 MHz, $CDCl_3$) δ 7.74 (2H, d, *J* = 8.5 Hz, Ar*H*), 7.63 (2H, d, *J* = 8.5 Hz, Ar*H*), 6.26 (1H, s, N*H*), 1.56 (6H, s, C(C*H*$_3$)$_2$). **^{13}C NMR** (126 MHz, $CDCl_3$) δ 175.82 (N*C*(O)C)), 154.82 (N*C*(O)N)), 139.48 – 114.06 (Ar*C*) 135.05 (Ar*C*), 130.15 (d, *J* = 32.9 Hz, Ar*C*), 126.35 (q, *J* = 3.7 Hz, Ar*C*), 126.16 (Ar*C*), 125.31 (q, *J* = 269.3 Hz, Ar*C*F_3), 58.93 (*C*(CH$_3$)$_2$), 25.53 (C(*C*H$_3$)$_2$). **^{19}F NMR** (470 MHz, $CDCl_3$) δ -62.71 (s, C*F*$_3$). **HRMS** (ESI): m/z calculated for $C_{12}H_{11}N_2O_3F_3$ requires 295.0670 for $[M+Na]^+$, found 295.0643.

Synthesis of **1h**

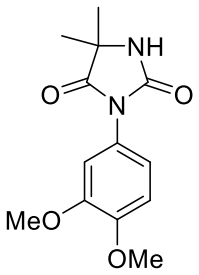

The above compound was obtained from the appropriate acyl azide synthesized previously following General Procedure **B** using the following reagents: acyl azide (1.19 g, 5.3 mmol), H-Aib-OMe.HCl (0.81 g, 5.3 mmol), triethylamine (0.81 mL, 5.83 mmol), potassium *tert*-butoxide (0.65 g, 5.83 mmol). The resulting crude mixture was purified via recrystallization using boiling ethanol to give a crystalline off-white solid, 93% from acyl azide, 41% from acid (1.40 g). **mp** (from $CHCl_3$): 196-198 °C **FTIR** (thin film): ν_{max} (cm^{-1}) = 3324.8, 2982.2,

1775.6, 1708.6. **^{1}H NMR** (300 MHz, $CDCl_3$) δ 6.94 (2H, s, Ar*H*), 6.88 (1H, s, Ar*H*), 6.35 (1H, s, N*H*), 3.89 (6H, app d, ArOCH_3), 1.53 (6H, s, C(CH_3)$_2$). **^{13}C NMR** (75 MHz, $CDCl_3$) δ 176.60 (N*C*(O)C), 155.96 (N*C*(O)N), 149.36 (Ar*C*OCH$_3$), 149.11 (Ar*C*OCH$_3$), 124.41 (Ar*C*), 119.10 (Ar*C*), 111.22 (Ar*C*), 110.03 (Ar*C*), 58.82 (*C*(CH$_3$)$_2$), 56.23 (ArO*C*H$_3$), 56.24 (ArO*C*H$_3$), 25.45 (C(*C*H$_3$)$_2$). **HRMS** (ESI): m/z calculated for $C_{13}H_{16}N_2O_4$ requires 287.1008 for $[M+H]^+$, found 287.0976.

Synthesis of **1i**

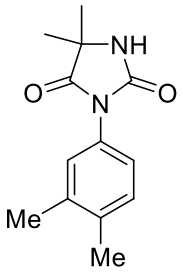

The above compound was obtained from the appropriate acyl azide synthesized previously following General Procedure **B** using the following reagents: acyl azide (1.37 g, 7.8 mmol), H-Aib-OMe.HCl (1.20 g, 7.8 mmol), triethylamine (1.20 mL, 8.58 mmol), potassium *tert*-butoxide (0.97 g, 8.58 mmol). The resulting crude mixture was purified via silica gel chromatography to give an off-white solid, 54% from acyl azide, 42% from acid (0.97 g). **mp** (from $CHCl_3$): 181-183 °C **FT-IR** (thin film): ν_{max} (cm^{-1}) = 3292.6, 1778.1, 1713.6. **^{1}H NMR** (500 MHz, $CDCl_3$) δ 7.22 (1H, d, *J* = 8.0 Hz, Ar*H*), 7.14 (1H, d, *J* = 1.9 Hz, Ar*H*), 7.09 (1H, dd, *J* = 8.0, 2.2 Hz, Ar*H*), 6.06 (1H, s, N*H*), 2.29 (3H, s, ArCH_3), 2.28 (3H, s, ArCH_3), 1.53 (6H, s, C(CH_3)$_2$). **^{13}C NMR** (126 MHz, $CDCl_3$) δ 176.50 (N*C*(O)C), 155.88 (N*C*(O)N), 137.85 (Ar*C*), 137.36 (Ar*C*), 130.45 (Ar*C*), 129.24 (Ar*C*), 127.59 (Ar*C*), 124.00 (Ar*C*), 58.85 (*C*(CH$_3$)$_2$), 25.50 (C(*C*H$_3$)$_2$), 20.05 (Ar*C*H$_3$), 19.71 (Ar*C*H$_3$). **HRMS** (ESI): m/z calculated for $C_{13}H_{16}N_2O_2$ requires 233.1290 for $[M+H]^+$, found 233.1272.

Synthesis of **1j**

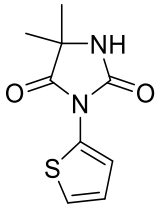

The above compound was obtained from the appropriate acyl azide synthesized previously following General Procedure **B** using the following reagents: acyl azide (0.40 g, 2.6 mmol), H-Aib-OMe.HCl (0.4 g, 2.6 mmol), triethylamine (0.40 mL, 2.9 mmol), potassium *tert*-butoxide (0.33 g, 2.9 mmol). The resulting crude mixture was purified via silica gel chromatography to give a light purple solid, 55% from acyl azide, 48% from acid (0.32 g). **^{1}H NMR** (500 MHz, $CDCl_3$) δ 7.50 (1H, dd, *J* = 3.9, 1.4 Hz, Ar*H*), 7.17 (1H, dd, *J* = 5.5, 1.4 Hz, Ar*H*), 7.00 (1H, dd, *J* = 5.5, 3.8 Hz, Ar*H*), 6.39 (1H, s, N*H*), 1.54 (6H, s, C(CH_3)$_2$). **^{13}C NMR** (126 MHz, $CDCl_3$) δ 174.77 (N*C*(O)C), 154.39 (N*C*(O)N), 132.42 (Ar*C*), 125.27 (Ar*C*), 121.87 (Ar*C*), 120.19 (Ar*C*), 58.68 (*C*(CH_3)$_2$), 25.52 (C(*C*H_3)$_2$). The data is in line with literature precedent.[2]

Synthesis of **1r**

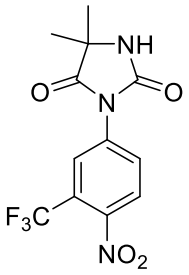

The above compound was obtained from the appropriate acyl azide synthesized previously following General Procedure **B** using the following reagents: acyl azide (1.94 g, 7.4 mmol), H-Aib-OMe.HCl (1.14 g, 7.4 mmol), triethylamine (1.14 mL, 8.14 mmol), potassium *tert*-butoxide (0.92 g, 8.14 mmol). The resulting crude mixture was purified via silica gel chromatography to give a crystalline yellow solid, 74% from acyl azide, 55% from acid (1.75 g). **^{1}H NMR** (500 MHz, $CDCl_3$) δ 8.14 (1H, s, Ar*H*), 8.01 (2H, d, *J* = 1.6 Hz, Ar*H*), 6.33 (1H, s, N*H*), 1.59 (6H, s, C(CH_3)$_2$). **^{13}C NMR** (126 MHz, $CDCl_3$) δ 175.31 (N*C*(O)C), 153.84 (N*C*(O)N), 146.32 (Ar*C*), 136.09 (Ar*C*), 129.11 (Ar*C*), 124.61 (q, *J* = 5.5 Hz, *C*F_3)., 122.83 (Ar*C*), 120.65 (Ar*C*), 59.08 (*C*(CH_3)$_2$), 25.52 (C(*C*H_3)$_2$). Data is in line with literature precedent.[3]

Synthesis of **1k**

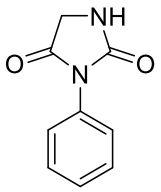

To a solution of glycine (2.25 g, 30 mmol) in NaOH (100 mL, 2M) was added phenyl isocyanate (3.25 mL, 30 mmol) dropwise at 0 °C. The solution was stirred at 0 °C for 15 mins before allowing the mixture to return to room temperature and stirred overnight. A small precipitate fell out of solution and was filtered off and discarded. The filtrate was acidified using concentrated HCl to pH 1. A precipitate fell out of solution and was filtered using a Buchner funnel. The solid collected was redissolved in HCl (100 mL, 1M) and heated to reflux for 2 hours. The reaction mixture was then allowed to return to room temperature where a further precipitate fell out of solution. This precipitate was collected via Buchner funnel to give Gly-Hyd, 52% (2.72 g). **^{1}H NMR** (500 MHz, $CDCl_3$) δ 7.55–7.45 (2H, m, Ar*H*), 7.40 (3H, dq, *J* = 3.1, 2.3 Hz, Ar*H*), 6.71 (1H, s, N*H*), 4.10 (2H, s, CH_2). **^{13}C NMR** (126 MHz, $CDCl_3$) δ 170.34 (N*C*(O)CH_2), 157.84 (N*C*(O)NH), 131.52 (Ar*C*), 129.42 (Ar*C*), 128.66 (Ar*C*), 126.42 (Ar*C*), 46.68 (*C*H_2). Data is in line with literature precedent.[4]

General Procedure **D** for the synthesis of amino acid derived *N*-phenylhydantoins.

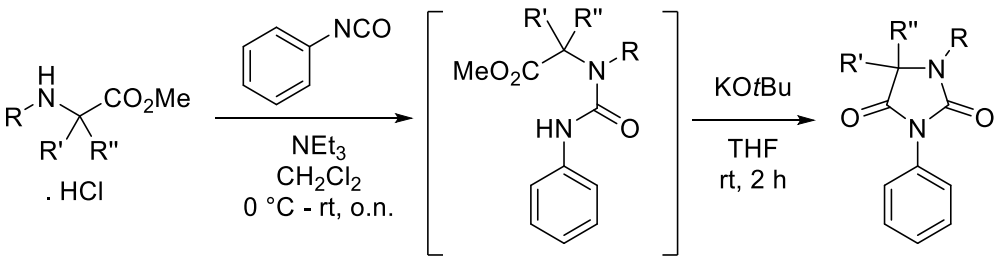

In an oven dried round bottom flask was added appropriate amino acid hydrochloride salt (10 mmol). The solid was dispersed in anhydrous CH_2Cl_2 (40 mL) and cooled to 0 °C. To the slurry was added triethylamine (1.53 mL, 1.11 g, 11 mmol) allowing for effervescence and the reaction mixture was allowed to stir for 5 minutes. To the resulting mixture was added phenyl isocyanate (1.09 mL, 1.19 g, 10 mmol) portionwise and the reaction mixture was allowed to return to room temperature and stir overnight. The flask was quenched with HCl (1M, 40 mL) and the organic layer separated. The organic layer was further washed with HCl (1M, 2 x 40 mL), was dried over $MgSO_4$ and concentrated *in vacuo* to give the crude urea. The resulting solid was dispersed in THF (40 mL) and was added potassium *tert*-butoxide (1.23 g, 11 mmol) and the mixture was stirred for ca. two hours, monitoring by TLC. The mixture was concentrated *in vacuo* and re-dispersed in a mixture of CH_2Cl_2 (40 mL) and H_2O (40 mL). The organic layer was separated and aqueous layer further extracted with CH_2Cl_2 (2 x 40 mL). The combined organics were dried over $MgSO_4$ and concentrated *in vacuo*. The resulting crude hydantoin was purified via silica gel chromatography (EtOAc:Petroleum Ether 40-60 °C) or via recrystallization from boiling ethanol.

Synthesis of **1l**

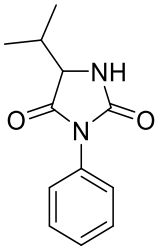

The above compound was obtained following General Procedure **D** from H-Val-OMe.HCl (1.68 g, 10 mmol). The resulting crude mixture was purified via recrystallization from boiling ethanol to give a crystalline white solid, 53% (1.16 g). **mp** (from $CHCl_3$): 121-123 °C. **FT-IR** (thin film): ν_{max} (cm^{-1}) = 3294.8, 2964.9, 1776.2, 1704.6. **^{1}H NMR** (300 MHz, $CDCl_3$) δ 7.53–7.42 (2H, m, Ar*H*), 7.38 (3H, m, Ar*H*), 6.54 (1H, s, N*H*), 4.07 (1H, d, *J* = 3.5 Hz, C*H*(*i*Pr), 2.33 (1H, dtd, *J* = 13.7, 6.8, 3.6 Hz, C*H*(CH_3)$_2$), 1.09 (3H, d, *J* = 7.0 Hz, CH(C*H*$_3$)$_2$), 1.01 (3H, d, *J* = 6.8 Hz, CH(C*H*$_3$)$_2$). **^{13}C NMR** (75 MHz, $CDCl_3$) δ 172.63 (N*C*(O)C), 157.33 (N*C*(O)N), 131.58 (Ar*C*), 129.33 (Ar*C*), 128.50 (Ar*C*), 126.39 (Ar*C*), 62.35 (*C*H(*i*Pr)), 30.80 (*C*H(CH_3)$_2$), 18.89 (CH(*C*H$_3$)$_2$), 16.19 (CH(*C*H$_3$)$_2$). **HRMS** (ESI): m/z calculated for $C_{12}H_{14}N_2O_2$ requires 241.0953 for $[M+Na]^+$, found 241.0951.

Synthesis of **1m**

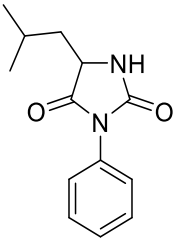

The above compound was obtained following General Procedure **D** from H-Leu-OMe.HCl (1.82 g, 10 mmol). The resulting crude mixture was purified via recrystallization from boiling ethanol to give a crystalline white solid, 80% (1.78 g). **mp** (from $CHCl_3$): 119-121 °C. **FT-IR** (thin film): ν_{max} (cm^{-1}) =,3288.4, 2958.6, 1777.7, 1713.7. **^{1}H NMR** (500 MHz, $CDCl_3$) δ 7.50–7.42 (2H, m, Ar*H*), 7.42–7.32 (3H, m, Ar*H*), 7.12 (1H, s, N*H*), 4.14 (1H, ddd, *J* = 9.1, 4.0, 1.3 Hz, NC*H*C=O), 1.89–1.75 (2H, m, C*H*$_2$(CH(CH_3)$_2$)), 1.63 (1H, dd, *J* = 9.3, 8.1 Hz, CH_2(C*H*(CH_3)$_2$)), 0.97 (3H, d, *J* = 6.2 Hz, CH(C*H*$_3$)$_2$), 0.94 (3H, d, *J* = 6.1 Hz, CH(C*H*$_3$)$_2$)). **^{13}C NMR** (126 MHz, $CDCl_3$) δ 173.61 (N*C*(O)C), 157.02 (N*C*(O)N), 131.65 (Ar*C*), 129.11 (Ar*C*), 128.24 (Ar*C*), 126.21 (Ar*C*), 55.80 (N*C*C=O), 41.03 (*C*H$_2$CH(CH_3)$_2$),

25.02($CH_2CH(CH_3)_2$), 23.08 ($CH_2CH(CH_3)_2$), 21.75 ($CH_2CH(CH_3)_2$). **HRMS** (ESI): m/z calculated for $C_{13}H_{16}N_2O_2$ requires 255.1109 for $[M+Na]^+$, found 255.1095.

Synthesis of **1n**

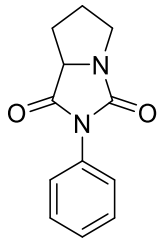

The above compound was obtained following General Procedure **D** from H-Pro-OMe.HCl (1.66 g, 10 mmol). The resulting crude mixture was purified via recrystallization from boiling ethanol to give a crystalline white solid, 60% (1.30 g). **mp** (from $CHCl_3$): 123-126 °C. **FT-IR** (thin film): ν_{max} (cm^{-1}) = 2980.6, 1774.6, 1707.5. **^{1}H NMR** (500 MHz, $CDCl_3$) δ 7.48–7.42 (2H, m, Ar*H*), 7.40–7.32 (3H, m, Ar*H*), 4.23 (1H, dd, *J* = 9.2, 7.5 Hz, NC*H*), 3.78 (1H, dt, *J* = 11.3, 7.8 Hz, NC*H*), 3.33 (1H, ddd, *J* = 11.3, 8.4, 4.6 Hz, NC*H*), 2.44–2.26 (1H, m, C*H*), 2.21–2.04 (2H, m, C*H*), 1.92–1.75 (1H, m, C*H*). **^{13}C NMR** (126 MHz, $CDCl_3$) δ 172.75 (N*C*(O)C), 159.50 (N*C*(O)N), 132.01 (Ar*C*), 129.21 (Ar*C*), 128.28 (Ar*C*), 126.06 (Ar*C*), 63.39 (N*C*H), 45.92 (N*C*H), 27.93 (*C*H_2), 27.03 (*C*H_2). **HRMS** (ESI): m/z calculated for $C_{12}H_{12}N_2O_2$ requires 239.0796 for $[M+Na]^+$, found 239.0798

Synthesis of **1o**

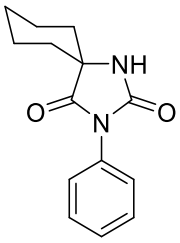

The above compound was obtained following General Procedure **D** from methyl 1-aminocyclohexane-1-carboxylate hydrochloride salt (1.94 g, 10 mmol). The resulting crude mixture was purified via recrystallization from boiling ethanol to give a crystalline white solid, 95% (2.32 g). **mp** (from $CHCl_3$): 225-227 °C. **FT-IR** (thin film): ν_{max} (cm^{-1}) = 3251.3, 2981.0, 1773.9, 1720.5 **^{1}H NMR** (500 MHz, $CDCl_3$) δ 7.48–7.44 (1H, m, Ar*H*), 7.43–7.40 (1H, m, Ar*H*), 7.39–7.33 (1H, m, Ar*H*), 6.88 (1H, s, N*H*), 1.96 (2H, m, Cy-CH_2), 1.78–1.65 (4H, m,

Cy-C*H*$_2$), 1.50–1.33 (2H, m, Cy-*CH*$_2$). **^{13}C NMR** (126 MHz, $CDCl_3$) δ 175.96 (N*C*(O)C), 156.06 (N*C*(O)N), 131.85 (Ar*C*), 129.19 (Ar*C*), 128.23 (Ar*C*), 126.32 (Ar*C*), 61.78 (*C*(Cy)), 33.85 (Cy*C*H$_2$), 24.68 (Cy*C*H$_2$), 21.89 (Cy*C*H$_2$). **HRMS** (ESI): m/z calculated for $C_{14}H_{16}N_2O_2$ requires 267.1109 for $[M+Na]^+$, found 267.1105.

Synthesis of **1p**

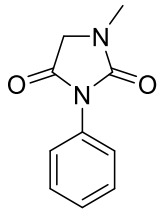

The above compound was obtained following General Procedure **D** from H-Sar-OMe.HCl (1.40 g, 10 mmol). The resulting crude mixture was purified via column chromatography to give a crystalline white solid, 38% (0.47 g). **^{1}H NMR** (500 MHz, $CDCl_3$) δ 7.49–7.43 (2H, m, Ar*H*), 7.42–7.33 (3H, m, Ar*H*), 4.03 (2H, d, *J* = 1.9 Hz, CC*H*$_2$N), 3.08 (3H, d, *J* = 1.9 Hz, NC*H*$_3$). **^{13}C NMR** (126 MHz,$CDCl_3$) δ 168.85 (N*C*(O)C), 155.96 (N*C*(O)N), 132.03 (Ar*C*), 129.27 (Ar*C*), 128.34 (Ar*C*), 126.24 (Ar*C*), 51.83 (C*C*H$_2$N), 30.09 (N*C*H$_3$). Data is in line with literature precedent.[5]

6.2.4: Synthesis of C–H Functionalized *N*-arylhydantoins

General procedure **E** for the synthesis of C–H alkenylated *N*-arylhydantoins

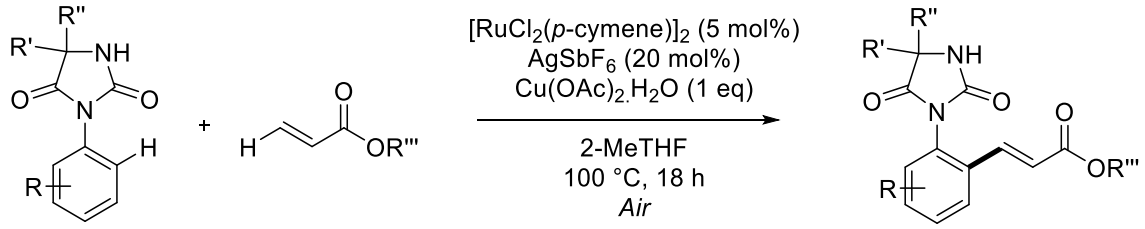

To an oven dried carousel tube was added *N*-arylhydantoin (0.5 mmol), $[RuCl_2(p\text{-cymene})]_2$ (0.016 g, 0.025 mmol), $AgSbF_6$ (0.035 g, 0.1 mmol) and $Cu(OAc)_2.H_2O$ (0.10 g, 0.5 mmol). The carousel tube was sealed with a Teflon cap leaving the tap open. To the tube was added 2-MeTHF (2 mL, 0.25 M) followed by appropriate acrylate coupling partner (1.5 mmol). The resulting mixture was stirred at 100 °C under reflux for 18 hours. The mixture was quenched with EtOAc (4 mL) and allowed to return to room temperature. The crude mixture was filtered using a short plug of silica, eluting with EtOAc. The filtrate was concentrated *in vacuo*. The crude mixture was purified using silica gel chromatography (EtOAc:Petroleum Spirit 40-60 °C) to give pure C–H alkenylated *N*-arylhydantoin.

Synthesis of **3aa**

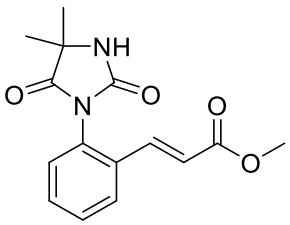

The above compound was synthesized using General Procedure **E** using *N*-arylhydantoin, **1a**, (0.10 g, 0.5 mmol) and methyl acrylate (0.14 mL, 1.5 mmol). Silica gel chromatography gave an off-white solid, 94%, (0.135 g). **mp** (from $CHCl_3$): 188-189 °C. **FT-IR** (thin film): ν_{max} (cm^{-1}) = 3311.0, 1782.6, 1712.9, 1638.4. **^{1}H NMR** (500 MHz, cdcl$_3$) δ 7.73 (1H, d, *J* = 7.3 Hz, Ar*H*), 7.55–7.44 (3H, m, ArC*H*=CHR), 7.27 (1H, d, *J* = 7.6 Hz, Ar*H*), 6.90 (1H, s, N*H*), 6.43 (1H, d, *J* = 15.9 Hz, ArCH=C*H*R), 3.76 (3H, s,CO_2CH_3), 1.57 (3H, s, $C(CH_3)_2$), 1.50 (3H, s, $C(CH_3)_2$). **^{13}C NMR** (126 MHz,$CDCl_3$) δ 176.62 (N*C*(O)C), 166.97 (*C*(O)O), 155.58 (N*C*(O)N), 139.01 (Ar*C*H=CHR), 132.91 (Ar*C*), 131.14 (Ar*C*), 130.81 (Ar*C*), 129.96 (Ar*C*), 129.49 (Ar*C*), 127.58 (Ar*C*), 120.85 (ArCH=*C*HR), 59.49 ($C(CH_3)_2$), 51.99 (CO_2CH_3), 25.76

($C(CH_3)_2$), 24.89 ($C(CH_3)_2$). **HRMS** (ESI): m/z calculated for $C_{15}H_{16}N_2O_4$ requires 289.1110 for $[M+H]^+$, found 289.1163.

Synthesis of **3ab**

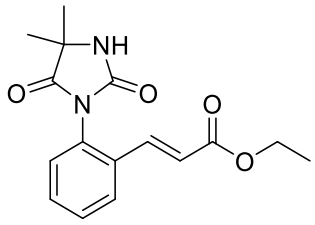

The above compound was synthesized using General Procedure **E** using *N*-arylhydantoin, **1a**, (0.10 g, 0.5 mmol) and ethyl acrylate (0.17 mL, 1.5 mmol). Silica gel chromatography gave an amorphous solid, 73% (0.192 g). **mp** (from $CHCl_3$): 105-107 °C. **FT-IR** (thin film): ν_{max} (cm^{-1}) = 3305.4, 2980.6, 1783.2, 1708.0, 1638.0. **^{1}H NMR** (500 MHz, $CDCl_3$) δ 7.79–7.68 (1H, m, Ar*H*), 7.53–7.43 (3H, m, Ar*H* & ArC*H*=CHR), 7.28 (1H, dd, *J* = 10.3, 8.8 Hz, Ar*H*), 6.97 (1H, s, N*H*), 6.43 (1H, d, *J* = 15.9 Hz, ArCH=C*H*R), 4.22 (1H, qd, *J* = 7.1, 2.3 Hz, $CO_2CH_2CH_3$), 1.56 (3H, s, $C(CH_3)_2$), 1.49 (3H, s, $C(CH_3)_2$), 1.29 (3H, t, *J* = 7.1 Hz, CO_2CH_3). **^{13}C NMR** (126 MHz, $CDCl_3$) δ 176.62 (N*C*(O)C), 166.48 (*C*(O)O), 155.59 (N*C*(O)N), 138.64 (Ar*C*H=CHR), 132.96 (Ar*C*), 131.05 (Ar*C*), 130.77 (Ar*C*), 129.92 (Ar*C*), 129.46 (Ar*C*), 127.51 (Ar*C*), 121.32 (ArCH=*C*HR), 60.82 ($C(CH_3)_2$), 59.45 ($CO_2CH_2CH_3$), 25.77 ($C(CH_3)_2$), 24.81 ($C(CH_3)_2$), 14.38 ($CO_2CH_2CH_3$). **HRMS** (ESI): m/z calculated for $C_{16}H_{18}N_2O_4$ requires 303.1267 for $[M+H]^+$, found 303.1312.

Synthesis of **3ac**

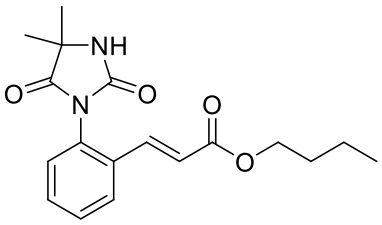

The above compound was synthesized using General Procedure **E** using *N*-arylhydantoin, **1a**, (0.10 g, 0.5 mmol) and butyl acrylate (0.22 mL, 1.5 mmol). Silica gel chromatography gave a thick oil, 94%, (inseparable mixture of 6:1 **3ac**:**1a**) (0.154 g). **^{1}H NMR** (500 MHz, $CDCl_3$) δ 7.73 (1H, dd, *J* = 7.6, 1.8 Hz, ArC*H*=CHR), 7.55–7.43 (3H, m, Ar*H*), 7.28–7.24

(1H, m, Ar*H*), 7.11 (1H, s, N*H*), 6.42 (1H, d, *J* = 15.9 Hz, ArCH=C*H*R), 4.16 (2H, td, *J* = 6.7, 3.9 Hz, $CO_2C\mathit{H}_2R$), 1.69–1.58 (2H, m, $CO_2CH_2C\mathit{H}_2R$), 1.54 (3H, s, $C(C\mathit{H}_3)_2$), 1.47 (3H, s, $C(C\mathit{H}_3)_2$), 1.44–1.34 (2H, m, $CO_2CH_2CH_2C\mathit{H}_2CH_3$), 0.92 (3H, t, *J* = 7.4 Hz, $CO_2CH_2CH_2CH_2C\mathit{H}_3$). **^{13}C NMR** (126 MHz, $cdcl_3$) δ 176.57 (N*C*(O)C), 166.48 (*C*(O)O), 155.50 (N*C*(O)N), 138.52 (Ar*C*H=CHR), 132.86 (Ar*C*), 130.93 (Ar*C*), 130.69 (Ar*C*), 129.79 (Ar*C*), 129.36 (Ar*C*), 129.08 (Ar*C*), 127.42 (Ar*C*), 126.26 (Ar*C*), 121.20 (ArCH=*C*HR), 64.63 ($CO_2\mathit{C}H_2R$), 59.33 ($\mathit{C}(CH_3)_2$), 30.71 ($CO_2CH_2\mathit{C}H_2R$), 25.60, ($C(\mathit{C}H_3)_2$), 24.69 ($C(\mathit{C}H_3)_2$), 19.19 ($CO_2CH_2CH_2\mathit{C}H_2R$), 13.73 ($CO_2CH_2CH_2CH_2\mathit{C}H_3$).

Synthesis of **3ad**

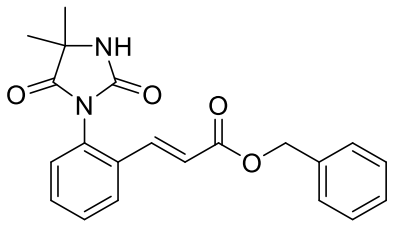

The above compound was synthesized using General Procedure **E** using *N*-arylhydantoin, **1a**, (0.10 g, 0.5 mmol) and benzyl acrylate (0.20 mL, 1.5 mmol). Silica gel chromatography gave an amorphous solid, 79% (0.144 g). **mp** (from $CHCl_3$): 143-145 °C. **FT-IR** (thin film): ν_{max} (cm^{-1}) = 3312.7, 2978.9, 1782.4, 1713.8, 1638.2. **^{1}H NMR** (300 MHz, $CDCl_3$) δ 7.75 (1H, dd, *J* = 7.3, 1.7 Hz, Ar*H*), 7.56 (d, *J* = 15.9 Hz, ArC*H*=CHR), 7.53–7.24 (10H, m, Ar*H* & N*H*), 7.21 (1H, s, Ar*H*), 6.51 (1H, d, *J* = 15.9 Hz, ArCH=C*H*R), 5.30–5.11 (2H, m, $CO_2C\mathit{H}_2Ph$), 1.46 (3H, s, $C(C\mathit{H}_3)_2$), 1.45 (3H, s, $C(C\mathit{H}_3)_2$). **^{13}C NMR** (75 MHz, $CDCl_3$) δ 176.65 (N*C*(O)C), 166.22 (*C*(O)O), 155.59 (N*C*(O)N), 139.06 (Ar*C*H=CHR), 135.76 (Ar*C*), 132.66 (Ar*C*), 131.17 (Ar*C*), 130.75 (Ar*C*), 129.89 (Ar*C*), 129.41 (Ar*C*), 129.17 (Ar*C*), 128.67 (Ar*C*), 128.39 (Ar*C*), 127.43 (Ar*C*), 126.33 (Ar*C*), 120.77 (ArCH=*C*HR), 66.68 ($CO_2\mathit{C}H_2Ph$), 59.36 ($\mathit{C}(CH_3)_2$), 25.54 ($C(\mathit{C}H_3)_2$), 24.66 ($C(\mathit{C}H_3)_2$). **HRMS** (ESI): m/z calculated for $C_{21}H_{20}N_2O_4$ requires 365.1501 for $[M+H]^+$, found 365.1484.

Synthesis of **3b**

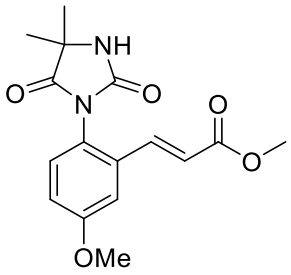

The above compound was synthesized using General Procedure **E** using *N*-arylhydantoin, **1b**, (0.081 g, 0.5 mmol) and methyl acrylate (0.14 mL, 1.5 mmol). Silica gel chromatography gave an off-white solid, 65% (0.101 g). **mp** (from $CHCl_3$): 167-169 °C. **FT-IR** (thin film): ν_{max} (cm^{-1}) = 3317.2, 1779.2, 1711.1, 1642.8. **^{1}H NMR** (500 MHz, $CDCl_3$) δ 7.45 (1H, d, *J* = 15.9 Hz, ArC*H*=CHR), 7.19 (1H, d, *J* = 2.8 Hz, Ar*H*), 7.17 (2H, d, *J* = 8.7 Hz, Ar*H*), 7.02 (2H, m, Ar*H*) 6.40 (1H, d, *J* = 15.9 Hz, ArCH=C*H*R), 3.83 (3H, s, CO_2CH_3), 3.76 (3H, s, ArOCH_3), 1.55 (3H, s, C(CH_3)$_2$), 1.48 (3H, s, C(CH_3)$_2$). **^{13}C NMR** (126 MHz, $CDCl_3$) δ 176.97 (N*C*(O)C), 166.89 (*C*(O)O), 160.40 (Ar*C*OMe), 155.99 (N*C*(O)N), 139.00 (Ar*C*H=CHR), 133.97 (Ar*C*), 130.58 (Ar*C*), 123.49 (Ar*C*), 121.01 (Ar*C*), 117.04 (Ar*C*), 112.20 (ArCH=*C*HR), 59.39 (*C*(CH_3)$_2$), 55.77 (ArO*C*H_3), 51.99 (CO_2CH_3), 25.71 (C(*C*H_3)$_2$), 24.81 (C(*C*H_3)$_2$). **HRMS** (ESI): m/z calculated for $C_{16}H_{18}N_2O_5$ requires 341.1112 for $[M+Na]^+$, found 341.1099.

Synthesis of **3c**

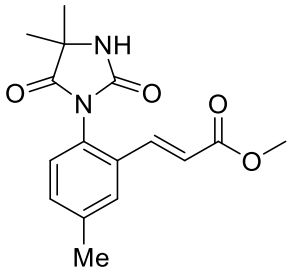

The above compound was synthesized using General Procedure **E** using *N*-arylhydantoin, **1c**, (0.109 g, 0.5 mmol) and methyl acrylate (0.14 mL, 1.5 mmol). Silica gel chromatography gave an off-white solid, 52% (0.079 g). **mp** (from $CHCl_3$): 191-193 °C. **FT-IR** (thin film): ν_{max} (cm^{-1}) = 3313.6, 1778.9, 1707.6, 1641.8. **^{1}H NMR** (500 MHz, $CDCl_3$) δ 7.53 (1H, s, Ar*H*), 7.49 (1H, d, *J* = 15.9 Hz, ArC*H*=CHR), 7.31 (1H, d, *J* = 7.5 Hz, Ar*H*), 7.15 (1H, d, *J* = 8.0 Hz, Ar*H*), 6.99 (1H, s, N*H*), 6.41 (1H, d, *J* = 15.9 Hz, ArCH=C*H*R), 3.76 (3H, s, CO_2CH_3),

2.40 (3H, s, ArCH_3), 1.56 (3H, s, C(CH_3)$_2$), 1.49 (3H, s, C(CH_3)$_2$). **^{13}C NMR** (126 MHz, $CDCl_3$) δ 176.78 (NC(O)C), 167.00 (*C*(O)O), 155.83 (NC(O)N), 140.09 (ArCH=CHR), 139.10 (Ar*C*), 132.53 (Ar*C*), 132.01 (Ar*C*), 129.22 (Ar*C*), 128.26 (Ar*C*), 128.06 (Ar*C*), 120.57 (ArCH=*C*HR), 59.44 (*C*(CH_3)$_2$), 51.93 (CO_2CH$_3$), 25.73 (C(*C*H$_3$)$_2$), 24.85 (C(*C*H$_3$)$_2$), 21.40 (Ar*C*H$_3$). **HRMS** (ESI): m/z calculated for $C_{16}H_{18}N_2O_4$ requires 325.1159 for $[M+Na]^+$, found 325.1154.

Synthesis of **3d**

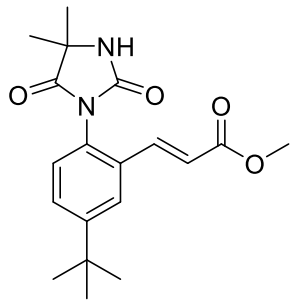

The above compound was synthesized using General Procedure **E** using *N*-arylhydantoin, **1d**, (0.130 g, 0.5 mmol) and methyl acrylate (0.14 mL, 1.5 mmol). Silica gel chromatography gave an off-white solid, 81% (0.140 g). **mp** (from $CHCl_3$): 161-164 °C. **FT-IR** (thin film): ν_{max} (cm^{-1}) = 3310.5, 1780.0, 1709.9, 1640.9. **^{1}H NMR** (500 MHz, $CDCl_3$) δ 7.71 (1H, s, Ar*H*), 7.59–7.47 (2H, m, ArC*H*=CHR & Ar*H*), 7.19 (1H, d, *J* = 8.2 Hz, Ar*H*), 7.08 (1H, s, N*H*), 6.43 (1H, d, *J* = 15.9 Hz, ArCH=C*H*R), 3.76 (3H, s, CO_2CH$_3$), 1.54 (3H, s, C(CH_3)$_2$), 1.47 (3H, s, C(CH_3)$_2$), 1.33 (9H, s, C(CH_3)$_3$). **^{13}C NMR** (126 MHz, $CDCl_3$) δ 176.82 (NC(O)C), 167.00 (*C*(O)O), 155.81 (NC(O)N), 152.92 (Ar*C*H=CHR), 139.62 (Ar*C*), 132.07 (Ar*C*), 128.89 (Ar*C*), 128.60 (Ar*C*), 128.14 (Ar*C*), 124.47 (Ar*C*), 120.34 (ArCH=*C*HR), 59.37 (*C*(CH_3)$_2$), 51.91 (CO_2CH$_3$), 35.02 (*C*(CH_3)$_3$), 31.29 (C(*C*H$_3$)$_3$), 25.67 (*C*(CH_3)$_2$), 24.79 (*C*(CH_3)$_2$). **HRMS** (ESI): m/z calculated for $C_{19}H_{24}N_2O_4$ requires 345.1809 for $[M+H]^+$, found 345.1783.

Synthesis of **3e**

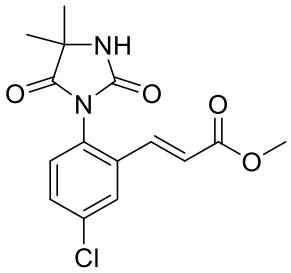

The above compound was synthesized using General Procedure **E** using *N*-arylhydantoin, **1e**, (0.119 g, 0.5 mmol) and methyl acrylate (0.14 mL, 1.5 mmol). Silica gel chromatography gave an off-white solid, 66% (0.106 g). **mp** (from $CHCl_3$): 193-195 °C. **FT-IR** (thin film): ν_{max} (cm^{-1}) = 3317.3, 1782.8, 1714.0, 1641.6. **^{1}H NMR** (500 MHz, $CDCl_3$) δ 7.69 (1H, d, *J* = 2.1 Hz, Ar*H*), 7.49–7.38 (2H. m, ArC*H*=CHR & Ar*H*), 7.22 (1H, d, *J* = 8.5 Hz, Ar*H*), 7.03 (1H, s, N*H*), 6.42 (1H, d, *J* = 15.9 Hz, ArCH=C*H*R), 3.76 (3H, s, CO_2CH_3), 1.56 (3H, s, $C(CH_3)_2$), 1.49 (3H, s, $C(CH_3)_2$). **^{13}C NMR** (126 MHz, $CDCl_3$) δ 176.40 (N*C*(O)C), 166.59 (*C*(O)O), 155.28 (N*C*(O)N), 137.76 (Ar*C*H=CHR), 135.97 (Ar*C*), 134.52 (Ar*C*), 131.02 (Ar*C*), 130.76 (Ar*C*), 129.18 (Ar*C*), 127.56 (Ar*C*), 122.05 (ArCH=*C*HR), 59.56 (*C*(CH_3), 52.11 (CO_2CH_3), 25.74 ($C(CH_3)_2$), 24.82 ($C(CH_3)_2$). **HRMS** (ESI): m/z calculated for $C_{15}H_{15}N_2O_4Cl_1$ requires 323.0799 for $[M+H]^+$, found 323.0770.

Synthesis of **3f**

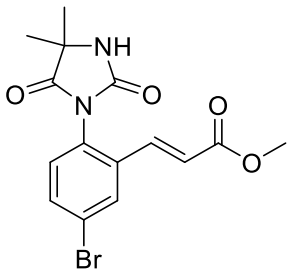

The above compound was synthesized using General Procedure **E** using *N*-arylhydantoin, **1f**, (0.142 g, 0.5 mmol) and methyl acrylate (0.14 mL, 1.5 mmol). Silica gel chromatography gave an off-white solid, 66% (0.122 g). **mp** (from $CHCl_3$): 181-183 °C. **FT-IR** (thin film): ν_{max} (cm^{-1}) = 3314.2, 1783.1, 1709.7, 1640.1. **^{1}H NMR** (500 MHz, $CDCl_3$) δ 7.85 (1H, d, *J* = 2.2 Hz, Ar*H*), 7.60 (1H, dd, *J* = 8.4, 2.2 Hz, Ar*H*), 7.41 (1H, d, *J* = 15.9 Hz, ArC*H*=CHR), 7.15 (1H, d, *J* = 8.4 Hz, Ar*H*), 7.06 (1H, s, N*H*), 6.42 (1H, d, *J* = 15.9 Hz, ArCH=C*H*R), 3.76 (3H, s, CO_2CH_3), 1.55 (3H, s, $C(CH_3)_2$), 1.48 (2H, s, $C(CH_3)_2$). **^{13}C NMR** (126 MHz, $CDCl_3$) δ

176.32 (N*C*(O)C), 166.59 (*C*(O)O), 155.26 (N*C*(O)N), 137.65 (Ar*C*H=CHR), 134.77 (Ar*C*), 133.96 (Ar*C*), 130.95 (Ar*C*), 130.53 (Ar*C*), 129.65 (Ar*C*), 123.97 (Ar*C*), 122.06 (ArCH=*C*HR), 59.58 (*C*(CH_3)$_2$), 52.12 (CO_2*C*H_3), 25.69 (C(*C*H_3)$_2$), 24.78 (C(*C*H_3)$_2$). **HRMS** (ESI): m/z calculated for $C_{15}H_{15}N_2O_4Br_1$ requires 367.0293 for $[M+H]^+$, found 367.0275.

Synthesis of **3g**

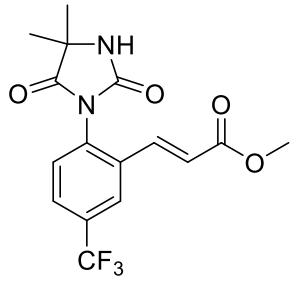

The above compound was synthesized using General Procedure **E** using *N*-arylhydantoin, **1g**, (0.136 g, 0.5 mmol) and methyl acrylate (0.14 mL, 1.5 mmol). Silica gel chromatography gave an off-white solid, 47% (0.084 g). **mp** (from $CHCl_3$): 175-178 °C. **FT-IR** (thin film): ν_{max} (cm^{-1}) = 3300.5, 1785.6, 1713.4, 1644.4. **^{1}H NMR** (500 MHz, $CDCl_3$) δ 7.97 (1H, s, Ar*H*), 7.75 (1H, d, *J* = 8.4 Hz, Ar*H*), 7.51 (1H, d, J = 15.9 Hz, ArC*H*=CHR), 7.43 (1H, d, *J* = 8.2 Hz, Ar*H*), 6.89 (1H, s, N*H*), 6.50 (1H, d, *J* = 15.9 Hz, ArCH=C*H*R), 3.79 (3H, s, CO_2C*H*$_3$), 1.60 (3H, s, C(C*H*$_3$)$_2$), 1.53 (3H, s, C(C*H*$_3$)$_2$). **^{13}C NMR** (126 MHz, $CDCl_3$) δ 176.09 (N*C*(O)C), 166.54 (*C*(O)O), 154.94 (N*C*(O)N), 137.75 (Ar*C*H=CHR), 133.77 (d, *J* = 26.9 Hz, Ar*C*), 132.18 (q, *J* = 33.2 Hz, Ar*C*), 130.22 (Ar*C*), 127.58 (d, *J* = 3.5 Hz, Ar*C*), 124.77 (d, *J* = 3.8 Hz, Ar*C*), 123.29 (q, *J* = 272.7 Hz, Ar*C*F_3). 122.59 (ArC=*C*HR), 59.75 (*C*(CH_3)$_2$), 52.20 (CO_2*C*H_3), 25.81 (C(*C*H_3)$_2$), 24.91 (C(*C*H_3)$_2$). **^{19}F NMR** (470 MHz, $CDCl_3$) δ -63.03 (s). **HRMS** (ESI): m/z calculated for $C_{16}H_{15}N_2O_4F_3$ requires 379.0882 for $[M+Na]^+$, found 379.0870.

Synthesis of **3h**

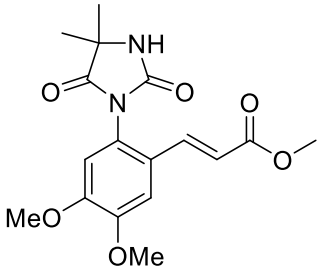

The above compound was synthesized using General Procedure **E** using *N*-arylhydantoin, **1h**, (0.132 g, 0.5 mmol) and methyl acrylate (0.14 mL, 1.5 mmol). Silica gel chromatography gave an off-white solid, 83% (0.145 g). **mp** (from $CHCl_3$): 196-198 °C. **FT-IR** (thin film): ν_{max} (cm^{-1}) = 3328.4, 1779.6, 1712.5, 1634.3. **^{1}H NMR** (500 MHz, $CDCl_3$) δ 7.41 (1H, d, *J* = 15.8 Hz, ArC*H*=CHR), 7.15 (1H, s, Ar*H*), 7.00 (1H, s, N*H*), 6.70 (1H, s, Ar*H*), 6.33 (1H, d, *J* = 15.8 Hz, ArCH=C*H*R), 3.92–3.88 (6H, m, ArOCH_3), 3.74 (3H, s, CO_2CH_3), 1.58 (3H, s, C(CH_3)$_2$), 1.50 (3H, s, C(CH_3)$_2$). **^{13}C NMR** (126 MHz, $CDCl_3$) δ 176.86 (N*C*(O)C), 167.20 (*C*(O)O), 155.84 (N*C*(O)N), 151.62 (Ar*C*OCH_3), 150.10 (Ar*C*OCH_3), 138.60 (Ar*C*H=CHR), 125.27 (Ar*C*), 124.39 (Ar*C*), 118.41 (ArCH=*C*HR), 111.74 (Ar*C*), 108.74 (Ar*C*), 59.43 (*C*(CH_3)$_2$), 56.36 (ArO*C*H_3), 56.26 (ArO*C*H_3), 51.87 (CO_2CH_3), 25.83 (C(*C*H_3)$_2$), 24.82 (C(*C*H_3)$_2$). **HRMS** (ESI): m/z calculated for $C_{17}H_{20}N_2O_6$ requires 349.1355 for $[M+H]^+$, found 349.1374.

Synthesis of **3i**

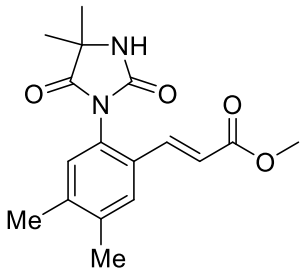

The above compound was synthesized using General Procedure **E** using *N*-arylhydantoin, **1i**, (0.116 g, 0.5 mmol) and methyl acrylate (0.14 mL, 1.5 mmol). Silica gel chromatography gave an off-white solid, 89%, (0.141 g). **mp** (from $CHCl_3$): 232-234 °C. **FT-IR** (thin film): ν_{max} (cm^{-1}) = 3327.5, 1783.6, 1728.0, 1636.1. **^{1}H NMR** (500 MHz, $CDCl_3$) δ 7.51 (1H, s, Ar*H*), 7.46 (1H, d, *J* = 15.9 Hz, ArC*H*=CHR), 7.04 (1H, s, Ar*H*), 6.79 (1H, s, N*H*), 6.39 (1H, d, *J* = 15.9 Hz, ArCH=C*H*R), 3.76 (3H, s, CO_2CH_3), 2.31–2.29 (6H, m, ArCH_3), 1.59 (3H, s, C(CH_3)$_2$), 1.52 (3H, s, C(CH_3)$_2$). **^{13}C NMR** (126 MHz, $CDCl_3$) δ 176.82 (N*C*(O)C), 167.21 (*C*(O)O), 155.92 (N*C*(O)N), 140.80 (Ar*C*H=CHR), 138.98 (Ar*C*), 130.27 (Ar*C*), 130.11 (Ar*C*), 128.50 (Ar*C*), 128.40 (Ar*C*), 119.59 (ArCH=*C*HR), 59.49 (*C*(CH_3)$_2$), 51.91 (CO_2CH_3), 25.80 (C(*C*H_3)$_2$), 24.96 (C(*C*H_3)$_2$), 19.96 (Ar*C*H_3), 19.82 (Ar*C*H_3). **HRMS** (ESI): m/z calculated for $C_{17}H_{20}N_2O_4$ requires 317.1496 for $[M+H]^+$, found 317.1462.

Synthesis of **3ja**

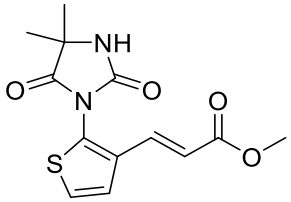

The above compound was synthesized using General Procedure **E** using *N*-arylhydantoin, **1j**, (0.105 g, 0.5 mmol) and methyl acrylate (0.14 mL, 1.5 mmol). Silica gel chromatography gave an off-white solid, 92% (0.135 g). **mp** (from $CHCl_3$): 172-174 °C. **FT-IR** (thin film): ν_{max} (cm^{-1}) = 3327.5, 1783.6, 1723.0, 1636.1. **^{1}H NMR** (500 MHz, $CDCl_3$) δ 7.33 (1H, d, *J* = 5.8 Hz, Ar*H*), 7.24–7.14 (3H. m, ArC*H*=CHR & Ar*H* & N*H*), 6.25 (1H, d, *J* = 15.9 Hz, ArCH=C*H*R), 3.72 (3H, s, CO_2CH_3), 1.48 (6H, s, $C(CH_3)_2$). **^{13}C NMR** (126 MHz, $CDCl_3$) δ 176.30 (N*C*(O)C), 167.30 (*C*(O)O), 154.59 (N*C*(O)N), 134.27 (Ar*C*H=CHR), 134.21 (Ar*C*), 131.65 (Ar*C*), 126.14 (Ar*C*), 124.35 (Ar*C*), 119.59 (ArCH=*C*HR), 59.46 ($C(CH_3)_2$), 51.91 (CO_2CH_3), 25.24 ($C(CH_3)_2$). **HRMS** (ESI): m/z calculated for $C_{13}H_{14}N_2O_4S_1$ requires 295.0708 for $[M+H]^+$, found 295.0706.

Synthesis of **3jb**

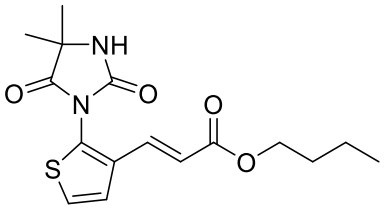

The above compound was synthesized using General Procedure **E** using *N*-arylhydantoin, **1j**, (0.105 g, 0.5 mmol) and butyl acrylate (0.22 mL, 1.5 mmol). Silica gel chromatography gave an amorphous solid, 84%, (0.140 g). **FT-IR** (thin film): ν_{max} (cm^{-1}) = 3317.5, 1788.6, 1728.0, 1634.1. **^{1}H NMR** (500 MHz, $CDCl_3$) δ 7.37–7.22 (3H, m, ArC*H*=CHR & Ar*H*), 6.99 (1H, s, N*H*), 6.27 (1H, d, *J* = 15.9 Hz, ArCH=C*H*R), 4.15 (2H, t, *J* = 6.6 Hz, CO_2CH_2R), 1.63 (2H, dt, *J* = 14.5, 6.7 Hz, $CO_2CH_2CH_2R$), 1.52 (6H, s, $C(CH_3)_2$), 1.38 (2H, dd, *J* = 15.0, 7.5 Hz, $CO_2CH_2CH_2CH_2CH_3$), 0.92 (3H, t, *J* = 7.4 Hz, $CO_2CH_2CH_2CH_2CH_3$). **^{13}C NMR** (126 MHz, $CDCl_3$) δ 176.21 (N*C*(O)C), 166.97 (*C*(O)O), 154.67 (N*C*(O)N), 134.45 (Ar*C*H=CHR), 133.94 (Ar*C*), 131.51 (Ar*C*), 126.16 (Ar*C*), 124.38 (Ar*C*), 120.16 (ArCH=*C*HR), 64.71 (CO_2CH_2R), 59.53 ($C(CH_3)_2$), 30.84 ($CO_2CH_2CH_2R$), 25.37 ($C(CH_3)_2$), 19.32

($CO_2CH_2CH_2CH_2CH_3$), 13.86. ($CO_2CH_2CH_2CH_2CH_3$). **HRMS** (ESI): m/z calculated for $C_{16}H_{20}N_2O_4S_1$ requires 337.1177 for $[M+H]^+$, found 337.1179.

Synthesis of **3k**

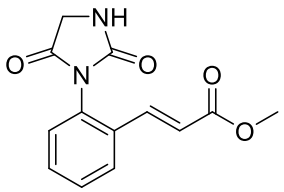

The above compound was synthesized using General Procedure **E** using *N*-arylhydantoin, **1k**, (0.088 g, 0.5 mmol) and methyl acrylate (0.14 mL, 1.5 mmol). Silica gel chromatography gave a white solid, 35% (0.045 g). **mp** (from $CHCl_3$): 154-157 °C **FT-IR** (thin film): ν_{max} (cm^{-1}) = 3301.9, 1778.4, 1708.4, 1638.3. **^{1}H NMR** (500 MHz, $CDCl_3$) δ 7.76 (1H, d, *J* = 7.5 Hz, Ar*H*), 7.59–7.45 (3H, m, Ar*H* & ArC*H*=CHR), 7.27 (1H, d, *J* = 7.9 Hz, Ar*H*), 6.81 (1H, s, N*H*), 6.47 (1H, d, *J* = 15.9 Hz, ArCH=C*H*R), 4.18 (1H, d, *J* = 17.8 Hz, CH_2), 4.09 (1H, d, *J* = 17.8 Hz, CH_2), 3.78 (3H, s, CO_2CH_3). **^{13}C NMR** (126 MHz, $CDCl_3$) δ 170.52 (N*C*(O)C), 167.11 (*C*(O)O), 157.53 (N*C*(O)N), 139.06 (Ar*C*H=CHR), 132.92 (Ar*C*), 131.24 (Ar*C*), 130.70 (Ar*C*), 130.05 (Ar*C*), 129.36 (Ar*C*), 127.66 (Ar*C*), 121.00 (ArCH=*C*HR), 52.07 (CO_2CH_3), 47.01 (CH_2). **HRMS** (ESI): m/z calculated for $C_{13}H_{12}N_2O_4$ requires 283.0697 for $[M+Na]^+$, found 283.0674.

Synthesis of **3l**

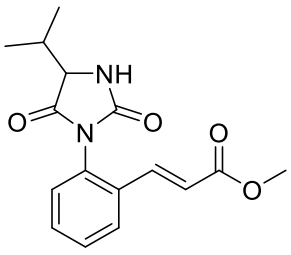

The above compound was synthesized using General Procedure **E** using *N*-arylhydantoin, **1l**, (0.109 g, 0.5 mmol) and methyl acrylate (0.14 mL, 1.5 mmol). Silica gel chromatography gave a white solid, 67% (0.101 g). **mp** (from $CHCl_3$): 178-180 °C. **FT-IR** (thin film): ν_{max} (cm^{-1}) = 3301.9, 1778.4, 1708.4, 1638.3. **^{1}H NMR** (400 MHz, DMSO-d_6, 368 K) δ 8.22 (1H, d, *J* = 25.3 Hz, ArC*H*=CHR), 7.93–7.86 (1H, m, Ar*H*), 7.57–7.45 (3H, m, Ar*H*), 7.28 (1H, s, N*H*), 6.53 (1H, d, *J* = 16.0 Hz, ArCH=C*H*R), 4.20 (1H, d, *J* = 2.7 Hz, C*H*(*i*Pr)), 3.73 (3H, s,

CO_2CH_3), 2.20 (1H, dtd, *J* = 13.7, 6.9, 3.9 Hz, C*H*$(CH_3)_2$), 1.10 (3H, d, *J* = 7.0 Hz, CH(C*H*$_3)_2$), 1.03 (3H, d, *J* = 6.8 Hz, CH(C*H*$_3)_2$). **^{13}C NMR** (101 MHz, DMSO-d_6, 368 K) 172.16 (N*C*(O)C), 165.5 (*C*(O)O), 155.32 (N*C*(O)N), 138.36 (Ar*C*H=CHR), 132.04 (Ar*C*), 131.14 (Ar*C*), 130.14 (Ar*C*), 129.04 (Ar*C*), 128.69 (Ar*C*), 126.66 (Ar*C*), 119.96 (ArCH=*C*HR), 50.75 (N*C*HC=O), 29.46 (C*H*$(CH_3)_2$), 17.67 (CH(C*H*$_3)_2$), 15.76 (CH(C*H*$_3)_2$). **HRMS** (ESI): m/z calculated for $C_{16}H_{18}N_2O_4$ requires 325.1167 for $[M+Na]^+$, found 325.1146.

Synthesis of **3m**

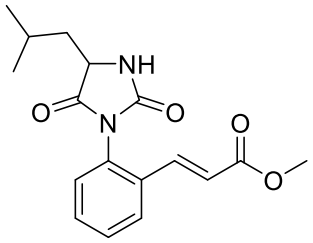

The above compound was synthesized using General Procedure **E** on half scale using *N*-arylhydantoin, **1m**, (0.63 g, 0.25 mmol) and methyl acrylate (0.07 mL, 0.75 mmol). Silica gel chromatography gave an white solid, 56% (0.044 g). **FT-IR** (thin film): ν_{max} (cm^{-1}) = 3298.62, 2957.1, 1780.9, 1716.5, 1638.7. **^{1}H NMR** (400 MHz, DMSO-d_6, 368 K) δ 8.41–8.29 (s, 1H, N*H*), 7.89 (1H, dd, *J* = 7.5, 1.9 Hz,Ar*H*), 7.59–7.41 (3H, m, Ar*H* & ArC*H*=CHR), 7.34–7.26 (1H, m, Ar*H*), 6.52 (1H, d, *J* = 16.0 Hz, ArCH=C*H*R), 4.31 (1H, app s, NC*H*C=O), 3.74 (3H, s, CO_2CH_3), 3.14–2.85 (2H, m, CH_2*i*Pr), 1.94 (1H, ddt, *J* = 14.6, 13.0, 6.6 Hz, C*H*$(CH_3)_2$), 1.00 (6H, app d, CH(C*H*$_3)_2$). **^{13}C NMR** (101 MHz, DMSO-d_6, 368 K) δ 173.17 (N*C*(O)C), 165.51 (*C*(O)O), 154.92 (N*C*(O)N), 138.27 (Ar*C*H=CHR), 132.01 (Ar*C*), 131.05 (Ar*C*), 130.09 (Ar*C*), 128.67 (Ar*C*), 126.83 (Ar*C*), 125.82 (Ar*C*), 119.99 (ArCH=*C*HR), 55.13 (N*C*HC=O), 50.78 (CO_2CH_3, 23.61 (*C*H*i*Pr), 22.34 (*C*H$(CH_3)_2$), 21.30 (CH(*C*H$_3)_2$). **HRMS** (ESI): m/z calculated for $C_{17}H_{20}N_2O_4$ requires 317.1501 for $[M+H]^+$, found 317.1493.

Synthesis of **3n**

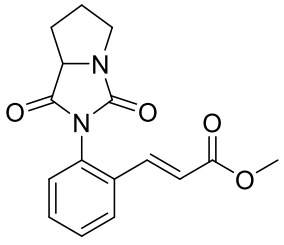

The above compound was synthesized using General Procedure **E** using *N*-arylhydantoin, **1n**, (0.108 g, 0.5 mmol) and methyl acrylate (0.14 mL, 1.5 mmol). Silica gel chromatography gave an amorphous solid, 69% (0.103 g). **FT-IR** (thin film): ν_{max} (cm^{-1}) = 2953.6, 1777.9, 1710.6, 1637.6. **^{1}H NMR** (500 MHz, DMSO-d_6, 368 K) δ 7.90 (1H, dd, *J* = 7.6, 1.8 Hz, Ar*H*), 7.60–7.48 (2H, m, Ar*H* & ArC*H*=CHR), 7.37 (1H, app s, Ar*H*), 7.39–7.34 (1H, m, Ar*H*), 6.53 (1H, d, *J* = 15.9 Hz, ArCH=C*H*R), 4.44 (1H, t, *J* = 8.3 Hz, NC*H*C=O), 3.74 (3H, s, CO_2CH_3), 3.69 (1H, q, *J* = 7.9 Hz, Pro*H*), 3.27 (1H, ddd, *J* = 11.1, 7.5, 5.7 Hz, Pro*H*), 2.50 (1H, p, *J* = 1.9 Hz, Pro*H*), 2.29 (1H, app s, Pro*H*), 2.11 (2H, m, Pro*H*), 1.89 (1H, app s, Pro*H*). **^{13}C NMR** (126 MHz, DMSO) δ 172.30 (N*C*(O)C), 165.61 (*C*(O)O), 158.37 (N*C*(O)N), 138.01 (Ar*C*H=CHR), 131.83 (Ar*C*), 130.88 (Ar*C*), 130.24 (Ar*C*), 128.98 (Ar*C*), 126.93 (Ar*C*), 120.19 (ArCH=*C*HR), 62.61 (N*C*HC=O), 50.92 (CO_2CH_3), 45.24 (Pro*C*), 26.66 (Pro*C*), 25.79 (Pro*C*). **HRMS** (ESI): m/z calculated for $C_{16}H_{16}N_2O_4$ requires 323.1010 for $[M+Na]^+$, found 323.1022.

Synthesis of **3oa**

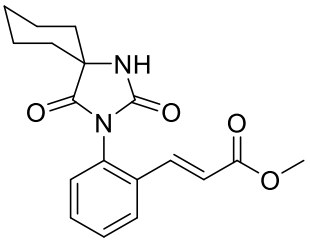

The above compound was synthesized using General Procedure **E** using *N*-arylhydantoin, **1o**, (0.122 g, 0.5 mmol) and methyl acrylate (0.14 mL, 1.5 mmol). Silica gel chromatography gave a white solid, 82% (0.135 g). **mp** (from $CHCl_3$): 228-229 °C **FT-IR** (thin film): ν_{max} (cm^{-1}) = 3288.9, 1777.8, 1708.3, 1638.1. **^{1}H NMR** (500 MHz, $CDCl_3$) δ 7.72 (1H, d, *J* = 7.4 Hz, Ar*H*), 7.61–7.42 (4H, m, Ar*H* & N*H* & ArC*H*=CHR), 7.25 (1H, d, *J* = 7.3 Hz, Ar*H*), 6.42 (1H, d, *J* = 15.9 Hz, ArCH=C*H*R), 3.75 (3H, s, CO_2C_{H3}), 2.07–1.67 (6H, m, Alkyl-C*H*), 1.61–1.23 (2H, m, Alkyl-C*H*). **^{13}C NMR** (126 MHz, $CDCl_3$) δ 176.21 (N*C*(O)C), 166.94 (*C*(O)O), 155.97 (N*C*(O)N), 139.15 (Ar*C*H=CHR), 132.85 (Ar*C*), 131.02 (Ar*C*), 130.89 (Ar*C*), 129.74 (Ar*C*), 129.47 (Ar*C*), 127.42 (Ar*C*), 120.60 (ArCH=*C*HR), 62.51 (*C*(Cyclohexyl)), 51.93 (CO_2CH_3), 34.30 (AlkC*H*), 33.44 (AlkC*H*), 24.63 (AlkC*H*), 21.70 (AlkC*H*), 21.61 (AlkC*H*). **HRMS** (ESI): m/z calculated for $C_{18}H_{20}N_2O_4$ requires 329.1496 for $[M+H]^+$, found 329.1289.

Synthesis of **3ob**

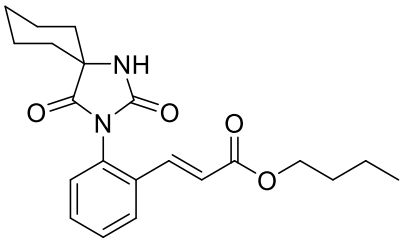

The above compound was synthesized using General Procedure **E** using *N*-arylhydantoin, **1o**, (0.122 g, 0.5 mmol) and butyl acrylate (0.14 mL, 1.5 mmol). Silica gel chromatography gave a white solid, 81% (0.150 g). **mp** (from $CHCl_3$): 157-159 °C **FT-IR** (thin film): ν_{max} (cm^{-1}) = 3284.3, 1778.3, 1707.8, 1638.0. **^{1}H NMR** (500 MHz, $CDCl_3$) δ 7.72 (1H, d, *J* = 7.3 Hz, Ar*H*), 7.68 (1H, s, Ar*H*), 7.53–7.37 (4H, m, N*H* & Ar*H* & ArC*H*=CHR), 7.25 (1H, d, *J* = 7.7 Hz, Ar*H*), 6.41 (1H, d, *J* = 15.9 Hz, ArCH=C*H*R), 4.22–4.09 (2H, m, CO_2CH_2R), 2.00–1.85 (2H, m, $CO_2CH_2CH_2$R), 1.83–1.53 (8H, m, Cyclohexyl-C*H* & *n*-Butyl-C*H*), 1.46–1.30 (5H, m, Cyclohexyl-C*H* & *n*-Butyl-C*H*), 0.92 (3H, t, *J* = 7.4 Hz, $CO_2CH_2CH_2CH_2CH_3$). **^{13}C NMR** (126 MHz, $CDCl_3$) δ 176.19 (N*C*(O)C), 166.53 (*C*(O)O), 156.00 (N*C*(O)N), 138.73 (Ar*C*H=CHR), 132.92 (Ar*C*), 130.90 (Ar*C*), 130.83 (Ar*C*), 129.70 (Ar*C*), 129.45 (Ar*C*), 129.05 (Ar*C*), 127.39 (Ar*C*), 126.31 (Ar*C*), 121.09 (ArCH=*C*HR), 64.65 (*C*(Cyclohexyl)), 62.49 (CO_2CH_2R), 34.34 (Alk*C*), 33.75 (Alk*C*), 33.39 (Alk*C*), 30.82 (Alk*C*), 24.62 (Alk*C*), 21.67 (Alk*C*), 21.62 (Alk*C*), 21.57 (Alk*C*), 19.29 (Alk*C*), 13.85 ($CO_2CH_2CH_2CH_2CH_3$). **HRMS** (ESI): m/z calculated for $C_{21}H_{26}N_2O_4$ requires 393.1793 for $[M+Na]^+$, found 393.1825.

Synthesis of **3p**

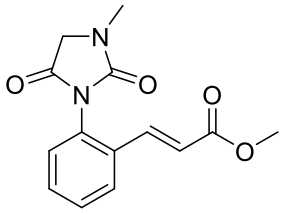

The above compound was synthesized using General Procedure **E** using *N*-arylhydantoin, **1p**, (0.095 g, 0.5 mmol) and methyl acrylate (0.14 mL, 1.5 mmol). Silica gel chromatography gave an amorphous solid, 45% (0.062 g). **FT-IR** (thin film): ν_{max} (cm^{-1}) = 1778.0, 1710.0, 1636.7. **^{1}H NMR** (500 MHz, $CDCl_3$) δ 7.73 (1H, dd, *J* = 7.6, 1.8 Hz, Ar*H*), 7.52 (1H, d, *J* = 15.9, 7.0 Hz, ArC*H*=CHR), 7.25–7.20 (2H, m, Ar*H*), 6.44 (1H. d, *J* = 15.9 Hz, ArCH=C*H*R), 4.15 (1H, d, *J* = 17.7 Hz, CCH_2N), 4.03 (1H, d, *J* = 17.7 Hz, CCH_2N), 3.76 (3H, s, CO_2CH_3),

3.06 (3H, s, NC*H*$_3$). **^{13}C NMR** (126 MHz,$CDCl_3$) δ 168.92 (N*C*(O)C), 167.08 (*C*(O)O), 155.71 (N*C*(O)N), 139.26 (Ar*C*H=CHR), 132.86 (Ar*C*), 131.17 (Ar*C*), 131.11 (Ar*C*), 129.81 (Ar*C*), 129.27 (Ar*C*), 127.53 (Ar*C*), 120.72 (ArCH=*C*HR), 52.03 (CO_2CH_3), 51.96 (CH_2), 30.15 (NCH_3). **HRMS** (ESI): m/z calculated for $C_{14}H_{14}N_2O_4$ requires 275.1032 for $[M+H]^+$, found 275.1018.

Synthesis of **3r**

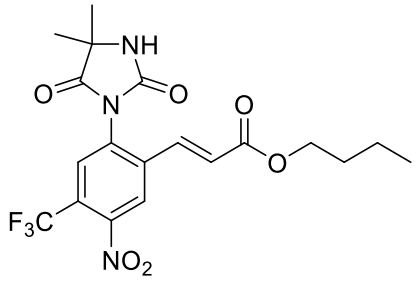

The above compound was synthesized using General Procedure **E** using *N*-arylhydantoin, **1r**, (0.159 g, 0.5 mmol) and butyl acrylate (0.22 mL, 1.5 mmol). Silica gel chromatography gave an off white anorphous solid, 14%, (0.030 g). **FT-IR** (thin film): ν_{max} (cm^{-1}) = 3310.8, 2964.6, 1789.8, 1722.1, 1643.8, 1546.1, 1387.0. **^{1}H NMR** (500 MHz, $CDCl_3$) δ 8.21 (1H, s, Ar*H*), 7.77 (1H, s, Ar*H*), 7.44 (1H, d, *J* = 15.9 Hz, ArC*H*=CHR), 6.57 (1H, d, *J* = 15.9 Hz, ArCH=C*H*R), 5.98 (1H, s, N*H*), 4.21 (2H, t, *J* = 6.6 Hz, CO_2CH_2R), 1.70–1.57 (8H, m, $C(CH_3)_2$ & $CO_2CH_2CH_2$R), 1.42 (2H, dq, *J* = 14.5, 7.3 Hz, $CO_2CH_2CH_2CH_2CH_3$), 0.95 (2H, t, *J* = 7.4 Hz, $CO_2CH_2CH_2CH_2CH_3$). **^{13}C NMR** (126 MHz, $CDCl_3$) δ 175.22 (N*C*(O)C), 165.43 (*C*(O)O), 153.49 (N*C*(O)N), 148.15 (Ar*C*H=CHR), 138.41 (Ar*C*NO_2), 135.34 (Ar*C*), 133.83 (Ar*C*), 129.65 (q, *J* = 5.3 Hz, Ar*C*F_3), 125.99 (Ar*C*), 125.28 (d, *J* = 35.3 Hz, Ar*C*), 124.45 (Ar*C*), 122.48 (Ar*C*), 120.30 (ArC=*C*HR), 65.47 ($C(CH_3)_2$), 60.04 (CO_2CH_2R), 30.80 ($CO_2CH_2CH_2$R), 25.99 ($C(CH_3)_2$), 25.14 ($C(CH_3)_2$), 19.34 ($CO_2CH_2CH_2CH_2CH_3$), 13.88 ($CO_2CH_2CH_2CH_2CH_3$). **^{19}F NMR** (470 MHz, $CDCl_3$) δ -60.06 (s, CF_3). **HRMS** (ESI): m/z calculated for $C_{19}H_{20}N_3O_6F_3$ requires 444.1377 for $[M+H]^+$, found 444.1355.

6.2.5: Competition Experiments

Intermolecular competition experiment between electron rich and electron poor substrates

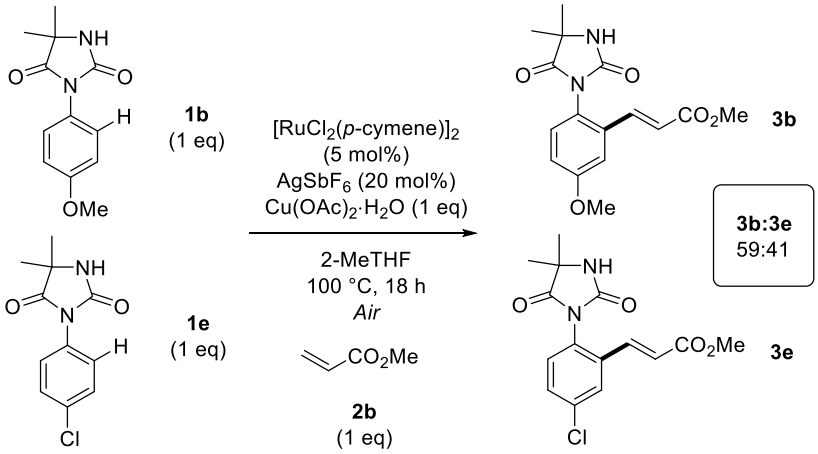

Overlaid Spectra of 3b (OMe, Red) and 3e (Cl, Blue)

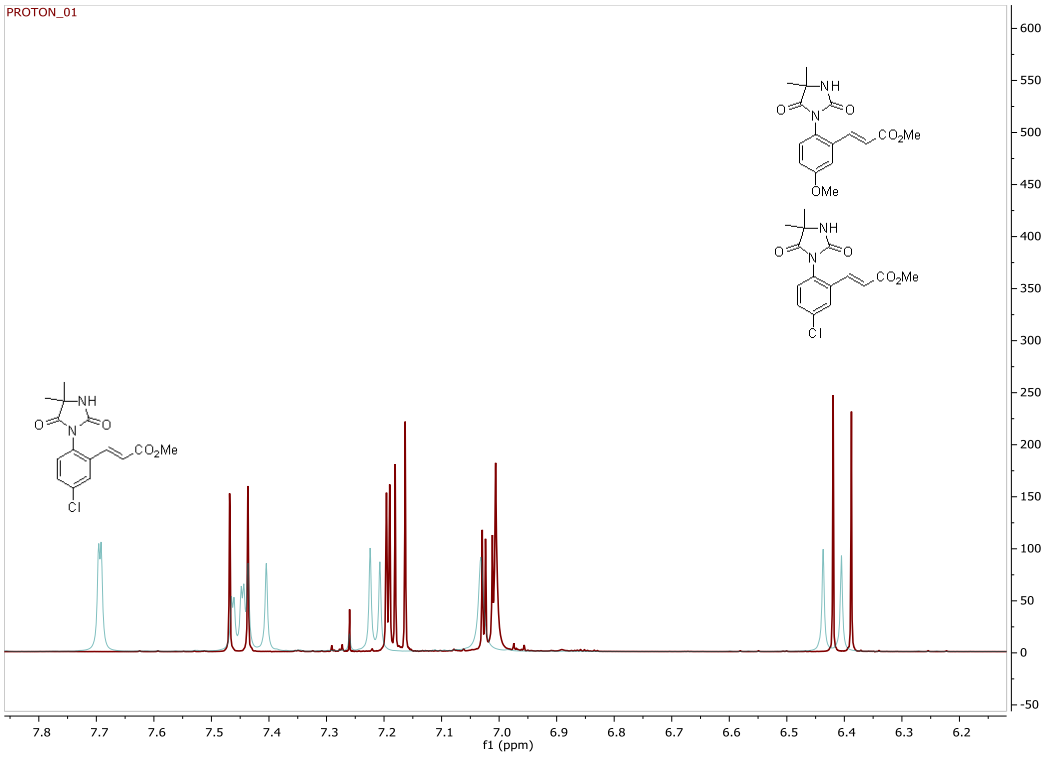

Crude Reaction Mixture of Competition Experiment Between 3b and 3e

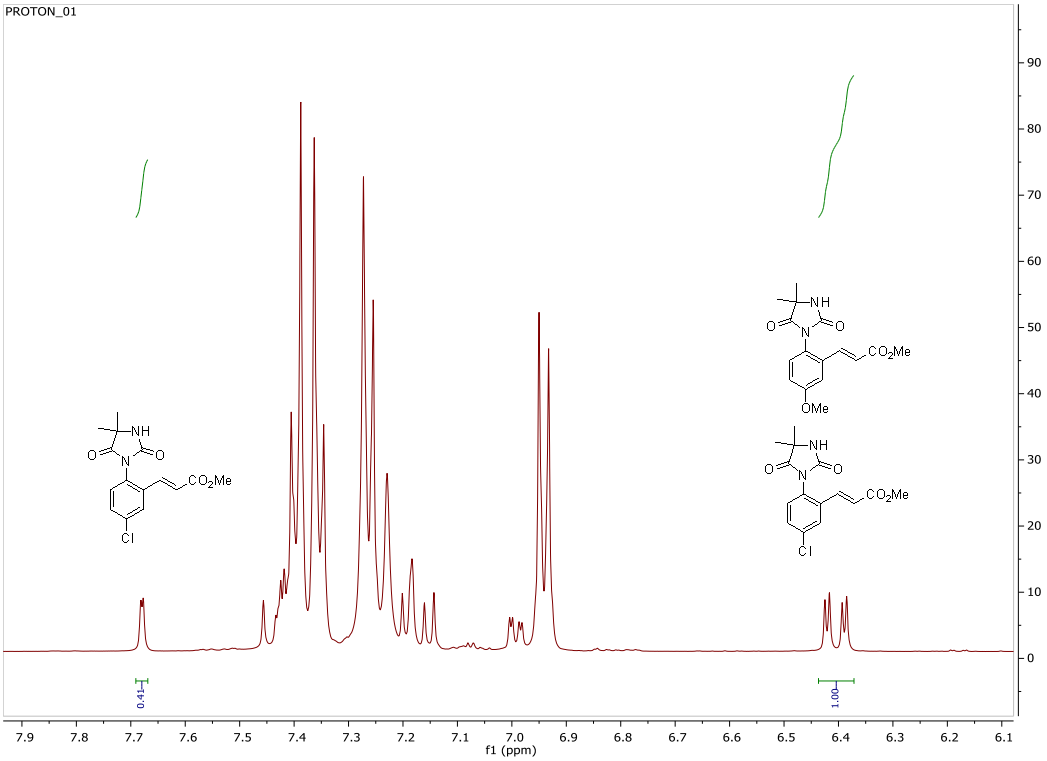

Competition experiment between hydantoin and oxazolidinone directing groups

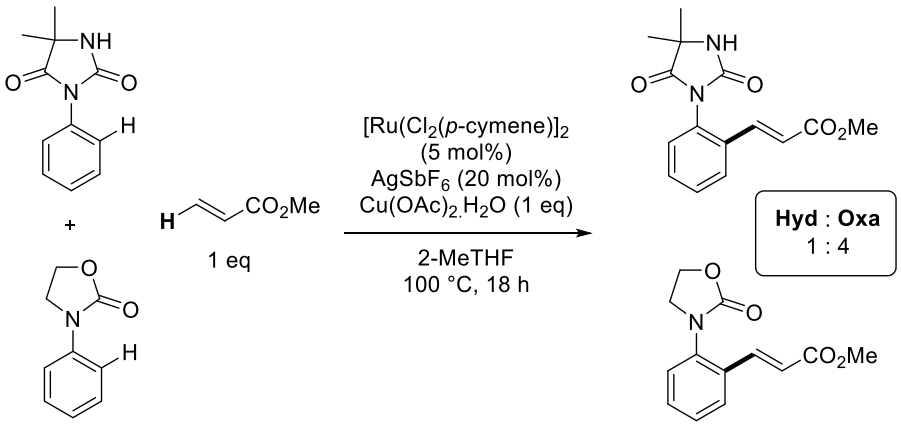

^{1}H NMR of crude mixture showing ratios between diagnostic protons showing ratio of Hyd:Oxa as 1:4. NMR signals are taken from this work and oxazolidinone reference.[6]

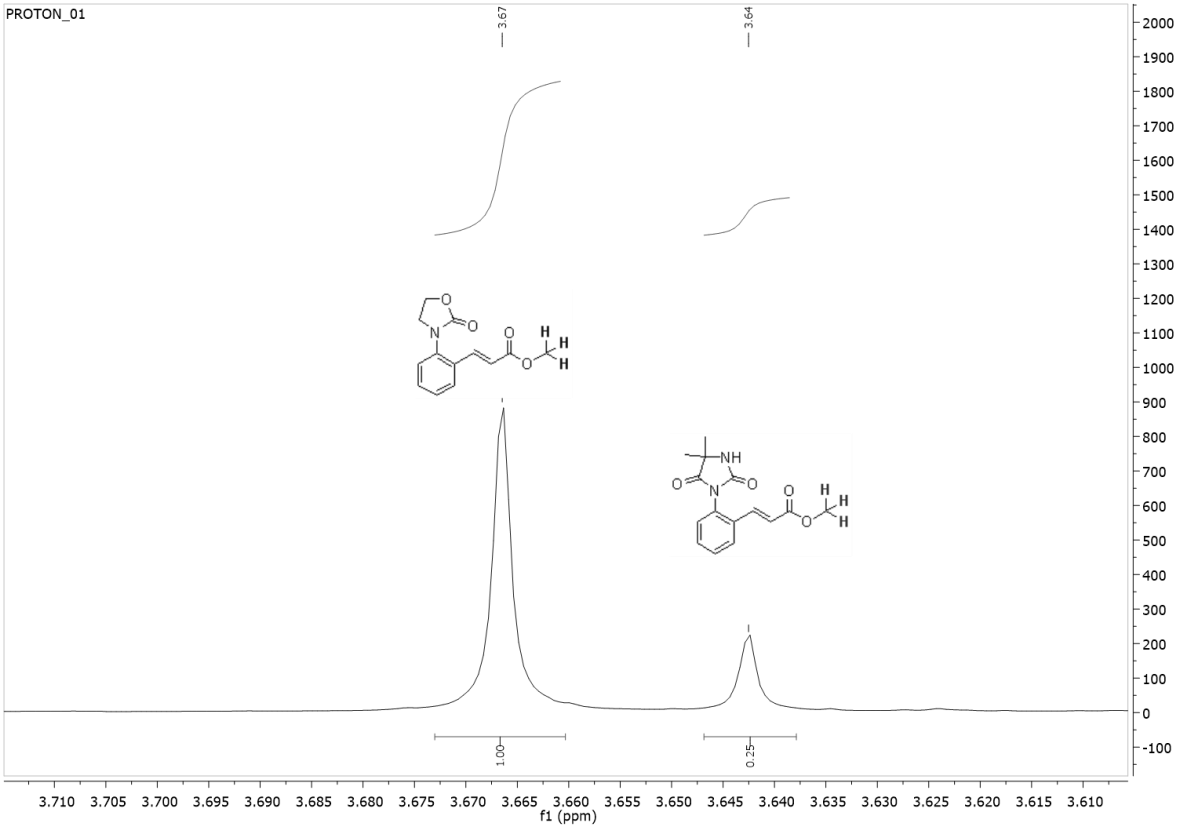

6.2.6: Mechanism

Scheme S1: Mechanism of Hydantoin Directed C–H Alkenylation

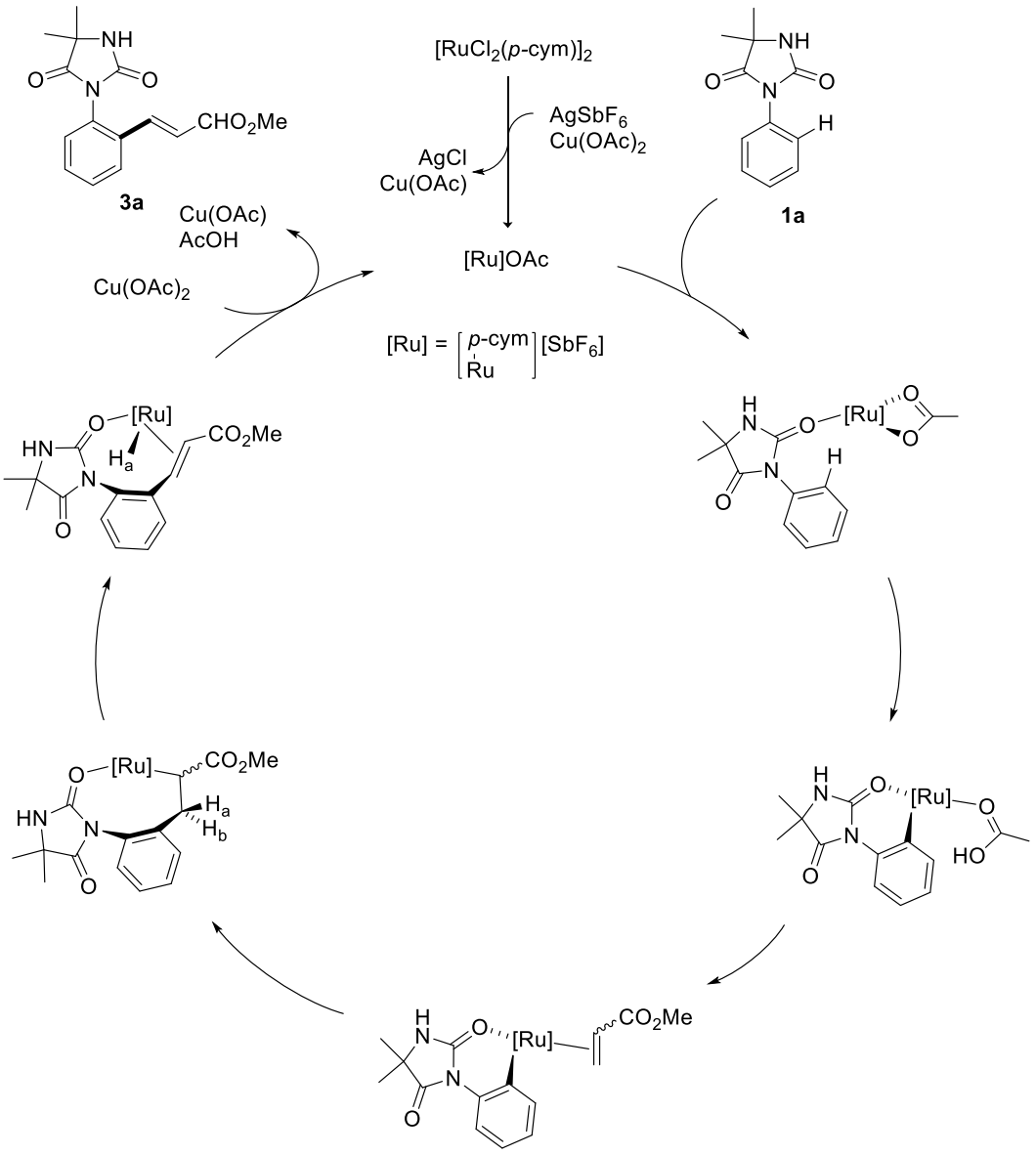

6.2.7: Synthesis of Succinimide Starting Materials

General Procedure **F** for the Formation of *N*-arylsuccinimides

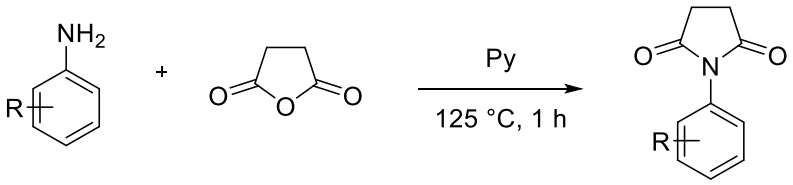

In an oven dried carousel tube, to a solution of substituted aniline (1.3 eq) in pyridine (1 mL) was added succinic anhydride (1 eq). The carousel tube was sealed with a Teflon cap with the tap closed and heated to 125 °C for 1 hr. The reaction was allowed to return to room temperature before quenching with H_2O (1 mL). HCl (1 M) was added until the aqueous solution was pH 3 and a crystalline solid falls out of solution. This solid was filtered and recrystallized from EtOH to give arylsuccinimide products.

Synthesis of **4a**

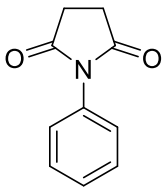

To a solution of freshly redistilled aniline (12 mL, 131.4 mmol) in pyridine (10 mL) was added succinic anhydride (10 g, 100 mmol) and the reaction was heated to reflux for 1 hr. The reaction was allowed to return to room temperature before quenching with H_2O (20 mL). HCl (1 M) was added until the aqueous solution was pH 3 and a crystalline solid falls out of solution. This solid was filtered and was recrystallized from EtOH to give crystalline white solid, **5c**, 56% (9.70 g). **^{1}H NMR** (500 MHz, $CDCl_3$) δ 7.51–7.45 (2H, m, Ar*H*), 7.42–7.37 (1H, m, Ar*H*), 7.30–7.27 (2H, m, Ar*H*), 2.89 (4H, s, CH_2). **^{13}C NMR** (126 MHz, $CDCl_3$) δ 176.32 (N*C*(O)CH_2), 132.07 (Ar*C*), 129.37 (Ar*C*), 128.82 (Ar*C*), 126.63 (Ar*C*), 28.59 (Ar*C*). Data is line with literature precedent.[7]

Synthesis of **4b**

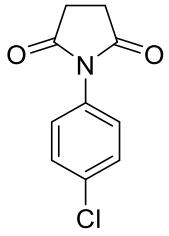

General Procedure **F** was followed using the following compounds: 4-chloroaniline, (1.66 g, 13 mmol), succinic anhydride (1 g, 10 mmol). Filtration gave a brown solid, 69% (1.45 g). **^{1}H NMR:** (500 MHz, $CDCl_3$ δ 7.46 – 7.43 (2H, d, J=8.6 Hz, Ar*H*), 7.25 (2H, d, J=8.6 Hz, Ar*H*), 2.89 (4H, s, C*H*$_2$). **^{13}C NMR:** (126 MHz, $CDCl_3$) δ 175.75 (N*C*(O)CH_2), 135.41 (Ar*C*), 129.35 (Ar*C*), 127.62 (Ar*C*), 28.35 (*C*H_2NC(O)). Data is in line with literature precedent.[8]

Synthesis of **4c**

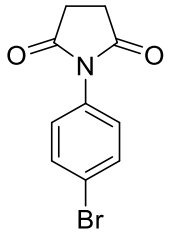

General Procedure **F** was followed using the following compounds: 4-bromoaniline, (2.33 g, 13 mmol), succinic anhydride (1 g, 10 mmol). Filtration gave an off-white solid, 82% (2.09 g). **^{1}H NMR:** (500 MHz, $CDCl_3$) δ 7.59 (2H, app d, Ar*H*), 7.19 (2H, app d, Ar*H*), 2.88 (4H, d, *J* = 4.3 Hz, CH_2). **^{13}C NMR:** (126 MHz, $CDCl_3$) δ 175.71 (N*C*(O)CH_2), 132.34 (Ar*C*), 130.85 (Ar*C*), 127.90 (Ar*C*), 122.44 (Ar*C*), 28.36 (*C*H_2NC(O)). Data is in line with literature precedent.[9]

Synthesis of **4d**

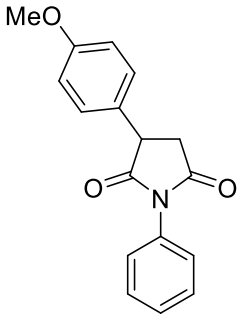

The combined solids: N-phenylmaleimide, (0.346 g, 2 mmol), 4-methoxyphenylboronic acid (0.911 g, 6 mmol) and $[RhCl(COD)]_2$ (0.049 g, 0.1 mmol) were added to an oven-dried carousel tube. The carousel tube was sealed with a Teflon cap ensuring the tap was closed. The solids were dissolved in de-oxygenated 1,4-dioxane (1.12 mL) and the solution stirred at room temperature for 15 minutes. To this solution was added KOH (50% in H_2O) (0.112 mL, 0.056 g, 1 mmol) and the solution heated to 50 °C for 18 h. The reaction mixture was diluted in EtOAc and filtered using a silica plug, eluting with EtOAc. The solvent was removed in vacuo and the crude mixture was purified using column chromatography (EtOAc:Hexanes) to yield a white solid, **4d**, 71% (0.401 g).**mp** (from $CHCl_3$) = 154-157 °C. **FT-IR:** (thin film): vmax (cm^{-1}) = 3060.1, 2996.6, 1701.8, 1642.1, 1609.0. **^{1}H NMR:** (500 MHz, $CDCl_3$) δ 7.48 (2H, t, *J* = 7.7 Hz, Ar*H*), 7.41 (1H, d, *J* = 7.4 Hz, Ar*H*), 7.34 – 7.31 (2H, m, Ar*H*), 7.24 (2H, d, *J* = 8.6 Hz, Ar*H*), 6.93 (2H, d, *J* = 8.7 Hz, Ar*H*), 4.14 (1, dd, *J* = 9.7, 4.8 Hz, C*H*), 3.81 (3H, s, OCH_3), 3.36 (1H, dd, *J* = 18.5, 9.7 Hz, CH_2), 2.97 (1 H, dd, *J* = 18.5, 4.8 Hz, CH_2). **^{13}C NMR:** (126 MHz, $CDCl_3$) δ 176.85 (N*C*(O)CHAr), 175.16 (N*C*(O)CH_2), 159.34 (Ar*C*), 131.95 (Ar*C*), 129.16 (Ar*C*), 129.04 (Ar*C*), 128.64 (Ar*C*), 128.43 (Ar*C*), 126.44 (Ar*C*), 114.68 (Ar*C*), 55.34 (O*C*H_3), 45.22 (Ar*C*HC(O)N), 37.31 (*C*H_2C(O)N). **HRMS:** (ESI): m/z calculated for $C_{17}H_{16}N_1O_3$ requires 282.1130 for $[M+H]^+$, found 282.1110

6.2.8: Synthesis of C–H Functionalized *N*-arylsuccinimides

General Procedure **G** for the Synthesis of C–H Alkenylated Succinimides

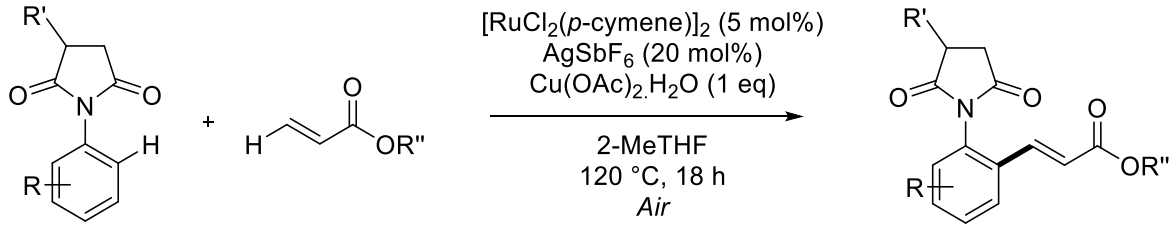

To an oven dried carousel tube was added *N*-arylsuccinimide (0.5 mmol), $[RuCl_2(p\text{-cymene})]_2$ (0.016 g, 0.025 mmol), $AgSbF_6$ (0.035 g, 0.1 mmol) and $Cu(OAc)_2.H_2O$ (0.10 g, 0.5 mmol). The carousel tube was sealed with a Teflon cap leaving the tap open. To the tube was added 2-MeTHF (2 mL, 0.25 M) followed by appropriate acrylate coupling partner (1.5 mmol). The resulting mixture was stirred at 100 °C under reflux for 18 hours. The mixture was quenched with EtOAc (4 mL) and allowed to return to room temperature. The crude mixture was filtered using a short plug of silica, eluting with EtOAc. The filtrate was concentrated *in vacuo*. The crude mixture was purified using silica gel chromatography (EtOAc:Petroleum Spirit 40-60 °C) to give pure C–H alkenylated *N*-arylsuccinimide.

Synthesis of **5a**

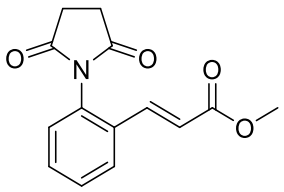

General Procedure **G** was followed using the following compounds: *N*-phenylsuccinimide, **4a,** (0.088 g, 0.5 mmol), methyl acrylate (0.14 mL, 0.13 g, 1.5 mmol), $[RuCl_2(p\text{-cymene})]_2$ (0.016 g, 0.025 mmol), $AgSbF_6$ (0.035 g, 0.1 mmol), $Cu(OAc)_2.H_2O$ (0.10 g, 0.5 mmol). The solvent was removed *in vacuo* and the crude mixture was purified using column chromatography (EtOAc:Hexanes) to yield a white solid, **5a**, 54% (0.14 g). **mp** (from $CHCl_3$) = 108-110 °C. **FT-IR** (thin film): vmax (cm-1) = 1708.6, 1638.1. **^{1}H NMR** (500 MHz, $CDCl_3$) δ 7.75 (1H, dd, *J* = 7.5, 1.8 Hz, Ar*H*), 7.53–7.47 (2H, m, Ar*H*), 7.41 (1H, d, *J* = 15.9 Hz, ArC*H*=CHR), 7.16 (1H, dd, *J* = 7.6, 1.5 Hz, Ar*H*), 6.44 (1H, d, *J* = 15.9 Hz, ArCH=C*H*R), 3.78 (3H, s, OCH_3), 3.07–2.91 (4H, m, CH_2). **^{13}C NMR** (126 MHz, $CDCl_3$) δ 176.21 (*C*(O)O), 166.98 (N*C*(O)C), 138.88 (Ar*C*H=CHR), 132.48 (Ar*C*), 131.21 (Ar*C*), 130.03 (Ar*C*), 129.00

(Ar*C*), 127.66 (Ar*C*), 126.65 (Ar*C*), 121.12 (ArCH=*C*HR), 52.04 (O*C*H_3), 28.85 (*C*H_2). **HRMS** (ESI): m/z calculated for $C_{14}H_{13}N_1O_4$ requires 282.0743 for $[M+Na]^+$, found 282.0713

Synthesis of **5b**

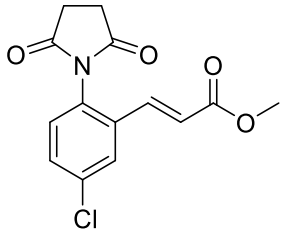

General Procedure **G** was followed using the following compounds: *N*-(4-chlorophenyl)succinimide, **4b,** (0.105 g, 0.5 mmol), methyl acrylate (0.14 mL, 0.13 g, 1.5 mmol), $[RuCl_2(p\text{-cymene})]_2$ (0.016 g, 0.025 mmol), $AgSbF_6$ (0.035 g, 0.1 mmol), $Cu(OAc)_2.H_2O$ (0.10 g, 0.5 mmol). Column chromatography gave a pale orange amorphous solid, **5c**, 32% (0.047 g). **mp** (from $CHCl_3$) = 101-103 °C. **FT-IR:** (thin film): vmax (cm^{-1}) = 3066.8, 2993.1, 1700.9, 1639.4, 1610.2. **^{1}H NMR:** (500 MHz, $CDCl_3$) δ 7.70 (1H, d, *J* = 2.1 Hz, Ar*H*), 7.45 (1H, dd, *J* = 8.4, 2.2 Hz, Ar*H*), 7.31 (1H, d, *J* = 15.9 Hz, ArC*H*=CHR), 7.10 (1H, d, *J* = 8.5 Hz, Ar*H*), 6.42 (1H, d, *J* = 15.9 Hz, ArCH=C*H*R), 3.77 (3H, s, OCH_3), 3.03 – 2.86 (4H, m, CH_2). **^{13}C NMR:** (126 MHz, $CDCl_3$) δ 175.75 (N*C*(O)CH_2), 166.40 (*C*(O)O), 137.48 (Ar*C*H=CHR), 135.84 (Ar*C*), 133.94 (Ar*C*), 130.87 (Ar*C*), 130.09 (Ar*C*), 129.77 (Ar*C*), 127.42 (Ar*C*), 122.07 (ArCH=*C*HR), 51.94 (O*C*H_3), 28.63 (*C*H_2). **HRMS:** (ESI): m/z calculated for $C_{14}H_{12}Cl_1N_1Na_1O_4$ requires 316.0352 for $[M+Na]^+$, found 316.0327

Synthesis of **5c**

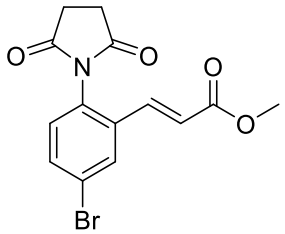

General Procedure **G** was followed using the following compounds: *N*-(4-bromophenyl)succinimide, **4c,** (0.127 g, 0.5 mmol), methyl acrylate (0.14 mL, 0.13 g, 1.5 mmol), $[RuCl_2(p\text{-cymene})]_2$ (0.016 g, 0.025 mmol), $AgSbF_6$ (0.035 g, 0.1 mmol), $Cu(OAc)_2.H_2O$ (0.10 g, 0.5 mmol). Column chromatography gave an off-white amorphous

solid, **25**, 26% (0.044 g). **mp** (from $CHCl_3$) = 98-101 °C. **FT-IR:** (thin film): vmax (cm^{-1}) = 3073.5, 2996.4, 1701.3, 1643.4, 1609.1. **^{1}H NMR:** (500 MHz, $CDCl_3$) δ 7.86 (1H, d, *J* = 1.9 Hz, Ar*H*), 7.60 (1H, dd, *J* = 8.4, 2.0 Hz, Ar*H*), 7.30 (1H, d, *J* = 15.9 Hz, ArC*H*=CHR), 7.03 (1H, d, *J* = 8.4 Hz, Ar*H*), 6.42 (1H, d, *J* = 15.8 Hz, ArCH=C*H*R), 3.78 (3H, s, OCH_3), 3.03 – 2.87 (4H, m, CH_2). **^{13}C NMR:** (126 MHz, $CDCl_3$) δ 175.66 (N*C*(O)CH_2), 166.38 (*C*(O)O), 137.38 (Ar*C*H=CHR), 134.23 (Ar*C*), 133.83 (Ar*C*), 130.43 (Ar*C*), 130.28 (Ar*C*), 123.86 (Ar*C*), 122.12 (ArCH=*C*HR), 51.95 (O*C*H_3), 28.63 (*C*H_2). **HRMS:** (ESI): m/z calculated for $C_{14}H_{12}Br_1N_1O_4$ requires 338.0004 for $[M+H]^+$, found 338.0028

Synthesis of **5d**

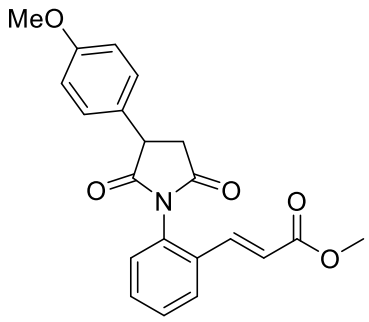

General Procedure **A** was followed using the following compounds: N-phenyl(4-methoxy)succinimide**, 4d,** (0.141 g, 0.5 mmol), methyl acrylate (0.14 mL, 0.13 g, 1.5 mmol), $[RuCl_2(p\text{-cymene})]_2$ (0.016 g, 0.025 mmol), $AgSbF_6$ (0.035 g, 0.1 mmol), $Cu(OAc)_2.H_2O$ (0.10 g, 0.5 mmol). Column chromatography gave an off-white amorphous solid, **33**, 24% (0.043 g). **mp** (from $CHCl_3$) = 92-94 °C. **FT-IR:** (thin film): vmax (cm^{-1}) = 3065.1, 2995.1, 2835.5, 1701.5, 1644.3, 1608.8. **^{1}H NMR:** (400 MHz, dmso-d_6, 368K) δ 7.90 (1H, d, *J* = 7.8 Hz, ArC*H*=CHR), 7.60 – 7.38 (4H, m, Ar*H*), 7.37 – 7.26 (2H, m, Ar*H*), 6.99 – 6.94 (2H, m, Ar*H*), 6.53 (1H, d, *J* = 15.9 Hz, ArCH=C*H*R), 4.39 – 4.26 (1H, m, C*H*), 3.80 (3H, s, CH_3), 3.76 (3H, s, CH_3), 3.02 – 2.96 (1H, m, CH_2), 2.93 – 2.86 (1H, m, CH_2). **^{13}C NMR:** (126 MHz, $CDCl_3$) δ 176.82, 175.20, 175.11, 166.80, 166.49, 159.37, 138.74, 138.58, 132.47, 132.34, 131.41, 130.97, 129.88, 129.86, 129.16, 128.93, 128.87, 128.81, 128.77, 128.67, 128.43, 127.48, 127.42, 126.44, 121.26, 120.95, 114.88, 114.71, 114.67, 55.34, 55.33, 51.85, 51.80, 45.86, 45.41, 45.22, 37.78, 37.42, 37.31, 28.41.(Mixture of peaks observed due to presence of rotamers). **HRMS:** (ESI): m/z calculated for $C_{21}H_{19}N_1O_5$ requires 388.1198 for $[M+Na]^+$, found 388.1143

Synthesis of **5e**

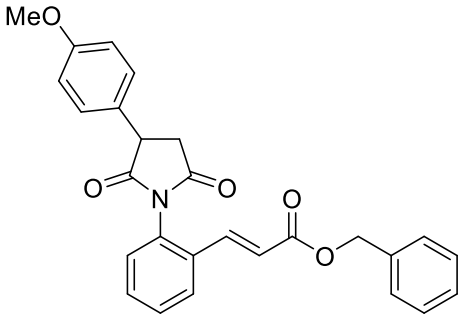

General Procedure **A** was followed using the following compounds: N-phenyl(4-methoxy)succinimide**, 4d,** (0.141 g, 0.5 mmol), benzyl acrylate (0.22 mL, 0.24 g, 1.5 mmol), $[RuCl_2(p\text{-cymene})]_2$ (0.016 g, 0.025 mmol), $AgSbF_6$ (0.035 g, 0.1 mmol), $Cu(OAc)_2.H_2O$ (0.10 g, 0.5 mmol). Column chromatography gave an off-white amorphous solid, **34**, 28% (0.061 g). **mp** (from $CHCl_3$) = 88-91 °C. **FT-IR:** (thin film): vmax (cm^{-1}) = 3074.0, 2996.4, 2837.5, 1700.9, 1643.4, 1608.8. **^{1}H NMR:** (400 MHz, dmso-d_6, 368K) δ 7.93 (1H, d, *J* = 7.4 Hz, ArC*H*-CHR), 7.62 – 7.45 (4H, m, Ar*H*), 7.44 – 7.31 (7H, m, Ar*H*), 6.96 (2H, dt, *J* = 9.8, 5.4 Hz, Ar*H*), 6.61 (1H, d, *J* = 15.9 Hz, ArCH=C*H*R), 5.26 (2H, d, *J* = 1.9 Hz, OCH_2Bn), 4.33 (1H, ddd, *J* = 27.2, 9.3, 5.1 Hz, C*H*), 3.77 (3H, s, CH_3), 2.98 – 2.87 (2H, m, CH_2). **^{13}C NMR:** (126 MHz, $CDCl_3$) δ 138.94, 131.02, 129.86, 128.83, 128.64, 128.59, 128.42, 128.05, 127.43, 126.44, 121.25, 114.91, 114.71, 77.25, 77.00, 76.75, 66.43, 55.34, 45.91, 45.39, 37.75. (Mixture of peaks observed due to presence of rotamers.). **HRMS:** (ESI): m/z calculated for $C_{27}H_{23}N_1O_5$ requires 464.1470 for $[M+Na]^+$, found 464.1484

6.2.9: References

(1) Hrocha, L.; Hruškováa, M.; Schmitza, J.; Schnakenburgb, G.; Gütschow, M. *Synthesis*, **2012**, *44*, 1907-1914

(2) Brouillette, Y.; Sujol, G.; Martinez, J.; Lisowski, V. *Synthesis*, **2009**, *3*, 389-394

(3) Brown, J. A.; Cochrane, A. R.; Irvine, S.; Kerr, W. J.; Mondal, B.; Parkinson, J. A.; Paterson, L. C.; Reid, M.; Tuttle, T.; Andersson, S.; Nilsson, G. N. *Adv. Synth. Catal.*, **2014**, *356*,, 3551-3562

(4) Ooms, F.; Wouters, J.; Oscari, O.; Happaerts, T.; Bouchard, G.; Carrupt, P-A.; Testa, B.; (5) Lambert, D. M. *J. Med. Chem.*, **2006**, *49*, 417-425

(6) Hoffman, R. V.; Reddy, M. M.; Cervantes-Lee, F. *J. Org. Chem.*, **2000**, *65*, 2591-2595

(7) Leitch, J. A.; Wilson, P. B.; McMullin, C. L.; Mahon, M. F.; Bhonoah, Y.; Williams, I. H.; Frost, C. G. *ACS Catal.*, **2016**, *6*, 5520-5529.

(8) Kim, H. J.; Kim, J.; Cho, S. H.; Chang, S. *J. Am. Chem. Soc.*, **2011**, *133*, 16382-16385

(9) Kobeissi, M.; Yazbck, O.; Chreim, Y. *Tetrahedron. Lett.*, **2014**, *55*, 2523-2526.

(10) Garad, D. N.; Tanpure, S. D.; Mhaske, S. B. *Beilstein J. Org. Chem.*, **2015**, *11*, 1008-1016.

6.3: Data and Supporting Information for “Remote C6-Selective Ruthenium-Catalyzed C–H Alkylation of Indole Derivatives via σ-Activation”

In the interest of presentation in a thesis, NMR spectra, computational data and crystallography data have not been included. However, in the interest of the reader these are available online at:
http://pubs.acs.org/doi/suppl/10.1021/acscatal.7b00038/suppl_file/cs7b00038_si_001.pdf
This supporting information has also been modified with the inclusion of data for preliminary results not included in publication however presented in this thesis, and ^{1}H and ^{13}C NMR assignments have been included. Formatting and colour changes have also been made.

6.3.1: General

Proton, carbon and fluorine NMR spectra were recorded on Bruker 300 MHz, or Agilent Technologies 500 MHz, spectrometer (^{1}H NMR at 500 MHz, or 300 MHz, $^{13}C\{^{1}H\}$ NMR at 126 MHz, or 75 MHz, and ^{19}F NMR at 470 MHz. Chemical shifts for protons are reported in parts per million downfield from $Si(CH_3)_4$ and are referenced to residual protium in the deuterated solvent ($CHCl_3$ at 7.26 ppm, or CH_3OH at 3.31 & 4.87 depending on solvent used). Chemical shifts for fluorines are reported in parts per million downfield from $CFCl_3$. NMR data are presented in the following format: chemical shift (number of equivalent nuclei by integration, multiplicity [app = apparent, br = broad, d = doublet, t = triplet, q = quartet, dd = doublet of doublets), dt = doublet of triplets), dq = doublet of quartets), ddd = doublet of doublet of doublets), m = multiplet], coupling constant [in Hz], assignment). Electrospray ionisation ultrahigh resolution time-of-flight mass spectrometry (ESI–UHR–TOF–MS) was performed on a Bruker maXis mass spectrometer. Electrospray ionisation high resolution time-of-flight mass spectrometry (ESI–HR–TOF–MS) was performed on a Bruker micrOTOF spectrometer. Infrared (IR) spectra were recorded on a Perkin–Elmer 1600 FT (Fourier transform), IR spectrophotometer, with absorbencies quoted as wavelength (v [in cm^{-1}]). Melting points were obtained on a Bibby Sterilin SMP10 melting point machine and are uncorrected.

Analytical thin-layer chromatography (TLC) was performed on aluminium-backed plates coated with Alugram® SIL G/UV254 purchased from Macherey–Nagel and visualised with UV light (254 or 365 nm), and/or KMnO4, 2,4-DNPH or I_2/Silica staining. Silica gel column chromatography was performed using 60 Å, 200-400 mesh particle size silica gel purchased

from Sigma–Aldrich. Samples were loaded as saturated solutions in an appropriate solvent system.

All reactions were performed using reagents obtained from Sigma-Aldrich, Acros Organics, Alfa Aesar, Fluorochem chemicals without further purification unless stated. $[RuCl_2(p\text{-cymene})]_2$ was purchased from STREM chemicals or Acros Organics. All water used was purified through a Merck Millipore reverse osmosis purification system prior to use. Anhydrous solvents were dried and degassed by passing through anhydrous alumina columns using an Innovative Technology Inc. PS-400-7 solvent purification system (SPS) and stored under an atmosphere of N_2 prior to use.

Reactions were performed in oven-dried glassware and under a blanket of N_2 if not stated. Temperatures quoted are external. Solvents were removed under reduced pressure using Büchi-Rotorvapor apparatus.

6.3.2: Optimization

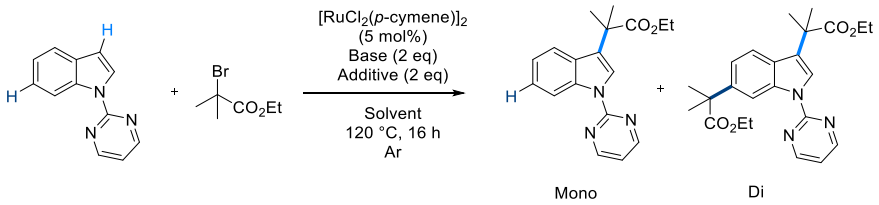

Entry	Base	Additive	Solvent	Temp	Time	CP (eq)	Base (eq)	Add. (eq)	Mono (%)	Di (%)
1	KOAc	-	1,4-dioxane	120	16	3	2	2	21	8
2	KOAc	AcOH	1,4-dioxane	120	16	3	2	2	49	47
3	-	AcOH	1,4-dioxane	120	16	3	2	2	26	0
4	KOAc	AcOH	2-MeTHF	120	16	3	2	2	62	32
5	KOAc	AcOH	DME	120	16	3	2	2	48	45
6	**KOAc**	**AcOH**	**AcOH**	**120**	**16**	**3**	**2**	**2**	**91**	**5**
7	**KOAc**	**AcOH**	**THF**	**120**	**16**	**3**	**2**	**2**	**39**	**57**
8	KOAc	AcOH	TBME	120	16	3	2	2	83	14
9	KOAc	AcOH	DCE	120	16	3	2	2	65	33
10	KOAc	AcOH	*t*-AmOH	120	16	3	2	2	12	6
11	KOAc	AcOH	PhMe	120	16	3	2	2	59	37
12	KOAc	AcOH	NMP	120	16	3	2	2	0	0
13	NaOAc	AcOH	THF	120	16	3	2	2	35	9
14	NBu_4OAc	AcOH	THF	120	16	3	2	2	0	0
15	K_2CO_3	AcOH	THF	120	16	3	2	2	6	3
16	K_2CO_3*	AcOH	THF	120	16	3	2	2	46	43
17	Na_2CO_3	AcOH	THF	120	16	3	2	2	0	0
18	KOPiv	AcOH	THF	120	16	3	2	2	17	9
19	KOAc	PivOH	THF	120	16	3	2	2	65	32
20	KOAc	$AdCO_2H$	THF	120	16	3	2	2	8	10
21	KOAc	$MesCO_2H$	THF	120	16	3	2	2	50	30
22	KOAc	Piv-Val-OH	THF	120	16	3	2	2	62	14
23	KOAc	TFA	THF	120	16	3	2	2	31	3
24	KOAc	KOAc	THF	120	16	3	2	2	55	40
25	KOAc	AcOH	THF	120	16	1	2	2	70	30
27	KOAc	AcOH	THF	120	16	5	2	2	36	26
28	KOAc	AcOH	THF	120	16	10	2	2	37	28
29	KOAc	AcOH	THF	100	16	3	2	2	55	43
30	KOAc	AcOH	THF	120	16	3	2	1	27	14
31	KOAc	AcOH	THF	120	16	3	2	3	56	46
32	KOAc	AcOH	THF	120	16	3	2	10	69	31
33	KOAc	AcOH	THF	120	16	3	1	2	71	17
34	KOAc	AcOH	THF	120	16	3	3	2	26	74
35**	KOAc	AcOH	THF	120	Time	3	2	2	0	0

Standard Conditions: Indole (0.25 mmol), ethyl α--bromoisobutyrate (0.75 mmol), $[RuCl_2(p\text{-cymene})]_2$ (5 mol%), Base (2 eq), Additive (2 eq), Solvent (1 mL), 120 °C, 16 h under Argon. * = KOAc (30 mol%) added. ** = $[RuCl_2(p\text{-cymene})]_2$ (0 mol%).

Scheme S1: Gram-scale synthesis of **3a** for reaction probing

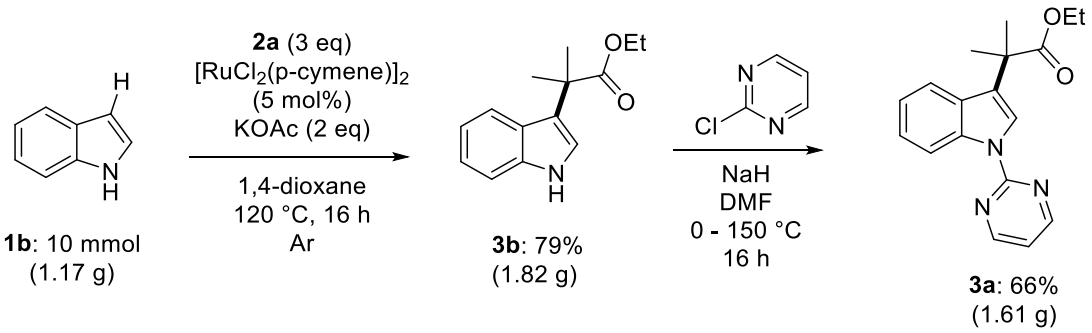

Scheme S2: Remote C-6 alkylation using [Ru(OAc)$_2$(*p*-cymene)] monomer as catalyst

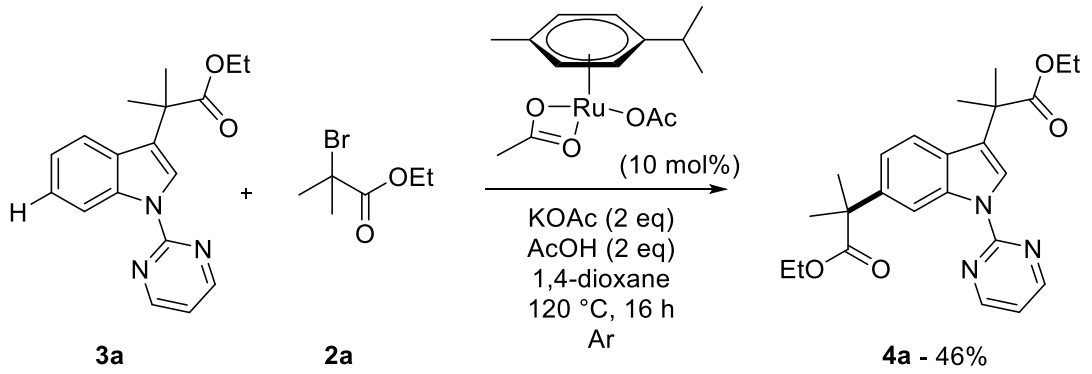

Scheme S3: Ruthenium Catalyzed C–H Alkylation of C4 Substituted Derivatives

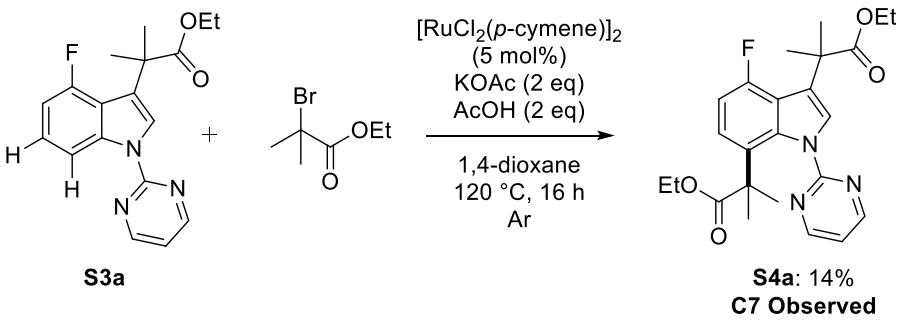

S3a

S4a: 14%
C7 Observed

C7 selectivity was exclusively observed in the C4-F derivative in low yields. This shows that the electronic nature of the fluorine strongly influences the selectivity of the product. This was investigated using the computational methods used previously (Figure S1) and this showed that this functionalization is likely to take place on an organic non-cyclometalated substrate. This C7 functionalization could then impact on potential C2 cyclometalation and C6 functionalisation.

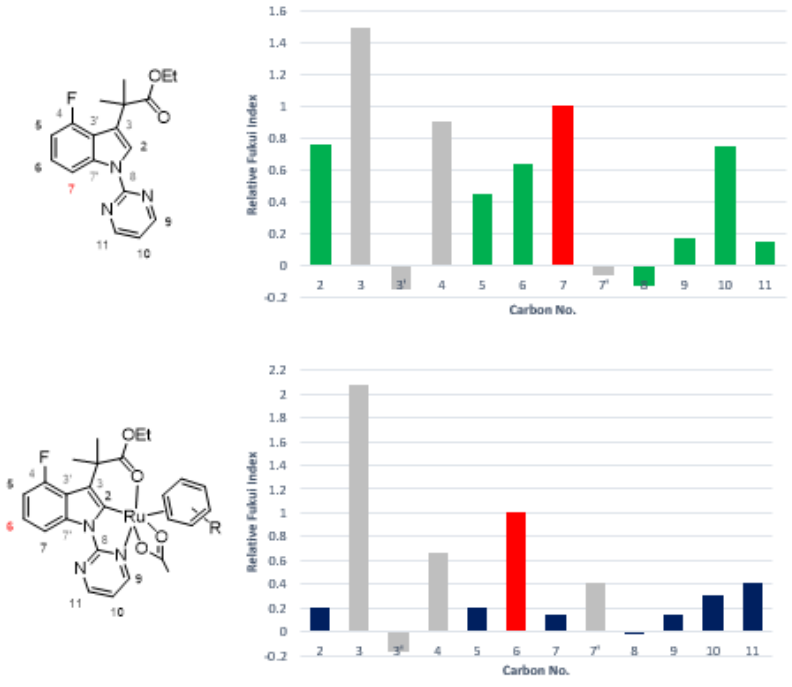

Figure S1: Relative nucleophilicity Fukui indices for organic and inorganic computed structures. Calculations were performed at the BP86/6-31G**&SDD(Ru) level of theory. Fukui indices were calculated with NBO total atomic charges from the optimized neutral structure. Most reactive vacant C–H position is highlighted in red.

6.3.3: Synthesis of Starting Materials

Synthesis of 1-(pyrimidin-2-yl)-1*H*-indole (**1a**)

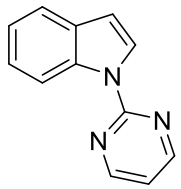

To a solution of indole (2.34 g, 20 mmol) in DMF (50 mL) was added sodium hydride (60% wt. in mineral oil, 1.2 g, 30 mmol) portion-wise. The reaction mixture was allowed to stir at room temperature for 1 hour. To the solution was added 2-chloropyrimidine (3.43 g, 30 mmol) and the reaction mixture was heated to 150 °C overnight. The reaction mixture was allowed to return to room temperature before being poured into brine (300 mL) and EtOAc (300 mL). The organic layer was separated and the aqueous layer was re-extracted with EtOAc (2 x 300 mL). The combined organic layers were dried over $MgSO_4$ and concentrated *in vacuo*. The crude mixture was purified *via* silica gel column chromatography (EtOAc/Petroleum Ether 40-60 °C) to give a white solid, 99% (3.88 g). **^{1}H NMR** (300 MHz, $CDCl_3$ δ 8.82 (1H, dq, *J* = 8.4, 0.9 Hz, In*H*), 8.71 (2H, d, *J* = 4.8 Hz, Pm*H*), 8.28 (1H, d, *J* = 3.7 Hz, In*H*), 7.69–7.58 (1H, m, In*H*), 7.35 (1H, ddd, *J* = 8.5, 7.1, 1.4 Hz, In*H*), 7.28–7.19 (1H, m, In*H*), 7.06 (1H, t, *J* = 4.8 Hz, Pm*H*), 6.71 (1H, dd, *J* = 3.7, 0.8 Hz, In*H*). **^{13}C NMR** (75 MHz, $CDCl_3$) δ 158.3 (Ar*C*), 154.9 (Ar*C*), 147.6 (Ar*C*), 131.4 (Ar*C*), 125.9 (Ar*C*), 123.8 (Ar*C*), 122.2 (Ar*C*), 121.0 (Ar*C*), 116.4 (Ar*C*), 116.2 (Ar*C*), 107.1 (Ar*C*). Data is in line with literature precedent.[1]

Synthesis of *tert*-butyl 1*H*-indole-1-carboxylate (**S1a**)

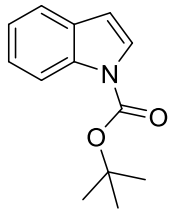

To a solution of 1*H*-indole (2.34 g, 20 mmol) and *N,N*-dimethylaminopyridine (0.244 g, 2 mmol) in CH_2Cl_2 (40 mL) was added di-*tert*-butyl dicarbonate (4.8 g, 22 mmol). The reaction was allowed to stir at room temperature overnight. Brine (100 mL) and CH_2Cl_2 (60 mL) were added to the reaction mixture and the organic layer extracted. The aqueous layer was re-extracted with CH_2Cl_2 (2 x 100 mL). The combined organic phases were dried over $MgSO_4$ and concentrated *in vacuo* to give a yellow oil, 90% (3.89 g). **^{1}H NMR** (500 MHz, $CDCl_3$) δ 8.21 (1H, d, *J* = 8.3 Hz, In*H*), 7.64 (1H, d, *J* = 3.8 Hz, In*H*), 7.60 (1H, ddd, *J* = 7.8, 1.3, 0.8 Hz, In*H*), 7.36 (1H, ddd, *J* = 8.3, 7.2, 1.3 Hz, In*H*), 7.30–7.22 (1H, m, In*H*), 6.61 (1H, dd, *J* = 3.7, 0.8 Hz, In*H*), 1.72 (9H, s, C*H*$_3$). **^{13}C NMR** (126 MHz, $CDCl_3$) δ 149.9 (Ar*C*), 135.3 (Ar*C*), 130.7 (Ar*C*), 126.0 (Ar*C*), 124.3 (Ar*C*), 122.7 (Ar*C*), 121.0 (Ar*C*), 115.3 (Ar*C*), 107.4 (Ar*C*), 83.7 (*C*(*t*Bu)), 28.3 (*C*H$_3$). Data is in line with literature precedent.[2]

Synthesis of 1-trimethylacetyl-1*H*-indole (**P1b**, p = pleminary)

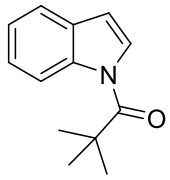

To a solution of 1*H*-indole (2.34 g, 20 mmol), *N*',*N*'-dimethylaminopyridine (244 mg, 0.2 mmol), and triethylamine (4.2 mL, 30 mmol) in anhydrous CH_2Cl_2 (40 mL) was added trimethylacetyl chloride (2.96 mL, 24 mmol) dropwise at 0 °C. The reaction mixture was allowed to return to room temperature and allowed to stir overnight. The reaction was quenched with brine (100 mL), and the organic layer extracted. The aqueous layer was re-extracted with CH_2Cl_2 (2 x 100 mL). The combined organics were dried over $MgSO_4$ and concentrated *in vacuo* to give the title compound, quantitative yield (4.01 g). **^{1}H NMR** (500 MHz, $CDCl_3$) δ 8.52 (1H, dq, *J* = 8.4, 0.8 Hz, Ar*H*), 7.74 (1H, dd, *J* = 3.9, 0.4 Hz, Ar*H*), 7.56 (1H, ddd, *J* = 7.7, 1.4, 0.8 Hz, Ar*H*), 7.35 (1H, dddd, *J* = 8.5, 7.2, 1.4, 0.4 Hz, Ar*H*), 7.29–7.24 (2H, m, Ar*H*), 6.62 (1H, dd, *J* = 3.8, 0.7 Hz, Ar*H*), 1.53 (9H, s, C(C*H*$_3$)$_2$). **^{13}C NMR** (126 MHz, $CDCl_3$) δ 177.2 (*C*O*t*Bu), 136.9 (Ar*C*), 129.5 (Ar*C*), 125.7 (Ar*C*), 125.2 (Ar*C*), 123.6 (Ar*C*), 120.6 (Ar*C*), 117.4 (Ar*C*), 108.3 (Ar*C*), 41.3 (*C*(CH$_3$)$_2$), 28.8 (C(*C*H$_3$)$_2$). Data is in line with literature precedent.[3]

Synthesis of 1-tosyl-1*H*-indole (**P1c**)

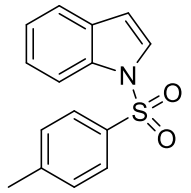

To a solution of indole (2.34 g, 20 mmol) in pyridine (5 mL) was added *p*-toluenesulfonyl chloride (4.58 g, 24 mmol) in CH_2Cl_2 (50 mL) dropwise. After addition was complete, the resulting mixture was allowed to stir at room temperature overnight. The mixture was quenched with 1M HCl (100 mL) and the organic phase extracted. The aqueous phase was re-extracted with CH_2Cl_2 (2 x 100 mL). The combine organic phases were dried over $MgSO_4$ and concentrated *in vacuo* to give the title compound, 2.99 g (55%). **^{1}H NMR** (500 MHz, $CDCl_3$) δ 7.99 (1H, dd, *J* = 8.3, 0.9 Hz, Ar*H*), 7.80–7.71 (2H, m, Ar*H*), 7.56 (1H, d, *J* = 3.7 Hz, Ar*H*), 7.52 (1H, dt, *J* = 7.8, 1.0 Hz, Ar*H*), 7.30 (1H, ddd, *J* = 8.4, 7.2, 1.3 Hz, Ar*H*), 7.25–7.19 (3H , m, Ar*H*), 6.65 (1H, dd, *J* = 3.7, 0.8 Hz, Ar*H*), 2.33 (3H, s, ArCH_3). **^{13}C NMR** (126 MHz, $CDCl_3$) δ 145.0 (Ar*C*), 135.5 (Ar*C*), 135.0 (Ar*C*), 130.9 (Ar*C*), 130.0 (Ar*C*), 127.0 (Ar*C*), 126.5 (Ar*C*), 124.7 (Ar*C*), 123.4 (Ar*C*), 121.5 (Ar*C*), 113.7 (Ar*C*), 109.1 (Ar*C*), 21.69 (Ar*C*H_3). Data is in line with literature precedent.[4]

Synthesis of 1-benzyl-1*H*-indole (**S1b**)

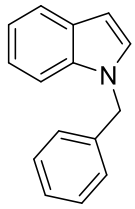

To a solution of 1*H*-indole (2.34 g, 20 mmol) in DMF (20 mL) was added sodium hydride (60% wt. in mineral oil, 2.85 g, 24 mmol). The reaction mixture was left to stir at room temperature for 1 hour. To the resulting slurry was added benzyl bromide (3.6 mL, 30 mmol) at 0 °C. The reaction mixture was allowed to stir at room temperature overnight. The resulting mixture was quenched with water (200 mL) and EtOAc (200 mL) was added. The organic layer was extracted and the aqueous layer was re-extracted with EtOAc (2 x 200 mL). The combined organic layers were dried over $MgSO_4$ and concentrated *in vacuo* to a yellow oil 95%, (3.93 g). **^{1}H NMR** (500 MHz, $CDCl_3$) δ 7.84 (1H, ddd, *J* = 7.7, 1.4, 0.8 Hz, Ar*H*), 7.58–7.48 (1H, m, Ar*H*), 7.46–7.38 (4H, m, Ar*H*), 7.38–7.26 (2H, m, Ar*H*), 7.27–7.19 (3H, m, Ar*H*), 5.39 (2H, d, *J* = 0.7 Hz, C*H*$_2$Ph). **^{13}C NMR** (126 MHz, $CDCl_3$) δ 137.6 (Ar*C*), 128.8 (Ar*C*), 128.8 (Ar*C*), 128.5 (Ar*C*), 128.3 (Ar*C*), 127.8 (Ar*C*), 127.7 (Ar*C*), 127.6 (Ar*C*), 126.8 (Ar*C*), 121.8 (Ar*C*), 121.1 (Ar*C*), 119.6 (Ar*C*), 109.8 (Ar*C*), 101.8 (Ar*C*), 50.1 (*C*H_2Ph). Data is in line with literature precedent.[2]

Synthesis of 3-methyl-1-(pyrimidin-2-yl)-1*H*-indole (**1c**)

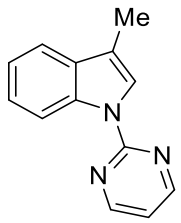

To a solution of 3-methylindole (2.62 g, 20 mmol) in DMF (20 mL) was added sodium hydride (60% wt. in mineral oil, 1.2 g, 30 mmol) portion-wise. The reaction mixture was allowed to stir at room temperature for 1 hour. To the solution was added 2-chloropyrimidine (3.43 g, 30 mmol) and the reaction mixture was heated to 150 °C overnight. The reaction mixture was allowed to return to room temperature before being poured into brine (300 mL) and EtOAc (300 mL). The organic layer was separated and the aqueous layer was re-extracted with EtOAc (2 x 300 mL). The combined organic layers were dried over $MgSO_4$ and concentrated *in vacuo*. The crude mixture was purified *via* silica gel column chromatography (EtOAc/Petroleum Ether 40-60 °C) to give a white solid, 24% (1.01 g). **^{1}H NMR** (500 MHz, $CDCl_3$) δ 8.78 (1H, dd, *J* = 8.5, 3.1 Hz, In*H*), 8.66 (2H, t, *J* = 4.3 Hz, Pm*H*), 8.04 (1H, dt, *J* = 2.7, 1.4 Hz, In*H*), 7.57 (1H, dd, *J* = 8.0, 3.0 Hz, In*H*), 7.36 (1H, tdd, *J* = 8.4, 3.9, 1.5 Hz, In*H*), 7.27 (1H, dt, *J* = 8.4, 3.4 Hz, In*H*), 6.98 (1H, q, *J* = 4.6 Hz, Pm*H*), 2.39–2.35 (3H, m, ArC*H*$_3$). **^{13}C NMR** (126 MHz, $CDCl_3$) δ 158.2 (Ar*C*), 135.8 (Ar*C*), 132.2 (Ar*C*), 123.8 (Ar*C*), 123.0 (Ar*C*), 121.9 (Ar*C*), 118.9 (Ar*C*), 116.3 (Ar*C*), 116.2 (Ar*C*), 115.7 (Ar*C*), 9.9 (Ar*C*H$_3$). Data is in line with literature precedent.[5]

Synthesis of 2-methyl1-(pyridin-2-yl)-1*H*-indole (**1d**)

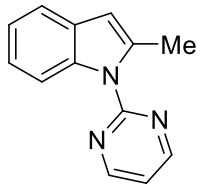

To a solution of 2-methylindole (0.65 g, 5 mmol) in DMF (5 mL) was added sodium hydride (60% wt. in mineral oil, 0.3 g, 7.5 mmol) portion-wise. The reaction mixture was allowed to stir at room temperature for 1 hour. To the solution was added 2-chloropyrimidine (0.84 g, 7.5 mmol) and the reaction mixture was heated to 150 °C overnight. The reaction mixture was allowed to return to room temperature before being poured into brine (75 mL) and EtOAc (75 mL). The organic layer was separated and the aqueous layer was re-extracted with EtOAc (2 x 75 mL). The combined organic layers were dried over $MgSO_4$ and concentrated *in vacuo*. The crude mixture was purified *via* silica gel column chromatography (CH_2Cl_2/Petroleum Ether 40-60 °C) to give a white solid, 5% (0.052 g). **^{1}H NMR** (500 MHz, $CDCl_3$) δ 8.77 (2H, d, *J* = 4.9 Hz, Pm*H*), 8.32 (1H, d, *J* = 8.1 Hz, In*H*), 7.54 (1H, d, *J* = 7.5 Hz, In*H*), 7.23 (2H, dt, *J* = 19.7, 6.9 Hz, In*H*), 7.10 (1H, t, *J* = 4.8 Hz, *Pm*H), 6.46 (1H, s, In*H*), 2.74 (3H, s, ArC*H*$_3$). **^{13}C NMR** (126 MHz, $CDCl_3$) δ 158.1 (Ar*C*), 137.9 (Ar*C*), 136.9 (Ar*C*), 129.5 (Ar*C*), 122.4 (Ar*C*), 121.9 (Ar*C*), 119.6 (Ar*C*), 117.0 (Ar*C*), 114.1 (Ar*C*), 106.8 (Ar*C*), 16.7 (Ar*C*H$_3$). Data is in line with literature precedent.[6]

Synthesis of ethyl 2-(1-(pyrimidin-2-yl)-1*H*-indol-3-yl)acetate (**3e**)

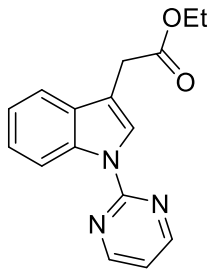

To a solution of indole-3-acetic acid (1.6 g, 9.1 mmol) in EtOH (40 mL) was added H_2SO_4 (2 mL). The reaction mixture was refluxed overnight. The reaction mixture was allowed to return to room temperature and was diluted in H_2O (100 mL) and EtOAc (100 mL). The organic layer was extracted, and the aqueous layer was re-extracted with EtOAc (100 mL). The combined organic layers were dried over $MgSO_4$ and concentrated *in vacuo*. The resulting residue was purified *via* silica gel column chromatography (EtOAc:Petroleum Ether 40-60 °C, 1:10 v:v) to afford a yellow oil. This yellow oil was diluted in DMF (7 mL) and sodium hydride (60% wt. in mineral oil, 0.39 g, 9.75 mmol) was added portionwise at 0 °C. The resulting slurry was allowed to stir for 1 hour. Following this 2-chloropyrimidine (1.12 g, 9.75 mmol) was added and the reaction was allowed to stir at room temperature overnight. The reaction mixture was concentrated *in vacuo*. The resulting residue was diluted in EtOAc (200 mL) and brine (200 mL). The organic layer was extracted and the aqueous layer was re-extracted with EtOAc (2 x 200 mL). The combined organic phases were filtered through a pad of cotton wool before being dried over $MgSO_4$ and concentrated *in vacuo*. The resulting residue was purified *via* silica gel column chromatography (EtOAc:Petroleum Ether 40-60 °C, 1:20 v:v) to afford a yellow oil, 14% from free acid (0.388 g). **^{1}H NMR** (500 MHz, $CDCl_3$) δ 8.80 (1H, dt, *J* = 8.4, 0.9 Hz, In*H*), 8.68 (2H, d, *J* = 4.8 Hz, Pm*H*), 8.26 (1H, t, *J* = 1.1 Hz, In*H*), 7.61 (1H, ddd, *J* = 7.8, 1.3, 0.7 Hz, In*H*), 7.36 (1H, ddd, *J* = 8.4, 7.1, 1.3 Hz, In*H*), 7.30–7.25 (1H, m, In*H*), 7.02 (1H, t, *J* = 4.8 Hz, Pm*H*), 4.19 (2H, q, *J* = 7.1 Hz, CO_2CH_2R), 3.80 (2H, d, *J* = 1.1 Hz, ArCH_2CO_2Et), 1.27 (3H, t, *J* = 7.1 Hz, $CO_2CH_2CH_3$). **^{13}C NMR** (126 MHz, $CDCl_3$) δ 171.4 (CO_2Et), 158.1 (Ar*C*), 135.7 (Ar*C*), 130.9 (Ar*C*), 124.6 (Ar*C*), 124.0 (Ar*C*), 122.1 (Ar*C*), 119.7 (Ar*C*), 119.0 (Ar*C*), 116.5 (Ar*C*), 116.1 (Ar*C*), 113.0 (Ar*C*), 111.3 (Ar*C*), 61.0 ($CO_2CH_2CH_3$), 31.6 (ArCH_2CO_2Et), 14.3 ($CO_2CH_2CH_3$). Data is in line with literature precedent.[7]

Synthesis of 1-(pyrimidin-2-yl)-1*H*-indol-3-yl acetate (**3f**)

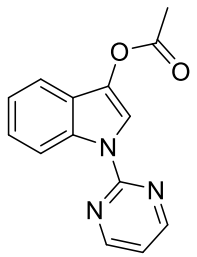

To an oven dried Schlenk flask was added 1-(pyrimidin-2-yl)-1*H*-indole (0.98 g, 5 mmol) and $PhI(OAc)_2$ (1.77 g, 5.5 mmol). The flask was evacuated and refilled with argon three times. Degassed acetic acid (3.5 mL) and acetic anhydride (1.5 mL) were added *via* septum. The reaction mixture was then heated to 60 °C and left to stir overnight. The mixture was allowed to return to room temperature and was quenched with water (25 mL) and subsequently saturated $NaHCO_3$ solution (75 mL). EtOAc (100 mL) was added and the organic layer was extracted. The aqueous layer was extracted with EtOAc (2 x 100 mL) and the combined organic phases were dried over $MgSO_4$ and concentrated *in vacuo*. The crude residue was purified *via* silica gel column chromatography (EtOAc/Petroleum Spirit 40-60 °C) to give a white solid, 61% (0.77 g). **^{1}H NMR** (500 MHz, $CDCl_3$) δ 8.82 (1H, dt, *J* = 8.5, 0.8 Hz, In*H*), 8.68 (2H, d, *J* = 4.7 Hz, Pm*H*), 8.43 (1H, s, In*H*), 7.56 (1H, ddd, *J* = 7.9, 1.3, 0.7 Hz, In*H*), 7.38 (1H, ddd, *J* = 8.5, 7.1, 1.3 Hz, In*H*), 7.30–7.21 (1H, m, In*H*), 7.02 (1H, t, *J* = 4.8 Hz, Pm*H*), 2.40 (3H, s, COC*H*$_3$). **^{13}C NMR** (126 MHz, $CDCl_3$) δ 168.2 (*C*(O)Me), 158.2 (Ar*C*), 157.9 (Ar*C*), 133.7 (Ar*C*), 133.0 (Ar*C*), 124.7 (Ar*C*), 124.2 (Ar*C*), 122.3 (Ar*C*), 117.6 (Ar*C*), 116.6 (Ar*C*), 116.2 (Ar*C*), 114.7 (Ar*C*), 21.2 (CO*C*H_3). Data is in line with literature precedent.[8]

Synthesis of 1-(pyrimidin-2-yl)-1*H*-indole-3-carbaldehyde (**3g**)

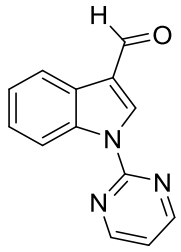

To a solution of indole-3-carboxaldehyde (0.725 g, 5 mmol) in DMF (10 mL) was added sodium hydride (60% wt. in mineral oil, 0.3 g, 7.5 mmol) portion-wise. The reaction mixture was allowed to stir at room temperature for 1 hour. To the solution was added 2-chloropyrimidine (0.863 g, 7.5 mmol) and the reaction mixture was heated to 150 °C overnight. The reaction mixture was allowed to return to room temperature before being poured into aqueous LiCl solution (5%, 100 mL) and EtOAc (100 mL). The organic layer was separated and the aqueous layer was re-extracted with EtOAc (2 x 100 mL). The combined organic layers were dried over $MgSO_4$ and concentrated *in vacuo*. The crude mixture was purified *via* silica gel column chromatography (EtOAc/Petroleum Ether 40-60 °C) and then recrystallized from EtOH to give a white fluffy solid, 22% (0.239 g). **mp** (from $CHCl_3$): 159-164 °C. **FT-IR** (thin film): ν_{max} (cm^{-1}) = 3138.5, 1673.5, 1569.5, 1547.9. **^{1}H NMR** (500 MHz, $CDCl_3$) δ 10.15 (1H, s, C*H*O), 8.91 (1H, s, In*H*), 8.79 (1H, dt, *J* = 8.4, 1.0 Hz, In*H*), 8.76 (2H, d, *J* = 4.8 Hz, Pm*H*), 8.34 (1H, ddd, *J* = 7.7, 1.5, 0.8 Hz, In*H*), 7.43 (1H, ddd, *J* = 8.5, 7.2, 1.5 Hz, In*H*), 7.41–7.35 (1H, m, In*H*), 7.20 (1H, t, *J* = 4.8 Hz, Pm*H*). **^{13}C NMR** (126 MHz, $CDCl_3$) δ 186.0 (*C*HO), 158.5 (Ar*C*), 157.1 (Ar*C*), 136.9 (Ar*C*), 136.5 (Ar*C*), 127.0 (Ar*C*), 125.7 (Ar*C*), 124.4 (Ar*C*), 122.1 (Ar*C*), 121.4 (Ar*C*), 118.0 (Ar*C*), 116.5 (Ar*C*). **HRMS** (ESI): m/z calculated for $C_{13}H_9N_3O_1$ requires 224.0824 for $[M+H]^+$, found 224.0809.

Synthesis of 5-methoxy-1-(pyrimidinyl-2-yl)-1*H*-indole (**1n**)

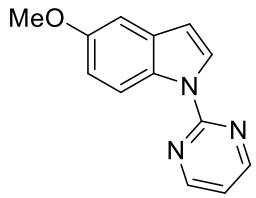

To a solution of 5-methoxyindole (0.735 g, 5 mmol) in DMF (10 mL) was added sodium hydride (60% wt. in mineral oil, 0.3 g, 7.5 mmol) portion-wise. The reaction mixture was allowed to stir at room temperature for 1 hour. To the solution was added 2-chloropyrimidine (0.863 g, 7.5 mmol) and the reaction mixture was heated to 150 °C over the weekend. The reaction mixture was allowed to return to room temperature before being poured into brine (100 mL) and EtOAc (100 mL). The organic layer was separated and the aqueous layer was re-extracted with EtOAc (2 x 100 mL). The combined organic layers were dried over $MgSO_4$ and concentrated *in vacuo*. The crude mixture was purified *via* silica gel column chromatography (EtOAc/Petroleum Ether 40-60 °C) to give a powdery white solid, 60% (0.670 g). **^{1}H NMR** (500 MHz, $CDCl_3$) δ 8.73–8.68 (1H, m, In*H*), 8.67 (2H, d, *J* = 4.8 Hz, Pm*H*), 8.25 (1H, d, *J* = 3.6 Hz, In*H*), 7.10 (1H, dd, *J* = 2.6, 0.5 Hz, In*H*), 7.00 (1H, t, *J* = 4.8 Hz, Pm*H*), 6.97 (1H, ddd, *J* = 9.1, 2.6, 0.5 Hz, In*H*), 6.63 (1H, dd, *J* = 3.7, 0.8 Hz, In*H*), 3.89 (3H, s, OC*H*$_3$). **^{13}C NMR** (126 MHz, $CDCl_3$) δ 158.2 (Ar*C*), 157.8 (Ar*C*), 155.6 (Ar*C*), 132.2 (Ar*C*), 130.4 (Ar*C*), 126.5 (Ar*C*), 117.2 (Ar*C*), 116.0 (Ar*C*), 112.7 (Ar*C*), 106.9 (Ar*C*), 103.3 (Ar*C*), 55.8 (O*C*H$_3$). Data is in line with literature precedent.[7]

Synthesis of 5-fluoro-1-(pyrimidin-2-yl)-1*H*-indole (**1o**)

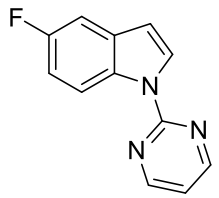

To a solution of 5-fluoroindole (0.675 g, 5 mmol) in DMF (10 mL) was added sodium hydride (60% wt. in mineral oil, 0.3 g, 7.5 mmol) portion-wise. The reaction mixture was allowed to stir at room temperature for 1 hour. To the solution was added 2-chloropyrimidine (0.863 g, 7.5 mmol) and the reaction mixture was heated to 150 °C over the weekend. The reaction mixture was allowed to return to room temperature before being poured into brine (100 mL) and EtOAc (100 mL). The organic layer was separated and the aqueous layer was re-extracted with EtOAc (2 x 100 mL). The combined organic layers were dried over $MgSO_4$ and concentrated *in vacuo*. The crude mixture was purified *via* silica gel column chromatography (EtOAc/Petroleum Ether 40-60 °C) to give a powdery white solid, 85% (0.897 g). **^{1}H NMR** (500 MHz, $CDCl_3$) δ 8.76 (1H, ddt, *J* = 9.1, 4.8, 0.6 Hz, In*H*), 8.69 (2H, d, *J* = 4.8 Hz, Pm*H*), 8.31 (1H, dd, *J* = 3.7, 0.5 Hz, In*H*), 7.32–7.20 (1H, m, In*H*), 7.10–7.02 (2H, m, Pm*H* & In*H*), 6.65 (1H, dd, *J* = 3.7, 0.8 Hz, In*H*). **^{13}C NMR** (126 MHz, $CDCl_3$) δ 159.1 (d, *J* = 237.8 Hz, Ar*C*), 158.3 (Ar*C*), 132.2 (d, *J* = 10.0 Hz, Ar*C*), 127.5 (Ar*C*), 117.4 (d, *J* = 8.6 Hz, Ar*C*), 116.4 (Ar*C*), 111.5 (d, *J* = 25.0 Hz, Ar*C*), 106.7 (d, *J* = 3.9 Hz, Ar*C*), 106.2 (d, *J* = 23.4 Hz, Ar*C*). **^{19}F NMR** (470 MHz, $CDCl_3$) δ -122.0 (td, *J* = 9.1, 4.9 Hz, Ar*F*). Data is in line with literature precedent.[9]

Synthesis of 5-bromo-1-(pyrimidin-2-yl)-1*H*-indole (**1p**)

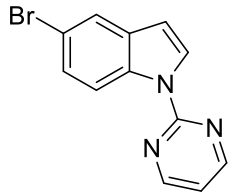

To a solution of 5-bromoindole (0.980 g, 5 mmol) in DMF (10 mL) was added sodium hydride (60% wt. in mineral oil, 0.3 g, 7.5 mmol) portion-wise. The reaction mixture was allowed to stir at room temperature for 1 hour. To the solution was added 2-chloropyrimidine (0.863 g, 7.5 mmol) and the reaction mixture was heated to 150 °C overnight. The reaction mixture was allowed to return to room temperature before being poured into aqueous LiCl solution (5%, 100 mL) and EtOAc (100 mL). The organic layer was separated and the aqueous layer was re-extracted with EtOAc (2 x 100 mL). The combined organic layers were dried over $MgSO_4$ and concentrated *in vacuo*. The crude mixture was purified *via* silica gel column chromatography (EtOAc/Petroleum Ether 40-60 °C) to give a powdery white solid, 86% (1.18 g). **^{1}H NMR** (500 MHz, $CDCl_3$) δ 8.73–8.66 (3H, m, Pm*H* & In*H*), 8.28 (1H, dd, *J* = 3.7, 0.4 Hz, In*H*), 7.74 (1H, dd, *J* = 2.1, 0.5 Hz, In*H*), 7.41 (1H, ddd, *J* = 8.8, 2.0, 0.4 Hz, In*H*), 7.07 (1H, t, *J* = 4.8 Hz, Pm*H*), 6.63 (1H, dd, *J* = 3.7, 0.8 Hz, In*H*). **^{13}C NMR** (126 MHz, $CDCl_3$) δ 158.3 (Ar*C*), 157.6 (Ar*C*), 134.2 (Ar*C*), 133.2 (Ar*C*), 127.1 (Ar*C*), 126.5 (Ar*C*), 123.5 (Ar*C*), 117.9 (Ar*C*), 116.6 (Ar*C*), 115.6 (Ar*C*), 110.2 (Ar*C*), 106.2 (Ar*C*). Data is in line with literature precedent.[2]

Synthesis of 1-(pyridine-2-yl)-1*H*-indole (**1h**)

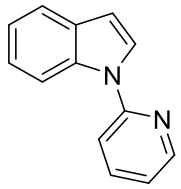

To a solution of indole (1.17 g, 10 mmol) in DMF (15 mL) was added sodium hydride (60% wt. in mineral oil, 0.6 g, 15 mmol) portion-wise. The reaction mixture was allowed to stir at room temperature for 1 hour. To the solution was added 2-bromopyridine (1.14 mL, 1.90 g, 12 mmol) and the reaction mixture was heated to 150 °C overnight. The reaction mixture was allowed to return to room temperature before being poured into brine (100 mL) and EtOAc (100 mL). The organic layer was separated and the aqueous layer was re-extracted with EtOAc (2 x 100 mL). The combined organic layers were dried over $MgSO_4$ and concentrated *in vacuo*. The crude mixture was purified *via* silica gel column chromatography (EtOAc/Petroleum Ether 40-60 °C) to give a light brown oil, 56% (1.08 g). **^{1}H NMR** (500 MHz, $CDCl_3$) δ 8.64–8.48 (1H, m, Ar*H*), 8.22 (1H, dd, *J* = 8.4, 0.9 Hz, Ar*H*), 7.82 (1H, ddd, *J* = 8.2, 7.4, 2.0 Hz, Ar*H*), 7.74 (1H, d, *J* = 3.4 Hz, Ar*H*), 7.68 (1H, ddd, *J* = 7.8, 1.3, 0.8 Hz, Ar*H*), 7.50 (1H, dt, *J* = 8.2, 0.9 Hz, Ar*H*), 7.31 (1H, dd, *J* = 8.4, 7.1, 1.3 Hz, Ar*H*), 7.22 (1H, ddd, *J* = 8.1, 7.1, 1.0 Hz, Ar*H*), 7.17 (1H, ddd, *J* = 7.4, 4.9, 0.9 Hz, Ar*H*), 6.73 (1H, dd, *J* = 3.5, 0.8 Hz, Ar*H*). **^{13}C NMR** (126 MHz, $CDCl_3$) δ 152.6 (Ar*C*), 149.1 (Ar*C*), 138.5 (Ar*C*), 135.2 (Ar*C*), 130.6 (Ar*C*), 126.1 (Ar*C*), 123.2 (Ar*C*), 121.4 (Ar*C*), 121.2 (Ar*C*), 120.2 (Ar*C*), 114.7 (Ar*C*), 113.1 (Ar*C*), 105.7 (Ar*C*), 105.6 (Ar*C*). Data is in line with literature precedent.[10]

Synthesis of 1-(5-chloropyrimidin-2-yl)-1*H*-indole (**1i**)

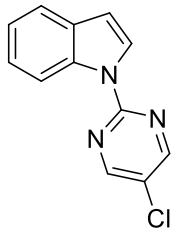

To a solution of indole (0.585 g, 5 mmol) in DMF (5 mL) was added sodium hydride (60% wt. in mineral oil, 0.3 g, 7.5 mmol) portion-wise. The reaction mixture was allowed to stir at room temperature for 1 hour. To the solution was added 2,5-dichloropyrimidine (1.39 g, 7.5 mmol) and the reaction mixture was heated to 150 °C overnight. The reaction mixture was allowed to return to room temperature before being poured into brine (100 mL) and EtOAc (100 mL). The organic layer was separated and the aqueous layer was re-extracted with EtOAc (2 x 100 mL). The combined organic layers were dried over $MgSO_4$ and concentrated *in vacuo*. The crude mixture was purified *via* silica gel column chromatography (EtOAc/Petroleum Ether 40-60 °C) to give a powdery white solid, 36% (0.416 g). **mp** (from $CHCl_3$) = 115-117 °C. **FT-IR** (thin film): ν_{max} (cm^{-1}) = 3051.4, 727.5 (C-Cl). **^{1}H NMR** (500 MHz, $CDCl_3$) δ 8.71 (1H, dt, *J* = 8.4, 0.9 Hz, In*H*), 8.62 (2H, d, *J* = 1.0 Hz, Pm*H*), 8.19 (1H, dd, *J* = 3.7, 1.0 Hz, In*H*), 7.62 (1H, ddd, *J* = 7.8, 1.3, 0.8 Hz, In*H*), 7.35 (1H, ddd, *J* = 8.5, 7.3, 1.3 Hz, In*H*), 7.30–7.18 (1H, m, In*H*), 6.71 (1H, dd, *J* = 3.7, 0.8 Hz, In*H*). **^{13}C NMR** (126 MHz, $CDCl_3$) δ 156.4 (Ar*C*), 155.7 (Ar*C*), 135.2 (Ar*C*), 131.3 (Ar*C*), 125.8 (Ar*C*), 125.0 (Ar*C*), 123.8 (Ar*C*), 122.4 (Ar*C*), 120.9 (Ar*C*), 116.1 (Ar*C*), 107.5 (Ar*C*). **HRMS** (ESI): m/z calculated for $C_{12}H_9N_3Cl_1$ requires 230.0485 for $[M+H]^+$, found 230.0480.

6.3.4: Synthesis of C3 Functionalized Materials

General Procedure **A** for the radical C-3 alkylation of indoles

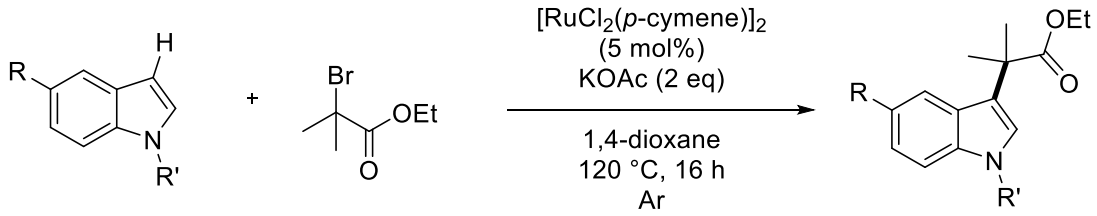

To an oven dried flask was charged relevant indole (2 mmol), ethyl α-bromo isobutyrate (0.95 L, 6 mmol), $[RuCl_2(p\text{-cymene})]_2$ (0.061 g, 0.1 mmol), potassium acetate (0.392 g, 4 mmol), and 1,4-dioxane (8 mL). The vessel was evacuated and refilled with argon three times. The reaction mixture was heated to 120 °C and left to stir for 16 h. The reaction mixture was allowed to return to room temperature and diluted with EtOAc (80 mL) and sat. $NaHCO_3$ solution (80 mL). The organic layer was extracted and the aqueous layer was re-extracted with EtOAc (2 x 20 mL). The combined organic layers were dried over $MgSO_4$ and concentrated *in vacuo*. The crude residue was purified *via* silica gel column chromatography using EtOAc/Petroleum Ether 40-60 °C (1:20-1:10, *v:v*) to give pure C-3 functionalized product.

General Procedure **B** for the pyrimidination/pyridination C3 alkylated indoles

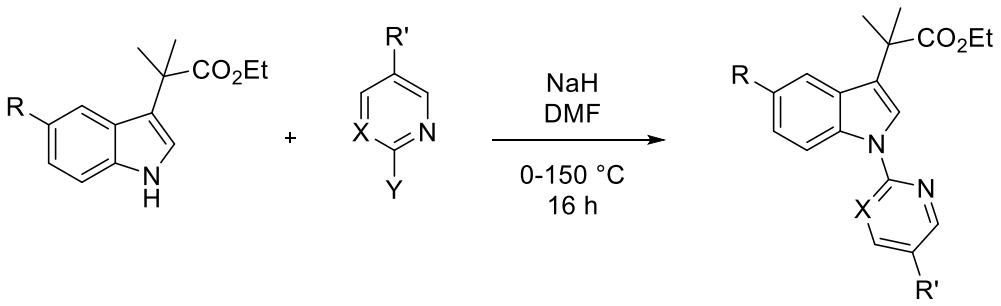

To a solution of C-3 alkylated indole (1 eq) in DMF (0.5-1 M), was added sodium hydride (60% wt. in mineral oil, 1.5 eq) portion-wise. The reaction mixture was allowed to stir at room temperature for 1 hour. To the solution was added 2-chloropyrimidine/2,5-dichloropyrimidine/2-bromopyridine (1.5 eq) and the reaction mixture was heated to 150 °C overnight. The reaction mixture was allowed to return to room temperature before being poured into aqueous LiCl solution (5%, 100 mL) and EtOAc (100 mL). The organic layer was separated and the aqueous layer was re-extracted with EtOAc (2 x 100 mL). The combined organic layers were dried over $MgSO_4$ and concentrated *in vacuo*. The crude mixture was purified *via* silica gel column chromatography (EtOAc/Petroleum Ether 40-60 °C, 10-20:90-80 *v:v*) to give *N*-substituted products.

Synthesis of 3-(*tert*-butyl)-1-(pyrimidin-2-yl)-1*H*-indole (**P3a**)

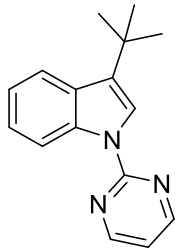

To an oven-dried carousel tube was charged with 1-(pyrimidin-2-yl)-1*H*-indole (49 mg, 0.25 mmol), potassium acetate (49 mg, 0.25 mmol), and $[RuCl_2(p\text{-cymene})]_2$ (8 mg, 0.0125 mmol, 5 mol%). The flask was sealed with a Teflon cap, evacuated and refilled with argon three times. 1,4-dioxane (1 mL) and 2-bromo-2-methylpropane (0.084 mL, 103 mg, 0.75 mmol) were added *via* septum and the reaction flask was heated to 120 °C for 16 h. The reaction mixture was allowed to return to room temperature and was diluted with EtOAc (30 mL) and sat. $NaHCO_3$ solution (30 mL). The organic phase was extracted and the aqueous phase re-extracted with EtOAc (2 x 30 mL). The combined organics were dried over $MgSO_4$ and concentrated *in vacuo*. The crude residue was purified *via* silica gel column chromatography (EtOAc:Petroleum Spirit 40-60 °C – 10:90 v:v) to give an amorphous off-white solid, 13% (8 mg). **FT-IR** (thin film): ν_{max} (cm^{-1}) = 2961.0, 1580.0, 1560.4. **^{1}H NMR** (500 MHz, $CDCl_3$) δ 8.86 (1H, dt, *J* = 8.4, 1.0 Hz, Ar*H*), 8.68 (2H, d, *J* = 4.8 Hz, Ar*H*), 8.01 (1H, s, Ar*H*), 7.89–7.77 (1H, m, Ar*H*), 7.33 (1H, ddd, *J* = 8.4, 7.1, 1.3 Hz, Ar*H*), 7.28–7.18 (1H, m, Ar*H*), 6.99 (1H, t, *J* = 4.8 Hz, Ar*H*), 1.52 (9H, s, $C(CH_3)_3$). **^{13}C NMR** (126 MHz, $CDCl_3$) δ 158.1 (Ar*C*), 158.1 (Ar*C*), 136.8 (Ar*C*), 130.5 (Ar*C*), 130.0 (Ar*C*), 123.3 (Ar*C*), 121.5 (Ar*C*), 121.4 (Ar*C*), 120.9 (Ar*C*), 116.6 (Ar*C*), 115.7 (Ar*C*), 31.9 ($C(CH_3)_3$), 30.5 ($C(CH_3)_2$). **HRMS** (ESI): m/z calculated for $C_{16}H_{17}N_3$ requires 274.1315 for $[M+Na]^+$, found 274.1337.

Synthesis of ethyl 2-methyl-2-(1-(pyrimidin-2-yl)-1*H*-indol-3-yl)propanoate (**3a**)

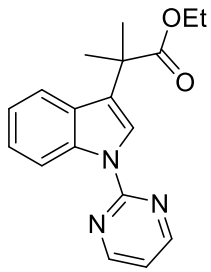

The above compound was synthesized using General Procedure **B** using ethyl 2-(1*H*-indol-3-yl)-2-methylpropanoate (1.16 g, 5 mmol), sodium hydride (60% wt. dispersion in mineral oil, 0.3 g, 7.5 mmol), 2-chloropyrimidine (0.863 g, 7.5 mmol) and DMF (5 mL) Silica gel chromatography gave a white solid, 89% (0.412 g). **mp** (from $CHCl_3$): 113-117 °C. **FT-IR** (thin film): ν_{max} (cm^{-1}) = 2981.1, 1725.6, 1579.3, 1562.7. **^{1}H NMR** (500 MHz, $CDCl_3$) δ 8.82 (1H, dt, *J* = 8.4, 0.9 Hz, In*H*), 8.69 (2H, d, *J* = 4.8 Hz, Pm*H*), 8.17 (1H, s, In*H*), 7.60 (1H, ddd, *J* = 7.9, 1.3, 0.7 Hz, In*H*), 7.33 (1H, ddd, *J* = 8.4, 7.1, 1.3 Hz, In*H*), 7.21 (1H, ddd, *J* = 8.1, 7.1, 1.1 Hz, In*H*), 7.02 (1H, t, *J* = 4.8 Hz, Pm*H*), 4.13 (2H, q, *J* = 7.1 Hz, CO_2CH_2R), 1.73 (6H, s, $C(CH_3)_2$), 1.13 (3H, t, *J* = 7.1 Hz, $CO_2CH_2CH_3$). **^{13}C NMR** (126 MHz, $CDCl_3$) δ 176.8 (CO_2Et), 158.2 (Ar*C*), 157.8 (Ar*C*), 136.3 (Ar*C*), 129.5 (Ar*C*), 123.8 (Ar*C*), 122.1 (Ar*C*), 122.0 (Ar*C*), 120.3 (Ar*C*), 116.6 (Ar*C*), 116.0 (Ar*C*), 61.1 (CO_2CH_2R, 42.2 ($C(CH_3)_2$), 26.1 ($C(CH_3)_2$), 14.3 ($CO_2CH_2CH_3$). **HRMS** (ESI): m/z calculated for $C_{18}H_{19}N_3O_2$ requires 310.1556 for $[M+H]^+$, found 310.1554.

Synthesis of ethyl 2-(1*H*-indol-3-yl)-2-methylpropanoate (**3b**)

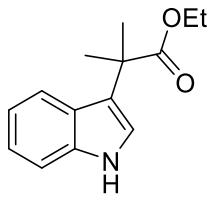

The above compound was synthesized using General Procedure **A** using 1*H*-indole (**1c**), 0.234 g). Silica gel chromatography gave a white solid, 89% (0.412 g). **mp** (from $CHCl_3$): 106-110 °C. **FT-IR** (thin film): ν_{max} (cm^{-1}) = 3409.7, 2979.5, 1709.6. **^{1}H NMR** (500 MHz, $CDCl_3$) δ 8.02 (1H, s, N*H*), 7.68 (1H, dq, *J* = 8.0, 0.9 Hz, In*H*), 7.34 (1H, dt, *J* = 8.2, 1.0 Hz, In*H*), 7.18 (1H, ddd, *J* = 8.2, 7.0, 1.1 Hz, In*H*), 7.09 (1H, ddd, *J* = 8.1, 7.1, 1.1 Hz, In*H*), 7.04 (1H, d, *J* = 2.5 Hz, In*H*), 4.13 (2H, q, *J* = 7.1 Hz, CO_2CH_2R), 1.70 (6H, s, $C(CH_3)_2$), 1.16 (3H, t, *J* = 7.1 Hz, $CO_2CH_2CH_3$). **^{13}C NMR** (126 MHz, $CDCl_3$) δ 177.2 (CO_2Et), 137.0 (Ar*C*), 125.8

(Ar*C*), 122.0 (Ar*C*), 121.1 (Ar*C*), 120.6 (Ar*C*), 120.6 (Ar*C*), 119.5 (Ar*C*), 111.4 (Ar*C*), 60.9 (CO_2CH_2R), 42.2 ($C(CH_3)_2$), 26.3 ($C(CH_3)_2$), 14.3 ($CO_2CH_2CH_3$). **HRMS** (ESI): m/z calculated for $C_{14}H_{17}N_1O_2$ requires 232.1338 for $[M+H]^+$, found 232.1317.

Synthesis of 2-methyl-2-(1-(pyridin-2-yl)-1*H*-indol-3-yl)propanoate (**3h**)

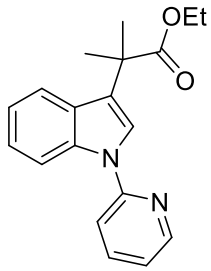

The above compound was synthesized using General Procedure **B** using ethyl 2-(1*H*-indol-3-yl)-2-methylpropanoate (0.231 g, 1 mmol), sodium hydride (60% wt. dispersion in mineral oil, 0.06 g, 1.5 mmol), 2-bromopyridine (0.143 mL, 1.5 mmol, 0.237 g) and DMF (2 mL) Silica gel chromatography gave an amorphous oil, 19% (0.060 g). **FT-IR** (thin film): ν_{max} (cm^{-1}) = 2980.0, 1723.0, 1591.1. **^{1}H NMR** (500 MHz, $CDCl_3$) δ 8.56 (1H, ddd, *J* = 4.9, 1.9, 0.9 Hz, Ar*H*), 8.13 (1H, dt, *J* = 8.3, 0.9 Hz, Ar*H*), 7.81 (1H, ddd, *J* = 8.2, 7.4, 1.9 Hz, Ar*H*), 7.71–7.63 (2H, m, Ar*H*), 7.52 (1H, dt, *J* = 8.3, 0.9 Hz, Ar*H*), 7.33–7.24 (1H, m, Ar*H*), 7.21–7.13 (2H, m, Ar*H*), 4.13 (2H, q, *J* = 7.1 Hz, CO_2CH_2R), 1.74 (6H, s, $C(CH_3)_2$), 1.15 (3H, t, *J* = 7.1 Hz, $CO_2CH_2CH_3$). **^{13}C NMR** (126 MHz, $CDCl_3$) δ 176.9 (CO_2Et), 152.4 (Ar*C*), 149.1 (Ar*C*), 138.4 (Ar*C*), 135.9 (Ar*C*), 128.5 (Ar*C*), 123.7 (Ar*C*), 123.2 (Ar*C*), 122.6 (Ar*C*), 121.0 (Ar*C*), 120.7 (Ar*C*), 120.1 (Ar*C*), 114.8 (Ar*C*), 112.9 (Ar*C*), 61.0 (CO_2CH_2R), 42.2 ($C(CH_3)_2$), 26.2 ($C(CH_3)_2$), 14.3 ($CO_2CH_2CH_3$). **HRMS** (ESI): m/z calculated for $C_{19}H_{20}N_2O_2$ requires 309.1603 for $[M+H]^+$, found 309.1610.

Synthesis of ethyl 2-methyl-2-(1-(5-chloropyrimidin-2-yl)-1*H*-indol-3-yl)propanoate (**3i**)

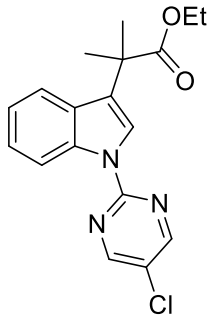

The above compound was synthesized using General Procedure **B** using ethyl 2-(1*H*-indol-3-yl)-2-methylpropanoate (0.231 g, 1 mmol), sodium hydride (60% wt. dispersion in mineral oil, 0.06 g, 1.5 mmol), 2,5-dichloropyrimidine (0.22 g, 1.5 mmol) and DMF (5 mL) Silica gel chromatography gave a white solid, 66% (0.225 g). **mp** (from $CHCl_3$): 120-124 °C. **FT-IR** (thin film): ν_{max} (cm^{-1}) = 2980.3, 1725.00, 1573.4, 1543.1. **^{1}H NMR** (500 MHz, $CDCl_3$) δ 8.72 (1H, dt, *J* = 8.5, 0.9 Hz, In*H*), 8.61 (2H, s, Pm*H*), 8.09 (1H, s), 7.60 (1H, ddd, *J* = 8.0, 1.2, 0.7 Hz, In*H*), 7.33 (1H, ddd, *J* = 8.4, 7.1, 1.3 Hz, In*H*), 7.22 (1H, ddd, *J* = 8.1, 7.2, 1.1 Hz, In*H*), 4.14 (2H, q, *J* = 7.1 Hz, CO_2CH_2R), 1.73 (6H, s, $C(CH_3)_2$), 1.14 (3H, t, *J* = 7.1 Hz, $CO_2CH_2CH_3$). **^{13}C NMR** (126 MHz, $CDCl_3$) δ 176.7 (CO_2Et), 156.5 (Ar*C*), 155.7 (Ar*C*), 136.2 (Ar*C*), 129.6 (Ar*C*), 125.6 (Ar*C*), 124.9 (Ar*C*), 124.0 (Ar*C*), 122.3 (Ar*C*), 122.1 (Ar*C*), 120.4 (Ar*C*), 116.4 (Ar*C*), 61.1 (CO_2CH_2R), 42.2 ($C(CH_3)_2$), 26.1 ($C(CH_3)_2$), 14.3 ($CO_2CH_2CH_3$). **HRMS** (ESI): m/z calculated for $C_{18}H_{18}Cl_1N_3O_2$ requires 344.1166 for $[M+H]^+$, found 344.1159.

Synthesis of ethyl 2-(5-methoxy-1*H*-indol-3-yl)-2-methylpropanoate (**S3b**)

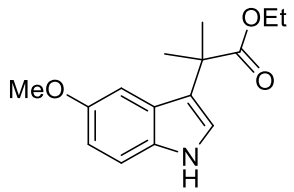

The above compound was synthesized using General Procedure **A** using 5-methoxyindole, 0.294 g). Silica gel chromatography gave a white solid, 69% (0.362 g). **mp** (from $CHCl_3$): 121-126 °C. **FT-IR** (thin film): ν_{max} (cm^{-1}) = 3412.9, 2981.9, 1715.8, 1624.8, 1582.5. **^{1}H NMR** (500 MHz, $CDCl_3$) δ 7.99 (1H, s, N*H*), 7.21 (1H, dd, *J* = 8.8, 0.6 Hz, In*H*), 7.13 (1H, dd, *J* = 2.5, 0.7 Hz, In*H*), 7.01 (1H, dd, *J* = 2.7, 0.4 Hz, In*H*), 6.85 (1H, ddd, *J* = 8.8, 2.5, 0.5 Hz, In*H*), 4.13 (2H, q, *J* = 7.1 Hz, CO_2CH_2R), 3.84 (3H, s, OCH_3), 1.68 (6H, s, $C(CH_3)_2$), 1.17 (3H, t, *J* = 7.1 Hz, $CO_2CH_2CH_3$). **^{13}C NMR** (126 MHz, $CDCl_3$) δ 177.2 (CO_2Et), 153.8 (Ar*C*), 132.1 (Ar*C*), 126.1 (Ar*C*), 121.4 (Ar*C*), 120.6 (Ar*C*), 112.2 (Ar*C*), 112.1 (Ar*C*), 102.5 (Ar*C*), 60.9 (CO_2CH_2R), 56.0 ($ArOCH_3$), 42.1 ($C(CH_3)_2$), 26.1 ($C(CH_3)_2$), 14.3 ($CO_2CH_2CH_3$). **HMRS** (ESI): m/z calculated for $C_{15}H_{19}N_1O_3$ requires 284.1263 for $[M+Na]^+$, found 284.1284.

Synthesis of ethyl 2-(5-methoxy-1-(pyrimidin-2-yl)-1*H*-indol-3-yl)-2-methylpropanoate (**3n**)

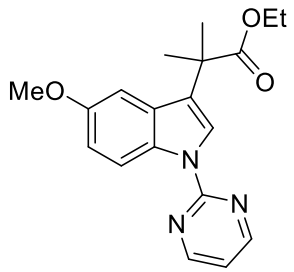

The above compound was synthesized using General Procedure **B** using ethyl 2-(5-methoxy-1*H*-indol-3-yl)-2-methylpropanoate (0.342 g, 1.3 mmol), sodium hydride (60% wt. dispersion in mineral oil, 0.078 g, 1.95 mmol) and 2-chloropyrimidine (0.224 g, 1.95 mmol). Silica gel column chromatography gave a white solid, 82% (0.361 g). **mp** (from $CHCl_3$): 71-75 °C. **FT-IR** (thin film): ν_{max} (cm^{-1}) = 2981.2, 1725.5, 1578.8, 1561.6. **^{1}H NMR** (500 MHz, $CDCl_3$) δ 8.71 (1H, d, *J* = 9.0 Hz, In*H*), 8.65 (2H, d, *J* = 4.8 Hz, Pm*H*), 8.14 (1H, s, In*H*), 7.06 (1H, d, *J* = 2.5 Hz, In*H*), 6.99 (1H, t, *J* = 4.8 Hz, Pm*H*), 6.95 (1H, dd, *J* = 9.1, 2.6 Hz, In*H*), 4.14 (2H, q, *J* = 7.1 Hz, CO_2CH_2R), 3.86 (3H, s, ArOC*H*$_3$), 1.72 (6H, s, C(C*H*$_3$)$_2$), 1.15 (3H, t, *J* = 7.1 Hz, $CO_2CH_2CH_3$). **^{13}C NMR** (126 MHz, $CDCl_3$) δ 176.8 (*C*O_2Et), 158.1 (Ar*C*), 157.7 (Ar*C*), 155.3 (Ar*C*), 131.2 (Ar*C*), 130.3 (Ar*C*), 124.8 (Ar*C*), 122.6 (Ar*C*), 117.35 (Ar*C*), 115.8 (Ar*C*), 112.5 (Ar*C*), 103.0 (Ar*C*), 61.1 (CO_2CH_2R), 55.8 (ArOCH_3), 42.1 (*C*$(CH_3)_2$), 26.0 (C(*C*$H_3)_2$), 14.3 ($CO_2CH_2CH_3$). **HRMS** (ESI): m/z calculated for $C_{19}H_{21}N_3O_3$ requires 340.1661 for $[M+H]^+$, found 340.1670.

Synthesis of ethyl 2-(5-fluoro-1*H*-indol-3-yl)-2-methylpropanoate (**S3c**)

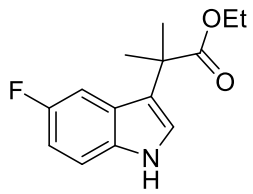

The above compound was synthesized using General Procedure **A** using 5-fluoroindole, 0.270 g). Silica gel chromatography gave an off-white solid, 74% (0.366 g). **mp** (from $CHCl_3$): 97-102 °C. **FT-IR** (thin film): ν_{max} (cm^{-1}) = 3370.7, 2980.0, 1705.3, 1630.2, 1580.5. **^{1}H NMR** (500 MHz, $CDCl_3$) δ 8.08 (1H, s, N*H*), 7.34 (1H, ddt, *J* = 10.3, 2.6, 0.6 Hz, In*H*), 7.23 (1H, ddd, *J* = 8.8, 4.5, 0.5 Hz, In*H*), 7.07 (1H, d, *J* = 2.5 Hz, In*H*), 6.92 (1H, td, *J* = 9.0, 2.5 Hz, In*H*), 4.14 (2H, q, *J* = 7.1 Hz, CO_2CH_2R), 1.67 (6H, s, C(C*H*$_3$)$_2$), 1.18 (3H, t, *J* = 7.1 Hz, $CO_2CH_2CH_3$). **^{13}C NMR** (126 MHz, $CDCl_3$) δ 176.9 (*C*O_2Et), 157.6 (d, *J* = 234.1 Hz, Ar*C*), 133.5 (Ar*C*), 126.1 (d, *J* = 10.0 Hz, Ar*C*), 122.5 (Ar*C*), 121.1 (d, *J* = 4.9 Hz, Ar*C*), 111.9 (d,

J = 9.8 Hz, Ar*C*), 110.5 (d, *J* = 26.3 Hz, Ar*C*), 105.6 (d, *J* = 24.0 Hz, Ar*C*), 61.0 (CO_2CH_2R), 42.1 ($C(CH_3)_2$), 26.1 ($C(CH_3)_2$), 14.3 ($CO_2CH_2CH_3$). **^{19}F NMR** (470 MHz, $CDCl_3$) δ -124.5 (td, *J* = 9.8, 4.6 Hz). **HRMS** (ESI): m/z calculated for $C_{14}H_{16}N_1O_2F_1$ requires 250.1243 for $[M+H]^+$, found 250.1243.

Synthesis of ethyl 2-(5-fluoro-1-(pyrimidin-2-yl)-1*H*-indol-3-yl)-2-methylpropanoate (**3o**)

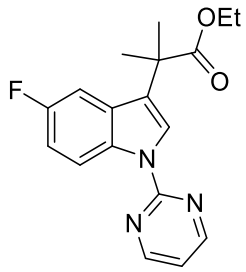

The above compound was synthesized using General Procedure **B** using ethyl 2-(5-fluoro-1*H*-indol-3-yl)-2-methylpropanoate (0.349 g, 1.4 mmol), sodium hydride (60% wt. dispersion in mineral oil, 0.084 g, 2.1 mmol) and 2-chloropyrimidine (0.242 g, 2.1 mmol). Silica gel column chromatography gave a white solid, 66% (0.302 g). **mp** (from $CHCl_3$): 110-114 °C. **FT-IR** (thin film): ν_{max} (cm^{-1}) = 2980.2, 1727.2, 1580.0, 1564.4. **^{1}H NMR** (500 MHz, $CDCl_3$) δ 8.84–8.74 (1H, m, In*H*), 8.67 (2H, d, *J* = 4.8 Hz, Pm*H*), 8.21 (1H, s, In*H*), 7.31–7.22 (1H, m, In*H*), 7.10–6.97 (2H, m, In*H* & Pm*H*), 4.14 (2H, q, *J* = 7.1 Hz, CO_2CH_2R), 1.71 (6H, s, $C(CH_3)_2$), 1.16 (3H, t, *J* = 7.1 Hz, $CO_2CH_2CH_3$). **^{13}C NMR** (126 MHz, $CDCl_3$) δ 176.5 (CO_2Et), 158.8 (d, *J* = 238.0 Hz, Ar*C*), 158.2 (Ar*C*), 157.6 (Ar*C*), 132.7 (Ar*C*), 130.3 (d, *J* = 9.6 Hz, Ar*C*), 124.7 (d, *J* = 4.2 Hz, Ar*C*), 123.6 (Ar*C*), 117.5 (d, *J* = 9.0 Hz, Ar*C*), 116.2 (Ar*C*), 111.5 (d, *J* = 24.8 Hz, Ar*C*), 105.9 (d, *J* = 24.2 Hz, Ar*C*), 61.2 (CO_2CH_2R), 42.1 ($C(CH_3)_2$), 26.0 ($C(CH_3)_2$), 14.3 ($CO_2CH_2CH_3$). **^{19}F NMR** (470 MHz, $CDCl_3$) δ -121.4 (td, *J* = 9.6, 5.1 Hz, Ar*F*). **HRMS** (ESI): m/z calculated for $C_{18}H_{18}N_3O_2F_1$ requires 328.1461 for $[M+H]^+$, found 328.1453.

Synthesis of ethyl 2-(5-bromo-1*H*-indol-3-yl)-2-methylpropanoate (**S3d**)

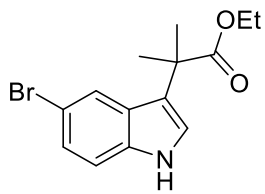

The above compound was synthesized using General Procedure **A** using 5-bromoindole, (0.392 g). Silica gel chromatography gave a light brown solid, 79% (0.490 g). **FT-IR** (thin film): ν_{max} (cm^{-1}) = 3352.4, 2979.1, 1703.4. **^{1}H NMR** (500 MHz, $CDCl_3$) δ 8.15 (1H, s, N*H*), 7.82 (1H, dd, *J* = 1.9, 0.6 Hz, Ar*H*), 7.24 (1H, dd, *J* = 8.6, 1.9 Hz, Ar*H*), 7.19–7.15 (1H, m, Ar*H*), 4.20–4.09 (2H, m, $CO_2CH_2CH_3$), 1.67 (6H, s, $C(CH_3)_2$), 1.20 (3H, t, *J* = 7.1 Hz, $CO_2CH_2CH_3$). **^{13}C NMR** (126 MHz, $CDCl_3$) δ 176.92 (CO_2Et), 135.59 (Ar*C*), 127.48 (Ar*C*), 124.89 (Ar*C*), 123.12 (Ar*C*), 121.99 (Ar*C*), 120.62 (Ar*C*), 112.82 (Ar*C*), 112.78 (Ar*C*), 61.14 ($CO_2CH_2CH_3$), 42.14 ($C(CH_3)_2$), 26.25 ($C(CH_3)_2$), 14.27 ($CO_2CH_2CH_3$). **HRMS** (ESI): m/z calculated for $C_{14}H_{16}N_1O_2Br_1$ requires 310.0443 for $[M+H]^+$, found 310.0430.

Synthesis of ethyl 2-(5-bromo-1-(pyrimidin-2-yl)-1*H*-indol-3-yl)-2-methylpropanoate (**3p**)

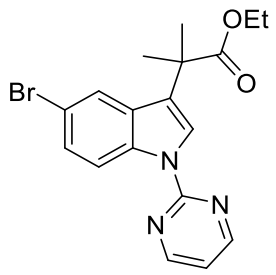

The above compound was synthesized using General Procedure **B** using ethyl 2-(5-bromo-1*H*-indol-3-yl)-2-methylpropanoate (0.440 g, 1.4 mmol), sodium hydride (60% wt. dispersion in mineral oil, 0.084 g, 2.1 mmol) and 2-chloropyrimidine (0.242 g, 2.1 mmol). Silica gel column chromatography gave a white solid, 43% (0.215 g). **mp** (from $CHCl_3$): 113-118 °C. **FT-IR** (thin film): ν_{max} (cm^{-1}) = 2981.2, 1723.9, 1575.5, 1563.5. **^{1}H NMR** (500 MHz, $CDCl_3$) δ 8.70 (1H, dd, *J* = 8.9, 0.5 Hz, In*H*), 8.68 (2H, d, *J* = 4.8 Hz, Pm*H*), 8.17 (1H, s, In*H*), 7.74 (1H, dd, *J* = 2.0, 0.5 Hz, In*H*), 7.40 (1H, dd, *J* = 8.9, 2.0 Hz, In*H*), 7.04 (1H, t, *J* = 4.8 Hz, Pm*H*), 4.16 (2H, q, *J* = 7.1 Hz, $CO_2CH_2CH_3$), 1.71 (6H, s, $C(CH_3)_2$), 1.18 (3H, t, *J* = 7.1 Hz, $CO_2CH_2CH_3$). **^{13}C NMR** (126 MHz, $CDCl_3$) δ 176.39 (CO_2Et), 158.23 (Ar*C*), 157.51 (Ar*C*), 135.00 (Ar*C*), 131.19 (Ar*C*), 126.58 (Ar*C*), 124.28 (Ar*C*), 123.29 (Ar*C*), 122.98 (Ar*C*), 118.06 (Ar*C*), 116.40 (Ar*C*), 115.42 (Ar*C*), 61.24 ($CO_2CH_2CH_3$), 42.14 ($C(CH_3)_2$), 26.07 ($C(CH_3)_2$), 14.25 ($CO_2CH_2CH_3$). **HMRS** (ESI): m/z calculated for $C_{18}H_{18}N_3O_2Br_1$ requires 388.0661 for $[M+H]^+$, found 388.0660.

Synthesis of ethyl 2-(4-fluoro-1-(pyrimidin-2-yl)-1*H*-indol-3-yl)-2-methylpropanoate (**S3a**)

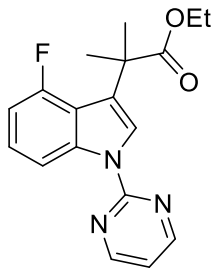

The above compound was synthesized using General Procedure **A** using 4-fluoroindole (0.405 g, 3 mmol) and other reagents scaled respectively. Silica gel chromatography gave a white solid which was immediately submitted to General Procedure **B** without analysis. This procedure was followed using sodium hydride (60% wt. dispersion in mineral oil, 0.072 g, 1.8 mmol), 2-chloropyrimidine (0.344 g, 3 mmol) and DMF (5 mL). Silica gel column chromatography gave a white solid, 40% over two steps (0.360 g). **mp** (from $CHCl_3$): 119-121 °C. **FT-IR** (thin film): ν_{max} (cm^{-1}) = 2979.9, 2923.8, 1727.0, 1578.6, 1563.2, 1445.3. **^{1}H NMR** (300 MHz, $CDCl_3$) δ 8.69 (2H, d, *J* = 4.8 Hz, Pm*H*), 8.64 (1H, d, *J* = 8.4 Hz, In*H*), 8.13 (1H, s, In*H*), 7.33–7.15 (1H, m, In*H*), 7.05 (1H, t, *J* = 4.8 Hz, Pm*H*), 6.89 (1H, ddd, *J* = 11.0, 8.0, 0.8 Hz, In*H*), 4.16 (2H, q, *J* = 7.1 Hz, $CO_2C\mathit{H}_2CH_3$), 1.72 (6H, s, $C(C\mathit{H}_3)_2$), 1.16 (2H, t, *J* = 7.1 Hz, $CO_2CH_2C\mathit{H}_3$). **^{13}C NMR** (75 MHz, $CDCl_3$) δ 177.1 ($\mathit{C}O_2R$), 158.2 (Ar*C*), 157.6 (d, *J* = 5.8 Hz, Ar*C*), 154.3 (Ar*C*), 138.5 (d, *J* = 10.5 Hz, Ar*C*), 124.6 (d, *J* = 8.0 Hz, Ar*C*), 124.2 (d, *J* = 3.5 Hz, Ar*C*), 122.2 (Ar*C*), 118.2 (d, *J* = 19.9 Hz, Ar*C*), 116.4 (Ar*C*), 112.6 (d, *J* = 3.6 Hz, Ar*C*), 107.9 (d, *J* = 20.6 Hz, Ar*C*), 61.0 ($CO_2\mathit{C}H_2CH_3$), 42.5 ($\mathit{C}(CH_3)_2$), 26.9 ($C(\mathit{C}H_3)_2$), 26.9 ($C(\mathit{C}H_3)_2$), 14.2 ($CO_2CH_2\mathit{C}H_3$). **^{19}F NMR** (470 MHz, $CDCl_3$) δ -123.66 (dd, *J* = 10.9, 5.2 Hz). **HRMS** (ESI): m/z calculated for $C_{24}H_{28}N_3O_4$ requires 442.2142 for $[M+H]^+$, found 442.2162.

6.3.5: Synthesis of C6 Functionalized Materials

General Procedure **C** for the C-3 Stabilised C-6 C–H Radical Alkylation of Indole Derivatives

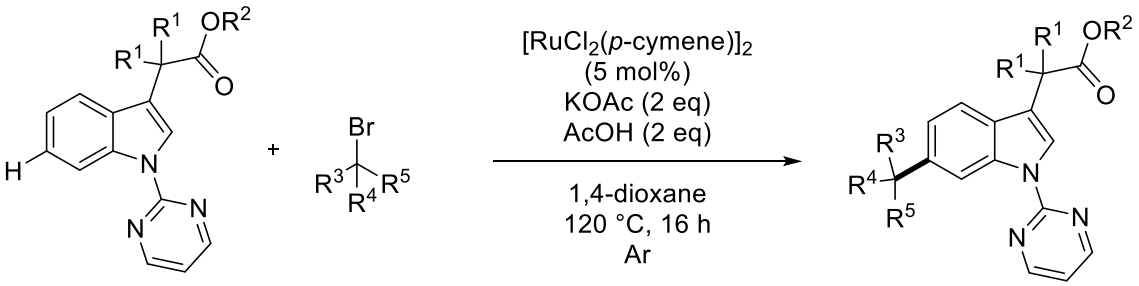

To an oven dried carousel tube was charged relevant C-3 functionalized material (0.25 mmol), α-bromo ester (0.75 mmol), $[RuCl_2(p\text{-cymene})]_2$ (0.0077 g), potassium acetate (0.049 g, 0.5 mmol), acetic acid (0.029 mL, 0.5 mmol, 0.030 g) and 1,4-dioxane (1 mL). The vessel was evacuated and refilled with argon three times. The reaction mixture was heated to 120 °C and left to stir for 16 h. The reaction mixture was allowed to return to room temperature and diluted with EtOAc (20 mL) and sat. $NaHCO_3$ solution (20 mL). The organic layer was extracted and the aqueous layer was re-extracted with EtOAc (2 x 20 mL). The combined organic layers were dried over $MgSO_4$ and concentrated *in vacuo*. The crude residue was purified *via* silica gel column chromatography using EtOAc/Petroleum Ether 40-60 °C (1:20-1:10, *v:v*) to give pure C-6 functionalized product.

General Procedure **D** for the One-Pot Sequential C3/C6 Alkylation of Indole Derivatives

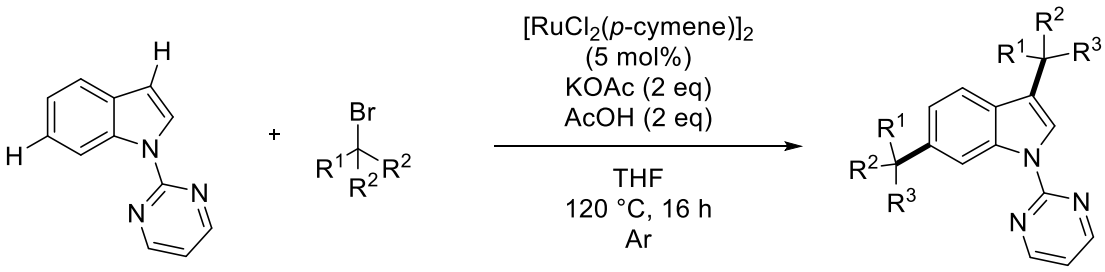

To an oven dried carousel tube was charged relevant indole derivative (0.25 mmol), α-bromo ester (0.75 mmol), $[RuCl_2(p\text{-cymene})]_2$ (0.0077 g), potassium acetate (0.049 g, 0.5 mmol), acetic acid (0.029 mL, 0.5 mmol, 0.030 g) and THF (1 mL). The vessel was evacuated and refilled with argon three times. The reaction mixture was heated to 120 °C and left to stir for 16 h. The reaction mixture was allowed to return to room temperature and diluted with EtOAc (20 mL) and sat. $NaHCO_3$ solution (20 mL). The organic layer was extracted and the aqueous layer was re-extracted with EtOAc (2 x 20 mL). The combined organic layers were dried over $MgSO_4$ and concentrated *in vacuo*. The crude residue was purified *via* silica gel column chromatography using EtOAc/Petroleum Ether 40-60 °C (1:20-1:10, *v:v*) to give a mixture of C-3 functionalized and C-3/C-6 di-functionalized products.

Synthesis of **4a**

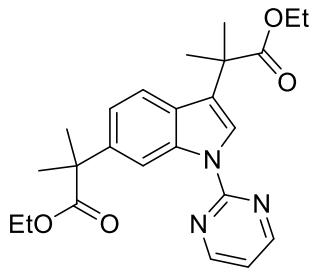

The above compound was synthesized using General Procedure **C** using **3a** (0.077 g) and ethyl α-bromoisobutyrate (0.12 mL, 0.75 mmol) as coupling partner. Silica gel chromatography gave a white solid, 80% (0.085 g). **mp** (from $CHCl_3$): 94-99 °C. **FT-IR** (thin film): ν_{max} (cm^{-1}) = 2978.7, 1725.1, 1578.1, 1562.8. **^{1}H NMR** (500 MHz, $CDCl_3$) δ 8.88 (1H, dd, *J* = 1.8, 0.6 Hz, In*H*), 8.68 (2H, d, *J* = 4.8 Hz, Pm*H*), 8.14 (1H, s, In*H*), 7.54 (1H, dd, *J* = 8.4, 0.6 Hz, In*H*), 7.19 (1H, dd, *J* = 8.4, 1.8 Hz, In*H*), 7.01 (1H, t, *J* = 4.8 Hz, Pm*H*), 4.14 (4H, m, $CO_2C\mathit{H}_2CH_3$), 1.71 (6H, s, $C(C\mathit{H}_3)_2$), 1.67 (6H, s, $C(C\mathit{H}_3)_2$), 1.20 (3H, t, *J* = 7.1 Hz, $CO_2CH_2C\mathit{H}_3$), 1.15 (3H, t, *J* = 7.1 Hz, $CO_2CH_2C\mathit{H}_3$). **^{13}C NMR** (126 MHz, $CDCl_3$) δ 177.4 ($\mathit{C}O_2Et$), 176.7 ($\mathit{C}O_2Et$), 158.2 (Ar*C*), 157.8 (Ar*C*), 140.9 (Ar*C*), 136.5 (Ar*C*), 128.1 (Ar*C*), 124.8 (Ar*C*), 122.4 (Ar*C*), 120.0 (Ar*C*), 116.0 (Ar*C*), 113.7 (Ar*C*), 61.0 ($CO_2\mathit{C}H_2R$), 60.9 ($CO_2\mathit{C}H_2R$), 47.0 ($\mathit{C}(CH_3)_2$), 42.2 ($\mathit{C}(CH_3)_2$), 27.2 ($C(\mathit{C}H_3)_2$), 26.1 ($C(\mathit{C}H_3)_2$), 14.2 ($CO_2CH_2\mathit{C}H_3$), 14.2 ($CO_2CH_2\mathit{C}H_3$). **HRMS** (ESI): m/z calculated for $C_{24}H_{29}N_3O_4$ requires 424.2236 for $[M+H]^+$, found 424.2254.

Synthesis of **4g**

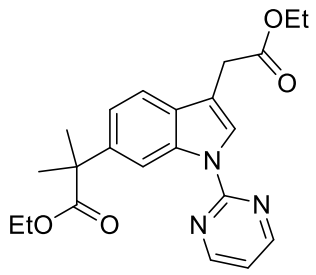

The above compound was synthesized using General Procedure **C** using **3a** (0.070 g) and ethyl α-bromoisobutyrate (0.12 mL, 0.75 mmol) as coupling partner. Silica gel chromatography gave an off white amorphous solid, 40% (0.040 g). **FT-IR** (thin film): ν_{max} (cm^{-1}) = 2979.5, 1727.6, 1577.8, 1567.6. **^{1}H NMR** (500 MHz, $CDCl_3$) δ 8.87 (1H, d, *J* = 1.8 Hz, In*H*), 8.68 (2H, d, *J* = 4.8 Hz, Pm*H*), 8.28 (1H, s, In*H*), 7.54 (1H, d, *J* = 8.4 Hz, In*H*),

7.28–7.22 (2H, m, In*H*), 7.03 (1H, t, *J* = 4.8 Hz, Pm*H*), 4.45 (2H, d, *J* = 1.4 Hz, C*H*$_2$CO$_2$Et), 4.24–4.09 (4H, m, CO$_2$C*H*$_2$CH$_3$), 1.68 (6H, s, C(C*H*$_3$)$_2$), 1.17-1.13 (3H, m, CO$_2$CH$_2$C*H*$_3$), 0.95–0.85 (3H, m, CO$_2$CH$_2$C*H*$_3$).**^{13}C NMR** (126 MHz, $CDCl_3$) δ 177.3 (*C*O$_2$Et), 172.7 (*C*O$_2$Et), 158.2 (Ar*C*), 141.0 (Ar*C*), 135.5 (Ar*C*), 130.1 (Ar*C*), 126.4 (Ar*C*), 120.3 (Ar*C*), 119.2 (Ar*C*), 116.3 (Ar*C*), 113.78 (Ar*C*), 113.6 (Ar*C*), 61.0 (CO$_2$*C*H$_2$R), 60.9 (CO$_2$*C*H$_2$R), 48.9, 45.6, 27.2 (C(*C*H$_3$)$_2$), 14.3 (CO$_2$CH$_2$*C*H$_3$), 14.2 (CO$_2$CH$_2$*C*H$_3$). **HRMS** (ESI): m/z calculated for $C_{22}H_{25}N_3O_4$ requires 418.1745 for $[M+Na]^+$, found 418.1775.

Synthesis of **4h**

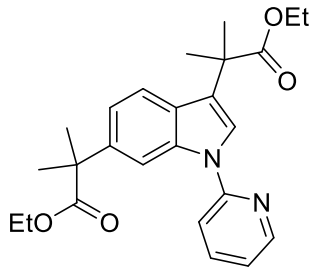

The above compound was synthesized using General Procedure **C** and using 1-(pyridinyl-1-yl)-1*H*-indole (0.049 g) and ethyl α-bromoisobutyrate (0.12 mL, 0.75 mmol) as coupling partner. Silica gel chromatography gave an amorphous solid, 55% (0.058 g). **FT-IR** (thin film): ν_{max} (cm^{-1}) = 2979.7, 1723.2, 1589.8, 1555.1. **^{1}H NMR** (500 MHz, $CDCl_3$) δ 8.56 (1H, ddd, *J* = 4.9, 2.0, 0.9 Hz, Ar*H*), 8.14 (1H, dd, *J* = 1.7, 0.7 Hz, Ar*H*), 7.82 (1H, ddd, *J* = 8.2, 7.4, 2.0 Hz, Ar*H*), 7.60 (2H, d, *J* = 8.9 Hz, Ar*H*), 7.48 (1H, dt, *J* = 8.2, 0.9 Hz, Ar*H*), 7.22–7.12 (2H, m, Ar*H*), 4.17–4.08 (4H, m, CO$_2$C*H*$_2$CH$_3$), 1.71 (6H, s, C(C*H*$_3$)$_2$), 1.64 (6H, s, C(C*H*$_3$)$_2$), 1.22–1.14 (6H, m, CO$_2$CH$_2$C*H*$_3$). **^{13}C NMR** (126 MHz, $CDCl_3$) δ 177.2 (*C*O$_2$Et), 176.8 (*C*O$_2$Et), 152.4 (Ar*C*), 149.2 (Ar*C*), 140.2 (Ar*C*), 138.5 (Ar*C*), 136.0 (Ar*C*), 127.1 (Ar*C*), 123.4 (Ar*C*), 122.9 (Ar*C*), 120.5 (Ar*C*), 120.1 (Ar*C*), 119.3 (Ar*C*), 114.9 (Ar*C*), 109.8 (Ar*C*), 61.0 (CO$_2$*C*H$_2$R), 60.9 (CO$_2$*C*H$_2$R), 46.8 (*C*(CH$_3$)$_2$), 42.2 (*C*(CH$_3$)$_2$), 27.1 (C(*C*H$_3$)$_2$), 26.2 (C(*C*H$_3$)$_2$), 14.3 (CO$_2$CH$_2$*C*H$_3$), 14.2 (CO$_2$CH$_2$*C*H$_3$). **HRMS** (ESI): m/z calculated for $C_{25}H_{30}N_2O_4$ requires 445.2103 for $[M+Na]^+$, found 445.2112.

Synthesis of **4i**

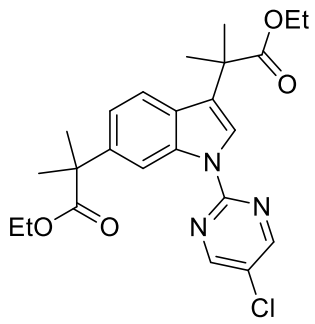

The above compound was synthesized using General Procedure **C** using 1-(5-chloropyrimidin-2yl)-1*H*-indole (0.057 g, 0.25 mmol) and ethyl α-bromoisobutyrate (0.12 mL, 0.75 mmol) as coupling partner. Silica gel chromatography gave a white solid, 40% (0.046 g). **mp** (from $CHCl_3$): 129-133 °C. **FT-IR** (thin film): ν_{max} (cm^{-1}) = 2980.0, 1725.6, 1573.3. **^{1}H NMR** (500 MHz, $CDCl_3$) δ 8.77 (1H, dd, *J* = 1.9, 0.6 Hz, In*H*), 8.62 (2H, s, Pm*H*), 8.06 (1H, s), 7.53 (1H, dd, *J* = 8.4, 0.6 Hz, In*H*), 7.21 (1H, dd, *J* = 8.4, 1.8 Hz, In*H*), 4.18-4.10 (4H, m, CO_2CH_{2R}), 1.71 (6H, s, $C(CH_3)_2$), 1.66 (6H, s, $C(CH_3)_2$), 1.20 (3H, t, *J* = 7.1 Hz, $CO_2CH_2CH_3$), 1.15 (3H, t, *J* = 7.1 Hz, $CO_2CH_2CH_3$). **^{13}C NMR** (126 MHz, $CDCl_3$) δ 177.2 (CO_2Et), 176.6 (CO_2Et), 156.5 (Ar*C*), 155.7 (Ar*C*), 141.1 (Ar*C*), 136.3 (Ar*C*), 128.16 (Ar*C*), 125.4 (Ar*C*), 124.9 (Ar*C*), 122.4 (Ar*C*), 120.4 (Ar*C*), 120.2 (Ar*C*), 113.6 (Ar*C*), 61.1 (CO_2CH_2R), 60.9 (CO_2CH_2R), 47.0 ($C(CH_3)_2$), 42.2 ($C(CH_3)_2$), 27.1 ($C(CH_3)_2$), 26.0 ($C(CH_3)_2$), 14.2 ($CO_2CH_2CH_3$), 14.1 ($CO_2CH_2CH_3$). **HRMS** (ESI): m/z calculated for $C_{24}H_{28}Cl_1N_3O_4$ requires 458.1847 for $[M+H]^+$, found 458.1855.

Synthesis of **4j**

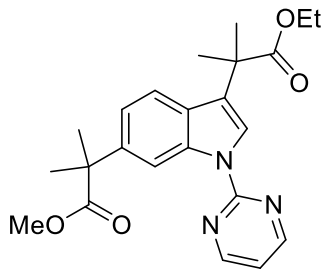

The above compound was synthesized using General Procedure **C** using **3a** (0.077 g) and ethyl α-bromoisobutyrate (0.12 mL, 0.75 mmol) as coupling partner. Silica gel chromatography gave a white solid, 65% (0.066 g). **mp** (from $CHCl_3$): 81-85 °C. **FT-IR** (thin film): ν_{max} (cm^{-1}) = 2977.6, 1727.5, 1578.0, 1562.7. **^{1}H NMR** (500 MHz, $CDCl_3$) δ 8.88 (1H,

dd, *J* = 1.9, 0.6 Hz, In*H*), 8.68 (2H, d, *J* = 4.8 Hz, Pm*H*), 8.14 (1H, s, In*H*), 7.54 (1H, dd, *J* = 8.4, 0.6 Hz, In*H*), 7.18 (1H, dd, *J* = 8.4, 1.9 Hz, In*H*), 7.01 (1H, t, *J* = 4.8 Hz, Pm*H*), 4.12 (2H, q, *J* = 7.1 Hz, CO_2CH_2R), 3.67 (3H, s, CO_2CH_3), 1.71 (6H, s, $C(CH_3)_2$), 1.68 (6H, s, $C(CH_3)_2$), 1.15 (3H, t, *J* = 7.1 Hz, $CO_2CH_2CH_3$). **^{13}C NMR** (126 MHz, $CDCl_3$) δ 177.9 (CO_2R), 176.7 (CO_2R), 158.2 (Ar*C*), 157.8 (Ar*C*), 140.6 (Ar*C*), 136.5 (Ar*C*), 128.2 (Ar*C*), 124.8 (Ar*C*), 122.4 (Ar*C*), 120.1 (Ar*C*), 120.1 (Ar*C*), 116.0 (Ar*C*), 113.6 (Ar*C*), 61.0 (CO_2CH_2R), 52.3 (CO_2CH_2R), 47.0 ($C(CH_3)_2$), 42.2 ($C(CH_3)_2$), 27.1 ($C(CH_3)_2$), 26.1 ($C(CH_3)_2$), 14.2 ($CO_2CH_2CH_3$). **HRMS** (ESI): m/z calculated for $C_{23}H_{27}N_3O_4$ requires 432.1902 for $[M+Na]^+$, found 432.1947.

Synthesis of **4k**

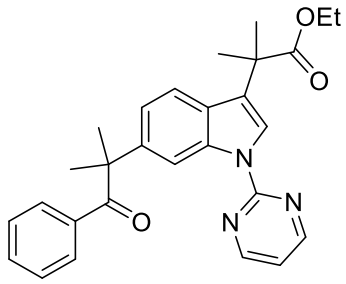

The above compound was synthesized using General Procedure **C** using **3a** (0.077 g) and 2-bromo isobutyrophenone (0.15 mL, 0.75 mmol) as coupling partner. Silica gel chromatography gave an amorphous solid, 26% (0.030 g). **FT-IR** (thin film): ν_{max} (cm^{-1}) = 2980.8, 1727.3, 1676.5, 1577.8, 1565.8. **^{1}H NMR** (500 MHz, CD_3OD) δ 8.94 (1H, dd, *J* = 1.8, 0.6 Hz, In*H*), 8.72 (2H, d, *J* = 4.8 Hz, Pm*H*), 8.20 (1H, s, In*H*), 7.52 (1H, dd, *J* = 8.4, 0.6 Hz, Ar*H*), 7.50–7.47 (2H, m, Ar*H*), 7.36–7.28 (1H, m, Ar*H*), 7.20–7.16 (2H, m), 7.14 (1H, t, *J* = 4.8 Hz, Pm*H*), 7.11 (1H, dd, *J* = 8.3, 1.8 Hz, Ar*H*), 4.10 (2H, q, *J* = 7.1 Hz, CO_2CH_2R), 1.69 (6H, s, $C(CH_3)_2$), 1.66 (6H, s, $C(CH_3)_2$), 1.08 (3H, t, *J* = 7.1 Hz, $CO_2CH_2CH_3$). **^{13}C NMR** (126 MHz, CD_3OD) δ 178.2 (*C*O), 159.62 (*C*O), 158.8 (Ar*C*), 142.2 (Ar*C*), 138.1 (Ar*C*), 137.9 (Ar*C*), 132.8 (Ar*C*), 130.7 (Ar*C*), 129.4 (Ar*C*), 129.0 (Ar*C*), 125.7 (Ar*C*), 123.7 (Ar*C*), 121.5 (Ar*C*), 121.1 (Ar*C*), 117.7 (Ar*C*), 114.7 (Ar*C*), 62.1 (CO_2CH_2R), 52.8 ($C(CH_3)_2$), 43.2 ($C(CH_3)_2$), 28.7 ($C(CH_3)_2$), 26.3 ($C(CH_3)_2$), 14.4 ($CO_2CH_2CH_3$). **HRMS** (ESI): m/z calculated for $C_{28}H_{29}N_3O_3$ requires 456.2287 for $[M+H]^+$, found 456.2307.

Synthesis of **4l**

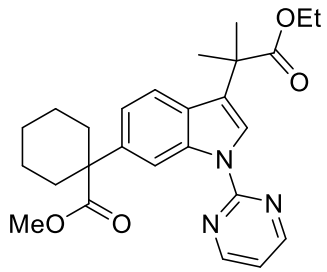

The above compound was synthesized using General Procedure **C** using **3a** (0.077 g) and methyl 1-bromo-1-cyclohexanecarboxylate (0.12 mL, 0.75 mmol) as coupling partner. Silica gel chromatography gave an amorphous solid, 14% (0.016 g). **FT-IR** (thin film): ν_{max} (cm^{-1}) = 2924.8, 2854.9, 1726.0, 1578.0, 1562.6, 1438.7. **^{1}H NMR** (300 MHz, $CDCl_3$) δ 8.93 (1H, dd, *J* = 1.8, 0.6 Hz, In*H*), 8.70 (2H, d, *J* = 4.8 Hz, Pm*H*), 8.13 (1H, s, In*H*), 7.52 (1H, dd, *J* = 8.5, 0.6 Hz, In*H*), 7.37–7.13 (1H, m, In*H*), 7.03 (1H, t, *J* = 4.8 Hz, Pm*H*), 4.12 (2H, q, *J* = 7.1 Hz, $CO_2C\mathit{H}_2CH_3$), 3.65 (3H, s, $CO_2C\mathit{H}_3$).2.61 (2H, d, J = 13.0 Hz, Cy*H*), 1.96–1.55 (10H, m, Cy*H* & $C(C\mathit{H}_3)_2$), 1.55–1.47 (2H, m, Cy*H*), 1.37–1.28 (2H, m, Cy*H*), 1.15 (3H, t, J = 7.1 Hz, $CO_2CH_2C\mathit{H}_3$), 0.94–0.79 (2H, m, Cy*H*). **^{13}C NMR** (75 MHz, $CDCl_3$) δ 176.8 ($\mathit{C}O_2R$), 176.3 ($\mathit{C}O_2R$), 158.2 (Ar*C*), 157.8 (Ar*C*), 139.9 (Ar*C*), 136.6 (Ar*C*), 128.2 (Ar*C*), 124.7 (Ar*C*), 122.4 (Ar*C*), 120.10 (Ar*C*), 116.0 (Ar*C*), 114.0 (Ar*C*), 67.9 ($CO_2\mathit{C}H_2R$), 66.2 ($CO_2\mathit{C}H_2R$), 61.1 ($\mathit{C}(CH_3)_2$), 52.1 (*C*(Cy)), 51.4 (Alk*C*H), 42.2 (Alk*C*H), 35.4 (Alk*C*H), 29.8 (Alk*C*H), 26.1 (Alk*C*H), 24.0 (Alk*C*H), 14.3 (Alk*C*H). **HRMS** (ESI): m/z calculated for $C_{27}H_{33}N_3O_4$ requires 472.2215 for $[M+Na]^+$, found 472.2216.

Synthesis of **4m**

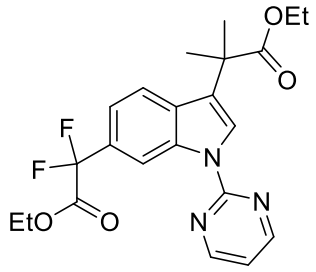

The above compound was synthesized using General Procedure **C** using **3a** (0.077 g) ethyl bromodifluoroacetate (0.096 mL, 0.75 mmol) as coupling partner. Silica gel chromatography gave an amorphous solid, 16% (0.017 g). **FT-IR** (thin film): ν_{max} (cm^{-1}) = 2983.7, 2922.8, 1764.4, 1727.4, 1578.2, 1566.7, 1452.9. **^{1}H NMR** (300 MHz, $CDCl_3$) δ 9.15 (1H, dd, *J* = 1.7,

0.8 Hz, *In*H), 8.73 (2H, d, *J* = 4.8 Hz, Pm*H*), 8.28 (1H, s, In*H*), 7.66 (1H, dd, *J* = 8.4, 0.8 Hz, In*H*), 7.44 (1H, dd, *J* = 8.4, 1.7 Hz, In*H*), 7.09 (1H, t, *J* = 4.8 Hz, Pm*H*), 4.32 (2H, q, *J* = 7.1 Hz, $CO_2CH_2CH_3$), 4.12 (2H, q, *J* = 7.1 Hz, $CO_2CH_2CH_3$), 1.72 (6H, s, $C(CH_3)_2$), 1.32 (3H, t, *J* = 7.2 Hz, $CO_2CH_2CH_3$), 1.14 (3H, t, *J* = 7.1 Hz, $CO_2CH_2CH_3$). **^{13}C NMR** (75 MHz, $CDCl_3$) δ 176.6 (CO_2R), 158.3 (CO_2R), 157.5 (Ar*C*), 135.6 (Ar*C*), 124.7 (Ar*C*), 124.2 (Ar*C*), 120.5 (Ar*C*), 119.0 (Ar*C*), 116.6 (Ar*C*), 114.3 (Ar*C*), 63.2 ($CO_2CH_2CH_3$), 61.2 ($CO_2CH_2CH_3$), 42.1 ($C(CH_3)_2$), 28.0 (d, *J* = 285.6 Hz, $C(F_2)$), 14.3 ($CO_2CH_2CH_3$), 14.1 ($CO_2CH_2CH_3$). **^{19}F NMR** (470 MHz, $CDCl_3$) δ -101.51. **HRMS** (ESI): m/z calculated for $C_{22}H_{23}N_3O_4F_2$ requires 432.1758 for $[M+H]^+$, found 432.1735.

Synthesis of **4p**

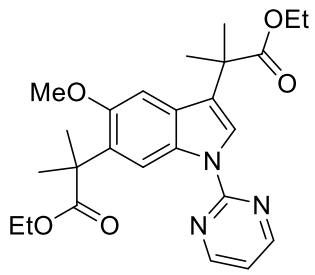

The above compound was synthesized using General Procedure **C**, using ethyl 2-(5-methoxy-1-(pyrimidin-2-yl)-1*H*-indol-3-yl)-2-methylpropanoate (0.085 g, 0.25 mmol), and ethyl α-bromoisobutyrate (0.12 mL, 0.75 mmol). Silica gel column chromatography gave a white solid, 92% (0.104 g). **mp** (from $CHCl_3$): 122-128 °C. **FT-IR** (thin film): ν_{max} (cm^{-1}) = 2980.9, 1726.2, 1578.5, 1562.7. **^{1}H NMR** (500 MHz, $CDCl_3$) δ 8.84 (1H, s, In*H*), 8.66 (2H, d, *J* = 4.7 Hz, Pm*H*), 8.11 (1H, s, In*H*), 7.01 (1H, s, In*H*), 6.98 (1H, t, *J* = 4.8 Hz, Pm*H*), 4.12 (4H, app qd, *J* = 7.1, 2.4 Hz, $CO_2CH_2CH_3$), 3.80 (3H, s, $ArOCH_3$), 1.71 (6H, s, $C(CH_3)_2$), 1.62 (6H, s, $C(CH_3)_2$), 1.15 (6H, app td, *J* = 7.1, 1.8 Hz, $CO_2CH_2CH_3$). **^{13}C NMR** (126 MHz, $CDCl_3$) δ 178.42 (CO_2Et), 176.81 (CO_2Et), 158.14 (Ar*C*), 157.73 (Ar*C*), 152.87 (Ar*C*), 131.40 (Ar*C*), 130.93 (Ar*C*), 128.58 (Ar*C*), 124.54 (Ar*C*), 122.11 (Ar*C*), 115.76 (Ar*C*), 113.89 (Ar*C*), 101.38 (Ar*C*), 61.01 ($CO_2CH_2CH_3$), 60.36 (CO_2CH_3), 55.40 ($ArOCH_3$), 44.91 ($C(CH_3)_2$), 42.13 ($C(CH_3)_2$), 26.21 ($C(CH_3)_2$), 25.96 ($C(CH_3)_2$), 14.34 ($CO_2CH_2CH_3$), 14.30 ($CO_2CH_2CH_3$). **HRMS** (ESI): m/z calculated for $C_{25}H_{31}N_3O_5$ requires 454.2342 for $[M+H]^+$, found 454.2371.

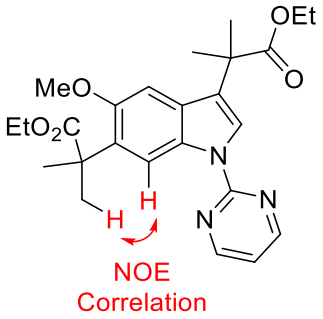

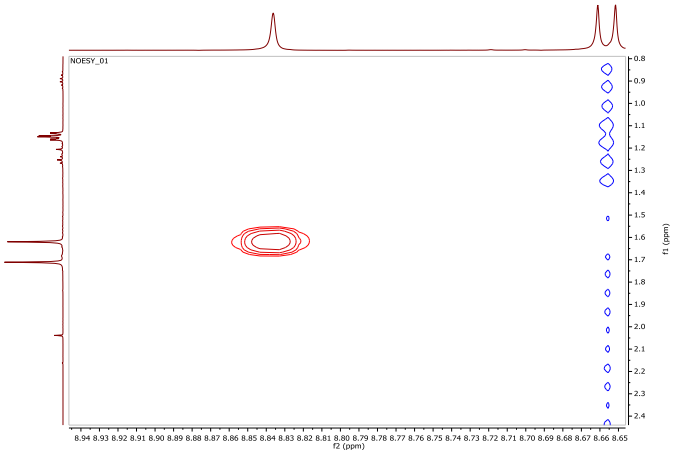

Synthesis of **4q**

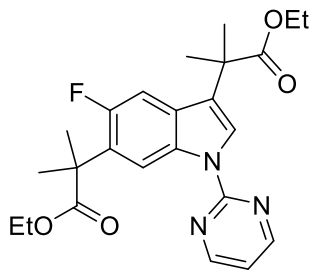

The above compound was synthesized using General Procedure **C**, using ethyl 2-(5-fluoro-1-(pyrimidin-2-yl)-1*H*-indol-3-yl)-2-methylpropanoate (0.082 g, 0.25 mmol), and ethyl α-bromoisobutyrate (0.12 mL, 0.75 mmol). Silica gel column chromatography gave a white solid, 87% (0.096 g). **mp** (from $CHCl_3$): 117-121 °C. **FT-IR** (thin film): ν_{max} (cm^{-1}) = 2981.0, 1729.3, 1579.0, 1565.0. **^{1}H NMR** (500 MHz, $CDCl_3$) δ 8.88 (1H, d, *J* = 7.2 Hz), 8.68 (2H, d, *J* = 4.8 Hz), 8.18 (1H, s), 7.25 (1H, d, *J* = 12.0 Hz), 7.04 (1H, t, *J* = 4.8 Hz), 4.15 (4H, app dq, *J* = 15.5, 7.1 Hz, $CO_2CH_2CH_3$), 1.70 (6H, s, $C(CH_3)_2$), 1.66 (6H, s, $C(CH_3)_2$), 1.17 (6H, app dt, *J* = 8.6, 7.1 Hz, $CO_2CH_2CH_3$). **^{13}C NMR** (126 MHz, $CDCl_3$) δ 177.32 (CO_2Et), 176.40 (CO_2Et), 158.21 (Ar*C*), 157.87 (Ar*C*), 156.79 (d, *J* = 207.0 Hz, Ar*C*F), 132.67 (Ar*C*), 129.14 (d, *J* = 16.2 Hz, Ar*C*), 128.79 (d, *J* = 10.1 Hz, Ar*C*), 124.48 (d, *J* = 3.9 Hz, Ar*C*), 123.37 (Ar*C*), 116.17 (Ar*C*), 114.27 (d, *J* = 5.1 Hz, Ar*C*), 106.24 (d, *J* = 25.8 Hz, Ar*C*), 61.04 (d, *J*

= 25.7 Hz, Ar*C*), 44.73 (*C*(CH_3)$_2$), 42.16 (*C*(CH_3)$_2$), 26.25 (C(*C*H_3)$_2$), 25.96 (C(*C*H_3)$_2$), 14.23 ($CO_2CH_2CH_3$), 14.19 ($CO_2CH_3CH_3$). **^{19}F NMR** (470 MHz, $CDCl_3$) δ -120.99 (dd, *J* = 12.0, 7.2 Hz). **HRMS** (ESI): m/z calculated for $C_{24}H_{28}N_3O_4F_1$ requires 442.2142 for $[M+H]^+$, found 442.2173.

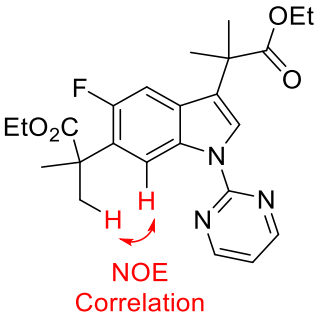

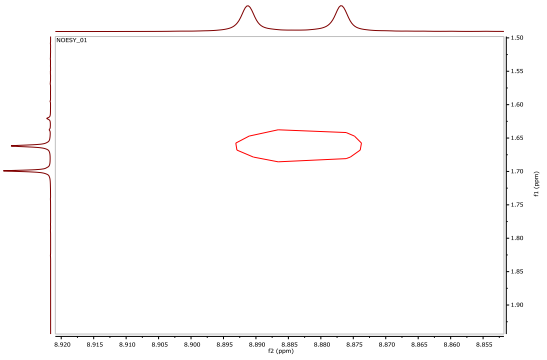

Synthesis of **4r**

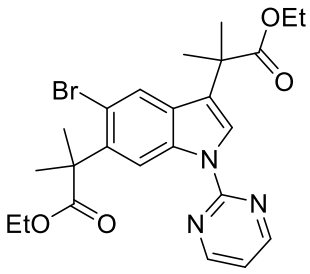

The above compound was synthesized using General Procedure **C**, using ethyl 2-(5-bromo-1-(pyrimidin-2-yl)-1*H*-indol-3-yl)-2-methylpropanoate (0.097 g, 0.25 mmol), and ethyl α-bromoisobutyrate (0.12 mL, 0.75 mmol). Silica gel column chromatography gave a white solid, 55% (0.069 g). **mp** (from $CHCl_3$): 130-134 °C. **FT-IR** (thin film): ν_{max} (cm^{-1}) = 2989.2, 1723.3, 1576.4, 1563.4, 1461.9, 1435.5. **^{1}H NMR** (500 MHz, $CDCl_3$) δ 9.03 (1H, s, In*H*), 8.67 (2H, d, *J* = 4.8 Hz, Pm*H*), 8.16 (1H, s, In*H*), 7.82 (1H, s, In*H*), 7.02 (1H, t, *J* = 4.8 Hz, Pm*H*), 4.16 (4H, dq, *J* = 11.0, 7.1 Hz, $CO_2CH_2CH_3$), 1.74 (6H, s, C(C*H*$_3$)$_2$), 1.71 (6H, s, C(C*H*$_3$)$_2$), 1.19 (6H, td, *J* = 7.1, 4.1 Hz, $CO_2CH_2CH_3$). **^{13}C NMR** (126 MHz, $CDCl_3$) δ 177.54

(*C*O_2Et), 176.29 (*C*O_2Et), 158.20 (Ar*C*), 157.52 (Ar*C*), 138.88 (Ar*C*), 135.54 (Ar*C*), 129.48 (Ar*C*), 125.53 (Ar*C*), 123.89 (Ar*C*), 123.40 (Ar*C*), 117.04 (Ar*C*), 116.28 (Ar*C*), 115.45 (Ar*C*), 61.19 ($CO_2CH_2CH_3$), 61.17 ($CO_2CH_2CH_3$), 48.53 ($C(CH_3)_2$), 42.14 ($C(CH_3)_2$), 27.05 ($C(CH_3)_2$), 26.07 ($C(CH_3)_2$), 14.22 ($CO_2CH_2CH_3$), 14.12 ($CO_2CH_2CH_3$). **HRMS** (ESI): m/z calculated for $C_{14}H_{28}N_3O_4Br_1$ requires 524.1160 for $[M+Na]^+$, found 524.1184.

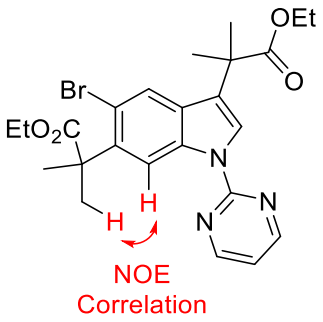

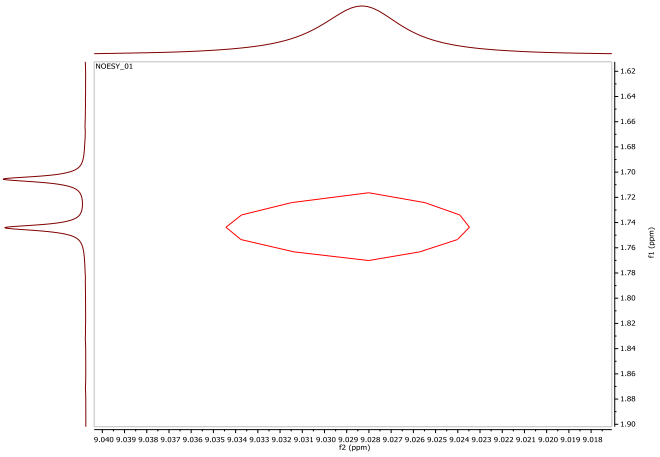

Synthesis of **S4a**

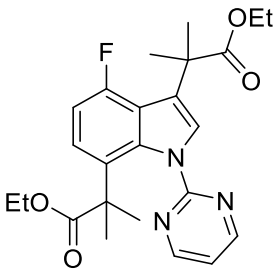

The above compound was synthesized using General Procedure **C**, using ethyl 2-(4-fluoro-1-(pyrimidin-2-yl)-1*H*-indol-3-yl)-2-methylpropanoate (0.082 g, 0.25 mmol), and ethyl α-bromoisobutyrate (0.12 mL, 0.75 mmol). Silica gel column chromatography gave an amorphous solid, 14% (0.015 g). **^{1}H NMR** (300 MHz, Chloroform-*d*) δ 8.76 – 8.60 (m, 3H), 8.10 (d, *J* = 0.6 Hz, 1H), 7.06 (t, *J* = 4.8 Hz, 1H), 6.90 (dd, *J* = 12.6, 1.5 Hz, 1H), 4.21 – 4.10 (m, 4H), 1.69 (s, 6H), 1.65 (s, 6H), 1.22 (d, *J* = 7.1 Hz, 2H), 1.22 – 1.11 (m, 4H). **^{13}C NMR**

(75 MHz, $CDCl_3$) δ 177.0 (*C*O_2R), 176.9 (*C*O_2R), 158.2 (Ar*C*), 157.4 (d, *J* = 41.5 Hz, Ar*C*), 153.9 (Ar*C*), 142.4 (d, *J* = 7.0 Hz, Ar*C*), 138.4 (d, *J* = 11.0 Hz, Ar*C*), 124.0 (d, *J* = 3.4 Hz, Ar*C*), 122.4 (Ar*C*), 116.8 (d, *J* = 20.5 Hz, Ar*C*), 116.4 (Ar*C*), 109.9 (d, *J* = 3.5 Hz, Ar*C*), 106.2 (d, *J* = 21.6 Hz, Ar*C*), 61.02 ($CO_2CH_2CH_3$) 61.00 ($CO_2CH_2CH_3$), 46.9 (d, *J* = 1.6 Hz, ($C(CH_3)_2$), 42.5 ($C(CH_3)_2$), 29.9 ($C(CH_3)_2$), 27.0 ($C(CH_3)_2$), 26.8 ($CO_2CH_2CH_3$), 14.2 ($CO_2CH_2CH_3$). **HRMS** (ESI): m/z calculated for $C_{24}H_{28}N_3O_4F_1$ requires 442.2142 for $[M+H]^+$, found 442.2162.

Unsuccessful Coupling Partners

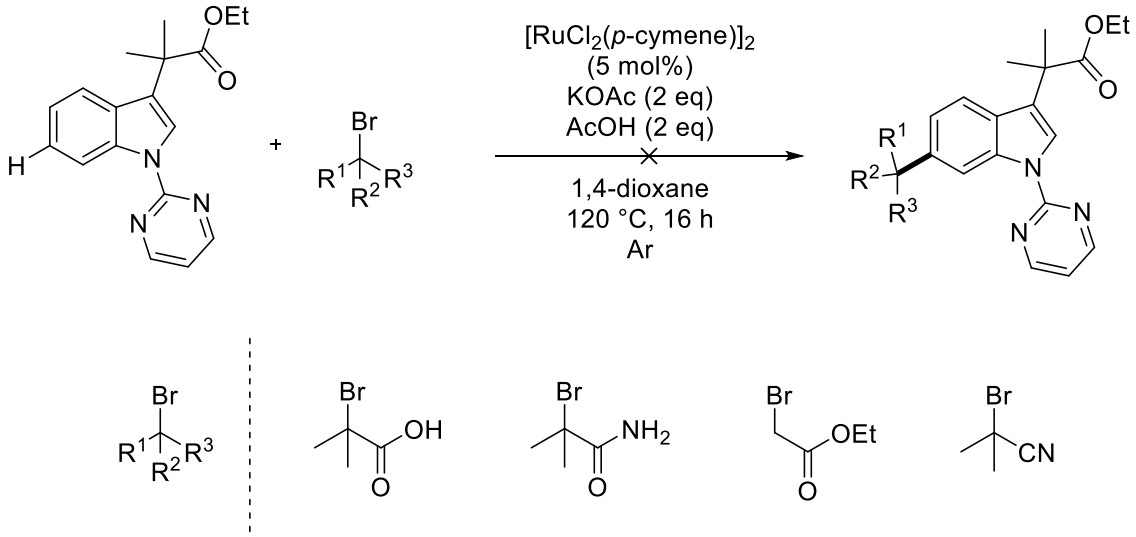

Synthesis of **3s** and **4s**

The above compounds were synthesized using General Procedure **D** using methyl α-bromoisobutyrate (0.10 mL, 0.75 mmol) as coupling partner. Silica gel chromatography gave two separable products **3s** (57%, 0.042 g) and **4s** (41%, 0.040 g).

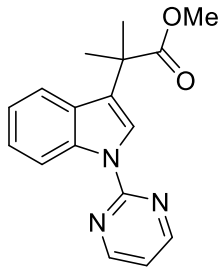

3s. mp (from $CHCl_3$): 110-114 °C. **FT-IR** (thin film): ν_{max} (cm^{-1}) = 2980.4, 1727.2, 1578.8, 1562.5. **^{1}H NMR** (500 MHz, $CDCl_3$) δ 8.84 (1H, d, *J* = 8.4 Hz, C-7*H*), 8.67 (2H, d, *J* = 4.8 Hz, Pm*H*), 8.19 (1H, s, C-2*H*), 7.58 (1H, d, *J* = 7.9 Hz, In*H*), 7.34 (1H, ddd, *J* = 8.4, 7.1, 1.3 Hz, In*H*), 7.23 (1H, ddd, *J* = 8.1, 7.1, 1.1 Hz, In*H*), 7.00 (1H, t, *J* = 4.8 Hz, Pm*H*), 3.66 (3H, s, CO_2CH_3), 1.75 (6H, s, $C(CH_3)_2$).**^{13}C NMR** (126 MHz,$CDCl_3$) δ 177.38 (CO_2R), 158.14 (Ar*C*), 158.13 (Ar*C*), 157.76 (Ar*C*), 136.29 (Ar*C*), 129.44 (Ar*C*), 124.85 (Ar*C*), 123.81 (Ar*C*), 122.10 (Ar*C*), 122.05 (Ar*C*), 120.02 (Ar*C*), 116.63 (Ar*C*), 116.04 (Ar*C*), 52.39 (CO_2CH_3), 42.13 ($C(CH_3)_2$), 26.10 ($C(CH_3)_2$). **HRMS** (ESI): m/z calculated for $C_{17}H_{17}N_3O_2$ requires 296.1399 for $[M+H]^+$, found 296.1383

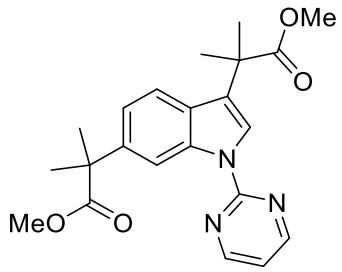

4s. mp (from $CHCl_3$): 108-112 °C. **FT-IR** (thin film): ν_{max} (cm^{-1}) = 2980.9, 1726.2, 1578.0, 1562.6 **^{1}H NMR** (500 MHz, $CDCl_3$) δ 8.89 (1H, dd, *J* = 1.8, 0.6 Hz, C-7*H*), 8.68 (2H, d, *J* = 4.8 Hz, Pm*H*), 8.15 (1H, s, C-2*H*), 7.52 (1H, dd, *J* = 8.4, 0.6 Hz, In*H*), 7.19 (1H, dd, *J* = 8.4, 1.8 Hz, In*H*), 7.01 (1H, t, *J* = 4.8 Hz, Pm*H*), 3.67 (3H, s, CO_2CH_3), 3.65 (3H, s, CO_2CH_3), 1.72 (6H, s, $C(CH_3)_2$), 1.69 (6H, s, $C(CH_3)_2$). **^{13}C NMR** (126 MHz, $CDCl_3$) δ 177.85 (CO_2R), 177.27 (CO_2R), 158.16 (Ar*C*), 157.77 (Ar*C*), 140.64 (Ar*C*), 136.46 (Ar*C*), 128.13 (Ar*C*), 124.58 (Ar*C*), 122.44 (Ar*C*), 120.17 (Ar*C*), 119.91 (Ar*C*), 116.03 (Ar*C*),

113.72 (Ar*C*), 52.39 (CO_2CH_3), 52.29 (CO_2CH_3), 47.01 ($C(CH_3)_2$), 42.13 ($C(CH_3)_2$), 27.13 ($C(CH_3)_2$), 26.09 ($C(CH_3)_2$). **HRMS** (ESI): m/z calculated for $C_{22}H_{25}N_3O_4$ requires 418.1800 for $[M+Na]^+$, found 418.1816.

Synthesis of **3t** and **4t**

The above compounds were synthesized using General Procedure **D** using benzyl α-bromoisobutyrate (0.13 mL, 0.75 mmol) as coupling partner. Silica gel chromatography gave two amorphous solids), **3t** (55%, 0.051 g) and **4t** (31%, 0.048 g).

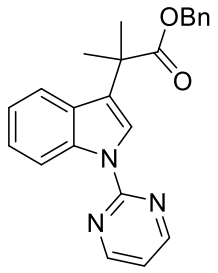

3t. FT-IR (thin film): ν_{max} (cm^{-1}) = 2980.9, 1726.2, 1578.7, 1562.0. **^{1}H NMR** (500 MHz, $CDCl_3$) δ 8.83 (1H, dt, *J* = 8.4, 0.9 Hz, C-7*H*), 8.67 (2H, d, *J* = 4.8 Hz, Pm*H*), 8.18 (1H, s, C-2*H*), 7.54 (1H, dt, *J* = 8.0, 0.9 Hz, In*H*), 7.33 (1H, ddd, *J* = 8.4, 7.1, 1.2 Hz, In*H*), 7.30–7.21 (2H, m, Ar*H*), 7.21–7.11 (3H, m, Ar*H*), 7.00 (1H, t, *J* = 4.8 Hz, Pm*H*), 5.12 (2H, s, CH_2Ph), 1.77 (6H, s, $C(CH_3)_2$). **^{13}C NMR** (126 MHz,$CDCl_3$) δ 176.62 (CO_2R), 158.15 (Ar*C*), 157.78 (Ar*C*), 136.28 (Ar*C*), 136.18 (Ar*C*), 129.42 (Ar*C*), 128.45 (Ar*C*), 128.01 (Ar*C*), 127.98 (Ar*C*), 127.97 (Ar*C*), 124.78 (Ar*C*), 123.78 (Ar*C*), 122.12 (Ar*C*), 122.04 (Ar*C*), 120.26 (Ar*C*), 116.54 (Ar*C*), 116.03 (Ar*C*), 66.70 (CH_2Ph), 42.31 ($C(CH_3)_2$), 26.07 ($C(CH_3)_2$). **HRMS** (ESI): m/z calculated for $C_{23}H_{21}N_3O_2$ requires 372.1712 for $[M+H]^+$, found 372.1727.

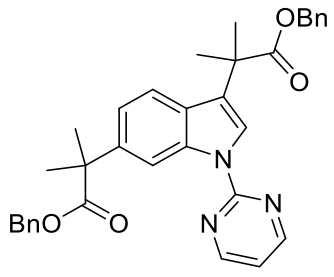

4t. FT-IR (thin film): ν_{max} (cm^{-1}) = 2978.1, 1725.8, 1577.5, 1562.4. **^{1}H NMR** (500 MHz, $CDCl_3$) δ 8.91 (1H, d, *J* = 1.7 Hz, C-7*H*), 8.65 (2H, d, *J* = 4.8 Hz, Pm*H*), 8.17 (1H, s, C-2*H*), 7.44 (1H, d, *J* = 8.4 Hz, *In*H), 7.30–7.19 (7H, m, Ar*H*), 7.18–7.10 (3H, m, Ar*H*), 7.00 (1H, t, *J* =

4.8 Hz, Pm*H*), 5.15 (2H, s, C*H*$_2$Ph), 5.12 (2H, s, C*H*$_2$Ph), 1.75 (6H, s, C(C*H*$_3$)$_2$), 1.73 (6H, s, C(C*H*$_3$)$_2$). **^{13}C NMR** (126 MHz, $CDCl_3$) δ 177.03 (*C*O_2R), 176.52 (*C*O_2R), 158.14 (Ar*C*), 157.76 (Ar*C*), 140.45 (Ar*C*), 136.45 (Ar*C*), 136.41 (Ar*C*), 136.16 (Ar*C*), 128.43 (Ar*C*), 128.10 (Ar*C*), 128.00 (Ar*C*), 127.97 (Ar*C*), 127.92 (Ar*C*), 127.75 (Ar*C*), 127.74 (Ar*C*), 124.51 (Ar*C*), 122.46 (Ar*C*), 120.15 (Ar*C*), 120.00 (Ar*C*), 115.97 (Ar*C*), 113.84 (Ar*C*), 66.66 (*C*H_2Ph), 66.46 (*C*H_2Ph), 47.08 (*C*(CH$_3$)$_2$), 42.30 (*C*(CH$_3$)$_2$), 27.08 (C(*C*H$_3$)$_2$), 26.04 (C(*C*H$_3$)$_2$). **HRMS** (ESI): m/z calculated for $C_{34}H_{33}N_3O_4$ requires 548.2549 for $[M+H]^+$, found 548.2539

Synthesis of **3u** and **4u**

The above compounds were synthesized using General Procedure **D** using 2-bromoisobutyrophenone (0.15 mL, 0.75 mmol) as coupling partner. Silica gel chromatography gave two off white solids), **3u** (38%, 0.032 g) and **4u** (12%, 0.015 g).

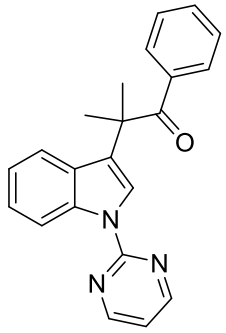

3u. mp (from $CHCl_3$): 120-128 °C. **FT-IR** (thin film): ν_{max} (cm^{-1}) = 2980.8, 1673.4, 1577.9, 1562.5. **^{1}H NMR** (500 MHz, $CDCl_3$) δ 8.82 (1H, dt, *J* = 8.4, 0.9 Hz, In*H*), 8.74 (2H, d, *J* = 4.8 Hz, Pm*H*), 8.34 (1H, s, In*H*), 7.79–7.71 (2H, m, Ar*H*), 7.45 (1H, ddd, *J* = 8.0, 1.2, 0.7 Hz, Ar*H*), 7.35–7.26 (2H, m, Ar*H*), 7.21–7.15 (2H, m, Ar*H*), 7.14–7.07 (2H, m, Ar*H*), 1.78 (6H, s, C(C*H*$_3$)$_2$). **^{13}C NMR** (126 MHz, $CDCl_3$) δ 204.54 (*C*OPh), 158.32 (Ar*C*), 137.29 (Ar*C*), 136.42 (Ar*C*), 131.90 (Ar*C*), 129.52 (Ar*C*), 129.09 (Ar*C*), 128.12 (Ar*C*), 125.78 (Ar*C*), 124.17 (Ar*C*), 122.39 (Ar*C*), 121.39 (Ar*C*), 120.39 (Ar*C*), 116.48 (Ar*C*), 116.26 (Ar*C*), 47.32 (*C*(CH$_3$)$_2$), 27.25 (C(*C*H$_3$)$_2$). **HRMS** (ESI): m/z calculated for $C_{22}H_{19}N_3O$ requires 364.1426 for $[M+Na]^+$, found 364.1417

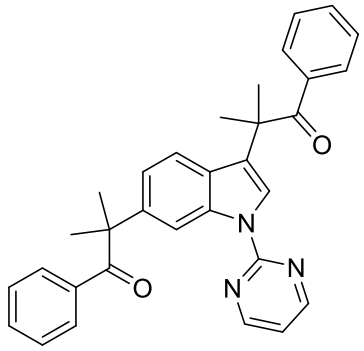

4u. mp (from $CHCl_3$): 106-110 °C. **FT-IR** (thin film): ν_{max} (cm^{-1}) = 2980.7, 1674.4, 1577.1, 1562.8. **^{1}H NMR** (500 MHz, $CDCl_3$) δ 8.86 (1H, dd, *J* = 1.8, 0.6 Hz, C-7*H*), 8.72 (2H, d, *J* = 4.8 Hz, Pm*H*), 8.33 (1H, s, C-2*H*), 7.72 (2H, dd, *J* = 8.5, 1.2 Hz, Ar*H*), 7.46–7.37 (3H, m, Ar*H*), 7.35–7.31 (1H, m, Ar*H*), 7.31–7.24 (2H, m, Ar*H*), 7.21–7.16 (2H, m, Ar*H*), 7.13–7.08 (2H, m, Ar*H*), 7.08–7.05 (2H, m, Ar*H* & Pm*H*), 1.77 (6H, s, C(C*H*$_3$)$_2$), 1.65 (6H, s, C(C*H*$_3$)$_2$). **^{13}C NMR** (126 MHz, $CDCl_3$) δ 204.58 (*C*OPh), 204.20 (*C*OPh), 158.35 (Ar*C*), 157.82 (Ar*C*), 141.35 (Ar*C*), 137.43 (Ar*C*), 136.98 (Ar*C*), 136.70 (Ar*C*), 131.80 (Ar*C*), 131.50 (Ar*C*), 129.83 (Ar*C*), 129.03 (Ar*C*), 128.33 (Ar*C*), 128.08 (Ar*C*), 127.94 (Ar*C*), 125.46 (Ar*C*), 121.88 (Ar*C*), 120.73 (Ar*C*), 120.45 (Ar*C*), 116.29 (Ar*C*), 113.84 (Ar*C*), 51.85 (*C*(CH$_3$)$_2$), 47.28 (*C*(CH$_3$)$_2$), 28.30 (C(*C*H$_3$)$_2$), 27.21 (C(*C*H$_3$)$_2$). **HRMS** (ESI): m/z calculated for $C_{32}H_{29}N_3O_2$ requires 488.2338 for $[M+H]^+$, found 488.2360

Synthesis of **3v** and **4v**

The above compounds were synthesized using General Procedure **A** using 1-(5-chloropyrimidin-2yl)-1*H*-indole (0.057 g, 0.25 mmol) and methyl α-bromoisobutyrate (0.10 mL, 0.75 mmol) as coupling partner. Silica gel chromatography gave two white solids), **3t** (39%, 0.032 g) and **4t** (30%, 0.032 g).

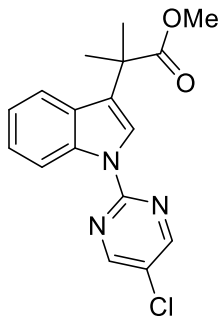

3v. mp (from $CHCl_3$): 151-153 °C. **FT-IR** (thin film): ν_{max} (cm^{-1}) = 2981.5, 1729.4, 1573.5, 1544.3. **^{1}H NMR** (500 MHz, Chloroform-*d*) δ 8.72 (1H, dd, *J* = 8.4, 0.9 Hz, C-7*H*), 8.60 (2H,

d, *J* = 0.7 Hz, Pm*H*), 8.10 (1H, d, *J* = 0.8 Hz, In*H*), 7.57 (1H, dd, *J* = 7.9, 1.1 Hz, In*H*), 7.34 (1H, dd, *J* = 8.3, 7.2 Hz, In*H*), 7.26–7.19 (1H, m, In*H*), 3.66 (3H, s, CO_2CH_3), 1.74 (6H, s, $C(CH_3)_2$). **^{13}C NMR** (126 MHz, $CDCl_3$) δ 177.23 (CO_2R), 156.44 (Ar*C*), 155.68 (Ar*C*), 136.15 (Ar*C*), 129.50 (Ar*C*), 125.45 (Ar*C*), 124.94 (Ar*C*), 124.05 (Ar*C*), 122.42 (Ar*C*), 122.06 (Ar*C*), 120.16 (Ar*C*), 116.50 (Ar*C*), 52.44 (CO_2CH_3), 42.14 ($C(CH_3)_2$), 26.06 ($C(CH_3)_2$). **HRMS** (ESI): m/z calculated for $C_{17}H_{16}Cl_1N_3O_2$ requires 352.0829 for $[M+Na]^+$, found 352.81800

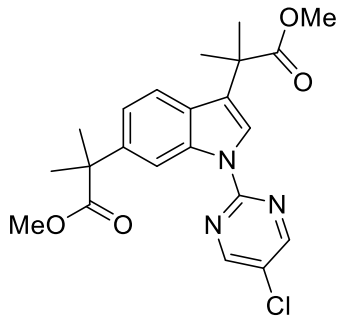

4v. mp (from $CHCl_3$): 142-148 °C. **FT-IR** (thin film): ν_{max} (cm^{-1}) = 2979.6, 1728.3, 1573.5, 1545.1. **^{1}H NMR** (500 MHz, $CDCl_3$) δ 8.78 (1H, dd, *J* = 1.8, 0.6 Hz, C-7*H*), 8.63 (2H, s, Pm*H*), 8.07 (1H, s, C-2*H*), 7.51 (1H, dd, *J* = 8.4, 0.6 Hz, In*H*), 7.20 (1H, dd, *J* = 8.4, 1.8 Hz, In*H*), 3.67 (3H, s, CO_2CH_3), 3.65 (3H, s, CO_2CH_3), 1.71 (6H, s, $C(CH_3)_2$), 1.68 (6H, s, $C(CH_3)_2$). **^{13}C NMR** (126 MHz, $CDCl_3$) δ 177.75 (CO_2R), 177.13 (CO_2R), 156.50 (Ar*C*), 155.71 (Ar*C*), 140.94 (Ar*C*), 136.35 (Ar*C*), 128.19 (Ar*C*), 125.20 (Ar*C*), 124.95 (Ar*C*), 122.45 (Ar*C*), 120.49 (Ar*C*), 120.06 (Ar*C*), 113.59 (Ar*C*), 52.45 (CO_2CH_3), 52.33 (CO_2CH_3), 47.01 ($C(CH_3)_2$), 42.14 ($C(CH_3)_2$), 27.11 ($C(CH_3)_2$), 26.06 ($C(CH_3)_2$). **HRMS** (ESI): m/z calculated for $C_{22}H_{24}Cl_1N_3O_4$ requires 452.1500 for $[M+Na]^+$, found 452.1374

6.3.6: Deuterium Experiments

Deuterium incorporation experiment on C-3 substituted indole

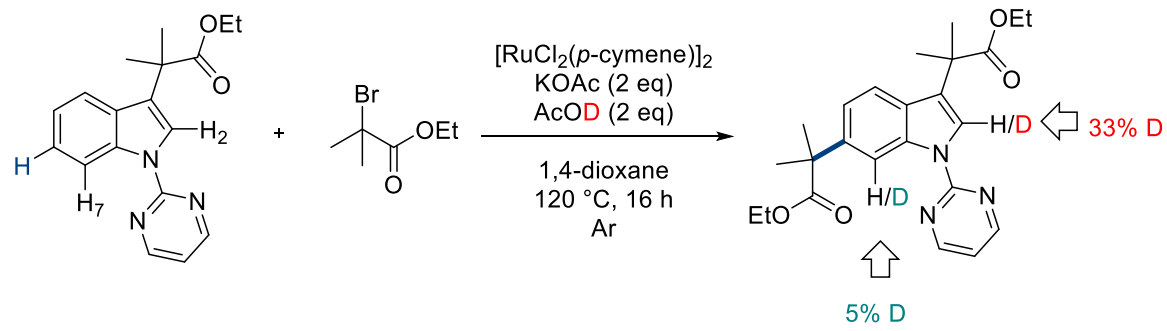

3a **2a** **4a**: 74%

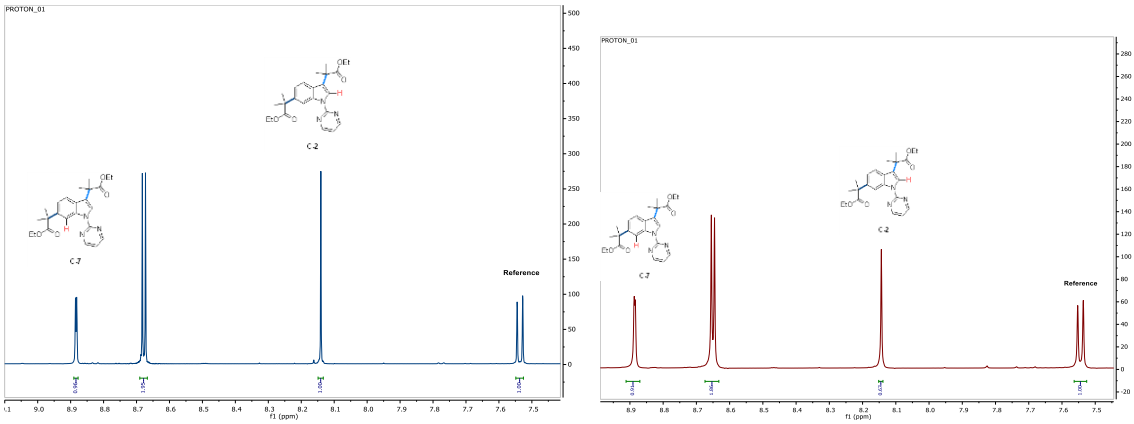

Regular Spectra	Deuterium Incorpoation Spectra
C2: 1.00	C2: 0.67
C7: 0.96	C7: 0.91

Deuterium incorporation at C2 = **33%**

Deuterium incorporation at C7 = **5%**

Deuterium incorporation experiment on one-pot C-3/C-6 alkylation

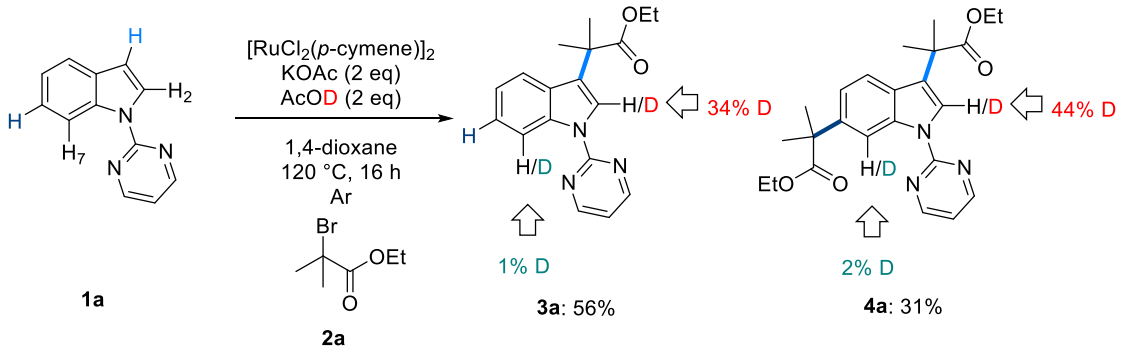

3a - Mono

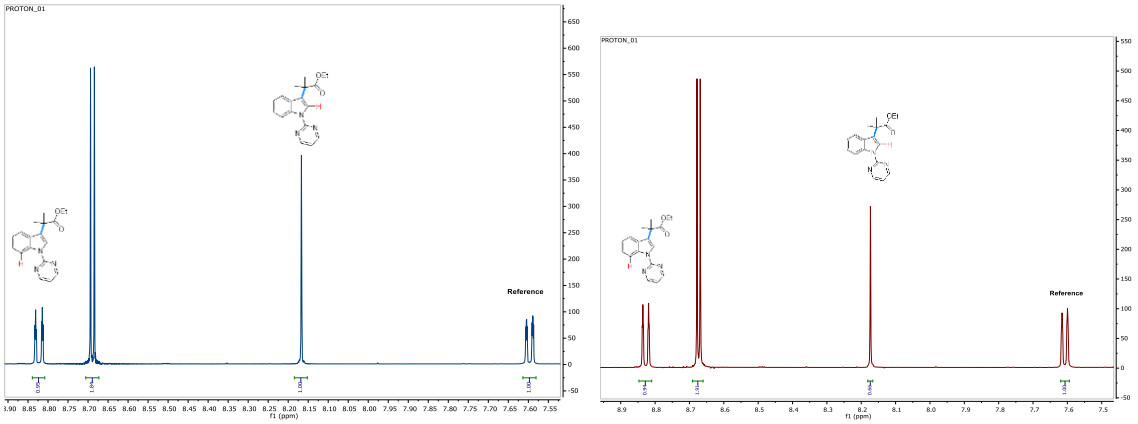

Regular Spectra	Deuterium Incorporation Spectra
C-2: 1.00	C-2: 0.66
C-7: 0.95	C-7: 0.94

Deuterium incorporation at C-2 = **34%**

Deuterium incorporation at C-7 = **1%**

4a - Di

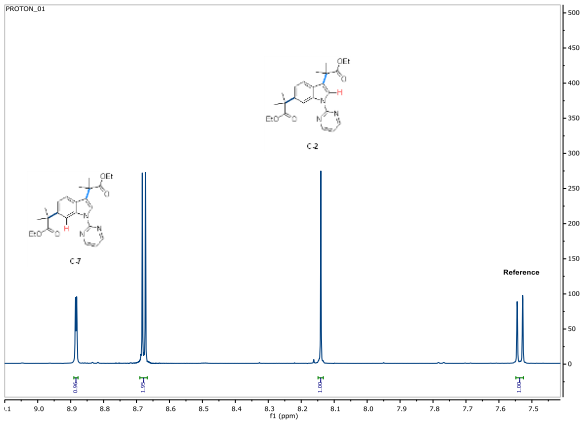

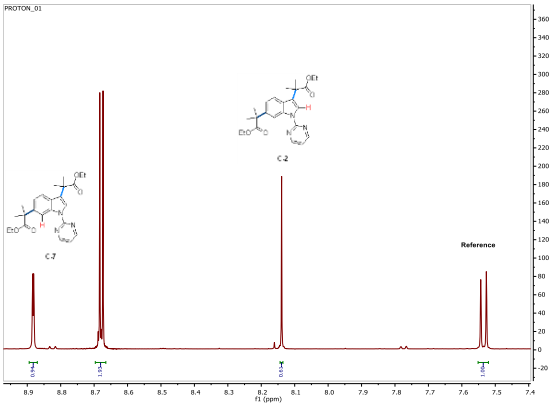

Regular Spectra	Deuterium Incorporation Spectra
C-2: 1.00	C-2: 0.61
C-7: 0.96	C-7: 0.94

Deuterium incorporation at C-2 = **39%**

Deuterium incorporation at C-7 = **2%**

6.3.7: Organometallic Work

Synthesis of **1a**-[Ru]-OAc

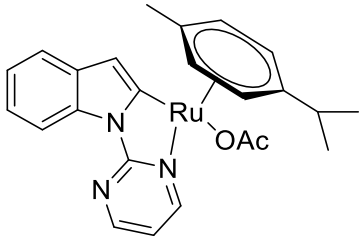

To an oven dried Schlenk flask was added $[RuCl_2(p\text{-cymene})]_2$ (0.239 g, 0.39 mmol), **1a** (0.150 g, 0.77 mmol) and potassium acetate (0.153 g, 1.56 mmol). The flask was evacuated and refilled with argon three times. Anhydrous methanol (5 mL) was then added *via* septum and the reaction mixture was stirred at 40 °C for 24 h. The mixture was filtered under a blanket of N_2, eluting with anhydrous methanol. The filtrate was then kept in the freezer for 7 days. The deep red crystals that formed in the filtrate were collected *via* vacuum filtration, giving **1a**-[Ru]-OAc, 32% (0.120 g). **^{1}H NMR** (500 MHz, $CDCl_3$) δ 9.10 (1H, dd, *J* = 5.6, 2.3 Hz), 8.61 (1H, dd, *J* = 4.6, 2.3 Hz), 8.37 (1H, dq, *J* = 8.0, 0.9 Hz), 7.40 (1H, ddd, *J* = 7.7, 1.2, 0.7 Hz), 7.19–7.09 (1H, m), 7.03 (1H, ddd, *J* = 8.3, 7.2, 1.2 Hz), 6.89–6.81 (2H, m), 5.72 (1H, dd, *J* = 6.0, 1.2 Hz), 5.54 (1H, dd, *J* = 6.0, 1.2 Hz), 5.28 (1H, dd, *J* = 6.0, 1.2 Hz), 5.12 (1H, dd, *J* = 6.0, 1.2 Hz), 3.47 (3H, s), Ac*H*), 2.62 (1H, hept, *J* = 6.9 Hz), C*H*$(CH_3)_2$), 2.07 (3H, s), ArC*H*$_3$), 1.11 (3H, d, *J* = 7.0 Hz), CH(C*H*$_3)_2$), 0.97 (3H, d, *J* = 6.9 Hz), CH(C*H*$_3)_2$). **^{13}C NMR** (126 MHz, $CDCl_3$) δ 165.59 (*C*=O), 162.47, 158.97, 136.45, 135.09, 122.55, 120.29, 117.67, 113.71, 113.65, 113.32, 103.17, 101.27, 89.67, 88.80, 83.29, 82.77, 50.84 (Ac*C*H_3), 30.67 (*C*H$(CH_3)_2$), 22.74 (Ar*C*H_3), 21.73 (CH(*C*$H_3)_2$), 18.75 (CH(*C*$H_3)_2$). Data is in line with literature precedent.[11]

6.3.8: References

(1) Xu, S.; Huang, X.; Hong, X.; Xu, B. *Org. Lett.*, **2012**, *14*, 4614

(2) Kim, J.; Kim, H.; Chang S. *Org. Lett.*, **2012**, *14*, 3924

(3) Islam, S.; Larrosa, I. *Chem. Eur. J.*, **2013**, *19*, 15093.

(4) Kim, J.; Kim, H.; Chang, C. *Org. Lett.*, **2012**, *14*, 3924.

(5) Reddy, V.; Qiu, R.; Iwasaki, T.; Kambe, N. *Org. Lett.*, **2013**, *15*, 1290

(6) Yu, D-G.; de Azambuja, F.; Glorius, F. *Angew. Chem. Int. Ed.*, **2014**, *53*, 2754

(7) Ackermann, L.; Lygin, A. V. *Org. Lett.*, **2011**, *13*, 3332

(8) Soni, V.; Patel, U. N.; Punji, B. *RSC Adv.*, **2015**, *5*, 57472

(9) Zhao, J.; Cheng, X.; Le, J.; Yang, W.; Xue, F.; Zhang, X.; Jiang, C. *Org. Biomol. Chem.*, **2015**, *13*, 9000

(10) Li, T.; Wang, Z.; Zhang, M.; Zhang, H-J.; Wen, T-B. *Chem. Commun.*, **2015**, *51*, 6777

(11) Sollert, C.; Devaraj, K.; Orthaber, A.; Gates, P. J.; Pilarski, L. T. *Chem. Eur. J.*, **2015**, *21*, 5380.

6.4: Data and Supporting Information for “Ruthenium-Catalyzed Remote C4-Functionalization of Carbazoles via σ-Activation”

In the interest of presentation in a thesis, NMR spectra and crystallography data have not been included. However, in the interest of the reader these are available online at: http://www.rsc.org/suppdata/c7/cc/c7cc07606a/c7cc07606a1.pdf
The supporting information has also been submitted to formatting and colour changes, however no changes in the data have been made.

6.4.1: General

Proton, carbon and fluorine NMR spectra were recorded on Bruker 300 MHz, or Agilent Technologies 500 MHz, spectrometer (^{1}H NMR at 500 MHz, or 300 MHz, ^{13}C NMR at 126 MHz, or 75 MHz, and ^{19}F NMR at 470 MHz. Chemical shifts for protons are reported in parts per million downfield from $Si(CH_3)_4$ and are referenced to residual protium in the deuterated solvent ($CHCl_3$ at 7.26 ppm, or CH_3OH at 3.31 & 4.87 depending on solvent used). Chemical shifts for fluorines are reported in parts per million downfield from $CFCl_3$. NMR data are presented in the following format: chemical shift (number of equivalent nuclei by integration, multiplicity [app = apparent, br = broad, d = doublet, t = triplet, q = quartet, dd = doublet of doublets), dt = doublet of triplets), dq = doublet of quartets), ddd = doublet of doublet of doublets), m = multiplet], coupling constant [in Hz], assignment). Electrospray ionisation ultrahigh resolution time-of-flight mass spectrometry (ESI–UHR–TOF–MS) was performed on a Bruker maXis mass spectrometer. Electrospray ionisation high resolution time-of-flight mass spectrometry (ESI–HR–TOF–MS) was performed on a Bruker micrOTOF spectrometer. Infrared (IR) spectra were recorded on a Perkin–Elmer 1600 FT (Fourier transform), IR spectrophotometer, with absorbencies quoted as wavelength (v [in cm^{-1}]). Melting points were obtained on a Bibby Sterilin SMP10 melting point machine and are uncorrected.
Analytical thin-layer chromatography (TLC) was performed on aluminium-backed plates coated with Alugram® SIL G/UV254 purchased from Macherey–Nagel and visualised with UV light (254 or 365 nm), and/or KMnO4, 2,4-DNPH or I_2/Silica staining. Silica gel column chromatography was performed using 60 Å, 200-400 mesh particle size silica gel purchased from Sigma–Aldrich. Samples were loaded as saturated solutions in an appropriate solvent system.
All reactions were performed using reagents obtained from Sigma-Aldrich, Acros Organics, Alfa Aesar, Fluorochem chemicals without further purification unless stated. [$RuCl_2$(*p*-

cymene)]$_2$ was purchased from STREM chemicals or Acros Organics. All water used was purified through a Merck Millipore reverse osmosis purification system prior to use. Anhydrous solvents were dried and degassed by passing through anhydrous alumina columns using an Innovative Technology Inc. PS-400-7 solvent purification system (SPS) and stored under an atmosphere of N_2 prior to use.
Reactions were performed in oven-dried glassware and under a blanket of N_2 if not stated.

Temperatures quoted are external. Solvents were removed under reduced pressure using Büchi-Rotorvapor apparatus.

6.4.2: Optimization

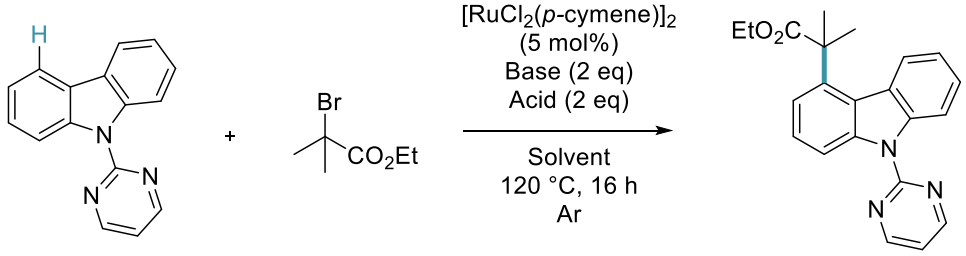

Entry	Base	Acid	Acid eq	Solvent	C4 % (IY)
1	KOAc	-	-	1,4-dioxane	53
2	KOAc	AcOH	2	1,4-dioxane	68 (48)
3	K_2CO_3 (+ $MesCO_2H$ 30%)	-	-	1,4-dioxane	7
4	K_2CO_3 (+ Piv-Val-OH 30%)	-	-	1,4-dioxane	7
5	K_2CO_3	AcOH	2	1,4-dioxane	-
6	K_3Citrate	AcOH	2	1.4-dioxane	45
7	K_2Oxalate	AcOH	2	1,4-dioxane	-
8	K_2Tartrate	AcOH	2	1,4-dioxane	56
9	KO_2CH	AcOH	2	1,4-dioxane	25
10	-	Piv-Val-OH	2	1,4-dioxane	Trace
11	$AdCO_2Na$	AcOH	2	1,4-dioxane	58
12	$MesCO_2K$	AcOH	2	1,4-dioxane	80 (61)
13	$MesCO_2K$	$MesCO_2H$	2	1,4-dioxane	64
14	$MesCO_2K$	$AdCO_2H$	2	1,4-dioxane	66
15	$MesCO_2K$	TFA	2	1,4-dioxane	15
16	$MesCO_2K$	HO_2CH	2	1,4-dioxane	34
17	$MesCO_2K$	conc. $HCl_{(aq)}$	2	1,4-dioxane	17
18	$MesCO_2K$	AcOH	2	2-MeTHF	55
19	$MesCO_2K$	AcOH	2	PhMe	-
20	$MesCO_2K$	AcOH	2	MeCN	72
21	$MesCO_2K$	AcOH	2	C_6H_6	39
22	$MesCO_2K$	AcOH	2	2-butanone	55
23	$MesCO_2K$	AcOH	2	AcOH	31
24	$MesCO_2K$	AcOH	2	DCE	38
25	$MesCO_2K$	AcOH	2	DME	49
26	$MesCO_2K$	AcOH	0.5	1,4-dioxane	80
27	**$MesCO_2K$**	**AcOH**	**1**	**1,4-dioxane**	**84 (68)**
28	$MesCO_2K$	AcOH	4	1,4-dioxane	68
29[a]	$MesCO_2K$	AcOH	1	1,4-dioxane	61
30[b]	$MesCO_2K$	AcOH	1	1,4-dioxane	76
31[c]	$MesCO_2K$	AcOH	1	1,4-dioxane	-
32[d]	**$MesCO_2K$**	**AcOH**	**1**	**1,4-dioxane**	**90 (76)**

General Conditions: 5CP-A (0.25-0.5 mmol), methyl α-bromoisobutyrate (0.75-1.5 mmol), $[RuCl_2(p\text{-cymene})]_2$ (5 mol%, 0.0125-0.025 mmol), solvent (1-2 mL), 120 °C, 16 h. [a] : Reaction carried out at 100 °C. [b] : Reaction carried out under air. [c] : Without $[RuCl_2(p\text{-cymene})]_2$. [d] : $[Ru(O_2CMes)_2(p\text{-cymene})]$ (10 mol%)

Further Experiments

We carried out further experiments to elucidate whether secondary and primary alkyl esters were amenable to the reaction methodology. Unfortunately, on using both the chloro and bromo ester coupling partners, no conversion to any product was observed.

Scheme S1: Ruthenium Catalysed C4-Alkylation using Primary and Secondary Alkyl Halides

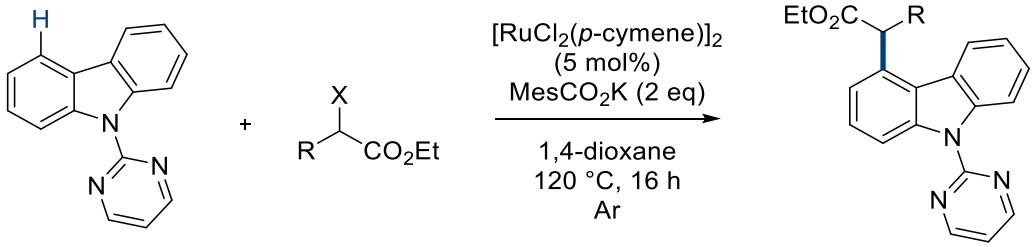

a: X = Br, R = Me
b: X = Cl, R = Me
c: X = Br, R = H
d: X = Cl, R = H

a-d: 0%

We were intrigued to investigate whether carbazole templates could be applied to other σ-activation protocols. To that end, we identified *meta*-sulfonation and *meta*-bromination methodologies as potentially the most amenable to this template. Unfortunately using the original conditions, the carbazole conditions from this report, and amalgamations, no C4-functionalised products were observed.

Scheme S2: Proposed Ruthenium-Catalysed C4-Sulfonation of *N*-pyrimidinylcarbazole

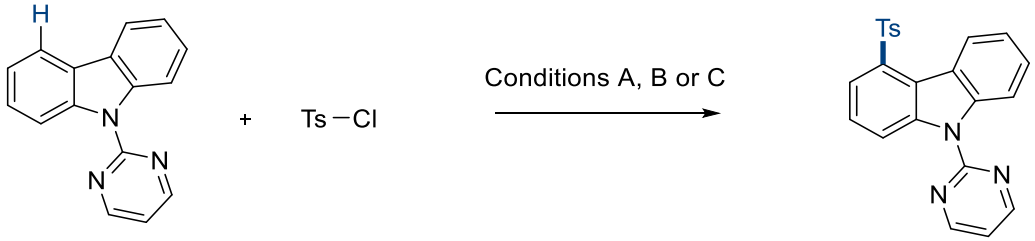

0%

A: $[RuCl_2(p\text{-cymene})]_2$ (5 mol%), $MesCO_2K$ (2 eq), 1,4-dioxane, 120 °C, 16 h
B: $[RuCl_2(p\text{-cymene})]_2$ (5 mol%), $MesCO_2K$ (2 eq), MeCN, 120 °C, 16 h
C: $[RuCl_2(p\text{-cymene})]_2$ (5 mol%), K_2CO_3 (2 eq), MeCN, 120 °C, 16 h

Scheme S3: Proposed Ruthenium-Catalysed C4-Bromination of *N*-pyrimidinylcarbazole

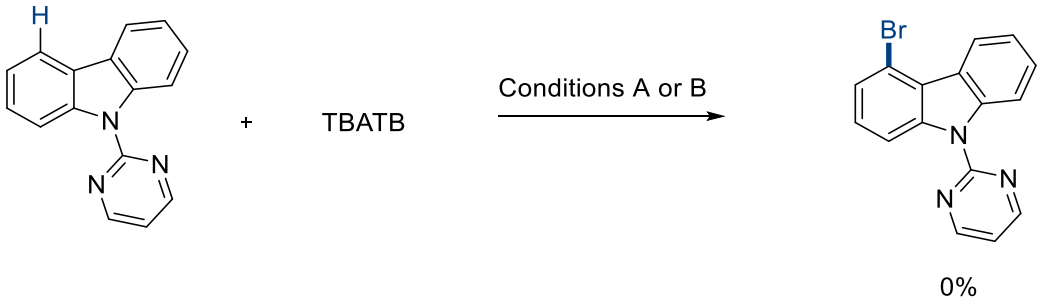

0%

TBATB = tetrabutylammonium tribromide
A: $[RuCl_2(p\text{-cymene})]_2$ (5 mol%), $MesCO_2H$ (30 mol%), K_2CO_3 (2 eq), 1,4-dioxane, 120 °C, 16 h
B: $[RuCl_2(p\text{-cymene})]_2$ (5 mol%), $MesCO_2K$ (2 eq), AcOH (2 eq), 1,4-dioxane, 120 °C, 16 h

6.4.3: Synthesis of Starting Materials

Synthesis of 9-(pyrimidin-2-yl)-9*H*-carbazole (**1a**)

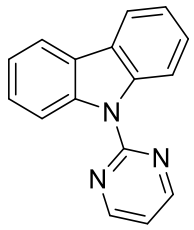

To a stirred solution of 9*H*-carbazole (1.67 g, 10 mmol) in DMF (10 mL) was added sodium hydride (60% wt. in mineral oil, 0.43 g, 11 mmol) at 0 °C. The reaction mixture was stirred at 0 °C for 1 hour. The reaction mixture was allowed to return to room temperature and 2-chloropyrimidine (1.38 g, 12 mmol) was added. The reaction mixture was heated to 150 °C overnight. After returning to room temperature the solution was poured into a separating funnel containing brine (150 mL). EtOAc (150 mL) was added and the organics were extracted. The resulting aqueous mixture was reextracted with EtOAc (2 x 150 mL). The combined organics were dried over $MgSO_4$ and concentrated *in vacuo*. The crude residue was purified *via* silica gel column chromatography (EtOAc:Petroleum Spirit 40-60 °C, 10:90 v:v) to give a white powdery solid, **1a**, 32% (790 mg). **^{1}H NMR** (500 MHz, $CDCl_3$) δ 8.93–8.80 (4H, m, Ar*H*), 8.21–7.76 (2H, m, Ar*H*), 7.51 (2H, ddd, *J* = 8.5, 7.2, 1.3 Hz, Ar*H*), 7.38 (2H, ddd, *J* = 8.1, 7.2, 1.0 Hz, Ar*H*), 7.13 (1H, t, *J* = 4.7 Hz, Ar*H*). **^{13}C NMR** (126 MHz, $CDCl_3$) δ 159.3 (Ar*C*), 158.0 (Ar*C*), 139.3 (Ar*C*), 126.7 (Ar*C*), 125.9 (Ar*C*), 122.4 (Ar*C*), 119.7 (Ar*C*), 116.4 (Ar*C*), 116.1 (Ar*C*). Data is in line with literature precedent.[1]

Synthesis of 3-bromo-9*H*-carbazole

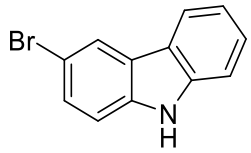

To a solution of 9*H*-carbazole (4 g, 24 mmol) in CH_2Cl_2 (75 mL) was added *N*-bromosuccinimide (4.25 g, 24 mmol) in DMF (8 mL) dropwise at room temperature. The reaction mixture was stirred for 4 hours before H_2O (100 mL) was added. The organic phase extracted, dried over $MgSO_4$, and concentrated *in vacuo*. The crude residue was purified *via* recrystallization from EtOH to give a crystalline white solid, 55% (3.26 g). **^{1}H NMR** (500 MHz, DMSO-d_6) δ 11.43 (1H, s, N*H*), 8.35 (1H, dd, *J* = 2.0, 0.6 Hz, Ar*H*), 8.16 (1H, dt, *J* = 7.9, 1.1 Hz, Ar*H*), 7.53–7.45 (3H, m, Ar*H*), 7.42 (1H, ddd, *J* = 8.2, 7.1, 1.2 Hz, Ar*H*), 7.17 (1H,ddd, *J* = 8.0, 7.1, 1.0 Hz, Ar*H*). **^{13}C NMR** (126 MHz, DMSO-d_6) δ 140.1 (Ar*C*), 138.4 (Ar*C*), 127.8 (Ar*C*), 126.3 (Ar*C*), 124.4 (Ar*C*), 122.7 (Ar*C*), 121.4 (Ar*C*), 120.7 (Ar*C*), 118.9 (Ar*C*), 112.9 (Ar*C*), 111.2 (Ar*C*), 110.5 (Ar*C*). Data is in line with literature precedent.[2]

Synthesis of 3-chloro-9*H*-carbazole

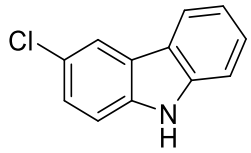

To a solution of 9*H*-carbazole (2 g, 12 mmol) in CH_2Cl_2 (20 mL) was added SO_2Cl_2 (1.0 mL, 800 mg, 12 mmol) dropwise at 0 °C. After addition was complete the reaction mixture was allowed to return to room temperature and stir overnight. The mixture was then diluted in CH_2Cl_2 (80 mL) and sat. $NaHCO_3$ solution (100 mL). The organic layer was separated and washed with aq. $NaHSO_3$ solution (100 mL), and brine (100 mL). The organic phase was dried over $MgSO_4$ and concentrated *in vacuo*. The crude residue was purified *via* silica gel column chromatography (EtOAc:Petroleum Spirit 40-60 °C, 10:90 v:v) to give mono-chlorinated product as a powdery white solid, 37% (900 mg). **^{1}H NMR** (500 MHz, DMSO-d_6) δ 11.41 (1H, s, N*H*), 8.22 (1H, d, *J* = 2.1 Hz, Ar*H*), 8.16 (1H, d, *J* = 7.8 Hz, Ar*H*), 7.50 (2H, dd, *J* = 8.4, 2.2 Hz, Ar*H*), 7.44–7.37 (2H, m, Ar*H*), 7.21–7.11 (1H, m, Ar*H*). **^{13}C NMR** (126 MHz, DMSO-d_6) δ 140.3 (Ar*C*), 138.1 (Ar*C*), 126.3 (Ar*C*), 125.2 (Ar*C*), 123.7 (Ar*C*), 122.8 (Ar*C*), 121.5 (Ar*C*), 120.7 (Ar*C*), 119.7 (Ar*C*), 118.8 (Ar*C*), 112.4 (Ar*C*), 111.2 (Ar*C*). Data is in line with literature precedent.[3]

Synthesis of 1,3,6-trichloro-9*H*-carbazole

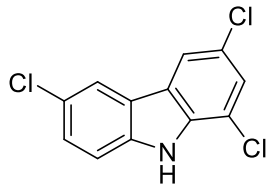

To a solution of 9*H*-carbazole (4 g, 24 mmol) in CH_2Cl_2 (40 mL) was added SO_2Cl_2 (4.0 mL, 6.4 g, 48 mmol) dropwise at 0 °C. After addition was complete the reaction mixture was allowed to return to room temperature and stir overnight. A further portion of SO_2Cl_2 (2.0 mL, 3.2 g, 24 mmol) was added at room temperature and allowed to stir for a further 4 hours. The mixture was then diluted in CH_2Cl_2 (80 mL) and sat. $NaHCO_3$ solution (200 mL). The organic layer was separated and washed with aq. $NaHSO_3$ solution (200 mL), and brine (200 mL). The organic phase was dried over $MgSO_4$ and concentrated *in vacuo*. The crude residue was purified *via* silica gel column chromatography (EtOAc:Petroleum Spirit 40-60 °C, 10:90 v:v) to give di-chlorinated product as a powdery white solid, 42% (2.7 g). **^{1}H NMR** (500 MHz, DMSO-d_6) δ 11.91 (1H, s, N*H*), 8.32 (2H, dd, *J* = 8.1, 2.0 Hz, Ar*H*), 7.61 (1H, d, *J* = 1.9 Hz, Ar*H*), 7.56 (1H, d, *J* = 8.6 Hz, Ar*H*), 7.48 (1H, dd, *J* = 8.7, 2.1 Hz, Ar*H*). **^{13}C NMR** (126 MHz, DMSO-d_6) δ 138.9 (Ar*C*), 135.9 (Ar*C*), 127.0 (Ar*C*), 125.0 (Ar*C*), 124.1 (Ar*C*), 124.0 (Ar*C*), 123.3 (Ar*C*), 123.0 (Ar*C*), 120.8 (Ar*C*), 119.5 (Ar*C*), 116.1 (Ar*C*), 113.3 (Ar*C*). Data is in line with literature precedent.[4]

General Procedure **A** for N-Arylation of Substituted Carbazoles

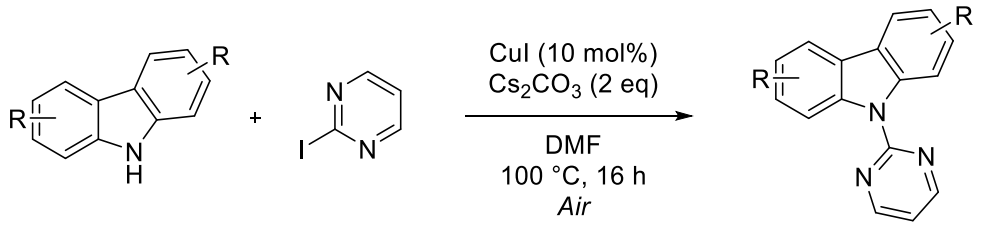

To an oven-dried carousel tube was charged relevant carbazole derivative (2 mmol), copper iodide (38 mg, 0.2 mmol, 20 mol%), caesium carbonate (1.3 g, 4 mmol) and 2-iodopyrimidine (824 mg, 4 mmol). The tube was sealed with a Teflon cap and anhydrous DMF (6 mL) was added *via* syringe. The reaction mixture was heated to 100 °C for 16 h. After this time the reaction mixture was allowed to return to room temperature. The mixture was diluted in EtOAc and filtered through a plug of celite, eluting with EtOAc. The filtrate was then concentrated *in vacuo*. The resulting crude residue was purified *via* silica gel column chromatography (EtOAc:Petroleum Spirit 40-60 °C, 10:90 v:v) to give desired arylated carbazole derivative. Note: The efficiency of this Ullmann reaction is directly affected by the quality of the 2-iodopyrimidine.

Synthesis of **1b**

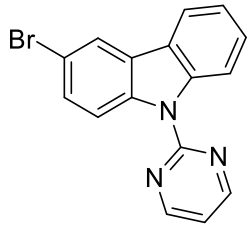

General Procedure **A** was followed using 3-bromo-9*H*-carbazole (492 mg, 2 mmol). Silica gel column chromatography gave a powdery white solid, 34% (220 mg). **mp** (from $CHCl_3$): 167-170 °C. **FT-IR** (thin film): ν_{max} (cm^{-1}) = 1581.7, 1558.2. **^{1}H NMR** (500 MHz, DMSO-d_6) δ 8.96 (2H, d, *J* = 4.8 Hz, Ar*H*), 8.77 (1H, d, *J* = 8.5 Hz, Ar*H*), 8.70 (1H, d, *J* = 8.9 Hz, Ar*H*), 8.45 (1H, d, *J* = 2.1 Hz, Ar*H*), 8.25 (1H, d, *J* = 7.7 Hz, Ar*H*), 7.62 (1H, dd, *J* = 8.9, 2.1 Hz, Ar*H*), 7.53 (1H, ddd, *J* = 8.4, 7.2, 1.3 Hz, Ar*H*), 7.43–7.34 (2H, m, Ar*H*). **^{13}C NMR** (126 MHz, DMSO-d_6) δ 158.6 (Ar*C*), 157.9 (Ar*C*), 138.7 (Ar*C*), 137.1 (Ar*C*), 129.0 (Ar*C*), 127.4 (Ar*C*), 127.0 (Ar*C*), 123.7 (Ar*C*), 122.5 (Ar*C*), 122.5 (Ar*C*), 120.4 (Ar*C*), 117.9 (Ar*C*), 117.2 (Ar*C*), 116.1 (Ar*C*), 114.60 (Ar*C*). **HRMS** (ESI): m/z calculated for $C_{16}H_{10}Br_1N_3$ requires 345.9950 for $[M+Na]^+$, found 345.9968.

Synthesis of **1c**

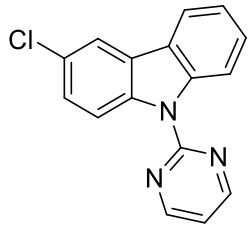

General Procedure **A** was followed using 3-chloro-9*H*-carbazole (403 mg, 2 mmol). Silica gel column chromatography gave a powdery white solid, 88% (492 mg). **mp** (from $CHCl_3$): 156-159 °C. **FT-IR** (thin film): v_{max} (cm^{-1}) = 2980.9, 1582.9, 1558.1. **^{1}H NMR** (500 MHz, DMSO-d_6) δ 8.98 (2H, d, *J* = 4.8 Hz, Ar*H*), 8.78 (2H, dd, *J* = 8.7, 7.4 Hz, Ar*H*), 8.34 (1H, d, *J* = 2.2 Hz, Ar*H*), 8.30–8.25 (1H, m, Ar*H*), 7.61–7.49 (2H, m, Ar*H*), 7.47–7.33 (2H, m, Ar*H*). **^{13}C NMR** (126 MHz, DMSO-d_6) δ 158.7 (Ar*C*), 157.9 (Ar*C*), 138.8 (Ar*C*), 136.8 (Ar*C*), 127.5 (Ar*C*), 126.7 (Ar*C*), 126.5 (Ar*C*), 126.3 (Ar*C*), 123.9 (Ar*C*), 122.6 (Ar*C*), 120.4 (Ar*C*), 119.6 (Ar*C*), 117.5 (Ar*C*), 117.3 (Ar*C*), 116.2 (Ar*C*). **HRMS** (ESI): m/z calculated for $C_{16}H_{10}N_3Cl_1$ requires 280.0636 for $[M+H]^+$, found 280.0652.

Synthesis of **1d**

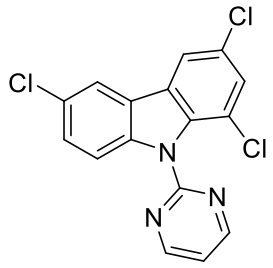

General Procedure **A** was followed using 1,3,6-trichloro-9*H*-carbazole (540 mg, 2 mmol). Silica gel column chromatography gave a powdery white solid, 41% (289 mg). **mp** (from $CHCl_3$): 175-179 °C. **FT-IR** (thin film): v_{max} (cm^{-1}) = 2981.1, 1565.3. **^{1}H NMR** (500 MHz, $CDCl_3$) δ 8.90 (2H, d, *J* = 4.8 Hz, Ar*H*), 7.94 (1H, dd, *J* = 19.7, 2.0 Hz, Ar*H*), 7.88 (1H, d, *J* = 8.8 Hz, Ar*H*), 7.48 (1H,d, *J* = 1.9 Hz, Ar*H*), 7.42 (1H, dd, *J* = 8.8, 2.1 Hz, Ar*H*), 7.33 (1H, t, *J* = 4.8 Hz, Ar*H*). **^{13}C NMR** (126 MHz,$CDCl_3$) δ 158.7 (Ar*C*), 157.3 (Ar*C*), 140.4 (Ar*C*), 135.7 (Ar*C*), 128.5 (Ar*C*), 128.3 (Ar*C*), 128.12 (Ar*C*), 128.08 (Ar*C*), 127.9 (Ar*C*), 124.9 (Ar*C*), 120.3 (Ar*C*), 120.2 (Ar*C*), 119.1 (Ar*C*), 118.9 (Ar*C*), 113.8 (Ar*C*). **HRMS** (ESI): m/z calculated for $C_{16}H_8N_3Cl_3$ requires 369.9684 for $[M+Na]^+$, found 369.9666.

Synthesis of 9-benzyl-9*H*-carbazole (**1e**)

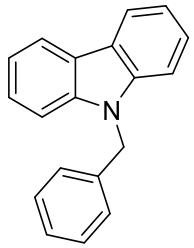

To a solution of 9*H*-carbazole (3 g, 18 mmol) in toluene (20 mL) was added sodium hydroxide (12 M in H_2O, 23 mL) and the reaction mixture allowed to stir at room temperature for 10 mins. After this time, tetebutylammonium iodide (650 mg, cat.) and subsequently benzyl bromide (2.6 mL, 3.69 g, 21.6 mmol) were added in one portion. The reaction mixture was left to stir overnight. The organic and aqueous phases were then separated and aqueous layer re-extracted with CH_2Cl_2 (2 x 50 mL). The combined organics were dried over $MgSO_4$ and concentrated *in vacuo*. The crude residue was purified *via* recrystallization from EtOH to give a crystalline white solid, 81% (3.76 g). **^{1}H NMR** (500 MHz, $CDCl_3$) δ 8.15 (2H, dt, *J* = 7.8, 1.0 Hz, Ar*H*), 7.44 (2H, ddd, *J* = 8.3, 7.1, 1.2 Hz, Ar*H*), 7.38 (2H, dt, *J* = 8.2, 0.9 Hz, Ar*H*), 7.31–7.23 (4H, m, Ar*H*), 7.16 (2H, ddd, *J* = 7.6, 2.0, 1.0 Hz, Ar*H*), 5.52 (2H, s, CH_2Ph). **^{13}C NMR** (126 MHz, $CDCl_3$) δ 140.8 (Ar*C*), 137.3 (Ar*C*), 128.9 (Ar*C*), 127.6 (Ar*C*), 126.5 (Ar*C*), 126.0 (Ar*C*), 123.2 (Ar*C*), 120.5 (Ar*C*), 119.3 (Ar*C*), 109.0 (Ar*C*), 46.68 (*C*H_2Ph). Data is in line with literature precedent.[5]

Synthesis of 1-(9*H*-carbazol-9-yl)-2,2-dimethylpropan-1-one (**1f**)

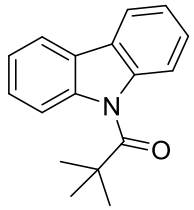

To a stirred solution of 9*H*-carbazole (1.67 g, 10 mmol), triethylamine (2.1 mL, 1.52 g, 15 mmol), and *N',N'*-dimethylaminopyridine (DMAP, 122 mg, 1 mmol) in anhydrous CH_2Cl_2 (30 mL) was added trimethylacetyl chloride (pivaloyl chloride, 1.5 mL, 1.45 g, 12 mmol) dropwise at 0 °C. After addition was complete, the reaction mixture was allowed to return to room temperature and stirred overnight. The reaction mixture was concentrate *in vacuo*, and the resulting residue was partitioned between EtOAc (100 mL) and brine (100 mL). The organic layer was extracted and the aqueous phase was re-extracted with EtOAc (2 x 100 mL). The combined organics were dried over $MgSO_4$ and concentrated *in vacuo*. The resulting residue was purified *via* silica gel column chromatography (EtOAc:Petroleum Spirit, 5:95 v:v) to give (on standing at 4 °C overnight) a crystalline white solid, 65% (1.62 g). **^{1}H NMR** (500 MHz, $CDCl_3$) δ 8.04 (2H, dd, *J* = 7.6, 1.4 Hz, Ar*H*), 7.75–7.63 (2H, m, Ar*H*), 7.45 (2H, ddq, *J* = 8.3, 7.1, 1.3 Hz, Ar*H*), 7.37–7.29 (2H, m, Ar*H*), 1.54 (6H, app d, Piv*H*). **^{13}C NMR** (126 MHz, $CDCl_3$) δ 184.2 (C*O*t*B*u), 139.4 (Ar*C*), 126.5 (Ar*C*), 124.9 (Ar*C*), 122.0 (Ar*C*), 120.2 (Ar*C*), 113.9 (Ar*C*), 43.9 (*C*(CH_3)$_3$), 28.5 (C(*C*H_3)$_3$). Data is in line with literature precedent.

Synthesis of 2,3-diethyl-1-(pyrimidin-2-yl)-1*H*-indole (**4a**)

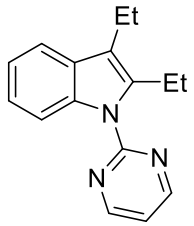

To an oven dried carousel tube was charged *N*-(2-bromophenyl)pyrimidin-2-amine (62.5 mg, 0.25 mmol), palladium(II) acetate (5.6 mg, 0.025 mmol), lithium chloride (1.1 mg, 0.025 mmol) and sodium carbonate (132 mg, 1.25 mmol). The reactor tube was evacuated and refilled with argon three times. Dimethylformamide (1 mL) and hex-3-yne (0.085 mL, 0.75 mmol) were then added *via* septum. The vessel was heated to 100 ^{o}C for 16 hours. Then the reaction mixture was cooled to room temperature, and EtOAc and 5 % LiCl solution (100 mL) were added. The organic layer was separated and the aqueous was washed with further EtOAc (3 × 100 mL). The organic layer was dried over $MgSO_4$ and the solvents were removed under vacuum. The resulting residue was purified by silica gel column chromatography (EtOAc:Petroleum Ether 40-60 °C, 5:95 v:v) to give as an orange oil in 56 % yield (35 mg). **FT-IR:** (thin film): vmax (cm^{-1}) = 3044, 2963, 2929, 2871, 2160, 2008, 1694, 1560, 1455, 1422. **^{1}H NMR:** (500 MHz, $CDCl_3$) δ 8.79 (2H, d, *J* = 4.8 Hz, Ar*H*), 8.22 (1H, d, *J* = 7.1 Hz, Ar*H*), 7.54 (1H, d, *J* = 6.7 Hz, Ar*H*), 7.24–7.16 (2H, m, Ar*H*), 7.12 (1H, t, *J* = 4.8 Hz, Ar*H*), 3.19 (2H, q, *J* = 7.4 Hz, C*H*$_2$CH$_3$), 2.78 (2H, q, *J* = 7.6 Hz, C*H*$_2$CH$_3$), 1.28 (3H, t, *J* = 7.5 Hz, CH$_2$C*H*$_3$), 1.11 (3H, t, *J* = 7.4 Hz, CH$_2$C*H*$_3$). **^{13}C NMR:** (126 MHz, CDCl3) δ 165.8 (Ar*C*), 158.1 (Ar*C*), 138.3 (Ar*C*), 136.4 (Ar*C*), 129.6 (Ar*C*), 122.5 (Ar*C*), 121.3 (Ar*C*), 118.8 (Ar*C*), 118.0 (Ar*C*), 116.7 (Ar*C*), 113.5 (Ar*C*), 19.3 (*C*H$_2$CH$_3$) , 17.4 (*C*H$_2$CH$_3$), 15.4 (CH$_2$*C*H$_3$), 15.0 (CH$_2$*C*H$_3$). **HRMS:** (ESI): m/z calculated for $C_{16}H_{17}N_4$ required 274.1315 for $[M+Na]^+$ and found 274.1302.

Synthesis of 1-(pyrimidin-2-yl)indoline (**4b**)

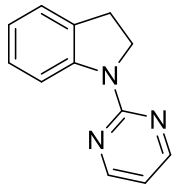

To a solution of indoline (0.56 mL, 5 mmol) and 2-chloropyrimidine (0.69 g, 5 mmol) in EtOH (40 mL) and water (20 mL) was added conc. HCl (1 mL). The reaction mixture was then refluxed overnight. The EtOH and water were then removed *in vacuo*. The crude residue was partitioned between water (100 mL) and CH_2Cl_2 (100 mL) and the organic layer extracted. The aqueous layer was re-extracted with CH_2Cl_2 (2 x 100 mL). The combined organic phases were dried over $MgSO_4$ and concentrated *in vacuo*. The crude residue was purified *via* silica gel column chromatography to give a bronze oil, 65% (0.632 g). **FT-IR** (thin film): ν_{max} (cm^{-1}) = 3041.9, 2955.9, 1557.0, 1548.0. **^{1}H NMR** (500 MHz, $CDCl_3$) δ 8.49 (2H, d, *J* = 4.7 Hz, Ar*H*), 8.40 (1H, d, *J* = 8.1 Hz, Ar*H*), 7.25–7.18 (2H, m, Ar*H*), 6.94 (1H, td, *J* = 7.4, 1.1 Hz, Ar*H*), 6.68 (1H, t, *J* = 4.8 Hz, Ar*H*), 4.24 (2H, dd, *J* = 9.2, 8.2 Hz, CH_2), 3.31–3.13 (2H, m, CH_2). **^{13}C NMR** (126 MHz, $CDCl_3$) δ 157.57 (Ar*C*), 143.74 (Ar*C*), 132.31 (Ar*C*), 127.38 (Ar*C*), 124.74 (Ar*C*), 121.63 (Ar*C*), 115.46 (Ar*C*), 111.52 (Ar*C*), 48.87 (*C*H_2), 27.41 (*C*H_2). **HRMS** (ESI): m/z calculated for $C_{12}H_{11}N_3$ requires 220.0853 for $[M+Na]^+$, found 220.0891.

6.4.4: Synthesis of C4-Functionalized Carbazoles

General Procedure **B** for the Remote C4-Alkylation of Carbazole Derivatives

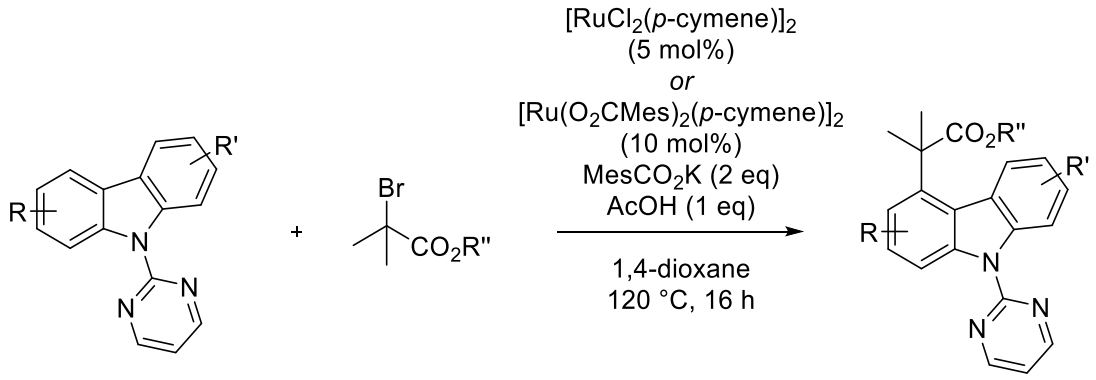

To an oven dried carousel tube was charged with relevant carbazole derivative (0.25 mmol), $[RuCl_2(p\text{-cymene})]_2$ (8 mg, 0.0125 mmol, 5 mol%) or $[Ru(O_2CMes)_2(p\text{-cymene})]$ (14 mg, 0.025 mmol, 10 mol%), and potassium 2,4,6-trimethylbenzoate ($MesCO_2K$, 102 mg, 0.5 mmol). The reaction vessel was then sealed with a Teflon cap, and then evacuated and refilled with Argon three times. 1,4-dioxane (1 mL), acetic acid (0.015 mL, 15 mg, 0.25 mmol) and relevant coupling partner (0.75 mmol) were added *via* syringe. The flask was then heated at 120 °C for 16 h. The reaction mixture was allowed to return to room temperature and was then diluted in EtOAc (20 mL) and sat. $NaHCO_3$ solution (20 mL). The organic layer was extracted and the aqueous layer was re-extracted with EtOAc (2 x 20 mL). The combined organics were dried over $MgSO_4$ and concentrated *in vacuo*. The crude residue was then purified *via* silica gel column chromatography (EtOAc:Petroleum Spirit 40-60 °C, 10:90-20:80 v:v), to give pure C4-alkylated structures.

Synthesis of **3a**

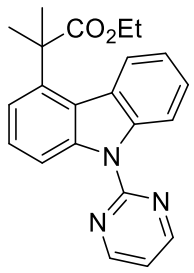

General Procedure **B** was followed using **1a** (61 mg, 0.25 mmol) and ethyl α-bromoisobutyrate (0.12 mL, 146 mg, 0.75 mmol). Silica gel column chromatography gave a white solid. $[RuCl_2(p\text{-cymene})]_2$ as catalyst: 68% (61 mg). $[Ru(O_2CMes)_2(p\text{-cymene})]$ as catalyst: 76% (68 mg). **mp** (from $CHCl_3$): 127-129 ^oC. **mp** (from $CHCl_3$): 130-133 °C. **FT-IR:** (thin film): vmax (cm^{-1}) = 3040, 2983, 2874, 2164, 1725, 1580, 1564, 1427. **^{1}H NMR:** (500 MHz, $CDCl_3$) δ 8.87 (2H, d, *J* = 4.78 Hz, Ar*H*), 8.69 (2H, d, *J* = 8.37 Hz, Ar*H*), 8.02 (1H, d, *J* = 8.11 Hz, Ar*H*), 7.46 (3H, m, Ar*H*), 7.32 (1H, t, *J* = 7.63 Hz, Ar*H*), 7.17 (1H, t, *J* = 4.77 Hz, Ar*H*), 4.04 (2H, q, *J* = 7.10 Hz, $CO_2CH_2CH_3$), 1.88 (6H, s, $C(CH_3)_2$), 0.95 (3H, t, *J* = 7.11 Hz, $CO_2CH_2CH_3$). **^{13}C NMR:** (126 MHz, CDCl3) δ 178.3 (CO_2Et), 158.7 (Ar*C*), 158.0 (Ar*C*), 140.0 (Ar*C*), 139.5 (Ar*C*), 139.0 (Ar*C*), 126.0 (Ar*C*), 125.7 (Ar*C*), 124.5 (Ar*C*), 123.5 (Ar*C*), 123.2 (Ar*C*), 121.8 (Ar*C*), 119.5 (Ar*C*), 116.7 (Ar*C*), 114.4 (Ar*C*), 113.7 (Ar*C*), 61.1 ($CO_2CH_2CH_3$), 47.0 ($C(CH_3)_2$), 27.0 ($C(CH_3)_2$), 13.9 ($CO_2CH_2CH_3$). **HRMS:** (ESI): found m/z calculated for $C_{22}H_{21}N_3O_2$ required 360.1707 for $[M+H]^+$, found 360.1715.

Synthesis of **3aa**

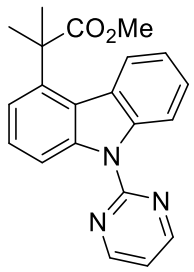

General Procedure **B** was followed using **1a** (61 mg, 0.25 mmol) and methyl α-bromoisobutyrate (0.10 mL, 136 mg, 0.75 mmol). Silica gel column chromatography gave a white solid, $[RuCl_2(p\text{-cymene})]_2$ as catalyst: 70% (60 mg). $[Ru(O_2CMes)_2(p\text{-cymene})]$ as catalyst: 65% (56 mg). **FT-IR** (thin film): v_{max} (cm^{-1}) = 2981.1, 1726.1, 1561.3. **mp** (from $CHCl_3$): 162-165 °C. **^{1}H NMR** (500 MHz, $CDCl_3$) δ 8.85 (2H, d, *J* = 4.8 Hz, Ar*H*), 8.74–8.66

(2H, m, Ar*H*), 7.54–7.45 (1H, m, Ar*H*), 7.45–7.41 (2H, m, Ar*H*), 7.38–7.32 (1H, m, Ar*H*), 7.14 (1H, t, *J* = 4.8 Hz, Ar*H*), 3.53 (3H, s, CO_2CH_3), 1.91 (6H, s, $C(CH_3)_2$). **^{13}C NMR** (126 MHz, $CDCl_3$) δ 179.1 (CO_2Me), 158.8 (Ar*C*), 158.2 (Ar*C*), 140.1 (Ar*C*), 139.5 (Ar*C*), 139.1 (Ar*C*), 126.1 (Ar*C*), 125.9 (Ar*C*), 124.6 (Ar*C*), 123.3 (Ar*C*), 123.2 (Ar*C*), 122.1 (Ar*C*), 119.5 (Ar*C*), 116.9 (Ar*C*), 114.6 (Ar*C*), 114.0 (Ar*C*), 52.65 (CO_2CH_3), 47.1 ($C(CH_3)_2$), 27.2 ($C(CH_3)_2$). **HRMS** (ESI): m/z calculated for $C_{21}H_{19}N_3O_2$ requires 346.1550 for $[M+H]^+$, found 346.1583.

Synthesis of **3ab**

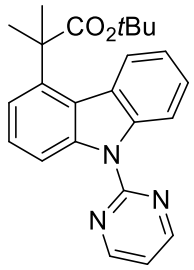

General Procedure **B** was followed using **1a** (61 mg, 0.25 mmol) and *tert*-butyl α-bromoisobutyrate (0.14 mL, 167 mg, 0.75 mmol). Silica gel column chromatography gave a white solid, $[RuCl_2(p\text{-cymene})]_2$ as catalyst: 72% (69 mg). $[Ru(O_2CMes)_2(p\text{-cymene})]$ as catalyst: 92% (89 mg). **mp** (from $CHCl_3$): 180-183 °C. **FT-IR** (thin film): ν_{max} (cm^{-1}) = 2980.8, 1717.2, 1561.2 **^{1}H NMR** (500 MHz, $CDCl_3$) δ 8.84 (2H, d, *J* = 4.8 Hz, Ar*H*), 8.72–8.63 (2H, m, Ar*H*), 8.18–8.15 (1H, m, Ar*H*), 7.50–7.43 (1H, m, Ar*H*), 7.40 (1H, dd, *J* = 7.7, 1.0 Hz, Ar*H*), 7.36–7.31 (1H, m, Ar*H*), 7.13 (1H, t, *J* = 4.8 Hz, Ar*H*), 1.86 (6H, s, $C(CH_3)_2$), 1.27 (9H, s, $C(CH_3)_3$). **^{13}C NMR** (126 MHz, $CDCl_3$) δ 177.2 (CO_2R), 158.8 (Ar*C*), 158.1 (Ar*C*), 140.1 (Ar*C*), 140.1 (Ar*C*), 139.1 (Ar*C*), 126.0 (Ar*C*), 125.8 (Ar*C*), 124.6 (Ar*C*), 124.5 (Ar*C*), 123.3 (Ar*C*), 121.7 (Ar*C*), 119.7 (Ar*C*), 116.7 (Ar*C*), 114.4 (Ar*C*), 113.6 (Ar*C*), 80.9 (Alk*C*), 47.8 (Alk*C*) , 27.8 (Alk*C*), 26.9 (Alk*C*). **HRMS** (ESI): m/z calculated for $C_{24}H_{25}N_3O_2$ requires 388.1947 for $[M+H]^+$, found 388.2069.

Synthesis of **3ac**

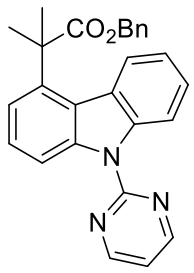

General Procedure **B** was followed using **1a** (61 mg, 0.25 mmol) and benzyl α-bromoisobutyrate (0.13 mL, 178 mg, 0.75 mmol). Silica gel column chromatography gave a white solid, $[RuCl_2(p\text{-cymene})]_2$ as catalyst: 51% (54 mg). $[Ru(O_2CMes)_2(p\text{-cymene})]$ as catalyst: 74% (78 mg). **mp** (from $CHCl_3$): 112-116 ^oC. **FTIR** (thin film): ν_{max} = 2968, 1718, 1583, 1563. **^{1}H NMR** (500 MHz, $CDCl_3$): δ 8.88 (2H, d, J = 4.8 Hz, Ar*H*), 8.69 (2H, dd, J = 8.3, 1.1 Hz, Ar*H*), 7.96 (1H, ddd, J = 8.2, 1.2, 0.6 Hz, Ar*H*), 7.48 (1H, dd, J = 8.4, 7.6 Hz, Ar*H*), 7.43-7.40 (2H, m, Ar*H*), 7.22-7.15 (5H, m, Ar*H*), 7.02-6.99 (2H, m, Ar*H*), 5.02 (2H, s, CH_2Ph), 1.90 (6H, s, C(CH_3)$_2$). **^{13}C NMR** (126 MHz, $CDCl_3$): δ 178.4 (CO_2Bn), 163.5 (Ar*C*), 158.4 (Ar*C*), 139.6 (Ar*C*), 139.1 (Ar*C*), 128.6 (Ar*C*), 128.2 (Ar*C*), 126.4 (Ar*C*), 126.0 (Ar*C*), 125.9 (Ar*C*), 124.8 (Ar*C*), 123.6 (Ar*C*), 123.5 (Ar*C*), 122.3 (Ar*C*), 119.9 (Ar*C*), 117.1 (Ar*C*), 114.8 (Ar*C*), 114.2 (Ar*C*), 67.2 CO_2CH_2Ph), 47.4 ($C(CH_3)_2$), 27.4 (C(CH_3)$_2$). **HRMS** (ESI): m/z calculated for $C_{27}H_{23}N_3O_2$ requires 422.1870 for $[M+H]^+$ found 422.1943.

Synthesis of **3ad**

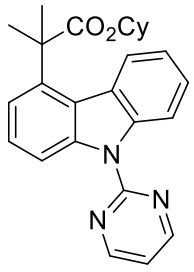

General Procedure **B** was followed using **1a** (61 mg, 0.25 mmol) and cyclohexyl α-bromoisobutyrate (147 mg, 0.75 mmol). Silica gel column chromatography gave an amorphous solid, $[RuCl_2(p\text{-cymene})]_2$ as catalyst: 54% (56 mg). $[Ru(O_2CMes)_2(p\text{-cymene})]$ as catalyst: 74% (76 mg). **FTIR** (thin film): ν_{max} = 2929, 2855, 1718, 1570. **^{1}H NMR** (500 MHz, $CDCl_3$): δ 8.88 (2H, d, J = 4.8 Hz,Ar*H*), 8.68 (2H, ddd, J = 8.4, 3.4, 1.0 Hz, Ar*H*), 8.05 (1H, dd, J = 8.2, 1.1 Hz, Ar*H*), 7.49-7.44 (2H, m, Ar*H*), 7.43-7.39 (1H, m, Ar*H*), 7.30 (1H,

ddd, *J* = 8.2, 7.2, 1.1 Hz, Ar*H*), 7.14 (1H, m, Ar*H*), 4.81-4.73 (1H, m, CO_2C*H*), 1.87 (6H, s, $C(CH_3)_2$), 1.56 (3H, broad s, Cy*H*), 1.45-1.32 (3H, m, Cy*H*), 1.22-1.00 (4H, m, Cy*H*). **^{13}C NMR** (126 MHz, $CDCl_3$): *δ* 178.2 (CO_2Cy), 163.3 (Ar*C*), 158.2 (Ar*C*), 139.4 (Ar*C*), 135.9 (Ar*C*), 128.4 (Ar*C*), 128.0 (Ar*C*), 126.2 (Ar*C*), 125.8 (Ar*C*), 124.6 (Ar*C*), 123.4 (Ar*C*), 122.1 (Ar*C*), 119.7 (Ar*C*), 116.9 (Ar*C*), 114.6 (Ar*C*), 114.0 (Ar*C*), 67.0 (CO_2*C*H), 47.2 ($C(CH_3)_2$), 27.2 ($C(CH_3)_2$), 27.1 (Cy*C*), 25.3 (Cy*C*), 24.6 (Cy*C*). **HRMS** (ESI): m/z calculated for $C_{26}H_{27}N_3O_2$ requires 436.1995 for $[M+Na]^+$ found 436.2027.

Synthesis of **3af**

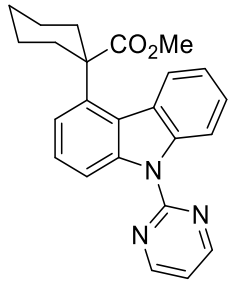

General Procedure **B** was followed using **1a** (61 mg, 0.25 mmol) and methyl 1-bromocyclohexane-1-carboxylate (0.12 mL, 166 mg, 0.75 mmol). Silica gel column chromatography gave a white solid, $[RuCl_2(p\text{-cymene})]_2$ as catalyst: 35% (34 mg). $[Ru(O_2CMes)_2(p\text{-cymene})]$ as catalyst: 42% (40 mg). **mp** (from $CHCl_3$): 182-185 °C. **FTIR** (thin film): ν_{max} = 2955, 2932, 2362, 2165, 2034, 1718, 1560. **^{1}H NMR** (500 MHz, $CDCl_3$): *δ* 8.89 (d, *J* = 4.8 Hz, 2H), 8.66–8.61 (2H, m, Ar*H*), 8.10–8.06 (1H, m, Ar*H*), 7.52–7.46 (2H, m, Ar*H*), 7.45 (1H, ddd, *J* = 8.4, 7.1, 1.2 Hz, Ar*H*), 7.45 (1H, ddd, *J* = 8.3, 7.1, 1.2 Hz, Ar*H*), 7.20 (1H, t, *J* = 4.8 Hz, Ar*H*), 3.49 (3H, s, CO_2CH_3), 2.48 (5H, s, Cy*H*), 1.81 (3H, s, Cy*H*), 1.26 (2H, s, Cy*H*). **^{13}C NMR** (126 MHz, $CDCl_3$) δ 178.6 (CO_2Me), 158.3 (Ar*C*), 140.5 (Ar*C*), 139.1 (Ar*C*), 138.5 (Ar*C*), 125.9 (Ar*C*), 125.8 (Ar*C*), 124.7 (Ar*C*), 124.2 (Ar*C*), 123.4 (Ar*C*), 122.0 (Ar*C*), 121.9 (Ar*C*), 117.0 (Ar*C*), 114.3 (Ar*C*), 113.5 (Ar*C*), 52.5 (CO_2CH_3), 50.9 (*C*(Cy)), 34.0 (Cy*C*), 25.9 (Cy*C*), 22.8 (Cy*C*). **HRMS** (ESI): m/z calculated for $C_{24}H_{23}N_3O_2$ requires 386.1870 for $[M+H]^+$ found 386.1922.

Synthesis of **3ah**

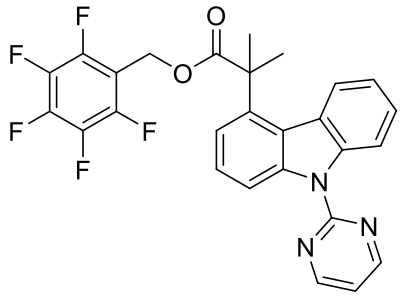

General Procedure **B** was followed using **1a** (61 mg, 0.25 mmol) and (perfluorophenyl)methyl-2-bromo-2-methylpropanoate (260 mg, 0.75 mmol),. Silica gel column chromatography gave a white solid, $[RuCl_2(p\text{-cymene})]_2$ as catalyst: 41% (52 mg). $[Ru(O_2CMes)_2(p\text{-cymene})]$ as catalyst: 39% (50 mg). **mp** (from $CHCl_3$): 165-168 ^oC. **FTIR** (thin film): ν_{max} = 2959, 1742, 1661, 1570, 1509. **^{1}H NMR** (500 MHz, $CDCl_3$): δ 8.88 (2H, d, *J* = 4.8 Hz, Ar*H*), 8.69 (2H, dd, *J* = 10.8, 8.4 Hz, Ar*H*), 7.78 (1H, d, *J* = 8.1 Hz, Ar*H*), 7.49 (1H, t, *J* = 8.0 Hz, Ar*H*), 7.43-7.38 (2H, m, Ar*H*), 7.18 (1H, t, *J* = 4.8 Hz, Ar*H*), 7.12 (1H, t, *J* = 7.6 Hz, Ar*H*), 5.06 (2H, s, C*H*$_2$Ar), 1.89 (6H, s, (C(C*H*$_3$)$_2$). **^{13}C NMR** (126 MHz, $CDCl_3$) δ 177.8 (*C*O_2R), 158.8 (Ar*C*), 158.2 (Ar*C*), 145.5 (dddd, *J* = 251.3, 11.3, 7.7, 4.0 Hz, Ar$_F$*C*), 143.0–140.2 (m, Ar$_F$C), 140.1 (Ar*C*), 139.0 (Ar*C*), 138.8 (Ar*C*), 138.4–135.7 (Ar$_F$*C*), 126.3 (Ar*C*), 125.6 (Ar*C*), 124.1 (Ar*C*), 123.0 (Ar*C*), 122.9 (Ar*C*), 121.5 (Ar*C*), 119.5 (Ar*C*), 116.9 (Ar*C*), 114.7 (Ar*C*), 114.2 (Ar*C*), 109.2 (td, *J* = 17.5, 3.7 Hz, Ar$_F$*C*), 53.9 (*C*H_2R), 47.1 (*C*(CH$_3$)$_2$), 29.8 (C(*C*H_3)$_2$). **^{19}F NMR** (470 MHz, $CDCl_3$): δ -141.85 (2F, dd, *J* = 22.4, 8.3 Hz, o-*F*), -153.06 (1F, s, *p*-F), -161.99 (2F, m, *m*-F). **HRMS** (ESI): m/z calculated for $C_{27}H_{18}F_5N_3O_2$ requires 512.1392 for $[M+H]^+$ found 512.1426.

Synthesis of **3b**

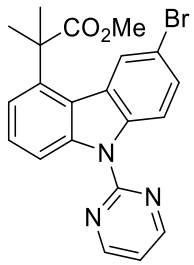

General Procedure **B** was followed using **1b** (81 mg, 0.25 mmol) and methyl α-bromoisobutyrate (0.1 mL, 136 mg, 0.75 mmol). Silica gel column chromatography gave a white solid, 54% (57 mg). **FT-IR** (thin film): ν_{max} (cm^{-1}) = 2981.2, 1727.8, 1567.3. **mp** (from

$CHCl_3$): 183-185 °C. **^{1}H NMR** (500 MHz, $CDCl_3$) δ 8.81 (2H, d, *J* = 4.8 Hz, Ar*H*), 8.71 (1H, dd, *J* = 8.4, 1.0 Hz, Ar*H*), 8.62 (1H, d, *J* = 8.9 Hz, Ar*H*), 8.09 (1H, d, *J* = 1.9 Hz, Ar*H*), 7.55 (1H, dd, *J* = 9.0, 1.9 Hz, Ar*H*), 7.52 (1H, dd, *J* = 8.5, 7.6 Hz, Ar*H*), 7.43 (1H, dd, *J* = 7.7, 1.0 Hz, Ar*H*), 7.14 (1H, t, *J* = 4.8 Hz, Ar*H*), 3.68 (3H, s, CO_2CH_3), 1.89 (6H, s, $C(CH_3)_2$). **^{13}C NMR** (126 MHz, $CDCl_3$) δ 178.3 (CO_2Me), 158.5 (Ar*C*), 158.2 (Ar*C*), 140.5 (Ar*C*), 139.8 (Ar*C*), 137.8 (Ar*C*), 128.4 (Ar*C*), 126.9 (Ar*C*), 126.4 (Ar*C*), 125.7 (Ar*C*), 122.1 (Ar*C*), 119.8 (Ar*C*), 117.0 (Ar*C*), 116.4 (Ar*C*), 115.0 (Ar*C*), 114.4 (Ar*C*), 52.6 (CO_2CH_3), 47.1 ($C(CH_3)_2$), 27.1 ($C(CH_3)_2$). **HRMS** (ESI): m/z calculated for $C_{21}H_{18}N_3O_2Br_1$ requires 446.0482 for $[M+Na]^+$, found 446.0554.

Synthesis of **3c**

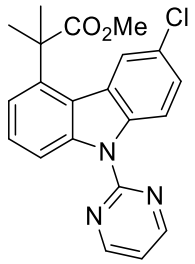

General Procedure **B** was followed using **1c** (70 mg, 0.25 mmol) and methyl α-bromoisobutyrate (0.1 mL, 136 mg, 0.75 mmol). Silica gel column chromatography gave a white solid, 60% (57 mg). **mp** (from $CHCl_3$): 200-203 °C. **FT-IR** (thin film): ν_{max} (cm^{-1}) = 2981.2, 1727.8, 1567.3. **^{1}H NMR** (500 MHz, $CDCl_3$) δ 8.82 (2H, d, *J* = 4.8 Hz, Ar*H*), 8.69 (2H, dd, *J* = 23.7, 8.9 Hz, Ar*H*), 7.95 (1H, s, Ar*H*), 7.51 (1H, d, *J* = 8.3 Hz, Ar*H*), 7.47–7.37 (2H, m, Ar*H*), 7.14 (1H, d, *J* = 4.9 Hz, Ar*H*), 3.66 (3H, s, CO_2CH_3), 1.89 (6H, s, $C(CH_3)_2$). **^{13}C NMR** (126 MHz, $CDCl_3$) δ 178.3 (CO_2Me), 158.5 (Ar*C*), 158.2 (Ar*C*), 140.6 (Ar*C*), 139.7 (Ar*C*), 137.5 (Ar*C*), 127.4 (Ar*C*), 126.9 (Ar*C*), 125.8 (Ar*C*), 125.7 (Ar*C*), 122.7 (Ar*C*), 122.3 (Ar*C*), 119.8 (Ar*C*), 117.0 (Ar*C*), 116.0 (Ar*C*), 114.4 (Ar*C*), 52.6 (CO_2CH_3), 47.1 ($C(CH_3)_2$), 27.1 ($C(CH_3)_2$). **HRMS** (ESI): m/z calculated for $C_{21}H_{18}N_3O_2Cl_1$ requires 402.0988 for $[M+Na]^+$, found 402.0918.

Synthesis of **3d**

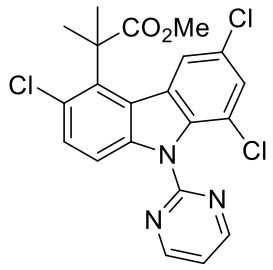

General Procedure **B** was followed using **1d** (87 mg, 0.25 mmol) and methyl α-bromoisobutyrate (0.1 mL, 136 mg, 0.75 mmol). Silica gel column chromatography gave a white solid, 10% (11 mg). **FT-IR** (thin film): ν_{max} (cm^{-1}) = 2950.9, 1731.1, 1566.7. **^{1}H NMR** (500 MHz, $CDCl_3$) δ 8.92 (2H, d, *J* = 4.9 Hz, Ar*H*), 8.03 (1H, d, *J* = 1.8 Hz, Ar*H*), 7.59 (1H, d, *J* = 8.9 Hz, Ar*H*), 7.45–7.41 (2H, m, Ar*H*), 7.38 (1H, t, *J* = 4.9 Hz, Ar*H*), 3.63 (3H, s, CO_2CH_3), 2.08 (6H, s, $C(CH_3)_2$). **^{13}C NMR** (126 MHz, $CDCl_3$) δ 178.2 (CO_2Me), 158.9 (Ar*C*), 137.0 (Ar*C*), 131.7 (Ar*C*), 127.7 (Ar*C*), 127.4 (Ar*C*), 126.8 (Ar*C*), 123.9 (Ar*C*), 122.8 (Ar*C*), 119.8 (Ar*C*), 119.2 (Ar*C*), 111.8 (Ar*C*), 52.69 (CO_2CH_3), 50.0 ($C(CH_3)_2$), 27.8 ($C(CH_3)_2$). **HRMS** (ESI): m/z calculated for $C_{21}H_{16}N_3O_2Cl_3$ requires 470.0200 for $[M+Na]^+$, found 470.0162.

Synthesis of **3g**

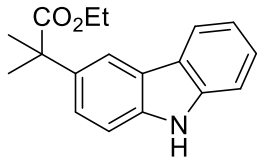

General Procedure **B** was followed using 9*H*-carbazole, **16** (87 mg, 0.25 mmol) and ethyl α-bromoisobutyrate (0.11 mL, 146 mg, 0.75 mmol). Silica gel column chromatography gave an amorphous solid, 14% (10 mg). **FT-IR** (thin film): ν_{max} (cm^{-1}) = 3419.2, 2928.7, 1715.5. **^{1}H NMR** (500 MHz, $CDCl_3$) δ 8.11–8.05 (2H, m, Ar*H*), 8.03 (1H, s, N*H*), 7.45–7.33 (4H, m, Ar*H*), 7.23 (1H, ddd, *J* = 8.0, 4.8, 3.4 Hz, Ar*H*), 4.14 (2H, q, *J* = 7.1 Hz, $CO_2CH_2CH_3$), 1.70 (6H, s, $C(CH_3)_2$), 1.18 (3H, t, *J* = 7.1 Hz, $CO_2CH_2CH_3$). **^{13}C NMR** (126 MHz, $CDCl_3$) δ 177.5 (CO_2Et), 140.1 (Ar*C*), 138.4 (Ar*C*), 136.3 (Ar*C*), 126.0 (Ar*C*), 124.1 (Ar*C*), 123.6 (Ar*C*), 123.4 (Ar*C*), 120.4 (Ar*C*), 119.6 (Ar*C*), 117.2 (Ar*C*), 110.78 (Ar*C*), 110.5 (Ar*C*), 60.9 ($CO_2CH_2CH_3$), 46.5 ($C(CH_3)_2$), 27.2 ($C(CH_3)_2$), 14.2 ($CO_2CH_2CH_3$). **HRMS** (ESI) m/z calculated for $C_{18}H_{19}N_1O_2$ requires 304.1316 for $[M+Na]^+$, found 304.1340.

Bromo and chloro disubstituted compounds were not amenable to the Ullmann coupling proceeding in low yields, due to perceived lack of solubility under the conditions. The small amounts brought through from these reactions were also not amenable to the C4-alkylation methodology, again due to lack of solubility.

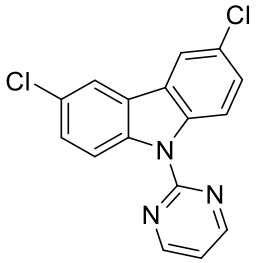

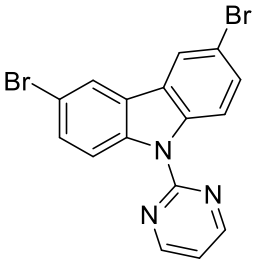

6.4.5: Mechanistic Studies

TEMPO Studies

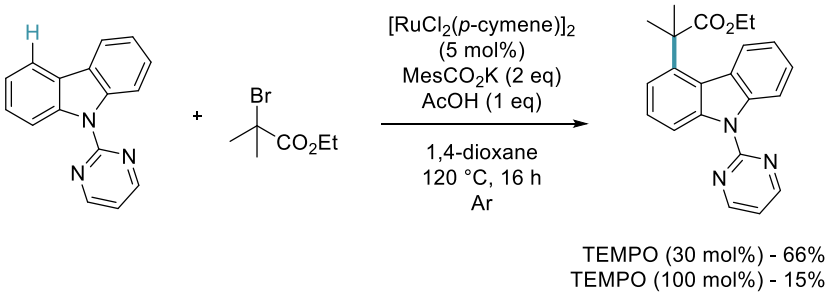

TEMPO (30 mol%) - 66%
TEMPO (100 mol%) - 15%

Deuterium Experiments

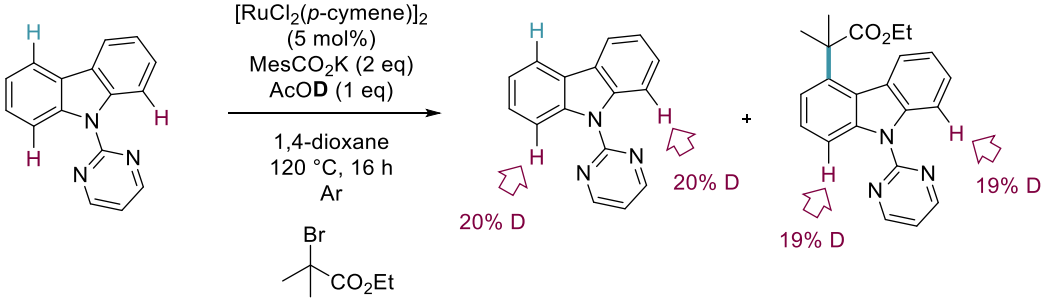

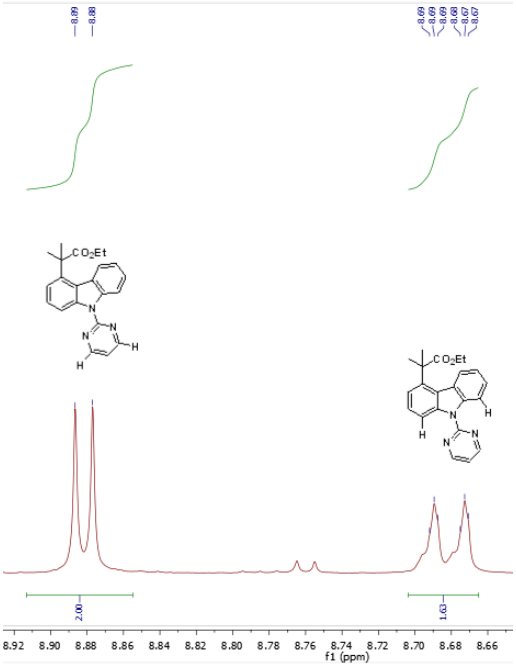

Product from D-Experiment

D incorporation = 18.5%

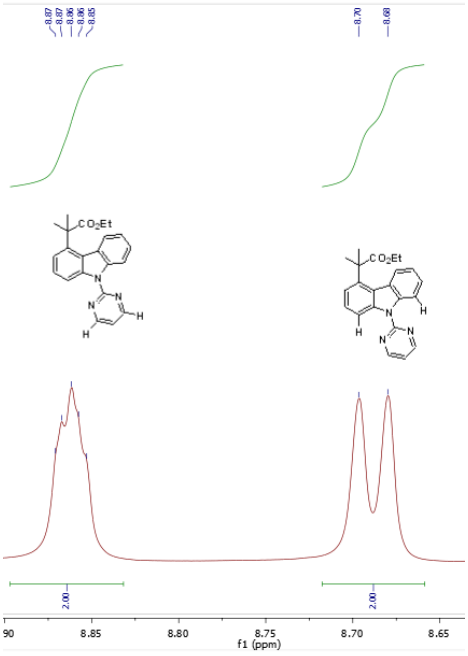

NMR 3a

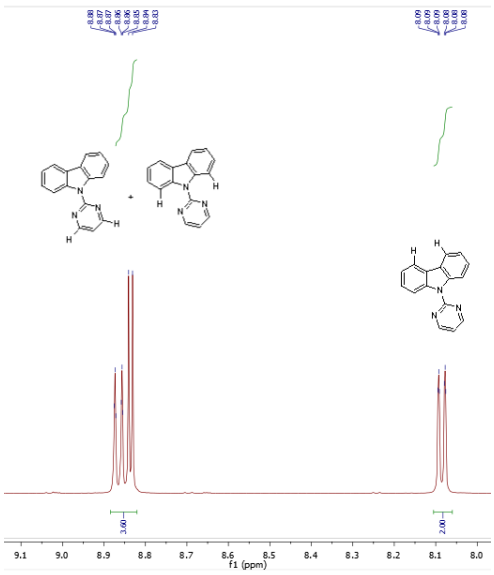

Product from D-Experiment

D incorporation = 10%

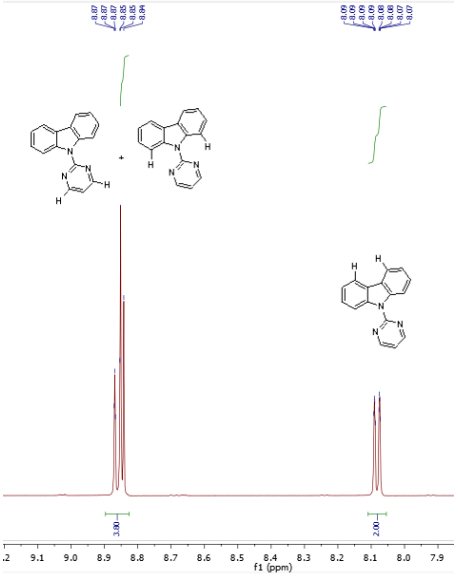

NMR 1a

6.5: Data and Supporting Information for “Ruthenium-Catalyzed *para*-Selective C–H Alkylation of Aniline Derivatives”

In the interest of presentation in a thesis, NMR spectra, crystallography data and computational data have not been included. However, in the interest of the reader these are available online at:
http://onlinelibrary.wiley.com/store/10.1002/anie.201708961/asset/supinfo/anie201708961-sup-0001-misc_information.pdf?v=1&s=f0fb5197df43fdbf5d975a9d52a1791e941ecc6a
The supporting information has also been submitted to formatting and colour changes, however no changes in the data have been made.

6.5.1: General

Proton, carbon and fluorine NMR spectra were recorded on Bruker 300 MHz, 400 MHZ or 500 MHz, or Agilent Technologies 500 MHz, spectrometer (^{1}H NMR at 500 MHz, 400 MHz, or 300 MHz, ^{13}C NMR at 126 MHz, 100 MHz, or 75 MHz, and ^{19}F NMR at 470 or 376 MHz. Chemical shifts for protons are reported in parts per million downfield from $Si(CH_3)_4$ and are referenced to residual protium in the deuterated solvent ($CHCl_3$ at 7.26 ppm). Chemical shifts for fluorines are reported in parts per million downfield from $CFCl_3$. NMR data are presented in the following format: chemical shift (number of equivalent nuclei by integration, multiplicity [app = apparent, br = broad, d = doublet, t = triplet, q = quartet, dd = doublet of doublets), dt = doublet of triplets), dq = doublet of quartets), ddd = doublet of doublet of doublets), m = multiplet], coupling constant [in Hz], assignment). Electrospray ionisation ultrahigh resolution time-of-flight mass spectrometry (ESI–UHR–TOF–MS) was performed on a Bruker maXis mass spectrometer. Electrospray ionisation high resolution time-of-flight mass spectrometry (ESI–HR–TOF–MS) was performed on a Bruker micrOTOF spectrometer. Infrared (IR) spectra were recorded on a Perkin–Elmer 1600 FT (Fourier transform), IR spectrophotometer, with absorbencies quoted as wavelength (v [in cm^{-1}]). Melting points were obtained on a Bibby Sterilin SMP10 melting point machine and are uncorrected.

Analytical thin-layer chromatography (TLC) was performed on aluminium-backed plates coated with Alugram® SIL G/UV254 purchased from Macherey–Nagel and visualised with UV light (254 or 365 nm), and/or KMnO4, 2,4-DNPH or I_2/Silica staining. Silica gel column chromatography was performed using 60 Å, 200-400 mesh particle size silica gel purchased

from Sigma–Aldrich. Samples were loaded as saturated solutions in an appropriate solvent system.

All reactions were performed using reagents obtained from Sigma-Aldrich, Acros Organics, Alfa Aesar, Fluorochem chemicals without further purification unless stated. $[RuCl_2(p\text{-cymene})]_2$ was purchased from STREM chemicals or Acros Organics. All water used was purified through a Merck Millipore reverse osmosis purification system prior to use. Anhydrous solvents were dried and degassed by passing through anhydrous alumina columns using an Innovative Technology Inc. PS-400-7 solvent purification system (SPS) and stored under an atmosphere of N_2 prior to use.

Reactions were performed in oven-dried glassware and under a blanket of N_2 if not stated. Temperatures quoted are external. Solvents were removed under reduced pressure using Büchi-Rotorvapor apparatus.

6.5.2: Optimization and Further Experiments

Scheme S1. Auxiliary Optimisation[a]

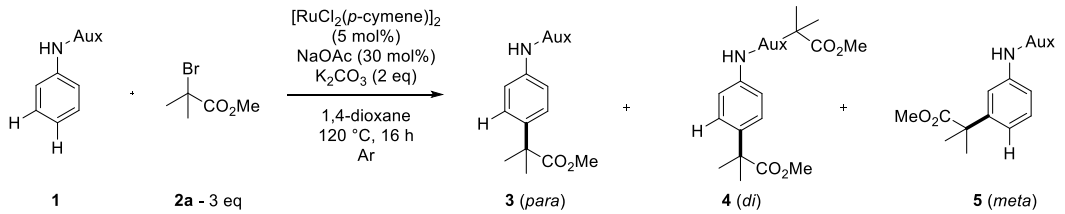

1 **2a** - 3 eq **3** (*para*) **4** (*di*) **5** (*meta*)

* denotes location of di-functionalization on Aux

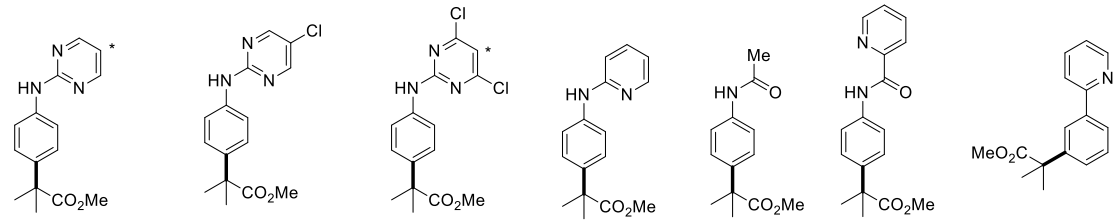

3b - 35%
4b - 6%

3c - 39%

3d - 16%
4d - 10%

3e - 0%

3f - 0%

3g - 0%

S5a - 38%[b]

[a] = ^{1}H NMR Conversions of Product Formation. [b] = Isolated Yield.

The use of dichloropyrimidine derivative (**1d**) led to increased ratio of formation of the di-substituted structure. This could be due to increased acidity at this position or the chloro substituents promoting radical interaction *via ortho*/*para*-direction.

The use of phenylpyridine under the exact same conditions leads to exclusively *meta*-selective products (**S5a**). This manifests the importance of the aniline substrate in enabling the *para*-C–H functionalisation.

Scheme S2. Conditions Optimisation

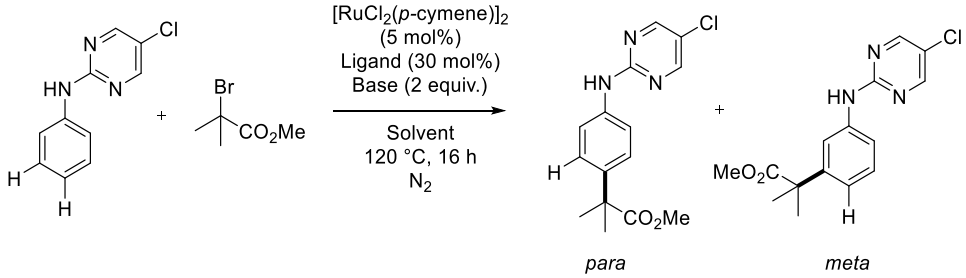

Entry	Ligand	Base	Solvent	Temp (°C)	Time (h)	Para % (IY)	Meta % (IY)
1	NaOAc	K_2CO_3	1,4-dioxane	120	16	39	-
2	NaOAc	K_2CO_3	PhMe	120	16	56	-
3	NaOAc	K_2CO_3	2-MeTHF	120	16	56	-
4	NaOAc	K_2CO_3	DME	120	16	28	-
5	NaOAc	K_2CO_3	CPME	120	16	35	-
6	NaOAc	K_2CO_3	TBME	120	16	81 (50)	-
7	NaOAc	K_2CO_3	DCE	120	16	59	-
8	NaOAc	K_2CO_3	MeCN	120	16	56	-
9	NaOAc	K_2CO_3	AcOH	120	16	Trace	-
10	NaOAc	K_2CO_3	DMA	120	16	-	-
11	NaOAc	K_2CO_3	*t*AmOH	120	16	41	-
12	NaOAc	K_2CO_3	*t*BuOH	120	16	24	-
13	KOAc	K_2CO_3	TBME	120	16	59	-
14	$MesCO_2H$	K_2CO_3	TBME	120	16	77	-
15	Piv-Val-OH	K_2CO_3	TBME	120	16	70	-
16	DMEDA	K_2CO_3	TBME	120	16	85	-
17	EN	K_2CO_3	TBME	120	16	28	-
18	TMEDA	K_2CO_3	TBME	120	16	7	-
19	Ac-Gly-OH	K_2CO_3	TBME	120	16	71	-
20	HCO_2K	K_2CO_3	TBME	120	16	52	-
21	*t*Bu Acac	K_2CO_3	TBME	120	16	4	-
22	DMEDA+NaOAc	K_2CO_3	TBME	120	16	72	-
23	**-**	**K_2CO_3**	**TBME**	**120**	**16**	**86 (55)**	**-**
24	-	Na_2CO_3	TBME	120	16	78	-
25	-	NaH	TBME	120	16	27	22
26	-	DIPEA	TBME	120	16	-	-
27	-	KOAc	TBME	120	16	57	43
28	-	Cs_2CO_3	TBME	120	16	69	-
29	-	Ag_2CO_3	TBME	120	16	-	-
30	-	-	TBME	120	16	-	-
31	-	K_2CO_3	TBME	60	16	-	-
32	-	K_2CO_3	TBME	100	16	63	-
33	-	K_2CO_3	TBME	110	16	80	-
34	-	K_2CO_3	TBME	130	16	80	10
35	-	K_2CO_3	TBME	140	16	55	38
36	-	K_2CO_3	TBME	120	16	-	-
40	-	K_2CO_3	TBME	120	2	32	-
41	-	K_2CO_3	TBME	120	4	66	-
42	-	K_2CO_3	TBME	120	6	59	-
43[a]	-	K_2CO_3	TBME	120	16	73	-
43[b]	-	K_2CO_3	TBME	120	16	71	-

General Conditions: Aniline Derivative (0.25-0.5 mmol), methyl α-bromoisobutyrate (0.75-1.5 mmol), $[RuCl_2(p\text{-cymene})]_2$ (5 mol%, 0.0125-0.025 mmol), solvent (1-2 mL), 120 °C, 16 h. a : K_2CO_3 (3 eq). b : Reaction carried out under air. CPME = cyclopentyl methyl ether. TBME = *tert*-butyl methyl ether *t*AmOH = 2-methyl-2-butanol. $MesCO_2H$ = 2,4,6-trimethylbenzoic acid. DMEDA = *N,N'*-dimethylethylenediamine, EN = ethylenediamine. TMEDA = *N,N'*-tetramethylethylenediamine. *t*Bu Acac = 2,2,6,6-tetramethylheptane-3,5-dione. DIPEA = *N,N*-diisoproylethylamine.

Scheme S3. Formation of Polymeric By-Products

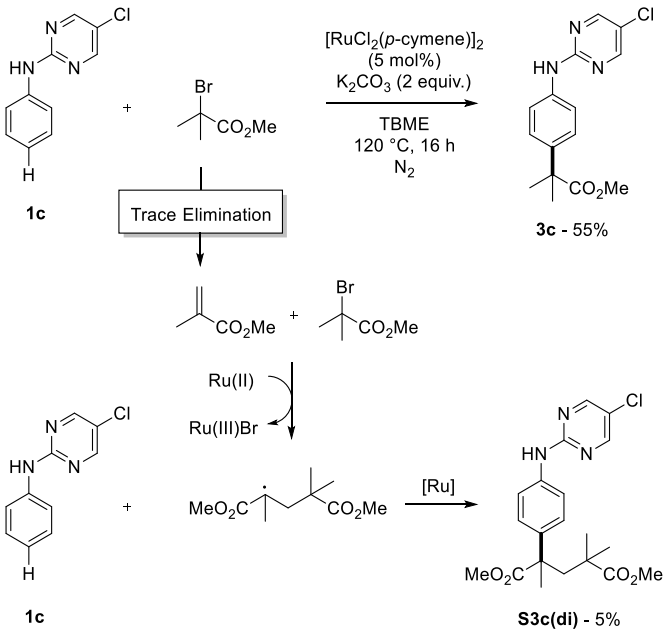

Disappointingly, the reaction conversions that were observed *via* crude NMR analysis were not readily converted in high isolated yields. We isolated polymer by-products out of the reaction mixture, which were contributing to the NMR conversion. These polymers were suggested to be formed *via* the trace formation of the methyl methacrylate *in situ*, *via* base elimination or in the protodemetalation mechanism. Interaction of the tertiary alkyl radical formed *via* single electron transfer with this alkene forms a secondary radical which can then interact in the *para* position. The dimeric radical products were isolated and fully characterised, and presence of trimeric products was observed *via* LC-MS however were not able to be characterised effectively enough to report. These observations are in line with our previous studies on *meta*-functionalisation using alpha halo carbonyl coupling partners.[1] This reaction methodology has also had issues with ruthenium leeching which has led to reduction in yields.

Scheme S4: Ruthenium-Catalyzed *para*-C–H Alkylation – Low Yielding and Unsuccessful Coupling Partners.

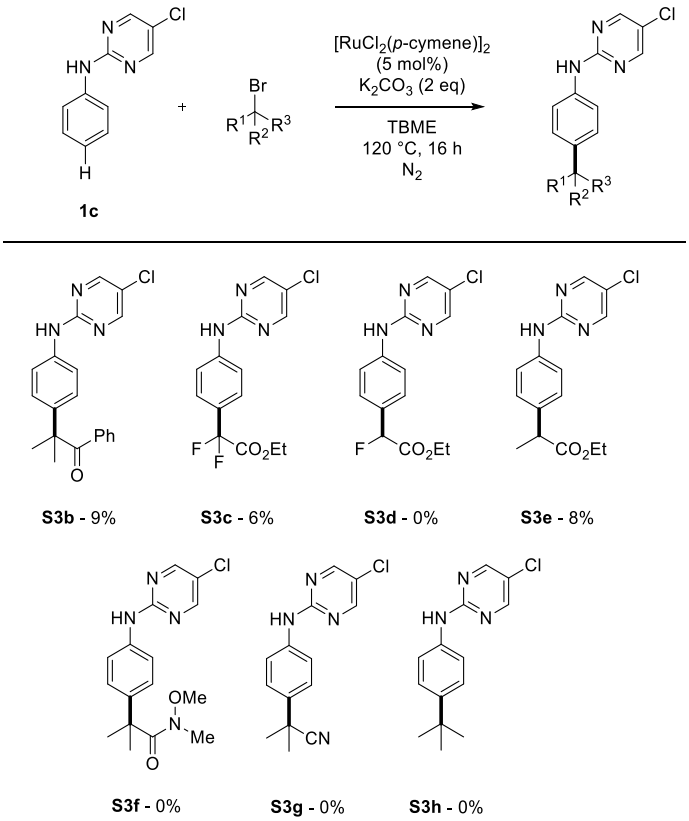

Scheme S5. Ruthenium-Catalysed C–H Alkylation of Methoxy Arene Derivatives

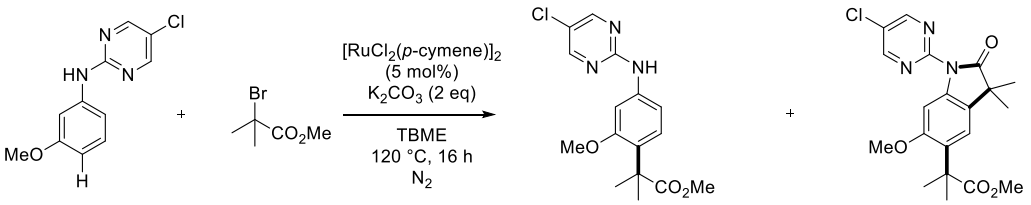

S1a **2a** **S3i** - 36%
Mono:**Di** - 1:1.8

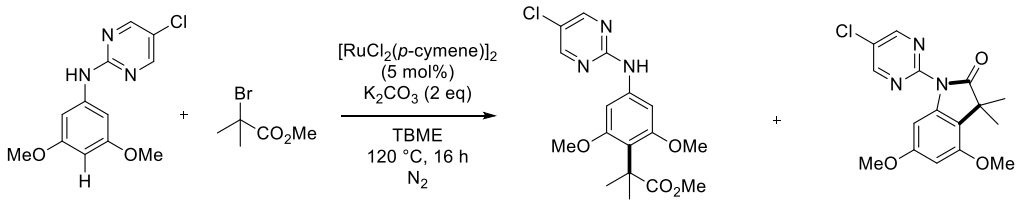

S1b **2a** **S3j** - 55%
para:**ortho** - 3.2:1

Scheme S6. Ruthenium Catalysed *para*-C–H Alkylation of *ortho*-substituted Anilines

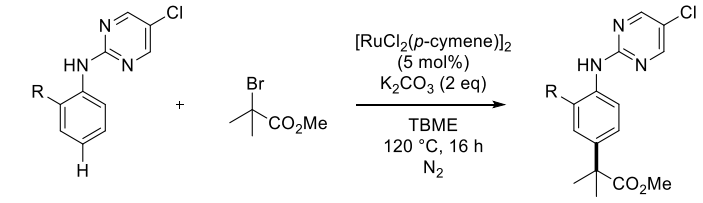

S1c-d **S3k-l**

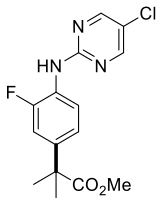

S3k - 0%

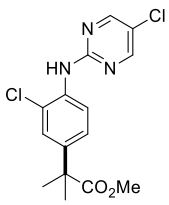

S3l - 0%

Scheme S7. Unsuccessful Substrates for Mechanistic Studies

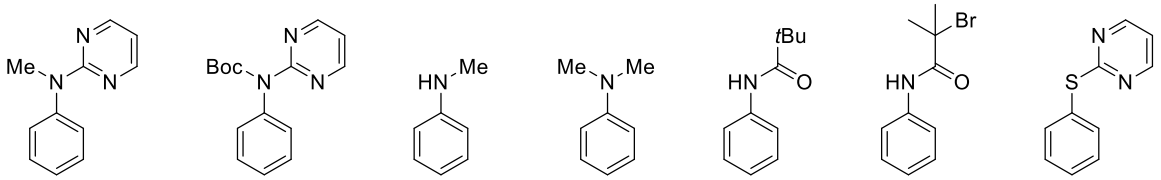

S1e **S1f** **S1g** **S1h** **S1i** **S1j** **S1k**

These investigations demonstrate that substitution of the *N–H* on the aniline structure with either a methyl (**S1e**), or boc (**S1f**) completely shuts down the reaction. *N*-methylaniline (**S1g**) and *N,N*-dimethylaniline were (**S1h**) unsuccessful substrates despite the demonstrated reactivity of free aniline previously. The use of pivanilide (**S1i**) and brominated derivative (**S1j**) were shown to incompatible with this methodology. The second of these results is of paramount importance as it suggests that the formation of the oxindoles do not proceed *via* an amidation reaction at the ester followed by radical ring closure. This demonstrates that these anilide derivatives are not capable of forming tertiary alkyl radicals. Exchange of the NH with a S linker (**S1k**) also are not tolerated. This manifests the importance of the free NH and that other electron rich anilines apart from aniline have any activity. This suggests that a general electron rich aniline C–H functionalisation protocol is not possible, and aniline is an outlier in this methodology due to innate reactivity *via* potentially a different mechanism.

6.5.3: Synthesis of Starting Materials

General Procedure **A** for the synthesis of *N*-functionalized anilines

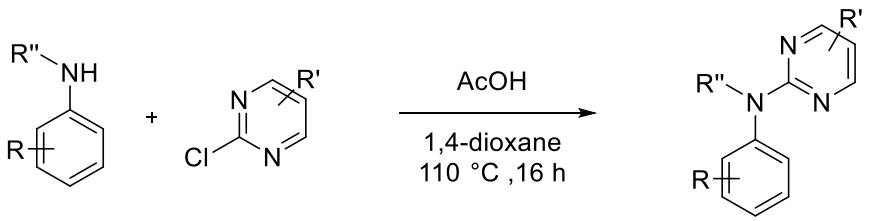

To a mixture of the relevant 2-chloropyrimidine derivative (1-1.5 eq) was added AcOH and 1,4-dioxane (1:3 solvent mixture at 0.25 M) and subsequently relevant aniline (1-1.5 eq). The reaction mixture was heated to reflux for 16 h. The flask was allowed to return to room temperature and diluted in EtOAc. To the solution was slowly added sat $NaHCO_3$ solution to quench the acetic acid, allowing for effervescence. The mixture was left to quench for 30 mins. After this time the mixture was poured into a separating funnel and the organic layer extracted. The organic layer was further washed with sat $NaHCO_3$ solution (2x) and brine (1x) and was then dried over $MgSO_4$ and concentrated *in vacuo*. The crude residue was purified using silica gel chromatography (EtOAc:Hexanes, 5:95-10:90 v:v) to give pure substituted aniline.

Synthesis of *N*-phenylpyrimidin-2-amine (**1b**)

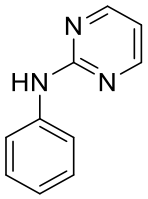

General Procedure **A** was followed using 2-chloropyrimidine (5.73 g, 50 mmol) and aniline (6.83 mL, 6.98 g, 75 mmol). Silica gel column chromatography gave a white solid, 69% (3.69 g). **^{1}H NMR** (500 MHz, $CDCl_3$) δ 8.42 (2H, d, *J* = 4.8 Hz, Ar*H*), 7.67 (1H, s, N*H*), 7.65–7.60 (2H, m, Ar*H*), 7.39–7.31 (2H, m, Ar*H*), 7.11–6.95 (1H, m, Ar*H*), 6.75–6.59 (1H, m, Ar*H*). **^{13}C NMR** (126 MHz, $CDCl_3$) δ 160.2 (Ar*C*), 158.1 (Ar*C*), 139.4 (Ar*C*), 129.1 (Ar*C*), 122.9 (Ar*C*), 119.7 (Ar*C*), 112.5 (Ar*C*). Data is line with literature precedent.[2]

Synthesis of 5-chloro-*N*-phenylpyrimidin-2-amine (**1c**)

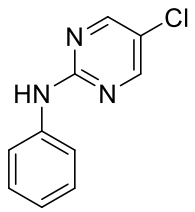

General Procedure **A** was followed using 2,5-dichloropyrimidine (17.88 g, 120 mmol) and aniline (7.29 mL, 7.44 g, 80 mmol). Silica gel column chromatography gave a white solid, 8.72 g (53%). **mp** (from $CHCl_3$): 129-132 °C. **FT-IR**: v_{max} (cm^{-1}) = 3255.7, 3107.4. **^{1}H NMR** (500 MHz, $CDCl_3$) δ 8.36 (2H, s, Ar*H*), 7.66–7.47 (2H, m, Ar*H*), 7.42 (1H, s, N*H*), 7.38–7.33 (2H, m, Ar*H*), 7.08 (1H, tt, *J* = 7.5, 1.1 Hz, Ar*H*). **^{13}C NMR** (126 MHz, $cdcl_3$) δ 158.4 (Ar*C*), 156.3 (Ar*C*), 139.04 (Ar*C*), 129.15 (Ar*C*), 123.30 (Ar*C*), 121.00 (Ar*C*), 119.69 (Ar*C*). **HRMS** (ESI): m/z calculated for $C_{10}H_8Cl_1N_3$ requires 206.0480 for $[M+H]^+$, found 206.0478.

Synthesis of 4,6-dichloro-*N*-phenylpyrimidin-2-amine (**1d**)

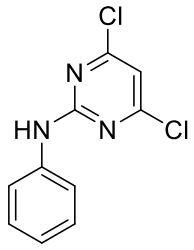

To a round bottom flask containing charged with 2,4,6-tichloropyrimidine (1.15 mL, 10 mmol) and THF 30 mL) was added aniline (1.37 mL, 1.40 g, 15 mmol) dropwise. Following this addition triethylamine (2.09 mL, 1.52 g, 15 mmol) was added in one portion. The reaction mixture was stirred at rt for 16 h. The mixture was poured into water (100 mL) and extracted with EtOAc (3 x 100 mL). The combined organics were washed with brine (100 mL), dried over $MgSO_4$ and concentrated *in vacuo*. The crude residue was purified *via* silica gel column chromatography (EtOAc/Hexanes - 5:95 v:v) to give a solid containing desired product and regioisomer (2,6-dichloro-*N*-phenylpyrimidin-4-amine). Trituration of the solid with hexane gave desired product, 19% (460 mg) **^{1}H NMR** (500 MHz, $CDCl_3$) δ 7.56 (2H, ddd, *J* = 4.0, 3.1, 1.7 Hz, Ar*H*), 7.36 (2H, dd, *J* = 8.5, 7.5 Hz, Ar*H*), 7.30 (1H, s, N*H*), 7.12 (1H, tt, *J* = 7.6, 1.1 Hz, Ar*H*), 6.79 (1H, s, *J* = 1.9 Hz, Ar*H*). **^{13}C NMR** (126 MHz, $CDCl_3$) δ 161.9 (Ar*C*), 159.1 (Ar*C*), 137.8 (Ar*C*), 129.1 (Ar*C*), 124.0 (Ar*C*), 119.9 (Ar*C*), 111.3 (Ar*C*). Recrystallization of the triturate from EtOH gave the pure regioisomer, 20%, (500 mg). **^{1}H NMR** (500 MHz, $CDCl_3$) δ 7.49–7.38 (3H, m, Ar*H*), 7.34–7.27 (3H, m, Ar*H*), 6.55 (1H, s, Ar*H*). **^{13}C NMR** (126 MHz, $CDCl_3$) δ 163.5 (Ar*C*), 161.3 (Ar*C*), 160.2 (Ar*C*), 136.4 (Ar*C*), 130.1 (Ar*C*), 127.0 (Ar*C*), 124.0 (Ar*C*), 100.9 (Ar*C*). Data for both compounds is in line with literature precedent.[3]

Synthesis of *N*-phenylpyridin-2-amine (**1e**)

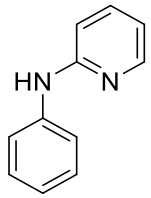

A mixture of aniline (2.73 mL, 2.79 g, 30 mmol) and 2-bromopyridine (2.86 mL, 4.75 g, 30 mmol) was heated to 160 °C for 16 h. The reaction mixture was allowed to cool and quenched with sat. $NaHCO_3$ solution (200 mL). The mixture was extracted with EtOAc (200 mL). The organic phase was washed with brine (200 mL) and dried over $MgSO_4$. The mixture was concentrated *in vacuo* to give a crude residue which was purified *via* silica gel column chromatography (EtOAc/Hexanes) to give an off-white solid, 3.15 g (62%). **^{1}H NMR** (500 MHz, $CDCl_3$) δ 8.21 (1H, dd, *J* = 4.9, 1.0 Hz, Ar*H*), 7.52–7.44 (1H, m, Ar*H*), 7.34 (2H, dd, *J* = 2.3, 0.6 Hz, Ar*H*), 7.33 (2H, d, *J* = 1.9 Hz, Ar*H*), 7.07–7.02 (1H, m, Ar*H*), 6.91–6.86 (1H, m, Ar*H*), 6.83 (1H, s, Ar*H*), 6.76–6.68 (1H, m, Ar*H*). **^{13}C NMR** (126 MHz, $CDCl_3$) δ 156.2 (Ar*C*), 148.6 (Ar*C*), 140.7 (Ar*C*), 137.8 (Ar*C*), 129.4 (Ar*C*), 122.9 (Ar*C*), 120.5 (Ar*C*), 115.1 (Ar*C*), 108.3 (Ar*C*). Data is in line with literature precedent.[4]

Synthesis of *N*-phenylpicolinamide (**1g**)

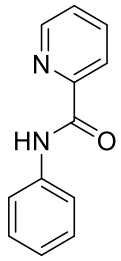

To a stirred solution of aniline (457 µL, 466 mg, 5 mmol) in anhydrous THF (10 mL) was added sequentially triethylamine (2.09 mL, 1.52 g, 15 mmol) and pyridine-2-carbonyl chloride hydrochloride (1.33 g, 7.5 mmol). The reaction mixture was stirred at rt for 2 h. After this time the reaction was concentrated *in vacuo*, diluted in EtOAc (100 mL) and washed with brine (100 mL) and sat. $NaHCO_3$ solution (100 mL). The aqueous layer was re-extracted with EtOAc (2 x 100 mL). The combined organic layers were dried over $MgSO_4$ and passed through a pad of silica using EtOAc as eluent. The solvent was concentrated *in vacuo* to give desired compound, 18% (171 mg). **^{1}H NMR** (400 MHz, $CDCl_3$) δ 10.03 (1H, s, N*H*), 8.62 (1H, ddd, *J* = 4.8, 1.6, 0.9 Hz, Ar*H*), 8.31 (1H, dt, *J* = 7.8, 1.0 Hz, Ar*H*), 7.91 (1H, td, *J* = 7.7, 1.7 Hz, Ar*H*), 7.79 (2H, dt, *J* = 8.7, 1.6 Hz, Ar*H*), 7.52–7.45 (1H, m, Ar*H*), 7.43–7.35 (2H, m, Ar*H*), 7.18–7.13 (1H, m, Ar*H*). **^{13}C NMR** (101 MHz, $CDCl_3$) δ 162.1 (Ar*C*), 150.0 (Ar*C*), 148.1 (Ar*C*), 137.9 (Ar*C*), 137.8 (Ar*C*), 129.23 (Ar*C*), 126.6 (Ar*C*), 124.5 (Ar*C*), 122.6 (Ar*C*), 119.8 (Ar*C*). Data is in line with literature precedent.[5]

Synthesis of 5-chloro-*N*-(3-(methylthio)phenyl)pyrimidin-2-amine (**1h**)

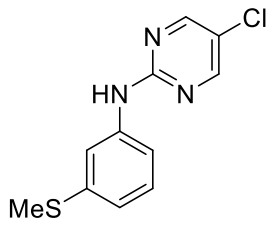

General Procedure **A** was followed using 2,5-dichloropyrimidine (4.47 g, 30 mmol) and 3-(methylthio)-aniline (2.46 mL, 2.78 g, 20 mmol). Silica gel column chromatography and subsequent recrystallization from EtOH gave a golden solid, 53% (2.67 g). **mp** (from $CHCl_3$): 121-123 °C. **FT-IR** (thin film): ν_{max} (cm^{-1}) = 3277.8, 2987.8, 2920.0. **^{1}H NMR** (400 MHz, $CDCl_3$) δ 8.39 (2H, s, Ar*H*), 7.61 (1H, t, *J* = 1.9 Hz, Ar), 7.33 (1H, ddd, *J* = 8.1, 2.0, 1.2 Hz, Ar*H*), 7.31-7.27 (2H, m, Ar*H* & N*H*), 7.01–6.95 (1H, m, Ar*H*), 2.53 (3H, s, SC*H*$_3$). **^{13}C NMR** (126 MHz, $CDCl_3$) δ 158.2 (Ar*C*), 156.3 (Ar*C*), 139.6 (Ar*C*), 129.4 (Ar*C*), 121.2 (Ar*C*), 121.1 (Ar*C*), 117.4 (Ar*C*), 116.3 (Ar*C*), 15.9 (S*C*H$_3$). **HRMS** (ESI): m/z calculated for $C_{11}H_{10}Cl_1S_1$ requires 252.0284 for $[M+H]^+$, found 252.0306.

Synthesis of 5-chloro-*N*-(*m*-tolyl)pyrimidin-2-amine (**1i**)

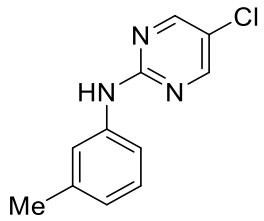

General Procedure **A** was followed using 2,5-dichloropyrimidine (4.47 g, 30 mmol) and *m*-toluidine (2.15 mL, 2.14 g, 20 mmol). Silica gel column chromatography gave a white solid, 53% (2.31 g). **mp** (from $CHCl_3$): 95-96 °C. **FT-IR** (thin film): ν_{max} (cm^{-1}) = 3351.2, 3048.4, 2922.0. **^{1}H NMR** (400 MHz, $CDCl_3$) δ 8.35 (2H, s, Ar*H* & N*H*), 7.43–7.36 (1H, m, Ar*H*), 7.26–7.18 (1H, m, Ar*H*), 6.90 (1H, d, *J* = 7.5 Hz, Ar*H*), 2.37 (3H, s, ArC*H*$_3$). **^{13}C NMR** (101 MHz, $CDCl_3$) δ 158.5 (Ar*C*), 156.4 (Ar*C*), 139.1 (Ar*C*), 138.9 (Ar*C*), 129.0 (Ar*C*), 124.2 (Ar*C*), 120.9 (Ar*C*), 120.3 (Ar*C*), 116.9 (Ar*C*), 21.7 (Ar*C*H$_3$). **HRMS** (ESI): m/z calculated for $C_{11}H_{10}Cl_1N_3$ requires 220.0636 for $[M+H]^+$, found 220.0646.

Synthesis of 5-chloro-*N*-(3-fluorophenyl)pyrimidin-2-amine (**1j**)

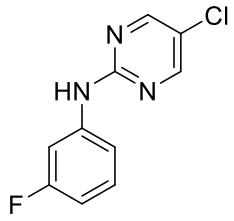

General Procedure **A** was followed using 2,5-dichloropyrimidine (4.47 g, 30 mmol) and 3-fluoroaniline (1.92 mL, 2.22 g, 20 mmol). Silica gel column chromatography gave a white solid 58% (2.58 g). **mp** (from $CHCl_3$): 112-114 °C. **FT-IR** (thin film): ν_{max} (cm^{-1}) = 3275.5. **^{1}H NMR** (400 MHz, $CDCl_3$) δ 8.38 (2H, s, Ar*H*), 7.65 (1H, dt, *J* = 11.5, 2.3 Hz, Ar*H*), 7.48 (1H, s, N*H*), 7.30–7.21 (1H, m, Ar*H*), 7.14 (1H, ddd, *J* = 8.1, 2.0, 0.7 Hz, Ar*H*), 6.76 (1H, tdd, *J* = 8.3, 2.5, 0.8 Hz, Ar*H*). **^{13}C NMR** (101 MHz, $CDCl_3$) δ 163.4 (d, *J* = 243.9 Hz, Ar*C*F), 162.1 (Ar*C*), 158.0 (Ar*C*), 156.4 (Ar*C*), 140.7 (d, *J* = 11.2 Hz, Ar*C*), 130.1 (d, *J* = 9.6 Hz, Ar*C*), 121.6 (Ar*C*), 114.6 (d, *J* = 2.8 Hz, Ar*C*), 109.6 (d, *J* = 21.5 Hz, Ar*C*), 106.5 (d, *J* = 26.8 Hz, Ar*C*). **^{19}F NMR** (376 MHz, $CDCl_3$) δ -106.60 – -114.82 (m, Ar*F*). **HRMS** (ESI): m/z calculated for $C_{10}H_7Cl_1F_1N_3$ requires 224.0385 for $[M+H]^+$, found 224.0384

Synthesis of 5-chloro-*N*-(3-chlorophenyl)pyrimidin-2-amine (**1k**)

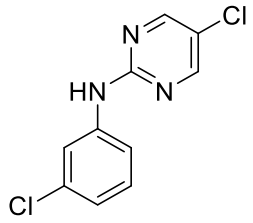

General Procedure **A** was followed using 2,5-dichloropyrimidine (4.47 g, 30 mmol) and 3-chloroaniline (2.12 mL, 2.55 g, 20 mmol). Silica gel column chromatography gave a white solid 57% (2.72 g). **mp** (from $CHCl_3$): 3286.9. **FT-IR** (thin film): ν_{max} (cm^{-1}) = 3286.9. **^{1}H NMR** (400 MHz, $CDCl_3$) δ 8.38 (2H, s, Ar*H*), 7.79 (1H, t, *J* = 2.0 Hz, Ar*H*), 7.43–7.31 (2H, m, Ar*H* & N*H*), 7.25 (1H, t, *J* = 8.0 Hz, Ar*H*), 7.03 (1H, ddd, *J* = 7.9, 1.9, 0.9 Hz, Ar*H*). **^{13}C NMR** (101 MHz, $CDCl_3$) δ 157.94, 156.39, 140.30, 134.83, 130.05, 123.01, 121.68, 119.21, 117.27, 77.48, 77.36, 77.16, 76.84. **HRMS** (ESI): m/z calculated for $C_{10}H_7Cl_2N_3$ requires 240.0090 for $[M+H]^+$, found 240.0099.

Synthesis of *N*-(3-bromophenyl)-5-chloropyrimidin-2-amine (**1l**)

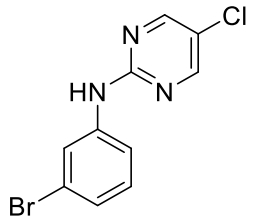

General Procedure **A** was followed using 2,5-dichloropyrimidine (2.24 g, 15 mmol) and 3-bromoaniline (1.09 mL, 1.72 g, 10 mmol). Silica gel column chromatography gave a pale pink solid, 44% (1.26 g). **mp** (from $CHCl_3$): 132-134 °C. **FT-IR** (thin film): ν_{max} (cm^{-1}) = 3311.2, 2977.8. **^{1}H NMR** (500 MHz, $CDCl_3$) δ 8.38 (2H, s, Ar*H*), 7.92 (1H, d, *J* = 1.0 Hz, Ar*H*), 7.47–7.37 (2H, m, Ar*H* & N*H*), 7.21–7.15 (2H, m, Ar*H*). **^{13}C NMR** (126 MHz, $CDCl_3$) δ 157.9 (Ar*C*), 156.4 (Ar*C*), 140.5 (Ar*C*), 130.3 (Ar*C*), 125.9 (Ar*C*), 122.9 (Ar*C*), 122.1 (Ar*C*), 121.7 (Ar*C*), 117.8 (Ar*C*). **HRMS** (ESI): m/z calculated for $C_{10}H_7Br_1Cl_1N_3$ requires 283.9512 for $[M+H]^+$, found 283.9566.

Synthesis of 5-chloro-*N*-(3,5-difluorophenyl)pyrimidin-2-amine (**1m**)

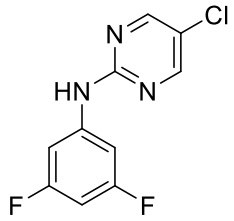

General Procedure **A** was followed using 2,5-dichloropyrimidine (2.24 g, 15 mmol) and 3,5-difluoroaniline (1.29 g, 10 mmol). Silica gel column chromatography gave a pale pink solid, 22% (530 mg). **mp** (from $CHCl_3$): 134-136 °C. **FT-IR** (thin film): ν_{max} (cm^{-1}) = 3296.9, 3167.5, 3127.5. **^{1}H NMR** (500 MHz, $CDCl_3$) δ 8.41 (2H, s, Ar*H*), 7.39 (1H, s, N*H*), 7.23 (2H, dd, *J* = 9.5, 2.2 Hz, Ar*H*), 6.49 (1H, tt, *J* = 8.9, 2.3 Hz, Ar*H*). **^{13}C NMR** (126 MHz, $CDCl_3$) δ 163.5 (d, *J* = 245.4 Hz, Ar*C*F), 163.4 (d, *J* = 245.4 Hz, Ar*C*F), 157.7 (Ar*C*), 156.4 (Ar*C*), 143.3–139.2 (m, Ar*C*), 122.3 (Ar*C*), 103.2–99.8 (m, Ar*C*), 98.0 (t, *J* = 25.8 Hz, Ar*C*). **^{19}F NMR** (471 MHz, $CDCl_3$) δ -109.20 (t, *J* = 8.7 Hz, Ar*F*). **HRMS** (ESI): m/z calculated for $C_{10}H_6Cl_1F_2N_3$ requires 242.0291 for $[M+H]^+$, found 242.0298.

Synthesis of *N*-phenylquinazolin-2-amine (**1n**)

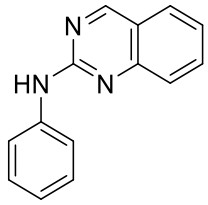

General Procedure **A** was followed using 2-chloroquinazoline (1.23 g, 7.5 mmol) and aniline (457 µL, 465 mg, 5 mmol). Silica gel column chromatography a yellow solid, 46% (513 mg). **^{1}H NMR** (500 MHz, Chloroform) δ 9.08 (1H, s, Ar*H*), 7.86–7.80 (2H, m, Ar*H*), 7.77–7.70 (3H, m, Ar*H*), 7.50 (1H, s, N*H*), 7.41–7.36 (2H, m, Ar*H*), 7.33 (1H, ddd, *J* = 8.0, 4.8, 3.2 Hz, Ar*H*), 7.07 (1H, t, *J* = 7.4 Hz, Ar*H*). **^{13}C NMR** (126 MHz, $CDCl_3$) δ 162.0 (Ar*C*), 157.0 (Ar*C*), 151.7 (Ar*C*), 139.8 (Ar*C*), 134.5 (Ar*C*), 129.1 (Ar*C*), 127.6 (Ar*C*), 126.5 (Ar*C*), 123.9 (Ar*C*), 122.7 (Ar*C*), 121.0 (Ar*C*), 119.2 (Ar*C*). Data is in line with literature precedent.[6]

Synthesis of 5-chloro-*N*-(3-methoxyphenyl)pyrimidin-2-amine (**S1a**)

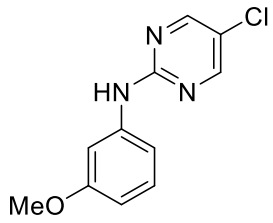

General Procedure **A** was followed using 2,5-dichloropyrimidine (4.47 g, 30 mmol) and *m*-anisidine (2.25 mL, 2.46 g, 20 mmol). Silica gel column chromatography and subsequent recrystallization from EtOH gave a white solid, 45% (2.15 g). **mp** (from $CHCl_3$): 133.136 °C. **FT-IR** (thin film) ν_{max} (cm^{-1}) = 3286.3, 2971.0. **^{1}H NMR** (400 MHz, $CDCl_3$) δ 8.36 (2H, s, Ar*H*), 7.35 (1H, t, *J* = 2.2 Hz, Ar*H*), 7.29 (1H, s, N*H*), 7.24 (1H, t, *J* = 8.3 Hz, Ar*H*), 7.05 (1H, dd, *J* = 8.0, 1.5 Hz, Ar*H*), 6.63 (1H, dd, *J* = 8.2, 1.9 Hz, Ar*H*), 3.83 (3H, s, O*CH$_3$*).**^{13}C NMR** (101 MHz, $CDCl_3$) δ 160.4 (Ar*C*), 158.3 (Ar*C*), 156.3 (Ar*C*), 140.3 (Ar*C*), 129.8 (Ar*C*), 121.1 (Ar*C*), 111.9 (Ar*C*), 108.3 (Ar*C*), 105.7 (Ar*C*), 55.44 (O*C*H_3). **HRMS** (ESI): m/z calculated for $C_{11}H_{10}Cl_1N_3O_1$ requires 248.0405 for $[M+Na]^+$, found 258.0414.

Synthesis of 5-chloro-*N*-(3,5-dimethoxyphenyl)pyrimidin-2-amine (**S1b**)

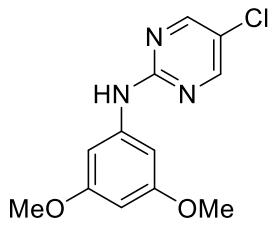

General Procedure **A** was followed using 2,5-dichloropyrimidine (2.24 g, 15 mmol) and 3,5-dimethoxyaniline (1.53 g, 10 mmol). Silica gel column chromatography gave a white solid, 33% (880 mg). **mp** (from $CHCl_3$): 121-124 °C. **FT-IR** (thin film): ν_{max} (cm^{-1}) = 3288.0, 3126.2, 2936.2, 2838.8. **^{1}H NMR** (500 MHz, $CDCl_3$) δ 8.35 (2H, s, Ar*H*), 7.43 (1H, s, N*H*), 6.83 (2H, d, *J* = 2.2 Hz, Ar*H*), 6.20 (1H, t, *J* = 2.2 Hz, Ar*H*), 3.80 (6H, s, ArOC*H*$_3$). **^{13}C NMR** (126 MHz, $CDCl_3$) δ 161.3 (Ar*C*), 158.3 (Ar*C*), 156.3 (Ar*C*), 140.8 (Ar*C*), 121.1 (Ar*C*), 98.0 (Ar*C*), 95.1 (Ar*C*), 55.5 (ArO*C*H_3). **HRMS** (ESI): m/z calculated for $C_{12}H_{12}Cl_1N_3O_2$ requires 266.0691 for $[M+H]^+$, found 266.0681.

Synthesis of *N*-methyl-*N*-phenylpyrimidin-2-amine (**S1e**)

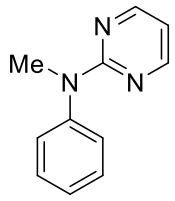

General Procedure **A** was followed using 2-chloropyrimidine (580 mg, 5 mmol) and *N*-methylaniline (810 µL, 800 mg, 7.5 mmol). Silica gel column chromatography gave a pale orange solid, 74% (685 mg). **^{1}H NMR** (500 MHz, $CDCl_3$) δ 8.34 (2H, d, *J* = 4.8 Hz, Ar*H*), 7.48–7.39 (2H, m, Ar*H*), 7.39–7.30 (2H, m, Ar*H*), 7.25 (1H, d, *J* = 7.3 Hz, Ar*H*), 6.56 (1H, t, *J* = 4.8 Hz, Ar*H*), 3.55 (3H, d, *J* = 0.5 Hz, NC*H*$_3$). **^{13}C NMR** (126 MHz, $CDCl_3$) δ 161.86 (Ar*C*), 157.54 (Ar*C*), 157.52 (Ar*C*), 145.46 (Ar*C*), 129.06 (Ar*C*), 126.48 (Ar*C*), 125.72 (Ar*C*), 110.68 (Ar*C*), 38.59 (N*C*H_3). Data is in line with literature precedent.[7]

Synthesis of *tert*-butyl phenyl(pyrimidin-2-yl)carbamate (**S1f**)

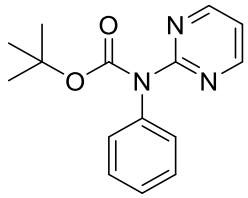

To a solution of *N*-phenylpyrimidin-2-amine (**1a**, 513 mg, 3 mmol) in DMF (20 mL) was added sodium hydride (60% wt. in mineral oil, 132 mg, 3.3 mmol) at 0 °C. After this addition the reaction mixture was allowed to return to room temperature and stir for 1 hour. After this time di-*tert*-butyldicarbonate (Boc_2O, 719 mg, 3.3 mmol) was added in one portion. The mixture was allowed to stir for a further hour. The solution was diluted with water (100 mL) and extracted with EtOAc (3 x 100 mL). The combined organic phases were dried over $MgSO_4$ and concentrated *in vacuo*. The crude residue was purified *via* silica gel column chromatography to give a white solid, 19% (156 mg). **^{1}H NMR** (500 MHz, $CDCl_3$) δ 8.65 (2H, d, *J* = 4.8 Hz, Ar*H*), 7.42–7.34 (2H, m, Ar*H*), 7.28 (2H, dt, *J* = 3.6, 1.5 Hz, Ar*H*), 7.22 (1H, dd, *J* = 8.5, 1.2 Hz, Ar*H*), 7.04 (1H, t, *J* = 4.8 Hz, Ar*H*), 1.45 (9H, s, C(CH_3)$_3$). **^{13}C NMR** (126 MHz, $CDCl_3$) δ 161.5 (Ar*C*), 158.35 (Ar*C*), 153.31 (Ar*C*), 141.41 (Ar*C*), 129.09 (Ar*C*), 127.83 (Ar*C*), 126.97 (Ar*C*), 117.29 (Ar*C*), 82.16 (*C*(CH_3)$_3$), 28.20 (C(*C*H_3)$_2$). Data is in line with literature precedent.[8]

Synthesis of *N*-phenylpivalamide (**S1i**)

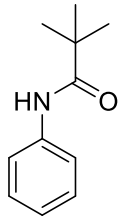

To a solution of aniline (0.91 mL, 930 mg, 10 mmol) and triethylamine (1.67 mL, 1.21 g, 12 mmol) in anhydrous CH_2Cl_2 (10 mL) was added trimethylacetyl chloride (1.24 mL, 1.21 g, 10 mmol) in anhydrous CH_2Cl_2 (10 mL) dropwise at 0 °C. After the addition was finished the reaction was stirred at 0 °C for 1 hour before being allowed to return to room temperature and stir overnight. The reaction mixture was quenched with 1M HCl (50 mL) and diluted in CH_2Cl_2 (30 mL). The organic layer was extracted and then washed with sat. $NaHCO_3$ solution (50 mL), brine (50 mL), dried over $MgSO_4$ and concentrated *in vacuo*. Petroleum Ether 40-60 °C (100 mL) was added and the mixture was allowed to crystallise at 0 °C for two hours. The pure product was collected *via* filtration to give a white solid, 84% (1.49 g). **^{1}H NMR** (500 MHz, $CDCl_3$) δ 7.57–7.47 (2H, m, Ar*H*), 7.36–7.28 (2H, m, Ar*H*), 7.10 (1H, td, *J* = 7.5, 0.8 Hz, Ar*H*), 1.32 (9H, s, C(C*H*$_3$)$_2$). **^{13}C NMR** (126 MHz, $CDCl_3$) δ 176.7 (N*C*(O)C), 138.2 (Ar*C*), 129.0 (Ar*C*), 129.0 (Ar*C*), 124.3 (Ar*C*), 120.1 (Ar*C*), 39.7 (*C*$(CH_3)_3$), 27.8 (C(CH$_3$)$_3$). Data is in line with literature precedent.[9]

Synthesis of 2-bromo-2-methyl-*N*-phenylpropanamide (**S1i**)

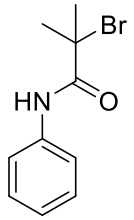

To a well stirred solution of aniline (0.91 mL, 930 mg, 10 mmol) and triethylamine (4.17 mL, 3.03 g, 30 mmol) in anhydrous CH_2Cl_2 (100 mL) was added 2-bromoisobutyryl bromide (1.23 mL, 2.29 g, 10 mmol) dropwise at 0 °C. After addition was complete the reaction was allowed to return to room temperature and stir overnight. The reaction mixture was concentrated and partitioned between EtOAc (100 mL) and H_2O (100 mL). The organic layer was extracted, dried over $MgSO_4$ and concentrated *in vacuo*, to give a light brown solid, 83% (2.01 g). **^{1}H NMR** (500 MHz, $CDCl_3$) δ 8.54–8.35 (1H, s, N*H*), 7.54 (2H, dt, *J* = 8.0, 1.1 Hz, Ar*H*), 7.41–7.30 (2H, m, Ar*H*), 7.15 (1H, t, *J* = 7.4 Hz, Ar*H*), 2.05 (6H, s, C(C*H*$_3$)$_2$). **^{13}C NMR** (126 MHz, $CDCl_3$) δ 170.1 (N*C*(O)C), 137.5 (Ar*C*), 129.2 (Ar*C*), 125.0 (Ar*C*), 120.1 (Ar*C*), 63.3 (*C*(CH$_3$)$_2$) , 32.7 (C(*C*H$_3$)$_2$). Data is in line with literature precedent.[10]

Synthesis of 2-(phenylthio)pyrmidine (**S1k**)

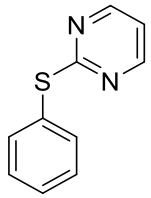

To a solution of thiophenol (8.15 mL, 8.80 g, 80 mmol) in acetic acid (20 mL) and 1,4-dioxane (40 mL) was added 2-chloropyrimidine (2.29 g, 20 mmol). The reaction mixture was heated to 120 °C overnight. After the reaction had returned to room temperature, saturated $NaHCO_3$ solution (20 mL) was added and the reaction was allowed to quench for 30 minutes. After this time, EtOAc (100 mL) and saturated $NaHCO_3$ solution (80 mL) were added. The organic layer was separated and the aqueous layer was extracted with EtOAc (2 x 100 mL). The combined organic layers were dried over $MgSO_4$ and concentrated *in vacuo*. The crude residue was purified *via* silica gel column chromatography (EtOAc/Petroleum Ether 40-60 °C) to give an off-white solid, 47% (1.77 g). **^{1}H NMR** (500 MHz, $CDCl_3$) δ 8.48 (2H, d, *J* = 4.9 Hz), 7.67–7.59 (2H, m), 7.47–7.37 (3H, m), 6.96 (1H, t, *J* = 4.8 Hz). **^{13}C NMR** (126 MHz, $CDCl_3$) δ 172.99, 157.68, 135.39, 129.54, 129.45, 129.35, 117.09. Data is in line with literature precedent.[11]

6.5.4: Synthesis of *para*-C–H Functionalized Materials

Synthesis of **3a** and **4a**

An oven-dried carousel tube was charged with *N*-phenylpyrimidin-2-amine (**1a**, 42 mg, 0.25 mmol), potassium carbonate (69 mg, 0.5 mmol), sodium acetate (6 mg, 0.075 mmol) and $[RuCl_2(p\text{-cymene})]_2$ (8 mg, 0.0125 mmol, 5 mol%) then sealed with a Teflon cap. The tube was evacuated and refilled three times with argon. 1,4-dioxane (1 mL) and methyl α-bromoisobutyrate (97 µL, 136 mg, 0.75 mmol) were added *via* septum and the reaction mixture heated to 120 °C for 16 h. After this time, the mixture was allowed to return to room temperature and was diluted in EtOAc (20 mL) filtered through a plug of celite. The filtrate was concentrated *in vacuo*. The crude residue was purified *via* silica gel column chromatography to give two products, **3a** (37%, 24 mg) and **4a** (6%, 5 mg) among a multitude of other products.

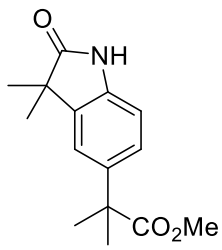

3a. Amorphous solid, 37% (24 mg). **FT-IR** (thin film): ν_{max} (cm^{-1}) = 3240.0, 2971.4, 1709.0, 1625.1. **^{1}H NMR** (500 MHz, $CDCl_3$) δ 8.79 (1H, s, N*H*), 7.17 (1H, dd, *J* = 8.1, 2.0 Hz, Ar*H*), 7.14 (1H, d, *J* = 1.9 Hz, Ar*H*), 6.88 (1H, d, *J* = 8.0 Hz, Ar*H*), 3.65 (3H, s, CO_2CH_3), 1.57 (6H, s, $C(CH_3)_2$), 1.38 (6H, s, $C(CH_3)_2$). **^{13}C NMR** (126 MHz, $CDCl_3$) δ 184.3 (*C*(O)N), 177.5 (*C*(O)O), 139.2 (Ar*C*), 138.7 (Ar*C*), 136.5 (Ar*C*), 125.1 (Ar*C*), 120.1 (Ar*C*), 109.7 (Ar*C*), 52.4 (CO_2CH_3), 46.4 ($C(CH_3)_2$), 45.0 ($C(CH_3)_2$), 26.9 ($C(CH_3)_2$) , 24.5 ($C(CH_3)_2$). **HRMS** (ESI): m/z calculated for $C_{15}H_{19}N_1O_3$ requires 284.1264 for $[M+Na]^+$, found 284.1257.

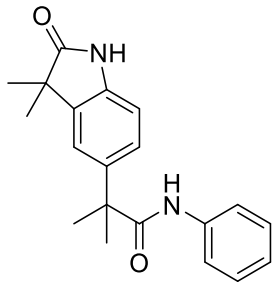

4a. Light yellow oil, 6% (5 mg). **FT-IR** (thin film): ν_{max} (cm^{-1}) = 3364.7, 2970.1, 1721.0, 1619.6, 1517.5. **^{1}H NMR** (500 MHz, $CDCl_3$) δ 7.97 (1H, s, N*H*), 7.23–7.17 (2H, m, Ar*H*), 7.16–7.09 (2H, m, Ar*H*), 7.04 (1H, td, *J* = 7.5, 1.1 Hz, Ar*H*), 6.90 (1H, dd, *J* = 8.1, 1.1 Hz, Ar*H*), 6.71–6.63 (2H, m, Ar*H*), 3.63 (3H, s, CO_2CH_3), 1.53 (6H, s, $C(CH_3)_2$), 1.40 (6H, s, $C(CH_3)_2$). **^{13}C NMR** (126 MHz, $CDCl_3$) δ 176.6 (*C*=O), 154.7 (*C*=O), 139.7 (Ar*C*), 136.4 (Ar*C*), 127.8 (Ar*C*), 126.7 (Ar*C*), 122.8 (Ar*C*), 122.6 (Ar*C*), 115.4 (Ar*C*), 109.8 (Ar*C*), 52.3 ($C(CH_3)_2$), 29.9 ($C(CH_3)_2$), 26.7 ($C(CH_3)_2$), 24.5 ($C(CH_3)_2$).

Synthesis of **3b** and **[4b]**

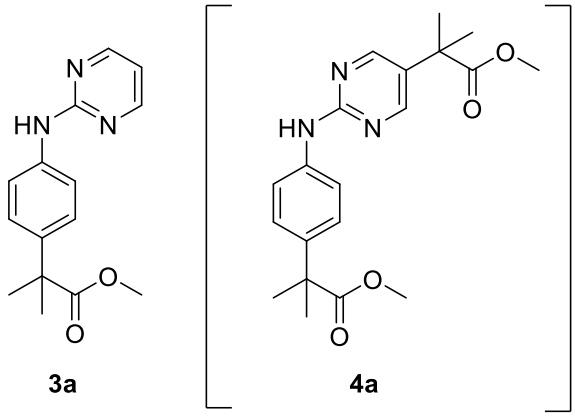

An oven-dried carousel tube was charged with *N*-phenylpyrimidin-2-amine (**1b**, 42 mg, 0.25 mmol), potassium carbonate (69 mg, 0.5 mmol), sodium acetate (6 mg, 0.075 mmol) and $[RuCl_2(p\text{-cymene})]_2$ (8 mg, 0.0125 mmol, 5 mol%) then sealed with a Teflon cap. The tube was evacuated and refilled three times with argon. 1,4-dioxane (1 mL) and methyl α-bromoisobutyrate (97 µL, 136 mg, 0.75 mmol) were added *via* septum and the reaction mixture heated to 120 °C for 16 h. After this time, the mixture was allowed to return to room temperature and was diluted in EtOAc (20 mL) and 5% ethylenediamine solution (20 mL). The organic layer was extracted and the aqueous phase we re-extracted with EtOAc (2 x 20 mL). The combined organic phases were dried over $MgSO_4$ and concentrated *in vacuo*. The crude residue was purified *via* silica gel column chromatography to give an inseparable mixture of **3b** and **4b**, 41% combined yield (Mixture of 85:15 **3b**:**4b**). **FT-IR** (thin film): ν_{max} (cm^{-1}) = 1730.3. **^{1}H NMR** (500 MHz, $CDCl_3$) δ 8.42 (2H, s, Ar*H*), 7.59 (1H, s, N*H*), 7.58–7.55 (2H, m, Ar*H*), 7.34–7.28 (2H, m, Ar*H*), 6.71 (1H, t, *J* = 4.7 Hz, Ar*H*), 3.64 (3H, s, CO_2CH_3), 1.57 (6H, s, $C(CH_3)_2$). **^{13}C NMR** (126 MHz, $CDCl_3$) δ 177.4 (CO_2Et), 160.3 (Ar*C*), 158.1 (Ar*C*), 156.1 (Ar*C*), 139.0 (Ar*C*), 138.1 (Ar*C*), 126.4 (Ar*C*), 119.7 (Ar*C*), 120.0 (Ar*C*), 112.6 (Ar*C*), 52.3 (CO_2CH_3), 46.1 ($C(CH_3)_2$), 26.7 ($C(CH_3)_2$). **HRMS** (ESI): m/z calculated for $C_{15}H_{17}N_3O_2$ (**3a**) requires 272.1394 for $[M+H]^+$, found 272.1382, $C_{20}H_{25}N_3O_4$ (**4a**) requires 394.1745 for $[M+Na]^+$, found 394.1759.

Reference HRMS showing two distinct products with both H and Na Adducts

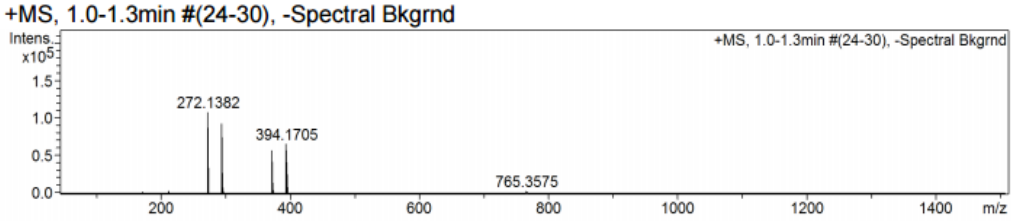

General Procedure **B** for the *para*-C–H alkylation of aniline derivatives.

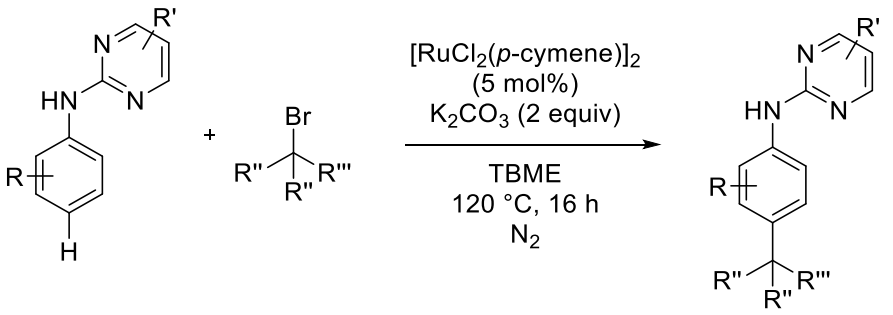

To a two-necked 25 mL round bottomed flask was added relevant aniline derivative (0.5 mmol), $[RuCl_2(p\text{-cymene})]_2$ (15.5 mg 0.025 mmol, 5 mol%), potassium carbonate (139 mg, 1 mmol) with stirring. The reaction vessel was sealed with a septum, a condenser equipped, and evacuated and refilled three times with nitrogen. To this mixture was added *tert*-butylmethyl ether (2 mL) and releveant coupling partner (1.5 mmol). The reaction mixture was heated to 120 °C for 16 h. After allowing the flask to return to room temperature, the mixture was diluted with EtOAc (20 mL) and filtered through a pad of cotton wool, rinsing with EtOAc. The resulting brown/green solution was concentrated *in vacuo*. The crude residue was loaded onto silica and purified *via* silica gel column chromatography (EtOAc:Hexanes, gradient to 10:90) to give pure *para*-alkylated product.

Synthesis of **3c**

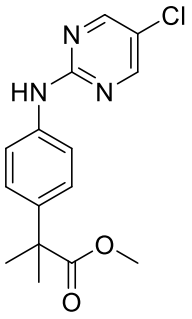

General Procedure **B** was followed using 5-chloro-*N*-phenylpyrimidin-2-amine (**1c**, 103 mg, 0.5 mmol) and methyl α-bromoisobutyrate (194 µL, 272 mg, 1.5 mmol). Silica gel column chromatography gave a white solid, 55% (84 mg). **mp** (from $CHCl_3$): 116-118 °C. **FT-IR** (thin film): ν_{max} (cm^{-1}) = 3269.8, 2950.5, 1726.1. **^{1}H NMR** (500 MHz, $CDCl_3$) δ 8.34 (2H, s, Ar*H*), 7.58–7.49 (2H, m, Ar*H*), 7.41 (1H, s, N*H*), 7.35–7.29 (2H, m, Ar*H*), 3.65 (3H, s, CO_2CH_3), 1.58 (6H, s, $C(CH_3)_2$). **^{13}C NMR** (126 MHz, $CDCl_3$) δ 177.4 (CO_2Me), 158.3 (Ar*C*), 156.3

(Ar*C*), 139.5 (Ar*C*), 137.6 (Ar*C*), 126.5 (Ar*C*), 121.0 (Ar*C*), 119.6 (Ar*C*), 52.33 (CO_2CH_3), 46.13 ($C(CH_3)_2$), 26.66 ($C(CH_3)_2$). **HRMS** (ESI): m/z calculated for $C_{15}H_{16}Cl_1N_3O_2$ requires 306.1004 for $[M+H]^+$, found 306.0984.

Synthesis of **3d** and **4d**

An oven-dried carousel tube was charged with 4,6-dichloro-*N*-phenylpyrimidin-2-amine (**1d**, 60 mg, 0.25 mmol), potassium carbonate (69 mg, 0.5 mmol), sodium acetate (6 mg, 0.075 mmol) and $[RuCl_2(p\text{-cymene})]_2$ (8 mg, 0.0125 mmol, 5 mol%) then sealed with a Teflon cap. The tube was evacuated and refilled three times with argon. 1,4-dioxane (1 mL) and methyl α-bromoisobutyrate (97 µL, 136 mg, 0.75 mmol) were added *via* septum and the reaction mixture heated to 120 °C for 16 h. After this time, the mixture was allowed to return to room temperature and was diluted in EtOAc (20 mL) and 5% ethylenediamine solution (20 mL). The organic layer was extracted and the aqueous phase we re-extracted with EtOAc (2 x 20 mL). The combined organic phases were dried over $MgSO_4$ and concentrated *in vacuo*. The crude residue was purified *via* silica gel column chromatography to give separable mono and di-functionalized materials, **3d** and **4d**, 25% combined yield (62:38 - **3d**:**4d**).

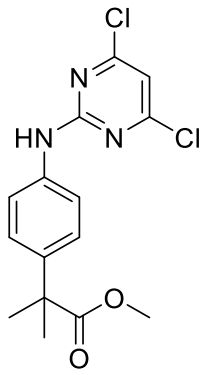

3d. Off-white amorphous solid. **FT-IR** (thin film): ν_{max} (cm^{-1}) = 3321.7, 2929.9, 1731.2. **^{1}H NMR** (500 MHz, $CDCl_3$) δ 7.57–7.46 (2H, m, Ar*H*), 7.36–7.31 (2H, m, Ar*H*), 7.28 (1H, s, N*H*), 6.78 (1H, s, Ar*H*), 3.65 (3H, s, CO_2CH_3), 1.58 (6H, s, $C(CH_3)_2$). **^{13}C NMR** (126 MHz, $CDCl_3$) δ 177.3 (CO_2Me), 162.0 (Ar*C*), 159.0 (Ar*C*), 140.4 (Ar*C*), 136.5 (Ar*C*), 126.6 (Ar*C*), 119.8 (Ar*C*), 111.4 (Ar*C*), 52.4 (CO_2CH_3), 46.2 ($C(CH_3)_2$), 26.66 ($C(CH_3)_2$). **HRMS** (ESI): m/z calculated for $C_{15}H_{15}Cl_2N_3O_2$ requires 340.0614 for $[M+H]^+$, found 340.0601

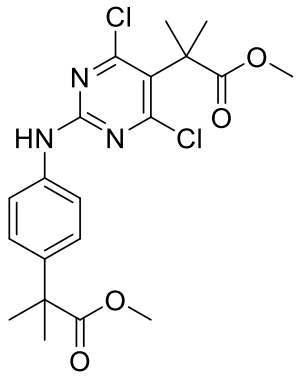

4d. Amorphous solid. **FT-IR** (thin film): ν_{max} (cm^{-1}) = 2978.7, 1732.4. **^{1}H NMR** (500 MHz, $CDCl_3$) δ 7.53–7.49 (2H, m, Ar*H*), 7.35–7.30 (2H, m, Ar*H*), 7.12 (1H, s, N*H*), 3.72 (3H, s, CO_2CH_3), 3.65 (3H, s, CO_2CH_3), 1.75 (6H, s, $C(CH_3)_2$), 1.57 (6H, s, $C(CH_3)_2$). **^{13}C NMR** (126 MHz, $CDCl_3$) δ 177.3 (CO_2Me), 177.2 (CO_2Me), 161.2 (Ar*C*), 155.6 (Ar*C*), 140.1 (Ar*C*), 136.6 (Ar*C*), 126.6 (Ar*C*), 119.44 (Ar*C*), 52.9 (CO_2CH_3), 52.4 (CO_2CH_3), 47.6 ($C(CH_3)_2$), 47.2 ($C(CH_3)_2$), 26.7 ($C(CH_3)_2$), 26.6 ($C(CH_3)_2$). **HRMS** (ESI): m/z calculated for $C_{20}H_{23}Cl_2N_3O_4$ requires 440.1138 for $[M+H]^+$, found 440.1113.

Synthesis of **3ca**

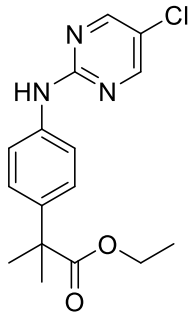

General Procedure **B** was followed using 5-chloro-*N*-phenylpyrimidin-2-amine (**1c**, 103 mg, 0.5 mmol) and ethyl α-bromoisobutyrate (220 µL, 293 mg, 1.5 mmol). Silica gel column chromatography gave a white solid, 39% (62 mg). **mp** (from $CHCl_3$): 93-96 °C. **FT-IR** (thin film): ν_{max} (cm^{-1}) = 2981.6, 1727.5. **^{1}H NMR** (500 MHz, $CDCl_3$) δ 8.34 (2H, s, Ar*H*), 7.59 (1H, s, N*H*), 7.56–7.46 (2H, m, Ar*H*), 7.38–7.29 (2H, m, Ar*H*), 4.12 (2H, q, *J* = 7.1 Hz, $CO_2CH_2CH_3$), 1.57 (6H, s, $C(CH_3)_2$), 1.19 (3H, t, *J* = 7.1 Hz, $CO_2CH_2CH_3$). **^{13}C NMR** (126 MHz, $CDCl_3$) δ 176.8 (CO_2Et), 158.4 (Ar*C*), 156.3 (Ar*C*), 139.6 (Ar*C*), 137.5 (Ar*C*), 126.5 (Ar*C*), 120.9 (Ar*C*), 119.5 (Ar*C*), 60.91 ($CO_2CH_2CH_3$), 46.06 ($C(CH_3)_2$), 26.62 ($C(CH_3)_2$), 14.18 $CO_2CH_2CH_3$). **HRMS** (ESI): m/z calculated for $C_{16}H_{18}Cl_1N_3O_2$ requires 342.0988 for $[M+Na]^+$, found 342.0981.

Synthesis of **3cb**

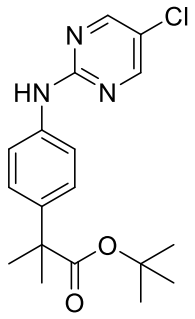

General Procedure **B** was followed using 5-chloro-*N*-phenylpyrimidin-2-amine (**1c**, 103 mg, 0.5 mmol) and *tert*-butyl α-bromoisobutyrate (280 µL, 335 mg, 1.5 mmol). Silica gel column chromatography gave a brown amorphous solid, 40% (70 mg). **FT-IR** (thin film): ν_{max} (cm^{-1}) = 2978.5, 1723.6. **^{1}H NMR** (500 MHz, $CDCl_3$) δ 8.33 (2H, s, Ar*H*), 7.60 (1H, s, N*H*), 7.54–7.49 (2H, m, Ar*H*), 7.35–7.29 (2H, m, Ar*H*), 1.52 (6H, s, C(C*H*$_3$)$_2$), 1.38 (9H, s, C(C*H*$_3$)$_3$). **^{13}C NMR** (126 MHz, $CDCl_3$) δ 176.0 (*C*O_2*t*Bu), 158.4 (Ar*C*), 156.3 (Ar*C*), 140.1 (Ar*C*), 137.3 (Ar*C*), 126.4 (Ar*C*), 120.8 (Ar*C*), 119.3 (Ar*C*), 80.38 ($CO_2C(CH_3)_3$), 46.65 (*C*(CH_3)$_2$), 27.94 (C(*C*H_3)$_3$), 26.64 (C(*C*H_3)$_2$). **HRMS** (ESI): m/z calculated for $C_{18}H_{22}Cl_1N_3O_2$ requires 370.1301 for $[M+Na]^+$, found 370.1314.

Synthesis of **3cc**

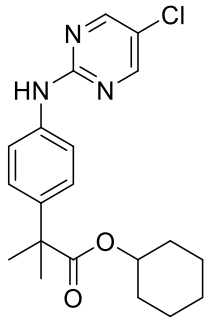

General Procedure **B** was followed using 5-chloro-*N*-phenylpyrimidin-2-amine (**1c**, 103 mg, 0.5 mmol) and cyclohexyl α-bromoisobutyrate (374 mg, 1.5 mmol). Silica gel column chromatography gave a white solid, 25% (46 mg). **mp** (from $CHCl_3$): 158-160 °C. **FT-IR** (thin film): ν_{max} (cm^{-1}) = 2935.1, 1722.8. **^{1}H NMR** (500 MHz, Chloroform) δ 8.34 (2H, s, Ar*H*), 7.55–7.47 (2H, m, Ar*H*), 7.44 (1H, s, N*H*), 7.36–7.29 (2H, m, Ar*H*), 4.82–4.73 (1H, m, OC*H*), 1.72 (2H, dt, *J* = 13.1, 7.2 Hz, Cy*H*), 1.65–1.58 (2H, m, Cy*H*), 1.56 (6H, s, C(C*H*$_3$)$_2$), 1.51–1.26 (6H, m, Cy*H*). **^{13}C NMR** (126 MHz, $CDCl_3$) δ 176.2 (*C*O_2Cy), 158.4 (Ar*C*), 156.3 (Ar*C*),

139.9 (Ar*C*), 137.4 (Ar*C*), 126.5 (Ar*C*), 120.9 (Ar*C*), 119.4 (Ar*C*), 72.6 (CO_2*C*H), 46.2 (*C*(CH_3)$_2$), 31.3 (Cy*C*), 26.6 (C(*C*H_3)$_2$), 25.5 (Cy*C*), 23.5 (Cy*C*). **HRMS** (ESI): m/z calculated for $C_{20}H_{24}Cl_1N_3O_2$ requires 396.1449 for $[M+Na]^+$, found 396.1468.

Synthesis of **3cd**

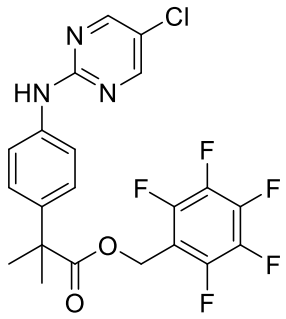

General Procedure **B** was followed using 5-chloro-*N*-phenylpyrimidin-2-amine (**1c**, 103 mg, 0.5 mmol) and perfluorobenzyl α-bromoisobutyrate (521 mg, 1.5 mmol). Silica gel column chromatography gave a white solid, 40% (93 mg). **mp** (from $CHCl_3$): 134-138 °C. **FT-IR** (thin film): ν_{max} (cm^{-1}) = 2975.9, 1736.9. **^{1}H NMR** (500 MHz, $CDCl_3$) δ 8.34 (2H, s, Ar*H*), 7.53 (1H, s, N*H*), 7.52–7.48 (2H, m, Ar*H*), 7.29–7.25 (2H, m, Ar*H*), 5.17 (2H, s, C*H*$_2$Ph^F), 1.57 (6H, s, C(C*H*$_3$)$_2$). **^{13}C NMR** (126 MHz, $CDCl_3$) δ 176.12 (*C*O_2Bn^F), 158.3 (Ar*C*), 156.3 (Ar*C*), 147.1–144.1 (m, Ar^F*C*), 143.3–140.4 (m, Ar^F*C*), 138.6 (Ar*C*), 137.8 (Ar*C*), 138.9–135.9 (m, Ar^F*C*), 126.4 (Ar*C*), 121.0 (Ar*C*), 119.5 (Ar*C*), 109.6 (td, *J* = 17.3, 3.7 Hz, Ar^F*C*), 54.0 (*C*H_2Ph^F), 46.2 (*C*(CH_3)$_2$), 26.4 (C(*C*H_3)$_2$). **^{19}F NMR** (471 MHz, Chloroform) δ -141.82 (dd, *J* = 21.9, 8.0 Hz, Ar*F*), -152.77 (t, *J* = 20.8 Hz, Ar*F*), -161.68 (td, *J* = 21.3, 7.8 Hz, Ar*F*). **HRMS** (ESI): m/z calculated for $C_{21}H_{15}Cl_1F_5N_3O_2$ requires 494.0673 for $[M+Na]^+$, found 494.0681.

Synthesis of **3ce**

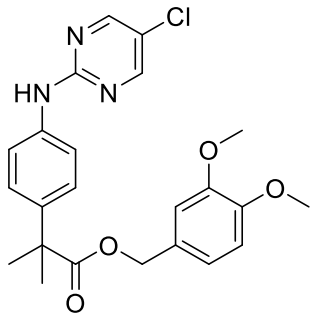

General Procedure **B** was followed using 5-chloro-*N*-phenylpyrimidin-2-amine (**1c**, 103 mg, 0.5 mmol) and 3,4-dimethoxybenzyl α-bromoisobutyrate (476 mg, 1.5 mmol). Silica gel column chromatography gave a golden oil, 43% (96 mg). **FT-IR** (thin film): ν_{max} (cm^{-1}) = 3344.0, 2936.9, 1781.3, 1726.9. **^{1}H NMR** (500 MHz, $CDCl_3$) δ 8.32 (2H, s, Ar*H*), 7.62 (1H, s, N*H*), 7.54–7.44 (2H, m, Ar*H*), 7.34–7.27 (2H, m, Ar*H*), 6.83–6.74 (2H, m, Ar*H*), 6.69 (1H, d, *J* = 2.0 Hz, Ar*H*), 5.04 (2H, s, C*H*$_2$Ar), 3.83 (3H, s, ArOC*H*$_3$), 3.76 (3, s, ArOC*H*$_3$), 1.58 (6H, s, C(C*H*$_3$)$_2$). **^{13}C NMR** (126 MHz, $CDCl_3$) δ 176.5 (*C*O_2Ar), 158.3 (Ar*C*), 156.2 (Ar*C*), 148.9 (Ar*C*), 148.9 (Ar*C*), 139.2 (Ar*C*), 137.6 (Ar*C*), 128.8 (Ar*C*), 126.5 (Ar*C*), 120.9 (Ar*C*), 120.6 (Ar*C*), 119.4 (Ar*C*), 111.1 (Ar*C*), 110.9 (Ar*C*), 66.47 (*C*H_2Ar), 55.9 (ArO*C*H_3), 55.8 (ArO*C*H_3), 46.1 (*C*(CH$_3$)$_2$), 26.5 (C(*C*H$_3$)$_2$). **HRMS** (ESI): m/z calculated for $C_{23}H_{24}N_3O_4Cl_1$ requires 464.1355 for $[M+Na]^+$, found 464.1350.

Synthesis of **3cf**

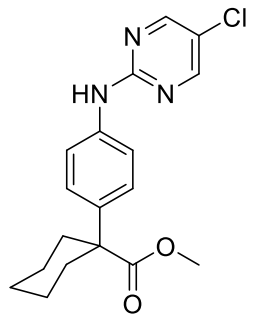

General Procedure **B** was followed using 5-chloro-*N*-phenylpyrimidin-2-amine (**1c**, 103 mg, 0.5 mmol) and methyl 1-bromo-1-cyclohexanecarboxylate (238 µL, 332 mg, 1.5 mmol). Silica gel column chromatography gave an amorphous white solid, 38% (66 mg). **mp** (from $CHCl_3$): 154-157 °C. **FT-IR** (thin film): ν_{max} (cm^{-1}) = 2937.4, 1726.8. **^{1}H NMR** (500 MHz, $CDCl_3$) δ 8.35 (2H, s, Ar*H*), 7.52 (2H, d, *J* = 8.7 Hz, Ar*H*), 7.37 (2H, d, *J* = 8.7 Hz, Ar*H*), 7.26 (1H, s, N*H*), 3.63 (3H, s, CO_2C*H*$_3$), 2.48 (2H, d, *J* = 12.9 Hz, Cy*H*), 1.75–1.61 (4H, m, Cy*H*), 1.51–1.42 (2H, m, Cy*H*), 1.32–1.23 (2H, m, Cy*H*). **^{13}C NMR** (126 MHz, $CDCl_3$) δ 175.9 (*C*O_2Me), 158.3 (Ar*C*), 156.4 (Ar*C*), 138.6 (Ar*C*), 137.6 (Ar*C*), 126.8 (Ar*C*), 121.1 (Ar*C*), 119.5 (Ar*C*), 119.5 (Ar*C*), 52.1 (CO_2*C*H$_3$), 50.5 (*C*Cy), 34.8 (Cy*C*), 25.7 (Cy*C*), 23.8 (Cy*C*). **HRMS** (ESI): m/z calculated for $C_{18}H_{20}Cl_1N_3O_2$ requires 346.1317 for $[M+H]^+$, found 346.1342.

Synthesis of **S3b**

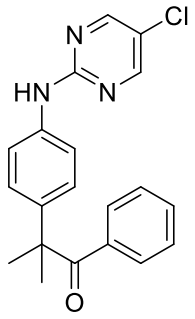

General Procedure **B** was followed using 5-chloro-*N*-phenylpyrimidin-2-amine (**1c**, 103 mg, 0.5 mmol) and 2-bromoisobutyrophenone (252 µL, 341 mg, 1.5 mmol). Silica gel column chromatography gave an amorphous white solid, 9% (16 mg). **FT-IR** (thin film): ν_{max} (cm^{-1}) = 1676.5. **^{1}H NMR** (500 MHz, $CDCl_3$) δ 8.35 (2H, s, Ar*H*), 7.58 (2H, d, *J* = 8.7 Hz, Ar*H*), 7.52 (2H, dd, *J* = 8.3, 1.1 Hz, Ar*H*), 7.36 (1H, t, *J* = 7.4 Hz, Ar*H*), 7.32–7.28 (3H, m, Ar*H* & N*H*), 7.23 (2H, t, *J* = 7.8 Hz, Ar*H*), 1.60 (6H, s, C(C*H*$_3$)$_2$). **^{13}C NMR** (126 MHz, $CDCl_3$) δ 203.9 (*C*OPh), 158.2 (Ar*C*), 156.4 (Ar*C*), 156.1 (Ar*C*), 139.8 (Ar*C*), 137.8 (Ar*C*), 136.5 (Ar*C*), 131.8 (Ar*C*), 129.9 (Ar*C*), 128.1 (Ar*C*), 126.5 (Ar*C*), 121.13 (Ar*C*), 119.8 (Ar*C*), 51.08 (*C*(CH$_3$)$_2$), 27.98 (C(*C*H$_3$)$_2$). **HRMS** (ESI): m/z calculated for $C_{20}H_{18}Cl_1N_3O_1$ requires 374.1038 for $[M+Na]^+$, found 374.1027.

Synthesis of **S3c**

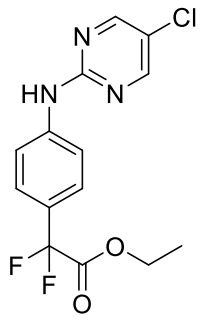

General Procedure **B** was followed using 5-chloro-*N*-phenylpyrimidin-2-amine (**1c**, 103 mg, 0.5 mmol) and ethyl bromodifluoroacetate (192 µL, 304 mg, 1.5 mmol). Silica gel column chromatography gave a white solid, 6% (10 mg). **mp** (from $CHCl_3$): 110-114 °C. **FT-IR** (thin film): ν_{max} (cm^{-1}) = 1755.2. **^{1}H NMR** (500 MHz, $CDCl_3$) δ 8.39 (2H, s, Ar*H*), 7.69 (2H, d, *J* = 8.7 Hz, Ar*H*), 7.58 (2H, d, *J* = 8.7 Hz, Ar*H*), 7.39 (1H, s, N*H*), 4.30 (2H, q, *J* = 7.1 Hz, $CO_2C\mathit{H}_2CH_3$), 1.31 (3H, t, *J* = 7.1 Hz, $CO_2CH_2C\mathit{H}_3$). **^{13}C NMR** (126 MHz, $CDCl_3$) δ 165.9–

162.3 (m, *C*CF_2), 157.9 (Ar*C*), 156.4 (Ar*C*), 141.46 (Ar*C*), 126.7 (t, *J* = 6.0 Hz, Ar*C*), 122.0 (Ar*C*), 118.7 (Ar*C*), 113.6 (Ar*C*), 63.2 (s, $CO_2CH_2CH_3$), 14.1 (s, $CO_2CH_2CH_3$). **^{19}F NMR** (471 MHz, $CDCl_3$) δ -103.05 (CF_2). **HRMS** (ESI): m/z calculated for $C_{14}H_{12}Cl_1F_2N_3O_2$ requires 350.0486 for $[M+Na]^+$, found 350.0480.

Synthesis of **S3e**

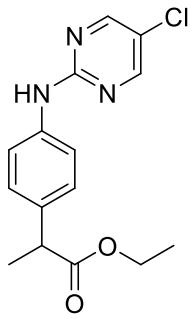

General Procedure **B** was followed using 5-chloro-*N*-phenylpyrimidin-2-amine (**1c**, 103 mg, 0.5 mmol) and ethyl 2-bromopropionate (195 µL, 272 mg, 1.5 mmol). Silica gel column chromatography gave an amorphous white solid, 8% (12 mg). **mp** (from $CHCl_3$): 113-116 °C. **FT-IR** (thin film): ν_{max} (cm^{-1}) = 1730.2. **^{1}H NMR** (500 MHz, $CDCl_3$) δ 8.34 (2H, s, Ar*H*), 7.54–7.47 (2H, m, Ar*H*), 7.34–7.27 (3H, m, Ar*H* & N*H*), 4.18–4.05 (2H, m, $CO_2CH_2CH_3$), 3.68 (1H, q, *J* = 7.2 Hz, $CH(CH_3)$), 1.49 (2H, d, *J* = 7.2 Hz, $CH(CH_3)$), 1.21 (3H, t, *J* = 7.1 Hz, $CO_2CH_2CH_3$). **^{13}C NMR** (126 MHz, $CDCl_3$) δ 174.7 (CO_2Et), 158.4 (Ar*C*), 156.4 (Ar*C*), 137.9 (Ar*C*), 135.6 (Ar*C*), 128.2 (Ar*C*), 121.0 (Ar*C*), 119.8 (Ar*C*), 60.87 ($CO_2CH_2CH_3$), 45.10 ($CH(CH_3)$), 18.72 ($CH(CH_3)$), 14.27 ($CO_2CH_2CH_3$). **HRMS** (ESI): m/z calculated for $C_{15}H_{16}Cl_1N_3O_2$ requires 306.1004 for $[M+H]^+$, found 306.0989.

Synthesis of **3h**

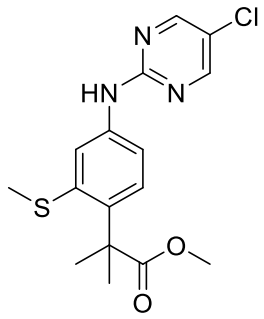

General Procedure **B** was followed using 5-chloro-*N*-(3-(methylthio)phenyl)pyrimidin-2-amine (**1h**, 126 mg, 0.5 mmol) and methyl α-bromoisobutyrate (194 µL, 272 mg, 1.5 mmol). Silica gel column chromatography gave an amorphous white solid, 38% (67 mg). **FT-IR** (thin film): v_{max} (cm^{-1}) = 3327.4, 2978.8, 1729.5. **^{1}H NMR** (500 MHz, $CDCl_3$) δ 8.35 (2H, s, Ar*H*), 7.72 (1H, d, *J* = 2.3 Hz, Ar*H*), 7.42 (1H, s, N*H*), 7.39 (1H, dd, *J* = 8.6, 2.3 Hz, Ar*H*), 7.32 (1H, d, *J* = 8.6 Hz, Ar*H*), 3.68 (3H, s, CO_2CH_3), 2.44 (3H, s, SCH_3), 1.60 (6H, s, $C(CH_3)_2$). **^{13}C NMR** (126 MHz, $CDCl_3$) δ 178.5 (CO_2Me), 158.2 (Ar*C*), 156.4 (Ar*C*), 139.9 (Ar*C*), 138.2 (Ar*C*), 138.0 (Ar*C*), 126.2 (Ar*C*), 122.2 (Ar*C*), 121.2 (Ar*C*), 117.5 (Ar*C*), 52.4 (CO_2CH_3), 46.8 ($C(CH_3)_2$), 27.3 (SCH_3), 19.1 ($C(CH_3)_2$). **HRMS** (ESI): m/z calculated for $C_{16}H_{18}Cl_1N_3O_2S_1$ requires 374.0708 for $[M+Na]^+$, found 374.0717.

Synthesis of **3i**

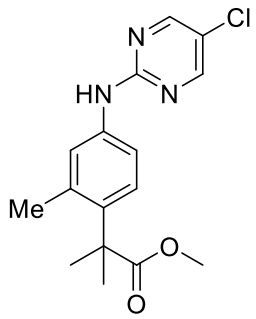

General Procedure **B** was followed using 5-chloro-*N*-(*m*-tolyl)pyrimidin-2-amine (**1i**, 110 mg, 0.5 mmol) and methyl α-bromoisobutyrate (194 µL, 272 mg, 1.5 mmol). Silica gel column chromatography gave an amorphous white solid, 21% (34 mg). **FT-IR** (thin film): v_{max} (cm^{-1}) = 2970.6, 1731.7. **^{1}H NMR** (500 MHz, Chloroform) δ 8.34 (2H, s, Ar*H*), 7.45 (1H, dd, *J* = 8.5, 2.4 Hz, Ar*H*), 7.33 (1H, d, *J* = 8.6 Hz, Ar*H*), 7.31–7.28 (2H, m, Ar*H* & N*H*), 3.67 (3H, s, CO_2CH_3), 2.21 (3H, s, $ArCH_3$), 1.57 (6H, s, $C(CH_3)_2$). **^{13}C NMR** (126 MHz, $CDCl_3$) δ 178.9 (CO_2Me), 158.4 (Ar*C*), 156.3 (Ar*C*), 137.9 (Ar*C*), 137.5 (Ar*C*), 136.9 (Ar*C*), 125.9 (Ar*C*), 122.7 (Ar*C*), 120.9 (Ar*C*), 117.1 (Ar*C*), 52.4 (CO_2CH_3), 46.1 ($C(CH_3)_2$), 27.1 ($ArCH_3$), 20.3 ($C(CH_3)_2$). **HRMS** (ESI): m/z calculated for $C_{16}H_{18}Cl_1N_3O_2$ requires 342.0988 for $[M+Na]^+$, found 342.0985.

Synthesis of **3j**

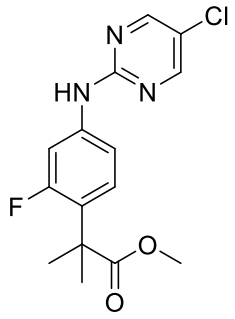

General Procedure **B** was followed using 5-chloro-*N*-(3-fluorophenyl)pyrimidin-2-amine (**1j**, 112 mg, 0.5 mmol) and methyl α-bromoisobutyrate (194 µL, 272 mg, 1.5 mmol). Silica gel column chromatography gave an amorphous white solid, 55% (89 mg). **mp** (from $CHCl_3$): 142-144 °C. **FT-IR** (thin film): ν_{max} (cm^{-1}) = 3338.3, 2981.2, 2951.1, 1726.9. **^{1}H NMR** (500 MHz, $CDCl_3$) δ 8.36 (2H, s, Ar*H*), 7.71 (1H, s, N*H*), 7.59 (1H, dd, *J* = 13.6, 2.2 Hz, Ar*H*), 7.24 (1H, t, *J* = 9.5 Hz, Ar*H*), 7.14 (1H, dd, *J* = 8.5, 2.2 Hz, Ar*H*), 3.68 (3H, s, CO_2CH_3), 1.56 (6H, s, $C(CH_3)_2$). **^{13}C NMR** (126 MHz, $CDCl_3$) δ 177.4 (CO_2Me), 160.8 (d, *J* = 245.2 Hz, Ar*C*F), 158.0 (Ar*C*), 156.3 (Ar*C*), 139.4 (d, *J* = 11.7 Hz, Ar*C*), 126.8 (d, *J* = 14.1 Hz, Ar*C*), 126.6 (d, *J* = 6.3 Hz, Ar*C*), 114.4 (d, *J* = 2.5 Hz, Ar*C*), 107.0 (d, *J* = 28.2 Hz, Ar*C*), 52.4 (CO_2CH_3), 43.8 ($C(CH_3)_2$), 25.9 ($C(CH_3)_2$). **^{19}F NMR** (471 MHz, $CDCl_3$) δ -111.88 (dd, *J* = 13.4, 8.9 Hz, Ar*F*). **HRMS** (ESI): m/z calculated for $C_{15}H_{15}Cl_1F_1N_3O_2$ requires 346.0737 for $[M+Na]^+$, found 346.0737.

Synthesis of **3k**

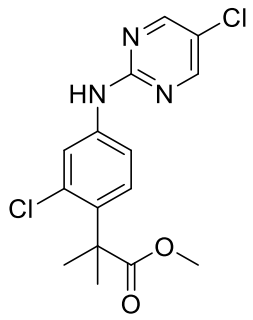

General Procedure **B** was followed using 5-chloro-*N*-(3-chlorophenyl)pyrimidin-2-amine (**1k**, 120 mg, 0.5 mmol) and methyl α-bromoisobutyrate (194 µL, 272 mg, 1.5 mmol). Silica gel column chromatography gave an amorphous white solid, 35% (60 mg). **mp** (from $CHCl_3$): 160-166 °C. **FT-IR** (thin film): ν_{max} (cm^{-1}) = 3345.2, 2923.2, 1733.2. **^{1}H NMR** (500

MHz, $CDCl_3$) δ 8.37 (2H, s, Ar*H*), 7.76 (1H, d, *J* = 2.3 Hz, Ar*H*), 7.42 (1H, s, N*H*), 7.40 (1H, dd, *J* = 8.6, 2.3 Hz, Ar*H*), 7.35 (1H, d, *J* = 8.6 Hz, Ar*H*), 3.68 (3H, s, $CO_2C\mathit{H_3}$), 1.61 (6H, s, $C(C\mathit{H_3})_2$). **^{13}C NMR** (126 MHz, $CDCl_3$) δ 177.7 ($\mathit{C}O_2Me$), 158.0 (Ar*C*), 156.4 (Ar*C*), 138.8 (Ar*C*), 136.7 (Ar*C*), 134.1 (Ar*C*), 127.1 (Ar*C*), 121.6 (Ar*C*), 121.1 (Ar*C*), 117.5 (Ar*C*), 52.6 ($CO_2\mathit{C}H_3$), 46.3 ($\mathit{C}(CH_3)_2$), 26.3 ($C(\mathit{C}H_3)_2$). **HRMS** (ESI): m/z calculated for $C_{15}H_{15}Cl_2N_3O_2$ requires 362.0441 for $[M+Na]^+$, found 362.0439.

Synthesis of **3l**

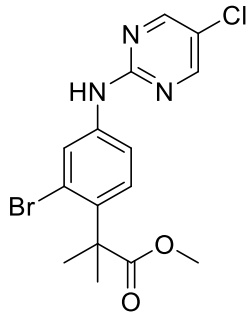

General Procedure **B** was followed using *N*-(3-bromophenyl)-5-chloropyrimidin-2-amine (**1l**, 137 mg, 0.5 mmol) and methyl α-bromoisobutyrate (194 µL, 272 mg, 1.5 mmol). Silica gel column chromatography gave an amorphous white solid, 29% (56 mg). **mp** (from $CHCl_3$): 150-155 °C. **FT-IR** (thin film): ν_{max} (cm^{-1}) = 2987.9, 1732.8. **^{1}H NMR** (500 MHz, $CDCl_3$) δ 8.37 (2H, s, Ar*H*), 7.92 (1H, d, *J* = 2.4 Hz, Ar*H*), 7.52 (1H, s, N*H*), 7.48 (1H, dd, *J* = 8.6, 2.4 Hz, Ar*H*), 7.35 (1H, d, *J* = 8.6 Hz, Ar*H*), 3.68 (3H, s, $CO_2C\mathit{H_3}$), 1.63 (6H, s, $C(C\mathit{H_3})_2$). **^{13}C NMR** (126 MHz, $CDCl_3$) δ 177.7 ($\mathit{C}O_2Me$), 157.9 (Ar*C*), 156.4 (Ar*C*), 138.8 (Ar*C*), 138.1 (Ar*C*), 127.4 (Ar*C*), 124.6 (Ar*C*), 123.9 (Ar*C*), 121.6 (Ar*C*), 118.1 (Ar*C*), 52.6 ($CO_2\mathit{C}H_3$), 47.7 ($\mathit{C}(CH_3)_2$), 26.6 ($C(\mathit{C}H_3)_2$). **HRMS** (ESI): m/z calculated for $C_{15}H_{15}N_3O_2Br_1Cl_1$ requires 405.9936 for $[M+Na]^+$, found 405.9955.

Synthesis of **3m**

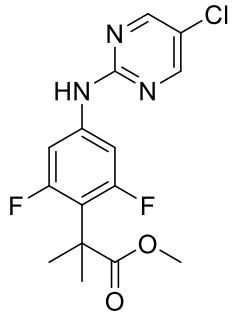

General Procedure **B** was followed using 5-chloro-*N*-(3,5-difluorophenyl)pyrimidin-2-amine (**1m**, 121 mg, 0.5 mmol) and methyl α-bromoisobutyrate (194 µL, 272 mg, 1.5 mmol). Silica gel column chromatography gave an amorphous white solid, 33% (57 mg). **mp** (from $CHCl_3$): 138-142 °C. **FT-IR** (thin film): ν_{max} (cm^{-1}) = 3293.7, 2988.4, 1734.3. **^{1}H NMR** (500 MHz, $CDCl_3$) δ 8.38 (2H, s, Ar*H*), 7.56 (1H, s, N*H*), 7.22–7.18 (1H, m, Ar*H*), 7.18–7.15 (1H, m, Ar*H*), 3.71 (3H, s, CO_2CH_3), 1.63 (6H, app t, $C(CH_3)_2$). **^{13}C NMR** (126 MHz, $CDCl_3$) δ 177.3 (CO_2Me), 161.3 (dd, *J* = 245.6, 11.7 Hz, Ar*C*F), 157.6 (Ar*C*), 156.3 (Ar*C*), 139.1 (t, *J* = 15.1 Hz, Ar*C*), 122.00 (Ar*C*), 114.5 (t, *J* = 16.3 Hz, Ar*C*), 103.4 – 101.5 (Ar*C*), 52.4 (CO_2CH_3), 44.1 ($C(CH_3)_2$), 26.4 (app t, *J* = 3.6 Hz, $C(CH_3)_2$). **^{19}F NMR** (471 MHz, $CDCl_3$) δ -109.37 (d, *J* = 12.3 Hz). **HRMS** (ESI): m/z calculated for $C_{15}H_{14}Cl_1F_2N_3O_2$ requires 342.0815 for $[M+H]^+$, found 342.0834.

Synthesis of **3na**

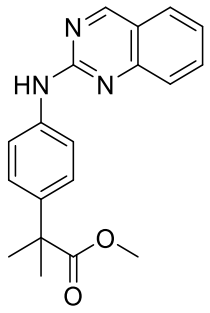

General Procedure **B** was followed using *N*-phenylquinazolin-2-amine (**1n**, 110 mg, 0.5 mmol) and methyl α-bromoisobutyrate (194 µL, 272 mg, 1.5 mmol). Silica gel column chromatography gave a white solid, 48% (77 mg). **mp** (from $CHCl_3$): 136-138 °C. **FT-IR** (thin film): ν_{max} (cm^{-1}) = 2978.3, 1729.0. **^{1}H NMR** (500 MHz, $CDCl_3$) δ 9.07 (1H, s, Ar*H*), 7.81–7.77 (2H, m, Ar*H*), 7.75–7.69 (4H, m, Ar*H* & N*H*), 7.38–7.34 (2H, m, Ar*H*), 7.32 (1H, ddd, *J* = 8.0, 5.0, 3.0 Hz, Ar*H*), 3.66 (3H, s, CO_2CH_3), 1.60 (6H, s, $C(CH_3)_2$). **^{13}C NMR** (126 MHz, $CDCl_3$) δ 177.5 (CO_2Me), 161.9 (Ar*C*), 156.9 (Ar*C*), 151.6 (Ar*C*), 138.8 (Ar*C*), 138.4 (Ar*C*), 134.5 (Ar*C*), 127.6 (Ar*C*), 126.4 (Ar*C*), 126.4 (Ar*C*), 123.9 (Ar*C*), 121.0 (Ar*C*), 119.1 (Ar*C*), 52.29 (CO_2CH_3), 46.09 ($C(CH_3)_2$), 26.66 ($C(CH_3)_2$). **HRMS** (ESI): m/z calculated for $C_{19}H_{19}N_3O_2$ requires 322.1550 for $[M+H]^+$, found 322.1569.

Synthesis of **3nb**

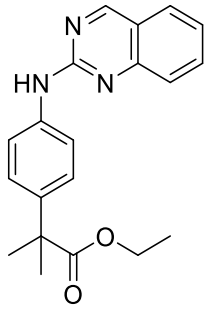

General Procedure **B** was followed using *N*-phenylquinazolin-2-amine (**1n**, 110 mg, 0.5 mmol) and ethyl α-bromoisobutyrate (220 µL, 293 mg, 1.5 mmol). Silica gel column chromatography gave a white solid, 28% (47 mg). **mp** (from $CHCl_3$): 100-102 °C. **FT-IR** (thin film): ν_{max} (cm^{-1}) = 3269.9, 2977.6, 1771.7. **^{1}H NMR** (500 MHz, $CDCl_3$) δ 9.08 (1H, s, Ar*H*), 7.81–7.77 (2H, m, Ar*H*), 7.75–7.68 (4H, m, Ar*H* & N*H*), 7.39–7.35 (2H, m, Ar*H*), 7.32 (1H, ddd, *J* = 8.0, 4.8, 3.2 Hz, Ar*H*), 4.13 (2H, q, *J* = 7.1 Hz, $CO_2CH_2CH_3$), 1.60 (6H, s, $C(CH_3)_2$), 1.20 (3H, t, *J* = 7.1 Hz, $CO_2CH_2CH_3$). **^{13}C NMR** (126 MHz, $CDCl_3$) δ 177.0 (CO_2Et), 161.9 (Ar*C*), 156.9 (Ar*C*), 151.6 (Ar*C*), 139.0 (Ar*C*), 138.2 (Ar*C*), 134.5 (Ar*C*), 127.6 (Ar*C*), 126.4 (Ar*C*), 123.8 (Ar*C*), 120.9 (Ar*C*), 119.0 (Ar*C*), 60.87 ($CO_2CH_2CH_3$), 46.05 ($C(CH_3)_2$), 26.66 ($C(CH_3)_2$), 14.19 ($CO_2CH_2CH_3$). **HRMS** (ESI): m/z calculated for $C_{20}H_{21}N_3O_2$ requires 336.1707 for $[M+H]^+$, found 336.1727.

Synthesis of **3nc**

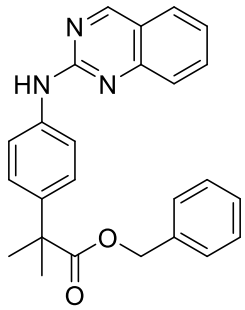

General Procedure **B** was followed using *N*-phenylquinazolin-2-amine (**1n**, 110 mg, 0.5 mmol) and benzyl α-bromoisobutyrate (386 mg, 1.5 mmol). Silica gel column chromatography gave a white solid, 53% (105 mg). **mp** (from $CHCl_3$): 98-102 °C. **FT-IR** (thin film): ν_{max} (cm^{-1}) = 3273.9, 2973.9, 1727.4. **^{1}H NMR** (500 MHz, $CDCl_3$) δ 9.09 (1H, s, Ar*H*), 7.81–7.76 (2H, m, Ar*H*), 7.76–7.72 (3H, m, Ar*H*), 7.59 (1H, s, N*H*), 7.39–7.35 (2H, m, Ar*H*), 7.35–7.23 (6H, m, Ar*H*), 5.13 (2H, s, CH_2Ph), 1.64 (6H, s, $C(CH_3)_2$). **^{13}C NMR** (126 MHz,

$CDCl_3$) δ 176.7 (*C*O_2Bn), 162.0 (Ar*C*), 156.9 (Ar*C*), 151.7 (Ar*C*), 138.6 (Ar*C*), 138.3 (Ar*C*), 136.4 (Ar*C*), 134.5 (Ar*C*), 128.5 (Ar*C*), 128.0 (Ar*C*), 127.8 (Ar*C*), 127.6 (Ar*C*), 126.5 (Ar*C*), 126.4 (Ar*C*), 123.9 (Ar*C*), 121.0 (Ar*C*), 119.1 (Ar*C*), 66.5 (CO_2*C*H_2Ph), 46.2 (*C*(CH_3)$_2$), 26.6 (C(*C*H_3)$_2$). **HRMS** (ESI): m/z calculated for $C_{25}H_{23}N_3O_2$ requires 398.1863 for $[M+H]^+$, found 398.1896.

Synthesis of **3nd**

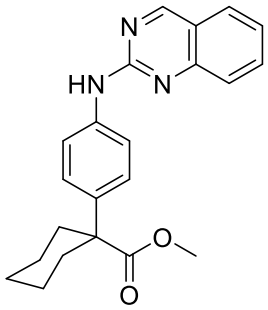

General Procedure **B** was followed using *N*-phenylquinazolin-2-amine (**1n**, 110 mg, 0.5 mmol) and methyl 1-bromo-1-cyclohexanecarboxylate (238 µL, 332 mg, 1.5 mmol). Silica gel column chromatography gave a white solid, 38% (69 mg). **mp** (from $CHCl_3$): 196-198 °C. **FT-IR** (thin film): ν_{max} (cm^{-1}) = 2988.6, 1720.6. **^{1}H NMR** (500 MHz, $CDCl_3$) δ 9.08 (1H, s, Ar*H*), 7.81–7.76 (2H, m, Ar*H*), 7.76–7.70 (3H, m, Ar*H*), 7.43 (1H, s, N*H*), 7.43–7.39 (2H, m, Ar*H*), 7.34 (1H, ddd, *J* = 8.1, 5.7, 2.4 Hz, Ar*H*), 3.65 (3H, s, CO_2C*H*$_3$), 2.50 (2H, d, *J* = 12.0 Hz, Cy*H*), 1.82–1.58 (6H, m, Cy*H*), 1.53–1.42 (2H, m, Cy*H*). **^{13}C NMR** (126 MHz, $CDCl_3$) δ 176.0 (*C*O_2Me), 162.0 (Ar*C*), 156.9 (Ar*C*), 151.7 (Ar*C*), 138.3 (Ar*C*), 137.9 (Ar*C*), 134.5 (Ar*C*), 127.6 (Ar*C*), 126.7 (Ar*C*), 126.5 (Ar*C*), 123.9 (Ar*C*), 121.0 (Ar*C*), 119.1 (Ar*C*), 52.1 (CO_2*C*H_3), 50.5 (*C*Cy), 34.8 (Cy*C*), 25.8 (Cy*C*), 23.8 (Cy*C*). **HRMS** (ESI): m/z calculated for $C_{22}H_{23}N_3O_2$ requires 362.1863 for $[M+H]^+$, found 362.1888.

Synthesis of **S3i*mono*** and **S3i*di***

General Procedure **B** was followed using 5-chloro-*N*-(3-methoxyphenyl)pyrimidin-2-amine (**S1a**, 118 mg, 0.5 mmol) and methyl α-bromoisobutyrate (194 µL, 272 mg, 1.5 mmol). Silica gel column chromatography gave two separable products, *para*-C–H-alkylated **S3i*mono***, 13% (22 mg) and *ortho/para*-C–H-alkylated-*ortho*-cyclised **S3i*di***, 23% (47 mg).

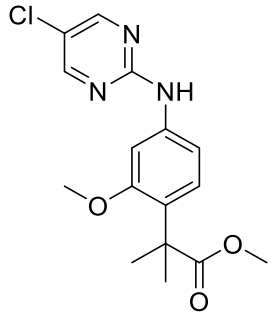

S3i*mono*. White Solid. **mp** (from $CHCl_3$): 132-134 °C. **FT-IR** (thin film): ν_{max} (cm^{-1}) = 2969.0, 1745.1. **^{1}H NMR** (500 MHz, $CDCl_3$) δ 8.35 (2H, s, Ar*H*), 7.35–7.31 (2H, m, N*H* & Ar*H*), 7.23 (1H, d, *J* = 8.3 Hz, Ar*H*), 7.04 (1H, dd, *J* = 8.3, 2.2 Hz, Ar*H*), 3.80 (3H, s, ArOCH_3), 3.62 (3H, s, CO_2CH_3), 1.51 (6H, s, C(CH_3)$_2$). **^{13}C NMR** (126 MHz, $CDCl_3$) δ 178.7 (CO_2Me), 158.3 (Ar*C*), 157.3 (Ar*C*), 156.4 (Ar*C*), 138.9 (Ar*C*), 129.1 (Ar*C*), 125.8 (Ar*C*), 121.0 (Ar*C*), 111.3 (Ar*C*), 103.2 (Ar*C*), 55.5 (CO_2CH_3), 52.0 (ArOCH_3), 44.0 (*C*(CH$_3$)$_2$), 25.9 (C(*C*H$_3$)$_2$). **HRMS** (ESI): m/z calculated for $C_{16}H_{18}Cl_1N_3O_3$ requires 336.1109 for $[M+H]^+$, found 336.1110.

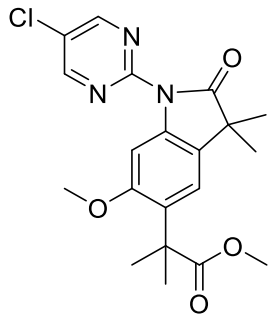

S3i*di*. Amorphous Solid. **FT-IR** (thin film): ν_{max} (cm^{-1}) = 2975.8, 1735.8. **^{1}H NMR** (500 MHz, $CDCl_3$) δ 7.29 (2H, s, Ar*H*), 7.15 (1H, s, Ar*H*), 3.77 (3H, s, ArOCH_3), 3.62 (3H, s, CO_2CH_3), 1.52 (6H, s, C(CH_3)$_2$), 1.49 (6H, s, C(CH_3)$_2$). **^{13}C NMR** (126 MHz, $CDCl_3$) δ 180.9 (CO_2Me), 178.4 (*C*ON), 157.0 (Ar*C*), 156.4 (Ar*C*), 154.1 (Ar*C*), 138.9 (Ar*C*), 130.5 (Ar*C*), 128.0 (Ar*C*), 126.4 (Ar*C*), 119.4 (Ar*C*), 97.6 (Ar*C*), 55.8 (ArOCH_3), 52.0 (CO_2CH_3), 44.6 (*C*(CH$_3$)$_2$), 44.28 (*C*(CH$_3$)$_2$), 26.0 (C(*C*H$_3$)$_2$), 25.5 (C(*C*H$_3$)$_2$). **HRMS** (ESI): m/z calculated for $C_{20}H_{22}N_3O_4Cl_1$ requires 426.1199 for $[M+Na]^+$, found 426.1200.

Synthesis of **S3j*para*** and **S3j*ortho***

General Procedure **B** was followed using 5-chloro-*N*-(3,5-dimethoxyphenyl)pyrimidin-2-amine (**S1b**, 133 mg, 0.5 mmol) and methyl α-bromoisobutyrate (194 µL, 272 mg, 1.5 mmol). Silica gel column chromatography gave two separable products, *para*-C–H-alkylated **S3j*para***, 42% (77 mg) and *ortho*-C–H-alkylated-cyclised **S3j*ortho***, 13% (21 mg).

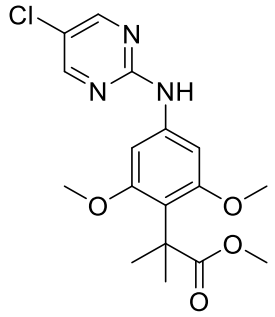

S3j*para*. Amorphous Solid. **FT-IR** (thin film): ν_{max} (cm^{-1}) = 3330.3, 2938.8, 1732.8. **^{1}H NMR** (500 MHz, Chloroform) δ 8.36 (2H, s, Ar*H*), 7.29 (1H, s, N*H*), 6.87 (2H, s, Ar*H*), 3.77 (6H, s, ArOC*H*$_3$), 3.65 (3H, s, CO_2CH_3), 1.57 (s, 6H). **^{13}C NMR** (126 MHz, $CDCl_3$) δ 179.6 (CO_2Me), 158.8 (Ar*C*), 158.3 (Ar*C*), 156.3 (Ar*C*), 138.8 (Ar*C*), 121.1 (Ar*C*), 116.6 (Ar*C*), 97.0 (Ar*C*), 55.9 (ArO*C*H$_3$), 51.8 (CO_2CH_3), 44.8 ($C(CH_3)_2$), 26.6 ($C(CH_3)_2$). **HRMS** (ESI): m/z calculated for $C_{17}H_{20}Cl_1N_3O_4$ requires 388.1035 for $[M+Na]^+$, found 338.1067.

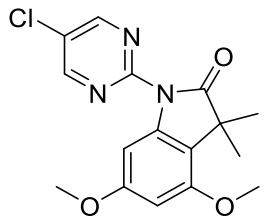

S3j*ortho*. Amorphous Solid. **FT-IR** (thin film): ν_{max} (cm^{-1}) = 2988.4, 1734.8. **^{1}H NMR** (500 MHz, $CDCl_3$) δ 8.80 (2H, s, Ar*H*), 6.84 (1H, d, *J* = 2.0 Hz, Ar*H*), 6.27 (1H, d, *J* = 2.0 Hz, Ar*H*), 3.86 (3H, s, ArOC*H*$_3$), 3.80 (3H, s, ArOC*H*$_3$), 1.54 (6H, s, $C(CH_3)_2$). **^{13}C NMR** (126 MHz, $CDCl_3$) δ 179.6 (*C*ON), 158.8 (Ar*C*), 158.3 (Ar*C*), 156.3 (Ar*C*), 138.8 (Ar*C*), 121.1 (Ar*C*), 116.6 (Ar*C*), 97.0 (Ar*C*), 55.9 (ArO*C*H$_3$), 51.8 (ArO*C*H$_3$), 44.8 ($C(CH_3)_2$), 26.6 ($C(CH_3)_2$). **HRMS** (ESI): m/z calculated for $C_{16}H_{16}Cl_1N_3O_3$ requires 356.0780 for $[M+Na]^+$, found 356.0772.

Data for **S3c(di)**

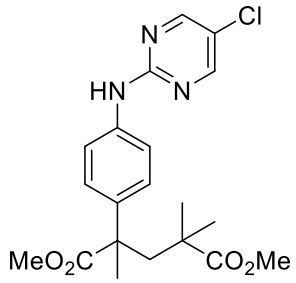

Amorphous Solid**. FT-IR** (thin film): ν_{max} (cm^{-1}) = 1734.3. **^{1}H NMR** (500 MHz, $CDCl_3$) δ 8.34 (2H, s, Ar*H*), 7.54–7.49 (2H, m, Ar*H*), 7.38–7.32 (2H, m, Ar*H*), 7.18 (1H, s, N*H*), 3.64 (3H, s, CO_2CH_3), 3.64 (3H, s, CO_2CH_3), 2.56 (1H, d, *J* = 14.5 Hz, CH_2), 2.48 (1H, d, *J* = 14.5 Hz, CH_2), 1.48 (3H, s, CH_3), 1.17 (3H, s, CH_3), 1.12 (3H, s, CH_3). **^{13}C NMR** (126 MHz, $CDCl_3$) δ 178.9 (CO_2Me), 176.7 (CO_2Me), 158.3 (Ar*C*), 156.4 (Ar*C*), 139.1 (Ar*C*), 137.7 (Ar*C*), 126.7 (Ar*C*), 121.1 (Ar*C*), 119.3 (Ar*C*), 52.3 (CO_2CH_3), 52.0 (CO_2CH_3), 48.9 ($C(CH_2R)_2$), 48.2 ($C(CH_2R)_2$), 41.8 (CH_2), 29.2 (CH_3), 24.0 (CH_3), 20.9 (CH_3). **HRMS** (ESI): m/z calculated for $C_{20}H_{24}Cl_1N_3O_4$ requires 406.1564 for $[M+H]^+$, found 406.1564.

6.5.5: Synthesis of *meta*-C–H Functionalized Materials

Synthesis of **S5a**

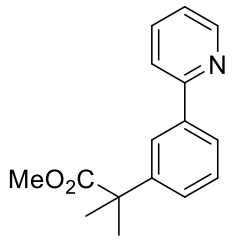

An oven-dried carousel tube was charged with phenylpyridine (36 µL, 39 mg, 0.25 mmol), potassium carbonate (69 mg, 0.5 mmol), sodium acetate (6 mg, 0.075 mmol) and $[RuCl_2(p\text{-cymene})]_2$ (8 mg, 0.0125 mmol, 5 mol%) then sealed with a Teflon cap. The tube was evacuated and refilled three times with argon. 1,4-dioxane (1 mL) and methyl α-bromoisobutyrate (97 µL, 136 mg, 0.75 mmol) were added *via* septum and the reaction mixture heated to 120 °C for 16 h. After this time, the mixture was allowed to return to room temperature and was diluted in EtOAc (20 mL) and 5% ethylenediamine solution (20 mL). The organic layer was extracted and the aqueous phase we re-extracted with EtOAc (2 x 20 mL). The combined organic phases were dried over $MgSO_4$ and concentrated *in vacuo*. The crude residue was purified *via* silica gel column chromatography to give *meta*-substituted structure, 36% (23 mg). **FT-IR** (thin film): ν_{max} (cm^{-1}) = 2978.2, 1782.0, 1731.6. **^{1}H NMR** (500 MHz, $CDCl_3$) δ 8.73–8.65 (1H, m, Ar*H*), 7.98 (1H, t, *J* = 1.8 Hz, Ar*H*), 7.90–7.80 (1H, m, Ar*H*), 7.77–7.66 (2H, m, Ar*H*), 7.42 (1H, t, *J* = 7.7 Hz, Ar*H*), 7.38 (1H, ddd, *J* = 7.8, 1.8, 1.3 Hz, Ar*H*), 7.22 (1H, ddd, *J* = 7.2, 4.8, 1.3 Hz, Ar*H*), 3.65 (3H, s, *J* = 8.9 Hz, CO_2CH_3), 1.65 (6H, s, *J* = 1.1 Hz, $C(CH_3)_2$). **^{13}C NMR** (126 MHz, $CDCl_3$) δ 177.2 (CO_2Me), 173.1 (Ar*C*), 157.5 (Ar*C*), 149.6 (Ar*C*), 145.2 (Ar*C*), 139.56 (Ar*C*), 136.7 (Ar*C*), 128.8 (Ar*C*), 126.4 (Ar*C*), 125.4 (Ar*C*), 124.2 (Ar*C*), 122.1 (Ar*C*), 120.7 (Ar*C*), 52.3 (CO_2CH_3), 46.6 ($C(CH_3)_2$), 26.6 ($C(CH_3)_2$)). **HRMS** (ESI): m/z calculated for $C_{16}H_{17}N_1O_2$ requires 256.1332 for $[M+H]^+$, found 256.1351.

Synthesis of **5c**

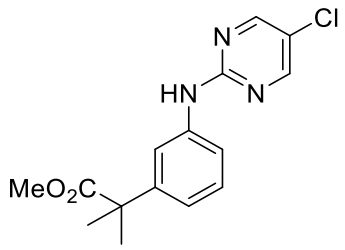

To an oven dried carousel tube was charged 5-chloro-*N*-phenylpyrimidin-2-amine (**1c**, 52 mg, 0.25 mmol), $[RuCl_2(p\text{-cymene})]_2$ (15.5 mg, 0.025 mmol, 10 mol%) and potassium acetate (49 mg, 0.5 mmol). The reaction vessel was sealed with a Teflon cap and evacuated and refilled three times with argon. To the carousel tube was then added DME (1 mL), acetic acid (29 µL, 30 mg, 0.5 mmol) and methyl α-bromoisobutyrate (97 µL, 136 mg, 0.75 mmol) were added *via* septum and the reaction mixture heated to 120 °C for 16 h. After this time, the mixture was allowed to return to room temperature and was diluted in EtOAc (20 mL) and sat. $NaHCO_3$ solution (20 mL). The organic layer was extracted and the aqueous phase we re-extracted with EtOAc (2 x 20 mL). The combined organic phases were dried over $MgSO_4$ and concentrated *in vacuo*. The crude residue was purified *via* silica gel column chromatography to give *meta*-substituted structure, 47% (36 mg, mixture of *meta*:*para* of 99:1. **FT-IR** (thin film): ν_{max} (cm^{-1}) = 3348.3, 2978.1, 1731.4. **^{1}H NMR** (500 MHz, $CDCl_3$) δ 8.35 (2H, s, Ar*H*), 7.55 (1H, ddd, *J* = 8.1, 2.2, 0.9 Hz, Ar*H*), 7.49 (1H, t, *J* = 2.0 Hz, Ar*H*), 7.31 (1H, t, *J* = 8.0 Hz, Ar*H*), 7.05 (1H, ddd, *J* = 7.8, 1.9, 0.9 Hz, Ar*H*), 3.67 (3H, s, CO_2CH_3), 1.59 (6H, s, $C(CH_3)_2$). **^{13}C NMR** (126 MHz, $CDCl_3$) δ 177.2 (CO_2Me), 158.4 (Ar*C*), 156.3 (Ar*C*), 145.8 (Ar*C*), 139.1 (Ar*C*), 129.1 (Ar*C*), 121.0 (Ar*C*), 120.6 (Ar*C*), 118.1 (Ar*C*), 117.2 (Ar*C*), 52.4 (CO_2CH_3), 46.7 ($C(CH_3)_2$), 26.6 ($C(CH_3)_2$). **HRMS** (ESI): m/z calculated for $C_{15}H_{16}Cl_1N_3O_2$ requires 328.0823 for $[M+Na]^+$, found 328.0831.

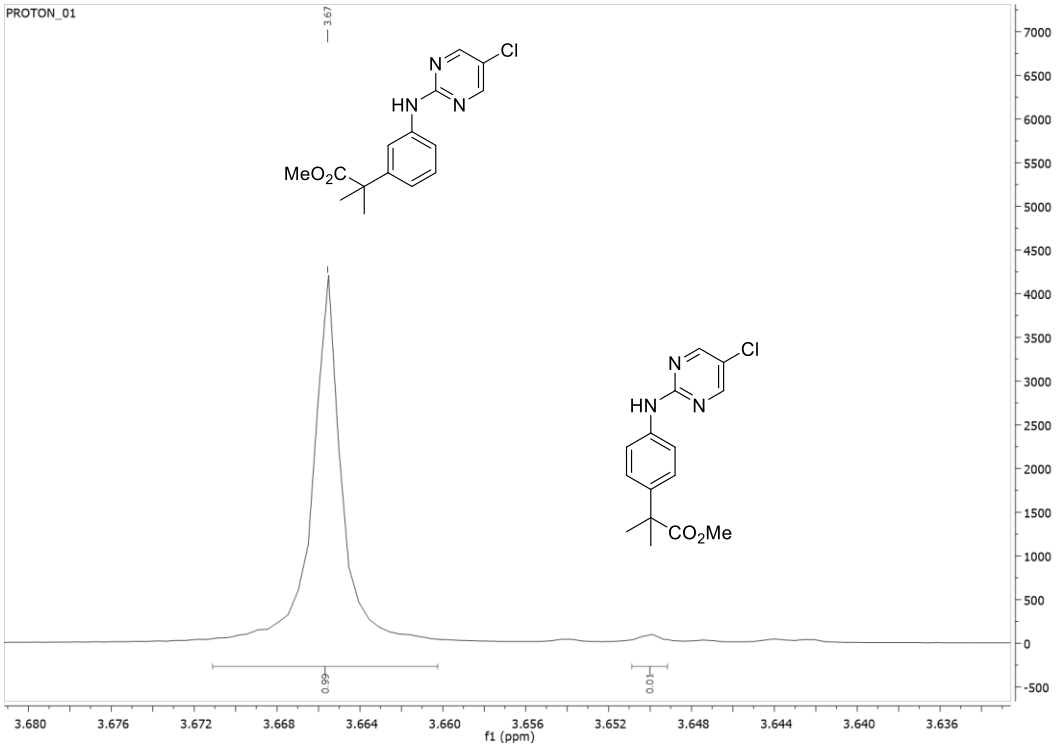
PROTON_01
3.67
Cl
N
HN
N
MeO2C
Cl
N
HN
N
CO2Me
0.99
0.01
7000
6500
6000
5500
5000
4500
4000
3500
3000
2500
2000
1500
1000
500
0
-500
3.680
3.676
3.672
3.668
3.664
3.660
3.656
3.652
3.648
3.644
3.640
3.636
f1 (ppm)

6.5.6: Deuterium Experiments

Synthesis of **1c-*d*$_5$**

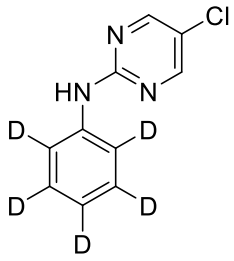

To a 250 mL three-necked round bottomed flask was charged 2-amino-4-chloroaminopyrimidine (1.42 g, 11 mmol), copper iodide (952 mg, 5 mmol, 50 mol%) and potassium carbonate (2.76 g, 20 mmol). A condenser was equipped and the flask was evacuated and refilled with nitrogen three times. d_5-bromobenzene (1.05 mL, 1.62 mL, 10 mmol), *N,N'*-dimethylethylenediamine (538 µL, 441 mg, 5 mmol, 50 mol%) and 1,4-dioxane (40 mL) were then added *via* septum. The reaction mixture was heated to 100 °C for 72 h. After this time, the reaction mixture was allowed to cool to room temperature and concentrated ammonia solution (20 mL) and brine (80 mL) were added and extracted with EtOAc (3 x 100 mL). The combined organic phases were dried over $MgSO_4$ and concentrated *in vacuo*. The crude residue was purified *via* silica gel column chromatography (EtOAc/Hexanes, 5:95 v:v) to give pure white solid, 35% (706 mg). *Note: The corresponding palladium-catalyzed Buchwald amination did not give any conversion to product. **^{1}H NMR** (400 MHz, $CDCl_3$) δ 8.36 (2H, s, Ar*H*), 7.63 (1H, s, N*H*). **^{13}C NMR** (101 MHz, $CDCl_3$) δ 158.4 (Ar*C*), 156.3 (Ar*C*), 138.9 (Ar*C*), 129.2–128.2 (m, Ar*C*), 123.2–122.0 (m, Ar*C*), 120.9 (Ar*C*), 119.30 (m, Ar*C*).

1c-*d*$_5$ – ^{1}H NMR (400 MHz, $CDCl_3$)

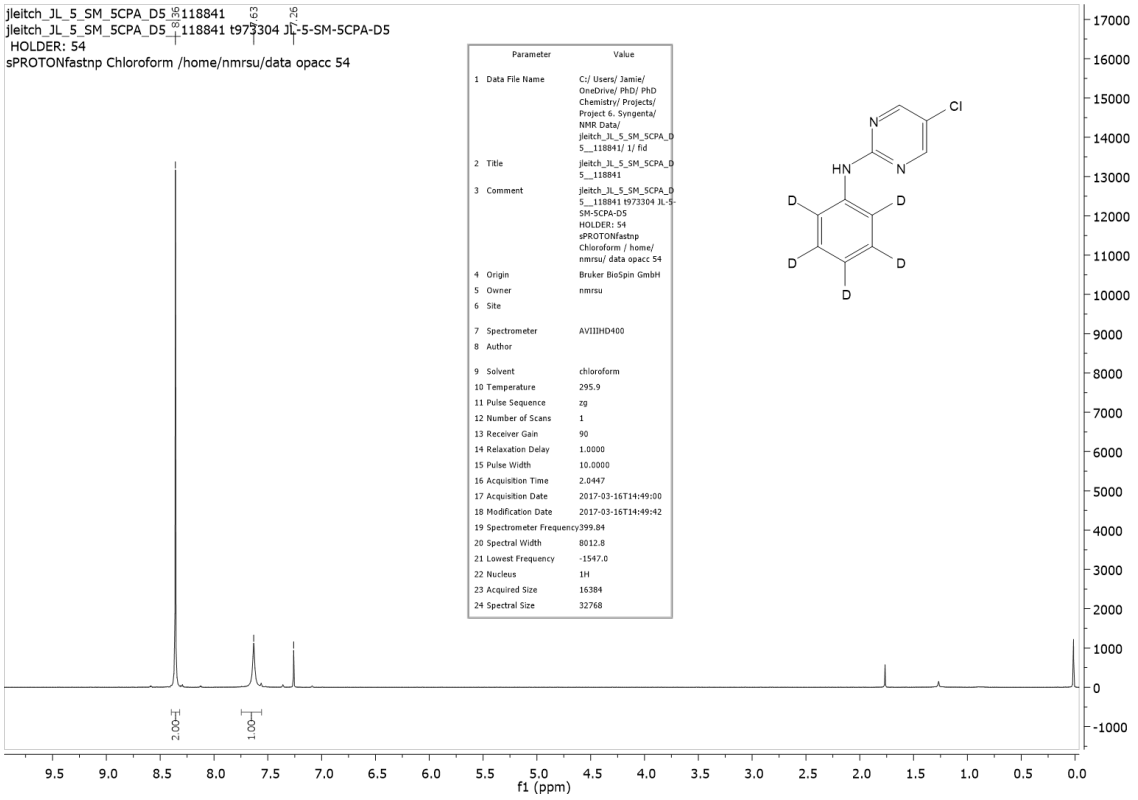

	Parameter	Value
1	Data File Name	C:/ Users/ Jamie/ OneDrive/ PhD/ PhD Chemistry/ Projects/ Project 6. Syngenta/ NMR Data/ jleitch_JL_5_SM_5CPA_D5__118841/ 1/ fid
2	Title	jleitch_JL_5_SM_5CPA_D5__118841
3	Comment	jleitch_JL_5_SM_5CPA_D5__118841 t973304 JL-5-SM-5CPA-D5 HOLDER: 54 sPROTONfastnp Chloroform / home/ nmrsu/ data opacc 54
4	Origin	Bruker BioSpin GmbH
5	Owner	nmrsu
6	Site	
7	Spectrometer	AVIIIHD400
8	Author	
9	Solvent	chloroform
10	Temperature	295.9
11	Pulse Sequence	zg
12	Number of Scans	1
13	Receiver Gain	90
14	Relaxation Delay	1.0000
15	Pulse Width	10.0000
16	Acquisition Time	2.0447
17	Acquisition Date	2017-03-16T14:49:00
18	Modification Date	2017-03-16T14:49:42
19	Spectrometer Frequency	399.84
20	Spectral Width	8012.8
21	Lowest Frequency	-1547.0
22	Nucleus	1H
23	Acquired Size	16384
24	Spectral Size	32768

1c-*d*$_5$ – ^{13}C NMR (101 MHz, $CDCl_3$)

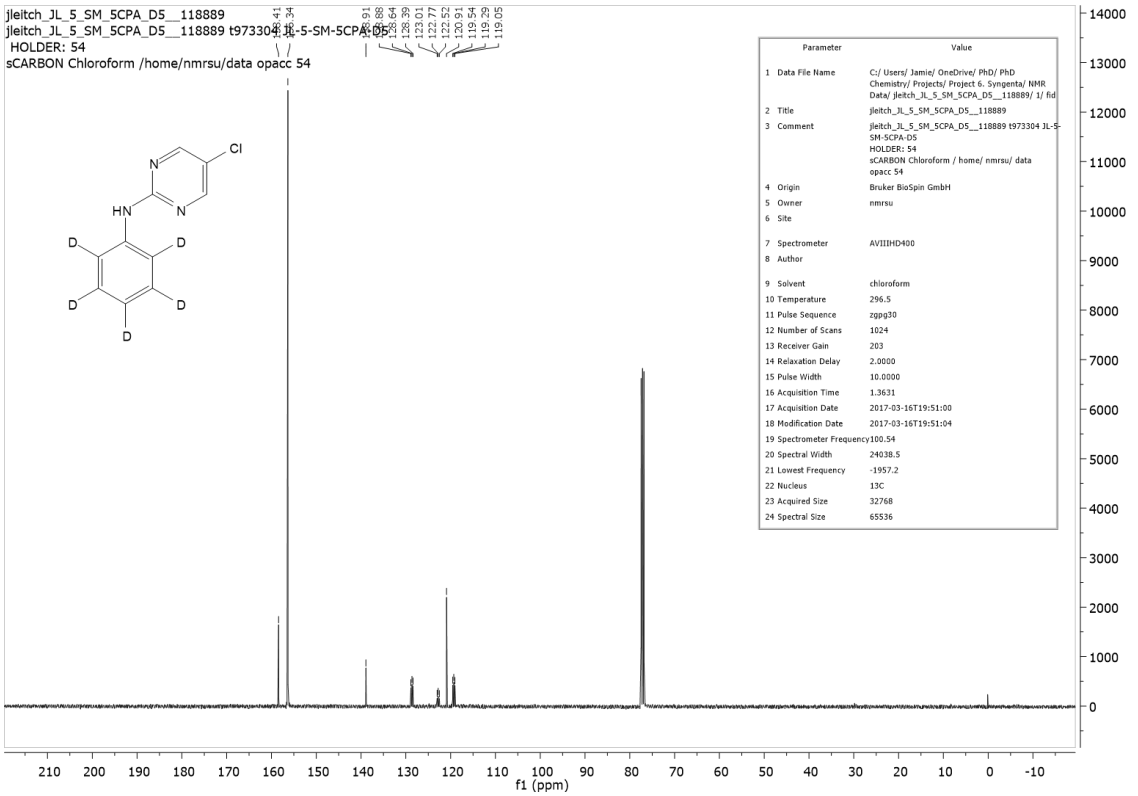

	Parameter	Value
1	Data File Name	C:/ Users/ Jamie/ OneDrive/ PhD/ PhD Chemistry/ Projects/ Project 6. Syngenta/ NMR Data/ jleitch_JL_5_SM_5CPA_D5__118889/ 1/ fid
2	Title	jleitch_JL_5_SM_5CPA_D5__118889
3	Comment	jleitch_JL_5_SM_5CPA_D5__118889 t973304 JL-5-SM-5CPA-D5 HOLDER: 54 sCARBON Chloroform / home/ nmrsu/ data opacc 54
4	Origin	Bruker BioSpin GmbH
5	Owner	nmrsu
6	Site	
7	Spectrometer	AVIIIHD400
8	Author	
9	Solvent	chloroform
10	Temperature	296.5
11	Pulse Sequence	zgpg30
12	Number of Scans	1024
13	Receiver Gain	203
14	Relaxation Delay	2.0000
15	Pulse Width	10.0000
16	Acquisition Time	1.3631
17	Acquisition Date	2017-03-16T19:51:00
18	Modification Date	2017-03-16T19:51:04
19	Spectrometer Frequency	100.54
20	Spectral Width	24038.5
21	Lowest Frequency	-1957.2
22	Nucleus	13C
23	Acquired Size	32768
24	Spectral Size	65536

Para C–H Alkylation of **1c-*d*$_5$**

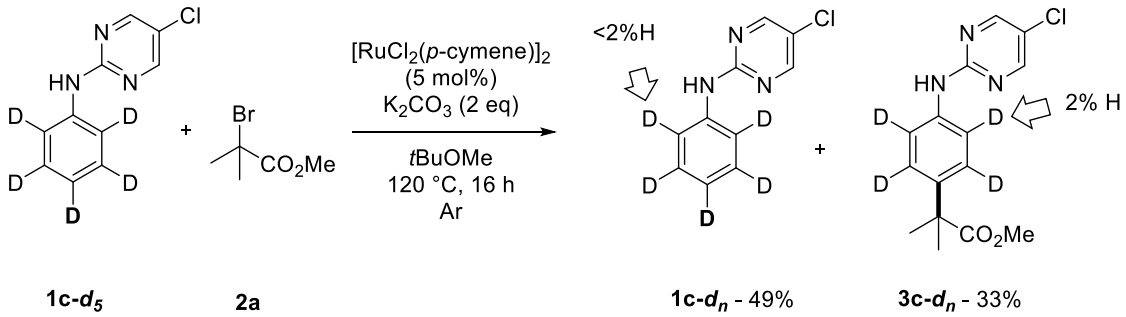

1c-*d*$_5$ **2a** **1c-*d*$_n$** - 49% **3c-*d*$_n$** - 33%

1c-*d*$_n$ – 1.5% H in each *ortho* position

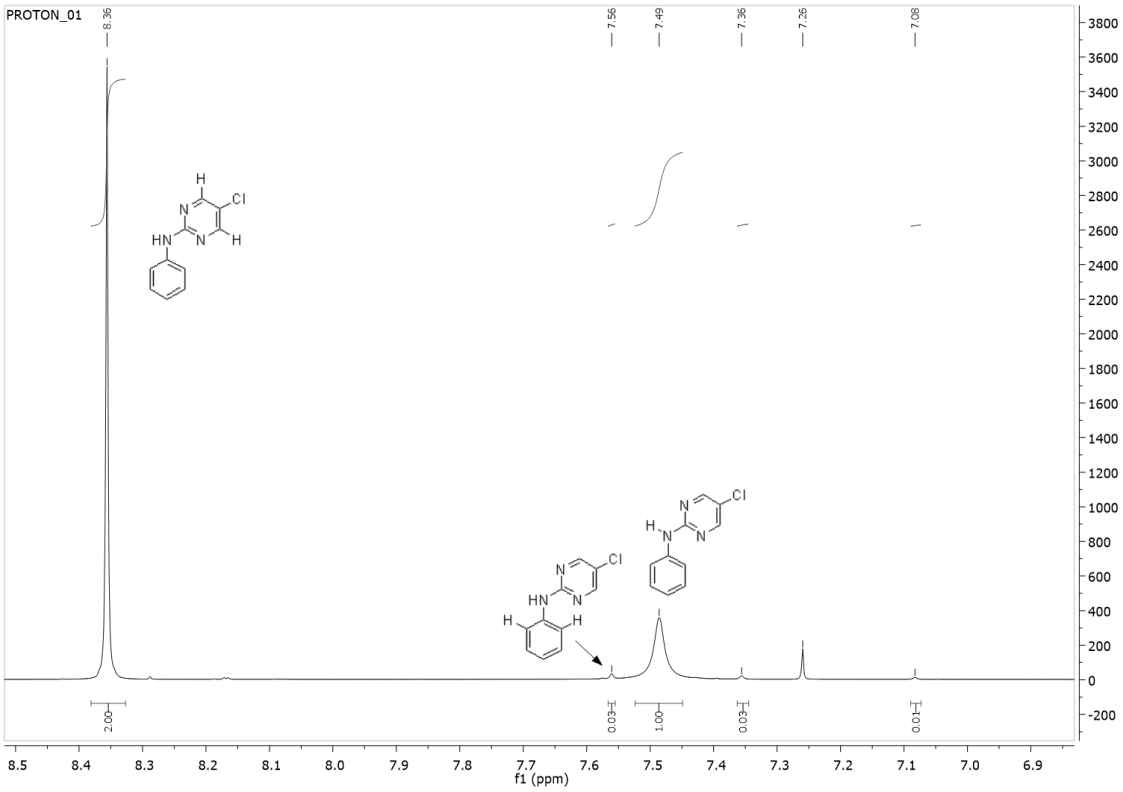

3c-d_n – 2% H in each *ortho* position

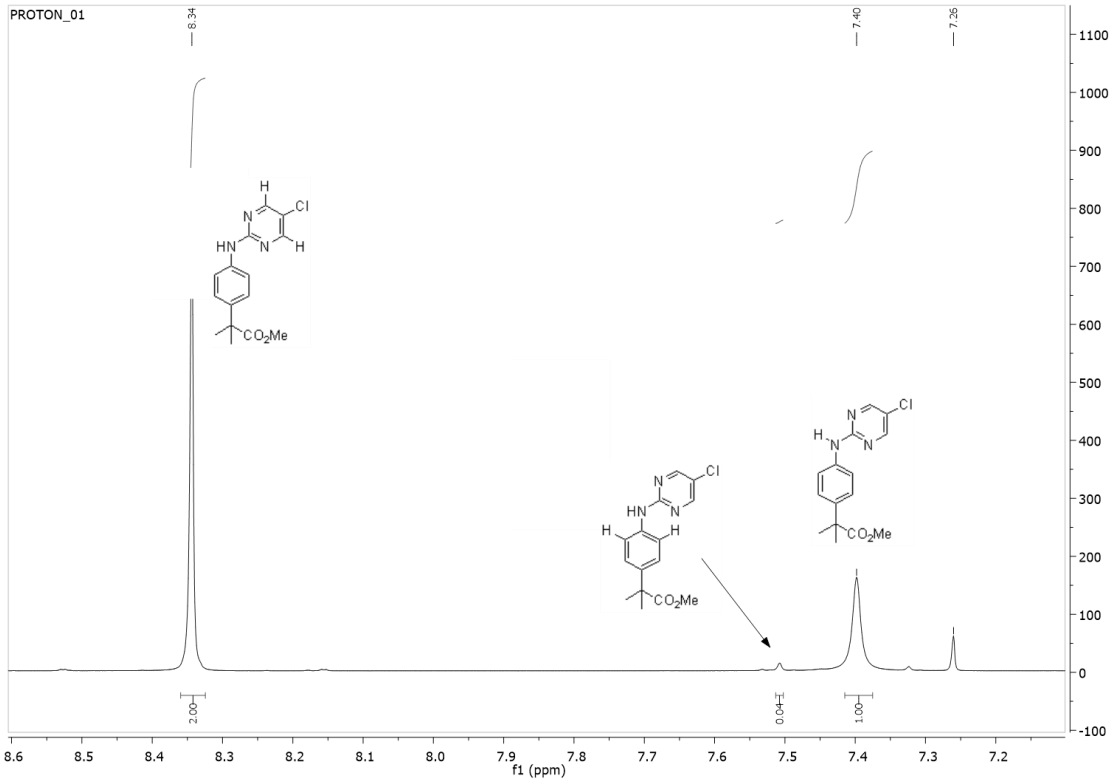

Meta C–H Alkylation of **3c**

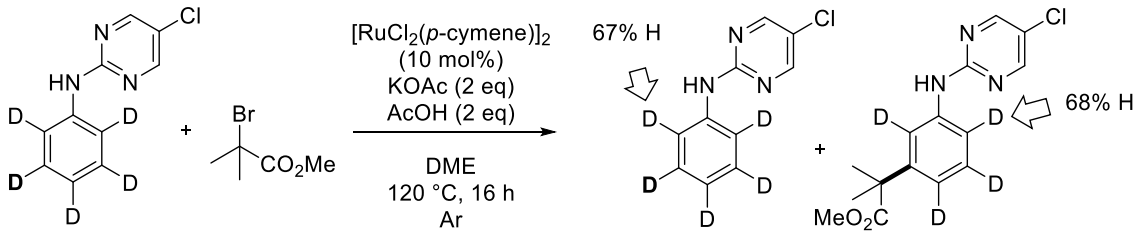

1c-*d*$_5$ **2a** **1c-*d*$_n$** - 21% **5c-*d*$_n$** - 29%

1c-*d*$_n$ – 67% H in each *ortho* position

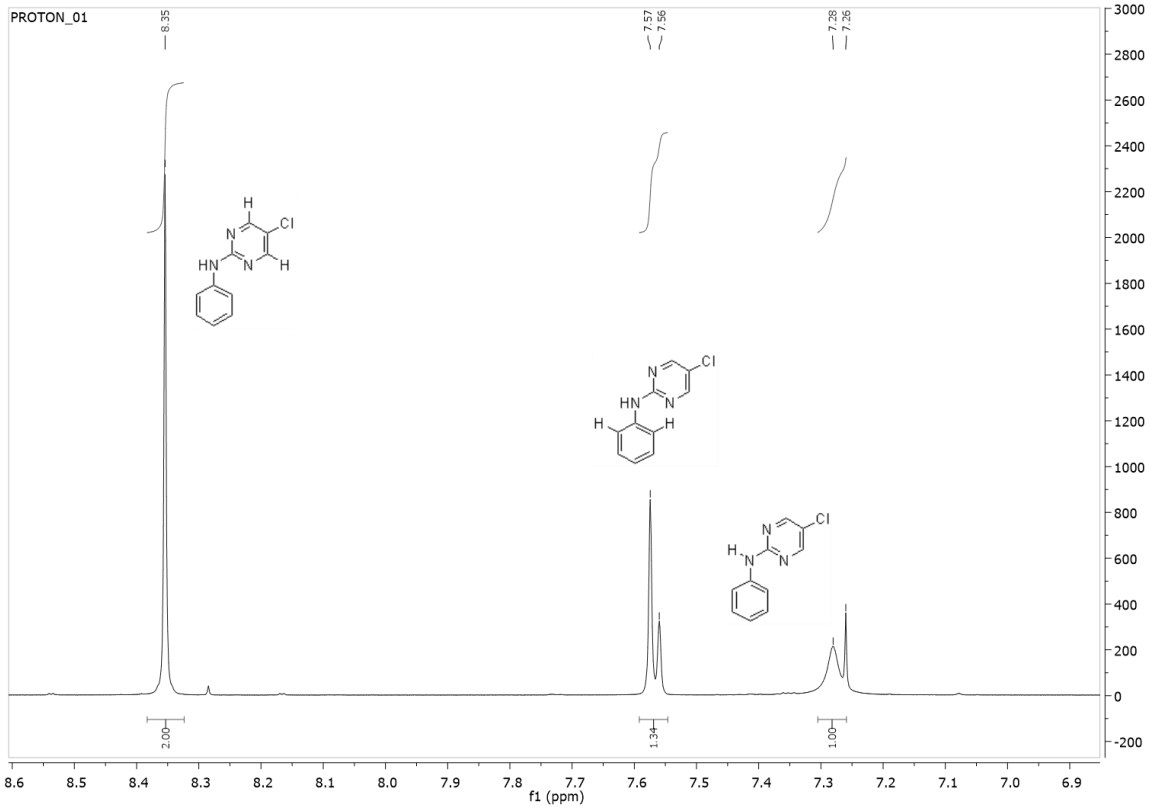

5c-d_n – 68% H in each *ortho* position

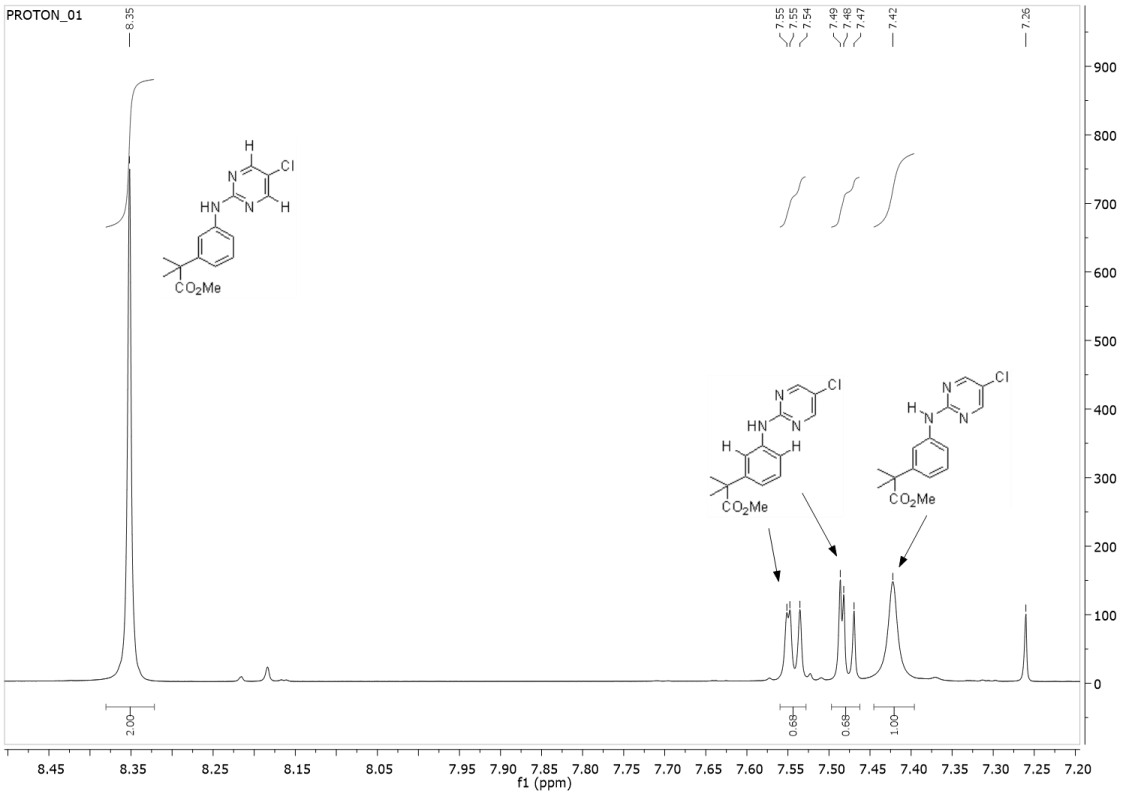

6.5.7: KIE Experiments

Scheme S8. Determination of Kinetic Isotope Effect *via* Intermolecular Competition

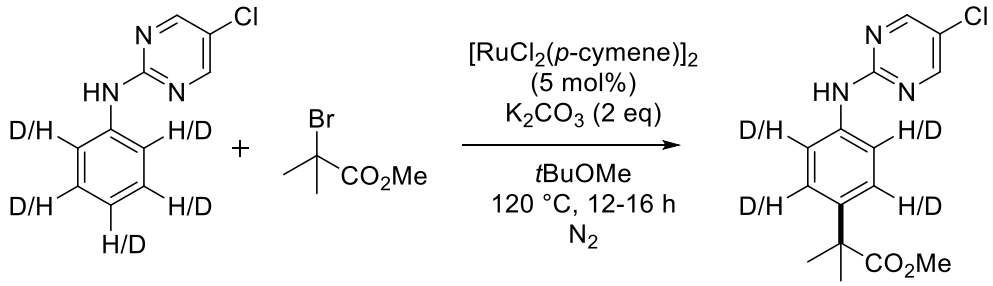

1c - 0.5 eq
[D]$_5$-1c - 0.5 eq

2a

h	Conversion	H	D	KIE
16	~70%	0.50	0.50	1.00
12	~50%	0.51	0.49	1.04
	Av.			1.02

70% Conversion:

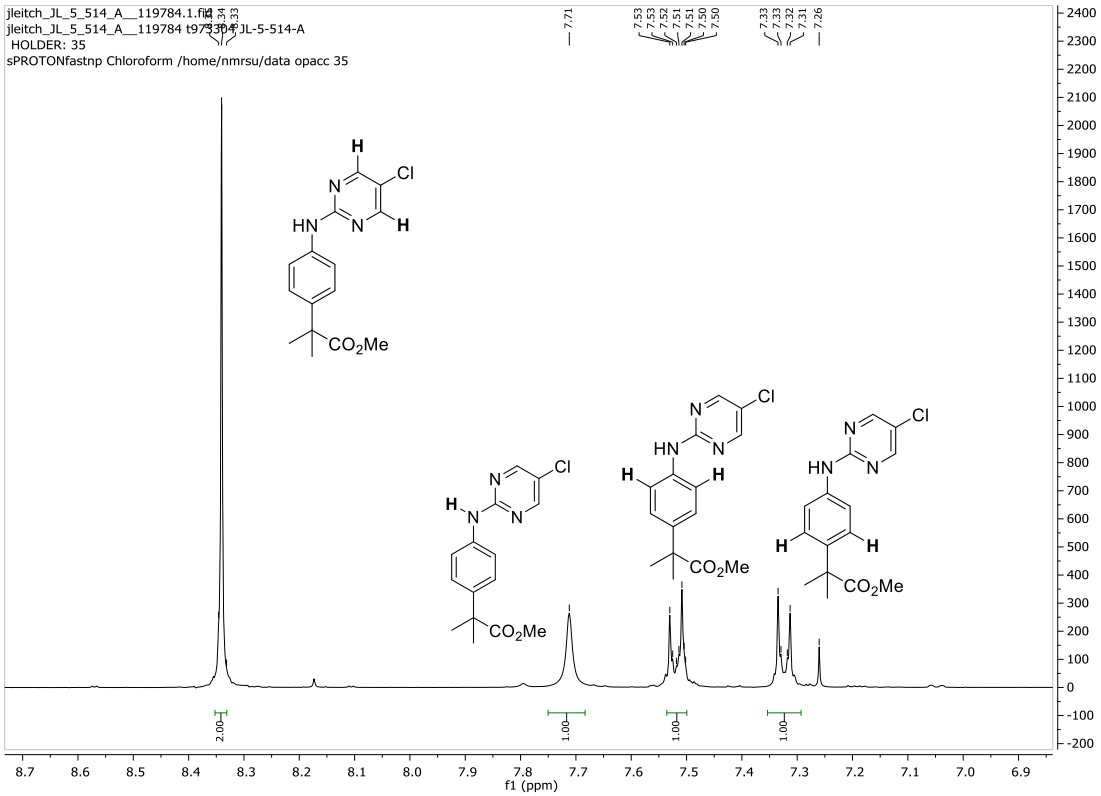

50% Conversion:

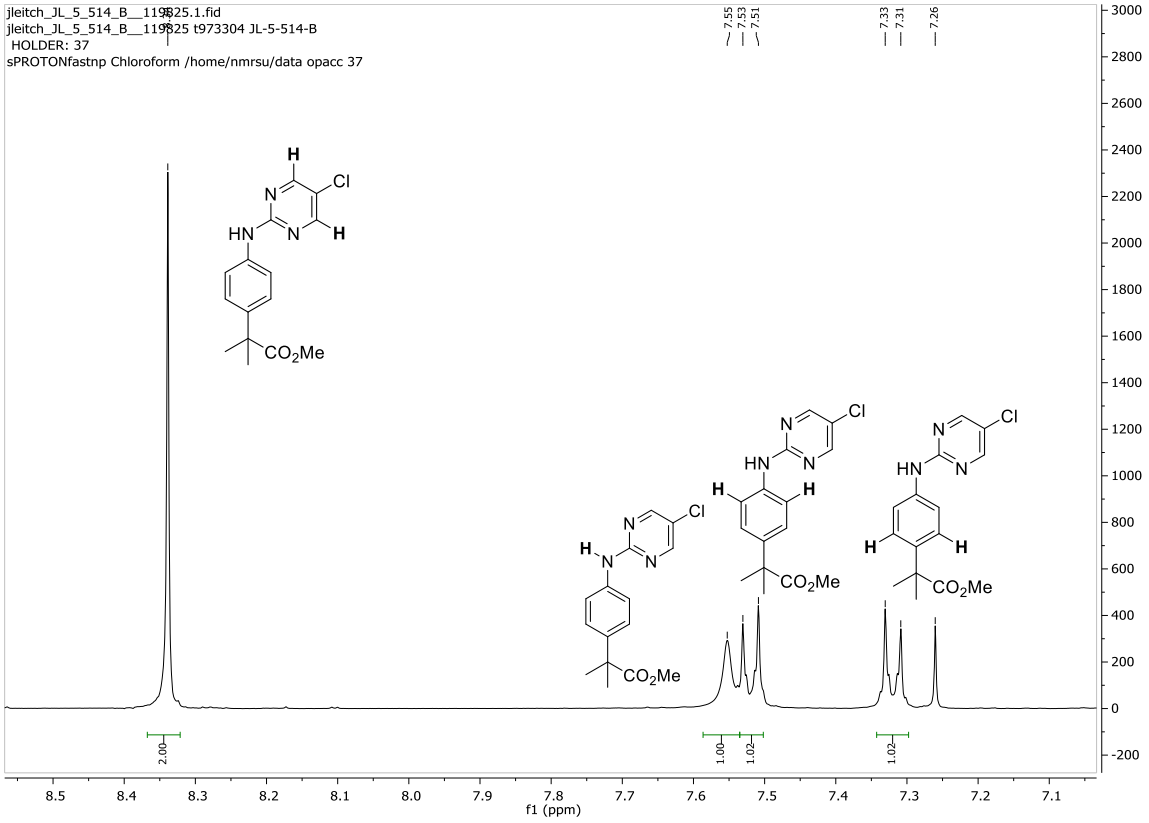

6.5.8: Crossover Experiment

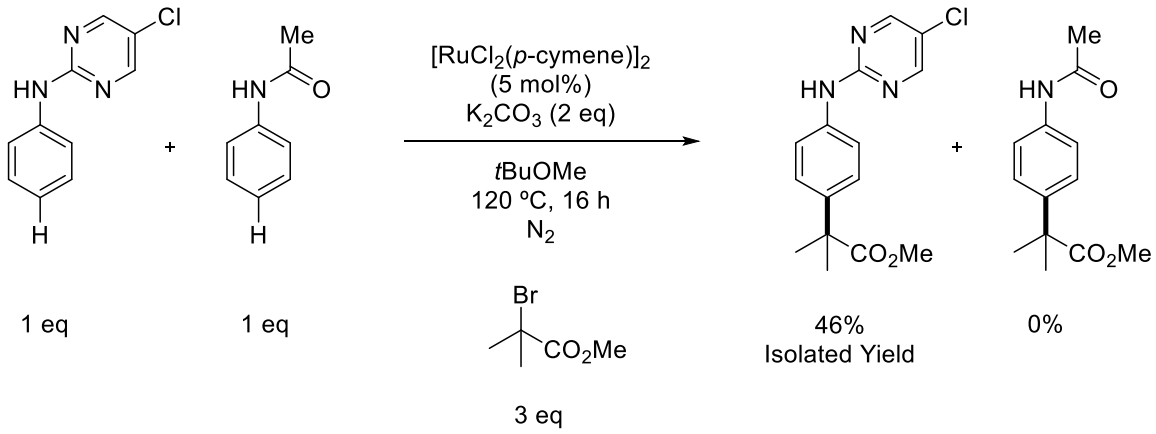

Crude LC-MS – No Observation of Substituted Acetanilide at any peak.

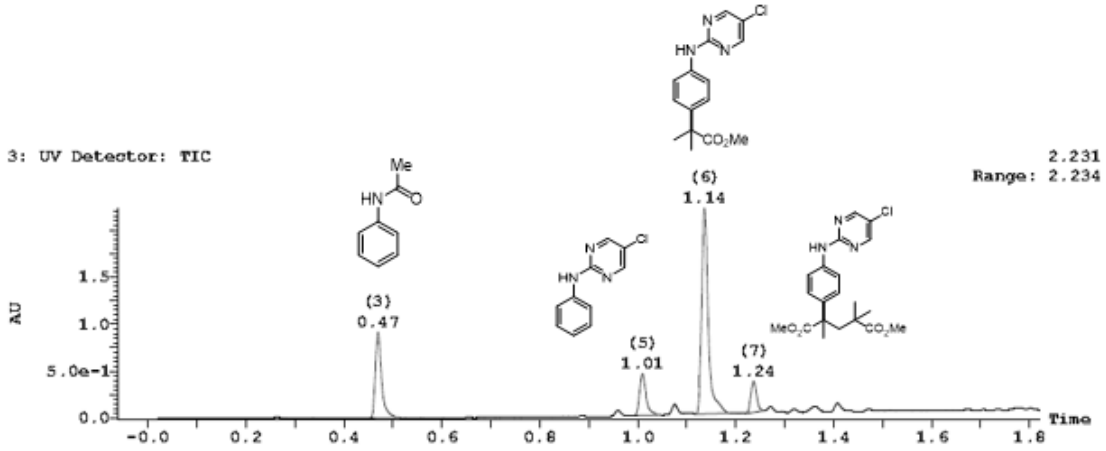

6.5.9: DFT Discussion

With a potential inner sphere ruthenium dictating the selectivity of functionalization, further Density Functional Theory (DFT) computations were employed to map the contrasting H-activation (cyclometalation) mechanisms for **1c** that result in complementary para or meta selectivity.

Using the same computational methodology we employed previously,[12] geometries were optimized in the gas phase with the BP86 functional using the basis set SDD for Ru and Cl, and 6-31G** on all other atoms. Additional single point corrections were applied for solvation (dioxane, ε = 2.2099), dispersion (Grimme's D3-BJ parameter set) and an extended basis-set (cc-pVTZ for Ru and 6-311++G** for all other atoms).

Initial coordination of the substrate **1c** to the *in situ* catalytically active cationic Ru intermediate (**A**), [Ru(η^6-*p*-cymene)(κ^2-O_2CR)(**1c**)]$^+$, occurs through one of the nitrogen atoms in the pyrimidine ring and affords two isomers; $\mathbf{A_C}$ and $\mathbf{A_N}$. The former ($\mathbf{A_C}$) has the phenyl group orientated towards the Ru centre and leads to X–H-activation occurring at the ortho carbon via a two-step concerted metalation deprotonation (CMD) mechanism and eventually forming the *meta* product. The latter, $\mathbf{A_N}$, is the more stable geometry with the phenyl group orientated away from Ru, positioning the N–H for activation and forming a four-membered ruthenacycle that ultimately leads to the para product. This intermediate ($\mathbf{A_N}$) has been chosen as the relative energy zero reference for both H-activation pathways.

Focusing first on acetate as the activating carboxylate base (see Figure S1, R = Me, bold), despite the preferred N–H orientation of **1c** by 3.3 kcal mol^{-1}, the barrier for reversible one-step N–H activation ($\mathbf{TS(A\text{-}B)_N}$) is 4.6 kcal mol^{-1} higher in free energy than the irreversible two-step CMD pathway. From $\mathbf{A_C}$ (ΔGcorr = +3.3 kcal mol^{-1}), the first C–H activation step ($\mathbf{TS(A\text{-}B)1_C}$) is the higher of the two CMD transition states (ΔG_{corr} = +10.9 kcal mol^{-1}), which involves the κ^2-κ^1 displacement of the base at Ru as the C–H bond of **1c** approaches the metal centre to form an agostic intermediate ($\mathbf{INT(A\text{-}B)_C}$; ΔG_{corr} = +7.0 kcal mol^{-1}), elongating the C–H bond from 1.091 Å to 1.151 Å. The lower second step, $\mathbf{TS(A\text{-}B)2_C}$, involves the cleavage of the C–H bond (ΔG_{corr} = +8.4 kcal mol^{-1}) and then exergonically forms a six-membered ruthenacycle acetic acid adduct, $\mathbf{B_C}$ (ΔG_{corr} = +2.0 kcal mol^{-1}). The preference for C–H activation over N–H activation agrees with our experimental observations for acetate reaction conditions.

Comparison of the acetate pathways with the carbonate equivalent structures was achieved by using bicarbonate (HCO_3^-, R = OH) in our computational model instead of the dianionic carbonate, CO_3^{2-}. This approach has been used in previous studies[13] and is not a perfect solution.[14] As shown in Figure S1 (R = OH, dashed / italic, '), the barrier to N–H activation is smaller for the bicarbonate pathway by 1.7 kcal mol^{-1}, (**TS(A-B)$_N$'**; ΔG_{corr} = +12.8 kcal mol^{-1}) and remains reversible with the four-membered ruthenacycle adduct **B$_N$'** endergonic by 2.6 kcal mol^{-1}. In fact, this barrier is now lower than the C–H activation pathway by 3.9 kcal mol^{-1}, with the N–H product, **B$_N$'**, 0.5 kcal mol^{-1} lower in energy than the C–H product complex **B$_C$'**. Despite **A$_C$'** being relatively more stable to **A$_N$'** for R = OH by 1.4 kcal mol^{-1} (**A$_C$'**; ΔG_{corr} = +1.9 kcal mol^{-1}), the first step in the CMD pathway (**TS(A-B)1$_C$'**) has increased significantly to ΔG_{corr} = +16.7 kcal mol^{-1}. The displacement of the distal oxygen in **TS(A-B)1$_C$'** leading to the loss of a Ru-O bond as the bicarbonate base at Ru changes from κ^2 to κ^1 raises the barrier by 5.8 kcal mol^{-1}. A shorter elongation of the C–H bond (1.122 Å) is observed in the agostic intermediate, **INT(A-B)$_C$'**; ΔG_{corr} = +3.1 kcal mol^{-1}, which after a small barrier to C–H cleavage in the second CMD step (**TS(A-B)2$_C$'**; ΔG_{corr} = +6.6 kcal mol^{-1}) endergonically forms the six-membered ruthenacycle adduct **B$_C$'** (ΔG_{corr} = +3.1 kcal mol^{-1}).

Therefore, by changing the base used to assist in the X–H-activation, we have mirrored computationally that which is seen experimentally - a change in mechanism and product selectivity is observed. When acetate is the base (R = Me), C–H activation is the lower pathway and forms the more stable product adduct **B$_C$**. However, when bicarbonate is the base (R = OH), the lower pathway involves N–H activation, and the more stable product adduct is **B$_N$'**.

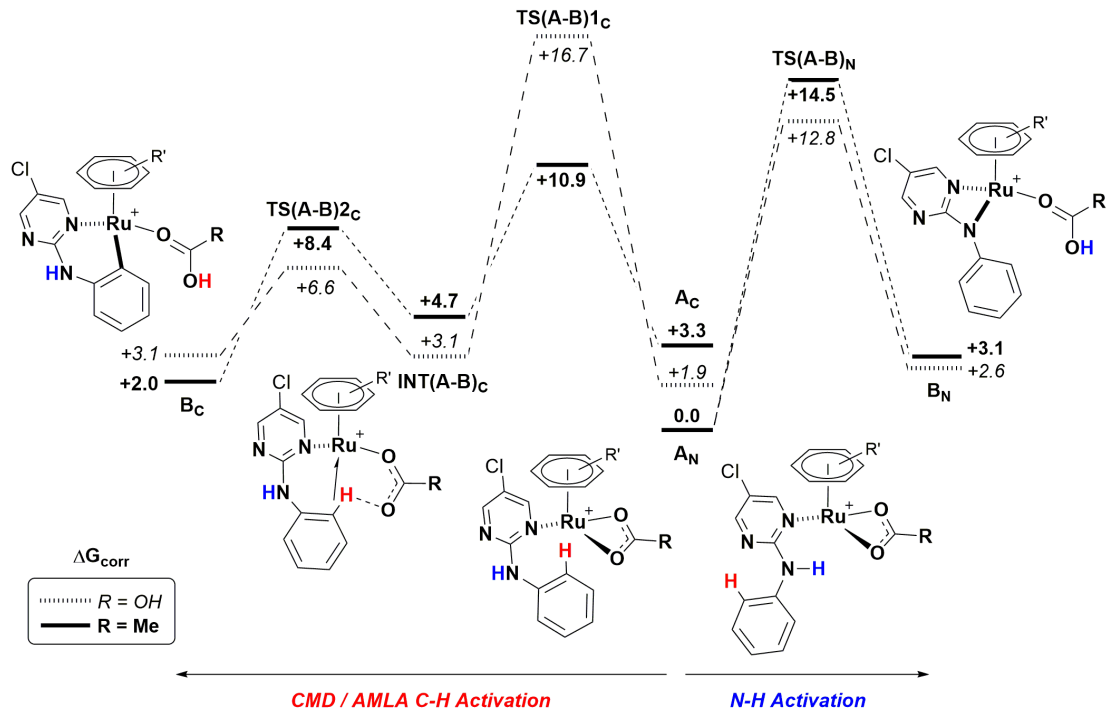

Figure S1. DFT calculated free energies (kcal mol^{-1}) relative to the most stable intermediate, A_N, for the competing C–H and N–H activations of 1c at [Ru(*p*-cymene)(O_2CR)]$^+$ in dioxane, when R = Me (acetate) or OH (carbonate).

Exchange of the coordinated acid in adduct **B** post X–H-activation for another carboxylate anion affords complex **C**, [Ru(η^6-*p*-cymene)(κ^1-O_2CR)(**1c***)], when **1c*** is the H-activated **1c**. For both carboxylates, the N–H activated intermediate (**C_N**/**C_N'**) is more stable; ΔΔG = 1.9 kcal mol^{-1} for acetate (R = Me) and 1.1 kcal mol^{-1} for bicarbonate (R = OH). Subsequently, the relative Fukui indices for the proposed N–H and C–H activated complexes were calculated (Figure S2). The N–H activated complex (**C_N**') was shown to have C3 (para-position) as the most activated position by a considerable amount. When the position of cyclometalation was switched to ortho C–H activation (**C_C**) a complete shift in the electronic nature of **1c**'s phenyl group is observed. Here the C2 (meta) position has increased relative nucleophilicity due the presence of the Ru-C σ-bond para to the C2 position. Likewise, an increase in the reactivity of the two *ortho* sites to the metal center (C4 and C6) reinforces the concept of the ruthenium behaving as a transient electronic *ortho*/*para* director. It is also worth noting that the nature of the ligand (R = OH vs Me) was shown to have negligible influence on the relative Fukui index (Figures S3-4)

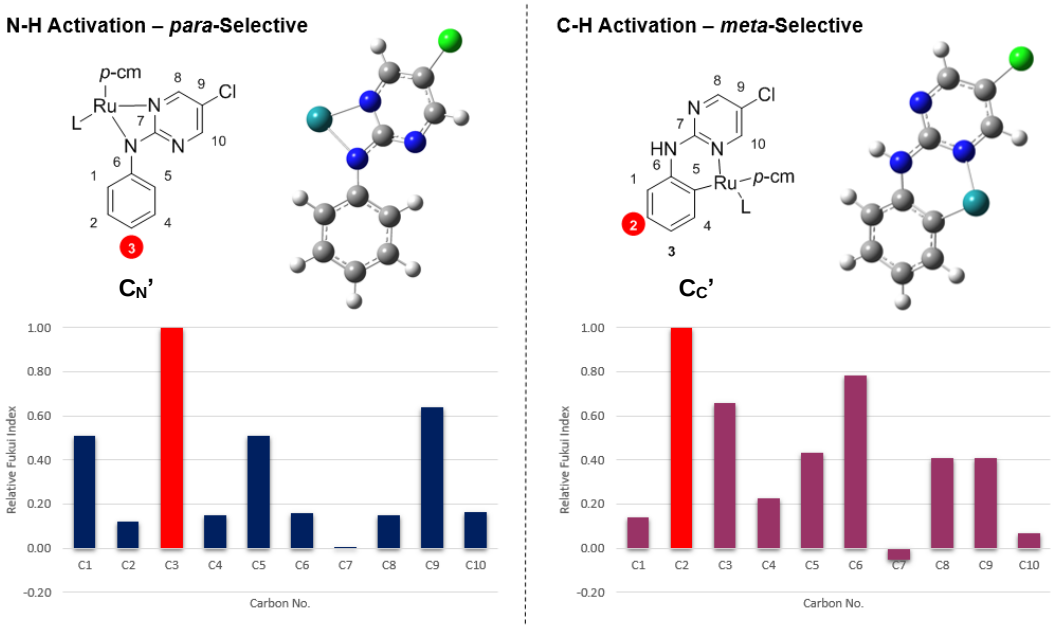

Figure S3. Relative nucleophilicity Fukui indices for inorganic computed structures C_N' (L = $O_2C(OH)$) and C_C (L = OAc) for (BP86/6-31G**&SDD(Ru,Cl); optimization and NBO), ball-and-stick figures of C_N' and C_C have the η^6-*p*-cymene and base ligands (L) omitted for clarity. The most reactive C–H position is highlighted in red

Varying the nature of the oxygen bound ligand to the ruthenium showed negligible influence in the electronic nature of the phenyl group of **1c**. This suggests that the complementary selectivity observed is not related to the different ligand set present in the reaction conditions (i.e. which base is used) but moreover on the position of cyclometalation and how these different ligand sets promote different selectivities.

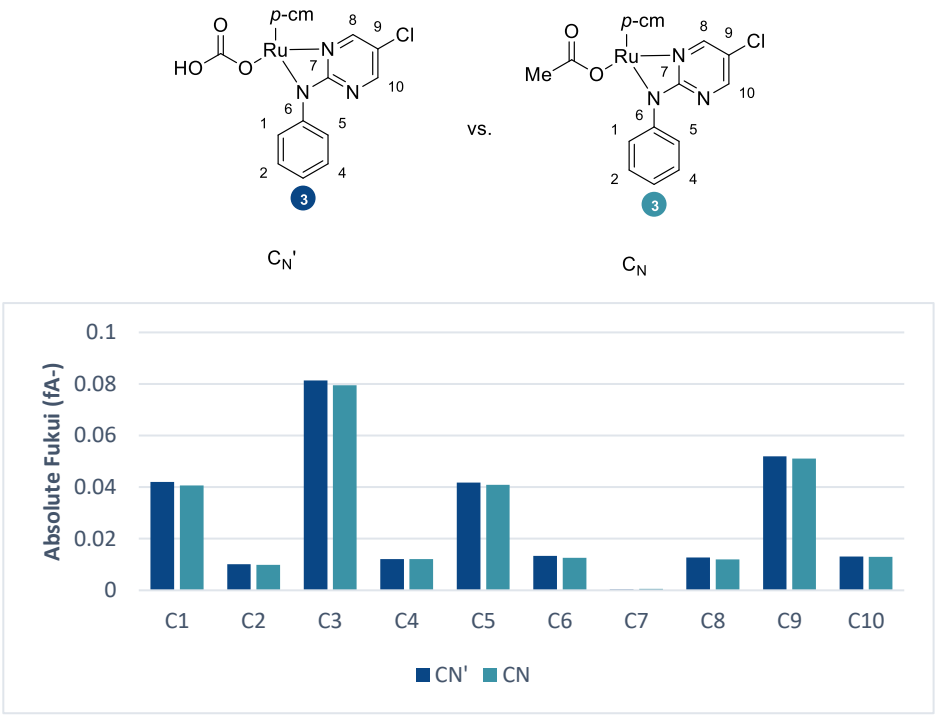

Figure S3 - Ligand Effects: Comparison of Absolute Fukui Indices from Ligand Exchange in N–H Activated Complexes.

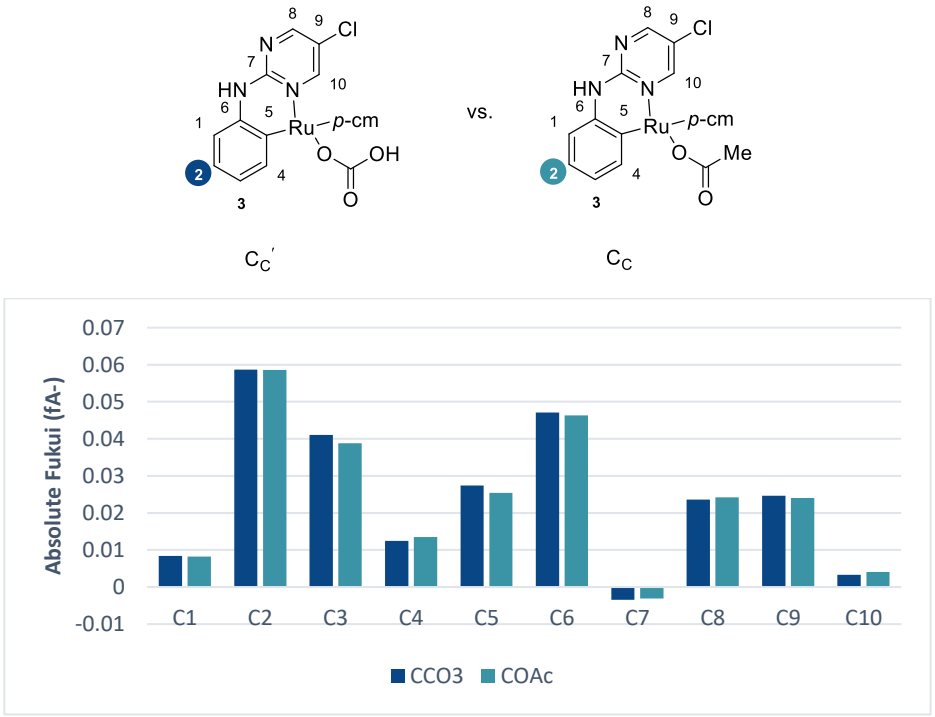

Figure S4 - Ligand Effects: Comparison of Absolute Fukui Indices from Ligand Exchange in C–H Activated Complexes.

6.5.10: References

(1) A. J. Paterson, S. St John-Campbell, M. F. Mahon, N. J. Press, C. G. Frost, *Chem. Commun.*, **2015**, *51*, 12807.

(2) X. Huang, S. Xu, Q. Tan, M. Gao, M. Li, B. Xu, *Chem. Commun.*, **2014**, *50*, 1465.

(3) Fukii, S.; Kobayashi, T.; Nakatsu, A.; Miyazawa, H.; Kagechika, H. *Chem. Pharm. Bull.*, **2014**, *62*, 700.

(4) S. Li, P. Peng, J. Wei, Y. Hu, J. Hu, R. Sheng, *Adv. Synth. Catal.*, **2015**, *357*, 3429.

(5) J. Zhou, B. Li, Z.-C. Qian, B.-F. Shi, *Adv. Synth. Catal.*, **2014**, *356*, 1038.

(6) R. Saari, J.-C. Toermae, T. Nevalainen, *Bioorg. Med. Chem.*, **2011**, *19*, 939.

(7) C. C. C. J. Seechurn, S. L. Parisel, T. J. Colacot, *J. Org. Chem.*, **2011**, *76*, 7918.

(8) E. Bellamy, O. Bayh, C. Hoarau, F. Trécourt, G. Quéguiner, F. Marsais, *Chem. Commun.*, **2010**, *46*, 7043.

(9) P. Wang, M. E. Farmer, X. Huo, P. Jain, P.-X. Shen, M. Ishoey, J. E. Bradner, S. R. Wisniewski, M. D. Eastgate, J.-Q. Yu, *J. Am. Chem. Soc.*, **2016**, *138*, 9269.

(10) B. A. Abel, C. L. McCormick, *Macromolecules*, **2016**, *49*, 465.

(11) I. M. Yonova, C. A. Osborne, N. S. Morrissette, E. R. Jarvo, *J. Org. Chem.*, **2014**, *79*, 1947.

(12) J. A. Leitch, P. B. Wilson, C. L. McMullin, M. F. Mahon, Y. Bhonoah, I. H. Williams, and C. F. Frost, *ACS Catal.*, **2016**, *6*, 5520.

(13) a) I, Özdemir, S. Demir, B. Çetinkaya, C. Gourlaouen, F. Maseras, C. Bruneau, P. H. Dixneuf, *J. Am. Chem. Soc*., **2008**, *130*, 1156. (b) Y. Boutadla, D. L. Davies, S. A. Macgregor, A. I. Poblador-Bahamonde, *Dalton Trans*., **2009**, *0*, 5887. (c) I. A. Sanhueza, A. M. Wagner, M. S. Sanford, F. Schoenebeck, *Chem. Sci.,* **2013**, *4*, 2767.

(14) a) C. E. Kefalidis, O. Baudoin, E. Clot, E. *Dalton Trans.,* **2010**, *39*, 10528. b) C. E. Kefalidis, M. Davi, P. M. Holstein, E. Clot, O. Baudoin, *J. Org. Chem*., **2014**, *79*, 11903.